

TEKA

KOMISJI MOTORYZACJI  
I ENERGETYKI ROLNICTWA  
I WSCHODNIUKRAIŃSKIEGO NARODOWEGO UNIwersYTETU  
IM. WOŁODYMYRA DAŁA W ŁUGAŃSKU

COMMISSION OF MOTORIZATION  
AND POWER INDUSTRY IN AGRICULTURE  
THE VOLODYMYR DAHL EAST-UKRAINIAN  
NATIONAL UNIVERSITY OF LUGANSK

POLSKA AKADEMIA NAUK ODDZIAŁ W LUBLINIE  
WSCHODNIUKRAIŃSKI NARODOWY UNIWERSYTET  
IM. WOŁODYMYRA DAŁA W ŁUGAŃSKU

TEKA

KOMISJI MOTORYZACJI I ENERGETYKI  
ROLNICTWA

I

WSCHODNIUKRAIŃSKIEGO NARODOWEGO  
UNIWERSYTETU  
IM. WOŁODYMYRA DAŁA W ŁUGAŃSKU

Tom XIC

LUBLIN 2011

POLISH ACADEMY OF SCIENCES BRANCH IN LUBLIN  
THE VOLODYMYR DAHL EAST-UKRAINIAN  
NATIONAL UNIVERSITY OF LUGANSK

TEKA

COMMISSION OF MOTORIZATION  
AND POWER INDUSTRY IN AGRICULTURE  
AND  
THE VOLODYMYR DAHL EAST-UKRAINIAN  
NATIONAL UNIVERSITY OF LUGANSK

Volume XIC

LUBLIN 2011

President of editorial and scientific committee

*Eugeniusz Krasowski*

Secretary

*Zbigniew Burski*

Editorial committee

*Jan Gliński, Karol Cupiał, Aleksandr Dashchenko, Sergiej Fedorkin, Aleksandr Holubenko, Anatolij Yakovenko, Janusz Laskowski, Ryszard Michalski, Aleksandr Morozow, Janusz Mysłowski, Iliia Nikolenko, Paweł Nosko, Valeriy Dubrowin, Marek Rozmus, Wołodymyr Snitynskiy, Stanisław Sosnowski, Aleksandr Sydorczuk, Giorgiy F. Tayanowski, Viktor Tarasenko*

Scientific committee

<i>Andrzej Ambrozik, Kielce, Poland</i>	<i>Ignacy Niedziółka, Lublin, Poland</i>
<i>Volodymyr Bulgakow, Kiev, Ukraine</i>	<i>Stanisław Niziński, Olsztyn, Poland</i>
<i>Valeriy Diadychev, Ługańsk, Ukraine</i>	<i>Janusz Nowak, Lublin, Poland</i>
<i>Kazimierz Dreszer, Lublin, Poland</i>	<i>Jurij Osenin, Ługańsk, Ukraine</i>
<i>Bohdan Hevko, Ternopil, Ukraine</i>	<i>Sergiej Pastushenko, Kherson, Ukraine</i>
<i>Marek Idzior, Poznań, Poland</i>	<i>Józef Sawa, Lublin, Poland</i>
<i>L.P.B.M. Jonssen, Groningen, Holland</i>	<i>Ludvikas Spokas, Kaunas, Lithuania</i>
<i>Dariusz Andrejko, Lublin, Poland</i>	<i>Povilas A. Sirvydas, Kaunas, Lithuania</i>
<i>Dariusz Dziki, Lublin, Poland</i>	<i>Jarosław Stryczek, Wrocław, Poland</i>
<i>Józef Kowalczyk, Lublin, Poland</i>	<i>Wojciech Tanaś, Lublin, Poland</i>
<i>Stepan Kovalyshyn, Lwów, Ukraine</i>	<i>Henryk Tylicki, Bydgoszcz, Poland</i>
<i>Elżbieta Kusińska, Lublin, Poland</i>	<i>Michaił Sukach, Kiev, Ukraine</i>
<i>Kazimierz Lejda, Rzeszów, Poland</i>	<i>Denis Viesturs, Ulbrok, Latvia</i>
<i>Nikołaj Lubomirski, Symferopol, Krym, Ukraine</i>	<i>Dmytro Voytiuk, Kiev, Ukraine</i>
<i>Jerzy Merkiś, Poznań, Poland</i>	<i>Janusz Wojdalski, Warszawa, Poland</i>
<i>Leszek Mościcki, Lublin, Poland</i>	<i>Bogdan Żółtowski, Bydgoszcz, Poland</i>
<i>Jerzy Grudziński, Lublin, Poland</i>	<i>Tadeusz Złoto, Częstochowa, Poland</i>

All the scientific articles received positive evaluations by independent reviewers

Linguistic consultant: *Małgorzata Wojcieszuk*

Technical editor: *Robert Kryński*

Typeset: *Hanna Krasowska-Kołodziej, Robert Kryński*

Cover design: *Barbara Jarosik*

© Copyright by Commission of Motorization and Power Industry in Agriculture 2011

© Copyright by Volodymyr Dahl East-Ukrainian National University of Ługańsk 2011

Commission of Motorization and Power Industry i Agriculture  
Wielkopolska Str. 62, 29-725 Lublin, Poland  
e-mail: [eugeniusz.krasowski@up.lublin.pl](mailto:eugeniusz.krasowski@up.lublin.pl)

ISSN 1641-7739

Edition 150 + 16 vol.

## RESEARCH ON RELIABILITY OF SUBSYSTEMS OF GRAIN HARVESTING COMBINE

Anatoliy Boyko\*, Kostyantyn Dumenko\*\*

\*National University of Life and Environmental Sciences of Ukraine,  
Kyiv, 15, Heroyiv Oborony, 03041, Ukraine

\*\*Mykolaiv State Agrarian University,  
Faculty of Farm Mechanization, Mykolaiv, 17 A Krylova street, 54040, Ukraine  
e-mail: dumenkokn@mail.ru

**Summary.** The results of theoretical research on reliability indices of combine harvesters subsystems for effective realization of harvesting in short periods of reaping have been considered.

**Key words:** Reaping-machine, count of transitions, intensity of refuses, technical system, chain connection.

### INTRODUCTION

Combine harvesters are difficult multioperational machines. A specific feature of their work is the intensive exploitation during the short period of a calendar year. They work approximately for one month in a year at harvesting grains and it stipulates the special requirements to their reliability.

The insufficient level of technologies of production and quality of materials used, that reduce the reliability of machines, cause the development of wear, fatigue, corrosive and other processes which extend the period of the increase of intensity of refuses [1]. Actually, the existent harvesting equipment mainly works at the gradual decline of the level of reliability of basic subsystems which provide the technological process of harvesting [2-4].

Due to instability of the state, condition and technical maintenance of agricultural equipment, including combine harvesters, the determination of their reliability indices is rather complicated.

### RESULTS AND DISCUSSION

The purpose of work is the research of reliability of subsystems of combine harvesters indices for the effective realization of field work in short periods of harvesting[1].

In accordance with classical chart the combine harvesters consist of the following basic knots which provide their functioning: reaping-machine (pickup) of grain mass, thresh vehicle, key straw shaker, crash, elevator, sieve state, bunker with on unloading device.

From the point of view of reliability such technical system is a successive chain connection of subsystems (Fig. 1).

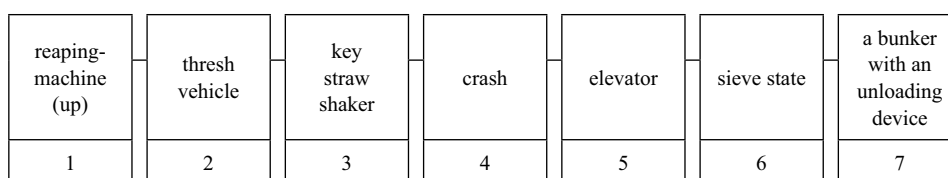


Fig. 1. General structural diagram of reliability of a grain harvester

The successive joining is known to be a basic joining for mechanical systems. The probability of faultless work in such case is determined according to the formula [3]:

$$P_c(t) = \prod_{i=1}^n P_i(t), \quad (1)$$

where:  $P_i(t)$  – probabilities of faultless work of subsystems components;  
 $i=1 \dots n$  - sequence number of subsystem.

The drawback of successive joining is that with the increase of amount of subsystems (due to the complication of equipment) the level of reliability without the application of special measures falls unavoidably[5-6].

In its turn, each of the combine subsystems can be presented as a system, consisting of subsystems of smaller grade, as well as separate elements. The hierarchy of a combine structure is in the total determined from the position of reliability, beginning from a general construction to its elements. The analysis of such structure makes it possible to determine the influence of the elements and structure constituents on the general level of reliability of a combine.

A reaping-machine (header) of a harvester combine is an independent subsystem aggregated with the basic part of machine. The constituents of the reaping-machine are a cutting vehicle, an auger, a reel and a chamber with a conveyer.

All mobile elements of the reaping-machine move due to a drive gear from a power plant of the combine. Thus, the reaping machine has the constituents which form a mechanical system, the flow diagram of reliability of which is represented on fig. 2.

Only the basic constituents which determine the possibility of carrying out the technological process of harvesting are presented on the chart. However, this chart, above all things, carries the information about the reliability connections in the system. It is evident, that, as well as in the previous chart, the successive connection of constituents is observed.

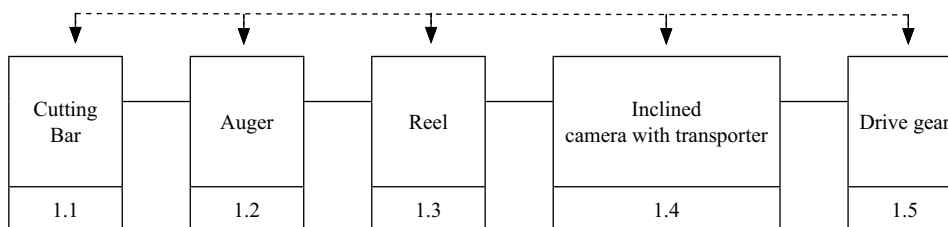


Fig. 2. Flowchart of reaper reliability

Such connection, peculiar to the mechanical systems, can be considered a basic one but at the same time the least reliable of all possible. Under the action of streams of events, related to the refuses and proceedings in a reaping-machine, the construction of trajectory of its conduct in transitions from state to state is possible (fig. 3).

The trajectory schematically represents the real situations of the possible states of the reaping machine in the periods of its operation, technical examination, adjustings and renewals. The trajectory of conduct is a composition of streams of random events and it is of stochastic character. The transition of the reaping machine to different possible states can be evidently presented as a graph of transitions (fig. 4). It takes into account not only the possible states conditioned by the action of streams of refuses and renewals, but also sets ties between the states as the orientation of events and intensity of their origin[7-8].

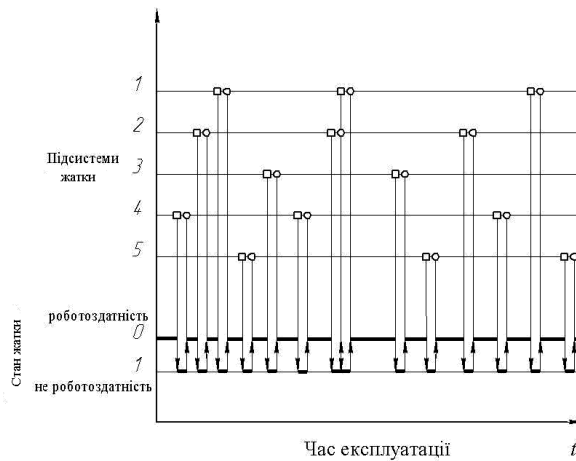


Fig. 3. Trajectory behavior of the reaping machine and its transition to different states:  
 □ - the moment of failure; ○ - the time of restoration.

Thus, the state of working ability is marked as “0”, and the refuse state “1”. The intensity of refuses is characterized by  $\lambda$  with an overhead index which specifies the number of subsystems and the reason for which the refuses occur, and the index below specifies the transition from the state of working ability to that of working disability. The intensity of renewals is marked accordingly as  $\mu$  with the index above, which specifies the number of a renewed subsystem, and the lower index specifies a transition from disabled to capable working state.

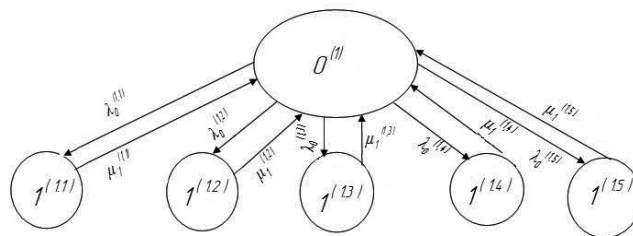


Fig. 4. Graph of reaper conversion to different states, in the state of disability and recovery

The next step of the combine elements differentiation within the reaper is to introduce the elements of the latest separately [5]. From the point of reliability the cutting device can be structured as follows (Fig. 5):



Fig. 5. Flowchart of reliability of reaper cutting device

Successive connection of elements makes a construction vulnerable to any types of refuses, and refuses form the certain streams of events, changing the system (the reaping machine) from a disabled state to a capable of working one. Operating under renewal forms the counterstreams which change the construction from the stage of repair to the capable of working state[9].

For the auger of the reaping machine, the basic characteristic damages are a bend of screws tearing them away at the places of welding, a bend of the pipe with pins and a wear of pins necks.

The wear of pins necks, as a typical damage, is also observed in reels. Alongside with it, there are cases of back pipe bend and key slot wear.

Most damages in a sloping chamber are observed in a chain conveyer which in case of wear is prolonged, and there are breaks of chain at development of cracks of fatigue. Lengthening is compensated by proper tension of chain, foreseen by periodic adjusting at technical examination.

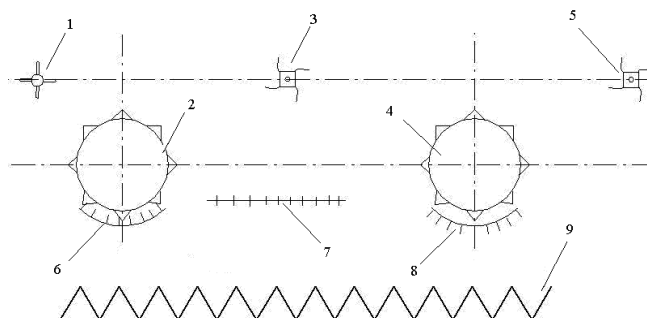


Fig. 6. Scheme of two drum threshing devices of combine harvester:

1 - receiving biter 2 - the first pulley, 3 - intermediate biter; 4 - pulley, 5 - jack biter, 6 - the first deck, 7 - support grid, 8 - the second deck, 9 - transport board cleaning.

The subsystem of a thresh vehicle consists of knots and details functionally combined between themselves. However, from the point of view of reliability the thresh vehicle is a mechanical system, intended for extracting grains from the ear. The refuse of any of the constituents of this subsystem results in the refuse of all aggregate. Therefore, the flowchart of reliability can be presented by the successive connection of elements (fig. 7).

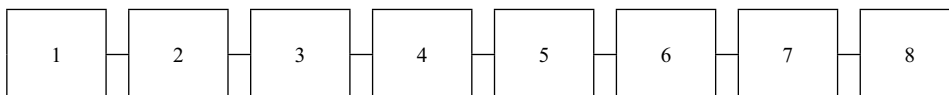


Fig. 7. Flowchart of reliability of threshing combine harvesters (designation according to Fig. 6)



The construction differs in minimum the possible amount of elements which are needed for implementation of functions for threshing grain. It also structurally meets the requirements reliability. Such construction of threshing machine requires highly reliable component elements. Otherwise, as a result of successive connection and in obedience to formula (1), a general level of probability of faultless work will be considerably low.

Graph of transitions of the thresh vehicle subsystem in different possible states at the loss of efficiency of component elements is presented in fig. 8.

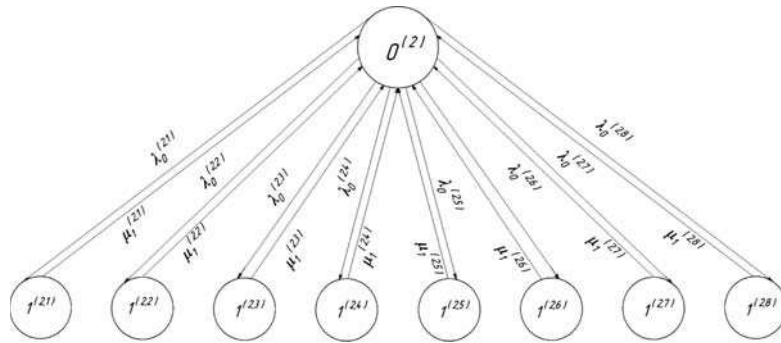


Fig. 8. Graph of conversion to possible states of threshing machine subsystem (designation according to Fig. 6)

As it is evident from the structural chart (fig. 6) and flowchart of reliability (fig. 7) the thresh vehicle subsystem differs in many elements. However, the elements of the subsystem can be grouped together according to their structural features and performed operations technology.

The first group includes the receiving, intermediate and pneumatic biter. Their characteristic defects are such as the deformation of blades, and break combs. These damages will be liquidated at renewals by smoothing the deformed details and welding at the places of breakage.

The second group is the thresh drums. The reasons of their break can be a wear of bill to a maximum state (appearance  $\Delta \leq 4$  mm), or destruction at emergency damages. In any case, the whips of the drums must be changed for the new ones. Thus, such operation of renewal must be executed in a specialized workshop, as the drum at replacement of serial whips needs subsequent dynamic balancing. The consequences of emergency damages can be decreased by changing the construction of the drum and providing it with short whips. At certain calculations it is possible to replace the damaged whips in the field conditions keeping the balance of the drum in the limits of possible disbalance. The application of the system of automatic balancing is also, possible.

A similar situation, but with its own  $\lambda$  and  $\mu$  features, occurs for the concaves, which are the counteractive elements in relation to the drums at beating out the grain. A difference only lies in the method of renewing the working elements of slats. To continue the work at a maximum wear they turn to a new working verge and at achievement of complete wear they are put out of operation and fixed as a refuse. However, such operation of renewal at the existent construction of concave can be made only once.

The key straw, crash and sieve state. An important subsystem for separation of grains from a straw is a key straw shaker. The keys of the straw shaker execute a difficult spatial motion which provides the divisions of fractions and their moving in the streams.

The principle of work of the subsystems of straw shaker and sieve lies in the restoration of oscillatory and forward motion necessary for division of fractions. Except for rare refuses, due to the

materials, defects development of cracks or insufficient level of technological culture of production, the principal reasons for loss of efficiency in the indicated subsystems is a wear of slide bearings in a driving gear mechanism. In general, such refuses can be considered on the example of the slide bearing of strawshaker[10].

In the wide-spread Soviet combines made at Rostov-on the-Don factory «Rostselmash» the wooden lubricated bearings are used. The advantage of such bearings is the simplicity of construction, possibility of adjusting a gap and easy replacement at achievement of maximum wear[11].

Summarizing the presented analysis of structural construction of subsystems of combine harvesters it is possible to conclude, that their classical structural solutions are executed mainly on the linear chart of successive connections of elements. It is the simplest realization of the machine as a technical system fairly adapted to the real terms of the long-term effective exploitation. At such construction of difficult agricultural equipment the achievement of the necessary level of reliability is possible only due to the use of high-quality and proper materials for the details, as well as the timely regulation of servicing work.

## CONCLUSIONS

The problem of support of the necessary level of reliability of combine harvesters becomes complicated due to the change of their physical condition in the process of details exploitation. Physical and chemical processes of wear of details, accumulation of damages, as a result of fatigue of materials, different types of hammerings, overloads, corrosive processes are quite common. The equipment gradually loses the initial level of readiness to the implementation of harvest work. These are natural processes which take place in the machines after the increase of their running time and the term of exploitation. The alternative can be the improvement of construction and timely skilled technical maintenance of the combine systems. Due to such actions it is possible to support the necessary level of reliability of the equipment for efficient field work and harvesting in short periods of reaping.

## REFERENCES

1. **Boyko A.I.:** Research of function of readiness of the mechanical systems at the accumulation of damages / A.I. Boyko, K.M. Dumenko of // Problem of calculable mechanics and durability of constructions: Bulletin of scientific works, Dnipropetrovsk : Science and education, 2010. — /issue.14. — pp. 72-78.
2. **Pogorily L.V.:** Harvesting Equipment: problems, alternatives, prognosis / L.V. Pogorily, S.M. Koval // Technika APK. — 2003. — №7. — pp.4—7.
3. **Ushakov I.A.:** Theory of Reliability Systems / I.A. Ushakov. — M.: Drofa, 2008. — 239 p.
4. **Nekiporenko V.I.:** Structural Analysis of systems / V.I. Nekiporenko. M. : Sovetskoe radio, 1977. — 214 p.
5. **Gritsishin M.:** Requirements to Combine Harvesters / M. Gritsishin, V. Amons, P. Grinko // Technika APK. — 2003.—№2— of 33. 9—15.
6. **Sudakov P.S.:** Ispytaniya sistem: vubor ob'emov i prodolgitelnosti. M.: Mashinostroenie, 1988. p. — 445.
7. **Truhanov V.M.:** Metodu obespecheniya nadezhnosti izdeliy mashinostroeniya. M.: Mashinostroenie, 1995. p. — 304.
8. **Truhanov V.M.:** Nadezhnost' v tehnike. M.: Mashinostroenie, 1999. p. — 598.

9. **Truhanov V.M.:** Nadegnost' izdeliy mashinostroeniya: Teoriya i praktika. M.: Mashinostroenie, 1996. p. – 336.
10. **Hald A.:** Matematicheskaya statistika s tehniceskimi prilozheniyami. M.: Inostrannaya literatura, 1956. p. – 379.
11. **Truhanov V.M., Zubkov V.F., Kruhtin U.I., Geltobruhov V.F.:** Transmisii gusenichnuh kole-snuh mashin. M.: Mashinostroenie, 2001. p. – 736.

#### BADANIA NIEZAWODNOŚCI PODSYSTEMÓW ZBOŻOWEGO KOMBAJNU

**Streszczenie.** Rezultaty badań teoretycznych na indeksach niezawodności podsystemów zbożowego kombajnu dla realizacji zbioru efektywnego ziarna w najkrótszym okresie.

**Słowa kluczowe:** grafy przemieszczeń, efektywność, techniczne systemy, związki koniudżow.

## MODELLING OF TRAFFIC FLOW IN AN URBAN TRANSPORTATION SYSTEM

Norbert Chamier-Gliszczyński

Politechnika Koszalińska, Zakład Mechatroniki i Mechaniki Stosowanej  
norbert.chamier-gliszczyński@tu.koszalin.pl

**Summary.** The present study covers proposals related to the formation of the traffic flow in an urban transportation system. An analysis was also presented of the traffic flow in a urban transportation system within two selected days of the week.

**Key words:** urban transportation system, traffic flow.

### INTRODUCTION

The movements of city dwellers in a transport system of a given city is represented by the traffic flow through the junctions and arcs of the urban transport network. The traffic flows to the transport network through those points that constitute the flow sources, it moves through the individual indirect junctions and connections in the transport network and leaves the network at the outlet point of the traffic flow. In the case of travels in the city area, the residents move from sending points (set  $A$ ) through a number of intermediate points (set  $V$ ) to collection points (set  $B$ ) (Fig. 1). There occurs a condition between the individual points [1, 2, 3, 4, 5]:

$$W = A \cup V \cup B, \quad (1)$$

where:

$W$  – set of components urban transport network,

$A$  – set of sending points,

$V$  – set of intermediate points,

$B$  – set of collection points.

The relationship between an ordered pair of points from sets  $A$  and  $B$  constitutes a transport relation [3, 5, 7]:

$$A \subset W, \quad B \subset W. \quad (2)$$

On this basis, we can define a set of all transport relations  $E$  in the urban transport network [2, 3, 5]:

$$E \subset (A \times B) = \{(a, b) : a \in A, b \in B\}. \tag{3}$$

At the same time, for each transport relation, a set of connections between the individual vertices of the graph of the urban transport network is defined. This set is marked as  $P^{ab}$ , where  $P$  is the set of all the routes in the urban transport network [2, 3, 5]:

$$P = \bigcup_{(a,b) \in E} P^{ab}. \tag{4}$$

The size of the traffic flow in the urban transport network between a distinguished pair of vertices  $(a, b)$  on the set of transport relations  $E$  is defined as:

$$x(a, b) \equiv x^{ab} \tag{5}$$

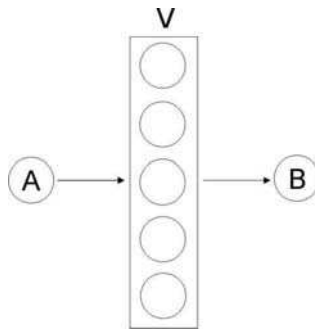


Fig. 1. Diagram of the movement of the traffic flow in the urban transport network: A – set of sending points, V – set of intermediate points, B – set of collection points

### INVESTIGATION THE TRAFFIC FLOW IN THE URBAN TRANSPORTAION SYSTEM

The investigations into the traffic flow in the urban transportation system were divided into two stages:

- the first stage is the definition of the basic parameters which characterize the traffic flow,
- the second stage is a direct analysis of the communication behaviors of city dwellers.

#### Stage 1

At the same time, the graph in the following form represents the transport tasks realized on Saturdays and Sundays [6] (Fig. 2):

$$G2 = \langle W2, L2 \rangle, \tag{6}$$

where:

$W2$  – set of components of graph  $G2$ :

$$W2 = \{w2_1, w2_2, w2_3, w2_4, w2_5, w2_6\}, \quad (7)$$

where:

$w2_1$  – home,

$w2_2$  – purchase,

$w2_3$  – amusement,

$w2_4$  – school,

$w2_5$  – workplace,

$w2_6$  – other,

$L$  – set of connections of graph  $G2$ :

$$L2 = \{l2_1, l2_2, l2_3, l2_4, l2_5, l2_6, l2_7, l2_8\}, \quad (8)$$

where:

$l2_1$  – connection  $w2_1$ - $w2_2$ ;  $w2_2$ - $w2_1$ ,

$l2_2$  – connection  $w2_4$ - $w2_1$ ,

$l2_3$  – connection  $w2_5$ - $w2_1$ ,

$l2_4$  – connection  $w2_1$ - $w2_3$ ;  $w2_3$ - $w2_1$ ,

$l2_5$  – connection  $w2_1$ - $w2_6$ ;  $w2_6$ - $w2_1$ ,

$l2_6$  – connection  $w2_2$ - $w2_3$ ,

$l2_7$  – connection  $w2_4$ - $w2_3$ ,

$l2_8$  – connection  $w2_3$ - $w2_5$ .

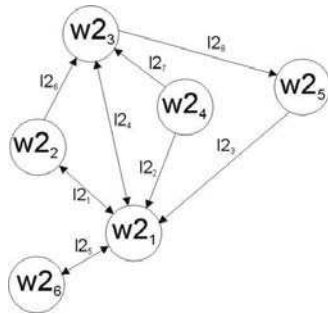


Fig. 2. The graph  $G2$  in the following form represents the transport tasks realized on Saturdays and Sundays

In the research carried out, four parameters were defined which have a direct influence on the traffic flow. These parameters include the following: time of the day, transport distances, the duration time of a transport task and the type of the means of transport.

Time of the day.

We assume that on Cartesian product  $X^{ab} \times W \times W$ ,  $dt$  representation is given of the following form:

$$dt : X^{ab} \times W \times W \rightarrow \mathbb{R}^+, \quad (9)$$

where quantity  $dt(a, b)$  is a non-negative real number with an interpretation of time interval  $(i, j)$  which determines the time of the day in the relation of transport  $(a, b)$ . For the purpose of clarity, we will use the notation as below:

$$dt((a, b), (i, j)) \equiv dt^{(a, b)}, \quad dt^{(a, b)} \geq 0. \quad (10)$$

Transport distances.

Quantity  $d(a, b)$  is a non-negative real number with an interpretation of the distance covered  $(i, j)$  in the relation of transport  $(a, b)$ :

$$d: X^{ab} \times W \times W \rightarrow \mathbb{R}^+, \quad d((a, b), (i, j)) \equiv d^{(a, b)}, \quad d^{(a, b)} \geq 0. \quad (11)$$

Duration time of a transport.

Quantity  $t(a, b)$  is a non-negative real number with an interpretation of the duration time of a transport  $(i, j)$  of the relation of transport  $(a, b)$ :

$$t: X^{ab} \times W \times W \rightarrow \mathbb{R}^+, \quad t((a, b), (i, j)) \equiv t^{(a, b)}, \quad t^{(a, b)} \geq 0, \quad (12)$$

Means of transport.

Quantity  $mt(a, b)$  is a non-negative real number with an interpretation of the selected means of transport  $(k)$  in the relation of transport  $(a, b)$ :

$$mt: X^{ab} \times W \times W \rightarrow \mathbb{R}^+, \quad mt((a, b), (k)) \equiv mt^{(a, b)}, \quad mt^{(a, b)} \geq 0, \quad (13)$$

## Stage 2

The investigations into the traffic flow were carried out based on the monitoring of social attitudes concerning a sustainable transport [8], they covered an analysis of the communication behavior of city dwellers. The research was narrowed down to two days of the week, i.e. Saturday and Sunday.

The largest traffic flow which moves at the connections of  $G2$  graph was observed in  $dI$  transport distances and involved 274 people. Out of this, 27% of people moved on foot and 70% of people traveled by passenger car (Fig. 3).

When analyzing the traffic flow moving on Saturday and Sunday on the connections of  $G2$  graph, an observation was made that every third transport task fell into in  $t2$  time interval, i.e. from 6 to 10 minutes. Out of this, 34% people moved on foot and 24% people traveled by car. The remaining data with respect to the duration time of the transport task taking into consideration the type of the means of transport can be found in fig. 4.

While taking into account  $dt$  parameter, i.e. time of the day, it was observed that during the day, the majority of transport tasks (82-87%) were realized by passenger car (Fig. 5). In the evening and at night, 79% and 74% of transport tasks respectively were performed with the use of a passenger car (Fig. 5).

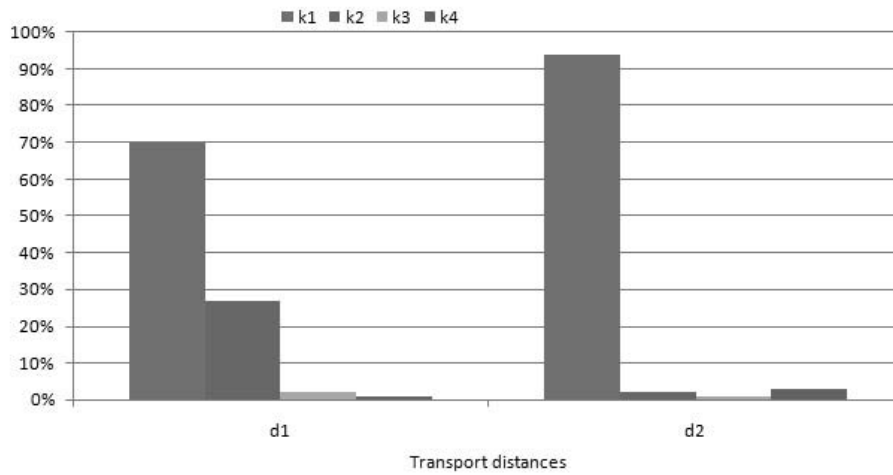


Fig. 3. The percentage share of those means of transport which are used to satisfy the transport needs of city dwellers – transport distances [8]: d1 – up to 5 km, d2 – over 5 km, k1 – passenger car, k2 – on foot, k3 – public transport, k4 – other

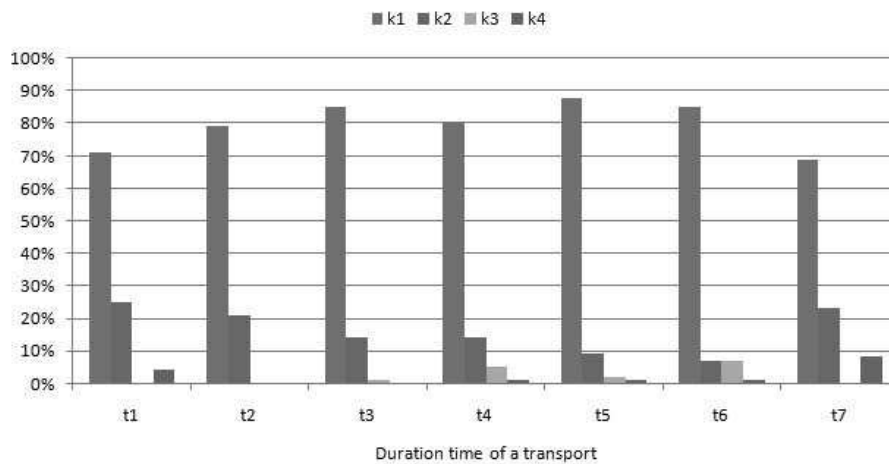


Fig. 4. The percentage share of those means of transport which are used to satisfy the transport needs of city dwellers – duration time of a transport [8]: t1 – up to 5 min, t2 – 6-10 min, t3 – 11-15 min, t4 – 16-20 min, t5 – 21-30 min, t6 – 31-60 min, t7 – over 60 min, k1 – passenger car, k2 – on foot, k3 – public transport, k4 – other



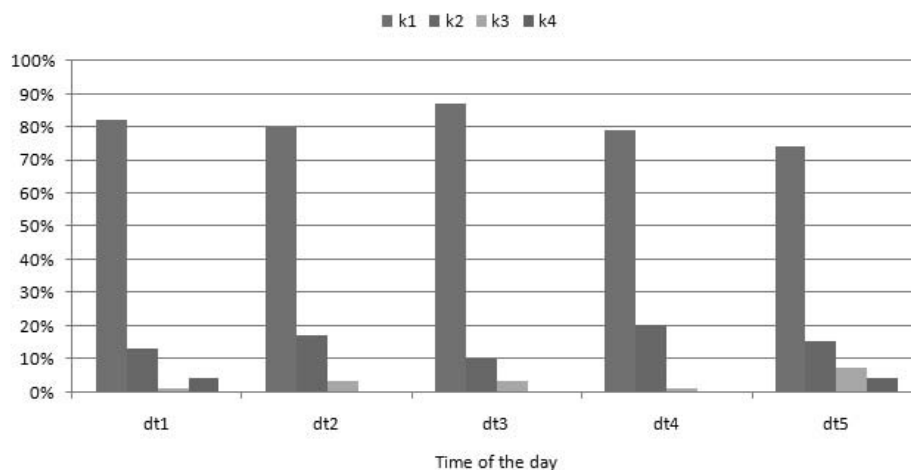


Fig. 5. The percentage share of those means of transport which are used to satisfy the transport needs of city dwellers – time of the day [8]: dt1 – 6:00am-9:59am, dt2 – 10:00am-2:59pm, dt3 – 3:00pm-5:59pm, dt4 – 6:00pm-9:59pm, dt5 – 10:00pm-5:59am, k1 – passenger car, k2 – on foot, k3 – public transport, k4 – other

## CONCLUSIONS

The formation process of the traffic flow in a urban transportation system which is presented in the study constitutes a separated fragment of a larger project whose task is to build a sustainable urban transportation system. Research concerning the traffic flow in a urban in relation to the four parameters distinguished, i.e. time of the day, transport distances, the duration time of a transport task, the type of the means of transport, is one the constituents of the construction of a sustainable urban transportation system. The results of these investigations were also presented in the study.

## REFERENCES

1. Ambroziak T.: Modelowanie procesów technologicznych w transporcie. Prace Naukowe, Transport 40, Oficyna Wydawnicza Politechniki Warszawskiej, Warszawa 1998.
2. Crainic T., Laporte G.: Planning models for freight transportation. European Journal of Operational Research, vol. 97, no 3 1997.
3. Jacyna M.: Modelowanie i ocena systemów transportowych. Oficyna Wydawnicza Politechniki Warszawskiej, Warszawa 2009.
4. Jacyna M.: Modelowanie wielokryterialne w zastosowaniu do oceny systemów transportowych. Prace Naukowe, Transport z. 47, Oficyna Wydawnicza Politechniki Warszawskiej, Warszawa 2001.
5. Jarzębińska-Dziegciar A.: Optymalizacja nieliniowych sieci transportowych z wykorzystaniem algorytmów genetycznych. Rozprawa doktorska, Politechnika Warszawska, Wydział Transportu, Warszawa 2004.

6. Korzan B.: Elementy teorii grafów i sieci. Metody i zastosowanie. Wydawnictwo Naukowo-Techniczne, Warszawa 1978.
7. Leszczyński J.: Modelowanie systemów i procesów transportowych. Oficyna Wydawnicza Politechniki Warszawskiej, Warszawa 1999.
8. Raport: Monitorowanie postaw społecznych w zakresie zrównoważonego transport. Pierwszy etap. PBS DGA/Ministerstwo Środowiska, Sopot 06.2010.

### MODELOWANIE POTOKU RUCHU W MIEJSKIM SYSTEMIE TRANSPORTOWYM

**Streszczenie.** W pracy przedstawiono propozycje kształtowania potoku ruchu w miejskim systemie transportowym. Zaprezentowano również analizę potoku ruchu w miejskim systemie transportowym w przeciągu dwóch wybranych dni tygodnia.

**Słowa kluczowe:** miejski system transportowy, potok ruchu.

## SELECTED ASPECTS OF MODELLING OF SUSTAINABLE URBAN TRANSPORTATION SYSTEM

Norbert Chamier-Gliszczyński

Politechnika Koszalińska, Zakład Mechatroniki i Mechaniki Stosowanej  
norbert.chamier-glisczynski@tu.koszalin.pl

**Summary.** The article refers to a system approach which is used in an analysis of transport issues. A proposal for the construction of a model of a sustainable urban transportation system was presented.

**Keywords:** urban transportation system, sustainable urban transportation system.

### INTRODUCTION

The dominating issue in the European transport policy is a vision to create a future oriented sustainable transport system with a high level of safety, one which is environment friendly and energy-efficient [11]. The so-called clean city transport constitutes a distinguished area in this policy. An implementation was initiated of a sustainable urban transport system, one which does not involve any hazards to the health of communities and ecosystems, and at the same time fulfils the needs connected with the mobility of the residents of a urban structure, while making use of the following [2]:

- renewable resources on the level of their regeneration,
- non-renewable resources on the level of replacing them with renewable substitutes.

All the activities related to the realization of a sustainable development of a urban transport system can be defined as the realization of the following objectives [10]:

- a reduction of the quantity of the pollution emitted by the means of transport up to such a level which is not dangerous to health and does not cause a reduction of the quality of the environment,
- a limitation of the emissions of those greenhouse gases from transport,
- an improvement of safety in transport,
- an improvement of the acoustic climate through actions leading to a reduction of the noise from transport,
- a minimization of the results of the congestion phenomenon,
- an elimination of bottlenecks and deficiencies in the infrastructure in the individual EU Member States,

- an improvement of the mobility of citizens and overcoming differences in the access to the transport infrastructure.

### URBAN TRANSPORTATION SYSTEM

The object whose description is defined as a set of interrelated elements and the environment in a manner which permits the achievement of a specific goal is known as a system [9]. The system analyzed in this study is a transport system whose purpose is a migration of people. This migration concerns both the residents of a given city and areas which surround a given city. By isolating the urban transport system from the existing reality, we have divided this reality into the system and the environment. The process carried out in this way results in an establishment of the boundaries of the system, i.e. a determination of those elements (objects) which are included among the elements of the system and those which are included in the environment. Obviously enough, this depends from the purpose the of research and therefore those relations which due to the defined purpose of the research are not essential, are omitted. At the same time, the impact of the environment on the transport system and vice versa occurs through external stimuli (input quantities) and reactions (output quantities) [5].

Taking into account the assumption that the system is a distinguished set of elements and a set of relations that are determined on its elements in the present deliberations, the structure of the transport system will be defined as an arranged pair in the following form [1, 5, 6, 9]:

$$S = \langle A, R \rangle, \quad (1)$$

where:

S – transport system,

A – a set of elements of the transport system [5],

$$A = \{a_i : i = 1, 2, \dots, n\}, \quad (2)$$

R – a set of relations defined on the elements of the transport system [5],

$$R = \{R_j : j = 1, 2, \dots, m\}, \quad (3)$$

for whom  $R_j$  relation is a subset of the Cartesian product in the following form [5],

$$R_j \subset A \times A \quad \text{dla } j = 1, 2, \dots, m. \quad (4)$$

The set of relations defined on the elements of the transport system depends from the purpose or the purposes which a given system realizes, which may include the following [6]:

- finding of the rules which decide about the processes which occur in the system analyzed, which will permit obtaining information that may constitute data for further research,
- an identification and optimization of the structure and control of the system analyzed.

## MODEL OF A SUSTAINABLE URBAN TRANSPORTATION SYSTEM

The model of a sustainable urban transportation system will be written as an arranged triple in the following form [1, 5, 7, 8, 9]:

$$\text{MZMST} = \langle G, F_w, F_o \rangle, \quad (5)$$

where:

MZMST – model of a sustainable urban transportation system,

$G$  – graph,

$F_w$  – the set of the functions determined on the set of the vertices of graph  $G$ ,

$$F_w = \{\phi_1, \phi_2, \dots, \phi_u\}, \quad u = 1, 2, \dots, U, \quad (6)$$

$U$  – the number of representations determined on the set of the vertices of graph  $G$ ,

$F_o$  – the set of the functions determined on the set of the connections of graph  $G$ ,

$$F_o = \{\gamma_1, \gamma_2, \dots, \gamma_z\}, \quad z = 1, 2, \dots, Z. \quad (7)$$

$Z$  – the set of the representations determined on the set of the connections of graph  $G$ .

The structure of a sustainable urban transportation system will be presented by means of graph  $G$ , where each connection is represented in the form of a graph arc. Destination points will be represented in the form of the vertices of this graph. This graph is written in the following form [1, 5, 7, 8, 9]:

$$G = \langle W, L, R \rangle, \quad (8)$$

where:

$W$  – set of components of graph  $G$ ,

$L$  – set of connections of graph  $G$ ,

$R$  – relation  $W \times L \times W$ .

For the purpose of the uniqueness of further considerations, we accept the following notation of the vertices and connections in graph  $G$ :

$$W = \{w(i) \equiv i: i = 1, 2, \dots, I\}; \quad i = \{1, 2, \dots, i, j, \dots, I\}, \quad (9)$$

$$L = \{(w(i), w(j)): w(i), w(j) \in W, w(i) \neq w(j) \quad i, j \in I\}. \quad (10)$$

As it can be seen from the above, the sustainable transport system in question possesses  $I$  graph vertices and  $K$  graph connections. Representation  $R$  transforms Cartesian product  $W \times O \times W$  into set  $\{0, I\}$  [1, 2, 3, 5, 7]:

$$R: W \times L \times W \rightarrow \{0, I\}. \quad (11)$$

Any triplet  $(w(i), o(k), w(j)) \in W \times L \times W$  such that  $R(w(i), l(k), w(j)) = I$  is interpreted in the following manner: arc  $l(k)$  which connects vertex  $w(i)$  with vertex  $w(j)$ ,  $w(i) \neq w(j)$  or arc  $l(k)$  is included

between vertices  $w(i)$  and  $w(j)$ . At the same time, any triplet  $(w(i), l(k), w(j)) \in W \times L \times W$  such that  $R(w(i), l(k), w(j)) = 0$  is interpreted in the following manner: arc  $l(k)$  does not connect vertex  $w(i)$  with vertex  $w(j)$ ,  $w(i) \neq w(j)$  or arc  $l(k)$  is not included between vertices  $w(i)$  and  $w(j)$ .

At the same time, graph  $G$  needs to possess an asymmetry property and an acclivity property in the meaning of roads [5, 7, 9]. Graph  $G$  is known as an asymmetric graph if the following condition is fulfilled for the arches of this graph:

$$\begin{aligned} \forall (l(k) \in L) \quad \exists (w(i), w(j) \in W : w(i) \neq w(j)), \\ R(w(i), l(k), w(j)) = 1 \Rightarrow \forall (l(k') \in L : l(k') \neq l(k)), \\ R(w(j), l(k'), w(i)) = 0. \end{aligned} \quad (12)$$

### INVESTIGATIONS INTO THE INITIAL STATE OF URBAN TRANSPORTATION SYSTEM

The investigations into the initial state of the urban transport system were carried out based on the monitoring of social attitudes concerning a sustainable transport [12], they covered an analysis of the communication behavior of city dwellers. The communication behavior of the city dwellers constitutes the realization of the given transport tasks with a division into two following scopes:

- transport tasks realized in the period from Monday to Friday,
- transport tasks realized on Saturdays and Sundays.

The graph in the following form represents the transport tasks realized from Monday to Friday (Fig. 1):

$$G1 = \langle W1, L1 \rangle, \quad (13)$$

where:

W1 – set of components of graph  $G1$ ,

$$W1 = \{w1_1, w1_2, w1_3, w1_4, w1_5, w1_6, w1_7, w1_8\}, \quad (14)$$

L1 – set of connections of graph  $G1$ ,

$$L1 = \{l1_1, l1_2, l1_3, l1_4, l1_5, l1_6, l1_7, l1_8, l1_9, l1_{10}, l1_{11}\}. \quad (15)$$

At the same time, the graph in the following form represents the transport tasks realized on Saturdays and Sundays (Fig. 2):

$$G2 = \langle W2, L2 \rangle, \quad (16)$$

where:

W2 – set of components of graph  $G2$ ,

$$W2 = \{w2_1, w2_2, w2_3, w2_4, w2_5, w2_6\}. \quad (17)$$

L2 – set of connections of graph G2:

$$L2 = \{l2_1, l2_2, l2_3, l2_4, l2_5, l2_6, l2_7, l2_8\}. \tag{18}$$

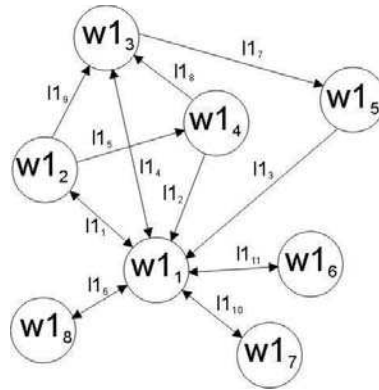


Fig. 1. The graph G1 in the following form represents the transport tasks realized from Monday to Friday

### CONCLUSIONS

A model approach to the urban transport system may successfully be used to solve optimization problems concerning a limitation of the environmental impact of the city transport. Such investigations are conducted by the author of this article, and the purpose of this research is a sustainable migration of city dwellers in the aspect of a minimization of the external costs of the urban transport. The external costs are costs connected with the negative environmental effects of the functioning of a urban transport system, and in particular costs connected with the following [4, 13]:

- air, water and soil pollution [14],
- noise emission,
- traffic collisions and road accidents,
- the occupancy of the area.

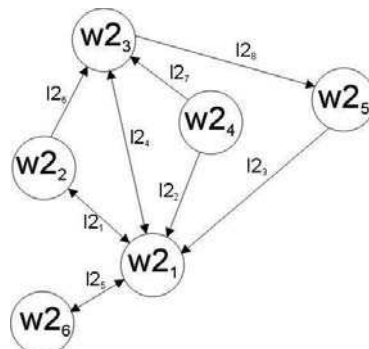


Fig. 2. The graph G2 in the following form represents the transport tasks realized on Saturdays and Sundays

## REFERENCES

1. Ambroziak T.: Modelowanie procesów technologicznych w transporcie. Prace Naukowe, Transport 40, Oficyna Wydawnicza Politechniki Warszawskiej, Warszawa 1998.
2. Cisowski T., Szymanek A.: Zrównoważony rozwój transportu miejskiego. Eksploatacja i Niezawodność 1/2006.
3. Crainic T., Laporte G.: Planning models for freight transportation. European Journal of Operational Research, vol. 97, no 3 1997.
4. Jacyna M.: Kształtowanie systemu transportowego w aspekcie zrównoważonego rozwoju. Badania operacyjne i systemowe 2006. Analiza systemowa w globalnej gospodarce opartej na wiedzy: e-wyzwania pod redakcją Urbańczyka E., Straszaka A., Owińskiego J.W. Akademicka Oficyna Wydawnicza EXIT, Warszawa 2006.
5. Jacyna M.: Modelowanie i ocena systemów transportowych. Oficyna Wydawnicza Politechniki Warszawskiej, Warszawa 2009.
6. Jacyna M.: Modelowanie wielokryterialne w zastosowaniu do oceny systemów transportowych. Prace Naukowe, Transport z. 47, Oficyna Wydawnicza Politechniki Warszawskiej, Warszawa 2001.
7. Jarzębińska-Dziegciar A.: Optymalizacja nieliniowych sieci transportowych z wykorzystaniem algorytmów genetycznych. Rozprawa doktorska, Politechnika Warszawska, Wydział Transportu, Warszawa 2004.
8. Korzan B.: Elementy teorii grafów i sieci. Metody i zastosowanie. Wydawnictwo Naukowo-Techniczne, Warszawa 1978.
9. Leszczyński J.: Modelowanie systemów i procesów transportowych. Oficyna Wydawnicza Politechniki Warszawskiej, Warszawa 1999.
10. Pawłowska B.: Analizowanie efektywności procesów równoważenia rozwoju transportu. Logistyka 2/2010.
11. Piekarski D.: Zrównoważony system transportowy: moda czy konieczność. Autobusy, Technika, Eksploatacja, Systemy transportowe, 6/2010.
12. Raport: Monitorowanie postaw społecznych w zakresie zrównoważonego transportu. Pierwszy etap. PBS DGA/Ministerstwo Środowiska, Sopot 06.2010.
13. Rydzyński P., Michajłow U.: Raport – Zewnętrzne koszty transportu. Rynek Kolejowy, 2/2004.
14. Zielińska E., Leja K.: Ecological problems of transport vehicles. TEKA, Commission of Motorization and Power Industry in Agriculture, Volume X, Lublin 2010.

WYBRANE ASPEKTY MODELOWANIA ZRÓWNOWAŻONEGO  
MIEJSKIEGO SYSTEMU TRANSPORTOWEGO

**Streszczenie.** Artykuł odwołuje się do systemowego podejścia wykorzystywanego w analizie zagadnień transportowych. Przedstawiona została propozycja budowy modelu zrównoważonego miejskiego systemu transportowego.

**Słowa kluczowe:** miejski system transportowy, zrównoważony miejski system transportowy.



## ENERGETIC AND TECHNOLOGICAL ANALYSIS OF THE PROCESS OF OIL PRESSING FROM WINTER RAPE

Adam Drosio\*, Marek Klimkiewicz\*, Remigiusz Mruk\*

\* Warsaw University of Life Sciences, Poland

**Summary.** There were carried out energetic and technical analysis of technology for winter rapeseed oil extraction designer for RME production in the farm. The technological process was subjected to optimization in respect to maximization of process productivity, minimization of energy demand, and maximization of rapeseed oil output.

The developed model of winter rape seed production in the farm is a tool that facilitates decision making on advisability of production undertaking or abandonment under conditions of the farm. It would facilitate a direct selection of machines and equipment for the defined production scale.

**Key words:** rapeseed oil, oil extraction, process energy consumption, winter rape, biofuels, raw material for RME production.

### INTRODUCTION

An increase in prices and petroleum shortage caused the interest in renewable fuels (biofuel) originated also from the oil plants. Biofuels for engine fuel systems should be, first of all, used in agriculture, since raw materials for biofuel production come mainly from agricultural production as a main crop or its by-products. The opinion that satisfaction of agricultural energetic needs should be achieved with the use of farm raw materials becomes more and more common [Drosio and Klimkiewicz 2009]. The efforts in this direction will enhance activity and restructuring of rural areas and allow for utilization of biofuel and its by-products directly by the producers. Fulfillment of this postulate can enhance stabilization of agricultural production and prices of agricultural products; it can also assure the energetic and food security of the country.

European Union maintains the agrarian policy that supports production of plant raw materials to be used in biofuel production [Kupczyk 2008]. These materials should not compete with food production and should be utilized directly on the farm; this will greatly reduce the logistic costs and technical infrastructure development, and improve energetic security in particular countries and UE.

The rapeseed oil can be widely used, since it can be fed to the self-ignition engines after minor modifications of fuel system [Bocheński and Bocheńska, 2008, Jakóbiec et al. 2009, Mruk 2006]. Striving at common application of rapeseed oil as a self-contained fuel (particularly in agriculture) is justified with its beneficial effect on natural environment and also with lower energy inputs in its production when compared to rapeseed methyl esters (RME).

Actuating the rapeseed oil extraction proves in farms can enhance the full use of production potential of seeds, straw and by-products (oil cakes). Part of seed crop can be used for food purposes, and the second part for biofuel production. The rape straw can be used for fabrication of highly-energetic fuel in the form of briquettes or pellets.

The oil output from the classical technology application can be high, which is a strong advantage of that method. However, it has some disadvantages also, namely the poor quality of post-extraction oil meal due to solvent residue and denatured protein content. Additionally, extraction equipment affects adversely the environment by emitting the aliphatic hydrocarbons into atmosphere (Tys et al. 2003).

During oil extraction with the use of screw presses the oil is not fully extracted, and its substantial part 8 – 14% remains in the oil cake (Jaswant and Bargale 2000).

Possibility of management of oil cake obtained in the oil extraction process, as an animal feed component, is very important; it enables to obtain a high-protein and high-energetic animal feed at reduced production costs.

Parameters of obtained oil, its chemical composition and the content of contaminants greatly depend on pressing parameters (Klimkiewicz and Wiechetek 2008, Klimkiewicz et al. 2010, Panasiewicz et al. 2009).

## PURPOSE AND METHODS

**The scientific aim** was to analyze effectiveness of oil extraction from winter rape seeds in a small farm, and evaluation of energy demand and oil output in this process. The process optimization affects directly effectiveness of oil extraction process, in respect of energetic and economic considerations.

The basic tool used in the work was process modeling that allowed for analysis and making variants. The developed optimization models were used in decision-making on selection of the best variant. The effect of press technical parameters on energy consumption and energetic effectiveness of the process was investigated (Gach, 2009; Jaros and Pabis 2007; Chmielecki 2006). Then, the process optimization for the assumed production scale was performed. The working parameters of equipment were taken according to manufacturer's recommendations.

**The utility aim** was to develop the information models for particular variants of oil extraction process that can be used by farmers to verify justification of a given variant application, together with determination of its effectiveness.

The process model developed for the farm is a tool facilitating decision making on undertaking production or its abandonment under the farm conditions. It would facilitate a direct selection of machines and equipment for the defined production scale and would allow for evaluation of effectiveness at assumed process parameters.

Numerical methods implemented in MatLab program were used in the modeling process. The active experiment on rapeseed oil extraction was aided by LabView program.

### **Methodology of investigations**

Each farm where the technological process is realized is characterized by different and specific production-site conditions and different activity aims. Therefore, evaluation criteria for technological processes are usually quite different (Banasiak 2008).

With respect to rapeseed oil extraction technology there were determined parameters of decision variables and constants for particular process variants. Then, there was performed the modeling of oil extraction process basing on the results obtained from oil seed extraction process with the use of the press of exchangeable die with various diameter of outlet hole. The change in screw rotational speed of press screw was considered also. There were developed three independent optimization models of the following objective functions: process productivity, energy demand and oil output.

Equipment of various design is available in the market; therefore, devices of output suitable for small farm conditions have been selected. The optimization process was carried out with the use of MATLAB program and function library **Optimization Toolbox**.

In optimization there were assumed the exemplary organization-site parameters for the farm of area 60 ha. It allows for agricultural commodity production under EU market position and is determined by technological, economic and social conditions. The 4-year rape succession and its 25% share in the crop structure were assumed in the farm. The remaining 75% were left for cereals.

The liquid fuel demand in the farm was assumed as 86 l/ha of diesel oil according to Council of Ministers' Decree of 8 Dec. 2009 on the excise tax refund included in diesel oil price used in agricultural production. No excise tax refund included in biofuels was considered in the Decree (Waszkiewicz, 2009). For such conditions there was proposed the machine fleet that allowed for execution of oil extraction process and biodiesel production to satisfy the fuel demand of own agricultural farm.

In investigations the screw press Farnet PSL UNO 7 (Farnet, 2010) was used; the 1.1 kW motor parameters were controlled with the inverter Hitachi SJ100 (Hitachi 2001) that allowed for current frequency adjustment with accuracy  $\Delta f \pm 0,01\text{Hz}$ .

Besides screw rotational speed  $n_v$ , the diameter of oil cake output die was changed; the die diameters of  $\varnothing 6$  [mm],  $\varnothing 8$  [mm] and  $\varnothing 10$  [mm] were used.

## RESULTS AND DISCUSSION

### **Own investigations – optimization of rapeseed oil extraction process in small farm.**

In agricultural activity of commodity production scale the manager follows the principle of rational farming. The resources of a given farm are limited, therefore, they should be utilized in the way that provides the maximal realization of assumed economic objectives. This principle applies to situation when both the means and objective can be determined in terms of quantity. It can be then called the principle of highest effectiveness (Tarnowski, 2009).

Realization of this principle can be twofold. In the first manner, the maximal objective can be obtained at a given input of resources or means. In the second one, the level of resources or means is maximized at the assumed objective.

Development of production system mathematical model to follow the above principles is possible with application of optimization methods (Tarnowski 1998; Tarnowski 1999, Kiczkowiak 2005; Tarnowski, 2001).

There was developed the optimization model for exemplary model agricultural farm that aims at winter rapeseed extraction for own internal needs.

Analysis of the obtained material and evaluation of objective function variability with consideration to the set of decision variables showed that particular optimization iteration processes correctly found the local minima for defined combination of decision variables.

To illustrate clearly the obtained results, the full set of optimization results for particular iterations and the selected objective function surfaces related to extreme values were marked on diagrams.

### **Investigations on objective function course with consideration to oil extraction productivity**

The Farnet PSL UNO 7 press oil extraction productivity were measured at 1 second intervals with the use of LabVIEW computer program. Duration of experiment depended on the press productivity. The oil extraction of rapeseeds of moisture content 7% was executed for seed sample of 1 kg.

Basing on the obtained results there was developed the model that determined the press productivity with consideration to die diameter variability and changes in the screw rotational speed:

$$W_w = A_1\phi_b^2 + A_2\phi_b + A_3n_w^2 + A_4n_w + A_5\phi \cdot n_w + A_6, \quad (1)$$

- $W_w$  – productivity [kg/h],
- $A_1, \dots, A_6$  – model coefficient [-],
- $\phi$  – die diameter [mm],
- $n_w$  – screw rotational speed [rpm].

As a result of regression model development there was obtained the equation of fitting degree  $R^2=0.956$  [-] of the form:

$$W_w = 0,128\phi_b + 0,685n_w - 4,53, \quad (2)$$

- $W_w$  – productivity [kg/h],
- $\phi$  – die diameter [mm],
- $n_w$  – screw rotational speed [rpm].

The model of mathematical course of changes in productivity according to screw rotational speed and die diameter is presented in Figure 1.

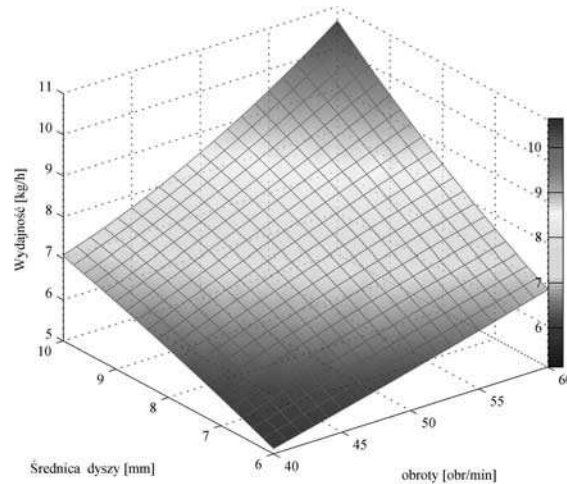


Fig. 1. Model determining press productivity at various screw rotational speed [rpm] and various die outlet hole diameter [mm]

The change in screw rotational speed  $n_w$  ranged from 40 to 60 [rpm], while in die diameter from 6 to 10 [mm].

### Results of extraction optimization process with respect to productivity

Basing on carried out experiment and the obtained results of rapeseed oil extraction, there was performed the process optimization with respect to productivity.

#### Structure of modeling process:

1. **The optimization subject** is productivity of technological process of winter rapeseed oil extraction.
2. **The optimization scope** takes into consideration changes in:
  - rotational speed.
  - die diameter.
3. **Criteria** – in optimization process the following criteria were assumed:  
 $W_w$  – process productivity [kg/h].
4. **Determination of decision variables:**
  - $\varnothing$  – die diameter (from 6 to 10 [mm]).
  - $n$  – screw rotational speed (from 40 to 60 [rpm]),
5. **Inequality limitations:**
  - $n - 40 \leq n \leq 60$  [rpm].
  - $\varnothing - 6 \leq \varnothing \leq 10$  [mm].

Objective function:

$$W_{wcelu} = A_1\phi_b^2 + A_2\phi_b + A_3n_w^2 + A_4n_w + A_5\phi \cdot n_w + A_6, \quad (3)$$

- $W_{wcelu}$  – objective function of oil extraction process productivity [kg/h],  
 $A_1, \dots, A_6$  – model coefficients [-],  
 $\phi$  – die diameter [mm],  
 $n_w$  – screw rotational speed [rpm].

The subject of worked out optimization is searching for maximal values of objective function according to dependence:

$$\max(W_{wcelu}(n_w, \phi)), \quad (4)$$

- $W_{wcelu}$  – objective function of oil extraction process productivity [kg/h],  
 $\phi$  – die diameter [mm],  
 $n_w$  – screw rotational speed [rpm].

Optimization results for extraction process productivity are presented in Figure 2 as averages of measurement series.

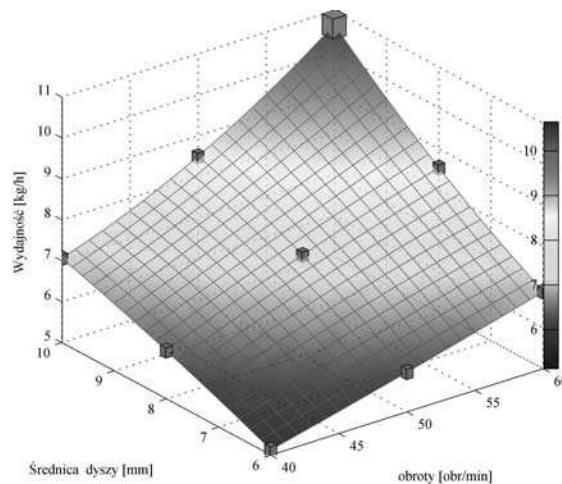


Fig. 2. Productivity [kg/h] according to die diameter-  $\phi$  [mm] and screw rotational speed [rpm]).

For the sample of parameters: die diameter  $\phi$  - 10 mm and rotational speed  $n_w$  - 60 rpm there was obtained the highest productivity, thus, the optimal value of technical parameters for the process on investigated device. This value is distinguished on diagram as the cube of magenta colour. The lowest productivity was obtained at technical parameters: die diameter  $\phi$  - 6 mm and rotational speed 40 rpm.

Extraction process productivity with the use of exemplary press increases with an increase in die diameter  $\phi$  – from 6 mm to 10 mm, and also with an increase in screw rotational speed  $n_w$  - from 40 to 60 rpm.

### Investigations on objective function course with consideration to energy demand

The Farnet PSL UNO 7 press energy demand was also measured at 1 second intervals with the use of LabView computer program. The results are presented in Figure 3 as the specific electric energy consumption [kJ/kg].

Basing on the obtained results there was developed the model that determined the extraction process energy consumption with consideration to die diameter variability and changes in the screw rotational speed.

$$E_w = A_1\phi_b^2 + A_2\phi_b + A_3n_w^2 + A_4n_w + A_5\phi \cdot n_w + A_6, \quad (5)$$

- $E_w$  – energy demand [kJ/kg],  
 $A_1, \dots, A_6$  – model coefficients [-],  
 $\phi$  – die diameter [mm],  
 $n_w$  – screw rotational speed [rpm].

As a result of regression model development there was obtained the equation of fitting degree  $R^2=0.909$  [-] of the form:

$$E_w = -1,82\phi_b + 2,02n_w^2 - 54,7n_w - 0,612\phi \cdot n_w + 1240, \quad (6)$$

- $E_w$  – energy demand [kJ/kg],  
 $\phi$  – die diameter [mm],  
 $n_w$  – screw rotational speed [rpm].

Figure 3 presents changes in energy demand of oil extraction process.

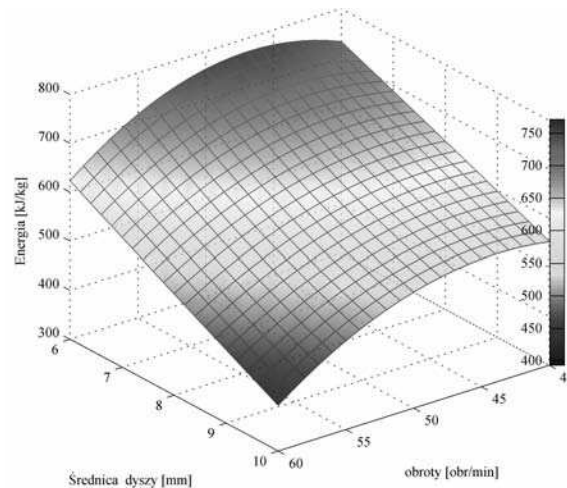


Fig. 3. Model of energy demand of rapeseed oil extraction with Farnet PSL UNO 7 press at various working parameters of device

As it is evident from the above model, the energy inputs are not directly proportional to the values of working parameters of the device: screw rotational speed [rpm] and die diameter [mm].

### Results of extraction optimization process with respect to energy demand

Basing on carried out experiment and the obtained results of rapeseed oil extraction, there was performed the process optimization with respect to process energy consumption.

#### Structure of modeling process:

1. **The optimization subject** is energy consumption in technological process of winter rapeseed oil extraction.
2. **The optimization scope** takes into consideration changes in:
  - rotational speed,
  - die diameter.
3. **Criteria** - in optimization process the following criteria were assumed:  
 $E_w$  – energy inputs in rapeseed oil extraction process [kJ/h].
4. **Determination of decision variables** of oil extraction process
  - $\phi$  – die diameter (from 6 to 10 [mm]),
  - $n_w$  – screw rotational speed (from 40 to 60 [rpm]).
5. **Inequality limitations:**
  - $n_w - 40 \leq n \leq 60$  [rpm],
  - $\phi - 6 \leq \phi \leq 10$  [mm].

Objective function:

$$E_{wcelu} = A_1\phi_b^2 + A_2\phi_b + A_3n_w^2 + A_4n_w + A_5\phi \cdot n_w + A_6, \quad (7)$$

- $E_{wcelu}$  – objective function of energy demand [kg/h],  
 $A_1, \dots, A_6$  – model coefficients [-],  
 $\phi$  – die diameter [mm],  
 $n_w$  – screw rotational speed [rpm].

The subject of worked out optimization is searching for minimal values of objective function according to dependence:

$$\min(E_{wcelu}(n_w, \phi)), \quad (8)$$

- $E_{wcelu}$  – objective function of energy demand [kg/h],  
 $\phi$  – die diameter [mm],  
 $n_w$  – screw rotational speed [rpm].

The lowest energy consumption was found at  $n_w$  - 60 rpm. This value is marked on Fig. 4 with the cube of magenta colour.

There is also another cube on the diagram 4 marked by magenta colour for technical parameters: die diameter  $\phi$  - 10 mm and rotational speed  $n_w$  - 40 obr/min, however, the value of that point is higher than optimal. For the sample of parameters: die diameter  $\phi$  - 6 mm and rotational speed  $n_w$  40 rpm, the highest energy consumption per 1 kg of pressed rapeseeds was obtained.



The energy consumption of extraction process with the use of exemplary press increases with a decrease in die diameter  $\phi$  – from 10 mm to 6 mm, and also with a decrease in screw rotational speed  $n_w$  - from 60 to 40 rpm.

Distribution of energy consumption values is marked with a net; its filling colour changes from dark blue to dark red along with an increase in energy demand.

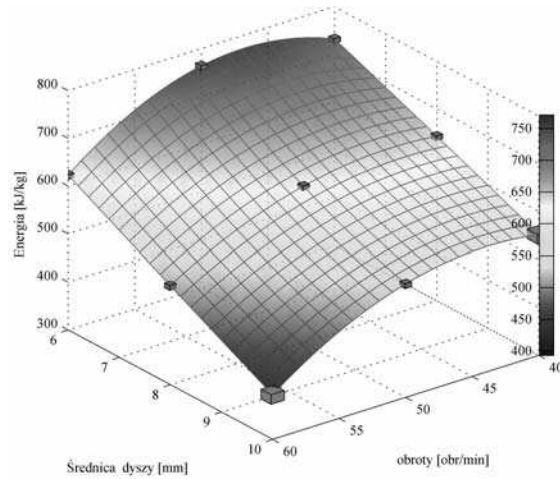


Fig. 4. Electric energy consumption [kJ/kg] according to die diameter  $\phi$  and screw rotational speed  $n_w$  [rpm].

As it is evident from Fig. 4, the process energy inputs are not directly proportional to the values of technical parameters of the device.

#### Investigations on objective function with consideration to oil output

During measurements on energy demand and device productivity, its effectiveness was also verified by the measurements of rapeseed oil output.

Basing on the obtained results there was developed the model that determined the oil output at various press working parameters with consideration to die diameter variability and changes in the screw rotational speed:

$$U_w = A_1\phi_b^2 + A_2\phi_b + A_3n_w^2 + A_4n_w + A_5\phi \cdot n_w + A_6, \quad (9)$$

- $U_w$  – oil output [kg/kg],
- $A_1, \dots, A_6$  – model coefficients [-],
- $\phi$  – die diameter [mm],
- $n_w$  – screw rotational speed [rpm].

As a result of regression model development there was obtained the equation of fitting degree  $R^2=0.987$  [-] of the form:

$$U_w = 0,0300\phi_b^2 - 2,97\phi_b + 2,00n_w^2 - 30,5n_w + 0,100\phi \cdot n_w + 420, \quad (10)$$

- $U_w$  – oil output [kg/kg],  
 $\phi$  – die diameter [mm],  
 $n_w$  – screw rotational speed [rpm].

Various amount of oil was obtained at different press adjustments. The obtained values related to changes in press working parameters are presented in Figure 5.

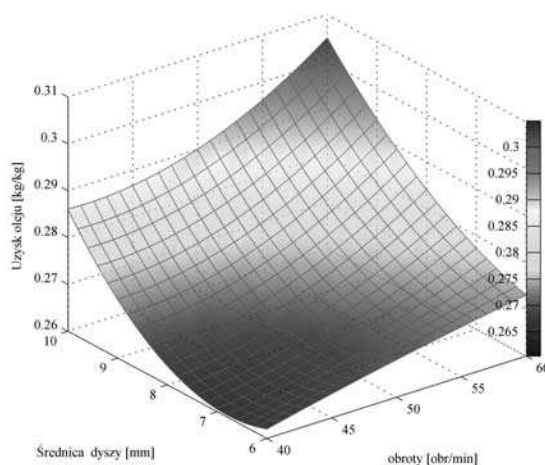


Fig. 5. Model of extraction process effectiveness expressed by oil output

The oil output value is not directly proportional to particular press parameters, but the growing trend can be found.

### Results of extraction optimization process with respect to oil output

Basing on carried out experiment and the obtained results of rapeseed oil extraction, there was performed the process optimization with respect to oil output.

Particular samples were obtained at defined settings of press working parameters. The sample mass was determined by weighing. Basing on this active experiments, the optimization process was carried out.

#### Structure of modeling process:

1. **The optimization subject** is oil output in technological process of winter rapeseed oil extraction.
2. **The optimization scope** takes into consideration changes in:
  - rotational speed,
  - die diameter.
3. **Criteria** - in optimization process the following criteria were assumed:  
 $U_w$  – oil output in rapeseed oil extraction process [kg/kg],
4. **Determination of decision variables:**

- $\phi$  – die diameter (from 6 to 10 [mm]),
- $n_w$  – screw rotational speed (from 40 to 60 [rpm]).

##### 5. Inequality limitations:

- $n_w - 40 \leq n \leq 60$  [rpm],
- $\phi - 6 \leq \phi \leq 10$  [mm].

Objective function:

$$U_{wcelu} = A_1\phi^2 + A_2\phi + A_3n_w^2 + A_4n_w + A_5\phi \cdot n_w + A_6, \quad (11)$$

- $U_{wcelu}$  – objective function of oil output [kg/h],  
 $A_1, \dots, A_6$  – model coefficients [-],  
 $\phi$  – die diameter [mm],  
 $n_w$  – screw rotational speed [rpm].

The subject of worked out optimization is searching for maximal values of objective function according to dependence:

$$\max(U_{wcelu}(n_w, \phi)), \quad (12)$$

- $U_{wcelu}$  – objective function of oil output [kg/kg],  
 $\phi$  – die diameter [mm],  
 $n_w$  – screw rotational speed [rpm].

The highest oil output was obtained for the sample at press working parameters: die diameter  $\phi$  - 10 mm and crew rotational speed  $n_w$  - 60 rpm. This value is marked on the diagram with magenta colour. The minimal oil output value was found for the sample at parameters: die diameter  $\phi$  - 6 mm and screw rotational speed  $n_w$  - 40 rpm.

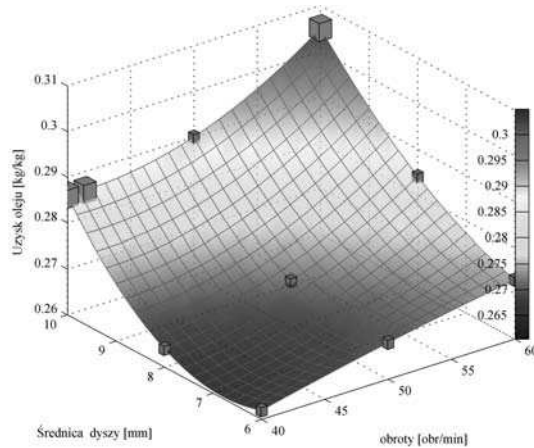


Fig. 6. Oil output [kg/kg] according to die diameter [ $\phi$ ] and screw rotational speed [rpm]

The effect of rapeseed oil extraction experiment with the use of Farnet PSL UNO 7 press is determination of press setting optimal parameters of in respect to productivity, energy inputs and oil output (Table 1), that amount to: die diameter  $\varnothing$  - 10 mm and screw rotational speed  $n_w$  - 60 rpm.

Table 1. Criteria of optimization and criteria of rapeseed oil extraction process

Criteria of optimization	Values	Unit
Productivity- maximal	10.65	kg/h
Energy consumption - minimal	0.393	MJ/kg
Oil output - maximal	0.305	kg/kg

Considering the investigated parameters: productivity, process energy consumption and oil output one can find that the optimization process points out at the need for proper selection of parameters (the increased screw rotational speed and die diameter), since working parameters recommended by manufacturer differ from the results obtained in optimization process.

## CONCLUSIONS

Basing on carried out optimization process of winter rapeseed oil extraction (at assumed limitations) and on the basis of performed active experiment one can find that:

- maximal possible process productivity amounts to 10.65 [kg/h],
- minimal energy demand amounts to 393 [kJ/kg],
- maximal rapeseed oil output amounts to 305 [g/kg].

To reach these results one should apply the press die diameter  $\varnothing$  - 10 [mm] and screw rotational speed  $n_w$  - 60 [rpm].

## REFERENCES

1. Banasiak J., 2008: Wydajnościowa analiza w procesach eksploatacji maszyn rolniczych. s. 63-68, Inżynieria Rolnicza 4(102)/2008, Wrocław.
2. Bocheński C. I., Bocheńska A., 2008: Ocena zasobów ropy naftowej i perspektywy jej substytucji biopaliwami. Motorol, s. 23-30, Lublin.
3. Chmielecki R., 2006: Rozwój form zespołowego użytkowania maszyn w rolnictwie Niemiec zachodnich., Instytut Ekonomiki Rolnictwa, Uniwersytet w Getyndze, Inżynieria Rolnicza Nr 13 (88) s. 37-45.
4. Drosio A., Klimkiewicz M. 2009: Efektywność i samowystarczalność energetyczna rolnictwa. w. Ekonomiczne uwarunkowania stosowania odnawialnych źródeł energii. Wydawnictwo Wieś Jutra, Warszawa.
5. Farnet 2010: Parametry techniczne. <http://www.farnet.pl>.
6. Gach S., 2009: Metody oceny technologii zbioru i konserwacji zielonych roślin paszowych., SGGW, Inżynieria Rolnicza Nr 4/2009 s. 67- 74.
7. Hitachi, 2001: Serja SJ100. Instrukcja obsługi. <http://www.kapeko.com.pl/falowniki.php>.
8. Jakóbiec J., Konstantynowicz L., Janik R., Ambroziak A., 2009: Wpływ właściwości fizykochemicznych paliw ropopochodnych i pochodzenia roślinnego na właściwości rozruchowe

- silników ZS. Eksploatacja silników spalinowych., Rozruch silników spalinowych. Zeszyt Nr 18, Szczecin.
9. Jaros M, Pabis S., 2007: Inżynieria systemów. SGGW. Warszawa.
  10. Jaswant S., Bargale P.C., 2000: Development of a small capacity double stage compression screw press for oil expression. Journal of Food Engineering 43.
  11. Kiczkowiak T., 2005: Algorytmy i modele w projektowaniu pneumatycznych układów napędowych. Wydawnictwo Uczelniane Politechniki Koszalińskiej. Koszalin.
  12. Klimkiewicz M., Jobbágy J., Simoník J., 2010: Analiza czynników warunkujących efektywną pracę silnika o zapłonie samoczynnym zasilanego nieprzetworzonym olejem rzepakowym. SGGW 2010, Warszawa.
  13. Klimkiewicz M., Wichetek J., 2008: The influence of selected pressing parameters on amount and properties of production of rapeseed oil. Zbornik z 13. międzynarodowej vedeckej konferencie Quality and reliability of technical systems 2008. SPU Nitra.
  14. Kupczyk A., 2008: Stan Aktualny i perspektywy wykorzystania biopaliw transportowych w Polsce na tle UE, Cz. IV. Aktualne Uwarunkowania i wykorzystanie biopaliw transportowych w Polsce. Biopaliwa II generacji. Energia i Ekologia, Warszawa.
  15. Mruk R., 2006: Badanie procesów spalania oleju napędowego oraz biopaliw rzepakowych. Inżynieria Rolnicza 7/2006, s. 333-342, Warszawa.
  16. Panasiewicz M., Mazur J., Zawisłak K., Sobczak P., 2009: An influence of preliminary rapeseed processing on oil extrusion. s., TEKA Kom. Mot. Energ. Rol., 9.
  17. Tarnowski W., 1998: Polioptymalizacja jako ośrodek integracji w nowoczesnych systemach CAD. Zeszyty naukowe Wydziału Mechanicznego Politechniki Koszalińskiej nr 23, s. 364-371, Koszalin.
  18. Tarnowski W., 2001: Symulacja i optymalizacja w MATLAB'ie. s. 206, Sopot.
  19. Tarnowski W., 2009: Optymalizacja i Polioptymalizacja w Mechatronice, Koszalin.
  20. Tys J., Piekarski W., Jackowska I., Kaczor A., Zajac G., Starobrad P., 2003: Technologiczne i ekonomiczne uwarunkowania produkcji biopaliwa rzepakowego. s., Acta Agrophysica, Lublin.
  21. Waszkiewicz,., 2009: Rynek wybranych narzędzi i maszyn rolniczych do produkcji roślinnej w Polsce w latach 2001-2007. Problemy Inżynierii Rolniczej Nr 1. s. 51-56, Warszawa.

## ANALIZA ENERGETYCZNO-TECHNICZNA TECHNOLOGII WYTŁACZANIA OLEJU Z NASION RZEPAKU OZIMEGO.

**Streszczenie.** Przeprowadzono analizę energetyczną i ocenę technologii wyciągania nasion rzepaku z przeznaczeniem na produkcję RME w gospodarstwie rolnym. Proces technologiczny poddano optymalizacji ze względu na: maksymalizację wydajności procesu, minimalizację zapotrzebowania na energię, maksymalizację uzysk oleju rzepakowego.

Opracowany model procesu wyciągania oleju z nasion rzepaku ozimego w gospodarstwie rolnym jest narzędziem ułatwiającym podejmowanie decyzji o celowości podjęcia produkcji lub zaniechania jej w warunkach gospodarstwa rolnego. Ułatwi on bezpośredni dobór maszyn i urządzeń dla określonej skali produkcji.

**Słowa kluczowe:** olej rzepakowy, wyciąganie oleju, energochłonność procesu, rzepak ozimy, biopaliwa, surowiec do produkcji RME.

## MODELLING AND VERIFICATION FAILURES OF A COMBUSTION ENGINE INJECTION SYSTEM

Mieczysław Dziubiński, Jacek Czarnigowski

Lublin University of Technology, Faculty of Mechanical Engineering  
20-618 Lublin, Nadbystrzycka 36 Str.  
E-mail: m.dziubinski@pollub.pl, j.czarnigowski@pollub.pl

**Summary.** Growing pressure to improve the performance of IC engines has resulted in development of improved control systems. These requirements, combined with the introduction of control algorithms that could only be simulated experimentally were the foundations of control-oriented modelling techniques. The paper presents the assumptions and requirements toward control oriented models and a model of an idling SI engine. Some results of identification and verification tests of the model are presented for the 1.5 GLI engine. On the basis of the engine model, the simulation of sensor failures had been carried out.

**Key words:** internal combustion engine, idle speed, control, simulation of sensors failures.

### 1. INTRODUCTION

During recent years, the main advances in internal combustion engine technology have been the reduction of toxic gas emissions and fuel consumption, in addition to improvement of engine work stability and reliability in steady and dynamic state.

These targets have been dictated by environment protection regulations. Neither engine construction development with optimisation of particular components, nor introduction of new materials and technologies were enough to reach these targets. Therefore, new control systems allowing for variable working conditions and dynamic changes of engine characteristics have had to be introduced and developed.

Simple control algorithms (e.g. PID) whose synthesis is based on the system transmittance analysis proved insufficient in these circumstances. This is due to their inability to account for the characteristics of the object of control. Thus, algorithms based on simple linear engine models were implemented such as LQR and H-infinity algorithms, where the selection of settings is based on mathematical processing of engine models. These algorithms have also their limitations: firstly, the model is linear and therefore only a rough approximation, and secondly, it is also stationary i.e. identified for a certain engine in a stated moment of its life cycle.

At the same time some complex algorithms emerged that, due to their nonlinearity could not be synthesized by means of mathematical transformations. Examples of these are algorithms based on adaptation theory. The settings of the regulator need to be determined empirically. A proper

synthesis requires repeatable conditions of the experiments which is highly difficult or even impossible to achieve either in the test-bed or during normal operation. A solution to this problem may be simulation tests, whose results can be verified empirically on the test bed.

This method is less time-consuming and allows reduced costs of control system algorithm synthesis. This is why modelling gained on importance and control-oriented models are being developed.

## 2. MODEL OF THE ENGINE

Our intention was to create a mathematic model by means of which parameters of control algorithms could be determined and tests of individual algorithms of the simulated SI engine idle speed control could be conducted. In order to meet the assumptions of the object oriented model, a mean value model allowing for inertia of the engine and its control system was developed. The object of modelling was a 1.5 GLI car engine – a four-stroke four-cylinder spark ignition single point injection engine, cubic capacity of  $1496 \text{ cm}^3$ . The model was calculated twice for each rotation of the crankshaft (frequency of ignition control). The model was programmed using a C++ object programming technique. It was divided into 3 modules:

- Fuel film,
- Manifold,
- Cylinder and crankshaft.

The nonstationarity and variability of the engine was expressed by changes of indicated torque determined in the last module.

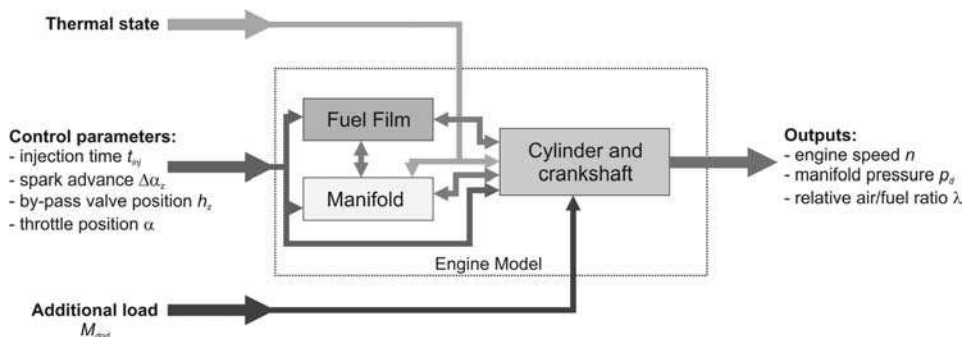


Fig. 1. Block diagram of the engine model

### 2.1. Fuel film module

Fuel film results from the deposit of condensed fuel on the manifold walls. It is particularly distinct in single point injection engines. The fuel film evaporates during the engine work adding to the injected dose, thus increasing the amount of fuel reaching the cylinder. In particular conditions the rate of vaporisation (and the amount of vaporised fuel) depends on the mass of fuel film.

The input to this module is the injection time  $t_{inj}$  recalculated into the mass of fuel supplied by a single injection  $m_{inj}$ . This injected fuel is divided into two parts:  $m_p$  – mass of fuel evaporised directly, and  $m_{ff}$  – mass of fuel deposited in the manifold as fuel film:

$$m_{ip} = (1 - X) \cdot m_{inj}, \quad (1)$$

$$m_{if} = X \cdot m_{inj}, \quad (2)$$

$m_{if}$  increases the total mass of fuel film  $m_{film}$ . At the same time, some fuel vaporises from the fuel film ( $m_{fp}$ ) adding to the fuel supplying the cylinder. Thus, the mass of fuel reaching the cylinder may be described by the following equation:

$$m_{fuel} = m_{ip} + m_{fp}. \quad (3)$$

The dynamic of fuel film is formulated by the equation describing change of fuel mass evaporating from the film:

$$\dot{m}_{fp} = \frac{1}{\tau} (-m_{fp} + X \cdot m_{inj}). \quad (4)$$

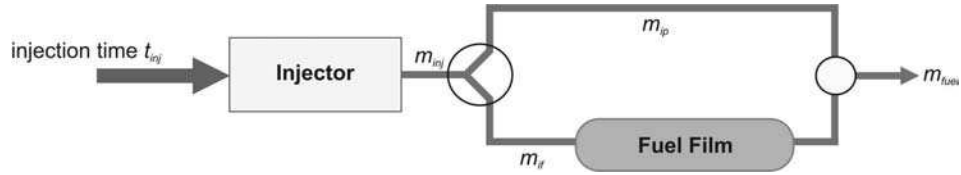


Fig. 2. Calculations in the fuel film module

## 2.2. Manifold module

This module is based on the mass balance in the manifold:

$$\frac{dm_{mf}}{dt} = \dot{m}_r + \dot{m}_{bp} + \dot{m}_{fuel} - \dot{m}_{cyl}. \quad (5)$$

The mass flow rates entering the manifold through the throttle and the by-pass valve are described by equations of subcritical or critical flow through a Venturi throat:

$$\dot{m} = \frac{\mu \cdot F_{flow} \cdot P_0}{\sqrt{R \cdot T_0}} \cdot \psi, \quad (6)$$

where:

$$\psi = \begin{cases} \sqrt{\frac{2 \cdot \kappa}{\kappa - 1} \left[ \left( \frac{P_d}{P_o} \right)^{\frac{2}{\kappa}} - \left( \frac{P_d}{P_o} \right)^{\frac{\kappa+1}{\kappa}} \right]} & P_d > P_o \cdot \left( \frac{2}{\kappa + 1} \right)^{\frac{\kappa}{\kappa - 1}} \\ \sqrt{\kappa \cdot \left( \frac{2}{\kappa - 1} \right)^{\frac{\kappa+1}{\kappa - 1}}} & P_d \leq P_o \cdot \left( \frac{2}{\kappa + 1} \right)^{\frac{\kappa}{\kappa - 1}} \end{cases}. \quad (7)$$



The mass flow rate of air-fuel mixture leaving the manifold is defined by the sum of masses reaching particular cylinders and calculated according to the following equation:

$$\dot{m}_{cyl} = \frac{1}{\Delta t} \frac{p_0 \cdot V_{cyl}}{R_{mix} \cdot T_0} \cdot \eta_v. \quad (8)$$

The output from the manifold module is the pressure in the manifold calculated from the equation of state of gas in the manifold as follows:

$$p_d = \frac{m_{mf} \cdot R \cdot T_{mf}}{V_{mf}}. \quad (9)$$

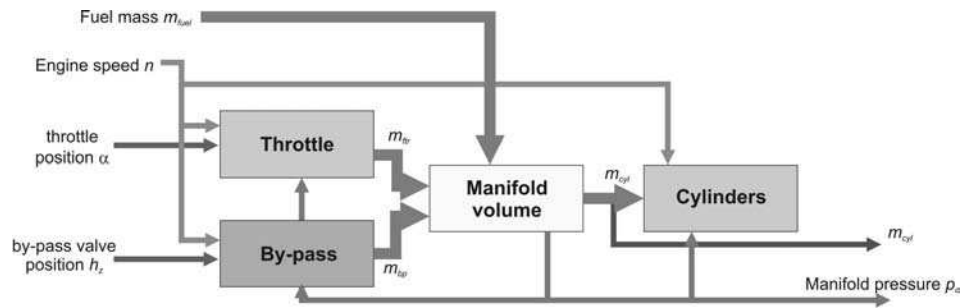


Fig. 3. Calculation of the manifold module: the algorithm

### 2.3. Cylinder and crankshaft module

The third module of the model is responsible for calculation of effects of engine operation, i.e. torque and combustion gases' composition. The inputs to this module are: spark advance  $\Delta\alpha_z$ , mass of air reaching the cylinder  $m_{air}$ , mass of fuel reaching the cylinder  $m_{fuel}$ , engine speed  $n$ , throttle position  $\alpha$  and additional load torque  $M_{load}$ . The parameters calculated by this module are engine speed and lambda sensor signal.

The module comprises four components:

- indicated torque ( $M_i$ ) calculation submodule,
- engine friction torque  $M_b$  calculation submodule,
- new engine speed calculation submodule,
- lambda sensor submodule.

### 2.4. Indicated torque (Mi) calculation submodule

The value of indicated torque is calculated on the basis of:

- engine speed  $n$ ,
- pressure in the manifold  $p_d$ ,
- spark advance  $\Delta\alpha_z$ .

The torque is calculated by means of artificial neural network MLP (3-5-5-1) BP. The result of calculation is corrected by a factor dependent on the air/fuel ratio coefficient  $\lambda$ , according to the following formula:

$$M_i = \beta(\lambda) \cdot M_{istch}. \quad (10)$$

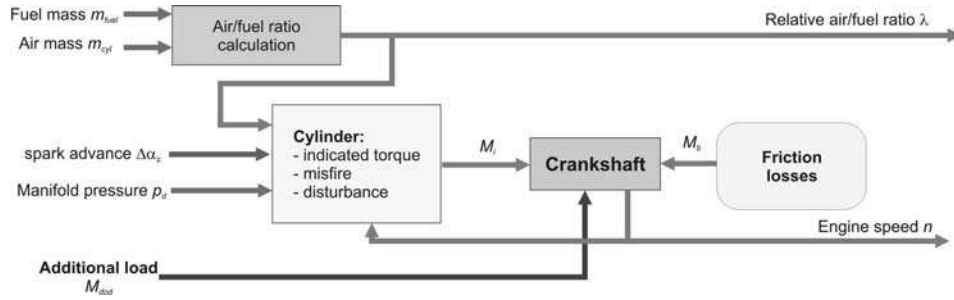


Fig. 4. Structure of the cylinder and crankshaft module

The author allowed for nonstationarity engine operation by modelling the following effects:

- misfire,
- uneven work of cylinders,
- stochastic nonstationarity of indicated torque.

The nonstationarity in this module is defined according [9]. To obtain a random value of normal distribution, of stated parameters of variability:

- mean value ,
- standard deviation  $\sigma_{M_i}$ ,

it may be calculated from the following equation:

$$M_{i\sigma} = \bar{M}_i + \sigma_{M_i} \cdot \cos(2 \cdot \pi \cdot RND) \cdot \sqrt{-2 \cdot \log(RND)}. \quad (11)$$

In order to bind the next value of  $M_i$  with the previous one, a back propagation of the value by means of functional binding values of  $M_i(k-1)$  and  $M_i(k)$  may be introduced:

$$M_i(k) = (1 - \xi^2) \cdot M_i(k-1) + z \cdot \xi \cdot M_{i\sigma}, \quad (12)$$

where:

$$z = 1 + 0.55 \cdot (1 - \xi)^{0.75}. \quad (13)$$

## 2.5. Engine friction torque calculation submodule

The value of engine friction torque is calculated from a dependency on engine speed  $n$ :

$$M_b = c_0 + c_1 \cdot n + c_2 \cdot n^2. \quad (14)$$

**2.6. Engine speed calculation submodule**

The engine speed of the engine is calculated based on the second principle of dynamics:

$$\frac{dn}{dt} \cdot I_b = M_i - M_b - M_{dod} \tag{15}$$

Additional load torque  $M_{dod}$  is the effect of engaging additional equipment during the engine work [1, 8]. On this basis, engine acceleration in a particular cycle and new engine speed are calculated.

**2.7. Lambda sensor submodule**

The last part of the cylinder and crankshaft module is the function calculating the lambda sensor signal (with signal time-lag). The function returns the voltage of the sensor on the basis of engine work parameters (actual air/fuel ratio in the cylinder). On the basis of the method presented in [Hawryluk 2001], the lag of signal was assumed to be 20 calculation cycles. The lambda sensor signal is modelled by a function described in [Pukrushpan 2004].

**3. IDENTIFICATION AND VERIFICATION OF THE MODEL**

The identification of the model covered idle speed as the model was designed for synthesizing and verification of idle speed control algorithms. The scope of verification was thus confined to:

- engine speed range from 600 to 1300 RPM,
- manifold pressure range from 30 to 60 kPa,
- spark advance range from 0 to 30 degrees before TDC,
- relative air/fuel ratio range from 0.8 to 1.2.

Subject to identification were parameters of the modules. Tests were conducted on the test bed equipped with a direct current brake that enabled both reception of the energy from the engine and to driving it. Fuel consumption, combustion gas composition, engine thermal state and in-cylinder pressure were measured. The cooling system allowed the engine to be kept in a steady thermal state. The conditions during the tests were steady in terms of thermal state and loads. A choice of results is presented below.

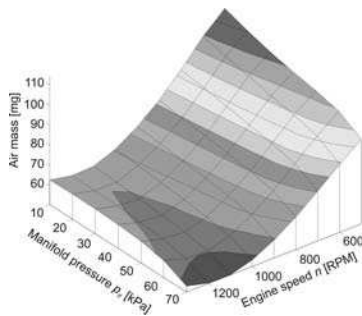


Fig. 5. Mass of air entering the manifold by closed throttle

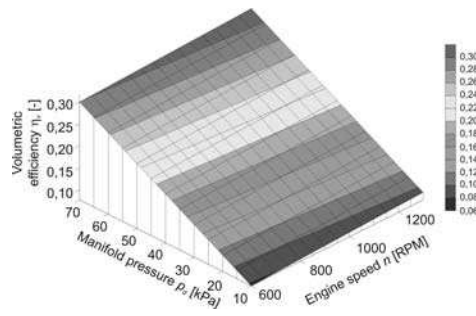


Fig. 6. Volumetric efficiency characteristics

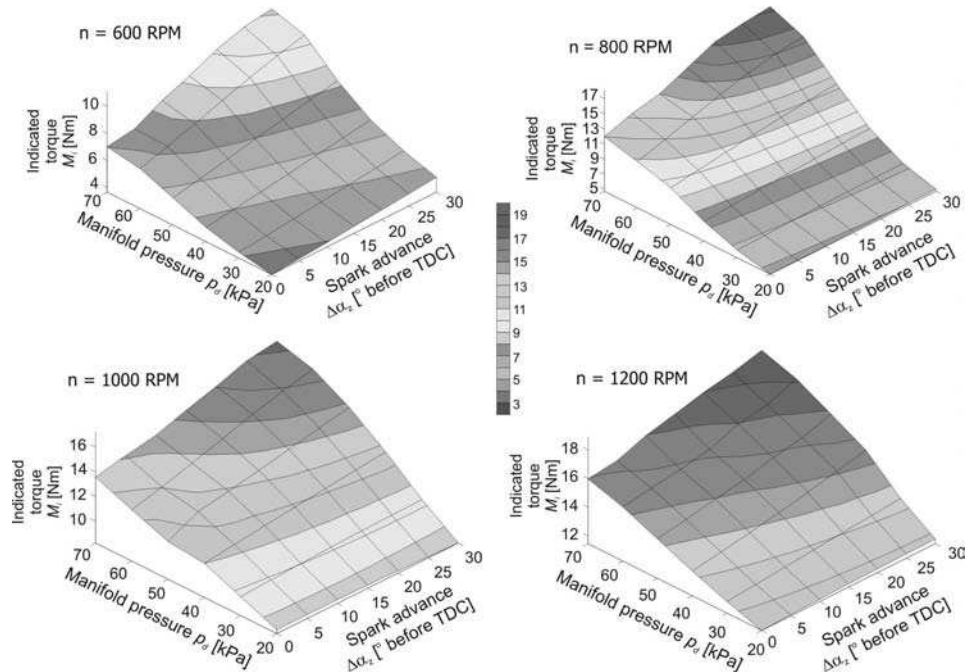


Fig. 7. Dependence of indicated torque from spark advance and engine speed by constant pressure in the manifold

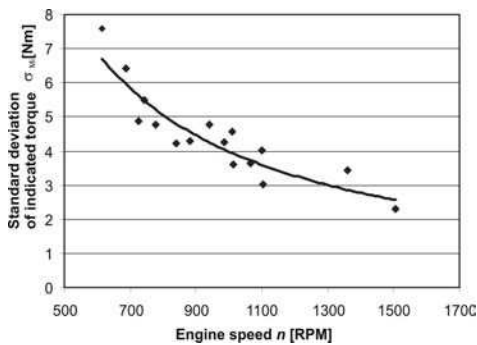


Fig. 8. Standard deviation of indicated torque

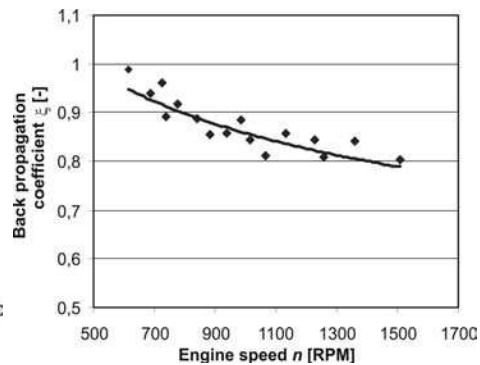


Fig. 9. Coefficient  $\xi$  of indicated torque

The last stage of the research was the verification of the model with regard to the steady state and sudden change of additional load specific to idle speed. As the main parameter of engine work was engine speed, the model adequacy analysis consisted in checking if the model correctly predicts the value of engine speed. In steady state, correlation of verification test results and model calculations was 0.95 (see Figure 12). This similarity of behaviour of the engine and its model was also clear in the case of sudden change of load without control (Figure 10).

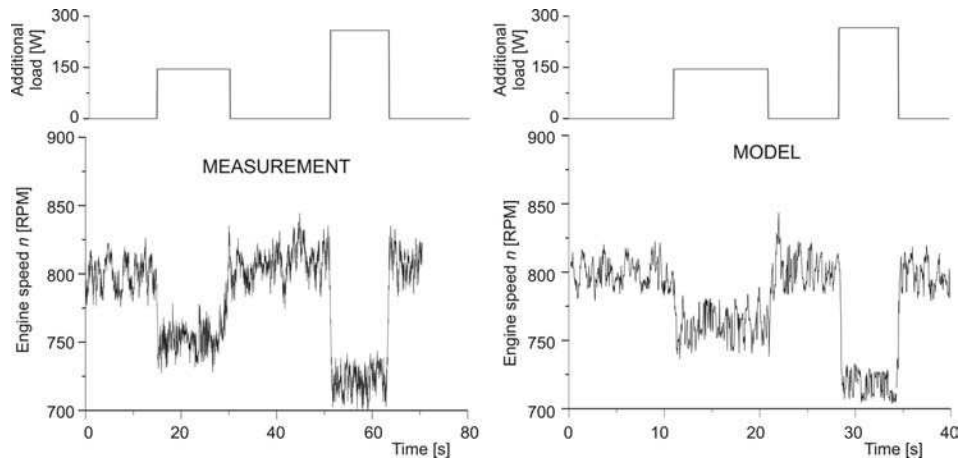


Fig. 10. Graph of rotational speed under additional load without control – test bed measurements and results of the simulation

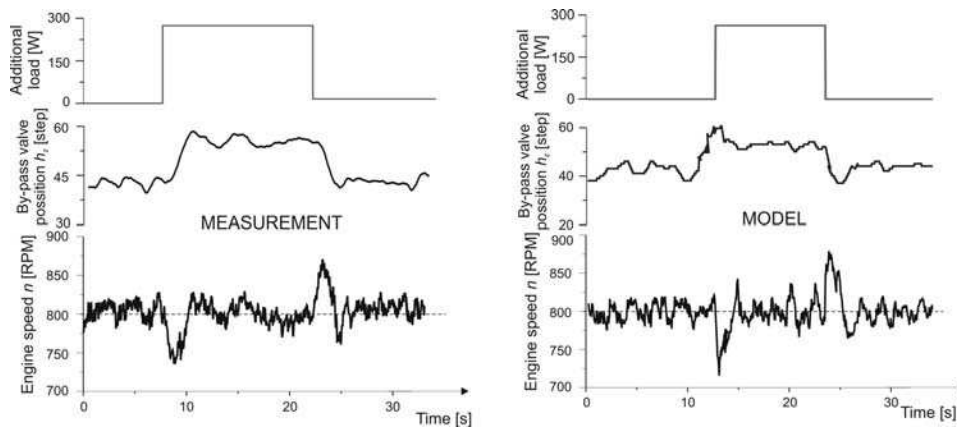


Fig. 11. Graph of rotational speed under additional load with adaptive control – test bed measurements and results of the simulation

The model was applied to simulation tests of adaptive and PID control algorithms [Smith 1995, Stefanopoulou 1998]. Exemplary results of these tests, confirming the adequacy of the model, can be seen in Figure 11.

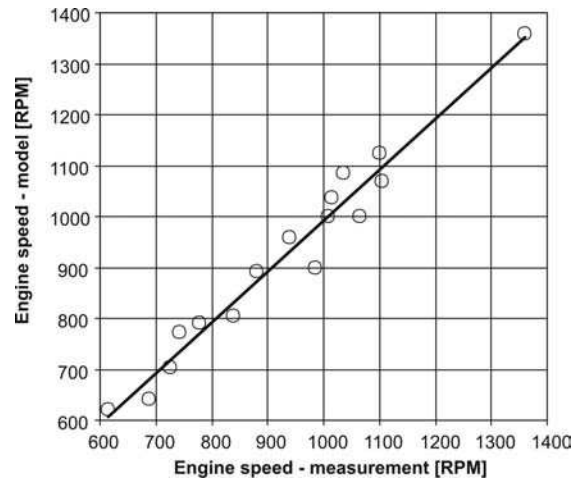


Fig. 12. Correlation of verification test results and model's calculations  
 LINE-BY-LINE EDITING CEASED HERE. ONLY RANDOM EDITING AFTER THIS POINT.

#### 4. MODELLING OF SENSOR FAILURES IN ENGINE INJECTION

The simulation model for sensor failures is presented in Fig. 13.

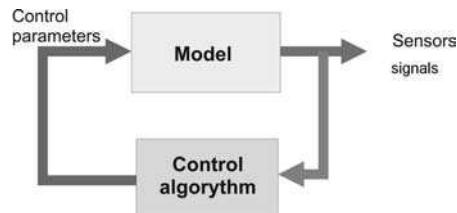


Fig. 13. Model of sensor failures simulation

##### 4.1. Models of sensors

Sensors were modeled as separate elements (modules) and described by the characteristics presented below:

- a) pressure sensor MAP,
 
$$U_{\text{MAP}} = 0.05294 \cdot \text{MAP} - 0.659,$$
 where:  $U_{\text{MAP}}$  - sensor voltage signal [V],  
 $\text{MAP}$  - pressure in suction manifold [kPa].
- b) temperature sensors:
 
$$U_{\text{Tem}} = 0.000002 \cdot T^3 - 0.0003 \cdot T^2 - 0.0305 \cdot T + 4.2796,$$
 where:  $U_{\text{Tem}}$  - sensor voltage signal [V],  
 $T$  - temperature [K],

The modules of cooling agent temperature and the temperature of air in the suction manifold were used in the model.

- c) throttling valve position sensor – potentiometric sensor:

$$U_{TP} = 0.05294 \cdot TP - 0.659,$$

where:  $U_{TP}$  - sensor voltage signal [V],  
 $TP$  – throttling valve position [%],

- d) mass air flowmeter MAF:

$$U_{MAF} = 0.6525 \cdot MAF^{0.3143},$$

where:  $U_{MAF}$  - sensor voltage signal [V],  
 $MAF$  – mass air flow [ $g \cdot s^{-1}$ ].

During simulation tests, it was possible to introduce failures of any sensor. In each case, it was possible to simulate the following failures:

- fault to frame:

$$U_{sen} = U_{gnd},$$

where:  $U_{sen}$  - sensor voltage signal [V],  
 $U_{gnd}$  - mass voltage level [V],

- fault to admission:

$$U_{sen} = U_{power},$$

where:  $U_{sen}$  - sensor voltage signal [V],  
 $U_{power}$  - admission voltage level [V],

- shift of the characteristic ( e.g. resulting from the shift of the sensor):

$$U_{sen} = U_{sen(m)} + \Delta U,$$

where:  $U_{sen}$  - sensor voltage signal [V],  
 $U_{sen(m)}$  - sensor voltage signal coming from the model without failures [V],  
 $\Delta U$  – level of sensor characteristic shift [V],

- characteristic tilt ( e.g. resulting from sensor ageing):

$$U_{sen} = U_{sen(m)} \cdot \alpha,$$

where:  $U_{sen}$  - sensor voltage signal [V],  
 $U_{sen(m)}$  - sensor voltage signal coming from the model without failures [V],  
 $\alpha$  – coefficient of sensor characteristic tilt [V].

#### 4.2. Controlling system

The engine control system model is presented in Fig. 14.

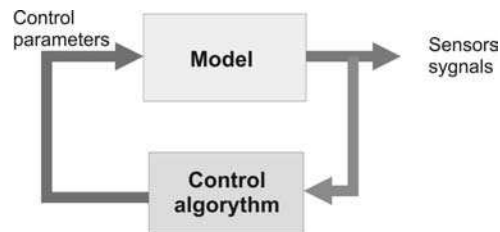


Fig. 14. Engine control system for chosen operation parameters

Signals and algorithm are misspelt fig 4.2 above.

In the range of studies, an algorithm of engine control based on maps and adaptation matching has been worked out. The control was carried out with three variables:

- ignition advance angle ( constant value during tests);
- by-pass valve position: in this case, adaptation control, whose aim was to stabilize engine speed on the assumed level was used. The algorithm of control, described in the paper: “Idle speed stabilization using competitive adaptation control of by-pass valve in SI engine” by Czarnigowski, Wendeker, Jakliński SAE-NA 34-2005, was used.
- Injection time:

In this case, the injection time is calculated according to the formula:

$$T_{inj} = k_{\alpha} \cdot t_{inj(m)} \cdot \alpha_{ET} \cdot \alpha_{MAT}$$

where:  $T_{inj}$  - injection time [ms],

$k_{\alpha}$  - correction factor calculated by adaptation algorithm,

$\alpha_{ET}$  - correction factor from engine temperature,

$\alpha_{MAT}$  - correction factor from the temperature of air in the suction manifold,

$t_{inj(m)}$  - basic injection time determined from the map [ms],

and:  $t_{inj(m)} = f(n, \text{LOAD})$ ,

where:  $n$  – engine speed[rpm].

LOAD - signal of engine load, depending on the tested sensor it is the degree to which the throttling valve opens, pressure in the suction manifold, the amount of air mass (mass flowmeter).

The disturbance of signals from sensors causes the change either of injection base dose or correction factor value (in case of temperature).

Figs. 15. – 20. present the course of rotational speed stabilization at the step increase and decrease of load in the case of efficient sensors.

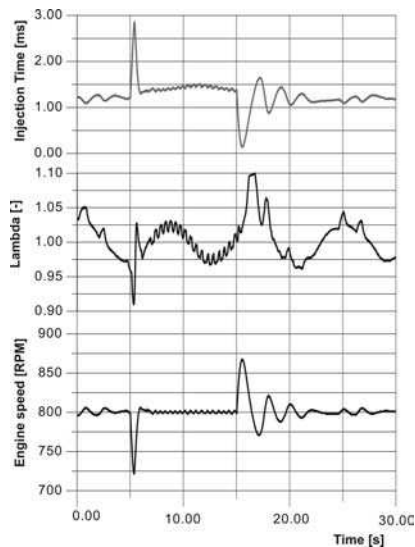


Fig. 15. Course of engine speed stabilization at the step increase and decrease of load in the case of efficient sensors

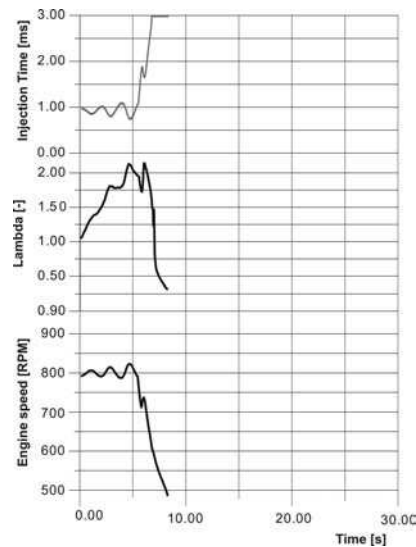


Fig. 16. Course of engine speed stabilization at the step increase and decrease of load for a pressure sensor failure in the suction manifold – fault to frame



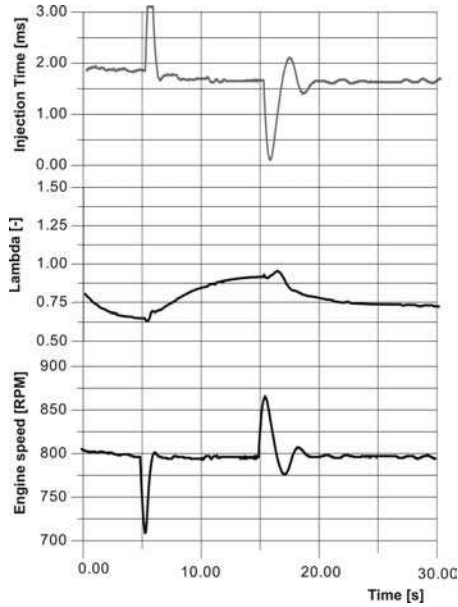


Fig. 17. Course of engine speed stabilization at the step increase and decrease of load for a pressure sensor failure in the suction manifold – fault to admission

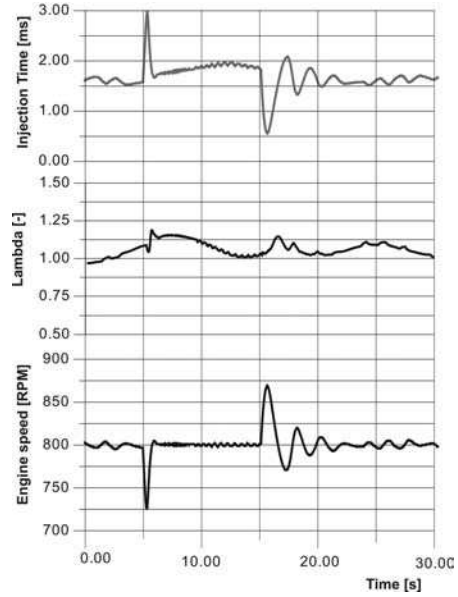


Fig. 18. Course of engine speed stabilization at the step increase and decrease of load for a pressure sensor failure in the suction manifold – characteristic shift

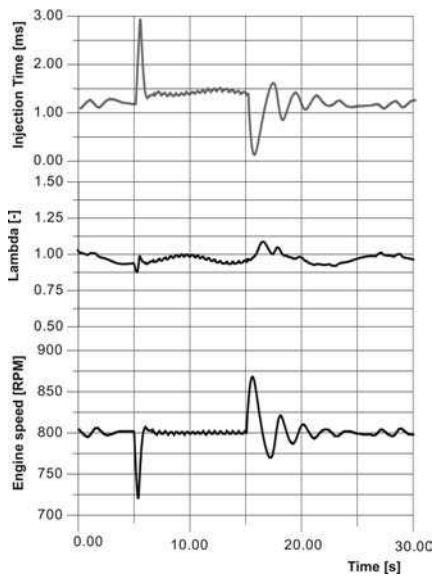


Fig. 19. Course of engine speed stabilization at the step increase and decrease of load for a pressure sensor failure in the suction manifold – characteristic tilt

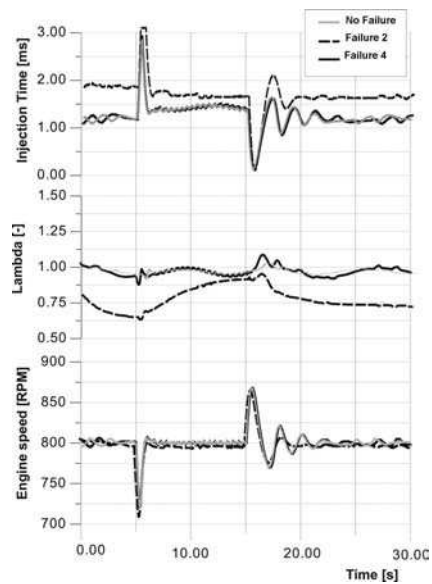


Fig. 20. Courses of engine speed stabilization at the step increase and decrease of load for the efficient sensor or its two failures

## CONCLUSIONS

Applying control oriented modelling to the synthesis of control algorithms enables us to conduct simulation tests to identify settings of regulators. Moreover, verification and comparative tests of particular control algorithms. Advantages of models based on mean values are ease of identification of parameters by satisfying level of adequacy in both steady and dynamic states and fast calculations.

In the case of developing idle speed control algorithms, allowing for nonstationarity and nonrepeatability of the engine is well-founded. Therefore, a special submodule has been introduced into the presented model allowing the researchers to closely approximate the actual behaviour of the engine. The adequacy of the model has been proved in tests.

The courses of engine speed stabilization at the step increase and decrease of load in the case of the efficient sensor or its two failures are not identical.

## REFERENCES

1. Ando H., Motomochi M.: Contribution of Fuel Transport Lag and Statistical Perturbation in Combustion to Oscillation of SI Engine Speed at Idle, *SAE Technical Paper*, nr 870545, 1987.
2. Ashhab M.-S. S., Stefanopoulou. A. G, Cook J. A., Levin M. B.: Control-Oriented Model for Camless Intake Process (Part I) *ASME Journal of Dynamic Systems, Measurement, and Control*, Vol 122, 2000, pp. 122-130.
3. Bidan P., Kouadio L.K, Valentin M, Montseny G.: Electrical assistance for S.I. idle-speed control, *Control Engineering Practice*, 6, 1998, pp. 829-836.
4. Cassidy J.F. , Athans M., Lee W.H.: On the Design of Electronic Automotive Engine Control Using Linear Quadratic Control Theory, *Transaction on Automatic Control*, IEEE 1980.
5. Dotoli M.: Fuzzy Idle Speed Control: A Preliminary Investigation, *Report on the research no. 97-E-858*, Department of Automation, Technical University of Denmark 1997.
6. Dziubiński M.: Reliability aspects in constructing vehicle electronic equipment, *Journal of Middle European Construction and Design of Cars*, pp. 2003, 44-48 Prague.
7. Dziubiński M.: Computer Control of Alternators Manufacture, *Manufacturing Engineering*, 4, 2003, pp.57-61.
8. Dziubiński M.: Investigations of ignition systems reliability, *Journal of KONES Internal Combustion Engines*, 2004, ,pp. 137-146 Warsaw.
9. Dziubiński M.: Reliability aspects in manufacturing of starter. *New Ways in Manufacturing Technologies*, 2004, pp.385-390 .
10. Jung M., Glover K.: Control-Oriented Linear Parameter Varying Modelling of a Turbocharged Diesel Engine, *Proceedings of the IEEE Conference on Control Applications*, Istanbul, Turkey, June 2003.
11. Gustaffson T.K., Makila P.M.: Modelling of Uncertain Systems with Application to Robust Process Contro, *Journal of Process Control*, No 11, 2001.
12. Han M., Loh R.N.K., Wang L., Lee A., Stander D.: Optimal Idle Speed Control of an Automotive Engine, *SAE Technical Paper* ,nr 981059, 1998.
13. Hawryluk B.: *Stochastyczny model silnika benzynowego w aspekcie stechiometrycznego składu spalin*, praca doktorska, Politechnika Lubelska, 2001.
14. Powell B.K., Cook J.A., Grizzle J.W.: Modeling and analysis of inherently multi-rate sampling fuel injected engin idle speed loop, *Proc. of 1987 American Control Conference*, Minneapolis, USA, 1987.

15. Powell B.K., Powers W.P.: Linear Quadratic Control Design for Nonlinear IC Engine Systems, *Proc: ISATA Conference*, Stockholm, Sweden, 1981.
16. Powell J.D.: A review of IC engine models for control system design, *Proc. of the 10<sup>th</sup> IFAC World Congress*, Munich, Germany, 1987.
17. Powers W.F., Powell B.K., Lawson G.P.: Application of optimal control and Kalman filtering to automotive systems, . *Int. J. Of Vehicle Design*, Special Publication SP4, 1983.
18. Pukrushpan J., Stefanopoulou A., Varigonda S.: *Control-Oriented Model of Fuel Processor for Hydrogen Generation in Fuel Cell Applications*” IFAC Symposium in Advances in Automotive Systems, Salerno, 2004.
19. Shim D., Khargonekar P.P., Ribbens W.: *Idle speed control for automotive engine*”. Proc. of 1995 American Control Conference, Seattle, USA, 1995.
20. Smith R.S. *Model Validation for Robust Control: an Experimental Process Control Application*. Automatica Vol. 31. No. 11, 1995.
21. Stefanopoulou A.G., Cook J.A., Freudenberg J.S., Grizzle J.W.: Control-Oriented Model of a Dual Equal Variable Cam Timing Spark Ignition Engine, *ASME Journal of Dynamic Systems, Measurement, and Control*, vol. 120,1998, pp. 257-266.
22. Wendeker M., Czarnigowski J.: Adaptive Control of the Idle Speed, *ICES2003-646 Proceedings of ICES03 2003 Spring Technical Conference of the ASME Internal Combustion Engine Division Salzburg*, Austria, May 11-14, 2003.
23. Wedeneker M., Czarnigowski J.: Adaptive Control Of The Idle Conditions Of Spark Ignition Engine, *SAE\_NA Technical Paper SAE\_NA 2003-01-15*, 2003.

## NOMENCLATURE

$F_{flow}$	– air flow area,
$h_z$	– by-pass valve position,
$I_b$	– engine moment of inertia,
$m_{air}$	– mass of air reaching the cylinder,
$M_b$	– engine friction torque,
$\dot{m}_{bp}$	– by-pass valve air mass flow rate,
$\dot{m}_{cyl}$	– cylinder mixture mass flow rate,
$M_{dod}$	– additional load torque,
$m_{film}$	– fuel film mass,
$\dot{m}_{fuel}$	– mass flow rate of fuel reaching the cylinder,
$m_{fp}$	– mass of fuel evaporated from fuel film,
$M_b$	– engine resistance torque,
$M_i$	– engine indicated torque,
$\bar{M}_i$	– mean value of indicated torque,
$M_{istich}$	– indicated torque by stoichiometric mixture,
$M_{\sigma}$	– indicated torque estimated by stochastic calculation,
$m_{if}$	– mass of fuel deposited in fuel film by single injection,
$m_{inj}$	– mass of fuel supplied by single injection ,
$m_{ip}$	– mass of fuel vaporized directly by single injection,
$m_{mf}$	– mixture mass in manifold,
$\dot{m}_{tr}$	– mass flow rate of air reaching the manifold by throttle,
$n$	– engine speed,
$p_o$	– atmospheric pressure,

$R$	– gas constant of air,
$R_{\text{mix}}$	– air/fuel mixture gas constant,
$RND$	– random variable (0-1),
$t_{inj}$	– injection time,
$T_{mf}$	– manifold air temperature,
$T_o$	– ambient air temperature,
$V_{cyl}$	– cylinder volume,
$V_{mf}$	– manifold volume,
$X$	– fuel deposited coefficient,
$\alpha$	– throttle position,
$\beta(\lambda)$	– air/fuel ratio correction,
$\Delta t$	– calculation period,
$\Delta\alpha_z$	– spark advance,
$\eta_v$	– volumetric efficiency,
$\mu$	– air flow coefficient,
$\lambda$	– relative air/fuel ratio,
$\zeta$	– back propagation coefficient,
$\psi$	– flow type coefficient,
$\tau$	– fuel film vaporisation time constant,
$\sigma_{M_i}$	– standard deviation of indicated torque.

## MODELOWANIE I WERYFIKACJA USZKODZEŃ UKŁADU WTRYSKOWEGO SILNIKA SPALINOWEGO

**Streszczenie.** Rosnące wymagania stawiane silnikom spalinowym przyczyniają się do wprowadzania nowych systemów sterowania. Wymagania te związane są z opracowaniem nowych algorytmów sterowania, które powinny być wyznaczone drogą eksperymentalną i w postaci modelowania. Artykuł przedstawia przyjęte założenia i wymagania dotyczące modelowania w aspekcie sterowania wolnych obrotów silnika. Wybrane badania identyfikacji i weryfikacji w postaci testów przeprowadzono dla modelu silnika 1.5 GLI. Na bazie modelu silnika przeprowadzono symulacje typowych uszkodzeń czujników.

**Słowa kluczowe:** silnik spalinowy, wolne obroty silnika, sterowanie, symulacja uszkodzeń czujników.

## REDUCING ENERGY CONSUMPTION DURING MANUFACTURE OF SEMI-FINISHED COMPONENTS OF THE PLANETARY GEAR THROUGH THE USE OF CASTINGS MADE BY RAPID PROTOTYPING

Andrzej Gil\*, Piotr Kowalski\*, Krzysztof Wańczyk\*

<sup>a</sup> Laboratory of Rapid Prototyping Techniques, Centre for Design and Prototyping,  
Foundry Research Institute ul. Zakopiańska 73, 31-418 Kraków, Poland

**Summary.** This paper proposes a reduction of energy consumption in the implementation of semi-finished components of the planetary gear through the use of foundry technology. The authors compared the calculated amount of sliced material for individual pieces made in technology to bring the full semi-solid and prototype castings. Next presents the selection of materials, development of casting technology parts analyzed, and the various stages of their execution. The final result was semifinished, which, after final machining are to be submitted for testing supplies.

**Key words:** Casting, planetary gears, rapid prototyping, machining.

### INTRODUCTION

The transmission components of machines and vehicles are usually made from various types of metal alloys using two different manufacturing techniques. The first technique is machining, where the required shape of the semi-finished product is obtained by removal of material from a solid workpiece. The second method is casting of components, which are next subjected to a finishing treatment. Naturally, each of these methods has its own advantages and drawbacks, but the choice of a more economical one depends on factors that characterise the currently produced component. A good example of the casting process used as an alternative solution to the fabrication of elements from solid blocks of materials are parts of the planetary gear used in motor vehicles designed for operation under heavy loads [2, 5, 9].

Typically, the primary planetary mechanism is composed of the three types of gears, meshed all the time. The wheel with external teeth, called sun wheel, is located in a central part of the transmission system. Around the sun wheel are arranged the intermediate wheels, or planets, whose axes of rotation are embedded in the yoke (or basket), and there are usually between two and five of them operating in the system. Planets are meshed with an outer gear with internal teeth, placed axially in relation to the sun gear. The planetary mechanism starts operating as a transmission gear allowing the transfer of torque as soon as one of the above mentioned elements is locked, thus

enabling movement of the other two elements, giving the required ratio resulting from the diameter of the individual gears. As a consequence, the three basic modes of operation are obtained:

- sun wheel locked – planets and the outer ring wheel rotate,
- planets yoke locked – the sun wheel and the outer ring wheel rotate,
- outer wheel ring locked – the sun wheel and planets rotate.

The advantage of a gear of this type is its compact design, which allows obtaining much higher ratios than the ratios obtainable in a standard gear, and also different ratios in different modes of operation.

Among the numerous applications of planetary gears, one of the possibilities is to use them as structural components of the drive system of motor vehicles. One of the solutions is to place the planetary gear inside the wheel hub, which enables using the gear mechanism to reduce the torque on the shaft. At the same time, by getting higher torque, the wheel decreases its rotational speed. In practical applications, the design of this mechanism is much more complex than the model example described here and consists of numerous mate parts.

## PURPOSIL AND METHODS

For designs of this type, three components of the mechanism were selected as parts that can be successfully made by casting. These parts are: gear body, ring wheel and cover. Until now, these components have been manufactured by subsequent operations of boring and turning from solid cylinder. Machining allows making items of good quality, free from any hidden material-related defects, but an evident drawback of the technology is the large volume of waste in the form of chips produced from the machined workpiece, as well as a high wear and tear of the cutting knives and lathe tools. The large quantity of the removed material is directly related to the overall dimensions of the machined elements; of some significance is also the fact that in the case of the ring and body, making the cylindrical shape also requires the removal of material from the cylinder interior.

Using casting technology as an alternative enables making these elements as semi-finished products, which after removal of a relatively small machining allowance will give the same shape as in the case of turning and boring from the solid body [1, 2].

To compare the volume of material removed in both processes, as a reference product, the components at a comparable stage of machining were used. The shape reflected the external and internal outlines of the finished product, but the blanks had no holes and final finishing which are usually done in subsequent operations. This allowed determining the difference in the volume of material removed at the first stage of machining, the outcome of which is obtaining the base product shape. At the same time it was assumed that the differences in energy consumption by the compared technologies should be analysed for and until this stage. To calculate the weight of the cylinders used as a starting stock for the machined components, their minimum dimensions were adopted, where outer diameter and height of the blanks were equal to the diameter and height of the ready components. In the case of castings, the weight of the raw components with machining allowances and drafts but without the gating and feeding systems was adopted.

The need for feeding the castings is a natural consequence of the cast metal contraction when it passes from the liquid to solid state; the additional problem in this case is the formation of hot spots in castings. The casting sole-to-casting with gating and feeding system ratio gives percent yield and determines the liquid alloy volume that should be ready to make one cast component. The gating and feeding systems separated from the casting make a good quality scrap used as a charge in the subsequent melting operations.[17-20]

Recycling of chips produced in the machining process is both complicated and energy consuming. Chips to be melted require deoiling and briquetting.

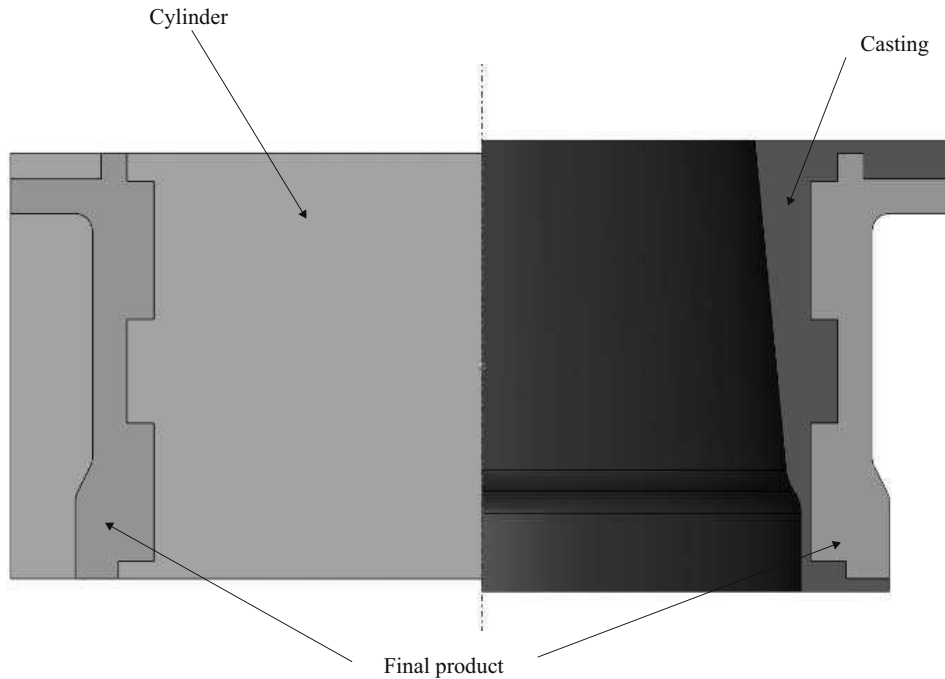


Fig.1. Comparing the waste material volume removed by machining and casting

Table 1. The weight of material consumed by comparable manufacturing technologies to make one set of the semi-finished products

	Estimated material consumption calculated in kg						Total waste in the form of chips
	Ring wheel		Body		Cover		
Element bored and turned	Starting material	Chips	Starting material	Chips	Starting material	Chips	
Cylinder	28,941	22,953	53,586	42,460	6,464	4,957	<b>70,370</b>
Casting	10,941	4,953	14,724	3,598	1,724	0,217	<b>8,768</b>

The calculation of energy consumed by the casting process is a very complex problem because of a large number of the different factors that take part in this process. It leaves no doubt that most of the energy is consumed by the melting process, but it is important to note that, besides the melted metal type and the furnace type and capacity, some impact on the energy consumption has

also the technical condition of the melting installation. Another issue is the process of foundry mould preparation, which can differ in terms of both technology and energy. Practically every foundry operates a technological line of its own design, and the efficiency and performance of devices can vary widely among each other. The additional factor influencing the solution adopted in the technical design of a moulding process is the size of the manufactured batch of castings. It is difficult to imagine that energy consumption might be the same for making a few pieces of the cast items only and a large batch of products, the more that the additional factor of the tooling cost and machine redesigning is also involved here.[2-7,14,16-18]

At the Foundry Research Institute in Cracow, studies have been conducted on the possibility of making several prototype cast semi-finished elements of the planetary gear for further performance tests. To achieve this goal, the method of rapid prototyping was used.[5,9,10,15]

Parts of the transmission gear were cast by the sand mould technology, which can be divided into the following stages:

- 1) designing of 3D foundry technology (allowances, the gating and feeding systems),
- 2) making virtual patterns and technical documentation for foundry tooling,
- 3) making foundry patterns (pattern plate or common foundry patterns),
- 4) making moulds from foundry patterns,
- 5) melting of selected cast alloy,
- 6) pouring of moulds,
- 7) cooling of castings and knocking out from foundry moulds,
- 8) fettling of castings, degating and removal of feeders.

## RESULTS AND DISCUSSIONS

The basis for the development of casting technology is the cast part shape, i.e. the overall dimensions and the degree of intricacy; of some importance is also the cast material type. First, based on the supplied documentation, 3D computer models of individual cast pieces were made, allowing for the necessary technological allowances and drafts. Because of the effect of linear contraction, patterns were enlarged by the values of this contraction, which is 1% and 2% for the cast iron and steel, respectively. Then, the gating and feeding systems were selected in sizes that guarantee making sound castings. Thus prepared documentation was used in the development of moulding technology, including various foundry patterns, core boxes and a configuration of feeding systems. Studies also included joining of individual tooling parts with alignment pins, the use of which ensures the correct assembly of foundry equipment [4, 9].



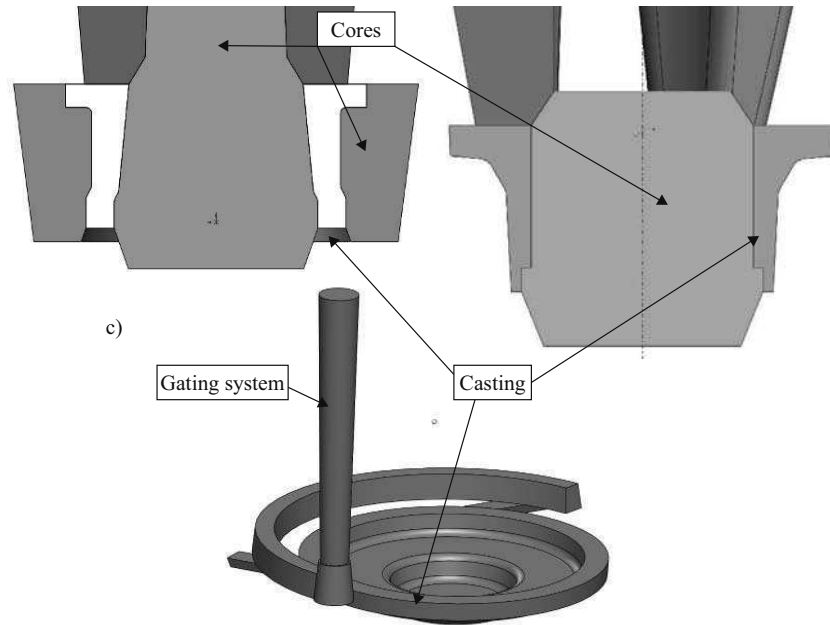
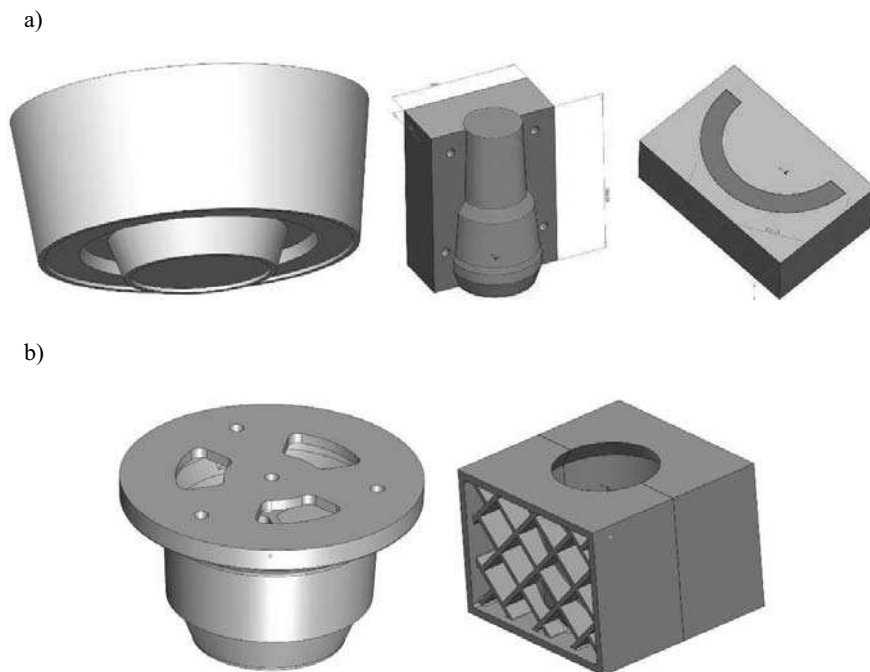


Fig. 2. Casting technology to make successive elements of the transmission gear: a) ring wheel, b) body, c) cover



c)



Fig. 3. Pattern tooling to make individual parts of the transmission gear: a) ring wheel, b) body, c) cover

Foundry patterns were made by the 3D Printing technology, i.e. three-dimensional printing on the layers of powder. The use of the technique of rapid prototyping allows making a real pattern directly from the 3D files of the prepared documentation. To minimise the volume of material used by the 3D printer, models were printed in the form of shells, and to increase their strength, a ribbed internal structure was designed. Patterns obtained by this technique were hardened soaking them with epoxy resin. Empty spaces inside patterns were filled with special fillers, and holders were attached to patterns to facilitate lifting them up from the ready mould. The last step was coating of patterns with a layer of protective paint [11].

a)



b)



c)



Fig. 4. Foundry patterns: a) ring wheel, b) body, c) cover,

As a material for moulds and cores to reproduce the casting of a cover, the self-hardening moulding mixtures based on silica sand with furan resin as a binder were used. In the case of bodies and rings, they were cast in common bentonite-bonded sand mixtures; cores were made in furan resin sand.

Moulds for casting of the cover were made as two halves, i.e. cope and drag, one half mould for casting one cover. The drag was made by placing patterns on the bottom plate with a frame, which was filled with moulding sand, compacted at the next step of operations. Then the whole was turned over, and after removal of the bottom plate, cope was moulded in the same way. After pulling the patterns out and adjustment of the gating system, the half moulds were assembled together and joined with a moulding glue. The glue was used to prevent molten metal from flowing out from the mould along the parting plane during pouring. The cast material was grey iron GJL200.



Fig. 5. Foundry moulds of cover

In moulds for casting of bodies and rings, inner cores had to be used. In the case of rings, moulds were additionally provided with pulled out outer parts. The casting shape was reproduced in core boxes filled with furan sand mixture. Mould cavities were reproduced by patterns with core prints. Moulds for bodies and rings were made from bentonite sand. In the upper part of mould, risers were placed, and their shape was reproduced with patterns joined to the pattern of the casting by means of centring pins. Risers were used to move the hot spots outside the casting area and feed them with liquid alloy during solidification.

To assemble moulds and make them ready for pouring, cores were first placed in the bottom part of mould and the mould was next closed with its upper counterpart and loaded. The bodies were cast from the GS-25CrMo4 steel (DIN 17205), while rings were cast from the L40HM steel (PN-88/H83160).

For casted components of the planetary gear, the alloys of metals have been melted in a medium-frequency induction furnace. Three different cast materials were melted, each of them being adjusted to the respective type of castings. The individual cast alloys and the respective pouring temperatures are compared in Table 2. [22,23]

Table 2. Alloy grades and pouring temperatures selected for individual castings

Casting	Material	Standard	Pouring temperature °C
Cover	Cast iron - GJL200	-	1380
Body	Cast steel - GS-25CrMo4	(DIN 17205)	1570
Ring	Cast steel - L40HM	(PN-88/H83160)	1550

After pouring and cooling, castings were knocked out from moulds and cleaned. Then the gating and feeding systems were cut off. Castings were evaluated for the presence of possible casting defects and checked for the dimensional accuracy. The results of the check have proved that castings are characterised by good surface quality, and are free from any serious defects, while their dimensions are consistent with expectations. Thus prepared cast parts of the planetary gear were handled for further machining.



Fig. 6. Semi-finished castings of the planetary gear

## CONCLUSIONS

The technology of casting semi-finished components of the planetary gear is regarded as a highly competitive process with the technology of machining these elements from a solid block of material. Comparing the volume of material removed during machining and casting (Table 1), it clearly follows that casting generates less chips and shortens the time of this operation. The difference in the amount of the machined material exceeds 60 kg for one set of gears; this value becomes particularly important in mass production of these elements, where it goes into tons.

The energy consumption by the manufacturing process should also be considered in terms of the possible recycling of the waste material. In the case of casting, a large part of the material allowance is process scrap in the form of gating and feeding systems, which can be easily reused within the same plant, while the same cannot be easily said of the chips formed during machining.

Last but not least, the reduced energy consumption is reflected in the price of the final product; lower production costs with high quality maintained raise the competitiveness of the company in the market. Today, the modern metalcasting industry pays more and more attention to the problem of energy consumption in the manufacturing processes, believing that its continuous reduction will bring even better economic results in future.

## REFERENCES

1. BUBICZ M.: *Raport: Szybkie prototypowanie cz. I – przegląd dostępnych rozwiązań. Maszyny, materiały, zastosowania.* / Projektowanie i Konstrukcje Inżynierskie 6(09) czerwiec, 2008, p. 14 - 21.
2. CHUA C.K., LEONG K.F., LIM C.S.: *Rapid Prototyping. Principles and Applications*, World Scientific, Singapore 2004.
3. PŁATEK P., Kret M.: *Techniki druku 3D – przykłady zastosowań metody FDM, warstwowe osadzania topionego materiału.* Seminarium techniki szybkiego prototypowania w cyklu życia produktu. „Mechanik” 2008, nr12.
4. DYBAŁA B.: *Technologie szybkiego prototypowania i wytwarzania*, W: „Raport. Rapid Prototyping & Reverse Engineering”, 2010.
5. SOBAŚ A.: *Od idei do produktu czyli rapid prototyping*, Warsztat, 2010.

6. BUBICZ M.: *Cyfrowe czy jednak fizyczne? Prototypowanie – wyzwanie XXI wieku*, Konstrukcje inżynierskie 2007, nr 1.
7. CHOJNOWSKA L.: *Model wirtualny wsparty wydrukiem 3D*. Desing News w Mechanice i Elektronice, 2008, nr 03.
8. CHUCHRO M., CZEKAJ J. RUSZAJ A.: *Wytwarzanie modeli funkcjonalnych i narzędzi metodą selektywnego spiekania laserowego (SLS, DMLS)*, Mechanik nr 12/2008, str. 1064
9. GUSTAFSON R.: *Rapid Prototyping: a tool for casting design and verification*, Mod.Casting 1999 Vol.89 nr 3 s.44-47.
10. HUMML W., HAEMERLE H.: *Metallische Prototypen in hoher Qualitaet durch innovative Feingiesstechniken*, Konstruieren+Giessen 2005 Jg.30 nr 1 s.10-13, bibliogr.1 poz.
11. KROKOSZ J., MŁODNICKI S., GIL A., KARWIŃSKI A., PABIŚ R., ĆWIKLAK R.: *Ocena możliwości wykorzystania technik szybkiego prototypowania w odlewnictwie oraz opracowanie założeń i wykonanie serii modeli i odlewów artystycznych*, Odlewnictwo współczesne – Polska i świat 2010, nr 1, str.3-13.
12. LEWANDOWSKI J.L.: *Postęp w zakresie szybkiego prototypowania*, Przegląd Odlewnictwa 3/2001 str. 116-117.
13. OCZOŚ K.E., *Rapid Prototyping - znaczenie, charakterystyka metod i możliwości*, Mechanik 1997, 70 nr 10 s.441 – 452.
14. PĄCZEK Z., KARWIŃSKI A., KROKOSZ J., PRZYBYLSKI J., PYSZ S.: *Zastosowanie technik LOM do wykonywania odlewów, możliwości, szanse, problemy*, wyd. Instytut Odlewnictwa – Kraków, Kraków, 2003.
15. WUENSCH R.: *Rapid Prototyping bei der Herstellung von Gussteilen*, Giesserei 2004 Jg.91 H.4 s.44-46.
16. CHLEBUS E.: *Innowacyjne technologie Rapid Prototyping – Rapid Tooling w rozwoju produktu*. Oficyna Wydawnicza Politechniki Wrocławskiej. Wrocław 2003, s.37-42,47-57,106-140,152-158.
17. RUSZAJ A.: *Niekonwencjonalne metody wytwarzania elementów maszyn i narzędzi*. Wydawca IOS w Krakowie. Kraków 1999,s.288,299.
18. OCZOŚ K.E.: *Rosnące znaczenie Rapid Manufacturing w przyrostowym kształtowaniu wyrobów*. Mechanik (2008)4, 256.
19. OCZOŚ K.E.: *Zastosowanie techniki Rapid Tooling do kontroli jakości wytwarzanych części samochodowych*. Mechanik (2008)12, 1022-1028.
20. OCZOŚ K.E.: *Rozwój kształtowania przyrostowego wyrobów*. Mechanik (2007)2,65
21. PLICHTA J., PLICHTA S.: *Techniki komputerowe w inżynierii produkcji*. Wydawnictwo Uczelniane Politechniki Koszalińskiej, Koszalin 2006.
22. Pirowski Z.,Gościański M.: *Consturcion and technology of production of casted shares for rotating and field ploughs* Teka komisji motoryzacji i energetyki rolnictwa, PAN O/Lublin, T. IX, s. 231-239.
23. Pysz S., Karwiński A., Czekaj E.: *An analysis and comparision of properties of Al-Si alloy automotive castings made by rapid prototyping and standard lot producton*. Teka komisji motoryzacji i energetyki rolnictwa, PAN O/Lublin, T. IX, s. 251-258.

ZMNIEJSZENIE ENERGOCHŁONNOŚCI WYKONANIA PÓLFABRYKATÓW  
ELEMENTÓW PRZEKŁADNI PLANETARNEJ POPRZEZ ZASTOSOWANIE  
ODLEWÓW OTRZYMANÝCH Z WYKORZYSTANIEM  
METOD SZYBKIEGO PROTOTYPOWANIA

**Streszczenie.** W artykule przedstawiono propozycję obniżenia energochłonności wykonania półfabrykatów elementów przekładni planetarnej poprzez zastosowania technologii odlewniczej. Porównano obliczone ilości skrawanego materiału dla poszczególnych detali wykonywanych w technologii wytaczania z pełnej bryły oraz z półfabrykatów odlewów prototypowych. W dalszej części przedstawiono dobór materiałów, opracowanie technologii odlewania analizowanych detali oraz poszczególne etapy ich wykonania. Efektem końcowym były półfabrykaty, które po ostatecznej obróbce skrawaniem mają być przekazane do testów eksploatacyjnych.

**Słowa kluczowe:** Odlewanie, przekładnia planetarna, szybkie prototypowanie, obróbka skrawaniem.

## A STORAGE TIME INFLUENCE ON MECHANICAL PARAMETERS OF TOMATO FRUIT SKIN

Bożena Gładyszewska, Anna Ciupak

Department of Physics, University of Life Sciences, ul. Akademicka 13, 20-950 Lublin  
e-mail: bozena.gladyszewska@up.lublin.pl

**Summary.** Presented work introduces the results of comparative analysis concerning selected mechanical properties of greenhouse Admiro and Encore and soil-grown Surya and Polset tomato's cultivars skin, stored at 13°C. A statistically significant effect of both: variety and storage time on the Young's modulus, critical stress and Poisson's ratio values was observed. The Young's modulus determined for greenhouse fruit's skin demonstrated considerably higher values than observed for the soil-grown varieties, in addition the highest values were set for an Encore while the lowest one for a Polset variety. The values of Young's modulus and critical stress decreased with the storage time growth while the Poisson's ratio remained in the range from 0.4 to 0.49. Poisson's ratio, established for greenhouse tomato's peel, took higher values than in the Encore variety case.

**Key words:** tomato skin, mechanical properties, Poisson's ratio, Young's modulus.

### INTRODUCTION AND RESEARCH GOAL

The subject of numerous researches ongoing in various scientific centers covers determination of mechanical properties for fruits and vegetables. The literature data shows that the most important and most often defined mechanical parameters are: the Young's modulus, the Poisson's ratio, the critical stress and strain, the biological yield point, and the rupture point [Sitkei 1986]. However, only a few works takes up the challenge of making the fruits and vegetables cover a research matter.

The tomato fruit's skin has a layered structure, functions mainly as a protection for the pulp, and is a kind of a border against external destructive factors, [Barrett et al. 1998; Telis 2004; Bargel and Neinhuis 2005, De los Reyes, 2007]. Probably the differences in the skin layers construction occurring among the tomato varieties, also decide on its mechanical properties. Fruit stores as well as food-processing plants are interested in fruits with a skin resistant to damage during e.g. transport and storage. However, from the perspective of the individual consumer, tomato fruit should have skin soft and easy to remove. Miles et al. (1969) also considered skin as the most important part of the tomato fruit, responsible for its mechanical strength.

Received strength parameters may thus allow the analysis of their changes depending on the tomato's variety and the growing environment as well as determine an attempt to assess the current state of physiological fruit. It can be expected, that on the basis of mechanical parameters variability, the fruit's shelf-life during the entire period of storage will be possible to assess.



The aim of this study was to examine the variability of selected strength parameters of tomato's fruit skin for the soil-grown and greenhouse varieties, stored at 13°C.

## MATERIALS AND METHODS

Tomato fruits of two greenhouse varieties: Admiro and Encore cultivated at "Leonów" (Niemce near Lublin, Poland) as well as tomato fruits of two soil-grown varieties: Polset and Surya cultivated in Ostrówek near Lublin were investigated.

Examined fruit material was delivered directly after harvesting. Tomato fruits were in the initial ripening stage with green-orange colored skin. The harvested fruits were similar in size. Fruits with visible defects and skin damages were rejected, and the remaining material was stored in a controlled environment chamber at temperature 13 °C. Tomatoes were removed from the controlled environment chamber and kept in a laboratory until fruit temperature became equal to ambient temperature (around 2 hours). After washing and drying the surface of the fruit, skin specimens were procured for tensile tests. The incision was made from the base of the tomato to the stalk. Longitudinal strips were sliced off from each fruit with a profiled, single-blade knife with a limiter. Parameters such as length, width and thickness were measured with the use of a caliper before the examination. The samples had the shape of a strip with the length of 30 mm ± 0.1 mm and the width of 10 mm ± 0.1 mm. The above values were measured with the use of a caliper. The thickness of each sample was measured under an optical microscope at 5 points in the central part of the strip on both sides with the accuracy of ± 0.05 mm. Prepared samples were placed in clamping grips of the tensile machine, which allows constant and measurable increase of the tensile force value which equalled 4.2 N min<sup>-1</sup>. Powdered graphite markers were randomly sprayed on the sample surface. The experiment was conducted on the measuring position assigned for the determination of mechanical properties of biological material [Gładyszewska 2006]. The method of random markers was applied to determine Young's modulus, Poisson's ratio and critical surface tension of the skin. This method relies on the analysis of the image of and the distance between points on the surface of the sample subjected to uniaxial stretching tests [Gładyszewska 2007]. The images of the stretched sample with graphite markers randomly sprayed on the sample surface and the value of the tensile force corresponding to each image were downloaded to the computer. The signal from the tensometer was transmitted to the computer with the use of an analogue-to-digital converter. The random marking method has fewer limitations and produces fewer errors than other techniques for testing the mechanical properties of biological materials. Its main advantage is that the obtained results are independent of the effects observed along the specimen's edges which are close to the clamping grips of the testing machine. The ends of the samples prepared directly before measurement were placed in the clamping grips of the tensile testing machine. The fixed clamping grip was connected to the Megaton Electronic (AG&Co) KT-1400 tensometer with a force measurement range of 0 -100 N, and the moving grip was flexibly connected to a transmission device for stretching the specimen. Using a CCD camera equipped with a microscope lens, the specimen was observed at 240 x 320 pixel resolution under 5x magnification.

Each measurement was performed in 30 replications. Young's modulus  $E$  is defined as the ratio of stress over strain in the direction of the applied force (x-axis) (equation 1). Young's modulus for each sample was determined based on the value of the slope of a straight line approximating individual dependence  $\varepsilon_x = f(\sigma)$ , where  $\varepsilon_x$  is the relative elongation in the direction of the x-axis (-), and  $\sigma$  is the value of stress (MPa):

$$E = \frac{\sigma}{\varepsilon_x}$$

The critical surface tension of a stretched specimen was determined using Eq. (2), and Poisson's ratio  $\nu$  was computed based on dependence (3):

$$\sigma = \frac{F}{S},$$

$$\nu = -\frac{\varepsilon_y}{\varepsilon_x},$$

where:  $F$  (N) is a force value corresponding to destruction of a sample,  $S = a \cdot b$ ,  $a$  and  $b$  are thickness and width of a sample, respectively (mm),  $\varepsilon_x$  is a relative elongation in the direction of the applied tensile force (-),  $\varepsilon_y$  is a relative elongation in a perpendicular direction to the applied force (-).

The results were processed statistically using the Statistica 6 application.

## RESULTS AND DISCUSSION

There is no possibility to determine unambiguously the physical features, characterizing the mechanical properties of tomato's fruit skin, without defining a thickness, for which these values were achieved. In the case of tomato fruits a visible, sharp boundary separating the skin from the flesh of the fruit is hard to define. The values should therefore be related to the average thickness of the samples accounting for 0.68 mm in case of greenhouse tomato fruit varieties and 0.77 mm for soil-grown ones [Ciupak 2010].

Changes in the average value of Young's modulus for the greenhouse (Admiro and Encore varieties) tomatoes' fruit skin, and skin of the Polset and Surya stored at 13 °C is presented on the figures 1 and 2 respectively.

The values of Young's modulus (Fig. 1a) determined for the greenhouse tomato fruit of Admiro variety on the harvesting day came to 4.15 MPa and after 14 days of storage reached 3.79 MPa, while in 21th day, its fall to a level of 3.04 MPa could be observed. On the final experimental day, the Young's modulus gained about 40 % lower values in comparison to the level from the first day of examination and accounted for 2.48 MPa.

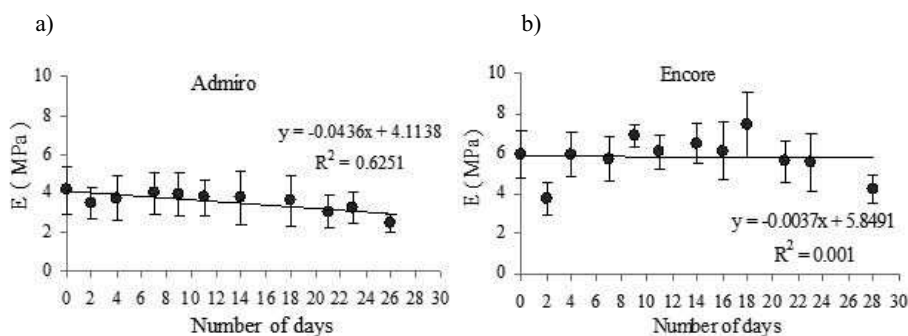
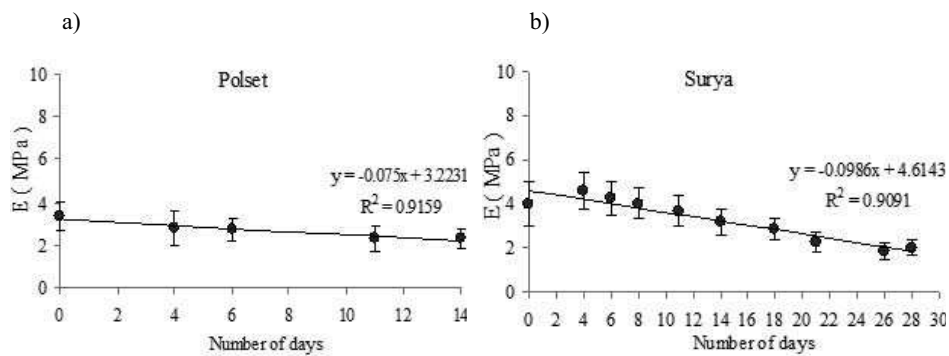


Fig. 1. The average values of Young's modulus for skin of greenhouse tomato fruit, Admiro (a) and Encore (b) varieties, stored at 13°C with a standard deviation

Figure 1b shows the changes of average Young's modulus values obtained for Encore tomato's fruit skin. During the four-week fruit storage, any clear upward trend or downward changes in the value of this parameter were not observed. On the harvesting day, Young's modulus average value came to 5.94 MPa. After two days of storage at 13 °C about 37 % decrease was noted, while on the fourth day increase to a value equal to that from the first day of research was registered. Gradual increase of the Young's modulus value during subsequent days was observed. On 18th day of storage, Young's modulus increased to 7.4 MPa while on the last day of testing (28th day of storage) 30 % decline of Young's modulus (to 4.19 MPa), in comparison with the first day values, was noticed (Fig. 1b).

Figure 2 illustrates the changes in Young's modulus values determined for tomato's skin of the soil-grown: Polset (Fig. 2a) and Surya (Fig. 2b) varieties, stored at 13 °C. In case of Polset variety of fruit only 14 days of measurements were possible to conduct. After this time, due to the progressive process of fruit softening and difficulties in the sample preparation, the studies were finished. The value of Young's modulus for Polset tomato skin came to 3.36 MPa on the harvesting day. This value slope to a level of 2.8 MPa was observed after 4 days of storage, while on the last day of measurement Young's modulus reached 2.31MPa, which was lower by over 30% from the initial rate (Fig. 2a).

Tomato fruits of Surya variety remain firm throughout the storage period and were tested for 4 weeks (Fig. 2b). On the harvesting day the average value of Young's modulus came to 3.99 MPa. After 4 days of storage, this value increased to 4.58 MPa, and then its clear downward trend with increasing storage time was observed. On the 14th day of storage the value of longitudinal modulus of elasticity fall to a level of 3.19 MPa was noticed, while on 21th day a clear decrease to the value of 2.25 MPa was noted. On the last testing day, the value of Young's modulus accounted only for 2.03 MPa



**Fig. 2.** The average values of Young's modulus determined for skin of soil-grown tomato fruit of Polset (a) and Surya (b) varieties, stored at 13°C with a standard deviation

The line graphs 3 and 4 (Fig. 3, Fig. 4) show the changes in the value of critical stress determined for tomato's skin for both greenhouse and soil-grown cultivars, stored at 13° C.

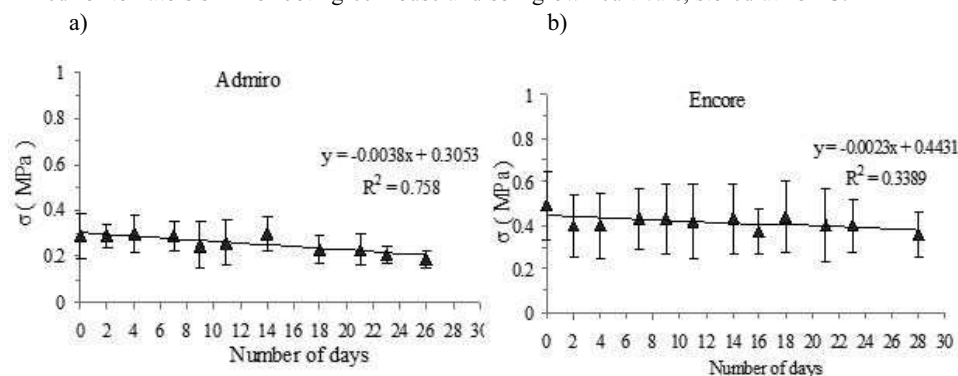


**Fig. 3.** The average values of critical stress determined for tomato's skin of greenhouse Admiro (a) and Encore (b) varieties, stored at 13°C with a standard deviation

Critical stress values calculated for the skin of the Admiro tomato during the harvesting day came to the 0.29 MPa and remained steady for over 14 storage days. On the last day of measurements, the parameter value decreased by over 30 % compared to the figure obtained in the first day of testing and reached 0.19 MPa (Fig. 3a). The average critical stress values at the date of harvesting for the Encore tomato fruits accounted for 0.49 MPa. Mentioned level was constant up to 23th day of fruit storage in a climate chamber. On the last day of the experiment, the critical stress values achieved 0.36 MPa (Fig. 3b).

The data on the figure 4 reflects the changes in critical stress values in addition to the skin of Polset and Surya varieties. On the first day of the experiment the values of the critical stress determined for Polset variety amounted to 0.29 MPa (Fig. 4a), while for the Surya variety came to 0.48 MPa (Fig. 4b).

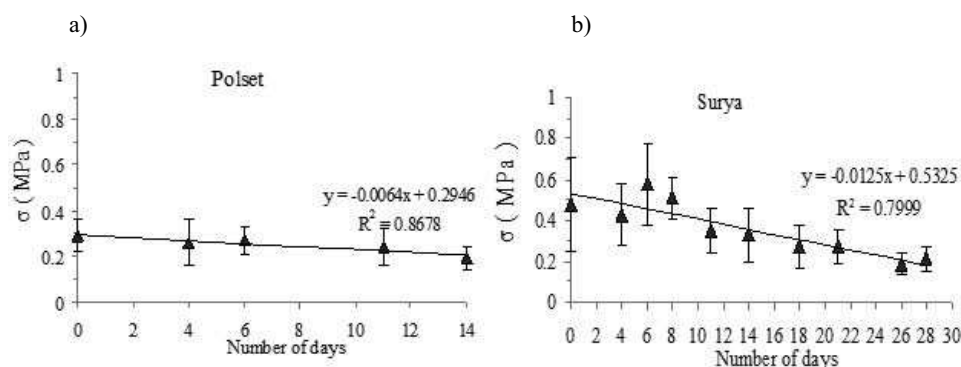


**Fig. 4.** The average values of critical stress determined for soil-grown tomato varieties: Polset (a) and Surya (b), stored at 13°C with a standard deviation

After four days of storage at a temperature of 13 ° C, the critical stress values for the Polset variety decreased slightly to 0.26 MPa. Similarly, for the Surya, the slight slope to a 0.43 MPa was

observed. On the last, 14th day of Polset storage, the critical stress value determined for the skin, declined to the 0.19 MPa while in case of the Surya variety this figure remained at the level of 0.33 MPa. On the last 28th day of Surya fruits storage, a critical stress values amounted to 0.21 MPa and were approximately about 56 % lower than during the first testing day (Fig. 4b).

The figure 5 shows changes in the value of Poisson's ratio in addition to the skin of greenhouse tomato fruit of Admiro and Encore varieties stored at 13 °C. The value of the parameter, in the instance of Admiro tomato skin, decreased by 22 % from 0.73 on the harvesting day to 0.57 after 26 days of storage (Fig. 5a).

The value of Poisson's ratio according to the Encore tomato skin has changed within 28 days of storage (Fig. 5b). On the harvesting day the ratio accounted for 0.56, while on the last day of storage, fell to a level of 0.43.

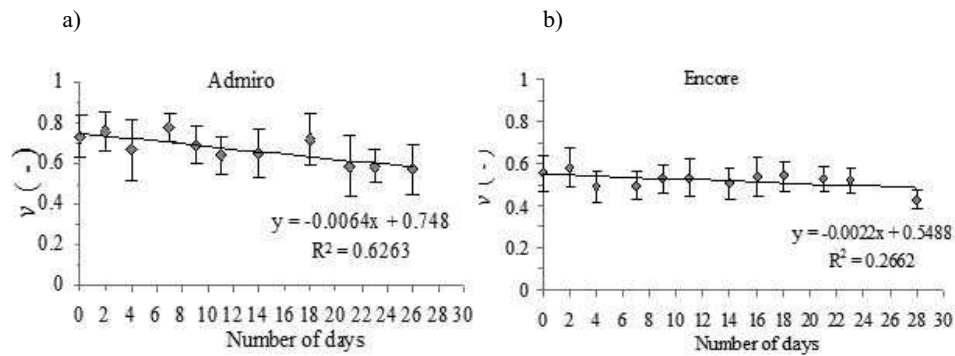


**Fig. 5.** The average values of the Poisson's ratio according to the skin of Admiro (a) and Encore (b) varieties, stored at 13°C with a standard deviation

Mean values of Poisson's ratio calculated for the skin of soil-grown tomato fruits of Surya and Polset varieties stored at 13 °C is given on the figures 6a and 6b respectively. The value of this parameter for a Polset variety ranged from 0.42 to 0.45 (Fig. 6a), while for Surya fruits the Poisson's ratio reached values between 0.4 - 0.49 (Fig. 6b).

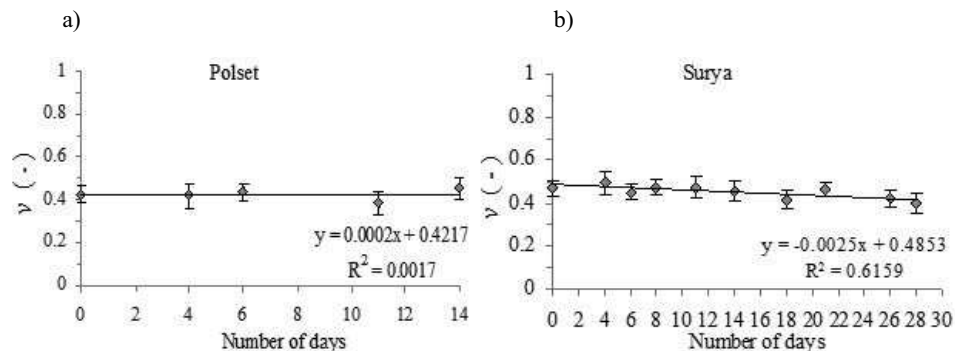


**Fig. 6.** The average values of the Poisson's ratio according to the skin of soil-grown tomato of Polset (a) and Surya (b) varieties, stored at 13°C with a standard deviation

Table 1 shows the Young's modulus, Poisson's ratio and critical stress values determined for the tomato skin of all tested cultivars, stored at 13°C, set during the entire study period. The values are given at intervals so that the upper limit of the range corresponds to the value determined at the date of fruits harvesting while the lower is the value on the last day of storage. In the case of soil-grown tomato fruit varieties (Surya and Polset) the Poisson's ratio value changed within the ranges given in Table 1.

**Table 1.** The average value of the parameters determined during conducted research

Storage temperature 13°C	Young's modulus E (MPa)	Poisson's ratio $\nu$ (-)	Critical stress $\sigma$ (MPa)	Storage time (days)
Admiro	4,15 – 2,48	0,73 – 0,57	0,29 – 0,19	26
Encore	5,94 – 4,19	0,56 – 0,43	0,49 – 0,36	28
Polset	3,36 – 2,31	0,42 – 0,45	0,29 – 0,19	14
Surya	3,99 – 2,03	0,40 – 0,49	0,48 – 0,21	28

Young's modulus determined for the skin of Admiro and Encore greenhouse varieties was higher than determined for the soil-grown Polset and Surya cultivars. On the harvesting day, the skin of Encore variety achieved the highest value of this parameter while the lowest were noted for the Polset cultivar (Table 1). Young's modulus, Poisson's ratio and critical stress calculated for the tomato's skin of the Surya variety are significantly higher than defined for the Polset fruits. The data reflects the decrease of the longitudinal elasticity modulus and critical stress values for the soil-grown tomato's skin stored at 13 °C over the whole storage time. The Poisson's ratio changes in the range from 0.4 to 0.49 could be observed (Table 1).

As it can be seen on the figure 1b for the Encore variety fruits, the Young's modulus demonstrates not only high fluctuations but also a significant scatter of results around the mean value. Similarly, a high coefficient of variation (more than 20 %) for Admiro variety could be observed (Fig. 1a). The largest spread of the critical stress values around the mean was determined for the skin of Surya and Encore tomato varieties (Fig. 3b and Fig 4b). For the Encore variety, Young's modulus and critical stress values fluctuation and scatter have been reflected in studies in which unequal softening and surface dying process was observed.

According to the literature data, the value of Young's modulus of tomato fruit skin is strongly dependent on the variety and can cover a wide range of values from about  $20 \cdot 10^{-3}$  MPa to 110 MPa and even 600 MPa for Beefsteak cultivar (Table 2).

**Table 2.** The Young's modulus values determined for the tomato fruit skin

Variety	Young's modulus E (MPa)	Literature position
Delicious Sunripe Oxheart	$25 \cdot 10^{-3}$ $21 \cdot 10^{-3}$ $17 \cdot 10^{-3}$	Hankinson and Rao 1979
[-]	5 – 50	Hamm et al 2008
[-] Beefsteak	10 – 110 600	Bargel and Neinhuis 2004a, 2005

Inbred 10	43	Matas et al 2004
Sweet 100	27	
Espero	70	Andrews et al 2002a
Scout, Viceroy	80 - 82	Voisey and Lyall 1965
Rideau	75	

A comparison of the values obtained on the basis of studies with available literature data (Table 2) indicates that the average values of Young's modulus determined for the skin of all tested tomato cultivars are similar and, together with a standard deviation, includes the lower limit of the values given by Hamm et al. (2008) (Table 2). Hankinson and Rao (1979) obtained much lower quantities than designated in this study. So much diversity may be caused by differences in cellular structure and strength properties of the skin.

The values of Poisson's ratio determined on the basis of the studies are summarized in Table 1. According to Hamm et al. (2008) for this value for skin of the tomato accounts for 0.5. Among the obtained results a scatter of Poisson's ratio are also observed, however for greenhouse fruits the ratio variability was greater than for the soil-grown cultivars (Fig. 5, Fig. 6).

## CONCLUSIONS

1. Statistically significant influence of both: fruits variety and storage time on the Young's modulus and critical stress values was defined.
2. Young's modulus determined for the skin of greenhouse Admiro and Encore varieties was higher than for the soil-grown Polset and Surya cultivars. The highest value was set for the skin of Encore while the lowest for Polset variety.
3. Surya variety is characterized by the higher values of Young's modulus, critical stress and Poisson's ratio than in case second (Polset) soil-grown cultivar.
4. The values of Young's modulus and critical stress determined for the skin of the soil-grown tomatoes decreased with the growth of the storage time, while Poisson's ratio run in the range of 0.40 - 0.49.
5. For greenhouse varieties greater dispersion of Young's modulus and Poisson's ratio values around the average was observed.
6. The further research are needed in order to evaluate a possible physiological state of fruits and their degree of maturity on the basis of changes in mechanical properties during the study period.

## REFERENCES

1. Ciupak A. 2010.: The influence of storage conditions on tomato's fruit skin mechanical properties. Doctoral/PhD thesis/dissertation (in Polish). University of Life Sciences in Lublin.
2. Andrews J., Adams S. R., Burton K. S., Edmondson R. N. 2002.: Partial purification of tomato fruit peroxidase and its effect on the mechanical properties of tomato fruit skin. *Journal of Experimental Botany* 53 (379), 2393-2399.
3. Bargel H., Neinhuis C. 2005.: Tomato (*Lycopersicon esculentum* Mill.) fruit growth and ripening as related to the biomechanical properties of fruit skin and isolated cuticle. *Journal of Experimental Botany* 56 (413), 1049-1060.

4. Bargel H., Neinhuis C. 2004.: Altered tomato (*Lycopersicon esculentum* Mill.) fruit cuticle biomechanics of pleiotropic non ripening mutant. *Journal of Plant Growth Regulation* 23, 61-75.
5. Barrett D., Garcia E., Wayne E. 1998.: Textural modification of processing tomatoes. *Critical Reviews in Food Science and Nutrition* 38 (3), 173-258.
6. Chung S. M., Yap A. U., Koh W. K., Tsai K. T., Lim C. T. 2004.: Measurement of Poisson's ratio of dental composite restorative materials. *Biomaterials* 25, 2455-2460.
7. De los Reyes R., Heredia A., Fito P., De los Reyes I. E., Andrés A. 2007.: Dielectric spectroscopy of osmotic solutions and osmotically dehydrated tomato products. *Journal of Food Engineering* 80, 1218-1225.
8. Etner S. A. 2003.: Twisting and bending of biological beams: distribution of biological beams in a stiffness. *The Biological Bulletin* 205, 36-46.
9. Gładyszewska B., 2007.: Method for testing selected mechanical properties of thin-film biomaterials (in Polish). *Rozprawy Naukowe* (325). Wydawnictwo Akademii Rolniczej, Lublin, 1-87.
10. Gładyszewska B. 2006.: Testing machine for assessing the mechanical properties of biological materials. *Technical Science* 9, 21-31.
11. Hamm E., Reis P., LeBlanc M., Roman B., Cerda E. 2008.: Tearing as a test for mechanical characterization of thin adhesive films. + Supplement. *Nature Materials* 7 (5), 386-390.
12. Hankinson B., Rao V. N. 1979.: Histological and physical behavior of tomato skins susceptible to cracking. *Journal of the American Society for Horticultural Science* 104 (5), 577-581.
13. Kader A. A., Stevens M. A., Albright-Holton M., Morris L. L., Algazi M. 1977.: Effect of fruit ripeness when picked on flavor and composition in fresh market tomatoes. *Journal of the American Society for Horticultural Science* 102 (6), 724-731.
14. Matas A. J., Cobb E. D., Bartsch J. A., Paolillo jr. D. J., Niklas K. J. 2004.: Biomechanics and anatomy of *Lycopersicon esculentum* fruit peels and enzyme-treated samples. *American Journal of Botany* 91 (3), 352-360.
15. Miles J. A., Fridley R. B., Lorenzen C. 1969.: Strength characteristics of tomatoes subjected to quasi-static loading. *Transactions of the ASAE* 12, 627-630.
16. Sitkei G. 1986.: *Mechanics of Agricultural Materials*. Budapest: Akademiai Kiado.
17. Steffe J. F. 1996.: *Rheological methods in food process engineering*. Freeman Press.
18. Telis V. R. N., Murari R. C. B. D. L., Yamashita F. 2004.: Diffusion coefficients during osmotic dehydration of tomatoes in ternary solutions. *Journal of Food Engineering* 61, 253-259.
19. Voisey P. W., Lyall L. H. 1965.: Methods of determining the strength of tomato skins in relation to fruit cracking. *Proceedings of the American Society for Horticultural Science* 86, 597-609.
20. Wojciechowski K. W. 2002.: Remarks on "Poisson ratio beyond the limits of the elasticity theory". *IC* 16, 1-6.

#### WPLYW CZASU PRZECHOWYWANIA NA PARAMETRY WYTRZYMAŁOŚCIOWE SKÓRKI OWOCÓW POMIDORA

**Streszczenie.** W pracy przedstawiono wyniki analizy porównawczej wybranych mechanicznych właściwości skórki owoców pomidora szklarniowego odmian Admiro i Encore oraz owoców pomidora gruntowego odmian Polset i Surya przechowywanych w temperaturze 13 °C. Stwierdzono statystycznie istotny wpływ odmiany i czasu przechowywania na wartość modułu Younga, naprężenia krytycznego i współczynnika Poissona. Moduł Younga skórki owoców szklarniowych był wyższy niż skórki owoców gruntowych. Najwyższą wartość wy-



znaczono dla owoców odmiany Encore, zaś najniższą dla owoców odmiany Polset. Wartość modułu Younga, naprężenia krytycznego skórki owoców gruntowych obniżała się wraz z wydłużaniem czasu przechowywania, zaś współczynnik Poissona zawierał się w przedziale 0,4 – 0,49. Współczynnik Poissona wyznaczony dla skórki owoców pomidora szklarniowego odmiany Admiro charakteryzował się wyższą wartością niż w przypadku odmiany Encore.

**Słowa kluczowe:** mechaniczne właściwości, moduł Younga, współczynnik Poissona, skórka owocu pomidora.

## IMPACT TESTING OF BIOLOGICAL MATERIAL ON THE EXAMPLE OF APPLE TISSUE

Krzysztof Gołacki, Paweł Kołodziej

Department of Machine Theory and Automatics, University of Life Science in Lublin

**Summary.** The study presents the measuring position for determination of the dynamical behavior of vegetables and fruit. The main element of the device is an instrumented rigid physical pendulum made of carbon fiber. The pendulum arm was developed as a double arch connected with the external links. This construction enables attaining the desirable value of the quotient of the mass moment of inertia of the pendulum arm with a fruit and the arm without it as well as appropriate rigidity. The studies with the pendulum device application simulated the apple drop from a required height. The tests measuring pendulum rotation angle and fruit response force in time facilitated determination of the force – displacement correlation at impact event. The obtained displacement and impact force courses in time were presented graphically.

**Key words:** bruise of apples, measuring stand, pendulum.

### INTRODUCTION

Losses of biological material caused by mechanical damage at harvest and post – harvest management constitute a severe problem for both, producers and industrial recipients. It is noteworthy that the losses include the quantitative decrease of fruit and vegetable weight as well as qualitative decrease of their trade value. That problem also concerns Polish producers of apples and processing plants that estimate their economic losses at hundreds of millions zlotys a year. Analyzing the mechanical damage of fruit and vegetable, Bollen [2006] found the following causes at fruit post – harvest handling: impact (at manual – mechanical harvest), compression ( harvest – initial packing and storage), vibration (transport).

However, the highest damage rate results from loads of a dynamic nature, that is impact. Dynamic load is the one whose attachment causes propagation in material stress in the form of a wave. The velocity initiating this character of stress propagation depends on density and rigidity of the impacted material. As for fruit and vegetables, even low impact height (a few centimeters) can cause bruises of a dynamic nature, hence a necessity to determine their susceptibility to bruising. The literature provides numerous impact damage tests [Garcia – Ramos et al., 2004, Blahovec 2006, Van Linden et al., 2006, Van Zeebroeck et al., 2003, 2007]. The impact tests may be grouped according to Sitkey [1986]:

- impact of fruit or vegetable against the fixed rigid flat plane perpendicular to the motion direction,
- impact of biological material on the fixed rigid flat or profile plane inclined to the motion orientation at the appropriate angle,
- fruit or vegetable striking the other fixed fruits or vegetables without their mass center displacement,
- biological material striking the plastic plane.

Biological material force responses obtained at a free-fall test enabled to verify the mathematical model of viscoelastic body [Lichtensteiger et al., 1988] as well as determine the effect of a surface kind and drop height on the impact damage rate [Chen et al., 1991]. However, the results of the impact testing with application of a sphere of known dimensions and mass allowed to evaluate fruit firmness in the sorting lines [Chen et al., 1985, Delwiche et al., 1989].

Apple resistance to impact bruising was also established using the method single fruit impact against single fruit” [Pang et al., 1996] as well as impacting against the accessory rigid surface [Holt and Schoorl 1977]. The advantages of these methods are their fastness, simplicity and a non – destructive nature. However the tests have certain drawbacks, too. One of them is that a sample gets impacted lying down on the substrate so impact energy dissipates in more than one site which does not allow for its correlation with bruising rate. Besides, substantial variation of mass, dimensions and elasticity of fruits and vegetables observed within even a variety affects impact force value at free fall as well as the accuracy of the studied trait (e.g. firmness).

Therefore, many researchers focused on experiments with pendulum and resistance area use for simulating free fall and functional impact of biological material. The studies with the pendulum were carried out by two methods. The first consisted in attaching the biological material to the arm end and measuring the damage – related parameters at the impact moment on the flat plane of the force sensor. Bajema and Hyde [1998] suggested construction of pendulum formed from two pairs of suspending Kevlar lines combined with a wafer and spikes for specimen mounting. In the other method, the values of force, acceleration or displacement were obtained as a result of pendulum impacting piece with a force sensor onto the fixed area of fruit or vegetable [Van Canneyt et al., 2003, Van Zeebrock et al., 2003, Yen et al., 2003, Blahovec et al., 2004]. However, Bajema et al., [1998] developed the concept of combination of the anvil with the built – in force sensor and pendulum as a rotating hammer with the force and acceleration sensors. Both elements made the device to measure both, impulse loading and stress wave responses in the cylindrical shape samples of definite dimensions.

Taking into account the above information, it should be highlighted that studies on sensitivity to impact loading need to be conducted under conditions most similar to free fall at full control of force and sample displacement. The conditions can be satisfied by a special pendulum that guarantees stiffness of the specimen mounted to the arm and its minimum mass that does not affect significantly the impact force course. Thus, the major task is to minimize pendulum arm mass while retaining high rigidity that ensures measurement of momentary angular position associated with sample displacement at impact event. The procedures described in literature allow for the measurement of only force response in time function. The present study has proposed the construction of measuring position for sample reaction force in the displacement function at the investigated sample impact against flat plane.

## MEASURING STAND CONSTRUCTION

The development of a measuring position followed the following design assumptions:

- technical feasibility of measurement head positioning along the vertical axis,
- regulation of measurement head position along the horizontal axis,
- providing a wide range of drop heights,
- measurement of pendulum angular position at definite accuracy,
- recording the impact force course,
- minimization of pendulum mass keeping appropriate rigidity of fruit attachment and its position stabilization at testing.

Besides, a possibility to mount acceleration sensors to both, the pendulum device and biological material studied. The measuring stand for impact testing, presented in Figure 1, is constructed from two rods mounted to the base and connected with three horizontal links. The rods were fitted with the measurement head with a piezoelectric force sensor Endeveco model 2311 – 10 of  $2,27 \text{ mV} \cdot \text{N}^{-1}$  sensitivity and measurement range  $\pm 2200 \text{ N}$ . The measuring head may be displaced in the vertical and horizontal plane and its position is set by adjusting screws. The pendulum arm is an operational element whose mass was minimized due to carbon fiber use. The arm construction ensures maintaining appropriate rigidity.

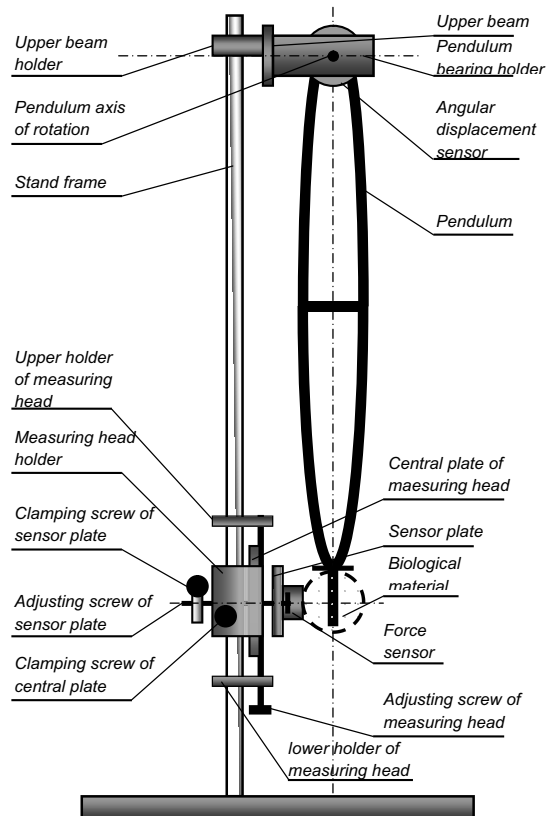


Fig. 1. Measuring stand to impact tests of biological materials

The pendulum is mounted on the axis of incremental optical encoder to record angular displacement Heidenhain model RON 275 at accuracy of  $0,005^{\circ}$ . The sensor was linked to the converter card National Instruments model SCB – 68 that performs data acquisition from the sensor to be afterwards processed by LabView ver. 8.6.1. program. The data measurement of pendulum angular displacement in time was released directly from the LabView programming system while recording of impact force course was initiated by means of a laser – detector gate as presented in Fig. 2.

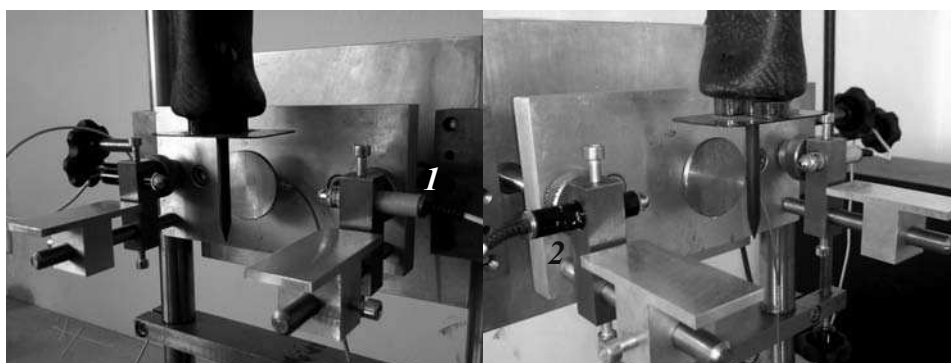


Fig 2. Release gate – laser (1), detector (2)

Construction of the pendulum arm is presented in Fig. 3. Two thin – walled tubes from carbon composite had their ends connected by links made of carbon laminate. They were filled with EPS – expanded polystyrene foam to ensure a suitable profile and shape of links. In the central part of the pendulum device, there was attached a connection stabilizer that at the same time stiffened the arm construction. The entire device was connected by liquid epoxy resin Epoxydharz L. In the pendulum top end, there was drilled a hole to mount the device at the axis of the angular displacement sensor, whereas the down end was equipped with a tang for research material mounting and its position stabilization. There was obtained uniform mass distribution of physical pendulum – 187g.

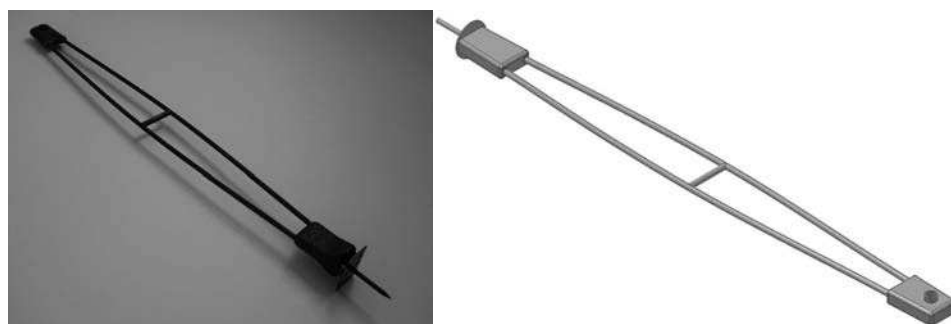


Fig 3. Pendulum arm

The mass moment of inertia of the arm with respect to the axis of rotation was  $0,072592419 \text{ kg} \cdot \text{m}^2$ , while the mass moment of inertia of the pendulum with fruit (average weight 240g) reached  $0,299417669 \text{ kg} \cdot \text{m}^2$ .

## DESCRIPTION OF TEST COURSE

The testing included apples of *Jonagold* variety. During the measurement, the fruits fixed to the pendulum device struck the vertical rigid flat plane of the force sensor measuring element. There was made the initial evaluation of apple diameter along the axis running through the point of fruit contact with force sensor measuring plane and fruit mass.

Appropriate positioning of apple contact point with operational area of the force sensor was possible through adjusting screws for horizontal and vertical displacement of the main plate and measuring head. Besides, before the testing onset, the pendulum device was set in the vertical position, angular displacement sensor reset and the arm deflection corresponding to required fruit drop height established.

Apples aimed for testing were placed at the room temperature. For seven successive days, 10 apples were taken to undergo the test. It consisted in 5 – time impact of apple against operational area of the sensor at the pendulum arm deflection of 18,5 that corresponded to the free – fall from 50 mm height. To record impact force and pendulum angular displacement profiles, there was applied a designed and constructed measuring path and computer with the LabView programming system. There were obtained the courses of the aforementioned values in time as digital data and in graphical form.

## TEST RESULTS

The impact tests performed provided the values of impact force and angular displacement, whose exemplary courses were presented in Figure 4.

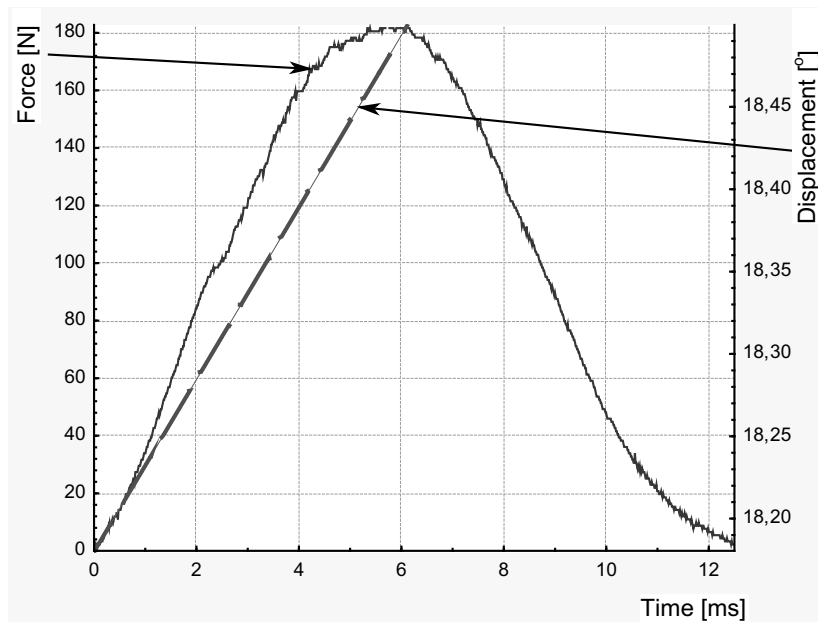


Fig 4. The values of impact force and angular displacement of the simple as independent time functions obtained in a single test

The measurement of impact force profile started at the moment of fruit contact with operational plane of force sensor (then  $F_u = 0$ ). At this point, the angular displacement value recorded by the pendulum rotation sensor was  $\delta = 0$  [°]. Then, impact force ( $F_u$ ) reached the peak value. Owing to apple surface deformation, after some time the displacement rate obtained the value  $\delta = \delta_{max}$  [°]. A recording mode of fruit displacement values during the impact moment was presented in Figure 5.

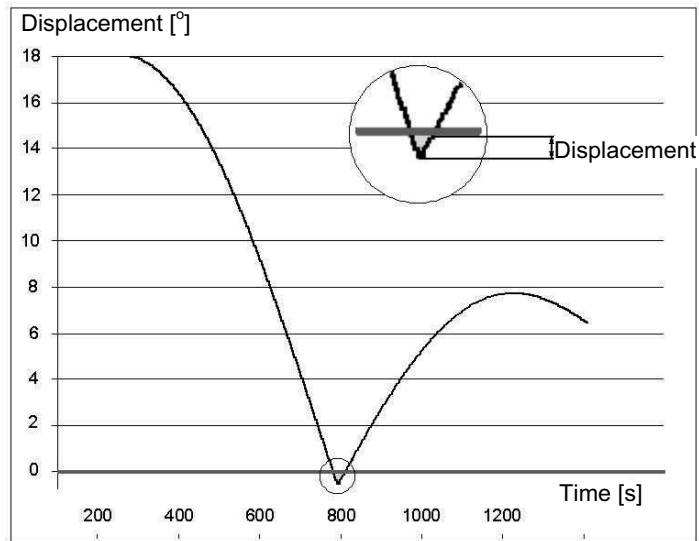


Fig. 5. Example of the angular displacement – time relationship for apple test during impact

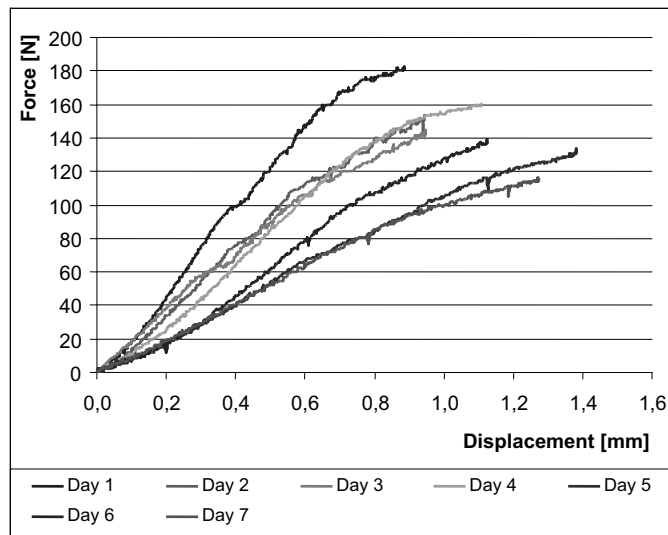


Fig. 6. Force – displacement relationship of the first impact for consecutive days of the test

Figure 6 illustrates the final measurement effect as response force – displacement relationship at the impact event. A detailed analysis of stress and deformation relationships will be possible to perform after including information about an apple shape in the contact area. Besides, it will be important to consider the regions in the contact area where the critical stress values were exceeded or not. Importantly, at this point it is possible to develop curves for different storage periods.

According to Figure 6 and 7, fresh fruits achieved higher values of reaction force at lower displacement rates and thus, the critical stress values were exceeded in them earlier. Stored apple deformation proved to be higher at lower maximum force values. Impact energy was higher in the case of fresh apples, which assuming similar critical stress values, implies the occurrence of greater areas of non – recoverable deformations.

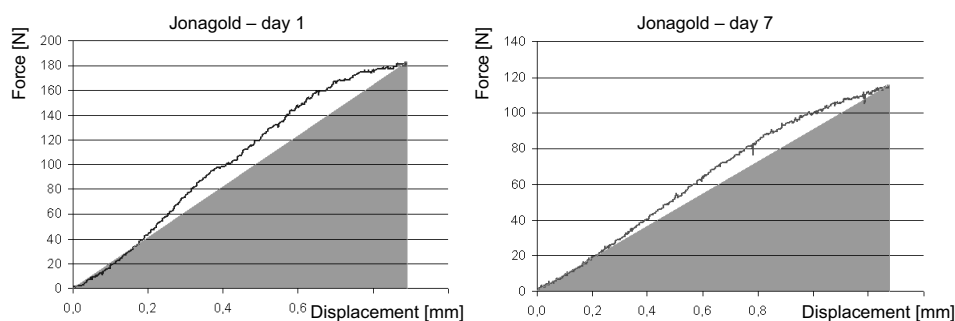


Fig. 7. Comparison of courses of force – displacement profiles for first and last day of testing

## CONCLUSIONS

- A designed and developed measuring stand ensures full regulation of the measuring head so that initial vertical position of the pendulum device with maintained sensor-fruit contact could be possible.
- The physical pendulum construction in the form of a double arch tied with external links combined with carbon laminate use allowed mass reduction to 185g at working length of 1m and to ensure required rigidity of mounting as well as stabilization of the studied material during impact.
- The measuring device applied facilitates simultaneous recording of the courses of arm angular displacement and impact force at high accuracy.
- The obtained force reaction profiles during impact event allowed for a comparison of apple sensitivity to dynamic loads in different storage periods.

## REFERENCES

1. Bajema R. W., Hyde G. M., Peterson K.: Instrumentation design for dynamic axial compression of cylindrical tissue samples. Transactions of the ASAE 41 (3), 1998, pp 747 – 754.
2. Bajema R. W., Hyde G. M.: Instrumented pendulum for impact characterization of whole fruit and vegetable specimens. Transactions of the ASAE 41 (5), 1998, pp 1399 – 1405.



3. Bollen A. F.: Technological innovations in sensor for assessment of postharvest mechanical handling systems, *International Journal Postharvest Technological And Innovation*, 2006, 1, pp 16 – 31.
4. Blahovec J., Mareš V., Paprštejn F.: Static and dynamic tests of pear bruise sensitivity. *Research Agricultural Engineering*. 50 (2), 2004, pp 54 – 60.
5. Blahovec J.: Shape of bruise spots in impacted potatoes. *Postharvest Biological Technologists*, 2006, 38, pp 278 – 284.
6. Chen P., Tang S., Chen S.: Instrument for testing the response of fruits to impact. *ASAE Paper No 85 – 3587*, 1985.
7. Chen P., Yazdani R.: Prediction of apple bruising due to impact on different surfaces. *Transactions of the ASAE* 43 (3), 1991, pp 956 – 961.
8. Delviche M. J., Tang S., Mehlschau J.: An impact force response fruit firmness sorter. *Transactions of the ASAE* 32 (1), 1989, pp 321 – 326.
9. Garcia – Ramos F. J., Ortiz – Canavate J., Ruiz – Altisent M.: Analysis of the factors implied in the fruit – to – fruit impacts on packing lines. *Applied Engineering Agriculture* 20, 2004, pp 671 – 675.
10. Holt J. E., Schoorl D.: Bruising and energy dissipation in apples. *Journal of Textures Studies* 7, 1977, pp 421 – 432.
11. Lichtensteiger M. J., Holmes R. G., Hamdy M. Y., Blaisdel J. L.: Evaluation of Kelvin model coefficients for viscoelastic spheres. *Transactions of the ASAE* 31 (1), 1988, pp 288 – 292.
12. Pang W., Studman C. J., Banks N. H., Baas P. H.: Rapid assessment of the susceptibility of apples to bruising. *Journal of Agricultural Engineering Research* 64, 1996, pp 37 – 48.
13. Sitkey G.: *Developments in Agricultural Engineering 8. Mechanics of Agricultural Materials*. Elsevier, Amsterdam, Oxford, New York, Tokio, 1986. pp 487.
14. Van Canneyt T., Tijsskens E., Ramon H., Verschoore R., Snock B.: Characterization of potato – shaped instrumented device. *Biosystems Engineering*, 86 (3), 2003, pp 275 – 285.
15. Van Linden V., De Ketelaere B., Desmet M., De Baerdemaeker J.: Determination of bruise susceptibility of tomato fruit means of an instrumented pendulum. *Postharvest Biological Technologists*, 2006, 40, pp 7 – 14.
16. Van Linden V., Scheerlinck N., Desmet M., De Baerdemaeker J.: Factors that affect tomato bruise development as a result of mechanical impacts. *Postharvest Biological Technologists*, 2006, 42, pp 260 – 270.
17. Van Zeebroeck M., Tijsskens E., Van Liedekerke P., Deli V., De Baerdemaeker J., Ramon H.: Determination of the dynamical behaviour of biological materials during impacts using pendulum device. *Journal Sound Vibr*, 2003, 266, pp 465 – 480.
18. Van Zeebroeck M., Van Linden V., Ramon H., De Baerdemaeker J., Nicolai B. M., Tijsskens E.: Impact damage of apples during transport and handling. *Postharvest Biological Technologists*, 2007, 45, pp 157 – 167.
19. Van Zeebroeck M., Van Linden V., Darius P., De Ketelaere B., Ramon H., Tijsskens E.: The effects of fruit factors on the bruise susceptibility of apples. *Postharvest Biological Technologists*, 2007, 46, pp 10 – 19.
20. Yen M., Wan Y.: Determination of textural indices of guava fruit using discriminate analysis by impact force. *Transactions of the ASAE* 46 (4), 2003, pp 1161 – 1166.

### TEST UDAROWY MATERIAŁU BIOLOGICZNEGO NA PRZYKŁADZIE TKANKI JABŁEK

**Streszczenie.** W pracy przedstawiono stanowisko do badań dynamicznych warzyw i owoców. Głównym elementem urządzenia jest sztywne wahadło fizyczne wykonane z włókien węglowych. Ramię wahadła zbudowano w postaci podwójnego łuku związanego zewnętrznymi łącznikami. Taka konstrukcja umożliwia uzyskanie korzystnej wartości ilorazu masowego momentu bezwładności ramienia wahadła wraz z owocem i ramienia bez owocu jak również odpowiednią sztywność. Badania z użyciem wahadła imitowały spadek jabłka z zadanej wysokości. Zastosowane testy pomiarowe kąta obrotu wahadła i siły reakcji owocu w czasie pozwoliły na wyznaczenie zależności siły w funkcji przemieszczenia podczas uderzenia. Uzyskane przebiegi przemieszczenia i siły uderzenia w czasie przedstawiono w formie graficznej.

**Słowa kluczowe:** obicia jabłek, stanowisko pomiarowe, wahadło.

## TRACTION QUALITIES OF A MOTOR CAR FIAT PANDA EQUIPPED WITH A 1.3 16 V MULTIJET ENGINE

Wawrzyniec Gołębiewski \*, Tomasz Stoeck \*

\* Department of Motor Vehicle Use, the West-Pomeranian University of Technology in Szczecin

**Summary.** In this paper was presented traction qualities of a Fiat Panda car equipped with a 1.3 16 V Multijet engine. Characteristics of the full power of the 1.3 JTD engine was prepared, along with a selection of the trend curves. On the basis of the moment curve from that graph and the car basic data, traction characteristic of the vehicle was created. It was proven a dependence of the propulsive force on the vehicle's linear velocity. On that basis, such traction qualities of the Fiat Panda, as its ability to accelerate, to drive upon hills and its achieving the maximum speed, were analyzed.

**Key words:** traction characteristics of a vehicle, theory of motion, combustion engines, external characteristic of an engine.

### INTRODUCTION

Accelerability is one of the most important traction qualities of a vehicle. It finds its reflection in urban traffic. A higher number of cars that manage to drive over a crossing in one light cycle results in a lower number of cars waiting before the crossing, which translates to a lower emission of combustion gases from engines working idle.

Moreover, quick passing is important to, as it shortens the time of the hazardous maneuver. This quality of the car is strongly affected by the external characteristics of the engine torque and selection of an appropriate power transmission system.

Overcoming heights by the vehicle at its maximum speed is meaningful too.

These traction qualities describe the essence of the vehicle work and the character of its use.

### PURPOSE OF THE RESEARCH

As the purpose of this research was accepted the performance of traction characteristic of a motor vehicle Fiat Panda, equipped with a 1.3 16 V Multijet engine. Based on it was taken analysis these traction qualities:

- ability to accelerate at individual gears,
- achieving the maximum velocity of vehicle,
- ability to overcome the hills.

## TESTING STATION

The testing station was composed of the following components:

- a fuel (diesel oil) tank – a 200 ltr fuel tank for diesel oil;
- a fuel pump – it was supposed to ensure fuel pressure from the tank and its delivery to the fuel pipes;
- an „Automex” fuel meter – it was an important component, necessary for measuring fuel consumption with the weighing method (not included in the scope of the tests). Uncombusted fuel returned to it through the engine;
- a Fiat Multijet 1,3 JTD engine – a four-stroke turbo-charged diesel engine with direct injection, provided with the Common Rail fuel delivery system;
- an „Automex” eddy current brake – which charged the engine with any chosen anti-torque at variable rotational speeds, using the rotary current phenomenon;
- a power panel with a Fiat Panda 2 switchboard with software and the fuel meter controlling system – was controlled the engine work and torque loading the engine via the brake, with a display of the basic operational parameters, including: power, engine torque, etc..

Below, on the figure 1 was presented the testing station arrangement.

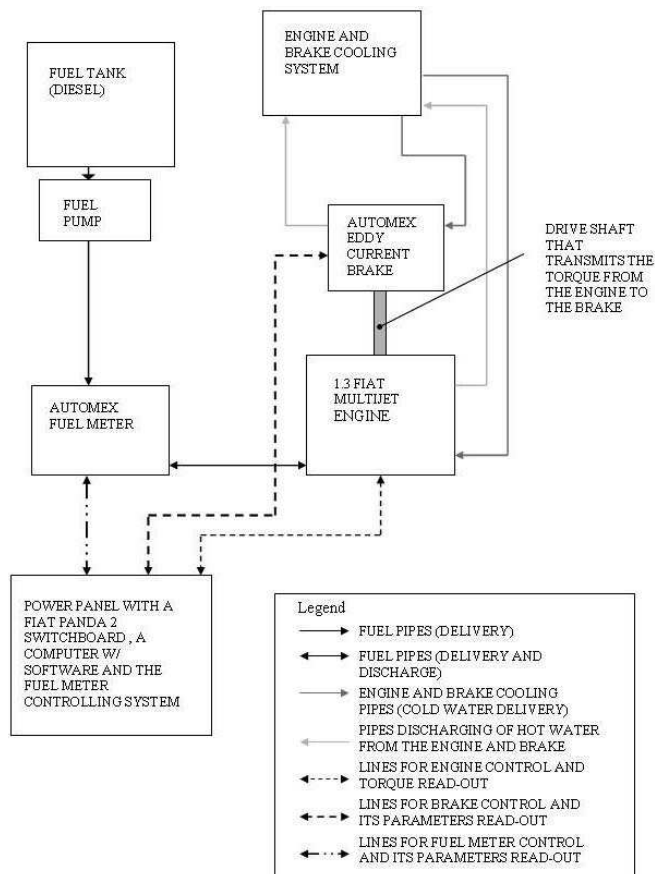


Fig.1. Arrangement of the testing station (plan)

COURSE OF THE TESTS

During the tests, measurements on a test engine bed were conducted, by performing the engine full power speed characteristic [6,9,16] for the Fiat Multijet 1,3 JTD.

It was appeared as follows:

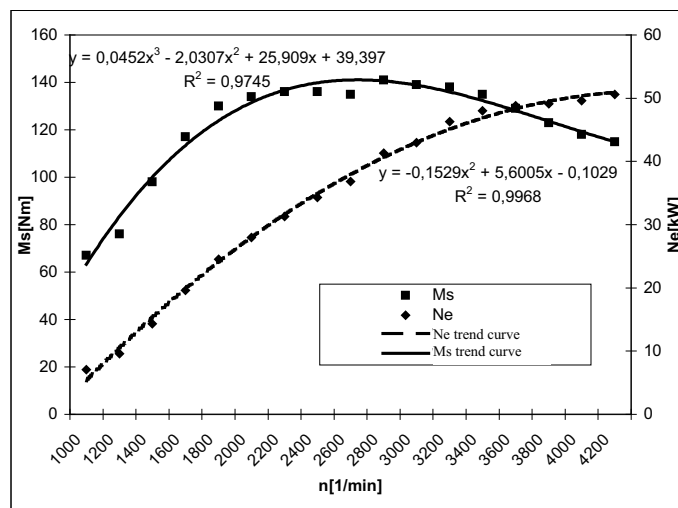


Fig.2. Speed characteristic of a Fiat Multijet 1,3 JTD engine;  $M_s$  – engine torque,  $N_e$  – engine power output,  $n$  – engine rotational speed,  $R^2$  – correlation coefficient

The measurements were made every 200 rpm, from 1000 rpm to 4200 rpm and the opposite. The result was counted as the mean of the two measurements. For these values, trend curves were matched. Equations characterizing those curves were shown on the graph, where  $x=1,2,3,... 17$  – the next measurement number. It was proven the good matching of the trend curves and the actual values by high values of the correlation coefficients ( $R^2$ ). In the table below, results of actual measurements with theoretic values obtained from equations of the matched trend curves were presented.

Table 1. Actual values and theoretical values of the engine torque and power output

	$n$ (rpm)	$M_s$ [Nm]	$M_{s,theor}$ [Nm]	$N_e$ [kW]	$N_{e,theor}$ [kW]
1	1000	67	63.3.2	7.1	5.34
2	1200	76	83.45	9.6	10.49
3	1400	98	100.07	14.3	15.32
4	1600	117	113.43	19.6	19.85
5	1800	130	123.82	24.5	24.08
6	2000	134	131.51	28	28.00
7	2200	136	136.76	31.3	31.61

8	2400	136	139.85	34.3	34.92
9	2600	135	141.04	36.8	37.92
10	2800	141	140.62	41.3	40.61
11	3000	139	138.84	43	43.00
12	3200	138	135.99	46.3	45.09
13	3400	135	132.33	48	46.86
14	3600	129	128.13	48.8	48.34
15	3800	123	123.67	49.1	49.50
16	4000	118	119.22	49.6	50.36
17	4200	115	115.05	50.6	50.92

where:  $M_s$  – values of actual engine torque,  $M_{s\ theor}$  – theoretical engine torque,  $N_e$  – actual engine power output,  $N_{etheor}$  – theoretical engine power output.

The next stage of the test it was made selection of parameters characterizing the vehicle and preparation of a traction graph based on the given above theoretical characteristic of the engine torque and its values from table 1.

## VEHICLE DATA

Below in table 2 the basic parameters that describe the vehicle were included.

Table 2. Basic data of the vehicle

Symbol	Value	Unit	where:
$Q$	19325.70	[N]	vehicle weight
$f$	0.012	-	rolling resistance coefficient
$c_x$	0.3	-	air resistance coefficient
$\gamma_p$	0.9	-	filling factor
$B$	1.578	[m]	vehicle width
$H$	1.54	[m]	vehicle height
$A$	2.19	[m <sup>2</sup> ]	vehicle end face area
$\eta$	0.9	-	propulsive system mechanical efficiency
$r_k$	0.27	[m]	wheel kinematic radius

Basic assumptions for selecting values for the vehicle data:

- it was assumed that the vehicle was fully loaded, hence its weight ( $Q$ ),

- the value of the rolling resistance coefficient  $f$  was adopted as for a surface similar to smooth asphalt,
- the value of the air resistance coefficient  $c_x$  was adopted as for a Fiat Panda car,
- the value of the filling factor  $\gamma_p$  was adopted as for motor cars,
- the values of the width and height of the car were adopted as for a Fiat Panda, version 4x2 Van,
- the vehicle end face area was calculated based on the dependence  $A = \gamma_p HB$ ,
- the value of the propulsive system mechanical efficiency was adopted as for motor cars,
- the wheel kinematic radius resulted from the tire size (at pressure recommended by the producer) and the ring, with consideration of static loads.

Table 3. Basic ratios of gearbox C514R and the final drive [18]

I gear	3.909
II gear	2.158
III gear	1.345
IV gear	0.974
V gear	0.766
Reverse gear	3.818
Final drive	3.438

### TRACTION CHARACTERISTIC OF THE CAR

Traction characteristic of the car was the dependence between the propelling force on the car wheels on its linear speed. The propelling force on the car wheels was calculated with the formula [12]:

$$F_N = (M_{s\ theor} \cdot i_{UN} \cdot \eta_{UN}) / r_k \quad (1)$$

where:

$F_N$  – propelling force [N],

$M_{s\ theor}$  – theoretical engine torque (value according to the trend curve) [Nm],

$i_{UN}$  – ratio of propelling system,

$\eta_{UN}$  – mechanical efficiency of propelling system,

$r_k$  – wheel kinematic radius [m].

Ratio of propelling system was described by dependence [12]:

$$i_{UN} = i_{PG} \cdot i_{SB} \cdot i_{SP} \quad (2)$$

where:

$i_{PG}$  – final drive ratio (permanent ratio),

$i_{SB}$  – ratio of the actual gear of the gearbox the car is driving at (selectable ratio),

$i_{SP}$  – ratio of the clutch.

It was adopted the value of ratio of full – switched clutch and it was matched 1.

The car velocity was described with the dependence [12]:

$$V=(2 \pi n_s r_k) / (60 i_{UV}), \quad (3)$$

where:

$V$  – car linear velocity [m/s],

$n_s$  – engine rotational speed [ $\text{min}^{-1}$ ].

Then was made a modification of units from [m/s] to [km/h] and formula which describe velocity of the vehicle were presented:

$$V=(2 \pi n_s r_k) / (60 i_{UV}) \quad 3,6. \quad (4)$$

The values of the propelling force and the linear velocity were calculated for five gears. The reverse gear was not taken into account.

On the graph it was shown the vehicle motion resistances, i.e. rolling resistance, air resistance and grade resistance. The resistance curves were drawn based on dependences available in the literature [1,4,8,12,14].

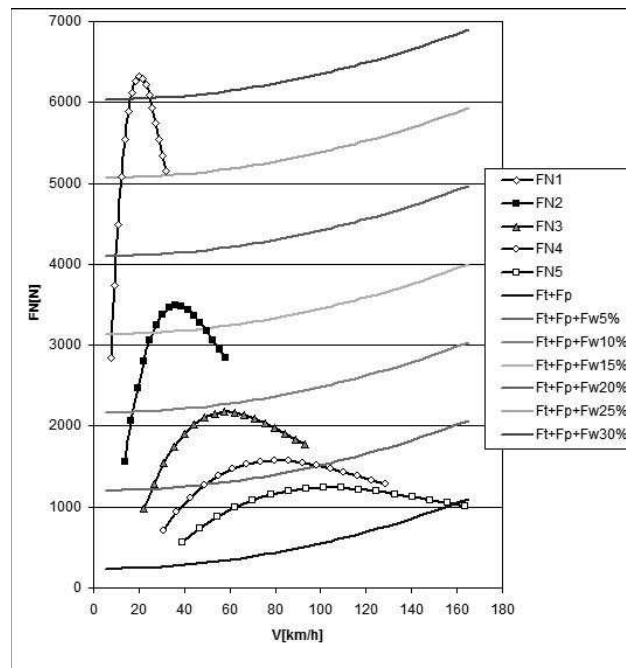


Fig.3. Traction graph of a Fiat Panda car equipped with a 1.3 JTD engine  
 FN1, FN2, FN3, FN4, FN5 – propelling force for the subsequent gears: 1, 2, 3, 4, 5;  
 Ft – rolling resistances; Fp – air resistance; Fw% – grade resistance  
 (e.g. Fw 5% – grade resistance at a 5% slope)



## RESULTS

Below it was gathered the results of the research:

- a) maximum velocity of the vehicle: 155 km/h,
- b) maximum propelling and acceleration forces at individual gears:

Table 4. Maximum propelling forces and accelerations at individual gears

	$FN_{max}$ [N]	$a$ [m/s <sup>2</sup> ]
gear 1	6318.28	3.21
gear 2	3488.07	1.77
gear 3	2173.98	1.10
gear 4	1574.32	0.80
gear 5	1238.12	0.63

where:  $FN_{max}$  – maximum value of propelling force at the given gear,  $a$  – maximum value of acceleration at the given gear

- c) ability to overcome the hills at gears 1, 2, 3 and 4:
  - steepest hill possible to overcome at gear 1: 30 %,
  - steepest hill possible to overcome at gear 2: 15 %,
  - steepest hill possible to overcome at gear 3: 5%,
  - steepest hill possible to overcome at gear 4: 5%.

## CONCLUSIONS

Considering the fact that it was not a profession car, its maximum velocity (155 km/h) was of a satisfactory level. Apart from the engine and propelling system design, that was strongly attributed to the aerodynamics of the vehicle. The air resistance factor had been effectively reduced throughout the years, thanks to which the car had been achieving higher and higher maximum speeds and using less and less fuel.

The ability to overcome a 30 % slope when fully loaded proved the good selection of the transmission ratio of gear 1 and utilization of the torque characteristics.

Acceleration values achieved at the other gears were important too, whereas the first selectable transmission had a high value.

It its worth consideration if it were not good to have the ratios of gears 2 and 3 increased slightly. This could make the car able to overcome steeper elevations at these gears and to achieve a better acceleration. Particularly, increasing the gear 3 ratio would make sense, as in urban traffic this gear is used most frequently.

On the other hand, increased ratios of gears 2 and 3 would result in increased fuel consumption while driving at them. That would entail a general increase of fuel consumption, and thus a higher emission of exhaust gases.

To sum up, in the view of the then ecology and economy, the engine and propelling system design should be qualified as good. Traction characteristics of the car result from its intended use.

## REFERENCES

1. Arczyński S.: Mechanika ruchu samochodu. Warsaw, WNT 1994. p. 45-64, 92-104.
2. Bogdański J.R.: Hamownia podwoziowa – kompendium wiedzy minimalnej cd. Auto Moto Serwis. No 10/2002. Wydawnictwo Instalator Polski. Warsaw 2002.
3. Bogdański J.R.: Ile koni „pod maską”? Auto Moto Serwis. No 6/2004. Wydawnictwo Instalator Polski. Warsaw 2004.
4. Dębicki M.: Teoria samochodu. Teoria napędu. WNT. Warsaw 1976. p. 19-27, 45-60, 106-120, 161-172.
5. Hozer J. red.: Statystyka. Katedra Ekonometrii i Statystyki Wydziału Nauk Ekonomicznych i Zarządzania Uniwersytetu Szczecińskiego. Szczecin 1998. p. 187-201.
6. Kijewski J.: Silniki spalinowe. WSiP Warsaw 1997. p.81-85.
7. Lisowski M.: Ocena własności trakcyjnych samochodu Jelcz 317 wyposażonego w silnik SW-680 z różnymi systemami doładowania. MOTROL. Lublin 1999.
8. Lisowski M.: Teoria ruchu samochodu. Teoria napędu. Politechnika Szczecińska. Szczecin 2003. p. 8-13, 17-19, 43-47, 64-67.
9. Luft S.: Podstawy budowy silników. WKiŁ. Warsaw 2006. p.45-46.
10. Mysłowski J.: Ocena własności eksploatacyjnych silników wysokoprężnych na podstawie jednostkowego zużycia paliwa. Praca doktorska. Szczecin 2005. p.18-26.
11. Mysłowski J., Mysłowski J.: Tendencje rozwojowe silników spalinowych o zapłonie samoczynnym. Wyd. AUTOBUSY. Radom 2006. p.70-77.
12. Prochowski L.: Mechanika ruchu. WKiŁ. Warszawa 2007.
13. Siłka W.: Energochłonność ruchu samochodu. WNT. Warszawa 1997. p.28-36.
14. Siłka W.: Teoria ruchu samochodu. WNT. Warszawa 2002. p.53-144.
15. Ubysz A.: Teoria trakcyjnych silników spalinowych. Politechnika Śląska. Gliwice 1991. p.203-210.
16. Wajand J. A., Wajand J. T.: Tłokowe silniki spalinowe. WNT. Warsaw 2005. p.159-162.
17. Zając P., Kołodziejczyk L. M.: Silniki spalinowe. WSiP. Warsaw 2001. p.108-114.
18. Zembowicz J.: Fiat Panda. WKiŁ. Warsaw 2005. p.12, 50-51, 136-138.
19. Instrukcja obsługi panelu mocy. Automex. Gdańsk 2007.
20. Instrukcja obsługi modułu programatora AMX 211. Automex. Gdańsk 2007.

### WŁASNOŚCI TRAKCYJNE SAMOCHODU FIAT PANDA WYPOSAŻONEGO W SILNIK 1,3 16 V MULTIJET

**Streszczenie.** W artykule przedstawiono własności trakcyjne samochodu Fiat Panda wyposażonego w silnik 1,3 16 V Multijet. Wykonano charakterystykę pełnej mocy silnika 1,3 JTD wraz z doborem krzywych trendu. Na podstawie krzywej momentu z tego wykresu oraz podstawowych danych pojazdu wyznaczono charakterystykę trakcyjną pojazdu. Była to zależność siły napędowej od prędkości liniowej pojazdu. Na jej podstawie analizowano własności trakcyjne pojazdu Fiat Panda, takie jak: zdolność przyspieszania, możliwość pokonywania wzniesień oraz uzyskiwanie maksymalnej prędkości.

**Słowa kluczowe:** własności trakcyjne pojazdu, teoria ruchu, silniki spalinowe, charakterystyka zewnętrzna silnika.

## APPLICATION OF MODERN ECOLOGICAL TECHNOLOGY LOST FOAM FOR THE IMPLEMENTATION OF MACHINERY

Aleksander Karwiński, Zdzisław Żółkiewicz

Foundry Research Institute In Cracow ul. Zakopiańska 73, Poland, kzs@iod.krakow.pl

**Summary.** At Królmet Iron Foundry some research and experimental studies have been carried out to develop technical and technological guidelines for the manufacture of pilot castings for machinery applications. The castings should be characterised by good mechanical properties, specially by good hardness, high abrasion wear resistance and impact resistance. Pilot castings have been made by lost foam technology on a modern casting installation. The output of the research and experimental work was designing and making of pattern tooling, determination of technical and technological parameters of the process, and making a batch of pilot castings. The produced castings had the required utilisation parameters.

**Key words:** casting, pattern, pattern made of foamed polystyrene, evaporation.

### INTRODUCTION

In the full form of model polystyrene, which fills a cavity forms in the course of its filling by the liquid metal is subjected to the influence of high temperature, passes from the solid through the liquid state, the gaseous state. Emit solid and gaseous products of thermal decomposition of polystyrene patterns. The kinetics of this process is significantly influenced by the gasification temperature, density and mass of the polystyrene patterns. One of the basic parameters is the amount and rate of gasses from the model polystyrene during its thermal decomposition. To ensure optimal conditions for obtaining a cast of the assumed shape and quality shall be the main characteristic parameters of the model making process, especially the chemical composition and density of the model. For the experimental trials were chosen cast rotor D8 - 11 / 2 (Figure 6). Models were made of polystyrene by Marbet. Were selected material pattern, its density, a method of forming and removing the model from the mold. Specified properties of polystyrene and a layer of ceramic used to do castings.

In order to reduce the maximum volume of gas separated in the process of gasification of the pattern assumes a constant density of  $20 \pm 2$  kg/m<sup>3</sup>. Elements of the pattern: in the matrix will be made and then combined into sets of pattern.

Forming and pouring implemented by the following scheme: the preparation of pattern → incorporate a ceramic layer → drying molding sand in a box of sand compaction → creating a vacuum in the form of flooding → spiking cooling.

Made pattern kits, parts, flooding the form shown in Figure 6.

### PROPERTY RESEARCH CERAMIC LAYER

Prior to research conducted tests of the ceramic layer including strength, permeability. Layers were studied by the manufacturer company and a film developed at the Foundry Research Institute. The results are shown in Figures 1, 2, 3. Developed liquid ceramic mass were checked for their rheological properties. These studies used rotational viscometer Bohlin Visco V88 manufactured by Bohlin Instruments Ltd. This is a rheometer with coaxial cylinders. Outer cylinder is stationary and is driven by an internal synchronous motor. The accuracy of measurements is - 3%.

The measurements are based on measuring the shear stress at a certain shear rate. Rheometer is controlled by a computer to analyze the results of the measurements used a computer program used to estimate the rheological parameters studied liquid adhesives and ceramic. The computer program also makes the necessary assessment of the quality estimation.

For the preparation of a liquid ceramic body used to ensure a small mixer agitator rotational speed (up to tens of revolutions per minute). To manufacturing molds - ceramic layer is used to cover:

- Disopast 4805,
- Kernrtop L87,
- Cyrkonar.

The measurements are based on measuring the shear stress at a certain shear rate. Rheometer is controlled by a computer to analyze the results of the measurements used a computer program used to estimate the rheological parameters studied liquid adhesives and ceramic. The computer program also makes the necessary assessment of the quality estimation.

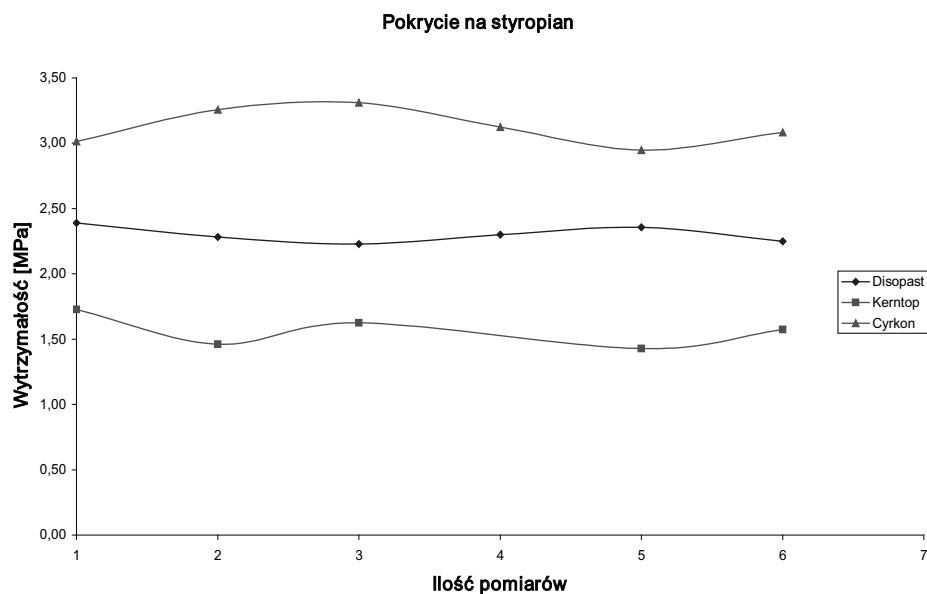


Fig. 1. Tensile strength for different layers of coverings

Such preliminary results of the technology resulted in the need to work on the development of the composition of the ceramic coating.

For oral liquid ceramic coating used to model the components used polystyrene similar to the method of lost wax models:

- as a solvent for adhesives - water,
- binder - colloidal silica - Sizol A30,
- composition, and butadiene latexes politetrafluoroetylenowego - sterynowego,
- composition of surfactants - anionic and nonionic active,
- an anti-foaming,
- meal ceramic refractory material - silicate or aluminosilicate molochite'u zirconia.

For test configurations to cover for serum resistance to tearing the thin ceramic layer and its permeability (Fig. 2, 3 and 4).

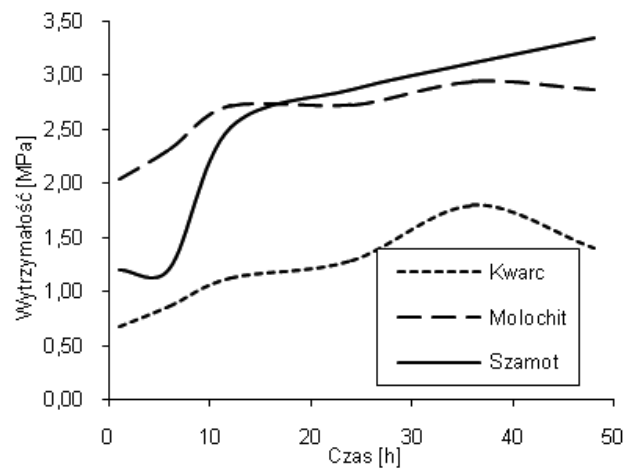


Fig. 2. Strength of thin ceramic layers made with different materials (raw sample) as a function of time

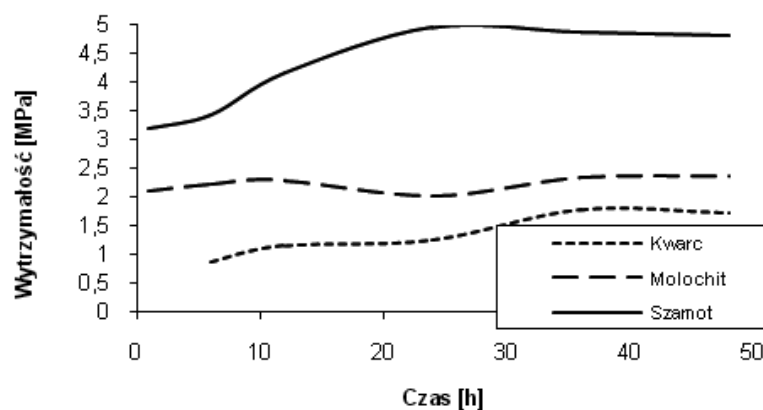


Fig. 3. Strength of thin ceramic layers made with different materials (sample annealed at 900°C) as a function of time

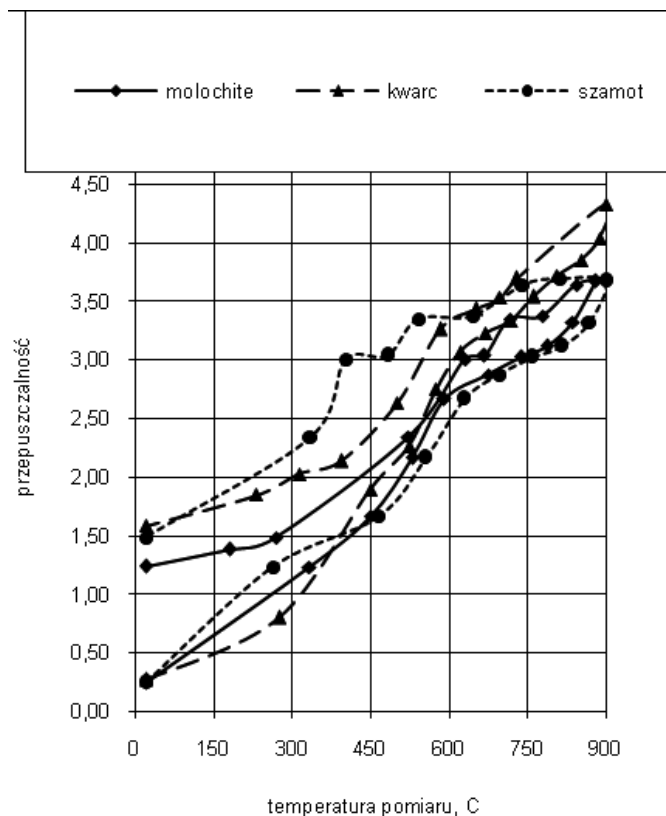


Fig. 4. Measuring changes in the permeability of the porcelain samples with different ceramic material used with changes in temperature

#### EXECUTION POLYSTYRENE PATTERN

For the production of cast pattern of different shapes and sizes of polystyrene is a property expansion at elevated temperatures. Properties of foamed polystyrene products depend on the species of the starting material and method of production. The most characteristic properties should include a very low density 15-60 kg/m<sup>3</sup>, and a low coefficient of thermal conductivity of about 0,024 kcal / m °C h.

Foaming polystyrene conducted preliminary and secondary treatment in an autoclave with bringing superheated steam at design pressure and temperature. It was found that the initial foaming time was dependent on the type of polystyrene. This time depends on the type of polystyrene, shape and weight of the pattern. The density of polystyrene made pattern ranged from 20 to 24 kg/m<sup>3</sup>.

An important factor influencing the process of pouring liquid metal form is a pattern of the gasification kinetics of polystyrene. During the process of flooding under the influence of temperature of molten metal followed by thermal gasification of the polystyrene pattern. In the cavity mold, emit gases. Volume dedicated gas depends on temperature and the pressure from the gas permeable form. The pressure directly affects the flow rate of the metal. In order to learn these parameters

were carried out tests to determine the kinetics of gasification of the experimental pattern. Sample results are shown in Figures 5, 6 and Table 1. With the increase of temperature increases the volume of released gases and gasification time is reduced.

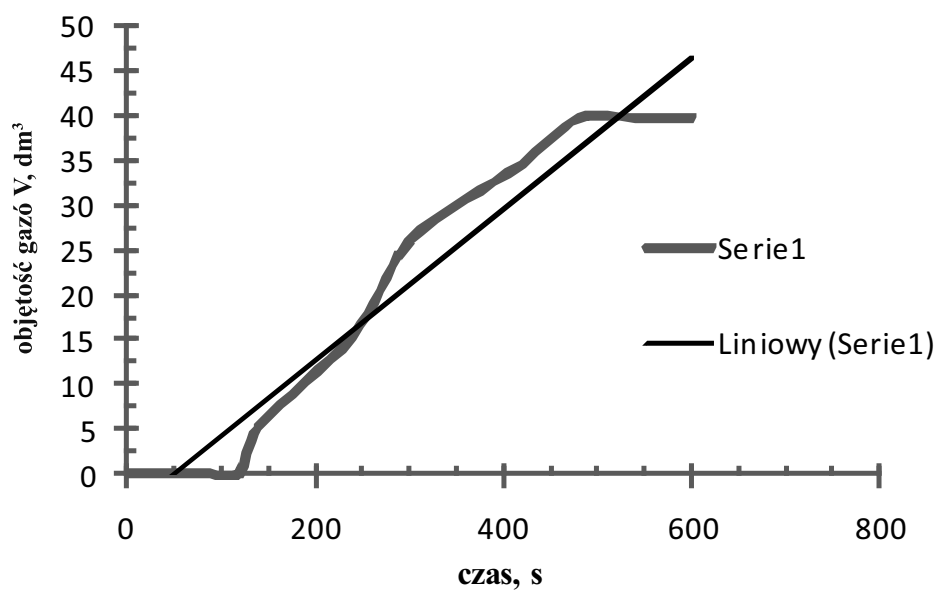


Fig. 5. The volume of gas separated from the EPS pattern, with a mass of 1 g at 400 °C, depending on the time, the density 20 kg / m<sup>3</sup> - Series 1

Table 1. The results of polystyrene

Property	Species polystyrene		
	Owipian 0308	Styrocell L830-3A	Styrocell L930-A
Relative viscosity $\eta$	1,81	1,94	2,17
Pentane content [%] according to the manufacturer's data	5,0	6,0	6,0
Pentane content [%] according to research	4,68	3,05	2,98
Ash content [%]	0,56	0,10	0,10

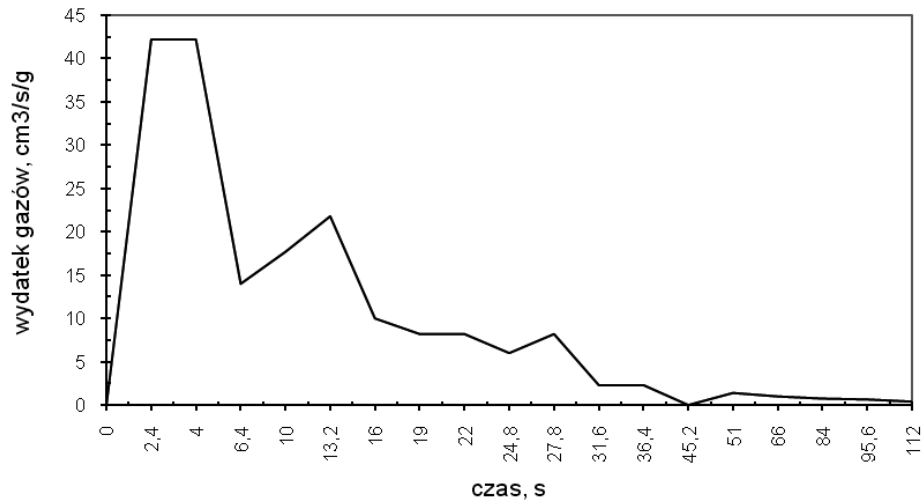


Fig. 6. Gas volume evolved from 1 g of the polystyrene pattern of 23 kg/m<sup>3</sup> density in function of time

The work undertaken was carried out measurements of compressive strength and tensile test samples cut from the models. The measurement was carried out in accordance with PN-B-20130. Results were as follows:

- compressive strength of 93 to 105 kPa,
- tensile strength of 115 to 140 kPa.

#### TECHNICAL IMPLEMENTATION OF TEST CASTINGS

The foundry KRÓLMET by heat EPS models, a series of experimental casting of rotor (Fig. 7, 8 and 9). Castings made of iron alloy.

During the study determined the optimal technological parameters of the process

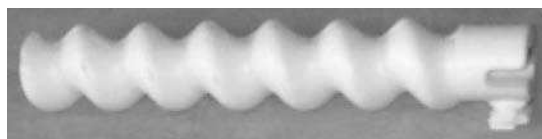


Fig. 7. Polystyrene pattern



a b



Fig. 8. Pilot castings, a - set of polystyrene patterns, b -in raw condition after pouring

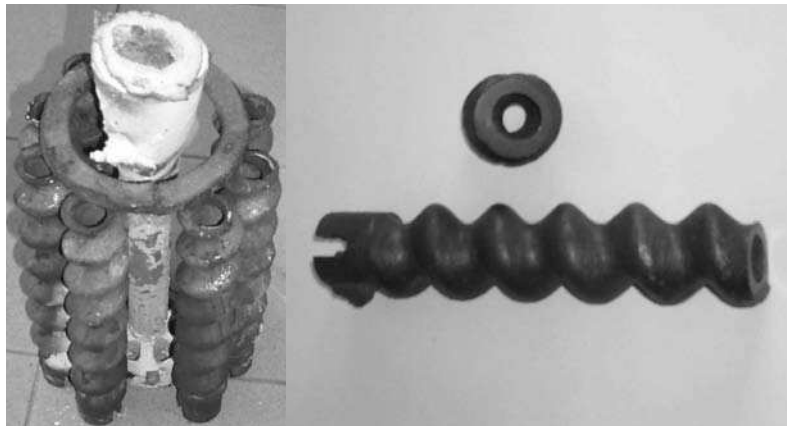


Fig. 9. Experimental rotor castings

## CONCLUSIONS

As a result of experimental research can be concluded that the technology of heat EPS pattern, in foundry castings Królmet you can do:

- With complex shapes,
- The cavities and holes,
- About the thickness of the casting below 10 mm,
- Cast alloy,
- Casting of high hardness above 40 HRC,

## REFERENCES

1. Karwiński A., Żółkiewicz Z., Żółkiewicz M., Król S.: Wykorzystanie technologii modeli cieplnie zgazowywanych do wykonania odlewów stosowanych w geotechnice. Archives of Foundry, 2006, rocznik 6, nr 18 ref. 120/18 s.225 I.
2. Karwiński A., Żółkiewicz Z., Żółkiewicz M., Król S.: „Ökologische und Ökonomische Aspekte des Einsatzes von LOST FOAM-Verfahren Statt des Wachsauerschmelzverfahrens ” Moulding Materials and Cost Reductions for Casting, 2005 Milovy, Czechy, s. 165 – 170, ISBN 80-02-01725-0.
3. Karwiński A., Żółkiewicz Z., Król S.: „Z.: „Application of the Evaporative Pattern Process in Making cast tools for Parts of Construction Machines”. Archives of Foundry - Archiwum Odlewnictwa 2004, rocznik 4, nr 11 ref. 33/11 s. 242 - 247.
4. Pirowski Z., Gościński M.: Construction and technology of production of casted shares for rotating and fird ploughs, TEKA, 2009, V. IX s.231-239 Lublin. PAN Lublin.
5. Pysz S., Karwiński A., Czekaj Cz.: An analyysis of the technical state of a stater Rusing the hall efekt-part II, TEKA , 2009, V. IX s.251-258Lublin. PAN Lublin.
6. Żółkiewicz Z., Żółkiewicz M.: Pattern evaporation process. Archives of Foundry Engineering Issue1, January-March 2007, V. 7, s. 49-52.
7. Żółkiewicz Z., Żółkiewicz M.: Characteristic properties of materials for evaporative patterns. Archives of Foundry Engineering V. 10, Special Issue, 2010, nr 3, s. 289-292.
8. Żółkiewicz Z.: Influence of Thermal Gasification of the Polystyrene Pattern on the Casting Surface. Archives of Foundry - Archiwum Odlewnictwa 2004, t 4, nr 11, s. 332 – 33.
9. Zdzisław Żółkiewicz, Marek Żółkiewicz, LOST FOAM PROCESS – THE CHANCE FOR INDUSTRY. TEKA , 2009, V. IX s.431-436 Lublin. PAN Lublin.
10. Żółkiewicz Z., Karwiński A., Żółkiewicz M., Pirowski Z., Uhl W., Stefański Z., Madej W., Krawiarz J.: „Trial Manufacture by the Lost Foam Process of Pilot Castings of High Abrasion Resistance Plates”, БИХИК Т. 1, 4. 2007 том 1 i 2 (94), s. 192. Chmielnicki 2007, zezwolenie Ministerstwa Ukrainy seria KB Nr 9722 , BAK Nr 2/2006.
11. Karwiński A., Pysz S., Krokosz J.: Komputerowe projektowanie procesu wykonania odlewów dla motoryzacji przy zastosowaniu nowej generacji ciekłych mas ceramicznych – V Międzynarodowa Konferencja „Motoryzacja i Energetyka Rolnictwa” MOTROL ‘2005, Odessa, Ukraina, 5 – 9 wrzesień 2005 – ISSN 1730-8658.
12. Karwiński A., Haratym R., Żółkiewicz Z.: Określenie zastosowania modeli zgazowywanych do wykonania odlewów precyzyjnych, MOTROL 2009, Komisja Motoryzacji i Energetyki PAN, tom 11, str. 97 – 103, Lublin 2009, ISSN 1730-8658.
13. Pysz S., Karwiński A., Czekaj E.: An Analysis and Comparison of Properties of Al-Si Alloy Automotive Castings Made by Rapid Prototyping and Standard Lot Production, Commission of Motorization and Power Industry Polish Academy of Science Branch in Lublin, TEKA, vol. IX, p. 251 – 258, Lublin 2009, ISSN 1641-7739.

**Scientific funded with centres on science work in summers 2009 – 2012 as investigative project No. N N507 270736**

## ZASTOSOWANIE NOWOCZESNEJ EKOLOGICZNEJ TECHNOLOGII LOST FOAM DO WYKONANIA CZĘŚCI MASZYN

**Streszczenie.** W odlewni żeliwa KRÓLMET w Zawierciu przeprowadzono prace badawczo doświadczalne związane z opracowaniem założeń techniczno technologicznych do produkcji odlewów części maszyn przy zastosowaniu metody zgazowanych modeli. Odlewy te charakteryzują się dobrymi właściwościami mechanicznymi, zwłaszcza twardością, odpornością na ścieranie i udarnością. Badania przeprowadzono w Instytucie Odlewnictwa a próby techniczne przeprowadzono w zmodernizowanym gnieździe odlewni KRÓLMET. W wyniku przeprowadzonych prac badawczych zoptymalizowano właściwości materiałów stosowanych w tej technologii oraz wykonano serię doświadczalnych odlewów. Otrzymano odlewy o założonych parametrach użytkowych.

**Słowa kluczowe:** technologia pełnej formy, odlewy, parametry.

## ANALYSIS OF WATER-WATER TYPE HEAT PUMP OPERATION IN A BUILDING OBJECT

Jarosław Knaga, Tomasz Szul

Department of Power Engineering and Agricultural Processes Automation,  
Agricultural University of Cracow, Balicka Str. 116B, 30-149 Kraków, Poland

**Summary.** The paper presents operation examination results of a heating system equipped with a heat pump, manufactured by the Sekut company, equipped with a scroll type compressor. The performed statistical analysis has shown a significant influence of external temperature and heat transfer coefficient to the COP value. Within the analysed period, the COP maintained a level of 2.6 at an average monthly temperature of  $-6^{\circ}\text{C}$ , with a transfer coefficient of 15%.

**Key words:** heating system, heat pump, operational effectiveness, central heating, hot domestic water.

Membership in the European Union obligates Poland to significantly increase the share of energy harvested from renewable sources in total consumption, which, in fact, is included within the scope of the so-called EU (3x20) climate package. It is assumed that by 2020, the European Union as the whole shall emit 20% less  $\text{CO}_2$ , the effectiveness of electric energy consumption shall increase by 20% and the share in the renewable energy sources (including those that use heat from low-temperature sources) within the energy balance shall also be 20%.

Use of heat pumps for heating purposes is one of the methods of harvesting renewable energy from natural the environment. A heat pump is a device using low-temperature and waste heat for heating, venting and preparation of hot domestic water. Its basic role consists in drawing heat from a source of lower temperature (bottom) and transferring in to a source of higher temperature (top). This process requires energy to be provided from outside [Zalewski 2001]. The ratio of thermal energy for heating to the work provided from outside is the measure of the heat efficiency of the device and is identified by the COP (Coefficient of Performance). It is desirable for that coefficient to be as high as possible.

The Decision of the Commission 2007/742/EC specifies the energy and ecology criteria that should be met by heat pumps. It provides minimum values of the COP that should consider the energy consumption value by the circulating pumps of bottom and top source of heat and introduces an additional coefficient for seasonal operational effectiveness. A heat pump may be considered to be a device that uses a renewable energy source if the final energy gain significantly exceeds the quantity of energy necessary to drive the pump. Significantly means that the assessed coefficient of the seasonal thermal (heating) efficiency of an SPF heat pump must meet the following requirements stated in Directive 2009/28/EC (1):

$$SPF > 1,15 \cdot \frac{1}{\eta}, \quad (1)$$

where:

*SPF* – seasonal performance factor of the heat pump,

$\eta$  – ratio of the total production of electric energy to the value of primary energy consumption within the whole European Union (acc. to Eurostat  $\eta=0.4$ ),

1.15 – effectiveness of electric energy consumption by final user.

Presently, the heat pump seasonal performance factor should be at least 2.87.

Manufacturers and distributors of heat pumps, as a rule, give the theoretical value of the COP determined under laboratory conditions for accurately specified parameters of bottom and top source temperatures at a given thermal load of the system. The value of such given coefficient does not take into consideration energy consumption by auxiliary devices. This is why, in order to specify the actual effectiveness of a heat pump, it is necessary to perform operational examinations [Knaga 2008, 2009, Kołaczkowski 2004, Skonieczna, Ciesielczyk 2009] that would enable determining the seasonal performance factor of the system under real conditions and the influence of different external parameters to this value.

## OBJECTIVE

The objective of the paper was to perform initial examinations of the operational nature of a water-water type compressor heat pump, which would allow one to determine the size and specify the variability of energy effectiveness of the heating system based on this type of heat pump in a real building object. The obtained examination results were used to develop the characteristics describing the energy effectiveness variability of the heating system.

## SUBJECT AND METHODOLOGY OF EXAMINATIONS

The subject of examinations was a newly built residential building with a total area of 157 m<sup>2</sup> and a cubage of 625 m<sup>3</sup>. The heated part of the building represents 55% of the total area, i.e. 86m<sup>2</sup>. This is a one floor building with a usable attic and a cellar under a part of the building. It is a wooden structure made of solid balk. Balks are placed on each other in a horizontal plane with insulation material between them made of wooden tow. The heating system of the building is based on the water-water type compressor heat pump that cooperates with central floor heating. Hot domestic water (h.d.w.) is prepared in the dispenser system with a volume of 250 m<sup>3</sup>, where the water is heated using a preliminary system of superheated steam cooling before the heat pump condenser (top source of heat). The bottom heat source is water drawn from an infiltration well with a depth of 4 m, where the water table is 1.5 m below the grade level. The temperature of the bottom source within the examined period was 9°C±0.5°C; thus for further analysis, its value is assumed to be constant. The heat pump selected for the examination, with a power rating of 11 kW on the heating side, with a Scroll type compressor, was manufactured by the Sekut company and was equipped with a Vizula control system made by Inveo (this system is a prototype model). The pump uses flat panel exchangers (compact construction) with a power rating of 13 kW. R407 is the cooling agent used in the compressor heat pump. The power of the circulating pump of the top heat source is 180 W and the bottom 370 W. Pt100 paired resistance sensors were used to measure the energy and power of the top heat source, and Pt100 and Pt500 sensors were used to measure the temperature at other points. The flow rate of the operating agent in the top and bottom source was measured by

a water meter with a GMDX-R type pulse transmitter, and the quantity of consumed hot water was measured by a single-flux water meter equipped with a GSD8-45R type pulse sensor, whereas the pulse value in the above mentioned flow meters, regardless of the type, was  $1\text{ dm}^3$ . Consumption of electric energy was measured by the LE-03 type pulse active energy counter within the first accuracy class. The measurement devices used meet the quality requirements of the laboratory examinations. The system operation parameters were read and recorded by the Visula operator's panel equipped with RS-232, RS-485, CAN interfaces and remote Ethernet communication.

At this stage, the paper was limited to determine the quantity of heat transferred to the object to cover the losses on penetration and ventilation and to prepare h.d.w. Electric energy consumption by the compressor and auxiliary devices, such as circulating pumps of bottom and top source and control system was monitored together with measurement of thermal comfort parameters indoors and the outside temperature. The quantity of heat given up to the object by the compressor heat pump was calculated based on dependence (2):

$$Q = \frac{1}{3,6} \int_{V_1}^{V_2} \rho \cdot c_w \cdot (t_{wej} - t_{wyj}) dV, \quad (2)$$

where:

$Q$  – heat [kWh],

$dV$  – change of the flowing operating medium volume [ $\text{dm}^3$ ],

$\rho$  – density of the operating medium [ $\text{kg} \cdot \text{dm}^{-3}$ ],

$c_w$  – specific heat of the operating medium [ $\text{MJ} \cdot (\text{kg} \cdot \text{deg})^{-1}$ ],

$t_{wej}$  – temperature at inlet to the system c.o. [ $^{\circ}\text{C}$ ],

$t_{wyj}$  – temperature at outlet from the system c.o. [ $^{\circ}\text{C}$ ].

Dependence (2) was also used to calculate the quantity of heat for preparation of h.d.w. The quantity of heat determined in dependence (2) referred to the sampling period and recording of data by the control and measurement system. The sampling frequency was established arbitrarily at a level of 1/60 Hz and resulted mostly from the significant inertia of the observed phenomena. The determined heat was subsequently compiled for 24 hours. The daily volume of heat supplied by a pump determined this way was used to specify the COP (3) of this heating device:

$$COP = \frac{Q_{CO24} + Q_{cww24}}{E_{tot}}, \quad (3)$$

where:  $COP$  – coefficient of performance of the heat pump,

$Q_{CO24}$  – heat given up by the heat pump to the central heating system within 24 hours [kWh],

$Q_{cww24}$  – heat given up by the heat pump to the h.d.w. system within 24 hours [kWh],

$E_{tot}$  – electric energy consumed by the compressor, circulating pumps and the control system of heat pump operation [kWh].

Analysis of operation of the compressor heat pump in the examined research object, at this stage, was limited to one month that was characterized by the highest variability of external temperature during the season. During the current heating season, this month was February. Calculations were performed using Excel and Statistica software, and all statistical hypotheses were verified at a level of significance of  $\alpha = 0.05$ .

## EXAMINATION RESULTS

The analysis of operation of the heat pump in the single family building was performed within one month characterized by the highest dynamics of external temperature variability within the heating season 2010/11. The graph (Fig. 1) presents the course of external and internal temperature variations in the residential building. The graph shows two points where the internal temperature significantly deviates from the set temperature (preferred by the user, i.e. 20°C). Point B shows a considerable drop of the internal temperature to 15°C, which was caused by a pump shut down due to pump failure at the bottom source. However, a deviation in point A amounting  $\pm 1.6^\circ\text{C}$  is related to a sudden change of external temperature.

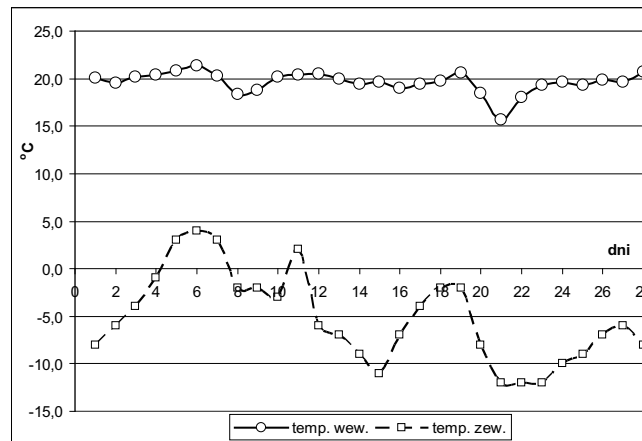


Fig. 1. Course of internal and external temperature changes within the analysed period

Energy characteristics were prepared for the analysed building based on the standard PN-EN 13790 [Decree of the Minister of Infrastructure 2008, Szul 2009]. This enabled theoretical determination of heat demand within individual days of the analysed month, considering the heating ( $Q_{co}$ ) and preparation of hot domestic water ( $Q_{cwu}$ ) [Trojanowska, Szul 2006]. The theoretical values were then compared with the values of actual heat consumption determined based on the measurements. Fig. 2 presents the comparable analysis results for preparation of hot domestic water. The apparent high amplitude of changes of actual heat demand for h.d.w. is the result of the variable nature of hot water consumption by the users. However, within the monthly balance, actual consumption of energy for h.d.w. only exceeds 5% of the calculated demand (Fig. 2).

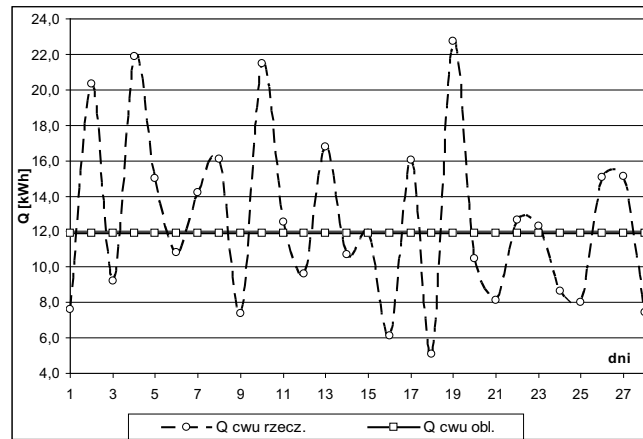


Fig. 2. Course of changes of actual and calculation heat consumption for preparation of hot domestic water

A similar analysis of heat demand was performed for the heating system. This allowed us to explain the causes of internal temperature changes in point A (Fig. 1). An increase of internal temperature in the object was caused by priority forcing of h.d.w. heating, which coincided with a sudden increase of external temperature. In spite of the fact that computational heat demand in the building decreases (Fig. 3), the central heating system had to supply heat due to h.d.w. forcing. This resulted in the system going into an intensified over-adjustment in the second phase by an external drop in temperature. After five days, the system returned to balance.

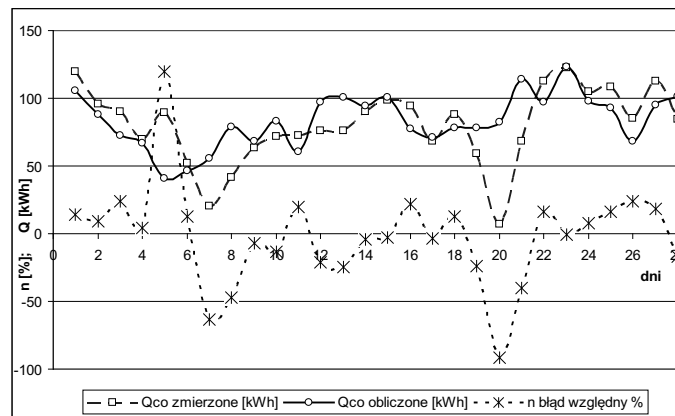


Fig. 3. Course of changes of actual and calculation heat consumption for heating



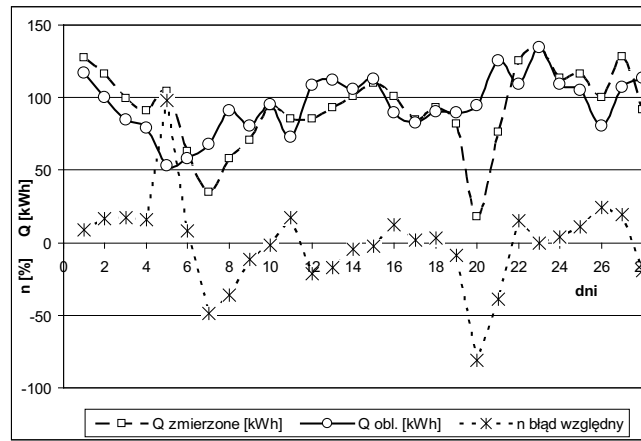


Fig. 4. Course of changes of actual and calculation heat consumption of the building

The course variations of total heat consumption (central heating + hot domestic water) within the analysed period is presented in Fig. 4. The relative error between the calculation and actual heat consumptions in relation to a 24 hour period does not exceed  $\pm 20\%$  (Fig. 4), except in the above described analysed cases. However, within the monthly balance, actual heat consumption is less by almost 3% than the calculated consumption. At this stage, it is safe to say that the heat pump is properly selected for the energy needs of the building and provides continuity of heating supply (except for an emergency case).

In the next stage of examinations, the energy efficiency of the heating system based on the compressor heat pump was specified. This analysis consists in determining the operational COP according to the adopted methodology (dependence 3). Statistical analysis within the basic scope allowed us to determine the factors influencing the COP value.

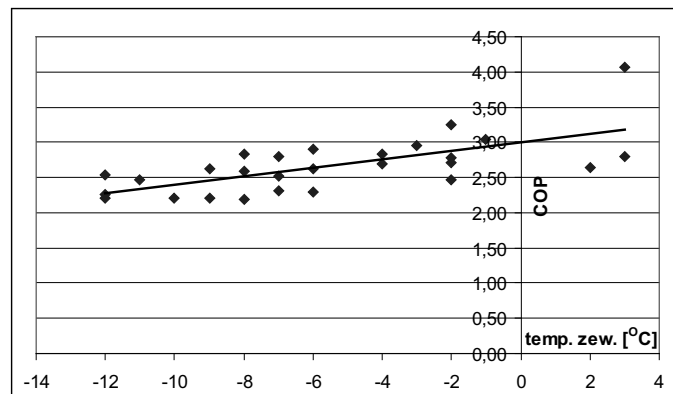


Fig. 5. COP dependence on external temperature

External temperature has a major influence on the COP value. This is described by dependence 4 determined with a determination coefficient of  $R^2$  at a level of 0.42.:

$$COP = 0,054 \cdot t_{zew} + 2,94, \quad (4)$$

where:

$t_{zew}$  – temperature outside the object  $^{\circ}C$ ,

Together with an increase of ambient temperature, the energy effectiveness of the heating system increases as well, and an increase of external temperature to  $10^{\circ}C$  translates to an increase of energy efficiency by 0.54. This effect can be explained by the low thermal inertia of the wooden building for which the time constant determined from the energy characteristics (calculated according to the standard PN – EN 13790) is 26 hours.

Parallel operation of the central heating system and hot domestic water system carried out by the examined heating system forced a coefficient to be determined that specifies the share of energy collected in the h.d.w. system in relation to the energy given up to central heating by the compressor heat pump.

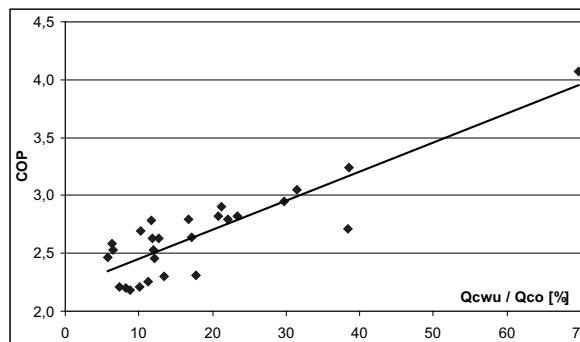


Fig. 6. COP dependence on the heat transfer coefficient

It appeared that this coefficient is closely correlated with the operational energy effectiveness of a heating system equipped with a heat pump. Based on this, dependence (5), which describes the operational effectiveness of the previously determined coefficient, was developed with adjustment of the model to data at a level of 73%:

$$COP = 0,025 \cdot w_{pc} + 2,2, \quad (5)$$

where:

$w_{pc}$  – heat transfer coefficient specified as  $w_{pc} = \frac{Q_{cwu24}}{Q_{co24}}$ ,

$Q_{CO24}$  – heat given up by the heat pump to the central heating system within 24 hours [kWh],

$Q_{cwu24}$  – heat given up by the heat pump to the h.d.w. system within 24 hours [kWh],

From the developed dependence and graph (6), it results that together with the increase of heat transfer coefficient, the energy effectiveness of the examined system increases as well, and it may reach an average value at a level of 3, which, in relation to the effectiveness of the national electric energy generation system, results in electric energy consumption by the final user at a level of 1.2. Moreover, it results from dependence (5) that in the case of a lack of energy consumption

by the h.d.w. system, the operational effectiveness of the heating system shall not drop below 2.2. The maximum value reached by the energy effectiveness of the heating system within the analysed period is 4, and this took place with a high coefficient of  $w_{cp} = 70\%$  and with relatively high external temperature. Due to the above, this point was not rejected at this stage of the analysis. Undoubtedly, further analysis should be performed in the direction of reduction of the operation cycle (activation of heat pump).

## CONCLUSIONS

As a result of the presented monthly analysis of operation, and subsequent determination of the operational energy effectiveness of the heating system based on the compressor heat pump, it can be ascertained that:

1. The heat pump was properly selected to the heating system of the residential building, providing continuity of heating supply within the considered period; this consisted of an energy stable bottom heat source and optimal selection of power for the heat pump.
2. Within the examined period, the average operational effectiveness COP of the entire system was 2.6. This can be acknowledged as good results due to the fact that the system worked at a relatively low average external temperature of  $-6^{\circ}\text{C}$  and a low average heat transfer coefficient of  $w_{cp} = 15\%$ .
3. External temperature significantly influences the energy effectiveness of the system, and together with its increase, the effectiveness increases, too. At an average ambient temperature of  $0^{\circ}\text{C}$ , the energy effectiveness of the heating system is at level 3.
4. At lower temperatures, thermal load of the h.d.w. system should be higher in order to maintain an optimum value of energy effectiveness or a bivalent system of cooling superheated steam should be employed.
5. Further analysis of the system should be performed within the operational cycle range, i.e. from the moment of activation to deactivation of the compressor heat pump. Such analysis would allow for the development of a more effective control system.

## REFERENCES

1. Decyzja Komisji z dnia 9 listopada 2007 r. 2007/742/WE określająca kryteria ekologiczne dotyczące przyznawania wspólnotowego oznakowania ekologicznego pompom ciepła zasilanym elektrycznie, gazowo lub absorpcyjnym pompom ciepła.
2. Directive of 23 April 2009 2009/28/EC OF THE EUROPEAN PARLIAMENT AND THE COUNCIL on the promotion of the use of energy from renewable sources and amending and subsequently.
3. Knaga J. 2008.: Energy efficiency of small compressor assisted air-water type heat pumps. TEKA Komisji Motoryzacji i Energetyki Rolnictwa Vol VIII. Lublin. S. 99-106.
4. Knaga J. 2009.: Efektywność sprężarkowej pompy ciepła powietrze-woda po modernizacji układu kierowniczego dolnego źródła ciepła. Inżynieria Rolnicza 6(115)/2009 s. 141-147.
5. Kołaczkowski B. 2004.: Badania eksploatacyjne pomp ciepła z pionowymi kolektorami grunutowymi. Mechanics / AGH University of Science and Technology T. 23, z. 3, s. 371-380.
6. PN-EN 13790 Energetyczne właściwości użytkowe budynków. Obliczanie zużycia energii do ogrzewania i chłodzenia.

7. Rozporządzenie Ministra Infrastruktury z dnia 6.11.2008 w sprawie metodologii obliczania charakterystyki energetycznej budynku i lokalu mieszkalnego lub części budynku stanowiącej samodzielną całość techniczno-użytkową oraz sposobu sporządzania i wzorów świadectw ich charakterystyki energetycznej. (Dz. U. nr 201, poz. 1240).
8. Skonieczna J., Ciesielczyk W. 2009.: Analiza pracy pomp ciepła z czynnikiem roboczym R407C. *Chemia – czasopismo techniczne*. Zeszyt 4. Wydawnictwo Politechniki Krakowskiej. s. 127-139.
9. Szul T. 2009.: Charakterystyka energetyczna budynków mieszkalnych na terenach wiejskich Polski południowej. *Technika Rolnicza, Ogrodnicza, Leśna* 2/2009. s. 19-21.
10. Trojanowska M., Szul T. 2006.: Modelling of energy demand for heating buildings, heating tap water and cooking in rural households. *TEKA Komisji Motoryzacji i Energetyki Rolnictwa*. Lublin Vol. VIa. s. 184-190.
11. Zalewski W. 2001.: Pompy ciepła sprężarkowe, sorpcyjne i termoelektryczne. IPPU Masta Gdańsk.

#### ANALIZA PRACY POMPY CIEPŁA TYPU WODA-WODA W OBIEKCIE BUDOWLANYM

**Streszczenie.** W opracowaniu przedstawiono wyniki badań eksploatacyjnych systemu grzewczego wyposażonego w pompę ciepła wyprodukowaną przez firmę Sekut ze sprężarką typu scroll. Przeprowadzona analiza statystyczna wykazała istotny wpływ temperatury zewnętrznej, oraz wskaźnika przekazania ciepła na wartość COP. W analizowanym okresie COP kształtowało się na poziomie 2.6 przy średniej miesięcznej temperaturze  $-6^{\circ}\text{C}$  i wskaźniku przekazania 15%.

**Słowa kluczowe:** system grzewczy, pompa ciepła, centralne ogrzewanie, ciepła woda użytkowa.

## MODELLING OF THE THERMAL CYCLE OF SI ENGINE FUELLED BY LIQUID AND GASEOUS FUEL

Arkadiusz Kociszewski

Internal Combustion Engines and Control Engineering  
Czestochowa University of Technology, al. Armii Krajowej 21, 42-201 Czestochowa,  
e-mail: kocisz@imtits.pcz.czyst.pl

**Summary.** Results of numerical analysis of methane and gasoline combustion in SI engine are presented in the paper. Work parameters of engine fuelled by gasoline and methane lean mixtures (excess air factor equals  $\lambda = 1.8$ ) are compared.

**Keywords:** combustion engine, modelling, lean mixture,  $\text{NO}_x$ ,  $\text{CO}_2$ .

### INTRODUCTION

In recent years, air quality has become a particularly severe problem in many countries. Growing concern with exhaust emissions from internal combustion engines has resulted in the implementation of strict emission regulations in many industrial areas such as the Europe and United States. Therefore, how to reduce hazardous emissions and greenhouse gases from engines has now become a research focus.

Improving fuel economy, using a fuel with higher hydrogen to carbon ratio (H/C) or using a renewable fuel can all reduce  $\text{CO}_2$  (greenhouse gas) emissions from engines [1]. Natural gas, which is primarily composed of methane ( $\geq 95\%$  vol. – [2]), is regarded as one of the most promising alternative fuels due to its interesting chemical properties with high H/C ratio and high research octane number (about 120 – [3]). Also, natural gas has relatively wide flammability limits (0.59-1.97 for pure methane – [4]) [1]. The exhaust of natural gas has characteristics such as low  $\text{NO}_x$  and low  $\text{CO}_2$ , natural gas has high potential as a clean energy source [5].  $\text{CO}_2$  and  $\text{NO}_x$  emissions of natural gas engines can be reduced by more than 20% compared with gasoline engines at equal power [1], [6], [7].

Combustion engine researches aimed at reducing of toxic components of exhaust (lean mixtures, alternative fuels) are carried out for many years in the Institute of Internal Combustion Engines and Control Engineering. Carried out are both experimental works and three-dimensional modelling of combustion process, using KIVA-3V and AVL FIRE programs [8-19].

The paper aims at analysis of the methane-air lean mixture combustion in SI engine and comparison of engine work parameters and  $\text{NO}$  (main component of  $\text{NO}_x$ ) and  $\text{CO}_2$  emission with work parameters of engine powered by gasoline as traditional fuel.

## NUMERICAL ANALYSIS OBJECT

The engine model was prepared according to the test engine data. The test engine was designed as the modified single-cylinder, high-pressure S320ER engine, which has been rebuilt in order to apply multipoint spark ignition. The application of multipoint spark ignition in the test engine allowed to fuel the engine with lean mixtures of liquid and gaseous fuels of air excess factor  $\lambda \leq 2.0$ , higher values of air excess factor were not possible to achieve [17], [18]. The main engine parameters are presented in Table 1. The location of spark plugs in the engine head is presented in Figure 1.

Table 1. Main engine parameters

Engine capacity	1810 cm <sup>3</sup>
Number of cylinders	1
Cylinder alignment	horizontal
Cylinder diameter	120 mm
Crank throw	80 mm
Crankshaft length	275 mm
Piston stroke	160 mm
Compression ratio	8.5
Rotational speed	1000 rev/min
Number of spark plugs	8

The numerical modelling was performed in KIVA-3V code [20]. The software is one of the more advanced numerical models, currently used to simulate the combustion process in piston engines. Program allows calculation of three-dimensional flow in the engine chambers of any geometry, including the effects of turbulence and heat exchange with the wall. KIVA-3V is an example of a three-dimensional field model. Combustion process (way and velocity the propagation of flame front) is the result of solving the basic conservation equations, and other dependencies that determine the flow field in the region of the front, the course of chemical reactions of combustion and instantaneous thermodynamic state of the medium. The model is based on solving the equations of conservation of mass, momentum, energy and quantities of ingredients, which describe the unsteady, three-dimensional flow field of chemical reaction (combustion). These equations are three-dimensional Navier-Stokes equations for the compressible fluid mixture. The model calculates separately the thermodynamic state of exhaust gases and the thermodynamic state of the unburned charge. The model calculates the temperature of each area and the average temperature.

The geometric mesh (Figure 1 b)) describing the combustion chamber of the test engine was generated in the pre-processor of KIVA-3V package.

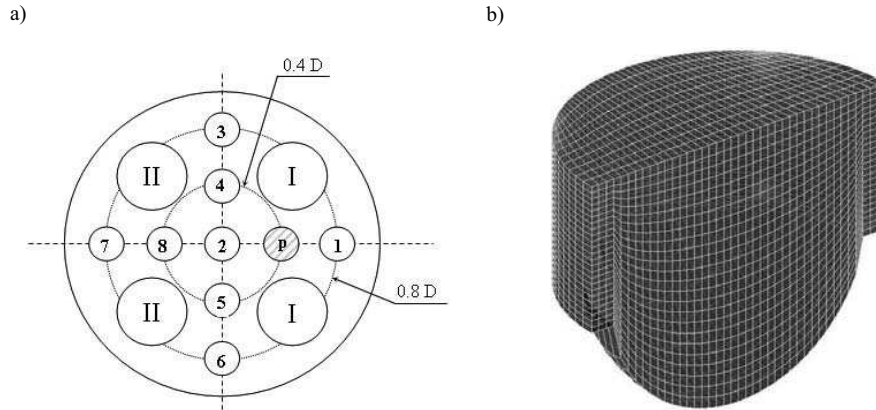


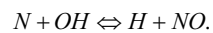
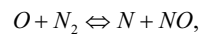
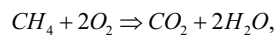
Fig. 1. Spark plug location legend in engine head, (I – inlet valves, II – outlet valves, D – cylinder bore, p – pressure sensor) - Fig. a) and geometric mesh in cartesian co-ordinate system – Fig. b)

## COMBUSTION MODELLING

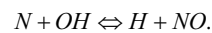
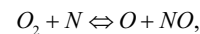
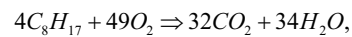
The simulation of combustion process was performed for lean mixtures of gaseous fuel (methane) and gasoline with air, for air excess factor values  $\lambda = 1.8$  for central spark plug no 2 (Fig. 1 a). The ignition advance angle was set to  $12^\circ$  CA before TDC for both fuels. Those parameters were derived from earlier numerical and experimental research [17], [18], where the main criterion in selecting the optimum value of ignition advance angle was the indicated work and exhaust emissions.

The chemical reaction of fuel combustion model in KIVA-3V takes into account one global reaction of fuel oxidation, three reactions of kinetics NO formation, according to extended Zeldowicz mechanism and six reactions of chemical equilibrium for intermediate species [21], [22]:

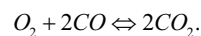
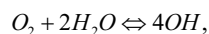
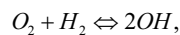
Methane



Gasoline



The reactions of chemical equilibrium are [21], [22]:



The coefficients of kinetic reaction rate of NO formation are necessary to perform the calculations and they were chosen on the basis of the literature studies [23]. However, the turbulence model used in the calculation is  $k-\varepsilon$  model.

The numerical simulation began at 220° CA and finished at 494° CA, which corresponds to experimental engine camshaft phases, which are inlet valves closure and beginning of outlet valves opening.

The results of numerical modelling of thermal cycle of model engine operated on methane and gasoline are compared in this work. The courses of pressure, temperature, NO and CO<sub>2</sub> concentration (averaged values for the volume of combustion chamber) in function of crank angle are presented. The distribution of temperature and nitric oxide concentration in the combustion chamber are presented in graphical form using Tecplot 360 postprocessing software [24].

### NUMERICAL ANALYSIS RESULTS

The following figures depict the distribution of temperature and nitric oxide concentration in the combustion chamber for the two analyzed fuels and courses of pressure, temperature, NO and CO<sub>2</sub> concentration (averaged values for the volume of combustion chamber) in function of crank angle. The temperature distribution is presented at crank angle equal 5° after top dead center (TDC). The NO distribution is presented at crank angle corresponding with the maximal concentration of this compound.

The temperature distribution as well as pressure and temperature courses (averaged values for the volume of combustion chamber) in function of crank angle for air excess factor  $\lambda=1.8$  are depicted in Fig.2 – Fig.4.

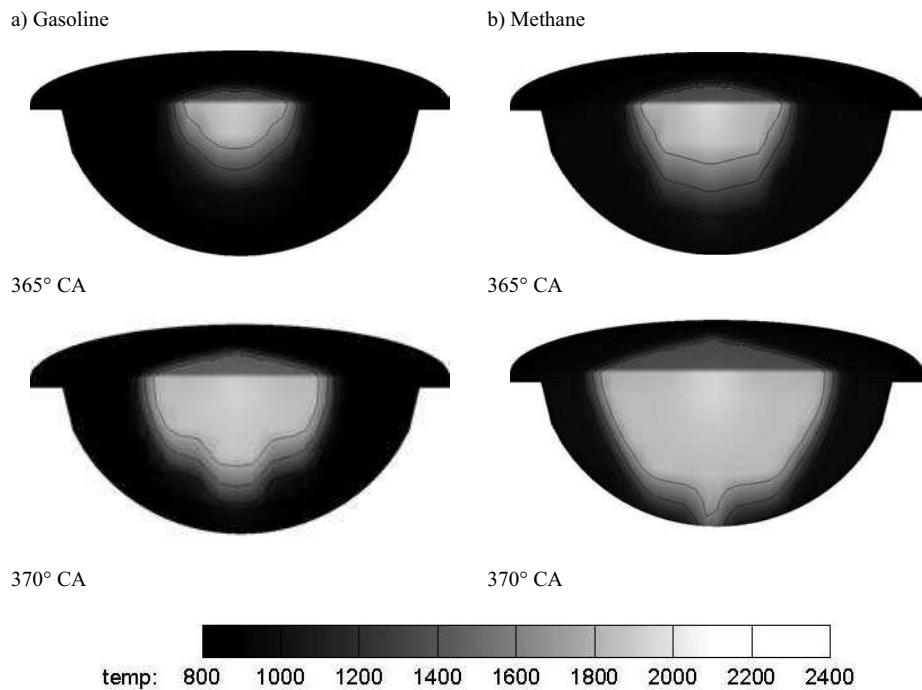


Fig. 2. Temperature distribution for 365° CA and 370° CA



Fig. 2. reveals, that the combustion process was accelerated by using methane as fuel. Greater portion of fuel was burnt and temperatures above 2000 K were reached. Such phenomenon is clearly seen in case of 10°CA after TDC piston position, where charge is burning in a large volume of the combustion chamber. The maximal instantaneous temperature in cylinder reached approx. 2200K for methane, which is approx. 100K more than in case of gasoline burning .

Fig. 3 and 4 depict pressure, heat release rate and temperature courses (averaged values for the volume of combustion chamber) in function of crank angle.

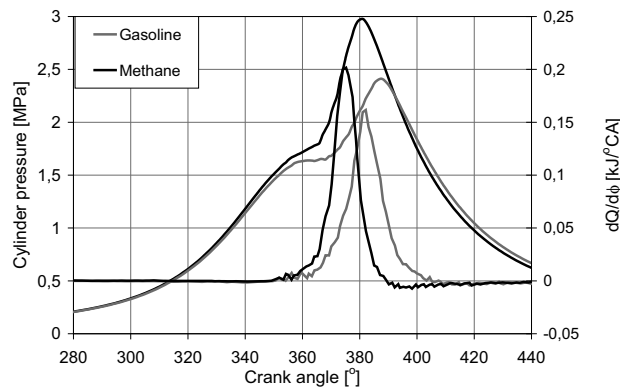


Fig. 3. In cylinder pressure and heat release rate courses for methane and gasoline

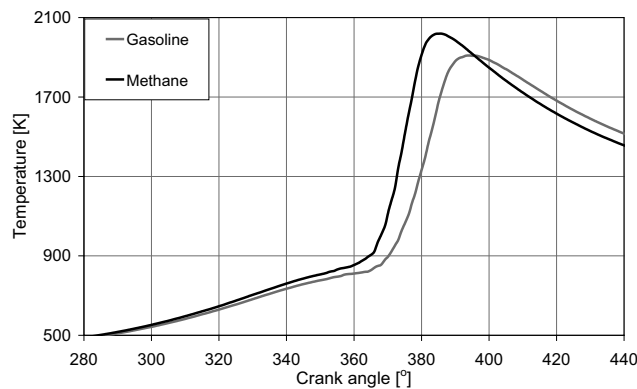


Fig. 4. In cylinder temperature courses for methane and gasoline

The pressure in the cylinder reaches its maximal value equal 2.4 MPa at 387°CA in case of gasoline burning. Using methane as fuel, causes the 24% increase in maximal pressure value to 2.97 MPa. The maximal pressure values occur earlier than in the case of engine powered by gasoline – the difference in crank angle is 6°CA. The combustion duration, defined on the basis of heat release rate, was 27° CA for methane and 34° CA for gasoline. The combustion duration was calculated as the crank angle interval from the spark timing to the end of combustion where the heat release reaches its maximum value – [25]. Above data prove that the combustion process was accelerated for the model

engine powered by methane. Also it is clearly seen on a chart depicting the pressure growth speed in the cylinder – Fig. 5. For gasoline, this parameter reaches maximal value of  $0.059 \text{ MPa}/^\circ$  at  $378^\circ\text{CA}$ , however for methane this factor value is almost two times higher and equals  $0.122 \text{ MPa}/^\circ$  at  $372^\circ\text{CA}$ .

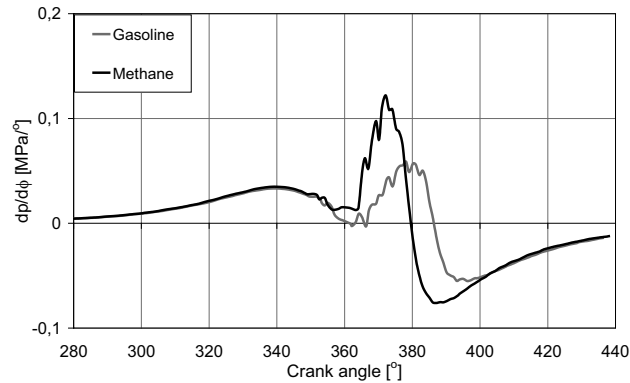


Fig. 5. Pressure growth speed courses in function of crank angle for methane and gasoline

Taking into consideration the above mentioned data, it can be stated that methane is better fuel for using in engine operating on ultra lean mixtures. The combustion process increases, which eliminates one of the main disadvantages of the use of lean mixtures - slow and very long burning.

The next objective of this paper was the numerical analysis of nitric oxide formation. Work of model engine powered by methane showed a decrease in emissions of NO, despite the higher temperature of combustion, cylinder pressure and pressure grow faster. Fig. 6 depicts the nitric oxide distribution in the combustion chamber for both fuels. The figures depict maximal values of nitric oxide concentration and are prepared in the same scale.

a) Gasoline –  $422^\circ\text{CA}$

b) Methane –  $400^\circ\text{CA}$

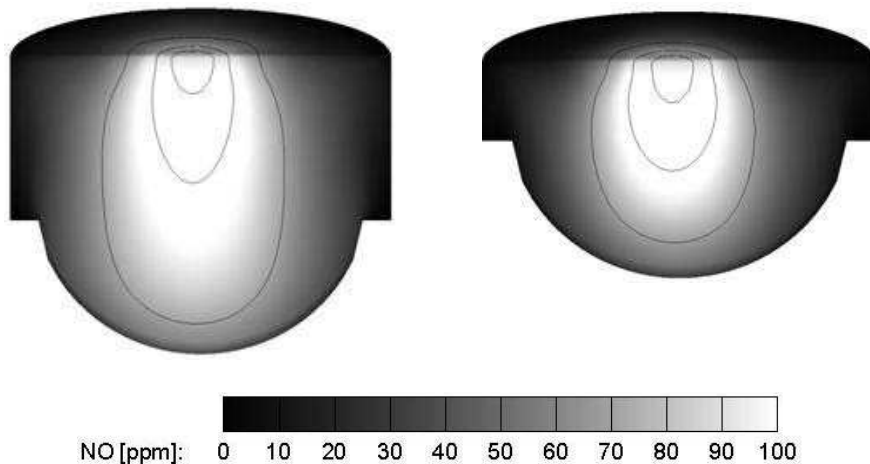


Fig. 6. NO distribution (actual maximum values) for gasoline and methane

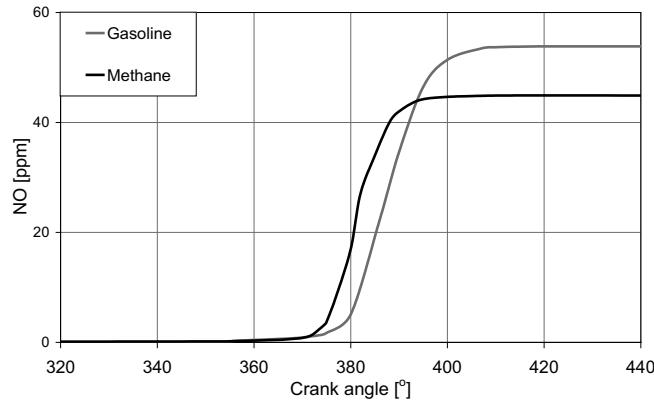


Fig. 7. Variations of NO concentration (mean values for cylinder volume) for methane and gasoline

For model engine fuelled by methane, the nitric oxide concentration (the averaged value for the volume of the combustion chamber – Fig. 7) reached its maximal value equal 45 ppm at 400°CA. However for gasoline as fuel, the NO concentration increased by 20% up to 54 ppm at 422°CA.

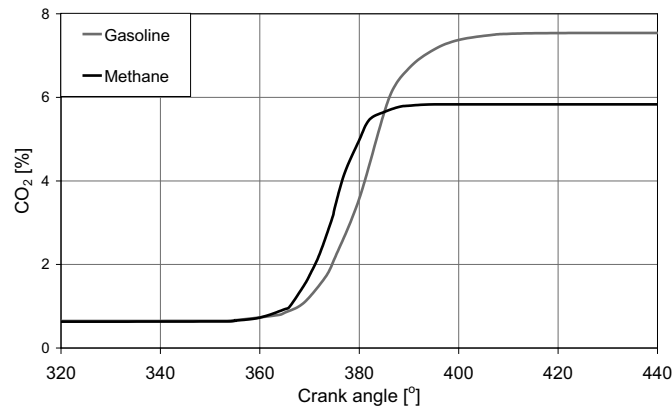


Fig. 8. Variations of CO<sub>2</sub> concentration (mean values for cylinder volume) for methane and gasoline

Above chart (fig.9) shows the variations of CO<sub>2</sub> concentration, which were occurred during modelled engine operation on methane and gasoline as fuels. The carbon dioxide emission values are mean values, calculated for the whole volume of cylinder. The maximal concentration of this compound was 7.5% at 407°CA and was obtained for engine fuelled by gasoline. However for methane as fuel, emission of CO<sub>2</sub> was decreased by about 23% and was 5.8% at 394°CA.

### CONCLUSIONS

The results of carried out analysis proved that using methane as fuel significantly improves engine work parameters. The combustion process was significantly accelerated in comparison with

engine fuelled with gasoline, combustion duration decreased by more than 20%. The pressure growth speed  $dp/d\phi$  was increased more than two times. Fuelling the engine with methane also decreases the concentration of nitric oxide in exhaust gases about 20%. The concentration of carbon dioxide in exhaust gases is also significantly lower in comparison with engine fuelled with gasoline. The difference was about 23%.

## REFERENCES

1. Cho M. H., He B-Q.: Spark ignition natural gas engines – A review, Elsevier Science, Energy Conversion and Management 48 (2007) 608–618, 2007.
2. Kowalewicz A.: Wybrane zagadnienia samochodowych silników spalinowych, Politechnika Radomska, Wydawnictwo, 2002.
3. Heywood J. B.: Internal combustion engine fundamentals, McGraw-Hill, 1988.
4. Kowalewicz A.: Podstawy procesów spalania, Wydawnictwa Naukowo-Techniczne, Warszawa 2000.
5. Goto Y., Narusawa K.: Combustion stabilization of spark ignition natural gas engine, Elsevier Science, JSAE Review 17 (1996), 251-258, 1996.
6. Semmin, Awang Idris, Rosli Abu Bakar: An Overview of Compressed Natural Gas as an Alternative Fuel and Malaysian Scenario, European Journal of Scientific Research, Vol.34, No.1, 2009.
7. Cho M. H., He B-Q.: Combustion and Emission Characteristics of a Natural Gas Engine under Different Operating Conditions, Korean Society of Environmental Engineers, Environ. Eng. Res. Vol. 14, No. 2, 95-101, 2009.
8. Szwaja S., Grab-Rogaliński K.: Hydrogen Combustion in a Compression Ignition Diesel Engine: Int.J.Hydrogen Energy Vol.34 nr 10, 4413-4421, 2009.
9. Szwaja S.: Hydrogen Rich Gases Combustion in the IC Engine. Journal of KONES Powertrain and Transport Vol.16 nr 4, 447-454, 2009.
10. Cupiał K., Szwaja S.: Producer Gas Combustion in the Internal Combustion Engine. Combustion Engines R.49 nr 2 (141), 27-32, 2010.
11. Borecki R. Szwaja S., Pyrc M.: Dual-Fuel Hydrogen-Diesel Compression Ignition Engine. Journal of KONES Powertrain and Transport Vol.15 nr 4, s.49-56, 2008.
12. Jamrozik A., Tutak W.: Modelling of combustion process in the gas test engine. Perspective Technologies and Methods in Memos Design, MEMSTECH, Lviv - Polyana, Ukraine. s. 14-17, 2010.
13. Szwaja S, Jamrozik A.: Analysis of Combustion Knock in the SI Engine. SILNIKI SPALINOWE/Combustion Engines, Mixture Formation Ignition & Combustion, Nr 2009-SC2, June 2009.
14. Tutak W., Jamrozik A.: *Numerical* analysis of some parameters of gas engine. Teka Komisji Motoryzacji i Energetyki Rolnictwa PAN, Volume X, 491-502, Polish Academy of Science Branch in Lublin, Lublin 2010.
15. Tutak W., Jamrozik A.: Modelling of the thermal cycle of gas engine using AVL FIRE Software. COMBUSTION ENGINES/Silniki Spalinowe, No. 2/2010 (141), 105-113, 2010.
16. Kociszewski A., Jamrozik A., Sosnowski M., Tutak W.: Simulation of combustion in multi spark plug engine in KIVA-3V. SILNIKI SPALINOWE/Combustion Engines, Mixture Formation Ignition & Combustion, 2007-SC2, 2007.

17. Cupiał K., Kociszewski A., Jamrozik A.: Multipoint spark ignition engine operating on lean mixture. Teka Komisji Motoryzacji i Energetyki Rolnictwa, PAN Oddział w Lublinie, Tom III, s. 70-78, Lublin 2003.
18. Kociszewski A., Cupiał K., Jamrozik A.: Możliwości spalania gazowych mieszanek zubożonych w silniku ZI. Journal of KONES. Internal Combustion Engines, Vol. 11, No. 1-2, 2004.
19. Tutak W., Jamrozik A., Kociszewski A., Sosnowski M.: Modelowanie obiegu cieplnego tłokowego silnika spalinowego o zapłonie iskrowym z uwzględnieniem recyrkulacji spali, Edukacja Techniczna i Informatyczna, Częstochowa 2010.
20. Amsden A.A.: KIVA-3V: A block-structured computer program for 3-D fluid flows with valves, chemical reactions, and fuel sprays. Los Alamos National Laboratory, Group T-3, March 1997.
21. Kesler M., Leżański T., Rychter T., Wolański P.: System spalania o zapłonie strumieniowym – analiza teoretyczna i badania silnikowe. International Scientific Conference on Internal Combustion Engines KONES'93, Gdańsk – Jurata, 1993.
22. Rychter T., Teodorczyk A.: Modelowanie matematyczne roboczego cyklu silnika tłokowego. Państwowe Wydawnictwo Naukowe, Warszawa 1990.
23. Jamrozik A.: Modelowanie procesu tworzenia tlenku azotu w komorze spalania gazowego silnika ZI. Materiały konferencyjne VII Międzynarodowej Konferencji Naukowej SILNIKI GAZOWE 2006 - konstrukcja, badania, eksploatacja, paliwa odnawialne. Zeszyty Naukowe Politechniki Częstochowskiej 162, Mechanika 26, 2006.
24. Tecplot Inc.: Tecplot 360 User's Manual. Bellevue, 2006.
25. Amr I., Saiful B.: An experimental investigation on the use of EGR in a supercharged natural gas SI engine. Fuel, Vol. 89, Issue 7, July 2010.

#### MODELOWANIE OBIEGU CIEPLNEGO SILNIKA ZI ZASILANEGO PALIWEM CIEKŁYM I GAZOWYM

**Streszczenie.** W artykule przedstawiono wyniki analizy numerycznej procesu spalania metanu oraz benzyny w silniku ZI. Porównano parametry pracy modelu silnika zasilanego ubogimi mieszankami benzyny i metanu, przy współczynniku nadmiaru powietrza  $\lambda = 1.8$ .

**Słowa kluczowe:** silnik spalinowy, modelowanie, mieszanka uboga,  $\text{NO}_x$ ,  $\text{CO}_2$ .

## RECRUITING AND USING AGRICULTURAL BIOGAS

Anna Kowalska

Katedra Inżynierii Środowiska i Przeróbki Surowców, Akademia Górniczo-Hutnicza w Krakowie

**Summary.** We are calling gas acquired of biomass, in particular from the installation alterations of animal wastes or plant, of the sewage treatment plant and landfill sites. The large potential of the biogas production has the farming. In farm households considerable quantities of waste which can be used in the fermentation are arising. Special agricultural cultivations and waste of the food production are a next source of biomass. In the article vital statistics were described about biogas, the process of the biogas production and conditions in which he should run.

**Key words:** biogas, biomass, renewable energy, biogasworks, farming.

### ADMISSION

Using the conventional sources of energy is connected with destroying natural resources and the environmental pollution. Petroleum, hard bituminous coal and dark brown are ranking the natural gas oneself to raw materials, of which stores are slowly ending. In the today seeking and applying alternative energy sources is an important call. According to the principle of the sustainable development we are obliged to use resources of the Earth this way in order to guarantee the equal access to them for future generations. Using on account of large stores arranged on the entire territory of the country the energy of biomass besides the wind power and solar is becoming increasingly common more and more. Biomass can be used in the form of the constant as fuel for direct burning, however subjected to specific processes can be processed into liquid or gas fuel. Biogas technologies apart from the production of the renewable energy enable the recycling of many troublesome waste in it from food-processing plants.

### BIOGAS AS ONE OF SOURCES OF THE RENEWABLE ENERGY

Renewable energy sources are widely available, boundlessly rich, renewable spontaneously in natural processes, having the smallest influence on the environment [11]. For electricity generated from renewable sources include heat or electricity generated from sources that produce energy from biomass, renewable generation from biogas, hydropower, wind power, solar collectors and geothermal sources.

Biogas is coming into existence in the biochemical process. In terms of physics he constitutes gas solution consisting mainly of methane and carbon dioxide. Particulates can be found in biogas also, water into forms of steam, the carbon monoxide, volatile hydrocarbons and trace amounts halocarbon whether volatile siloxanes (table 1) [8]. Methanogenesis process often occurs in natural conditions, among others on peat bogs, at the bottom of oceans and lakes, during volcanic eruptions, in paunches of ruminants and in liquid manure. He ranks among anthropogenic sources of methane: getting coal, natural gas and petroleum, landfill sites and sewage treatment plants and breeding of the domestic animals.

Table 1. Percentage composition of biogas [8]

element	content	
	scope %	on average %
methane (CH <sub>4</sub> )	42-85	methane (CH <sub>4</sub> )
carbon dioxide (CO <sub>2</sub> )	14-48	carbon dioxide (CO <sub>2</sub> )
hydrogen sulphide (H <sub>2</sub> S)	0,08-5,5	hydrogen sulphide (H <sub>2</sub> S)
hydrogen (H <sub>2</sub> )	0-5	hydrogen (H <sub>2</sub> )
carbon monoxide (CO)	0-2,1	carbon monoxide (CO)
nitrogen (N <sub>2</sub> )	0,6-7,5	nitrogen (N <sub>2</sub> )
oxygen (O <sub>2</sub> )	0-1	oxygen (O <sub>2</sub> )

The production and energy using agricultural biogas, even though he is one of the most favourable methods of acquiring the renewable energy, she didn't still find the universal application in Poland. In Europe the most for biogas is located in Germany, Denmark and Austria [21]. While in Germany amount for biogas in 2010 exceeded six thousand, in Poland it acted scarcely 150. Poland has the high potential of the biomass production, therefore the structure will enable biogas fulfilment of the obligations concerning achieving 15% to 2020 year of participation of the electric energy generated from the renewables. It is estimated that the agricultural products, liquid and solid manure and by-products and residues of agro-food industry can gain a sufficient amount of materials needed to produce approximately 5-6 billion m<sup>3</sup> of biogas per year, with a purity of methane gas [5,7].

Biogas obtained in the fermentation can be developed to a lot of ways. They most often use biogas for the production of electricity in engines ignition or turbine as well as of thermal energy in adapted gas boilers. From 1m<sup>3</sup> it is possible to produce biogas 2.1 kWh of the electric energy (at the assumed efficiency of arrangement 33%) or 5.4 kWh of the warmth (at the assumed efficiency of arrangement 85%) [23]. Arrangements associated, enabling the simultaneous production of electricity are also applied and thermal. A possibility of the transfer exists to the gas mains after prior treating [20].

## PROCESS OF COMING INTO EXISTENCE OF BIOGAS

Coming into existence of biogas is a multistage process occurring in anaerobic conditions at the participation of special micro-organisms and at the appropriate pH. The methane fermentation

is a step-by-step process, and in individual stages other group of micro-organisms is dominating [6]. We distinguish four stages in a process of coming into existence of biogas: hydrolytic phase, acid phase, acetate phase and methanogenic phase.

The hydrolytic phase relies on the schedule polymerized, largely of insoluble organic compounds, at the catalytic participation of enzymes of the bacterium from the group of relative anaerobes. Polysaccharides are surrendering to the hydrolysis to simple sugars, fats for alcohol polyhydric and of fatty acids, proteins to aminoacids.

In the phase of the acidity processing water-soluble chemical substances is taking place, in it of products of the hydrolysis through specialist micro-organisms in metabolic processes to simple organic acids, alcohol, aldehydes and hydrogen and carbon dioxide. The rest part is being bioreduced to acetates. Products from this phase are characterized by an intense unpleasant smell.

Acetogenic phase consists in processing bacterium of the ethanol and volatile fatty acids by appropriate species to acetic acid, and carbon dioxide and hydrogen, that is to substrates which in the next phase can to be converted into methane.

In the last phase, methanogenic bacteria produce methane, of which 70% is being generated of the acetic acid or alcohol, and 30% is coming into existence as a result of the reduction in the carbon dioxide in the reaction with hydrogen with the participation of some methanogenic bacteria [14]

As a result of the first and second stage acids are staple products (acetic acid, propionic acid, lactic acid, valerian acid), therefore they are often named fermentation sour. Two next stages closely are also connected with themselves from the consideration, the fact that they are directly responsible for the production of methane. Therefore the third and fourth determined stage is a name of the methanogenic fermentation. Considering above, it is possible to talk about the two-stage course of anaerobic transforming organic substance [9].

In the steadily proceeding fermentation the speed of creating intermediates in the determined phase is directly proportional to a velocity of their decay in the next phase. As a result almost an entire quantity of biomass biodegradable, is staying converted into final products: methane, ammonia, hydrogen sulphide and carbon dioxide [16].

## DIVISION OF METHODS OF THE BIOGAS PRODUCTION

Four criteria of identity of systems of the biogas production are most often applied. They belong to them: temperature, in which a process is proceeding, number of stages of the fermentation, dry matter content in substrates and mode of filling fermentation chambers.

On account of the temperature of the process we distinguish the fermentation psychrophilic, mesophilic and thermophilic. In the first stage of the fermentation bacteria are dominating, of which the optimum of the height is taking place in the temperature from 10°C to 20°C. in the phase mezophilic the scope of temperatures fluctuates from 37°C to 35°C. It is noteworthy, that in this temperature range is the most well-known active methane bacteria. The optimal temperature in the thermophilic phase is action of micro-organisms from 50°C to 60°C. Bacteria cultures participating in the last stage are applied in the event that it is necessary hygienisation leading for killing pathogenic bacteria [10].

Depending on the dry matter content in the fermentation chamber we are distinguishing the dry and wet fermentation. There is a speech about the wet fermentation, when substrate in the chamber through the entire duration of the process remains for the fermentation in the fluid state. Content of dry mass in fermenter is taking out from 12% to 15% and at such a consistency pumping and interspersing material is possible. If the number of dry mass will rise above 16%, then material is losing the ability to pump and we are ranking such a fermentation to dry [1].



In the dry fermentation the batch about the high dry matter content stored is having more free time in the state. The chamber of the fermentation has the cylinder shape, and it is made of steel or of reinforced concrete. In the chamber an agitator being used mixing up and transferring substrate is installed. Substrate is being dispensed into the container in the constant way, with the help of the agitator he is mixt up and moved toward the mouth from the chamber. An optimal use of the capacity of the chamber is an advantage of this method and relatively high productivity of the fermentation. Arable farms which don't have the sufficiency apply this technology manure.

Straight majority for biogas is working in the system of the wet fermentation, and integrated chambers of the fermentation and buffer containers of biogas are most often an applied technological solution. The container of the chamber as a rule is made of the reinforced concrete and he is covered gas-tight with roof. He is equipped with the pipework heating installed on the floor slab or on the wall of the tank. An agitator also has. Containers of chambers are low 6-8m and relatively wide – about the diameter coming up to 35m. Since the dispensed batch is in the way constant, chambers of the fermentation have the great capacity (a few thousand m<sup>3</sup>). A great stability of litigating is an advantage of the wet fermentation, applying conventional techniques of mixing up and the transport, possibility of partial separating individual fermentations, even decay of substrate, bacterial biomass and biogenic elements [7].

The number of applied containers and means of implementation in them of individual stages of the process influences the amount of stages of the technological process. An one-stage process is most often applied in agricultural biogasworkses, more rarely two - or multistage. The one-stage process is proceeding in one container, therefore between individual bevels a fermentation is lacking the physical division. A large number of containers enables to conduct the process two - or multistage [4,11,17].

Mode of filling fermenter depends on two factors: of access of substrate and the structure of the installation. Under the discontinuous procedure the container is being filled in the maximum amount with fresh substrate, and then hermetically closed. After the end of the stated time the container is staying emptied. It is important in order at the bottom to leave the sparseness of the batch for vaccinating the new process. A changeable amount and a quality of produced biogas are a great defect in this process. Filling fermenter under the discontinuous procedure can be held also with using two containers. The first container is being filled with substrate slowly and evenly in order to initiate the process of decaying. In the second container an appropriate fermentation is proceeding, after which for end the content is being removed, and into her place contents of the first container are being moved. Applying such a method lets the biogas production for increasing the evenness. Constant filling is characterized by repeated filling the container fermenter in the sequence of twenty-four hours. The amount of applied substrate for filling is equaling the quantity of post-fermentation waste chosen into the container of the storage payment. This method assures the regular biogas production and good using the capacity fermenter. A mode mixt up which is an alteration of the constant mode is also applied. In this case storage container of post-fermentation waste is also fulfilling the role fermenter, and covering the container allows for the assembly of gas coming into existence. In the process mixt up a productivity of substrate is increasing as well as a regularity of producing biogas is growing [18].

#### CONDITIONS OF THE COURSE OF THE PROCESS OF COMING INTO EXISTENCE OF BIOGAS

Methanogenic bacteria participating in the process of secreting biogas which we are ranking among: *Methanobacterium omelianski*, *Methanobacterium suboxydans*, *Methanobacterium sohnge-*

nii, *Methanobacterium propionicum*, *Methanobacterium formicicum*, *Methanococcus mazei*, *Methanococcus vannielii*, *Methanosarcinia barkeri* and *Methanosarcinia methanica*, are very sensitive to environmental conditions [3]. In order to assure for these micro-organisms optimum development, one should conduct the fermentation in closely named terms. We are ranking oxygen among important factors affecting the fermentation, temperature, reaction the pH, nutrients, inhibitors and mixing [4].

Methanogenic bacteria are compulsory or optional anaerobes. Therefore is important so that the process is conducted in fermentation containers closed tightly, without the access of oxygen from atmospheric air.

To a large extent the height of individual strains of bacteria participating in individual stages of the process depends on the pH of the environment. For acidic and hydrolyzing bacteria the pH has the sour reaction and he is ranging from 4,5 to 6,3. Higher pH in the scope from 6,8 to 7 is the best environment for bacteria producing acetic acid and methane. Carbon dioxide remains in the neutral pH range, but decreases if the buffer capacity is exhausted  $\text{CO}_2$ , causing a chain reaction. Stopping the activity of the bacterium causes reducing the reaction by the pH methanogenic, next is reaching the concentrations of acids associated with the acetic fermentation what in consequence is leading for even bigger lowering the reaction. At excessively alkaline reaction of the environment in bulks hydrogen sulphide and hydrogen are secreted, however in case of the sour reaction the fermentation is finding stopped, but in the extreme case given up [7,22].

Various types of bacteria involved in methane fermentation process developed at various temperatures and divide them into:

- psychrophile bacteria – they are cryophilic bacteria, below temperatures  $0^\circ\text{C}$  are dying and above  $30^\circ\text{C}$ , best are developing in temperature  $15^\circ\text{C}$ ;
- mezophilic bacteria - below temperatures  $10^\circ\text{C}$  are dying and above  $45^\circ\text{C}$  best are developing in the temperature:  $30 - 37^\circ\text{C}$ . pathogenic bacteria, for which the temperature of the human body is optimum are in this group;
- thermophilic bacteria - below temperatures  $40^\circ\text{C}$  are dying and above  $70^\circ\text{C}$ , best are developing in temperature  $52^\circ\text{C}$ . These bacteria live in sulphuric, ferric hot springs and in hot sewers [18].

For the majority of the methanogenic bacteria the optimal temperature is included in a mezophilic scope. With bioreactors the most spread on account of the largest outputs of biogas and the good stability of the process, are so which are working in temperatures mezophilic. If is essential higienisation, that is reduction in pathogenic bacteria, using thermophilic bacteria is necessary [1]. Conducting the process in high temperatures is guaranteeing the high output of gas relatively, however a quite great sensitivity of disruptions is his defect. Holding the adequate temperature in individual stages of the process is an important factor exquisitely. The change already against 10 steps in the sequence of twenty-four hours causes the thermal shock and dying of the methanogenic bacteria. Insufficiently heated may be due to the failure of the heating reactor. The drop in temperature directly affects the inhibition of bacteria, and indirectly to a decrease in pH and acidity.

To surviving and the height nutrients and trace elements are essential for the bacterium, so as: nickel, selenium, cobalt, iron, molybdenum and tungsten. A ratio of coal to nitrogen is also essential in applied base. To the correct course of the process relationship C:N should take out 1:30. If the relation is too high (much C, little N) coal isn't undergoing a complete transformation, causing the smaller output of methane. Applying base about the high protein content is disadvantageous, since big freeing ammonium nitrogen causes the market. In case of the too large nitrogen content, a threat of the harmful height to the process of ammonia exists. So that bacteria receive the sufficient portion of nutritional substances, ratio of C: N: P: S should be 600:15:5:1 [15].

We are calling every substance the inhibitor, pollutant in fermenter which is slowing down or is stopping the fermentation, for example: antibiotics (appearing in the urine of farm animals or the municipal waste) destroying methanogenic bacteria, ammonia and some metals (nickel, copper), if are appearing in the high concentration. Selecting substrates to the biogas production, one should take the possibility of appearing of inhibitors into consideration. Every storage substance of substrate given in greater concentrations can stop the fermentation. Even important trace elements can in high concentrations work on bacteria. The part of inhibitors is finding its way to the fermentation chamber together with the substratum, the rest part is products coming into existence in individual stages of the disintegration. The most harmful substances which even in sparsenesses can stop the process of the disintegration, it: antibiotics, disinfectants and herbicide, solvents and salts. Destructively heavy metals being found in a free figure also work on the fermentation. Their neutralization is possible thanks to the hydrogen sulphide coming into existence during the fermentation. The part of inhibitors is having an influence on other substances. Nitrogen is an essential nutrient for anaerobic micro-organisms, ammonia however coming into existence during the fermentation ( $\text{NH}_3$ ) in the little concentration is already litigating to the inhibition, of reducing the biogas production, the unpleasant smell and the low-quality of biogas. Since ammonia coming into existence is reacting with water, forming the ammonium ion and the ion ( $\text{OH}^-$ ), therefore he constitutes the balance for the concentration of ammonium ( $\text{NH}_4^+$ ). The height is moving the pH balance and an increase in the concentration of ammonia is taking place. Sulphur is also composing biomass. During the fermentation he can appear in the liquid form, or as the hydrogen sulphide in the mixture of liquid and gasses. Together with a rise in temperature a number of the freed hydrogen sulphide is rising in the liquid state, however together with the rise in the biogas production a pressure is growing in the bioreactor, and because of that content of freed compound. Hydrogen sulphide coming into existence during the fermentation ( $\text{H}_2\text{S}$ ) in the free figure at setting 50 mg/l is already cellular poison threatening the process of the disintegration. The effect slowing down or completely hindering of different substances depends on many factors. Very much for the establishment thresholds, from which stopping the process is beginning are difficult [22].

Standardizing the temperature and good contact of the bacterium and bases, and hence heightening the biogas production are guaranteeing mixing. The lack of effective mixing the content of the fermentation container causes delaminating fermenting substrate. Bacteria gathering at the bottom fermentora have the limited contact with base. The part of substance is rising to the surface, creating not very permeable layer for gasses coming into existence in the process. However it is worthwhile noticing, that both lack of mixing, as and are disturbing intensive mixing up process of the biogas production, therefore in fermenter free-rotational agitators are being assembled about the small cutting strength [19].

The change of for instance only one of exchanged factors causes the dismissal or in the extreme case stopping the activity of the bacterium, what the composition of biogas, that is contents in it are changing as a result of methane.

## CONCLUSIONS

Amount and composition of biogas depend mainly the chemical composition of organic compounds subjected to the fermentation, the temperature of litigating, the presence of inhibitors, mixing up and the time of keeping substrates in the reactor. Bacteria participating in the methane fermentation are very sensitive to the sequence of factors. Shaking at least one parameter is disturbing the process, and in extreme cases he can entirely break it. With important advantages of the

methane fermentation, beside he is providing with energy fuel in the form of biogas, reducing the environmental pollution and getting the valuable natural fertilizer.

## REFERENCES

1. Buraczewski G., Bartoszek B. 1990.: Biogaz wytwarzanie i wykorzystanie, Państwowe Wydawnictwo Naukowe, Warszawa.
2. Głodek E. (red.) 2007.: Pozyskiwanie i energetyczne wykorzystanie biogazu rolniczego. Wydawnictwo Instytut Śląski, Opole.
3. Janczur K. 2009.: Biogazownia rolnicza – inwestycja chroniąca klimat. *Czysta Energia* 1/2009.
4. Janczur K., Szymandera Z. 2010.: Efekt ekologiczny biogazowi rolniczej. *Czysta Energia* 11/2010.
5. Juško-Kowalczyk A. 2009.: Przegląd technologii produkcji biogazu. *Czysta Energia* 9/2009.
6. Kowalska A. 2010.: Overview of technological methods of energy production from biomass. *TEKA Kom. Mot. Energ. Roln.* Vol. 10.
7. Kujawski O. 2009.: Przegląd technologii produkcji biogazu (część pierwsza). *Czysta Energia* 12/2009.
8. Kujawski O. 2010.: Przegląd technologii produkcji biogazu (część trzecia), *Czysta Energia* 2/2010.
9. Kujawski O., Kujawski J. 2010.: Przegląd technologii produkcji biogazu (część druga). *Czysta Energia* 1/2010.
10. Lewandowski W.M. 2001.: Proekologiczne źródła energii odnawialnej. Wydawnictwo Naukowe – Techniczne Warszawa.
11. Lis T. 2009.: Rozwój sektora biogazu rolniczego w Polsce. *GLOBenergia Odnawialne Źródło Energii* 3/2009.
12. Małada A., Sobczyk W. 2005.: Uprawa roślin energetycznych jako forma aktywizacji środowisk wiejskich. *Zeszyty Naukowe Katedry Inżynierii Procesowej Uniwersytetu Opolskiego*, zeszyt II, Opole.
13. Mokrzycki E. (red.) 2005.: Podstawy gospodarki surowcami energetycznymi. Uczelniane Wydawnictwo Naukowe – Dydaktyczne AGH, Kraków.
14. Olesienkiewicz A. 2010.: Biogaz – szybko, wydajnie i opłacalnie. Sposoby modyfikacji technologii fermentacji metanowej. *GLOBenergia Odnawialne Źródło Energii* 4/2010.
15. Roszkowski A. 2006.: Agriculture and fuels of the future, *TEKA Kom. Mot. Energ. Roln.*, Vol. 6.
16. Schenkel Y., Crehay R., Delaunois C., Schummer J. 2003.: The agricultural sector and bio-energy production. *TEKA Kom. Mot. Energ. Roln*, Lublin, Vol. 3.
17. Sobczyk W. 2006.: The utilization of the biomass energy as the important factor of versatile development of agrosphere. *Folia Scientiarum Universitatis Technicae Resoviensis* nr 229. *Budownictwo i inżynieria środowiska*, z. 40.
18. Sobczyk W. 2008.: Wykorzystanie alternatywnych źródeł energii w Zawoi Przysłopie (Małopolska), *Folia Scientiarum Universitatis Technicae Resoviensis* nr 229, *Budownictwo i inżynieria środowiska*, z. 47.
19. Soliński I. 2001.: Biomasa energia odnawialna. Wydawnictwo Biblioteka Szkoły Eksploatacji Podziemnej, Kraków.
20. Szymańska M., Łabętowicz J. 2009.: Dostępność i zasoby substratów do produkcji biogazu w Polsce. *Czysta Energia* 5/2009.

21. Żmuda K., Czerniakowska-Bojko E. 2009.: Rolniczy potencjał energetyczny – biogazownie rolnicze przyszłością polskiej wsi. *Czysta Energia*, 9/2009.
22. [www.agroenergetyka.pl](http://www.agroenergetyka.pl).
23. [www.pga.org.pl](http://www.pga.org.pl).

**Publikacja zrealizowana w ramach pracy statutowej nr 11.11.100.280.**

### POZYSKIWANIE I WYKORZYSTANIE BIOGAZU ROLNICZEGO

**Streszczenie.** Biogazem nazywamy gaz pozyskany z biomasy, w szczególności z instalacji przeróbki odpadów zwierzęcych lub roślinnych, oczyszczalni ścieków oraz składowisk odpadów. Największy potencjał produkcji biogazu ma rolnictwo. W gospodarstwach hodowlanych powstają znaczne ilości odpadów, które mogą być wykorzystane w procesie fermentacji. Kolejnym źródłem biomasy są specjalne uprawy rolne oraz odpady produkcji spożywczej. W artykule przedstawiono podstawowe informacje na temat biogazu, procesu produkcji biogazu oraz warunków w jakich powinien przebiegać.

**Słowa kluczowe:** biogaz, biomasa, energia odnawialna, biogazownia, rolnictwo.

## AN APPLICATION OF BUTANOL AS A DIESEL FUEL COMPONENT AND ITS INFLUENCE ON EXHAUST EMISSIONS

Miłosław Kozak\*

\*Poznań University of Technology, Poland

**Summary.** The influence of oxygenated diesel fuel containing n-butanol on a passenger car exhaust emissions was tested over the NEDC transient cycle. The tests showed that a diesel fuel/butanol blend, containing 10% of n-butanol, caused a significant decrease in PM and smoke emissions, had no effect on NO<sub>x</sub> and CO<sub>2</sub> emissions and brought about higher CO and HC emissions. The most favourable fact resulting from the butanol application as diesel fuel component is that it produces desirable changes in PM/NO<sub>x</sub> trade-off.

**Key words:** Diesel Engines, Exhaust Emissions, Diesel Fuel, Butanol.

### INTRODUCTION

It is well known that fuel composition as well as its parameters have a significant influence on the exhaust emissions. The environmentally oriented changes in diesel fuel parameters boil down mainly to an increase in cetane number, decrease of density, sulphur and PAH content, and lower temperatures of fuel distillation. More unconventional, but also environmentally oriented diesel fuel modification is the oxygenation of the fuel. The process of oxygenation occurs by addition of oxygenated compounds to diesel fuel. The author carried out some research with oxygenated diesel fuels containing glycol ethers, maleates and carbonates. In most cases oxygenated fuels gave significant reductions in PM emissions, in some cases reductions in CO, HC, and NO<sub>x</sub> emissions were also achieved [1-3].

Alcohols also can be used as oxygenated compounds. Ethanol is commonly used as a gasoline component and there are also successful examples of its application in diesel engines. However ethanol, because of its very high octane number, low boiling temperature, low density, only partial miscibility with hydrocarbons, etc. is not actually the best candidate for oxygenation of diesel fuel. Another alcohol, which can be used as fuel component is butanol. Because of its high octane number (RON/MON = 96/78), butanol is a good fuel for spark-ignition engines. That is why the majority research deal with butanol application as a fuel for spark-ignition engines. The most recent examples of such works are items: [4-8]. Butanol can be also used as a diesel fuel component, and in this application it is significantly better than ethanol. It should be noticed that butanol has physical properties (density, viscosity) quite similar to those of diesel fuel and in contrast to ethanol, is very well miscible with hydrocarbons. High calorific value is another butanol advantage over ethanol. According to [9]: 1% of butanol decreases the diesel fuel's cetane number by 0.5 units only.

There are not many publications concerning the application of butanol as a diesel fuel component. Rakpulos et al. recently published some articles [10-12] on the application of diesel fuel/butanol blends. They tested exhaust emissions of a diesel engine, operating in stationary conditions, fuelled with different mixtures of diesel fuel and n-butanol. They generally noticed reductions in CO, NO<sub>x</sub> and smoke emissions but an increase in HC emissions. Similar changes in emissions of a small diesel engine were observed by Dogan [13]. Miers et al. [14] tested diesel fuel/butanol blends containing 20% and 40% by volume of n-butanol. Emission tests were carried out on a chassis dynamometer over the UDDS and HWFET dynamic cycles and during steady-state operation of a Euro 3 diesel passenger car. During the UDDS cycle a significant increase in CO and HC emissions, but also a reduction in NO<sub>x</sub> emissions was noticed. During highway drive cycle they observed 25% increase in NO<sub>x</sub> emissions when fuel contained 40% of butanol but CO and HC emissions remained unchanged. Neither PM nor smoke emissions were measured over dynamic cycles. During steady-state tests with different vehicle speeds and loads, the CO and NO<sub>x</sub> emissions remained at very similar level regardless of a fuel type, whereas smoke emissions decreased as butanol content increased. HC emissions were traditionally higher for fuels containing butanol.

## RESEARCH APPARATUS AND PROCEDURES

The New European Driving Cycle (NEDC) was selected as a representative test for this study. The test was Urban Driving Cycle (UDC) (cold start), followed by the high-speed Extra Urban Drive Cycle (EUDC) (hot start).

The tests were conducted on a passenger car equipped with a direct injection (Common Rail) turbocharged diesel engine, representing the latest technology in production at the start of the research program. Major data on the vehicle are shown in table 1.

Table 1. Specifications of the test vehicle

Vehicle Type	Passenger Car
Dry Weight	950 kg
Engine Type	Diesel, 4-cylinder in-line
Displacement	1.3 dm <sup>3</sup>
Max. Power	51 kW @ 4000 rpm
Max. Torque	145 Nm @ 1500 rpm
Injection / Combustion Type	Direct injection Common Rail, turbocharged (intercooled)
Exhaust Gas Recirculation EGR	Electronically controlled (closed-loop)
Emission Control	Oxidation catalyst DOC
Calibrated to	EURO 4

The test vehicle was fuelled with two fuels: conventional Euro 5 diesel fuel (DF) and the Bu10 fuel blend consisting of 90% by volume of DF and 10% of n-butanol. The properties of diesel fuel and n-butanol are given in table 2 and 3 respectively. The majority of properties of Bu10 blend

can be calculated from properties of DF and n-butanol. An exception is cetane number. The cetane number for Bu10 blend had been measured at a value of 47.2.

Table 2. Diesel fuel (DF) specifications

		Unit	Value
Cetane number		–	52.8
Cetane index		–	53.4
Density @ 20°C		kg/m <sup>3</sup>	827.7
Sulfur content		ppm	8.8
Oxygen content		%(m/m)	0.0
Viscosity	@ 20°C	mm <sup>2</sup> /s	4.096
	@ 40°C	mm <sup>2</sup> /s	2.607
Distillation	E250	%(v/v)	38.1
	E350	%(v/v)	–
	T95	°C	332.3
	FBP	°C	343.7
Aromatic hydrocarbons	Total aromatics	%(m/m)	20.7
	Monoaromatics	%(m/m)	18.8
	Diaromatics	%(m/m)	1.7
	Tri+ aromatics	%(m/m)	0.2
	Total PAH	%(m/m)	1.9

Table 3. Some properties of n-butanol

	Unit	Value
Molecular weight	amu	74
Oxygen content	%(m/m)	21.6
Boiling point	°C	117
Freezing point	°C	–90
Flash point	°C	34
Autoignition point	°C	343
Density @ 20°C	kg/m <sup>3</sup>	810
Viscosity @ 20°C	mm <sup>2</sup> /s	3.64
Cetane number	–	25 [14], 18 [15]



The tests were carried out at the Emissions Testing Laboratory using the emissions chassis dynamometer Schenck 500/GS60. The CVS AVL CEC system with full-flow dilution tunnel AVL CET-LD/20 type and particulate sampling system AVL CEP-LD/100 PTS 60 l/min, controlling system CESAR and Sartorius microbalance were used to measure exhaust emissions.

## TEST RESULTS AND DISCUSSION

In the first stage of the NEDC, i.e. in the UDC – Bu10 fuel blend caused considerable growth of CO emissions (fig. 1). The analysis of the results of continuous CO emissions measurement in the UDC revealed that the negative influence of Bu10 is mostly manifested during engine operation at high speed and load in steady conditions. Additionally, the analysis showed decreasing CO emissions during the realization of consecutive elementary cycles. The CO emissions drastically decrease in the last, i.e. fourth elementary cycle, which is connected with the start of effective operation of the catalytic converter. At the same time, this elementary cycle is characterized by the greatest relative differences in CO emissions between neat diesel fuel and Bu10.

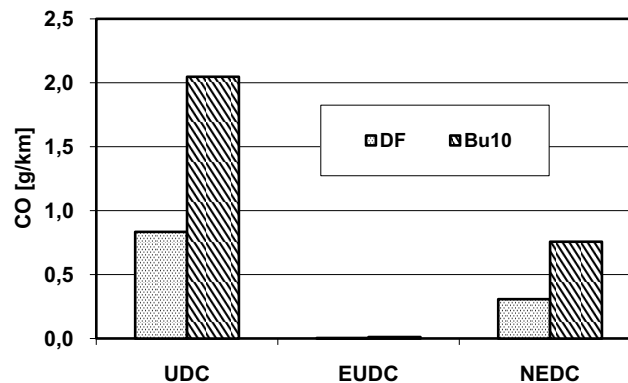


Fig. 1. CO emissions during UDC, EUDC and the whole NEDC for conventional diesel fuel (DF) and diesel fuel/butanol blend (Bu10)

The average CO emissions in the EUDC were over two orders of magnitude lower than in the UDC and amounted to less than 0.01 g/km for the both fuels. This confirms high effectiveness of removing of CO by the catalytic converter. Taking into account such a low emission of CO in the EUDC, the average emission in the entire NEDC is determined mainly by the UDC and the influence of fuel containing butanol is very similar to this in the UDC.

The results of increased CO emissions for diesel fuel/butanol blend described above are consistent with results obtained by Miers et al. [14], however they tested diesel fuel/butanol blends over different transient cycles, i.e. UDDS and HWFET. The results of tests carried out at steady-state conditions [10, 11, 13] show in principle decreases in CO emissions when a diesel fuel/butanol blend is applied.

The influence of the Bu10 fuel blend in the UDC is also unfavourable in the case of HC emissions (fig. 2). The analysis of the results of continuous measurement of HC in the UDC revealed that the negative influence of Bu10 fuel blend is the most evident, similarly to CO, during engine operation at high speed and load in steady conditions. The course of HC emissions during the first three elementary cycles is similar, which means that at that time the catalytic reactor had no influ-

ence upon the HC emissions. It is in the last, i.e. fourth elementary cycle that the catalytic converter starts to operate and the level of HC emitted considerably decreases. However, the Bu10 fuel still causes the growth of HC emissions.

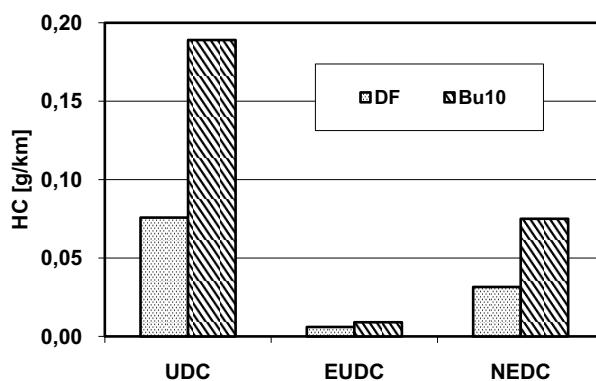


Fig. 2. HC emissions during UDC, EUDC and the whole NEDC for conventional diesel fuel (DF) and diesel fuel/butanol blend

The major benefit expected as a result of the use of oxygenated compounds, including butanol, is the decrease of PM emissions. At the same time it is known that the use of oxygenated compounds (especially those of low autoignition quality) may cause the growth of  $\text{NO}_x$  emissions as a result of intensification of “prompt  $\text{NO}_x$ ” production. However, most previous studies [10, 11, 12, 13, 14, 15] show, that in case of diesel fuel/butanol blends there is no increase in  $\text{NO}_x$  emission and possibly even a decrease. Figure 3 shows  $\text{NO}_x$  emission over the NEDC. One can notice that during the UDC  $\text{NO}_x$  emissions are lower when the test vehicle is fuelled with Bu10, next during the EUDC this emission is slightly lower when the vehicle is fuelled with neat diesel fuel. For the NEDC analyzed as a whole there is actually no difference in  $\text{NO}_x$  emissions.

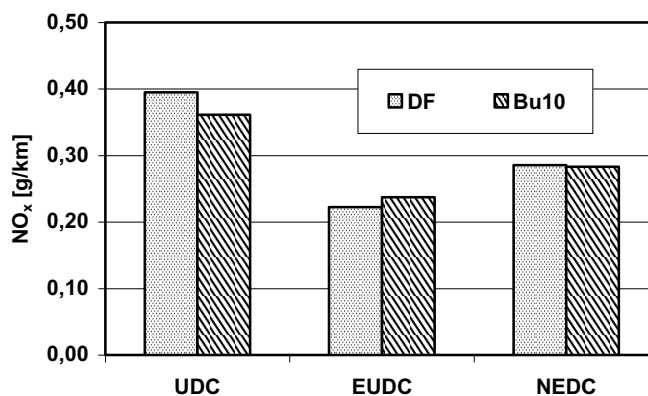


Fig. 3.  $\text{NO}_x$  emissions during UDC, EUDC and the whole NEDC for conventional diesel fuel (DF) and diesel fuel/butanol blend (Bu10)

The favourable influence of butanol on PM emissions has been confirmed over the whole NEDC (fig. 4). In the UDC – PM emission was lowered by 14%. In the EUDC PM emission reduction was even better and reached 25%. Average reduction in PM emissions in the complete NEDC was at a level of 21%. The analysis of the results of continuous smoke opacity measurement revealed that Bu10 fuel blend causes lower smoke emissions over the whole NEDC. Favourable influence of butanol on smoke emission was especially evident during vehicle's accelerations. In the available literature there are no results of diesel fuel/butanol blends influence on PM emissions during transient cycles. In stationary conditions a reduction in PM/smoke emissions is generally reported [10, 11, 12, 13, 14, 15].

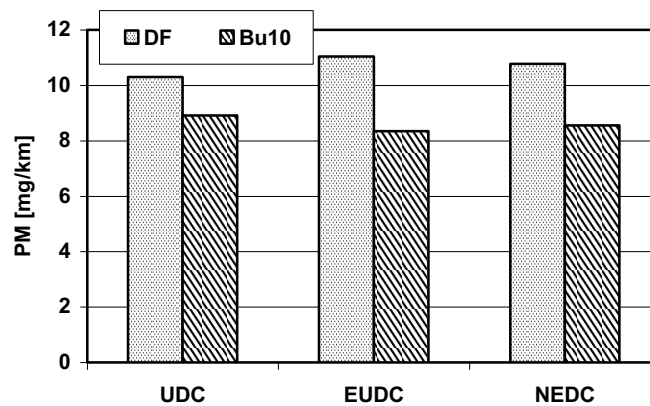


Fig. 4. PM emissions during UDC, EUDC and the whole NEDC for conventional diesel fuel (DF) and diesel fuel/butanol blend (Bu10)

Bu10 fuel blend has no influence on CO<sub>2</sub> emissions, neither in the UDC phase nor in the EUDC phase of the NEDC cycle (fig. 5).

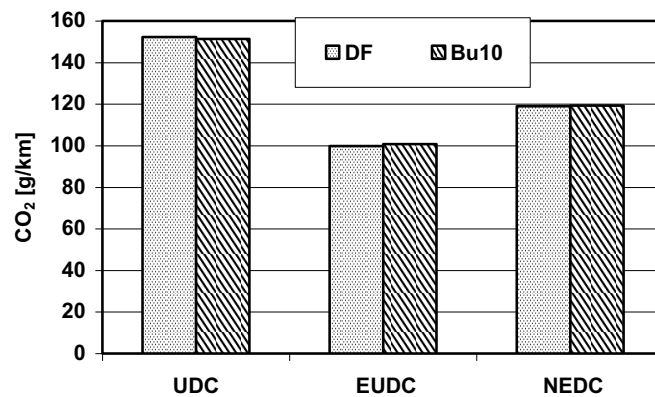


Fig. 5. CO<sub>2</sub> emissions during UDC, EUDC and the whole NEDC for conventional diesel fuel (DF) and diesel fuel/butanol blend (Bu10)

## CONCLUSIONS

Exhaust emissions from a diesel passenger car fuelled by diesel fuel/butanol blend (Bu10) were tested over the NEDC transient cycle. The test revealed a favourable influence of Bu10 fuel on the PM/NO<sub>x</sub> trade-off. Namely, a significant (by 21%) reduction of PM emissions was achieved with no change in NO<sub>x</sub> emissions. The reduction in PM emissions was confirmed by a considerable decrease in smoke emission. Application of Bu10 fuel had also some unfavourable effects, that are increases in CO and HC emissions. However, it should be emphasized, that after catalyst's light-off, which generally took place at the end of the UDC phase, the CO and HC emissions decreased to a very low level and then fuel type was of little importance. Bu10 fuel had no effect on CO<sub>2</sub> emissions.

The butanol can be regarded as a universal fuel component since it is applicable to gasoline and diesel fuel. In case of both fuels, butanol offers some favourable reductions in exhaust emissions. It can be expected that the role of butanol as a fuel component will be growing. Especially if butanol will be produced on a mass scale as a renewable fuel (second generation biofuel).

## REFERENCES

1. Kozak M., Merksiz J., Bielaczyc P. and Szczotka A.: The Influence of Oxygenated Diesel Fuels on a Diesel Vehicle PM/NO<sub>x</sub> Emission Trade-Off. SAE Technical Paper 2009-01-2696. 2009 SAE Powertrains, Fuels and Lubricants Meeting, San Antonio, Texas, USA, 02-05.11.2009.
2. Kozak M., Merksiz J., Bielaczyc P. and Szczotka A.: Low-Emissions Diesel Fuels Based on Oxygenated Compounds. APAC 15 Proceedings Vol. 1. 15th Asia Pacific Automotive Engineering Conference (APAC), Hanoi, Vietnam, 26-28.10.2009.
3. Kozak M., Merksiz J., Bielaczyc P. and Szczotka A.: Exhaust Emissions from a Diesel Passenger Car Fuelled with Oxygenated Fuels. Combustion Engines 2009-SC1.
4. Yang J., Wang Y. and Feng R.: The Performance Analysis of an Engine Fuelled with Butanol-Gasoline Blend. SAE Paper 2011-01-1191.
5. Wigg B., Coverdill R., Lee C. and Kyritsis D.: Emissions Characteristics of Neat Butanol Fuel Using a Port Fuel-Injected, Spark-Ignition Engine. SAE Paper 2011-01-0902.
6. Wallner T. and Frazee R.: Study of Regulated and Non-Regulated Emissions from Combustion of Gasoline, Alcohol Fuels and their Blends in a DI-SI Engine. SAE Paper 2010-01-1571.
7. Yang J., Yang X., Liu J., Han Z. and Zhong Z.: Dyno Test Investigations of Gasoline Engine Fueled with Butanol-Gasoline Blends. SAE Paper 2009-01-1891.
8. He X., Ireland J.C., Zigler B.T., Ratcliff M.A., Knoll K.E., Alleman T.L. and Tester J.T.: The Impacts of Mid-level Biofuel Content in Gasoline on SIDI Engine-out and Tailpipe Particulate Matter Emissions. SAE Paper 2010-01-2125.
9. Zöldy M., Hollo A. and Thernesz A.: Butanol as a Diesel Extender Option for Internal Combustion Engines. SAE Paper 2010-01-0481.
10. Rakopoulos D.C., Rakopoulos C.D., Giakoumis E.G., Dimaratos A.M. and Kyritsis D.C.: Effects of Butanol-Diesel Fuel Blends on the Performance and Emissions of a High-Speed DI Diesel Engine. Energy Conversion and Management no. 51 (2010).
11. Rakopoulos D.C., Rakopoulos C.D., Hountalas D.T., Kakaras E.C., Giakoumis E.G. and Papagiannakis R.G.: Investigation of the Performance and Emissions of Bus Engine Operating on Butanol/Diesel Fuel Blends. Fuel no. 89 (2010).

12. Rakopoulos D.C., Rakopoulos C.D., Papagiannakis R.G. and Kyritsis D.C.: Combustion heat release analysis of ethanol or n-butanol diesel fuel blends in heavy-duty DI diesel engine. Fuel no. 90 (2011).
13. Dogan O.: The Influence of n-butanol/Diesel Fuel Blends Utilization on a Small Diesel Engine Performance and Emissions. Fuel no. 90 (2011).
14. Miers S. A., Carlson R. W., McConnell S. S., Ng H. K., Wallner T. and LeFeber J.: Drive Cycle Analysis of Butanol/Diesel Blends in a Light-Duty Vehicle. SAE Paper 2008-01-2381.
15. Weiskirch C., Kaack M., Blei I. and Eilts P.: Alternative Fuels for Alternative and Conventional Diesel Combustion Systems. SAE Paper 2008-01-2507.

TYTUŁ

**Streszczenie.**

**Słowa kluczowe:**

## OPTIMIZATION OF ENERGY CONSUMPTION IN THE FREEZE DRYING PROCESS OF CHAMPIGNON (*AGARICUS BISPORUS L*)

Paweł Kozak, Dariusz Dziki, Andrzej Krzykowski, Stanisław Rudy

Department of Thermal Technology, University of Life Sciences in Lublin,  
Doświadczalna 44, 20-280 Lublin, Poland

**Summary.** In this paper, the influence of surface load of heating plates and degree of fineness of champignon fruits (*Agaricus bisporus L*) on the energy consumption in the freeze drying process was studied. The experimental researches were carried out for five material load levels of heating plates (6, 8, 10, 12, 14 kgm<sup>-2</sup>) and at the constant temperature (323K) and pressure of heating plates (63 Pa), after preliminary freezing of raw material to 248K. When the heating load was low (from 6 to 8 kgm<sup>-2</sup>), the degree of fineness of raw material had no influence on the specific energy requirements needed to heat of plates and to dry the raw material. However, the increase of heating load from 10 to 14 kgm<sup>-2</sup> resulted in the increase of specific energy inputs with the increasing degrees of fineness.

**Key words:** freeze drying, energy requirements, champignon fruits.

### INTRODUCTION

It is common knowledge that the freeze drying process is one of the most expensive methods of food conservation. The total cost of freeze-dried foods production is the sum of costs of equipment, materials, operating and energy consumption [Nastaj 1996]. The optimization of drying time and an increase of effectiveness of energy utilization could lead to a decrease of overall cost of freeze-drying [Millman 1984, 1985, Kumagai 1991, Yunfei 1996, Didukh, Kirchuk 2007, Liapis, Litchfield 1979].

The main costs of freeze-drying are divided as follows: the costs of freezing, ice sublimation and elimination of bound water, generation of hypoaerospheric pressure and condensation of water vapor [Lombrana i in. 1993, Ratti 2001].

The current costs of freeze-drying process are about four times higher than spray-drying and about eight times higher than convective drying. However, when the total energy consumption is taken into consideration, especially the preparation of raw material, these relations fundamentally change (the total cost of freeze-drying is only about 1.3 higher in comparison to convective drying) [Flink 1977, Lorentzen 1980, Benali, Amazouz 2006, Rudy 2009]. A decrease of energy consumption during the freeze-drying could be obtained by changing the conditions of the process – tem-

perature of heating plates and pressure in the drying chamber [Lis 1999a, 1999b, Lis i in. 2001, Depta, Lis 2001, Kozak 2001, Ivanova, Andonov 2001].

## MATERIALS AND METHODS

The aim of the work was to evaluate the influence of degree of fineness and the level of champignon load of heating plates on the freeze-drying energy consumption and the freeze-dryer capacity.

The scope of the work included the experimental research, relying on the freeze drying process of suitably prepared raw material samples, the analysis of energy consumption during drying and the statistical analysis of the obtained results.

The material for investigations was arable champignon (*Agaricus bisporus* L). The determination of dry matter in the fresh raw material was carried out according to PN-ISO 1026:2000. The champignons were taken directly after harvesting from mushroom growing cellar (600 kg capacity per 24 hours). The fresh fruits of first and second harvest phases were taken for investigations. Within the two hours after the harvesting, the raw material was washed in cold water, drained off water and selected according to cap diameter (from 25 to 35 mm) and appearance of fruits. The specimens of abnormal shape and exhibited signs of damage were discarded.

The experimental researches were carried out for five material load levels of heating plates (6, 8, 10, 12, 14 kg×m<sup>2</sup>). The heating plates were part of working area of freeze-dryer. The degree of fineness was as follows: chips, and cube (side length 4, 6, 8 and 10 mm). The freeze-drying process was carried out at the temperature of heating plates  $t = 50^{\circ}\text{C}$  at the pressure in the drying chamber  $p = 63$  Pa.

The champignon fruits were cut in order to obtain adequate degree of fineness (chips about 2 mm thickness). The laboratory food processor was used for mushrooms cutting. The ground samples of mushrooms were taken and formed according to the mass resulted from the level of load of freeze dryer heating plates. The samples were placed on aluminum plates in the freeze chamber. The process of preliminary freezing was monitored by using the thermocouple sensors placed in the geometrical center of samples. The freezing time of the individual samples was measured up to the temperature of  $-25^{\circ}\text{C}$ . The freezing time ranged from 4.5 to 9.0 hours according to the thickness of sample layers. The samples were stored in the dryer freezing chamber of dryer with the temperature  $25^{\circ}\text{C}$  during the 48 hours.

The lophylization process of champignon fruits was carried out in properly instrumented freeze-dryer by contact method of heat supply. The diagram of freeze-dryer was presented in Figure 1.

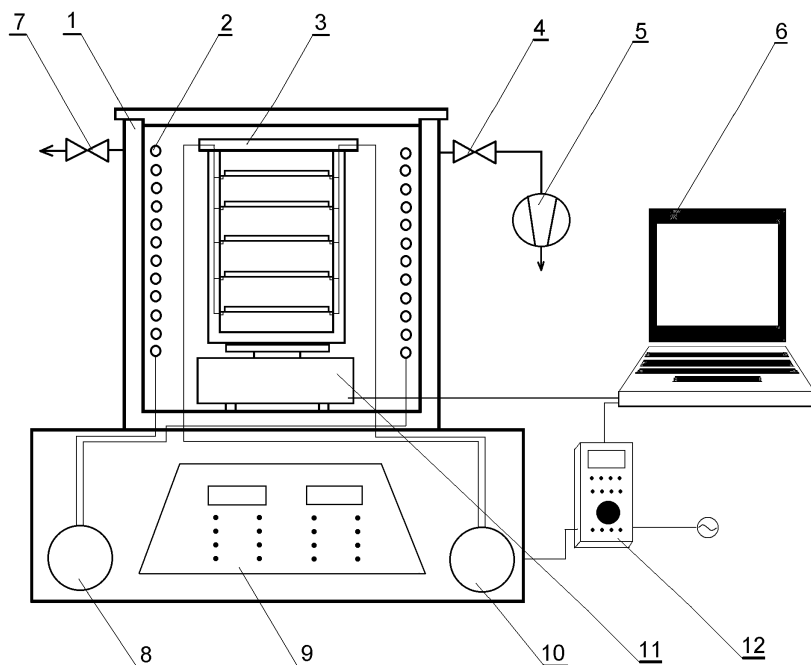


Fig. 1. Lyophilisator ALPHA 1-4: 1- drying chamber, 2- ice condenser, 3- frame with heating plates, 4- electro-magnetic valve, 5- vacuum pump, 6- computer, 7- aeration valve, 8- cooling system of ice condenser, 9- control and measuring system, 10- heating system, 11- tensometric balance, 12- electric meter

The prepared and frozen samples were placed on the five heating plates with the total surface of  $0,157 \text{ m}^2$ . The plates' kit was located on the balance frame in the drying chamber of lyophilisator. Three thermocouples were placed inside a frozen sample as follows: close by the surface, in the geometrical center and in the layer adhered to the heating plate. Such distribution of measuring points enabled proper control of drying process and observation of moving sublimation front.

The drying process was started when the plates' kit with drying material was located in the lyophilisator drying chamber and vacuum system was started. The plates heating system was started automatically when the assumed pressure in the drying chamber was attained.

During the drying process the values of material mass and temperature were monitored and recorded with a sampling constant of 60 s. The samples were dried until the moisture content reached about 3% wet basis.

The measurement of the electrical energy supply to particular sub-assemblies of the lyophilisator, was registered as the power distribution during the drying process with a sampling constant of 0.5 s. The measurement was performed using digital M-4660-M millimeter cooperating with DIGISCOP v. 2.05 software which recorded and converted the measuring data.

The total value of energy supply for particular sub-assemblies of the lyophilisator during one cycle of drying was calculated by using the numerical integration method and spreadsheet.

The investigations were replicated five times for each combination of load and degree of fineness. The obtained data was further subjected to a statistical analysis and the consequent evaluations were analyzed for a variance analysis. Statistical tests were evaluated by using the Statistica 6.0 software (StatSoft, Inc., Tulsa, USA). All the statistical tests were carried out at the significance level of  $\alpha = 0.05$ .



## RESULTS, ANALYSIS, AND DISCUSSION

The dry matter content in the fresh fruits of champignons was, on average, 9.7% w.b. The differences between the dry matter content of fruit selected according to the size and obtained from individual batches of first and second harvest phases were negligible ( $\pm 0,1\%$ ). The higher moisture content is characteristic for raw material obtained in the subsequent harvesting phases and for fruits with the cap diameter lower than 25 mm and higher than from 35 mm.

The electric energy inputs on freeze drying process are the sum of energy inputs of all lyophilisator systems necessary for the process realization. Thus the specific electric energy inputs ( $e$ ) is a sum of energy supply to ice condenser, vacuum and heating system, and automatic with reference to 1 kg of dried raw material.

The two-factor variance analysis was made for the evaluation of the significance of influence of degree of fineness and the load of heating plates on the specific energy inputs. The results showed that degree of fineness had a significant influence on  $e$ , however the level of load of heating plates was insignificant (Table 2). An increase of  $e$  with the decrease of degree of fineness resulted mainly from the increase of freeze drying time (Fig. 2).

Table 1. The results of variance analysis of degree of fineness and the load of heating plates on the specific energy inputs in the process of freeze drying of champignon

Variance source	SS	df	MS	F	p-value	F
Degree of fineness	7767,7	4	1941,9	4048,6	$1,3 \times 10^{-109}$	2,462613
Load	2,2171	4	0,5543	1,1556	0,33508	2,462613
Interaction	5,9307	16	0,3707	0,7728	0,71214	1,745647

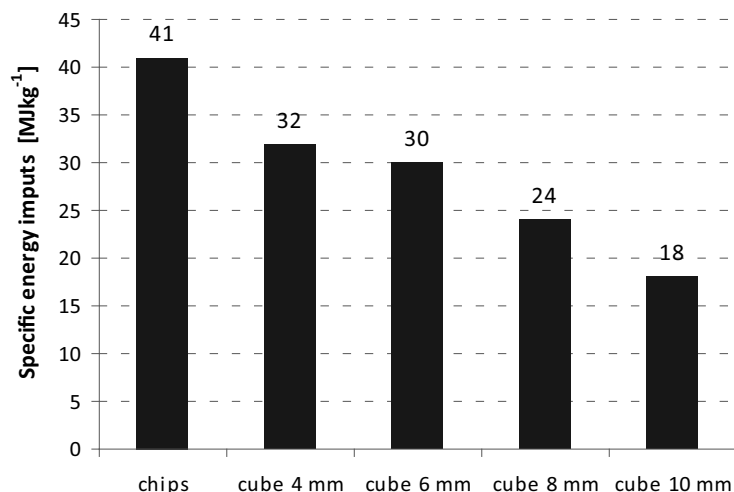


Fig. 2. The relation between the degree of fineness of champignon and the specific energy inputs in the process of freeze drying

The obtained average values of specific energy inputs can be useful only for proportional comparison between the energy consumption during the processes carried out in the given lyophilisator and in the changeable conditions of load of heating plates. Thus it can be concluded that the absolute values of specific energy inputs obtained in the laboratory-scale could not be comparable with the specific energy inputs obtained in the industrial conditions. However, the results showed that as the degree of fineness of champignons increases the energy consumption of freeze drying process increases, too. This tendency was also observed by other researches during the freeze-drying process of vegetables [Adams 1991, Genina et al 1996].

The measurements of the amount of energy supplied to the individual lyophilisator subassemblies showed that only the amount of energy supplied to the heating plates significantly depends on the analysed variables, such as the degree of fineness, load of heating plates and interactions between them. This energy is used for water phase change – at the beginning for ice sublimation and then vacuum evaporation. This was confirmed by the two-factor variance analysis (Table 2). The amount of electrical energy supplied for the other lyophilisator subassemblies resulted only from the running time.

Table 2. The results of variance analysis of degree of fineness and the load of heating plates on the specific energy inputs supplied to the heating plates of lyophilisator during the freeze drying process of champignon

Source of variance	SS	df	MS	F	p-value	F
Degree of fineness	6,0407	4	1,5102	5,5898	0,000421	2,462613
Load	58,694	4	14,673	54,313	$3 \times 10^{-24}$	2,462613
Interaction	25,5362	16	1,596	5,9075	$7,02 \times 10^{-9}$	1,745647

The results and analysis of energy used for heating of drying material (the energy supplied to heating plates) have proved that an increase of degree of fineness caused an increase of energy requirements of heating plates relatively to the unit of mass of dried material.

On the basis of the numerical data presented in Table 2 it can be stated that the decrease of specific energy inputs supplied to the heating plates of lyophilisator resulted in 82.5% form variation of plates load (range of load 6-14 kgm<sup>-2</sup>), in 8.5% from degree of fineness, and in 9% form the interactions of these two variables.

The variation of electric energy requirements used for the heating of lyophilisator plates was shown in Figure 3.

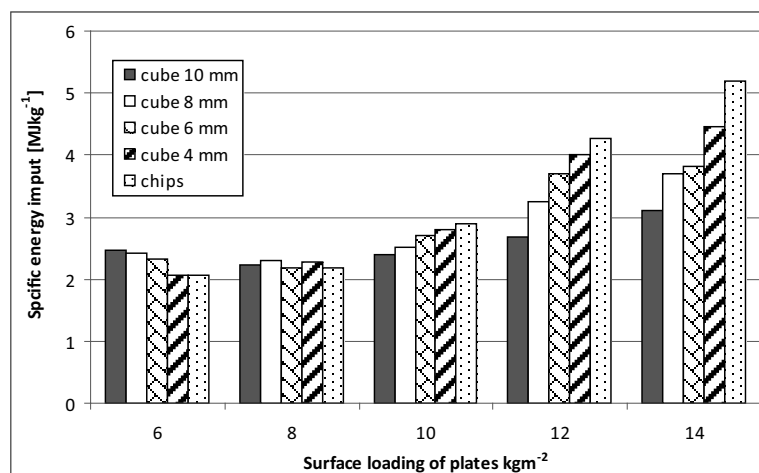


Fig. 3. The relation of specific energy input into surface loading of heating plates of lyophilisator to heating load and degree of fineness

The result showed that the degree of fineness of champignons has a negligible influence on specific energy inputs supplied into the lyophilisator when the heating load is 6 and 8 kgm<sup>-2</sup>. An increase of heating load of plates resulted in an increase of specific energy inputs with the increase of degrees of fineness.

## CONCLUSIONS

On the basis of the obtained results the following conclusions can be formulated:

1. When the heating load was low (from 6 to 8 kgm<sup>-2</sup>), the degree of fineness of champignons had no influence on the specific energy inputs needed to heat the plates and to dry the material. The increase of heating load from 10 to 14 kgm<sup>-2</sup> resulted in the increase of specific energy inputs with increasing degrees of fineness.
2. When the heating load of lyophilisator was 6-8 kgm<sup>-2</sup>, the lower energy consumption for heating of drying material and for water phase change was observed. The increase of the load from 8 to 14 kgm<sup>-2</sup> caused the increase of electric energy used for heating by approximately two times.
3. The theoretical energy requirements for water phase change in the raw material and at the drying chamber conditions are higher than the ones obtained during the experimental studies, and for the heating load below 8 kgm<sup>-2</sup>. The real amount of supplied energy to the plates ranged from 2.1 to 2.4 MJkg<sup>-1</sup> in the range of load from 6 to 8 kgm<sup>-2</sup>.
4. The significant increase of energy requirements for water phase change is caused by the increase of heating plates load above 10 kgm<sup>-2</sup> and the increase of the degree of fineness of raw material.

## REFERENCES

1. Adams G.D.J.: Freeze-drying of biological materials. *Drying Technology*, 9 (4), 1991, pp. 891-925.
2. Benali M., Amazouz M.: "Drying of vegetable starch solutions on inert particles: Quality and energy aspects", *Journal of Food Engineering*, Volume 74, 2006, pp. 484-489.
3. Depta M., Lis T.: Wpływ sposobu suszenia czosnku na jednostkowe zużycie energii i wskaźniki jakości suszu. *Inżynieria Rolnicza*, 2, 2001, pp. 25-29.
4. Didukh V., Kirchuk R.: Optimization of immovable material layer at drying. *TEKA Kom. Mot. Energ. Roln. - OL PAN 7 2007*, pp. 81-85.
5. Flink J.: Energy analysis id dehydration processes. *Food Technology*, 31, 1977, pp. 77-84.
6. Genin N., Rene F.: Influence of freezing rate and ripeness state of fresh courgette on the quality of freeze-dried products and freeze-drying time. *Journal of Food Engineering*, 1996, 29, pp. 201-209.
7. Ivanova, D.; Andonov, K.: "Analytical and experimental study of combined fruit and vegetable dryer". *Energy Conversion and Management*, Volume: 42, Issue: 8, May, 2001, pp. 975-983
8. Kozak P.: Wpływ warunków przechowywania liofilizatu z pieczarki na stopień zachowania witaminy C. *Inżynieria Rolnicza*, 2, 2001, pp. 143-146.
9. Kumagai H., Nakamura K., Toshimasa Y.: Rate analysis of the freeze-drying of liquid food by a modified uniformly retreation ice front model. *Agric. Bil. Chem.*, 55(3), 1991, pp. 737-742.
10. Liapis A.I., Litchfield R.J.: Optimal control of a freeze dryer I: Theoretical development and quasi steady state analysis. *Chemical Engineering Science*, 34, 1979, pp. 975-981.
11. Lis H., Lis T.: Temperatura sublimacyjnego suszenia jako czynnik wpływający na cechy jakościowe suszu jabłkowego oraz zużycie energii. *Inżynieria Rolnicza*, 4 (10), 1999, pp. 219-226.
12. Lis H., Lis T., Kozak P., Piwowarski E.: Wpływ temperatury na cechy jakościowe suszów, czas procesu liofilizacji i zużycie energii. *Inżynieria Rolnicza*, 5(11), 1999, pp. 21-27.
13. Lis H., Zarajczyk J.: Wyniki wieloczynnikowych badań liofilizacji jabłek. *Inżynieria Rolnicza*, 2, 2001, pp. 203-209.
14. Lombrana J.I., Elvira C., Villaran M.C., Izcarra J.: Simulation and design of heating profiles in heat controlled freeze-drying of pharmaceuticals in vials by the application of a sublimation semispherical model. *Drying Technology*, 11(3), 1993, pp. 471-487.
15. Lorentzen J.: Nowe metody suszenia i zagęszczania żywności, *Materiały Sympozjum zorganizowanego przez JUFoST. Nowe kierunki rozwoju liofilizacji*. 1980, WNT, Warszawa.
16. Millman M.J., Liapis A.I., Marchelo J.M.: Guidelines for the desirable operation of batch freeze-driers during the removal of free water. *J. of Food Technol.*, 19, 1984, pp. 725-738.
17. Millman M.J., Liapis A.I., Marchelo J.M.: Note on the economics of batch freeze-dryers. *J. of Food Technol.*, 20, 1985, pp. 541-551.
18. Nastaj J.F.: Some aspects of freeze-drying of dairy biomaterials. *Drying Technology*, 14(9), 1996, pp. 1967-2002.
19. Rudy S.: Energy consumption in the freeze - and convection-drying of garlic. *TEKA Kom. Mot. Energ. Roln. - OL PAN 9 2009*, pp. 259-266.
20. Yunfei L., Chengzhi W.: The optimal parameters of freeze-drying of food. *Drying '96 – Proceedings of the 10th International Drying Symposium (IDS'96)*, Kraków, 30 July-2 August, vol. B, 1996, pp. 801-804.

OPTYMALIZACJA NAKŁADÓW ENERGETYCZNYCH W PROCESIE  
SUBLIMACYJNEGO SUSZENIA OWOCNIKÓW PIECZARKI  
(*AGARICUS BISPORUS* L)

**Streszczenie.** Zbadano wpływ obciążenia powierzchni płyt grzejnych i stopnia rozdrobnienia owocników pieczarki *Agaricus bisporus* na energochłonność procesu sublimacyjnego suszenia. Badano wpływ warunków procesu sublimacyjnego suszenia na energochłonność procesu. Badania przeprowadzono dla pięciu ustalonych poziomów obciążenia płyt grzejnych surowcem (6, 8, 10, 12, 14 kg·m<sup>-2</sup>) i stałe temperatury płyt grzejnych (323 K) i ciśnienia (63Pa) po wstępnym zamrożeniu materiału do temperatury 248K. Kiedy obciążenie płyt grzejnych było niskie (od 6 do 8 kgm<sup>-2</sup>) stopień rozdrobnienia materiału nie miał wpływu na nakłady energii potrzebne do ogrzania płyt grzejnych. Jednakże wzrost stopnia obciążenia z 10 to 14 kgm<sup>-2</sup> powodował zwiększenie nakładów energii wraz ze wzrostem stopnia rozdrobnienia.

**Słowa kluczowe:** suszenie sublimacyjne, energochłonność procesu, owocniki pieczarki.

## INFLUENCE OF BLANCHING AND CONVECTIVE DRYING CONDITIONS OF PARSLEY ON PROCESS ENERGY CONSUMPTION

Andrzej Krzykowski, Stanisław Rudy, Paweł Kozak,  
Dariusz Dziki, Zbigniew Serwatka

Department of Thermal Technology, University of Life Sciences in Lublin,  
Doświadczalna 44, 20-280 Lublin, Poland

**Summary.** The aim of this study was to evaluate the influence of temperature (40, 50, 60, 70°C), flow velocity of the drying air (0,5 i 1 ms<sup>-1</sup>) and water blanching (3 min) on the specific energy during convective drying of parsley. The total process energy was also evaluated. The results showed that an increase of drying air temperature from 40 to 70°C caused a decrease of the total process energy by about 43% (1 ms<sup>-1</sup>s) and 31% (0,5 ms<sup>-1</sup>) for non-blanching parsley, and about 52% (1 ms<sup>-1</sup>), and 42% (0,5 ms<sup>-1</sup>) for blanching material. For each drying temperature the total drying energy was lower in the case of the flow velocity 1.0 ms<sup>-1</sup> and decreased after blanching. The lowest average total drying energy (10.5 MJkg<sup>-1</sup>) was obtained for blanched parsley dried at the temperature of 70°C, and for the air flow velocity of 1.0 ms<sup>-1</sup>.

**Key words:** convection-drying, energy consumption, parsley.

### **Nomenclature:**

e - specific drying energy [MJ·h<sup>-1</sup>·kg<sup>-1</sup>],  
E - total drying energy [MJ·kg<sup>-1</sup>],  
T - temperature [°C].

## INTRODUCTION

Vegetables are a necessary component of a healthy diet and should be consumed every day, but their seasonal occurrence and limit shelf life cause a necessity of using adequate food preservation methods [Pabis 2007, Jech et al. 2006].

The freeze drying is one of the best methods of food preservation. During this process the physical and chemical changes occurring in raw materials are minimized [Lis T. and Lis H. 1999, Lisowa et al. 1999, King 1980, Kawala et al. 1993, Ratti 2001, Rudy 2009]. However, the energy consumption during freeze drying is very high, which limits the application of this drying method. Therefore, convective drying is commonly chosen in food industry because of its simplicity and low cost [Nindo et al. 2003].

The minimization of energy requirements during drying depends on adequate methods of raw material preparation and selection of the optimum process parameters [Benali, Amazouz 2006, Flink 1977, Koyuncu et al. 2004, Tippayawong et al. 2009]. Among many methods of pre-treatment, blanching is among the most common ones. It is usually performed prior to drying, to inactivate enzymes responsible for various undesirable enzymatic reactions. Blanching also helps to remove the air from the intercellular spaces [Postolski 1987, Klimczak and Irzyniec 1994, Zadernowski and Oszmiański 1994]. Moreover, blanching can help increase the drying rate, hence reducing the drying time [Skorupska 1998, Depta and Lis 2001, Szarycz et al. 2003, Severini et al., 2005] and thus the energy consumption decreases. Due to the steadily rising costs of energy, the investigations of drying energy consumption are constantly required.

## MATERIALS AND METHODS

The aim of this study was to evaluate the influence of water blanching, temperature and flow velocity of the drying air on the energy consumption during convective drying of parsley.

The investigations were performed for two drying flow velocities, namely  $0.3$  and  $1 \text{ ms}^{-1}$ , at the temperature of  $40$ ,  $50$ ,  $60$ , and  $70^\circ\text{C}$ . The material for investigations was parsley (cv. Berlińska). Before drying, the material was cut into  $10 \text{ mm}$  cubes and blanched in water bath at the temperature of  $95^\circ\text{C}$  for  $3 \text{ min}$ . The second part of material was not blanched (control sample). The process of convection drying was continued until the mass of the sample reached the constant moisture ( $12\% \text{ w.b.}$ ) The convection dryer's load was  $12 \text{ kgm}^{-2}$ . The energy expenditure on the drying process was calculated at hourly intervals.

The convection drying was conducted using a vertical air-flow dryer (Fig. 1). The heating assembly of the dryer consisted of three heating elements and, more specifically, of heaters in chamotte casings, with a total strength of  $6.9 \text{ kW}$ . One of these heaters was connected into the circulation system of the temperature regulator. The axial ventilator, powered by an electric engine with a multi-stage regulation of rotation, ensured the air flow.

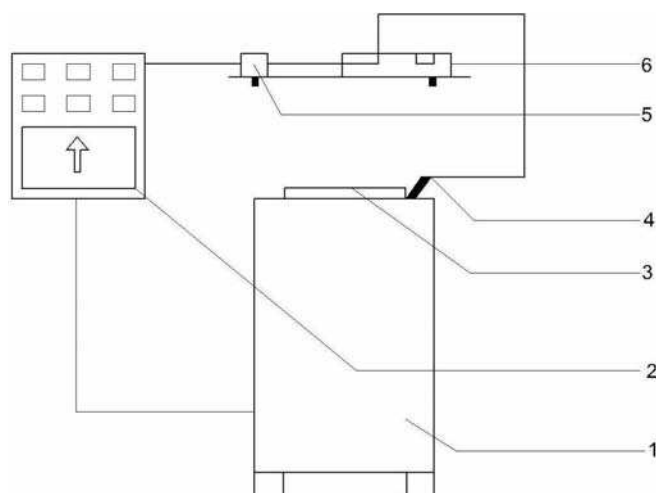


Fig. 1. The scheme of measuring stand for convective drying: 1 – dryer, 2 – switchboard, 3 – tray, 4 – contact thermometer, 5 – contactor, 6 – stabilizer

The measuring stand was also equipped with meter of electric power. The specific drying energy ( $e$ ) was calculated using the numerical integration method changes of power consumption as a function of time, related to the mass of the processed material, and expressed in  $\text{MJ}\cdot\text{h}^{-1}\cdot\text{kg}^{-1}$ . The total energy distributed to the convection dryers ( $E$ ) constituted the sum of energy inputs during the whole period, and was expressed in  $\text{MJ}\cdot\text{h}^{-1}$ . The measurements were replicated 5 times. The obtained data were further subjected to the statistical analysis and the consequent evaluations were analyzed with the variance analysis. The linear regression analysis was also carried out on these data. All the statistical tests were carried out at the significance level of  $\alpha = 0.05$ .

## RESULTS AND DISCUSSION

The significantly longest average drying time of parsley was noted for unblanched raw material and dried in the temperature of  $40^\circ\text{C}$ , and for the air flow velocity  $0,5\text{ ms}^{-1}$ . The use of blanching and an increase of drying air flow velocity reduced the drying time for each used temperature level (Fig. 2).

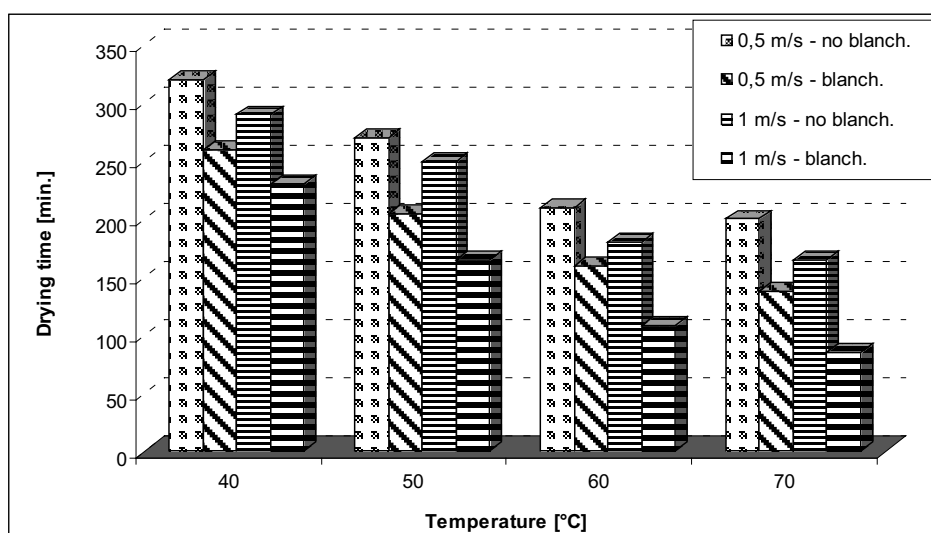


Fig. 2. The time of convective drying

The average values of specific drying energy ( $e$ ) in the consecutive stages of parsley convective drying and in the relation to drying temperature and air flow velocity, and by using blanching were presented in Figures 3-6. For each drying temperature, the inverse relationships were observed between the drying time and specific drying energy consumption. These relationships were described by the linear regression equations (Tables 1-4).



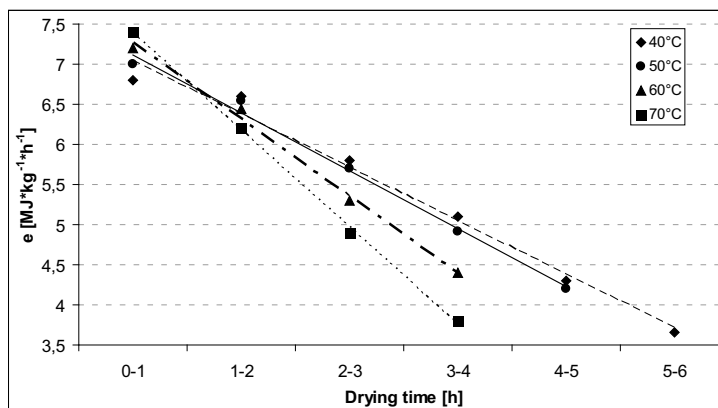


Fig. 3. Specific energy consumption during the drying of unblanched parsley (air flow velocity  $0.5 \text{ ms}^{-1}$ )

Table 1. Regression equations described the relations between the specific drying energy of unblanched parsley (e) and drying time (t) – air flow velocity  $0.5 \text{ ms}^{-1}$

t [°C]	The regression equation	R <sup>2</sup>
40	$e = -0.6657 \cdot t + 7.7067$	0.999
50	$e = -0.724 \cdot t + 7.844$	0.994
60	$e = -0.955 \cdot t + 8.225$	0.992
70	$e = -1.21 \cdot t + 8.6$	0.984

The water blanching of parsley before convective drying caused a decrease of specific energy consumption for each level of drying temperature and for two drying air flow velocities.

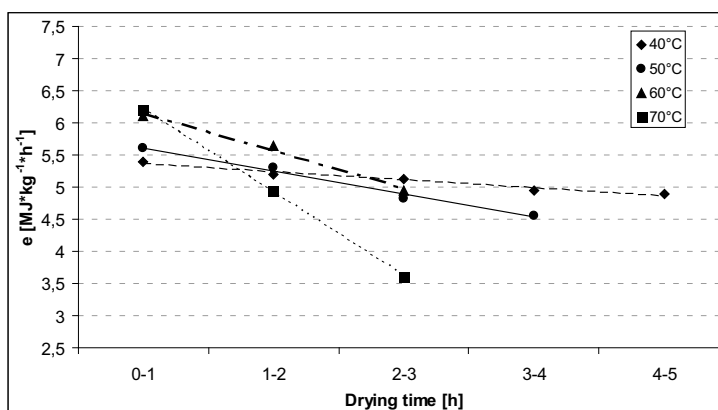
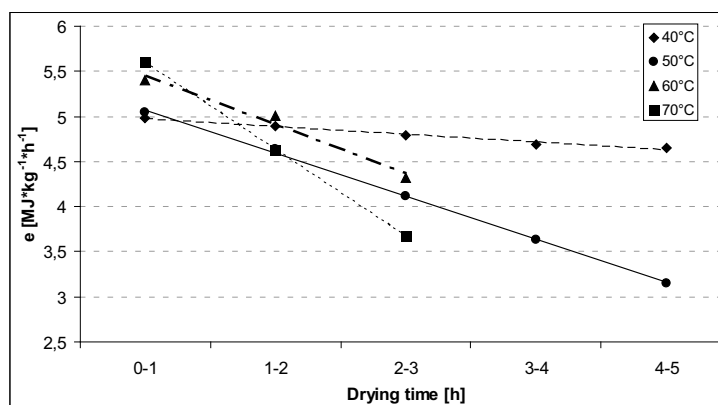


Fig. 4. Specific energy consumption during the drying of blanched parsley (air flow velocity  $0.5 \text{ ms}^{-1}$ )

Table 2. Regression equations described the relations between the specific drying energy of blanched parsley ( $e$ ) and drying time ( $t$ ) – air flow velocity  $0.5 \text{ ms}^{-1}$ 

$t$ [°C]	The regression equation	$R^2$
40	$e = -0,125 \cdot t + 5,491$	0,963
50	$e = -0,3586 \cdot t + 5,9691$	0,989
60	$e = -0,575 \cdot t + 6,7117$	0,988
70	$e = -1,3 \cdot t + 7,5165$	0,999

An increase of drying air temperature from  $40^\circ\text{C}$  to  $70^\circ\text{C}$ , for two flow velocities of drying factor, caused an increase of specific energy consumption during the first hour of drying (about  $0.6 \text{ MJkg}^{-1}$  and  $0.8 \text{ MJkg}^{-1}$ , respectively, in the case of unblanched and blanched parsley). In the subsequent time ranges, the specific energy consumption decreases, as the temperature of drying increases. It is caused by a faster decrease in water content at the higher process temperatures.

Fig. 5. Specific energy consumption during the drying of unblanched parsley (air flow velocity  $1.0 \text{ ms}^{-1}$ )Table 3. Regression equations described the relations between the specific drying energy of unblanched parsley ( $e$ ) and drying time ( $t$ ) – air flow velocity  $1.0 \text{ ms}^{-1}$ 

$t$ [°C]	The regression equation	$R^2$
40	$e = -0,086 \cdot t + 5,058$	0,983
50	$e = -0,4801 \cdot t + 5,5569$	0,998
60	$e = -0,541 \cdot t + 6,7117$	0,974
70	$e = -0,9625 \cdot t + 6,56$	0,999

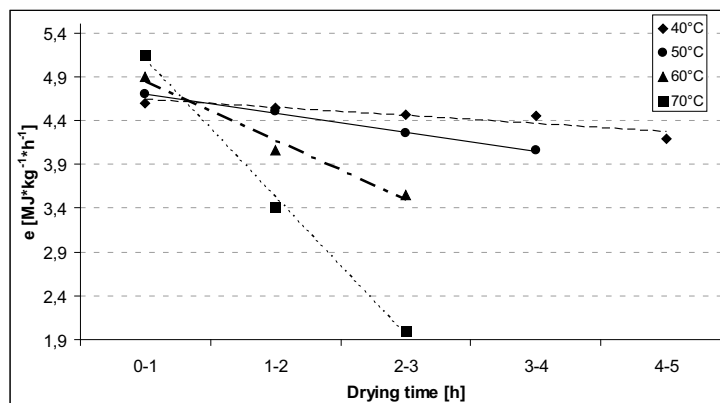


Fig. 6. Specific energy consumption during drying of blanched parsley (air flow velocity  $1.0 \text{ ms}^{-1}$ )

Table 4. Regression equations described the relations between the specific drying energy of blanched parsley ( $e$ ) and drying time ( $t$ ) – air flow velocity  $1.0 \text{ ms}^{-1}$

$t$ [°C]	The regression equation	$R^2$
40	$e = -0,0919 \cdot t + 4,7244$	0,835
50	$e = -0,217 \cdot t + 4,92$	0,997
60	$e = -0,673 \cdot t + 5,5163$	0,979
70	$e = -1,5752 \cdot t + 6,6719$	0,996

The increase of drying air flow velocity from  $0.5 \text{ ms}^{-1}$  to  $1 \text{ ms}^{-1}$ , at the given temperature level, caused the decrease of specific energy consumption during the drying process. The increase in air flow velocity in the first hour of the process duration, from  $0.5 \text{ ms}^{-1}$  to  $1 \text{ ms}^{-1}$  resulted in the decrease of electric energy from  $1.6$  to  $1.9 \text{ MJkg}^{-1}$  and from  $0.8$  to  $1.2 \text{ MJkg}^{-1}$  for unblanched and blanched parsley, respectively.

The increase of drying temperature and air flow velocity as well as the use of blanching caused a decrease of total drying energy necessary to dry  $1 \text{ kg}$  of parsley (Fig. 7).

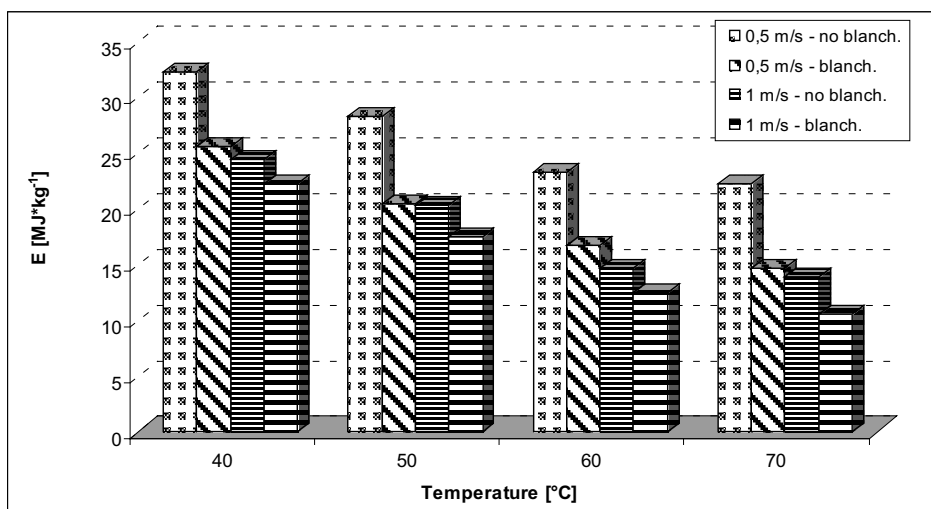


Fig. 7. Total drying energy of parsley

The highest average total drying energy ( $32.2 \text{ MJkg}^{-1}$ ) was obtained for unblanched parsley at  $40^\circ\text{C}$  and for the flow velocity of  $0.5 \text{ ms}^{-1}$ .

For each drying temperature, the total drying energy was lower in the case of the flow velocity  $1.0 \text{ ms}^{-1}$  and decreased after blanching. The lowest average total drying energy, at nearly  $10.5 \text{ MJkg}^{-1}$ , was obtained for blanched parsley dried at the temperature of  $70^\circ\text{C}$ .

## CONCLUSIONS

Based on the conducted analyses, the following conclusions can be drawn:

1. For each drying temperature blanching caused a significant decrease of parsley drying time.
2. The specific drying energy during convective drying linearly decreased as the drying time increased.
3. The increase of drying air temperature from  $40^\circ\text{C}$  to  $70^\circ\text{C}$  caused the decrease of total drying energy by nearly 43% (air flow  $1 \text{ ms}^{-1}$ ), and 31% (air flow  $1 \text{ ms}^{-1}$ ) for unblanched parsley, and by nearly 52%, and 42% (air flow  $0.5 \text{ ms}^{-1}$ ) in the case of blanched material.
4. The lowest average total drying energy, by nearly  $10.5 \text{ MJkg}^{-1}$ , was obtained for blanched parsley dried at the temperature of  $70^\circ\text{C}$ , and for the air flow velocity of  $1.0 \text{ ms}^{-1}$ .

## REFERENCES

1. Benali M., Amazouz M.: "Drying of vegetable starch solutions on inert particles: Quality and energy aspects", *Journal of Food Engineering*, Volume 74, 2006, pp. 484-489.
2. Depta M., Lis T.: "Wpływ sposobu suszenia czosnku na jednostkowe zużycie energii i wskaźniki jakości suszu", *Inżynieria Rolnicza*, nr 2, 2001, pp. 25-29.

3. Flink J.: Energy analysis id dehydration processes. *Food Technology*, Volume 31, 1977, pp. 77-84.
4. Kawala Z., Kapłon J., Kramkowski R.: „Ważniejsze aspekty suszenia sublimacyjnego”, *Przemysł Spożywczy*, nr 3, 1993, pp. 64-67.
5. King C.J.: „Nowe techniki odwadniania” [w:] Spicer A. „Nowe metody zagęszczania i suszenia żywności”. Materiały z Sympozjum zorganizowanego przez IUFoST. WNT, Warszawa 1980.
6. Klimczak J., Iżyniec Z.: „Blanszowanie warzyw. Kryteria wyboru warunków i metod prowadzenia procesu”. Cz. I. *Przemysł Fermentacyjny i Owocowo – Warzywny*, nr 9, 1994, pp. 25-26.
7. Koyuncu, T.; Serdar, U.; Tosun, I.: “Drying characteristics and energy requirement for dehydration of chestnuts (*Castanea sativa* Mill.)”, *Journal of Food Engineering*, Volume: 62, Issue: 2, April, 2004, pp. 165-168.
8. Jech J., Angelovič M., Poničan J., Židek B., Žitňák M.: Evaluation of drying-plant schief cbs 16-4 power parameters at drying maize. *TEKA Kom. Mot. Energ. Roln. - OL PAN 6A 2006*, pp. 92–100.
9. Lis T., Lisowa H.: „Temperatura sublimacyjnego suszenia jako czynnik wpływający na cechy jakościowe suszu jabłkowego oraz na zużycie energii”. *Inżynieria Rolnicza*, nr 4, 1999. pp. 219-226.
10. Lisowa H., Lis T., Kozak P., Piwowarski E.: „Wpływ temperatury na cechy jakościowe suszów, czas procesu liofilizacji i zużycie energii”, *Inżynieria Rolnicza*, nr 5, 1999, pp. 21-27.
11. Nindo C. I., Sun T., Wang S.W., Tang J.: Powers J.R. 2003. Evaluation of drying technologies for retention of physical quality and antioxidants in asparagus (*Asparagus officinalis* L.). *Lebesm.-Wiss. Technol.* 36, pp.507–516.
12. Pabis S.: Theoretical models of vegetable drying by convection, *Transp Porous Med* (2007) 66: s. 77-87.
13. Postolski J.: „Optymalizacja procesu blanszowania warzyw”. Cz. I. Uwarunkowania technologiczne jakości warzyw po blanszowaniu. *Przemysł Fermentacyjny i Owocowo – Warzywny*, nr 10, 1987, pp. 22-23.
14. Ratti C.: “Hot air and freeze-drying of high value foods: a review”, *Journal of Food Engineering*, Volume 49, 2001, pp. 311-319.
15. Rudy S.: Energy consumption in the freeze - and convection-drying of garlic. *TEKA Kom. Mot. Energ. Roln. - OL PAN 9 2009*, pp. 259–266.
16. Severini C., Baiano A., Pilli T.D., Carbone B.F., Derossi A., 2005.: Combined treatments of blanching and dehydration: study on potato cubes. *Journal of Food Engineering* 68, pp. 289–296.
17. Skorupska E.: „Wpływ blanszowania na proces suszenia warzyw”. VIII Konferencja Naukowo- Techniczna MUPS, Białystok- Białowieża, 1998, pp. 467- 474.
18. Szarycz M., Kamiński E., Jałoszyński K., Szponarska A.: „Analiza mikrofalowego suszenia pietruszki w warunkach obniżonego ciśnienia. Część I. Kinytyka suszenia pietruszki nieblanszowanej i blanszowanej”. *Technica Agraria* nr 2 (2), 2003, pp. 17 – 27.
19. Tippayawong N., Tantakitti C., Thavornun S., Peerawanitkul V.: Energy conservation in drying of peeled longan by forced convection and hot air recirculation. *Biosystems Engineering* 104 (2009), pp. 199-204.
20. Zadernowski R., Oszmiański J.: „Wybrane zagadnienia z przetwórstwa owoców i warzyw”. Wydawnictwo ART., Olsztyn 1994.

## ANALIZA WPŁYWU BLANSZOWANIA I WARUNKÓW KONWEKCYJNEGO SUSZENIA PIETRUSZKI NA ENERGOCHŁONNOŚĆ PROCESU

**Streszczenie.** Zbadano wpływ temperatury (40, 50, 60, 70°C) i szybkości przepływu powietrza suszącego (0,5 i 1 ms<sup>-1</sup>) oraz blanszowania wodnego (3 min.), na jednostkowe zużycie energii w czasie trwania suszenia konwekcyjnego oraz sumaryczną energochłonność procesu. Wzrost temperatury powietrza suszącego, w zakresie 40-70°C powoduje zmniejszenie całkowitych nakładów energetycznych o około 43% - 1 ms<sup>-1</sup> i 31% - 0,5 ms<sup>-1</sup> w przypadku pietruszki nie blanszowanej oraz o 52% - 1 ms<sup>-1</sup> i 42% - 0,5 ms<sup>-1</sup>, dla surowca blanszowanego. W całym zakresie temperatury całkowite nakłady energetyczne były niższe przy prędkości przepływu powietrza 1,0 ms<sup>-1</sup> i malały w wyniku blanszowania. Najniższe średnie nakłady energetyczne wynoszące około 10,5 MJkg<sup>-1</sup> uzyskano w przypadku pietruszki blanszowanej i suszonej w temperaturze 70°C, przy prędkości przepływu 1 ms<sup>-1</sup>.

**Słowa kluczowe:** suszenie konwekcyjne, energochłonność procesu, pietruszka.

## A COMPARISON OF MECHANICAL PARAMETERS OF TOMATO'S SKIN OF GREENHOUSE AND SOIL-GROWN VARIETIES

Izabela Kuna-Broniowska<sup>1</sup> Bożena Gładyszewska<sup>2</sup>, Anna Ciupak<sup>2</sup>

<sup>1</sup>Department of Applied Mathematics and Informatics,  
University of Life Sciences in Lublin, Akademicka 13, 20-950 Lublin, Poland  
e-mail: izabela.kuna@up.lublin.pl

<sup>2</sup>Departments of Physics, University of Life Sciences in Lublin,  
Akademicka 13, 20-950 Lublin, Poland  
e-mail: bozena.gladyszewska@up.lublin.pl

**Summary.** The paper presents the results of studies concerning the Young's modulus, critical stress, Poisson's ratio and thickness determined for the skin of greenhouse tomato cultivars (Admiro and Encore), and soil-grown varieties (Polset and Surya) comparison. Multivariate analysis of variance and one-dimensional tests [Hinkelmann 2008] were carried out. With the contrasts application the greenhouse varieties were compared with soil-grown ones. The comparison inside both: the greenhouse and soil-grown groups were also conducted. The homogeneity groups containing the average values of defined mechanical parameters of the tomato skin were determined.

**Key words:** skin, tomato fruit, Young's modulus, Poisson's ratio, multivariate analysis of variance, average homogeneity groups.

### INTRODUCTION

The need to define the fundamental characteristics of biological material, including its mechanical properties is mainly related to the evaluation of the final product. It seems to be especially important in the case of horticultural production. The scale of the considered problem is huge, due to the fact that fruits as well as vegetables are prone to damage at every stage of production [Dobrzański and Rybczyński, 2008, Machado 1999, Sargent 1992, Peleg 1984, O'Brien 1963]. Emerging loads and breaking stresses are a natural consequence of the above situation. Mechanical damage leads to products commercial value reduction while the physiological changes (e.g. softening) during the fruit and vegetables ripening affects the susceptibility to damage, in addition. Therefore, the outer surface of fruits and vegetables (peel) functions mainly as a protective barrier for the internal soft tissues, determines the physiological states of the whole product, and takes part in biochemical processes [Bargel and Neinhuis 2005, Andrews et al. 2002].

The basic physical parameters characterizing the plant material in terms of mechanical properties are Young's modulus, critical stress and Poisson's ratio [Mohsenin 1970].

The aim of this study was to determine the values and statistical dependence between the strength parameters set by the uniaxial tensile tests application for the skin of greenhouse and soil-grown tomato varieties, stored at 13°C.

## MATERIALS AND METHODS

The research material was a peel of greenhouse tomato varieties Encore and Admiro as well as the soil-grown's Surya and Polset cultivars, both stored at 13°C.

In each measurement series 30 repetitions were performed. Tomato fruits were selected randomly from among that, which skin was dyed in the orange and did not have any visible external damage. The specimens shape was established as rectangular strips, which were cut longitudinally in order to make the layer of pulp the thinnest possible. A profiled, single-blade knife with a limiter, ensuring repeatability of the specimens thickness was used for the skin biopsy.

The sample thickness was measured with the optical microscope application at 5 points in the central part of the strip on both sides with the accuracy of  $\pm 0.05$  mm after which the average value was calculated. The samples length and width were measured with the use of a caliper with the  $\pm 0.1$  mm accuracy. To eliminate the effect of sample drying, each test was performed immediately after specimen preparation.

In each single measurement the value of the force  $F$ , which followed the specimen rupture, was registered.

The method of random markers was applied to determine Young's modulus and Poisson's ratio of the tomato's fruit skin. Its main advantage is that the obtained results are independent of the effects observed along the specimen's edges, which are close to the clamping grips of the testing machine. Mentioned method relies on the analysis of the image and the distance between points on the surface of the sample subjected to uniaxial stretching tests. The random marking method allows measurements at well-defined location of the skin segment, which enables to eliminate the limitations occurring in typical strength tests such as cutting the samples with constant middle cross-section [Gładyszewska 2007].

The experiment was conducted on the measuring position assigned for the determination of mechanical properties of biological material [Gładyszewska 2006]. Prepared samples were placed in clamping grips of the tensile machine, after which powdered graphite markers were randomly sprayed on the sample surface. A CCD camera equipped with a microscope lens allowed the specimen observation at 240 x 320 pixel resolution under 5x magnification. The images from the camera as well as the value of the tensile force corresponding to each image were downloaded to the computer.

The critical surface tension  $\sigma_k$  of a stretched specimen was determined using Eq. (1), with the cross-section  $S$  knowledge:

$$\sigma_k = \frac{F}{S}, \quad (1)$$

where:  $F$  [N] is a force value corresponding to destruction of a sample,  $S = a \cdot b$ ,  $a$  and  $b$  [mm] specimen's thickness and width respectively.

Knowledge of the relative elongation in the direction of the x-axis  $\varepsilon_x$  for different stress values  $\sigma_x$  made it possible to determine the Young's modulus  $E$  (2):

$$E = \frac{\sigma_x}{\varepsilon_x}, \quad (2)$$



while the Poisson's ratio  $\nu$  was computed based on dependence (3):

$$\nu = -\frac{\varepsilon_y}{\varepsilon_x}, \quad (3)$$

where:  $\varepsilon_x$  is a relative elongation in the direction of the applied tensile force (-),  $\varepsilon_y$  is a relative elongation in a perpendicular direction to the applied force (-).

### STATISTICAL ANALYSIS

The statistical analysis was processed with the Statistica 6 application and included Young's modulus  $E$ , Poisson's ratio  $\nu$ , the critical stress  $\sigma_k$  and the thickness of the tomato fruit's skin determination for both: greenhouse Admiro and Encore and ground Surya and Polset varieties, stored at 13 ° C.

The distribution of Poisson's coefficient  $\nu$ , which is the ratio of longitudinal strain and transverse strain, was difficult to determine. The ratio of two independent variables with normal standard distributions has a Cauchy distribution [Feller 1966]. This bell-shaped, symmetrical distribution has a higher peak in the center and "fatter" tails in comparison with normal distribution. However, if two normal distributed variables have a nonzero mean, a form of their ratio distribution is more complicated [Hinkley 1969]. Under certain assumptions, the data can be transformed to produce a new variable with distribution close to normal distribution [Geary 1930]. Since the Cauchy distribution is similar to normal distribution, it can be assumed, that the distribution of Poisson's ratio will also be close to normal distribution. For this reason, the statistical tests were performed to examine the consistency between Poisson's ratio distribution and normal distribution. Normal distribution parameters  $\mu$  and  $\sigma$  were determined based on a sample, and for this reason the Shapiro-Wilk test was used [Shapiro and Wilk 1965]. The type of deviation of Poisson's ratio distribution from normality was analyzed based on probability plots [Thode 2002].

The results of the Shapiro-Wilk test, performed at the significance level of 0.01, indicate that there are no grounds for rejecting the assumed normality of Poisson's coefficient  $\nu$  distribution.

Young's modulus is a function of four variables: the force  $F$ , strain  $\varepsilon_x$ , sample thickness  $a$  and width  $b$ . Determination of the Young's modulus density function requires knowledge of other variables distributions and does not necessarily lead to a normal distribution, which is demanded for most statistical tests. The hypothesis, based on Shapiro-Wilk test, assuming that the Young's modulus distribution is the normal distribution, was not rejected, therefore the assumption of Young's modulus normality is recognized as a fulfilled (Kuna-Broniowska et al. 2011).

Tomato fruits were stored for at least 14 days, however, due to the incompatibility of the period of measurement for the individual varieties only four common terms of measurement could be distinguished. The experiment was conducted in two-way cross-classification system. The factors were experimental cultivars (Admiro, Encore, Polset and Surya) and the length of storage period (harvesting day, 4th day, 11th day and 14th day of storage).

Following linear model was adopted:

$$y_{ijk} = \mu + \alpha_j + \beta_k + \alpha\beta_{jk} + e_{ijk},$$

where:

$y_{ijk}$  – value of selected determinant of tomato fruit peel,

$\alpha_j$  – effect of  $j$ -th variety,  $j = 1, 2, 3, 4$ ,

$\beta_k$  – effect of  $k$ -th storage time length,  $k = 1, 2, 3, 4$ ,

$\alpha\beta_{jk}$  – interaction effect of varieties and shelf-life.

Three types of hypotheses concerning the parameters of the experimental model were tested:

1. Hypothesis assuming no significant diversity of the varieties due to the mechanical properties of processed tomato's fruit skins.
2. Hypothesis about no significant diversity of the storage periods due to the mechanical properties of processed tomato's fruit peels.
3. Hypothesis assuming no significant diversity of tested varieties storage periods due to the mechanical properties of processed tomato's fruit skins.

Table 1 presents the results of Wilks' multivariate tests of significance on which (at the level of significance  $\alpha = 0.01$ ) significant variation of mechanical properties of tomato fruit peel because of the variety and storage time was found. It was also stated that the investigated tomato varieties diversify during storage time, taking into account mechanical properties of their peel (the importance of interaction). Additionally, changes in the mechanical properties values extend to them differently during storage. Thus, determining the degree of ripeness of tomato fruits on the basis of changes in Young's modulus or Poisson's ratio values, which are basic determinants defining the material properties, should be carried out separately for each variety. The result of multivariate testing indicates that a comparison of average strength properties is essential (Tab. 1). In order to determine which characteristics diversify significantly due to experimental factors one-dimensional tests were carried out. Table 2 shows the results of tests for the four studied tomato fruit peel parameters.

The null hypothesis for the Young's modulus, Poisson's ratio and skin thickness were rejected at the significance level of  $\alpha = 0.01$ , based on unidimensional testing. It indicates the presence of significant diversity for each of three skin parameters due to the variety and storage time (Tab. 2). Critical stress values were significantly different between varieties, but did not diverse significantly during studied storage periods (Table 2). For Young's modulus, Poisson's ratio, skin thickness and the critical stress a significant interaction between the variety of tomatoes and their storage time was observed, which is synonymous with the need to analyze temporal changes in values of mechanical parameters separately for each variety.

Table 1. Wilks' multivariate tests of significance for the four varieties of tomatoes stored at 13°C

Effect	Test	Value	F	Effect	Error	p
Absolute term	Wilks	0.007	16212	3	343	0.000
Variety	Wilks	0.258	69	9	835	0.000
Storage time	Wilks	0.554	25	9	835	0.000
Interaction Variety x Time	Wilks	0.790	3	27	1002	0.000

Table 2. Unidimensional tests for Poisson's ratio  $\nu$ , the skin thickness, the critical stress  $\sigma_k$  and Young's modulus  $E$ 

Diversity sources	Degrees of freedom	SS	MS	F	p
<b>Poisson's ratio <math>\nu</math></b>					
Absolute term	1	96.802	96.802	15702.712	0.000
Variety	3	3.121	1.040	168.760	0.000
Time	3	0.079	0.026	4.293	0.000
Variety x Time	9	0.171	0.019	3.086	0.000
Error	345	2.127	0.006		
Generally	360	5.49734			
<b>Skin thickness</b>					
Absolute term	1	200.564	200.564	10619.693	0.000
Variety	3	2.066	0.689	36.460	0.000
Time	3	2.117	0.706	37.358	0.000
Variety x Time	9	0.773	0.086	4.546	0.000
Error	345	6.516	0.019		
Generally	360	11.4318			
<b>Critical stress <math>\sigma_k</math></b>					
Absolute term	1	45.180	45.180	1997.310	0.000
Variety	3	2.565	0.855	37.792	0.000
Time	3	0.166	0.055	2.442	<b>0.064</b>
Variety x Time	9	0.549	0.061	2.699	0.005
Error	345	7.804	0.023		
Generally	360	11.0494			
<b>Young's modulus <math>E</math></b>					
Absolute term	1	5769.497	5769.497	6688.028	0.000
Variety	3	507.704	169.235	196.178	0.000
Time	3	10.598	3.533	4.095	0.007
Variety x Time	9	34.556	3.840	4.451	0.000
Error	326	281.227	0.863		
Generally	341	824.135			

SS – sum of squares, MS- average square, Test F- Snedecor test, p – empirical probability (a posteriori)

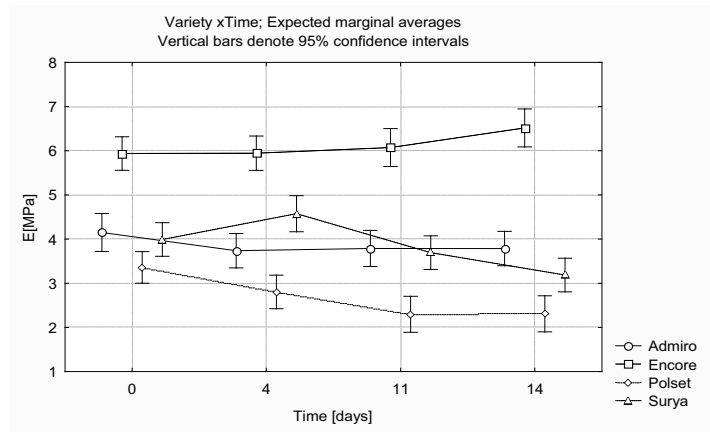


Fig. 1. The average values of Young's modulus in the selected four days of measurement

From the four tested tomato fruits cultivars, stored at 13 °C, the skin of Polset soil-grown cultivar was characterized by the lowest value of Young's modulus, while the highest one in the case of greenhouse Encore variety was received. Additionally, the value of the longitudinal modulus of elasticity for this variety increased with the growth of the storage time, while in the case of other varieties this value decreased in varying degrees (Fig. 1).

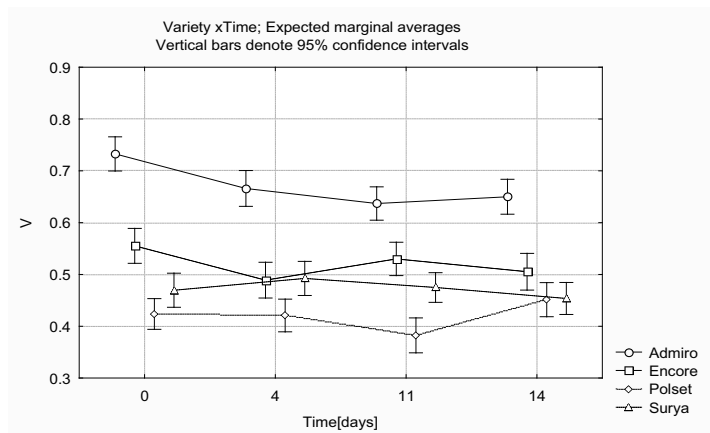


Fig. 2. Mean values of Poisson's ratio in the selected four days of measurement

The skin of greenhouse Admiro variety was characterized by the greatest value of Poisson's ratio  $\nu$ , while similar values of this parameter were observed in the case of the other 3 cultivars (Fig. 2).

The null hypotheses rejection for the studied mechanical properties of tomato fruit peel, indicates the significance of averages comparison in one case, at least. A study object was to compare the different varieties of soil-grown and greenhouse tomatoes. What is more, greenhouse Encore variety was compared with three others cultivars in the respect of Young's modulus E values while

the Admiro variety with three other varieties on account of the Poisson's ratio  $\nu$  value. Four types of comparisons were defined by the following contrasts in order to carry out mentioned task:

1. Differences among both: the values of Poisson's ratio  $\nu$  ( $\mu_{VE} - \mu_{VA}$ ) and Young's modulus  $E$  ( $\mu_{EE} - \mu_{EA}$ ) for Admiro and Encore greenhouse tomato's fruit peel.
2. Differences among both: the values of Poisson's ratio  $\nu$  ( $\mu_{ES} - \mu_{EP}$ ), and Young's modulus  $E$  ( $\mu_{VS} - \mu_{VP}$ ) for soil-grown Polset and Surya tomato's fruit peel.
3. Differences between the values of Young's modulus  $E$  in the case of the Encore tomato variety with three other cultivars together:  $3\mu_{EE} - (\mu_{EA} + \mu_{EP} + \mu_{ES})$ .
4. Differences between the values of Poisson's ratio  $\nu$  determined for tomato skin of Admiro variety with three other cultivars together:  $3\mu_{VA} - (\mu_{VE} + \mu_{VP} + \mu_{VS})$ .

Table 3. Confidence intervals for selected comparisons between the average values of Poisson's ratio  $\nu$  and Young's modulus  $E$

Comparison	Poisson's ratio $\nu$					
	Evaluation	SE	t	p	Confidence boundaries -95%	Confidence boundaries 95%
$\mu_{VE} - \mu_{VA}$	-0.606	0.048	-12.520	0.000	<b>-0.701</b>	<b>-0.511</b>
$\mu_{VS} - \mu_{VP}$	0.212	0.046	4.649	0.000	<b>0.122</b>	<b>0.302</b>
$3\mu_{VA} - (\mu_{VE} + \mu_{VP} + \mu_{VS})$	2.409	0.117	20.640	0.000	<b>2.179</b>	<b>2.639</b>
Young's modulus $E$						
$\mu_{EE} - \mu_{EA}$	8.951	0.584	15.340	0.000	<b>7.803</b>	<b>10.099</b>
$\mu_{ES} - \mu_{EP}$	4.677	0.559	8.365	0.000	<b>3.577</b>	<b>5.777</b>
$3\mu_{EE} - (\mu_{EA} + \mu_{EP} + \mu_{ES})$	31.737	1.424	22.287	0.000	<b>28.936</b>	<b>34.539</b>

All comparisons considering average Poisson's ratio  $\nu$  values as well as Young's modulus  $E$  averages proved to be significant (Tab. 3). The Encore variety turned out to be different from the other three cultivars in the respect of Young's modulus values.

Admiro variety showed to be significantly different from the other three cultivars in the respect of Poisson's ratio  $\nu$ .

Both the greenhouse and soil-grown tomato varieties differ significantly among themselves in terms of Poisson's ratio and Young's modulus values.

Table 4. Homogeneous averages groups of Poisson's ratio; HSD (unequal N); Homogeneous group,  $\alpha = 0.05$ ; Error: intergroup MS = 0.00616, df = 345 (degrees of freedom)

Cell number	Variety	Time	Poisson's ratio $\nu$	1	2	3	4	5	6	7
			Averages							
10	Polset	11	0.382	****						
11	Polset	4	0.421	****	****					
12	Polset	0	0.424	****	****					
9	Polset	14	0.451	****	****	****				
13	Surya	14	0.454	****	****	****				
16	Surya	0	0.470		****	****				
14	Surya	11	0.475		****	****	****			
7	Encore	4	0.489		****	****	****			
15	Surya	4	0.492		****	****	****			
5	Encore	14	0.505		****	****	****			
6	Encore	11	0.530			****	****			
8	Encore	0	0.555				****	****		
2	Admiro	11	0.637					****	****	
1	Admiro	14	0.650						****	****
3	Admiro	4	0.666						****	****
4	Admiro	0	0.733							****

Table 4 contains homogeneous average groups of Poisson's ratio  $\nu$  for four tested cultivars determined in four selected days of storage. Seven homogeneous groups were identified. Admiro Variety, characterized by the highest values of Poisson's ratio created two homogeneous groups while other groups were formed by the averages for two or three varieties. The largest group consists with averages for Encore, Polset and Surya varieties, where, in the majority, the Surya averages occur.

Table 5. Homogeneous averages groups of Young's modulus  $E$ ; HSD (unequal N); Homogeneous groups,  $\alpha = 0.05$ ; Error: intergroup MS = 0.00616, df = 345 (degrees of freedom)

Cell number	Variety	Time	$E$ Averages	1	2	3	4	5
11	Polset	12	2.297	****				
12	Polset	15	2.309	****				
10	Polset	5	2.803	****	****			
16	Surya	15	3.186	****	****	****		
9	Polset	1	3.360		****	****		
15	Surya	12	3.694		****	****	****	
2	Admiro	5	3.738		****	****	****	
4	Admiro	15	3.786			****	****	
3	Admiro	12	3.789		****	****	****	
13	Surya	1	3.991			****	****	
1	Admiro	1	4.149			****	****	
14	Surya	5	4.575				****	
5	Encore	1	5.879					****
6	Encore	5	5.944					****
7	Encore	12	6.073					****
8	Encore	15	6.517					****

The Tukey test (HSD) application allowed to distinguish five homogeneous averages groups of Young's modulus  $E$  for the four tested cultivars in four selected days of storage (Table 5). Encore variety, characterized by the highest values of Young's modulus parameter, created one homogeneous averages group. Other groups were formed by the averages for two or three varieties. The largest group consists of averages for Admiro, Polset and Surya varieties where, in the majority, the Admiro averages occur.

## CONCLUSIONS

1. Young modulus, Poisson's ratio, thickness and critical stress values determined for the skin of tested tomato cultivars differentiate significantly with the duration of storage time.
2. Designated strength parameters were significantly dependent on the tested variety.
3. Comparative analysis revealed much greater variation of Young's modulus and Poisson's ratio values for greenhouse tomato fruit than in the case of soil-grown cultivars.

## REFERENCES

1. Andrews J., Adams S. R., Burton K. S., Evered C. E. 2002.: Subcellular localization of peroxidase in tomato fruit skin and the possible implications for the regulation of fruit growth. *Journal of Experimental Botany* 53 (378), 2185-2191.
2. Bargel H., Neinhuis C. 2005.: Tomato (*Lycopersicon esculentum* Mill.) fruit growth and ripening as related to the biomechanical properties of fruit skin and isolated cuticle. *Journal of Experimental Botany* 56 (413), 1049-1060.
3. Dobrzański jr. B., Rybczyński R. 2008.: Właściwości fizyczne i biochemiczne materiałów roślinnych. Problemy pomiaru mechanicznych właściwości owoców w aspekcie oceny ich jędrności. Lublin: Wyd. Nauk. FRNA, Komitet Agrofizyki PAN.
4. Feller W. 1966. An introduction to probability theory and its applications”, 2, Wiley.
5. Geary R.C. 1930.: The Frequency Distribution of the Quotient of Two Normal Variates”. *Journal of the Royal Statistical Society* 93 (3), 442-446.
6. Gładyszewska B., 2007.: Method for testing selected mechanical properties of thin-film bio-materials (in Polish). *Rozprawy Naukowe* (325). Wydawnictwo Akademii Rolniczej, Lublin, 1-87.
7. Gładyszewska B. 2006.: Testing machine for assessing the mechanical properties of biological materials. *Technical Science* 9, 21-31.
8. Hinkelmann K. and Kempthorne O. 2008.: Design and Analysis of Experiments. Wiley.
9. Hinkley D. V. 1969. On the ratio of two correlated normal random variables. *Biometrika* 56 (3), 635-639.
10. Kuna - Broniowska I., Gładyszewska B., Ciupak A. 2011.: Storage temperature influence on Young modulus of tomato skin. *Teka Komisji Motoryzacji i Energetyki Rolnictwa – OL PAN*, (w druku).
11. Machado R. M., Rodriguez del Rincon A., Portas C. A. 1999.: Mechanical harvest of processing tomatoes: influence on percentage of damaged fruit and importance of the relation green fruit/rotten fruits. *Acta Horticulturae* 487, 237-241.
12. Mohsenin N. N. 1970.: Application of engineering techniques to evaluation of texture of solid food materials. *Journal of Texture Studies* 1, 133-154.
13. O'Brien M., Claypool L. L., Leonard S. J., York G. K., MacGillivray J. H. 1963.: Causes of fruit bruising on transport trucks. *Hilgardia* 35 (6), 113-124.
14. Peleg K. 1984.: A mathematical model produce damage mechanisms. *Transactions of the ASAE* 27 (1), 287-293.
15. Sargent S. A., Brecht J. K., Zoellner J. 1992.: Sensitivity of tomatoes at mature-green and breaker ripeness stages to internal bruising. *Journal of the American Society for Horticultural Science* 117 (1), 119-123.
16. Shapiro S. S., Wilk M. B. 1965.: An analysis of variance test for normality (complete samples). *Biometrika* 52 (3-4), 591-611.
17. Thode H. C. 2002.: Testing for normality. New York: Marcel Dekker.

PORÓWNANIE PARAMETRÓW WYTRZYMAŁOŚCIOWYCH SKÓRKI  
OWOCÓW POMIDORA SZKLARNIOWEGO I GRUNTOWEGO

**Streszczenie.** Praca zawiera wyniki badań dotyczących porównania wartości modułu Younga, naprężenia krytycznego, współczynnika Poissona i grubości skórki owoców pomidora szklarniowego odmian Admiro i Encore oraz gruntowego odmian Polset i Surya. W tym celu przeprowadzona została wielowymiarowa analiza wariancji



oraz testy jednowymiarowe (Hinkelmann 2008). Za pomocą kontrastów porównano odmiany szklarniowe z odmianami gruntowymi, przeprowadzono również porównania wewnątrz odmian szklarniowych i gruntowych. Wyznaczono także grupy jednorodne średnich wartości badanych parametrów skórki owoców pomidora.

**Słowa kluczowe:** skórka, owoc pomidora, moduł Younga, współczynnik Poissona, wielowymiarowa analiza wariancji, grupy jednorodne średnich.

## MECHANICAL PROPERTIES OF TEXTURE OF MIXED FLOUR BREAD WITH AN ADMIXTURE OF RYE GRAIN

Elżbieta Kusińska, Agnieszka Starek

Department of Food Engineering and Machinery, University of Life Sciences in Lublin, Poland,  
Doświadczalna 44, 20-236 Lublin, e-mail: elzbieta.kusinska@up.lublin.pl

**Summary.** The paper presents a comparison of the mechanical textural properties of mixed flour bread with an admixture of rye grain and without such an admixture (hardness, springiness, cohesiveness and chewiness) and its chemical properties (moisture and acidity). A discussion is given concerning the dough preparation and the baking of the bread. Additionally, based on sensory evaluation, the shelf life of the bread was determined, during which the bread is acceptable to the consumers.

**Key words:** mixed flour bread, textural properties, shelf life.

### INTRODUCTION

Bread is the most important food product and the most frequently consumed by man. Its unique sensory values caused that it is a universal food product, always up to date and irreplaceable [Adalla 1996].

The extensive range of consumers requires that the market is supplied with breads baked to varied recipes, as well as special and dietary breads [Diowksz 2010]. Mixed flour leaven-based bread, due to its sensory and nutritional values, is believed to be one of the best [Ambroziak 1988, Gąsiorowski 2004, Kot 2010, Piesiewicz 2008, Wojcieszak 1956].

The admixture of certain products to flour allows not only to produce bread with enhanced nutritional value, but also to develop a line of bakery products with health-promoting qualities [Bartnikowska 2007, Park Sang Ha and Morita 2004].

Nutrition and consumer studies show that an addition of rye grain to bread has many advantages. The grain is characterised by a high content of ballast substances, which determines its exceptional dietary value. The specific composition of rye has an effect on the intestinal flora and on optimum functioning of the digestive system. The consumption of rye bread, especially wholemeal, leads to the maintenance of optimum level of sugar in the blood [Staszewska 2008].

Next to the dietary values, the sensory traits are an important factor determining the acceptance of a product by consumers. Sensory evaluation plays a highly important role in the control of food quality [Pijanowski et al.]. Texture is a multi-parametric determinant of bakery products [Borowy and Kubiak 2010]. In certain cases it may even have a stronger effect on the consumer

than taste, flavour and colour [Szcześniak 1998]. Texture has also a high importance in transport and processing, as it determines the manner in which products can be handled [Brandt et al. 1963]. Thanks to studies of textural properties we can create better products that will be successful on the market [Pszczola 2009, Szcześniak 1977].

The texture of bread is the object of increasing interest of researchers from the field of bakery. It allows to obtain the most comprehensive estimation of bread quality [Surówka 2002].

Texture can be described in the physical sense as well as in the sensory one. In the physical sense, texture is the rheological property of products, comprising the relations of stress – strain – time [Billar 2005, Szcześniak 1963, 2002, Sherman 1970, ISO 1981]. In the sensory context, texture can be defined as a series of sensations or impression induced in the course of eating, related with the physical properties of the product [Korzeniowska-Ginter 2006, Marzec 2007].

### OBJECTIVE AND SCOPE OF STUDY

The objective of the study was the comparison of the textural properties of mixed flour bread with an admixture of rye grain and without such admixture, and determination of time of storage (shelf life) during which the bread is acceptable to the consumer. The scope of the study comprised the preparation and baking of the bread, determination of its mechanical properties, moisture and acidity, and sensory evaluation.

### METHOD

The experimental material was mixed flour bread and mixed flour bread with an admixture of rye grain. To obtain 10 kg of dough we used: 3.20 kg of wheat flour type 550, 1 kg of wholemeal wheat flour type 2000, 0.5 kg of wholemeal rye flour type 2000, 1.35 kg of rye leaven, 1.2 kg of rye grain, 50 g of salt and 8 g of instant yeast carefully dissolved in 3 l of water, and 225 ml of oil. The leaven was prepared earlier using rye flour type 2000 and water.

The rye grain was cooked in water and, after cooling down, kept under cover at temperature of 5°C for 24 hours. Dough was prepared with the two-phase method (intermediate). Flour to be used for bread baking was brought to ambient temperature and screened. Weighed portions were placed on a spiral mixer (model 15S). Next, yeast, salt, water and leaven were added, and mixed for 5 min using mixer speed of 110 min<sup>-1</sup>, then rye was added, and mixed for 3 min. at the same mixer speed. A control samples was prepared in an analogous manner (but without the addition of rye grain). The produced dough was divided into 1 kg portions and loaves were formed by hand (ten loaves each) in the form of dough balls; the loaves were placed in pans greased with edible oil. The height of dough in the pans was 70±3mm. Dough in the pans was covered with cloth and left for ca. 1 to rise. After that time the dough surface was wet with water and the pans were placed in the oven. The time of baking was 25 minutes at temperature of 180°C, and additionally 10 min. at 210°C. After taking the pans out of the oven, the surface of the loaves was again wet with water, and taken out of the pans. The bread was then left for 24 hours at ambient temperature without covering. Two loaves each (with and without rye grain addition) were subjected to textural and physicochemical tests on the same day. The remaining loaves were sealed in polyethylene bags and stored in a controlled climate chamber at 16°C. The analyses were repeated for the subsequent 4 days.

Instrumental analysis of the product studied was conducted using the texture tester TA.XT plus, coupled with a computer. The samples were cubes cut out from the bread crumb, with side of 2 cm (10 each from every loaf). The samples were subjected to double compression at tester head

travel speed of  $50 \text{ mm} \cdot \text{min}^{-1}$ . The compression process was conducted at constant deformation of the samples, of 50% of their height, with intervals between compression series being 5 s.

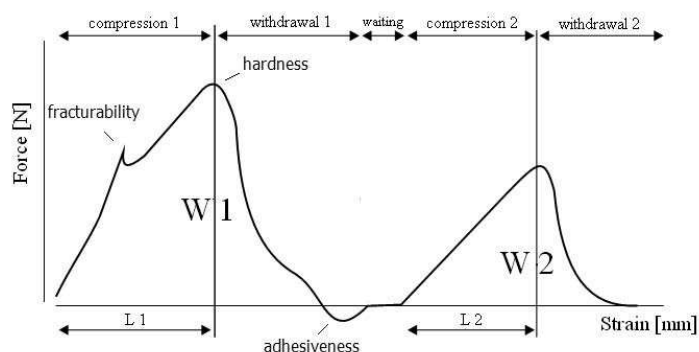


Fig. 1. Example of a graph obtained in the double compression test (TPA)

The TPA graphs (Fig. 1) were used for direct reading or for calculation of the following mechanical properties of the material tested:

- hardness [N], i.e. the maximum force during the first cycle of compression,
- springiness [-], that characterises the degree of recovery of the initial form; it is the quotient of sample deformations during the first and second compression ( $Spr=L2/L1$ ),
- cohesiveness [-], characterising the forces of internal bonds that hold the product in one piece; it is the quotient of the areas beneath the graphs of forces of the first and second compression of the sample ( $Koh=W2/W1$ ),
- chewiness [N], which is a measure of force required to chew a bite of food to make it ready for swallowing; it is defined as the product of hardness, cohesiveness and springiness.

The breads were also subjected to sensory evaluation in accordance with the standard PN-A-74252 [1998].

Measurements of acidity and moisture of the bread crumb were conducted in conformance with the standard PN-A-74108 [1996].

## RESULTS

The effect of rye grain addition on the textural properties of the bread is presented in Fig. 2-5.

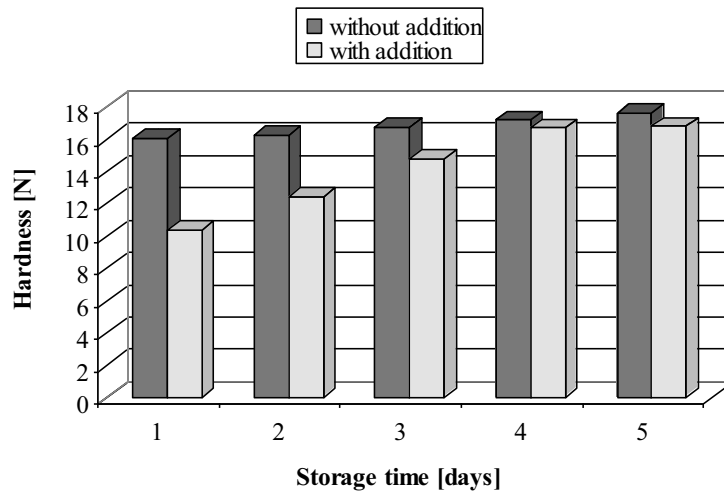


Fig. 2. Hardness of mixed flour bread without [ $H_1$ ] and with an admixture of rye grain [ $H_2$ ] versus time of storage

The relations presented in the Figure are described with equations (1) and (2):

$$H_1 = 0.407t + 15.533, \quad (1)$$

$$R^2 = 0.99,$$

$$H_2 = 10.25t^{0.323}, \quad (2)$$

$$R^2 = 0.98.$$

As can be seen from Fig. 2, after 1 day of storage the hardness of the bread without an admixture of rye grain was higher than of that of the bread with rye grain by 58%. Extension of the time of storage caused a reduction of the difference between the hardness levels of both products. The level of hardness of the bread with an admixture of rye grain increased with extension of storage time to 4 days. The value of that trait after 1 day from baking was 10.36 N, and after 5 days - 16.80 N. Whereas, the increase in the hardness of the bread without rye grain was slight, followed a linear function, and the value of that trait varied from 16.02 after 1 day of storage to 17.59 N after 5 days from baking. The equations describing the changes in bread hardness have a very high value of the coefficient of determination.

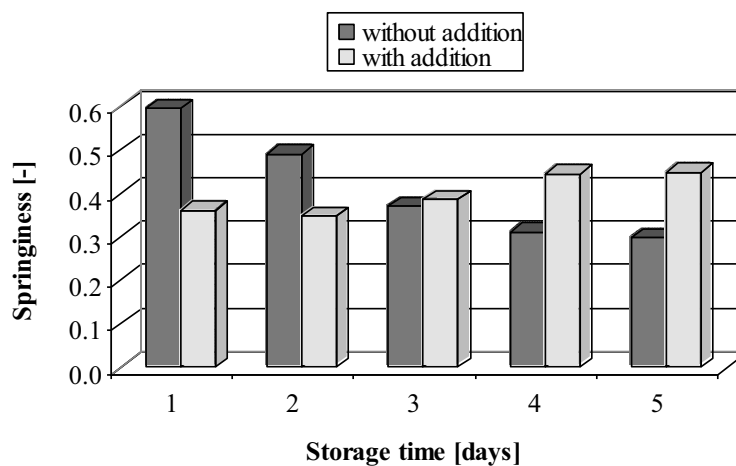


Fig. 3. Springiness of mixed flour bread without [ $Spr_1$ ] and with an admixture of rye grain [ $Spr_2$ ] versus time of storage

The relations presented in the Figure are described by equations (3) and (4):

$$Spr_1 = -0.1984 \ln(t) + 0.603, \quad (3)$$

$$R^2 = 0.98,$$

$$Spr_2 = 0.0039t^2 + 0.0041t + 0.3428, \quad (4)$$

$$R^2 = 0.86.$$

As follows from Fig. 3, presenting changes of springiness of mixed flour bread, the springiness of the bread without any admixture of rye grain decreased with extension of storage time, while that of the bread with such an admixture increased. The springiness of the bread without rye grain, after 1 day, was higher than that of the bread with an admixture of the grain (by 0.24). The value of that trait after 1 day from the time of baking was 0.57, and after 5 days – 0.29. Whereas, the springiness of the bread with an admixture of rye grain initially stayed at a constant level; an increase in the value of that trait was noted after 3 days from baking. The difference in springiness between breads tested after 2 and 3 days amounted to 0.04. Extension of the time of storage by another day caused further increase of springiness by 0.06, while after additional 24 hours the value of the trait was at the same level.

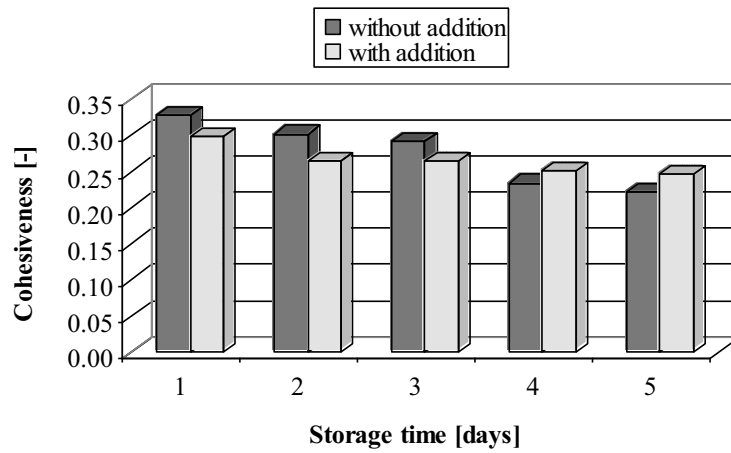


Fig. 4 presents the results of measurements of cohesiveness

Fig. 4. Cohesiveness of mixed flour bread without [ $Coh_1$ ] and with an admixture of rye grain [ $Coh_2$ ] versus time of storage

The relations presented in the Figure are described by equations (5) and (6):

$$Coh_1 = -0.0016t^2 - 0.0196t + 0.348, \quad (5)$$

$$R^2 = 0.95,$$

$$Coh_2 = 0.2955t^{-0.1163}, \quad (6)$$

$$R^2 = 0.96.$$

After 1 day of storage the cohesiveness of the bread without an admixture of rye grain was higher by 9% than that of the bread with such an admixture. The values of that trait decreased with the passage of time (from 1 to 5 days) for the bread without an admixture of rye grain, from 0.33 to 0.22. In the case of bread baked with an admixture of rye grain, the decrease in the level of cohesiveness was less pronounced, the difference between the product tested after 1 day from baking and that examined after 5 days of storage being 0.05.

Changes in the chewiness of the breads are illustrated in Fig. 5.

The chewiness of the mixed flour bread without rye grain, after 1 day, was higher than that of the bread enriched with that component. The difference was high at 2.5 N. In the case of the bread baked without an admixture of the grain the value of chewiness decreased with the time of storage.

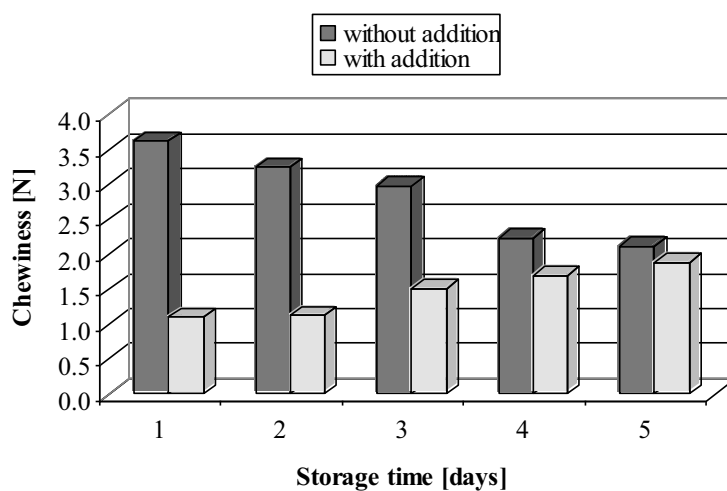


Fig. 5. Chewiness of mixed flour bread without [ $Ch_1$ ] and with an admixture of rye grain [ $Ch_2$ ] versus time of storage

The relations presented in the Figure are described by equations (7) and (8):

$$Ch_1 = 0.0043t^2 + 0.4279t + 4.0766, \quad (7)$$

$$R^2 = 0.96,$$

$$Ch_2 = 0.0088t^2 + 0.1601t + 0.8863, \quad (8)$$

$$R^2 = 0.95.$$

On the first and second day no significant differences were noted between the levels of chewiness of the bread with an admixture of rye grain. Further extension of storage time caused a significant increase in the level of chewiness, up to the value of 1.88 N.

Statistical analysis revealed that the obtained values of all mechanical properties of the breads were significantly related with the time of storage and with the recipe.



The results of assays of the chemical properties are presented in Fig. 6 and 7.

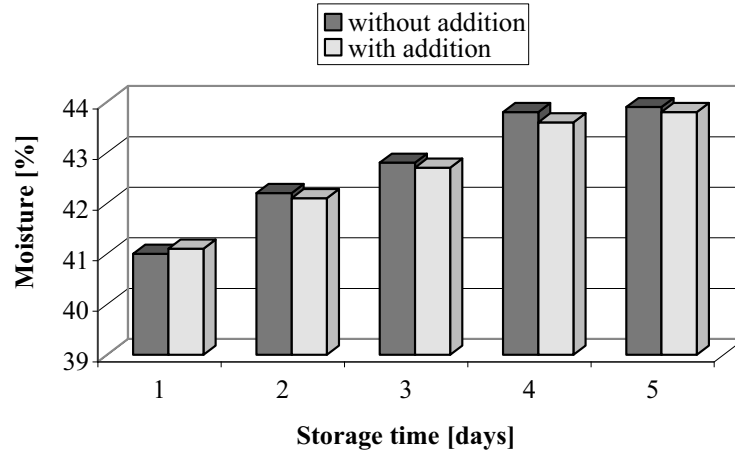


Fig. 6. Moisture content of mixed flour bread without [ $M_1$ ] and with an admixture of rye grain [ $M_2$ ] versus time of storage

The relations obtained are described by equations (9) and (10):

$$M_1 = 1.8744 \ln 9(t) + 40.945, \quad (9)$$

$$R^2 = 0.98,$$

$$M_2 = 0.69t + 40.59, \quad (10)$$

$$R^2 = 0.97.$$

The moisture content of both breads on particular days was at a similar level, with no significant differences. With the passage of the time of storage there was a slight increase, from about 41 to 43.9%, that being an effect of the tight sealing of the breads and their fermentation.

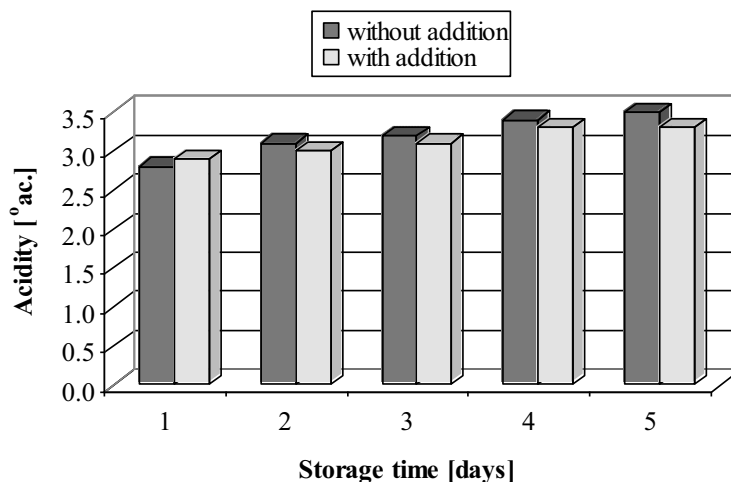


Fig. 7. Acidity of mixed flour bread without  $[A_1]$  and with an admixture of rye grain  $[A_2]$  versus time of storage

The relations presented in the Figure are described by equations (11) and (12):

$$A_1 = 0.17t + 2.69, \quad (11)$$

$$R^2 = 0.96,$$

$$A_1 = -0.0071t^2 + 0.1529t + 2.74, \quad (12)$$

$$R^2 = 0.95.$$

The acidity of both breads on particular days was at a very similar level, with no significant differences. During the storage the value of acidity increased from about 2.8 to 3.5° ac.

The sensory assessment ratings of the quality of the breads showed that the highest – first – level of quality was awarded to the bread without an admixture of rye grain on the first day after baking (33 points). On the second day the quality of that bread dropped to the second level (30 p.). Further storage of the bread resulted in a gradual decrease in its quality to the third level (25 p.). Notably better ratings were awarded to the bread with an admixture of rye grain. Up till the third day it was rated in the first class of quality (33 points), and on the fifth day it was classified in class two (29 p.). That bread can be stored for longer periods of time. It retains its freshness longer.

Using the instrumental analysis one can largely eliminate the sensory evaluation of bread, that being time-consuming and not overly objective. Control of the mechanical parameters of bread allows the estimation of the quality of the product, as it largely correlates with the sensory evaluation.

## CONCLUSIONS

1. The recipe of the breads and their storage time had a significant effect on the studied mechanical properties and on their sensory evaluation.

2. The bread with an admixture of rye grain had lower hardness and chewiness, which is a positive feature. The values of those traits increased with the time in storage.

3. In the course of storage, the admixture of rye grain caused a decrease in the springiness and cohesiveness, and an increase in the chewiness of the product. The mean values of those parameters after 1 day of storage were from 0.361, 0.299 and 1.104 N, respectively, for samples of bread with an admixture of rye grain, to 0.596, 0.327 and 3.625 N in the case of bread without that admixture.

4. Storage caused an increase in the moisture content and in the acidity of the breads.

5. Most recommended is the bread with an admixture of rye grain during the first three days of storage, and the bread without such an admixture during the first two days from baking.

6. Using instrumental analysis one can largely eliminate the sensory evaluation of bread, that evaluation being time-consuming and not really objective.

## REFERENCES

1. **Adalla M.**, 1996.: Chleb na Bliskim Wschodzie – wczoraj i dziś. *Przegląd Piekarski i Cukierniczy*, 22-23.
2. **Ambroziak Z.**, 1988.: *Piekarstwo i ciastkarstwo*. Wydawnictwo Naukowo-Techniczne, W-wa.
3. **Bartnikowska E.**, 2007.: Dodatki do pieczywa o działaniu prozdrowotnym. *Przegląd Piekarski i Cukierniczy*, 8, 6-8.
4. **Biller B.** 2005.: *Technologia Żywności- Wybrane zagadnienia*, SGGW, Warszawa.
5. **Borowy T., Kubiak M.**, 2010.: Tekstura wyróżnikiem jakości produktów piekarskich i cukierniczych. *Cukiernictwo i Piekarstwo*, 10, 33-36.
6. **Brandt M.A., Skinner E.Z., Coleman J.A.**, 1963.: Texture profile metod. *Journal Food Science*, 28, 404-409.
7. **Diowski A.**, 2010.: Pieczywo jako żywność funkcjonalna. Cz.II. Pieczywo dietetyczne. *Przegląd Piekarski i Cukierniczy*, 10, 12-14.
8. **Gąsiorowski H.**, 2004.: *Pszenica. Chemia i Technologia*. Państwowe Wydawnictwo Rolnicze i Leśne, Poznań.
9. **ISO**, 1981.: *Sensory Analysis Vocabulary, Part 4*, Genewa, Switzerland.
10. **Korzeniowska-Ginter R.**, 2006.: Wpływ jakości mąki tortowej na cechy biszkoptu. *Żywność, Nauka, Technologia, Jakość*, 37, 30-33.
11. **Kot M.**, 2010.: Kontrola procesu produkcji i ocena jakości pieczywa. *Przegląd Piekarski i Cukierniczy*, 2, 6-10.
12. **Marzec A.**, 2007.: Tekstura żywności. *Przemysł Spożywczy*, 5, 6-10.
13. **Park Sang Ha, Morita N.**, 2004.: Effect of enzymes on the dough properties and bread quality of wheat flour partly substituted for amaranth flour. *Food Science and Technology Research*, 10(2), 127-133.
14. **Piesiewicz H.**, 2008.: Nasz polski chleb powszedni-mieszany. *Przegląd Piekarski i Cukierniczy*, 9, 13-17.
15. **Pijanowski E., Dłużewski M., Dłużewska A., Jarczyk A.**, 1996.: *Ogólna Technologia Żywności*. WNT, Warszawa.
16. **PN-A-74108**, 1996.: *Pieczywo. Metody badań*. Polski Komitet Normalizacyjny.
17. **Pszczoła D.**, 2009.: Hooked on a mouthfeelind. *Food Technology*, 9,47-57.
18. **Sherman P.**, 1970.: *Industrial rheology*. Acad. Press, London.
19. **Staszewska E.**, 2008.: Żyto i produkcja pieczywa żytniego. *Przegląd Piekarski i Cukierniczy*, 11, 26-29.
20. **Surówka K.**, 2002.: Tekstura żywności i metody jej badania. *Przemysł Spożywczy*, 10, 12-17.

21. **Szcześniak A.S.**, 2002.: Texture is a sensory property. *Food Quality and Preference*, 13, 215- 225.
22. **Szcześniak A.S.**, 1998.: Sensory texture profiling-historical and sensory perspectives. *Food Technology* Vol. 52, No. 8, 54-57.
23. **Szcześniak A.S.**, 1977.: An overview of recent advances in food texture research. *Food Technology*, 31(4), 71-73.
24. **Wojcieszak P.** 1956.: *Fermentacja ciasta*. Wydawnictwo Przemysłu Lekkiego i Spożywczego.

#### MECHANICZNE WŁAŚCIWOŚCI TEKSTURY CHLEBA MIESZANEGO Z DODATKIEM ZIARNA ŻYTA

**Streszczenie.** W pracy porównano mechaniczne właściwości teksturalne pieczywa mieszanego z dodatkiem ziarna żyta i bez jego dodatku (twardość, sprężystość, kohezynność i żujność) oraz właściwości chemiczne (wilgotność i kwasowość). Omówiono przygotowanie ciasta i wypiek chleba oraz określono na podstawie oceny sensorycznej czas przechowywania, w którym pieczywo jest akceptowane przez konsumenta.

**Słowa kluczowe:** chleb mieszany, właściwości teksturalne, czas przechowywania.

## BAYESIAN NETWORKS AS KNOWLEDGE REPRESENTATION SYSTEM IN DOMAIN OF RELIABILITY ENGINEERING

Andrzej Kusz, Piotr Maksym, Andrzej W. Marciniak

University of Life Sciences in Lublin  
Department of Technology Fundamentals

**Summary.** The paper presents Bayesian Networks (BNs) in the context of methodological requirements for building knowledge representation systems in the domain of reliability engineering. BNs, by their nature, are especially useful as a formal and computable language for modeling stochastic and epistemic uncertainty intrinsically present in conceptualization and reasoning about reliability.

**Key words:** reliability models, probabilistic networks, Bayesian networks, knowledge representation system.

### INTRODUCTION

Expressiveness of Bayesian networks (BNs) is sufficient for modeling a wide class of systems that involve uncertainty [1, 2, 3]. Bayesian networks are already accepted as a useful modeling framework that is particularly well suited for reliability applications [4, 5]. The proposal of using BNs as a framework for reliability analysis has initiated a research trend of building BNs corresponding to and comparing with classical reliability formalisms. Features regarding both modeling as well as analysis of reliability block diagrams [6, 7] and fault-trees [8, 9, 10] have been compared to BNs, and it has been showed that BNs have significant advantages over the traditional frameworks [5, 11].

The aim of the paper is the presentation of methodology of building BNs reliability models as a process of translating reliability models represented in classical forms like block diagram, event trees, and fault trees to representation language based on Bayesian network. The reason for BN as reliability knowledge representation language comes from knowledge engineering approach where models are treated as formal and computational symbolic system [12]. Reliability models to be knowledge representation system should have property of being built and adapted with machine learning methods based on empirical data. The second requirement is possibility of functioning as a knowledge base, i.e. answering questions using probabilistic inference algorithms.

Application of BN in modelling both static and dynamic problems in reliability engineering is already well grounded. Authors showed on examples that BN language is at least as expressive as other formal systems used in reliability engineering.

## RELIABILITY MODELS AND THEIR BNS REPRESENTATION

Knowledge engineering approach to BN as knowledge representation symbolic system is exemplified as translation of structural reliability models like series, parallel, mixed, bridge and k-out-of-n structures to equivalent Bayesian networks and using them as questions answering system.

Let's assume a system that consists of  $n$  components each of them is non-renewable after failure and its reliability state is described by two-state random process:

$$X_{e_i}(t) = \begin{cases} 1 & \text{if component } e_i \text{ is in operating state at time } t, \\ 0 & \text{in failed state.} \end{cases} \quad t \geq 0, i = 1, 2, \dots, n \quad (1)$$

Reliability function of  $i$ -th component is defined as probability of random event, where is random variable representing time to failure of component, or alternately as expected value of:

$$R_i(t) = P\{\xi_i > t\} = EX_{e_i}(t); \quad i = 1, 2, \dots, n; \quad t \geq 0. \quad (2)$$

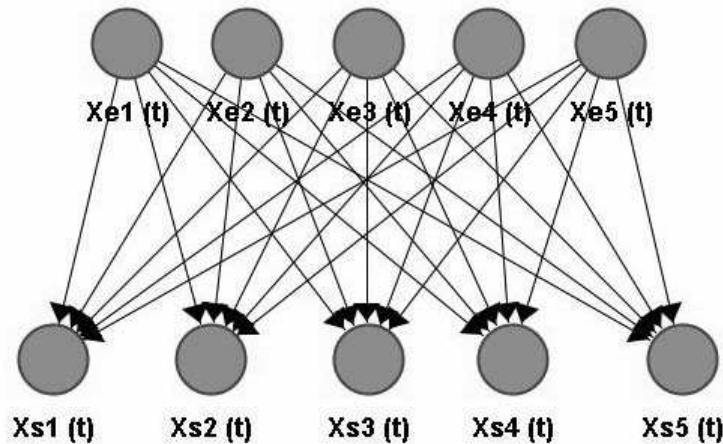
State of the system is a binary valued function (structure function)  $\varphi(\mathbf{X}(t))$  of its components states:  $\mathbf{X}(t) = (X_{e_1}(t), X_{e_2}(t), \dots, X_{e_n}(t))$ ;

$$\varphi(\mathbf{X}(t)) = \begin{cases} 1 & \text{if system is operable at time } t, \\ 0 & \text{in failed state.} \end{cases} \quad t \geq 0, i = 1, 2, \dots, n \quad (3)$$

Then system reliability is expressed as:

$$R_s(t) = E\varphi(\mathbf{X}_t). \quad (4)$$

All possible reliability structures can be represented as a single Bayesian network with root nodes representing state of components  $X_{e_i}(t)$  for required operation time (mission time)  $t \geq 0$  and target node representing state of system structure expressed as Boolean function of components states. Example BN representing the following reliability structures: S1 – series, S2 – parallel, S3 – “k-out-of-n”, S4 – bridge, S5 – mixed is shown on Fig. 1.



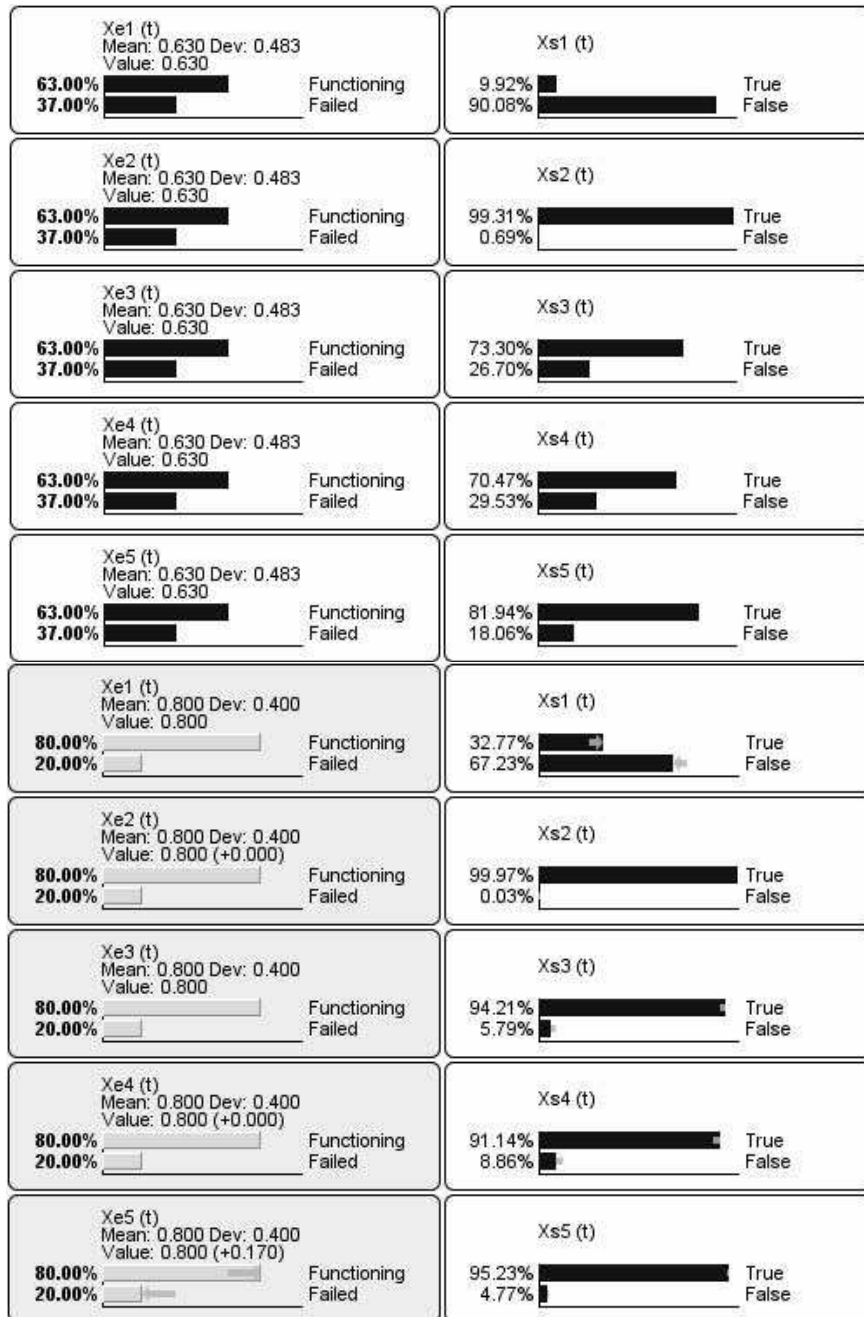


Fig. 1. Bayesian network representing reliability structures (a) and an example of inference (b)

Since BN representing structures contain nodes with conditional probability distribution defined as Boolean structure functions. Figure 1 presents inference to answer a question of how

changes the structure reliability when changing components reliability. For example, if we increase all components reliability (for a fixed mission time  $t$ ) from 0.63 to 0.8 then the structures reliability  $R_{s1}, R_{s2}, \dots, R_{s5}$  increases accordingly:  $0.099 \rightarrow 0.328$ ,  $0.993 \rightarrow 0.999$ ,  $0.733 \rightarrow 0.942$ ,  $0.747 \rightarrow 0.914$ ,  $0.819 \rightarrow 0.952$ .

For presentation system reliability as a function of its components reliability and a mission time we used dynamic BN with two time steps (Fig. 2).

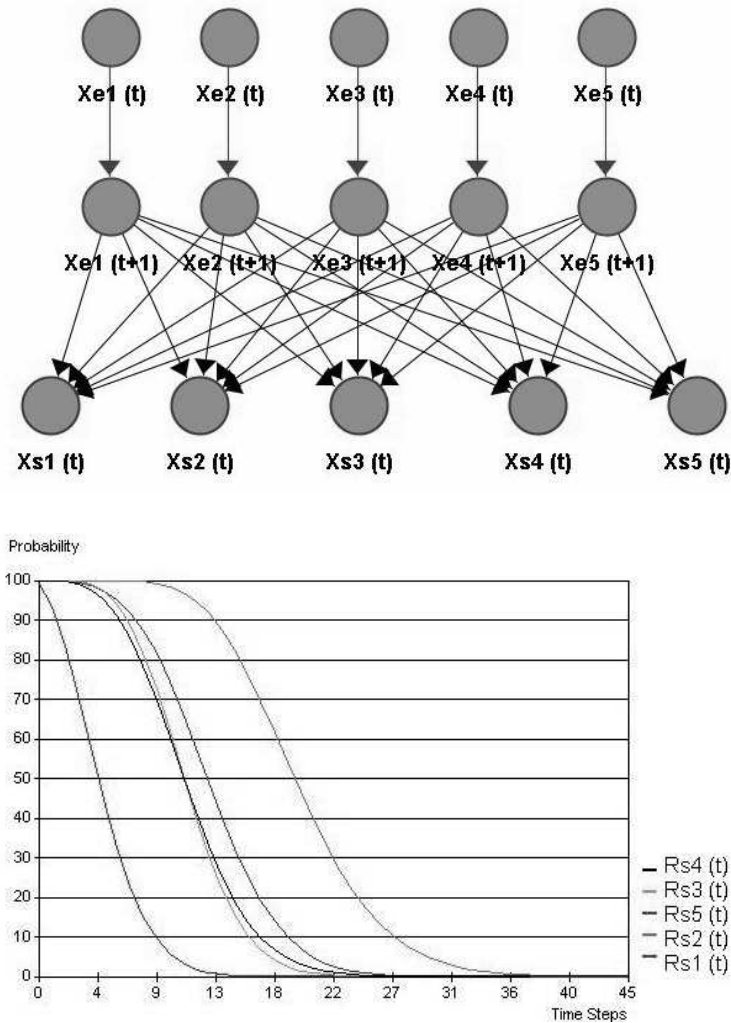


Fig. 2. Dynamic Bayesian network representing system (structure) reliability as a function of components reliability and a function of required operation time

The next figure (Fig. 3) presents a model where reliability is computed for random mission time. Corresponding BN is completed with node representing mission time of each element (not necessarily the same).



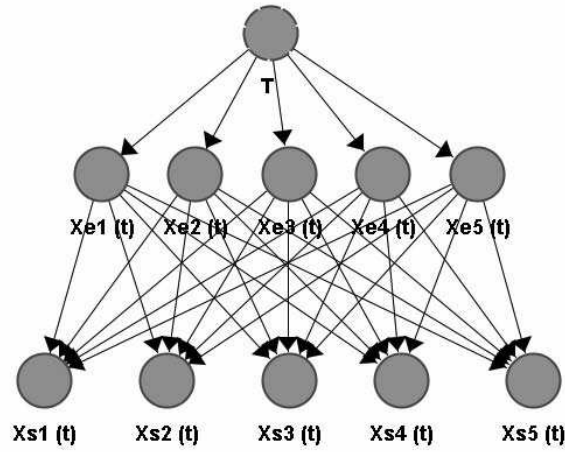


Fig. 3. Bayesian network representing system reliability for random mission time

Similarly simple is translation the event tree or failure tree models to equivalent Bayesian network models. It can be done by implementation in BN the logic gates used in ET or FT models [17], (Fig. 4).

$X_s = X_{e1} \text{ OR } X_{e2}$		<table border="1"> <thead> <tr> <th>B</th> <th>Xe1</th> <th>B</th> <th>Xe2</th> </tr> </thead> <tbody> <tr> <td>0</td> <td>20%</td> <td>0</td> <td>20%</td> </tr> <tr> <td>1</td> <td>80%</td> <td>1</td> <td>80%</td> </tr> </tbody> </table> <table border="1"> <thead> <tr> <th>B</th> <th>Xe1 OR Xe2</th> </tr> </thead> <tbody> <tr> <td>0</td> <td>4%</td> </tr> <tr> <td>1</td> <td>96%</td> </tr> </tbody> </table>	B	Xe1	B	Xe2	0	20%	0	20%	1	80%	1	80%	B	Xe1 OR Xe2	0	4%	1	96%
B	Xe1	B	Xe2																	
0	20%	0	20%																	
1	80%	1	80%																	
B	Xe1 OR Xe2																			
0	4%																			
1	96%																			
$X_s = X_{e1} \text{ AND } X_{e2}$		<table border="1"> <thead> <tr> <th>B</th> <th>Xe1</th> <th>B</th> <th>Xe2</th> </tr> </thead> <tbody> <tr> <td>0</td> <td>20%</td> <td>0</td> <td>20%</td> </tr> <tr> <td>1</td> <td>80%</td> <td>1</td> <td>80%</td> </tr> </tbody> </table> <table border="1"> <thead> <tr> <th>B</th> <th>Xe1 AND Xe2</th> </tr> </thead> <tbody> <tr> <td>0</td> <td>36%</td> </tr> <tr> <td>1</td> <td>64%</td> </tr> </tbody> </table>	B	Xe1	B	Xe2	0	20%	0	20%	1	80%	1	80%	B	Xe1 AND Xe2	0	36%	1	64%
B	Xe1	B	Xe2																	
0	20%	0	20%																	
1	80%	1	80%																	
B	Xe1 AND Xe2																			
0	36%																			
1	64%																			
<p>Fault - Tree OR Gate</p>	<p>Bayesian Network OR Node</p>	<p>Conditional probability distribution</p>																		
<p>Fault - Tree AND Gate</p>	<p>Bayesian Network AND Node</p>	<p>Conditional probability distribution</p>																		

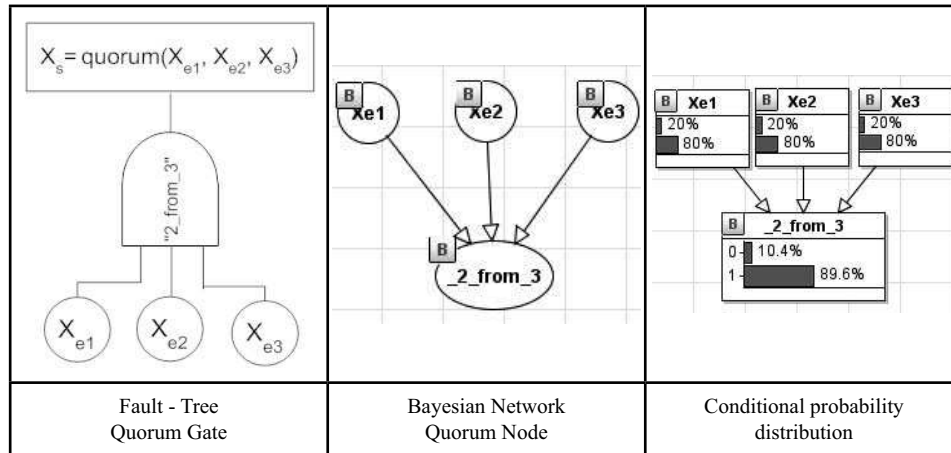


Fig. 4. Bayesian networks equivalents of Fault-Tree logic gates

Root nodes, in the BN terminology, correspond to the fault tree basic events. The undesired Top Event is represented in the BN model as a leaf node (i.e., a node without descendants)

Normal logic gate represents element failure when all its causes are known. In FTA and MFA, events aren't necessarily concerned with failed elements but can represent other events which only cause or contribute to system components failure. In that case, using BN as a model allows representing epistemic uncertainty being result of incomplete knowledge of all events that can influence resulting failures as their consequence. It can be done by modification the logic gates using Boolean gates with leakage. The effect of using Noisy-OR logic gate [2, 13, 14] is shown on Fig.5.

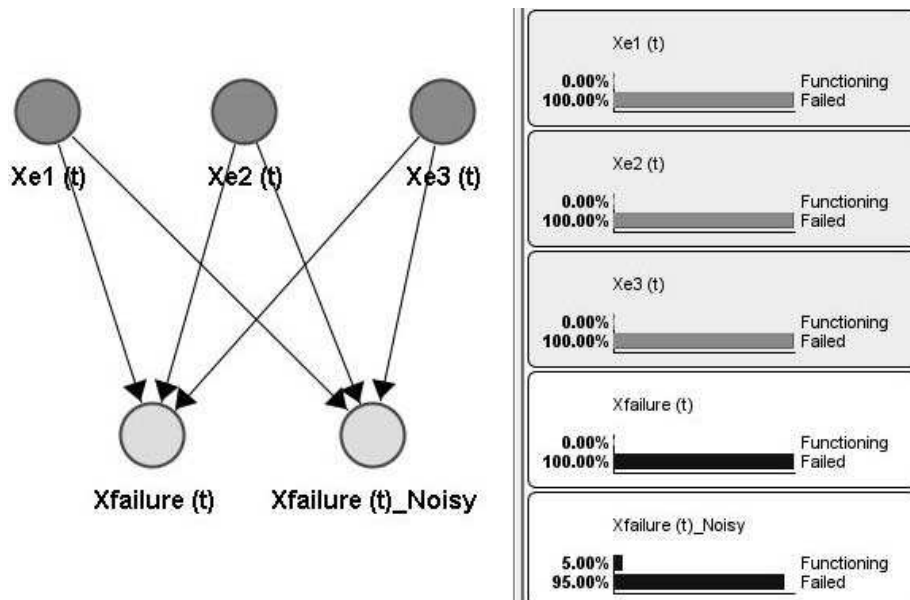


Fig. 5. Bayesian network representing epistemic uncertainty using Noisy-OR gate

Noisy logic function is a very constructive formalism for modelling diagnostic problems and diagnostic reasoning, [14, 15, 16].

## CONCLUSIONS

Application of Bayesian networks as reliability knowledge representation language unifies the reliability models building methods. Expressiveness of BN language is higher than probabilistic Boolean logic. Resulting BNs reliability models are automatically adaptable to new data using machine learning methods and efficient inference algorithms enable automate predictive and diagnostic reasoning. It would be very interesting to explore extended conceptualisations of reliability problems expressed in first-order logic Bayesian networks, [18,19,20].

## REFERENCES

1. Pearl J. (1986): Fusion, Propagation, and Structuring in Belief Networks. *Artificial Intelligence* 29(3), 241-288.
2. Pearl J. (1988): Probabilistic Reasoning in Intelligent Systems: Network of Plausible Inference. Morgan Kaufmann.
3. Halpern J., Y. (2005): Reasoning about uncertainty. The MIT Press Cambridge, Massachusetts, London.
4. Barlow RE.: Using influence diagrams. In: Clarotti CA, Lindley DV, editors. Accelerated life testing and experts' opinions in reliability; 1988. p. 145-57.
5. Langseth H., Portinale L., 2007.: Bayesian networks in reliability. *Reliability Engineering and System Safety* 92 (2007) 92-108.
6. Martz HF, Waller RA.: Bayesian reliability analysis of complex series/parallel systems of binomial subsystems and components. *Technometrics* 1990;32(4):407-16.
7. Torres-Toledano JG, Sucar LE.: Bayesian networks for reliability analysis of complex systems. *Lecture notes in artificial intelligence*, vol. 1484. Berlin, Germany: Springer; 1998.p. 195-206.
8. Solano-Soto J, Sucar, LE.: A methodology for reliable system design. In: Proceedings of the 4th international conference on industrial and engineering applications of artificial intelligence and expert systems. *Lecture notes in artificial intelligence*, vol. 2070. Berlin, Germany: Springer; 2001. p. 734-45.
9. Portinale L, Bobbio A.: Bayesian networks for dependability analysis: an application to digital control reliability. In: Proceedings of the fifteenth conference on uncertainty in artificial intelligence. San Francisco, CA: Morgan Kaufmann Publishers; 1999. p. 551-8.
10. Bobbio A, Portinale L, Minichino M, Ciancamerla E.: Improving the analysis of dependable systems by mapping fault trees into Bayesian networks. *Reliab Eng Syst Saf* 2001;71(3):249-60.
11. Tchangani AP.: Reliability analysis using Bayesian networks. *Stud. Inform. Control* 2001;10(3):181-8.
12. Sowa J., F. (2000): Knowledge representation, Logical, Philosophical, and Computational Foundations. Brooks/Cole.
13. Henrion M. (1986): Some practical issues in constructing belief networks. In L. N. Kanal, T. S. Levitt, and J. F. Lemmer, editors, *Uncertainty in Artificial Intelligence* 3, pages 161-173. North-Holland, Amsterdam, 1989.

14. Agosta J. M. (1991).: Conditional inter-causally independent node distributions, a property of “noisy-or” models. In Proc. Conf. on Uncertainty in Artificial Intelligence, pp. 9–16, San Francisco, 1991. Morgan Kaufmann.
15. Agosta J. M., Gardos T. (2004).: Bayes Network “Smart” Diagnostics. Intel Technology Journal, Volume 8, Issue 4, 2004.
16. Oniśko A., Marek J. Druzdzel M. J. Wasyluk H. (2001).: Learning Bayesian network parameters from small data sets: Application of noisy-or gates. International Journal of Approximate Reasoning, 27(2):165–182, 2001.
17. Vesely W., E., Goldberg F., F. et al. (1981).: Fault Tree Handbook. Systems and Reliability Research, Office of Nuclear Regulatory Research, U.S. Nuclear Regulatory Commission.
18. Poole, D., 2003.: „First-Order Probabilistic Inference.” Proceedings of the Eighteenth International Joint Conference on Artificial Intelligence.
19. Laskey K.B. (2007).: MEBN: A Language for First-Order Bayesian Knowledge Bases. Artificial intelligence 172(2-3).
20. Haenni R. (et al.) (2010).: Probabilistic Logic and Probabilistic Networks. Springer.

#### SIECI BAYESOWSKIE JAKO SYSTEM REPREZENTACJI WIEDZY W DZIEDZINIE INŻYNIERII NIEZAWODNOŚCI

**Streszczenie.** W artykule przedstawiono sieci bayesowskie (BNs) w kontekście wymogów metodologicznych do budowy systemów reprezentacji wiedzy w dziedzinie inżynierii niezawodności. Ze swej natury, sieci bayesowskie, są szczególnie przydatne jako formalny i obliczalny język do modelowania niepewności stochastycznej i epistemicznej. Takie rodzaje niepewności są istotną cechą konceptualizacji i rozumowania o niezawodność.

**Słowa kluczowe:** modele niezawodnościowe, sieci probabilistyczne, sieci bayesowskie, system reprezentacji wiedzy.

## OPERATING COSTS OF FARM BUILDINGS IN SELECTED ECOLOGICAL HOLDINGS

Urszula Malaga-Toboła

Institute of Agricultural Engineering and Informatics  
University of Agriculture in Krakow  
urszula.malaga-tobola@ur.krakow.pl

**Summary.** The aim of the article was to specify and analyze the replacement value of farm buildings and the annual and unitary costs of their operation in terms of labor productivity. For comparative analysis of the test objects, these objects were divided into area groups: to 10 ha, from 10.01 to 20.00 ha and above 20 ha of arable land. The scope of research included organic farms located in the mountain region specializing in livestock production.

**Keywords:** operating costs, farm buildings, organic farms, area groups, labor productivity.

### INTRODUCTION

One of the factors of production is capital, whose components are: working capital and assets capital, including buildings and structures. In order to be able to run efficient production processes, holdings must have livestock buildings, other buildings and warehouses adapted to the size and type of business and for the stored material [Tabor, Malaga-Toboła 2004; Tabor, Kuboń 2004; Kuboń 2006; Malaga-Toboła 2009]. In light of the ongoing structural changes and the possibility of implementing new technologies in agricultural production, especially livestock production, there is a natural need to balance the building stock and assess their technical and technological state. The demand for the various production buildings mainly determines the direction and the specialization of production. Holdings specializing in crop production are investing in barns, warehouses, sheds and silos. Horticultural farms - in warehouses, storehouses and sheds. However, holdings specializing in breeding and raising animals are building or modernizing production facilities, primarily cowsheds, piggeries and barns [Lorencowicz, Włodarczyk 2009]. The investment decisions of the farmers are influenced by the support for agriculture from both domestic and European legislation. It is expected that, thanks to the EU funds, the period of 2007-2013 financing will increase the level of construction investment in the countryside. This is confirmed by data from the first half of 2007, where the number of granted building permits for agricultural buildings was already 26.4% higher than in the corresponding period the previous year and continues to grow [Traffic Building ... 2008, 2010].

## PURPOSE, SCOPE AND METHODOLOGY OF WORK

Livestock is becoming a very attractive and effective method of improvement of the economic efficiency of organic farms, especially now in the era of increased interest in the quality of animal products, especially dairy production. However, wishing to acquire high-quality raw materials, breeding systems should be implemented in functional buildings, ensuring the welfare of animals. Buildings should be designed and implemented in accordance with the standards of technology and technological systems used in animal husbandry and should also minimally threaten the environment [Romaniuk and others 2007].

The aim of this study was therefore to determine the status of farm buildings in terms of number, age, size, and cost analysis of their operation, in terms of labor productivity and arable land.

The scope of study covered 25 ecological buildings, specializing in livestock production, mainly in milk production. Farms were located in the mountain region, in Hańczowa.

The study was conducted through interviews with the owners of the holdings. The information collected in order to achieve the goal of the work included: kinds of buildings, their surfaces, building material, material and energy inputs and also the volume of production and labor productivity. The data concerned the year 2010.

For comparative analysis, the surveyed holdings were divided into 2 groups, taking as the criterion for allocation the arable area (UAA). There were 7 objects with the area of 10 ha, 10 holdings from 10.01 to 20 ha and 8 with the area of more than 20 ha.

The buildings were divided into: livestock buildings, which included barns, piggeries and poultry houses, bifunctional buildings, warehouses, which also included barns, storages and refrigerators, garages and sheds, silos and dryers.

Replacement value of buildings was identified as the product of the surface and the current unitary cost of its construction, which was adopted by the current tables of PZU (Polish Insurance). The operating costs of production buildings and warehouses included amortization, insurance, electricity consumption, and repairs and maintenance [Kuboń 2007, Michałek et al. 1998]. Amortization was calculated as the ratio of the replacement value of buildings for the period of amortization, insurance costs were adopted on the basis of evaluation of buildings for insurance purposes (PZU 2010.), And the costs of electricity consumption, repairs and maintenance - according to the accounts.

Labour productivity is defined as the quotient of the value of clean production produced in the holding to the workload [Kierul 1986, Fereniec 1999, Gębska, Filipiak, 2006].

## CHARACTERISTICS OF THE SURVEYED HOLDINGS

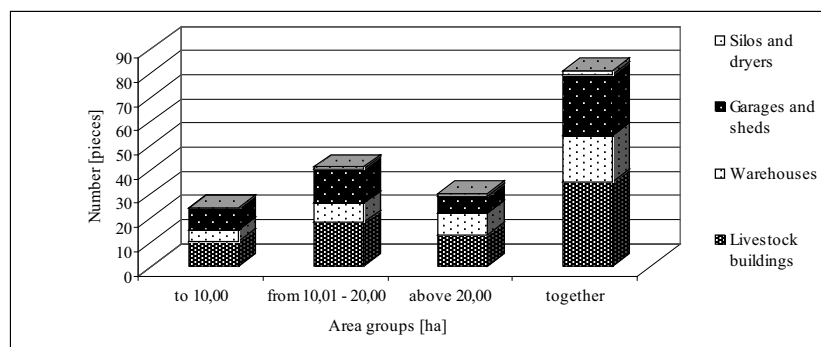
The average area of arable land in the surveyed holdings was 18.06 ha (Tab. 1). The structure of land use was dominated by permanent pasture, involving 75% of the total arable land. However, in the crop structure 65% of arable land was occupied by fodder, 28% - grain, while on the remaining area root crops were grown. Average density of livestock was 1.03 LU · ha<sup>-1</sup> of arable land. The main direction of activity of the surveyed holdings was the production of milk, hence 90% of stocking density were dairy cows.

Table 1. Characteristics of the surveyed holdings

Specification	Area groups [ha]			
	to 10,00	from 10,01 - 20,00	above 20,00	average
Number of holdings	7	10	8	25
Cropland [ha]	7,63	15,85	29,93	18,06
Arable land [ha], in it:	3,26	3,87	6,56	4,56
Grain crops	1,68	1,48	0,70	1,29
Root crops	0,39	0,37	0,14	0,30
Fodder crops	1,20	2,02	5,71	2,97
Grassland [ha]	4,37	11,98	23,38	13,50
Stocking [LU·ha <sup>-1</sup> of arable land]	1,02	1,16	0,86	1,03
Number of machines and tools [pieces · holding <sup>-1</sup> ]	14,14	14,10	15,15	14,45
Replacement value of park machine [t zł · ha <sup>-1</sup> of arable land]	21,64	14,00	7,80	14,16

Source: Author's calculations

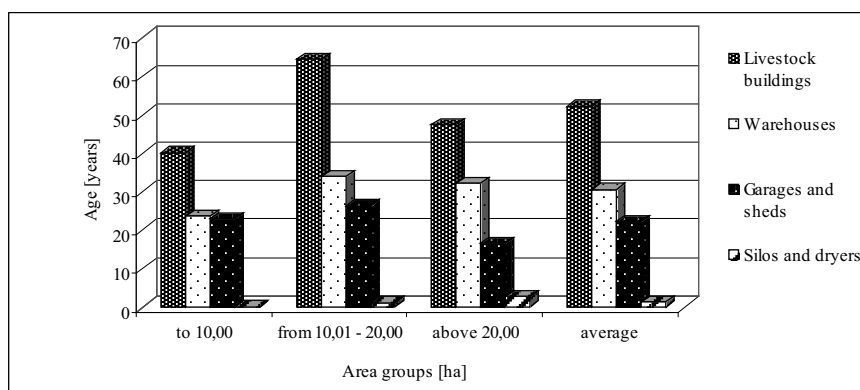
The machine park in the surveyed holdings was really diverse. On average, on one farm there were 14.45 units of machines and tools. It is worth noting that the technical background, in quantitative terms, was virtually the same both in small farms and in the objects of a large area of land, which proved the technical overinvestment of small farms and, in consequence their low profitability. You can see it very clearly, looking at the replacement value of the machine park, which in the smallest farms was almost 3-fold higher than in the larger farms. Machines for animal production were the leading group of the technical means, which was obvious from the specification of the surveyed holdings.



Source: Author's calculations

Fig. 1 Quantitative assessment of the farm buildings in the inspected holdings

The only data that give a picture of the current number of agricultural buildings are the data from the CSO census [Mulica, Hutnik, 2007]. In 25 surveyed holdings the total of 81 farm buildings was reported. Most of the buildings (41 units) were on the farms ranging in size from 10 to 20 ha of arable land (Fig. 1). On average, there were 2 livestock buildings, 1 warehouse and garage / shed per farm. Due to the direction of production, 42% were livestock buildings, 31% - garages and sheds, 25% - warehouses, including the vast majority of the barn, and only 2% - silos and dryers. Cattle was primarily fed by haylage, hence the small number of silos silage, in spite of the dairy direction of production.



Source: Author's calculations

Fig. 2. Age of buildings in the surveyed holdings

Stankiewicz [2003], the technical condition of livestock buildings and farm buildings was assessed as low, due to the fact that almost half of the buildings (46% sheds, 50% piggery and 44% barns) were built before 1960. In the surveyed holdings the average age of building was 27 years. The oldest buildings, with an average age of 31 occurred on farms with the area from 10 to 20 ha, while the youngest (22 years) at the smallest area. While taking into account the type of buildings, by far in all the area groups the oldest were livestock buildings, whose average age is 52 years and warehouses - 30 years old (Fig. 2)

Table 2. Surface of the buildings in the surveyed holdings [m<sup>2</sup>]

Specification	Area groups [ha]			
	to 10,00	from 10,01 - 20,00	above 20,00	average
Livestock buildings	147,60	199,50	218,10	190,90
Warehouses	57,10	81,40	94,60	78,80
Garages and sheds	83,40	85,20	86,50	85,10
Silos and dryers	0,00	2,00	3,80	2,00
Together	288,10	366,10	399,30	354,90

Source: Author's calculations



According to the Central Statistical Office, the area of production buildings used by Polish farmers is small, as the average size of a cowshed is 95 m<sup>2</sup> and of a barn - 128 m<sup>2</sup>. Only in the western and northern provinces the area is larger in the case of cowshed and piggery, which stems from the fact that in these regions a large proportion of arable land belonged to State Farms [Central Statistical Office 2007]. However, in the surveyed holdings the average size of livestock buildings was relatively high and amounted to more than 190 m<sup>2</sup>, but it resulted from the direction of activity (Tab. 2). However, a small warehouse space (78.8 m<sup>2</sup>) resulted from the feeding system of cattle. Farmers produced for haylage, which was stored in the field, so warehouses were used for storing fodder and hay, which were a dietary supplement.

### THE RESULTS OF THE RESEARCHES

Replacement value is the value which corresponds to the cost of replacement of the building, an asset that means restoration to the state of a new one, but not improved in view of the existing dimensions, construction and materials.

Average replacement value of buildings in the surveyed holdings stood at 132.12 t PLN (Tab. 3). More than half of this value (61%) were the livestock buildings, 21% - warehouses and 18% - garages and sheds. The replacement value is determined by the type of building material, in addition to surface. Most of the buildings, especially livestock buildings and garages were built with airbricks. Also wood was used, especially in the case of barns and occasionally also buildings from blocks of brick were reported. It is worth noting that the replacement value of the distinguished types of buildings grew along with the area of arable land.

Table 3. Replacement value of farm buildings [t PLN]

Specification	Area groups [ha]			
	to 10,00	from 10,01 - 20,00	above 20,00	average
Livestock buildings	64,07	84,52	90,61	80,74
Warehouses	20,68	28,53	31,51	27,28
Garages and sheds	22,71	23,64	24,61	23,69
Silos and dryers	0,0	0,40	0,75	0,40
Together	107,46	137,08	147,48	132,12

Source: Author's calculations

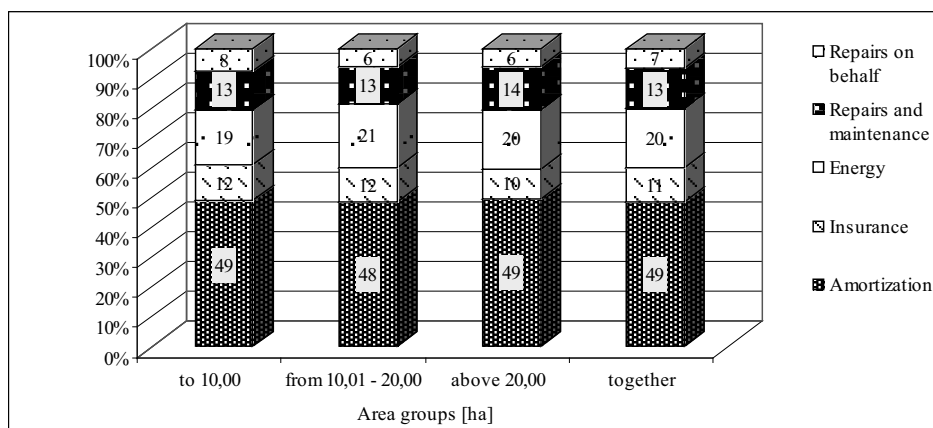
Farmers undertaking new investments or modernizing buildings were increasingly starting to pay attention to costs incurred for this purpose that did not cause the increasing of the financial outlays in production costs and those expenditures amortized in a relatively short time.

Table 4. The annual operating costs of buildings [t PLN·year<sup>-1</sup>]

Specification	Area groups [ha]			
	to 10,00	from 10,01 - 20,00	above 20,00	average
Livestock buildings	3,02	3,94	4,05	3,72
Warehouses	0,35	0,47	0,77	0,53
Garages and sheds	0,87	0,92	0,87	0,90
Silos and dryers	0	0,01	0,02	0,02
Together	4,24	5,34	5,66	5,15

Source: Author's calculations

On average, total annual operating costs of buildings amounted to 5.15 t zł (Tab. 4). These costs, like the replacement value, grew along the surface of arable land, therefore the highest costs were in the holdings above 20 ha of arable land. This regularity was noted for all the types of buildings, except garages and sheds, where the costs of their operation were the smallest, and the largest holdings were at the same level. As many as 72% of the total operating costs were spent on the livestock buildings. Garages and sheds absorbed 17% of the cost, and warehouses only 10%. The structure of total costs in the area groups was nearly identical (Fig. 3).



Source: Author's calculations

Fig. 3. The structure of the annual operating costs

The largest share in the structure of the total operation costs was amortization, accounting for almost half of them (49%) and energy costs constituting 20%. The share of other operating costs such as the performed repairs and maintenance, insurance, and repairs amounted to: 13, 11 and 7%.

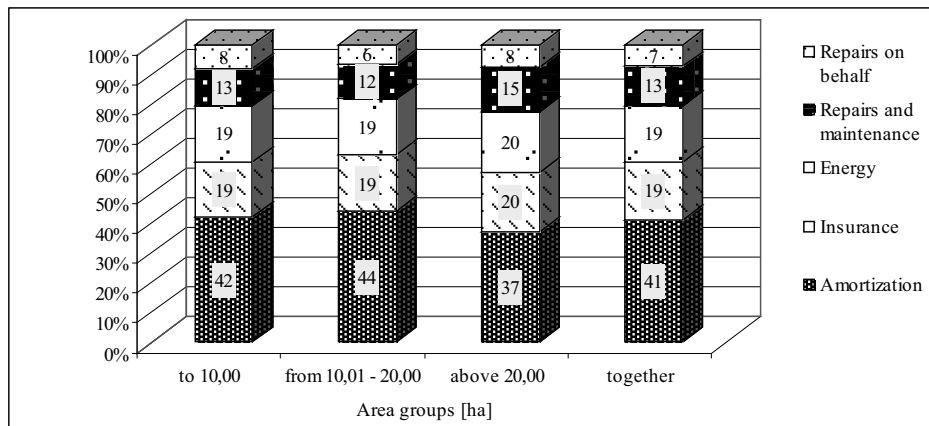
Table 5. Unitary operating costs of buildings [PLN·m<sup>-2</sup>·<sup>-1</sup>]

Specification	Area groups [ha]			
	to 10,00	from 10,01 - 20,00	above 20,00	average
Livestock buildings	23,92	22,91	22,99	23,22
Warehouses	4,75	5,05	15,61	8,34
Garages and sheds	13,10	13,59	10,41	12,44
Silos and dryers	0,00	0,65	0,71	0,49
Together	41,77	42,20	49,72	44,49

Source: Author's calculations

The total operation costs with respect to the surface of the buildings were 44.49 PLN·m<sup>-2</sup>·<sup>-1</sup> (Tab. 5). Comparing them in area groups it is worth noting that in the smallest farms up to 10 ha of arable land and average sectorally, with the area from 10 to 20 ha of arable land, unitary costs differed by only 0.43 PLN·m<sup>-2</sup>·<sup>-1</sup>, but in the largest farms they were 7.95 PLN·m<sup>-2</sup>·<sup>-1</sup> higher than the lowest. This difference was due to high operating costs of warehouses in this group which were more than 10 PLN·m<sup>-2</sup>·<sup>-1</sup> higher than those incurred in the smallest objects. On average, the highest unitary costs were incurred in the livestock buildings, garages and sheds.

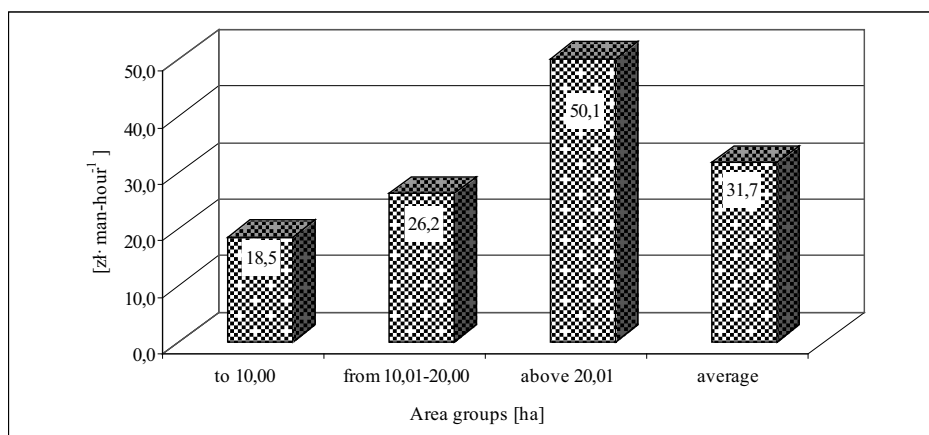
The structure of unitary costs was similar to the annual costs (Fig. 4).



Source: Author's calculations

Fig. 4. The structure of unitary operating costs

According to Myczko [1995] operation costs of buildings and technical equipment depends of labor productivity, which depends on the direction of production, techniques and animal welfare and adaptation of the premises and equipment to the implemented technology.



Source: Author's calculations

Fig. 5. Labour productivity in the surveyed holdings

Average labor productivity in the surveyed farms was 31.70 PLN · man-hour<sup>-1</sup> (Fig. 5). Noteworthy is the fact that this ratio in the largest objects was nearly 2-fold higher compared to the other two groups. Thus, the most effective work was only on the farms with the area exceeding 20 ha of arable land. In these holdings the highest value of pure production was obtained, at the lowest labor outlays.

A very big impact on the increase of the labor productivity is exerted, for example, by the mechanization of production processes [Winnicki 1995; Malaga-Toboła 2008; Michalek, Kuboń 2009; Slawinski 2010].

The paper analyzes the correlation considering independent variables of the replacement value of buildings and the costs of their operation as well as the dependent variable of labor productivity. The relationship between these variables was statistically insignificant. However, a statistically significant relationship was noted between the operating costs of buildings and their replacement value. The correlation coefficient was 0.90, so this relationship was very high.

The analysis of variance showed the significance of differences in labor productivity in each area group. In comparison, there were large deviations from the mean average value of labor productivity in the buildings with up to 10 ha and from 10.01 to 20 ha of arable land, compared with the objects of the largest area.

## CONCLUSIONS

In the surveyed holdings 81 farm buildings were reported, of which 42% were livestock buildings. With regard to the age of buildings in Poland, they were mostly relatively young objects, with an average age of 27. The average size of livestock buildings was 190.9 m<sup>2</sup>, garages and sheds - 85.1 m<sup>2</sup> and warehouses - 78.8 m<sup>2</sup>, while the holdings had at their disposal about 354.90 m<sup>2</sup>.

The average annual operational costs were at the level of 5.15 t PLN and were aligned in various area groups nevertheless they were the highest in the facilities with the largest area (although the differences were small).

Average unitary costs were  $44.49 \text{ PLN} \cdot \text{m}^{-2}$ . These costs were 10 PLN per  $\text{m}^2$  higher in the largest objects than in the holdings to 20 ha of arable land. In the cost structure of both the annual and unitary costs, the largest share belonged to the costs of amortization of buildings and energy.

The statistical analysis shows that the increase in the replacement value of buildings by 1 t PLN will increase annual operating costs by about 32.68 t zł.

The highest labor productivity ( $50.09 \text{ PLN per man-hour}^{-1}$ ) occurred on the holdings with over 20 ha of arable land and was statistically significantly different from that obtained in territorially smaller holdings. Therefore, the surface of 20 ha of arable land is a threshold at which the production starts to be economically justified.

The relationship between the replacement value of buildings, their operating costs and labor productivity proved to be statistically insignificant.

## REFERENCES

1. Fereniec J. 1999.: *Ekonomika i organizacja rolnictwa*. Wydawnictwo Key Text. Warszawa. s. 33-57.
2. Gębska M., Filipiak T. 2006.: *Podstawy ekonomiki i organizacji gospodarstw rolniczych*. Wydawnictwo SGGW. Warszawa. ISBN 83-7244-756-X.
3. Kierul Z. 1986. *Ekonomika i organizacja gospodarstw rolniczych*. Państwowe Wydawnictwo Rolnicze i Leśne. Warszawa. s. 193-197.
4. Kuboń M. 2006.: Potencjał magazynowy oraz jego wykorzystanie w gospodarstwach rolnych o wielokierunkowym profilu produkcji. *Inżynieria Rolnicza*. Nr 12(87). Kraków. s. 277-286.
5. Kuboń M. 2007.: Metodyczne aspekty szacowania kosztów infrastruktury logistycznej przedsiębiorstw rolniczych. *Problemy Inżynierii Rolniczej* 1(55). Warszawa. s. 125-133.
6. Lorencowicz E., Włodarczyk A. 2009.: Budownictwo inwentarskie w Polsce – stan i tendencje zmian. *Technica Agraria*. Nr 8 (1-2).s. 11-22.
7. Malaga-Toboła U. 2008.: Wskaźnik technicznego uzbrojenia a wydajność pracy w aspekcie uproszczenia produkcji roślinnej. *Inżynieria Rolnicza*. Nr 2 (100). s. 195-202.
8. Malaga-Toboła U. 2009.: Kierunek i uproszczenie produkcji a wyposażenie gospodarstw w budynki gospodarskie. *Inżynieria Rolnicza*. Nr 9(118). Kraków. s. 145-152.
9. Michałek R. i in. 1998.: Uwarunkowania technicznej rekonstrukcji rolnictwa. *Polskie Towarzystwo Inżynierii Rolniczej*. Kraków. ISBN 83-905219-1-1.
10. Michałek R., Kuboń M. 2009.: Postęp naukowo-techniczny i jego skutki społeczno-ekologiczne. *Inżynieria Rolnicza*. Nr 1 (110). s. 207-212.
11. Mulica E., Hutnik E. 2007.: Stan zasobów budowlanych gospodarstw rolnych w regionie dolnośląskim. *Problemy Inżynierii Rolniczej*. Nr 1. Warszawa. s. 131-138.
12. Myczko A. 1995.: Stan i perspektywy mechanizacji produkcji zwierzęcej. IBMER. Warszawa.
13. *Rocznik statystyczny rolnictwa i obszarów wiejskich*. 2007. GUS Warszawa.
14. Romaniuk W., Łukaszuk M., Domasiewicz T. 2007.: Projektowanie, ocena i wybór rozwiązań obiektów inwentarskich. *Problemy Inżynierii Rolniczej*. Nr 1. s. 57-65.
15. Ruch budowlany w 2007 i w 2010 roku. 2008, 2010. GUNB Warszawa. [http://www.gunb.gov.pl/pliki/inf\\_pras.pdf](http://www.gunb.gov.pl/pliki/inf_pras.pdf) z dnia 10 lipca 2011 r.
16. Sławiński K. 2010.: Analiza usług mechanicznych w gospodarstwach ekologicznych. *Inżynieria Rolnicza*. Nr 5 (123). s. 253-258.
17. Stankiewicz D. 2003.: Budynki produkcyjne na wsi [w:] *Infrastruktura techniczna wsi*. Kancelaria Sejmu – BSiE Warszawa. s.13–17.

18. Tabor S., Kuboń M. 2004.: Kierunek produkcji a koszty logistyki w wybranych gospodarstwach rolniczych. Inżynieria Rolnicza. Nr 4(59). Kraków. s. 241-247.
19. Tabor S., Malaga-Toboła U. 2004.: Kierunek produkcji a koszty magazynowania pasz. Wieś Jutra. Technika w produkcji zwierzęcej. Nr 11-12 (76-77). s. 44-45.
20. Winnicki S. 1995.: Uwarunkowania zootechniczne i weterynaryjne w produkcji zwierzęcej. Materiały pokonferencyjne – Podstawowe problemy w technice i technologii produkcji zwierzęcej z uwzględnieniem aspektów ekologicznych. IBMER. Warszawa. s. 23.

*Scientific work financed from funds for science in the years 2010-2013 as a development project nr NR12-0165-10*

### KOSZTY EKSPLOATACJI BUDYNKÓW GOSPODARCZYCH W WYBRANYCH GOSPODARSTWACH EKOLOGICZNYCH

**Streszczenie.** Celem artykułu było określenie i analiza wartości odtworzeniowej budynków gospodarskich i rocznych oraz jednostkowe koszty ich działalności w zakresie wydajności pracy. Do analizy porównawczej obiektów badań, obiekty te zostały podzielone na grupy wg powierzchni: do 10 ha, od 10.01 do 20.00 ha i powyżej 20 ha użytków rolnych. Zakres badań obejmował gospodarstwa ekologiczne znajdujące się w górskim regionie i specjalizujące się w produkcji zwierzęcej.

**Słowa kluczowe:** koszty operacyjne, budynki gospodarcze, gospodarstwa ekologiczne, grupy obszarowe, wydajność pracy.

## OPTIMIZATION OF A TRANSPORT APPLYING GRAPH-MATRIX METHOD

Andrzej Marczuk, Wojciech Misztal

Department of Agricultural Machines and Devices, University of Life Sciences in Lublin,  
1 Poniatowski Street, 20-060 Lublin, Poland

**Summary.** The paper presents the procedure for solving a transportation task. The optimization was carried out in two phases. In the first one, a preliminary flow matrix was achieved on a base of the information on the demands and supplies values as well as transport costs, whereas some shifts within the preliminary flow matrix were made. All changes resulted in an optimum matrix, for which  $Z_x$  function held the lowest possible value. Presented method appeared to be efficient for solving the transportation tasks of particular type.

**Key words:** transport, optimization, Vogel's Approximation Method, Graph-Matrix Method.

### INTRODUCTION

Transport is a very important element of any economy, because it makes possible to flow goods and services among its particular branches. It assures supplying raw materials, materials, semi-products, and final products, and becomes one of intermediate stages during production process, which makes various institutions closer to one another. Connections between transport and economy branches is not of a single-directional character; the transport uses economy's achievements such as road system, fuels, etc. [Basiewicz, Gołaszewski, Rudziński, 2007, Burski, Mijalska-Szewczak 2008, Towpik, Gołaszewski, Kukulski 2006, Zielińska, Lejda 2010]. Close inter-relations between transport and economy branches make the development level of the latter depends on development level of the former and vice versa [Pang 2004]. However, notion *development* should be understood not only as modernization of transport means, but also optimization of transporting tasks, the means take part in. The development determines not only the increase of weight of goods possible to transport during a time unit, but also the decrease of expended costs, which can be modified by means of route optimization, for instance [Jacyna 2009, Marczuk 2009].

The study aimed at presenting the procedure for solving the transportation tasks using selected optimization methods. The optimization was carried out in two phases. The objective of the first was to formulate a preliminary flow matrix  $X = [x_{ij}]$ , on a base of information related to the demand and supply data along with cost values for transporting goods between suppliers and receivers. The second phase focused on shifting within such achieved flow matrix in such a way to make matrices held lower or equal (not higher) values of function  $Z_x$ , which is the costs expended to all transportation operations. Many procedures were prepared both for the first and second phase

[Tiwari, Shandilya 2006, Kasana, Kumar 2004, Bernard 1999]. Among methods related to the first phase, such ones as The Northwest Corner Method, Vogel's Approximation Method, The Minimum Cost Method, etc. The Graph-Matrix Analysis with its modifications is counted to the second phase. Particular methods differ relating both to actions, and conditions, as well as complexity, difficulty in implementing, and precision of achieved results [Srinivasan 2008, Jain, Aggarwal 2009, Sen 2010].

### VOGEL'S APPROXIMATION METHOD

The method is a specific procedure leading to solve a transportation task; it allows for achieving a final solution. However, the result is not always optimum, because sometimes it is only some approximation of the optimum. Inaccuracy of the method makes that it can be efficiently applied only for defining the preliminary solution (achievement of preliminary flow matrix). Applying the Vogel's Approximation Method in the first phase of procedure contributes to time saving when the whole optimization action is performed. The method is usually much more accurate than other ones used in that phase, which results in lower number of iterations necessary to be made in subsequent phase.

The starting point for Vogel's Approximation Method – as similar as for other first-phase methods – is made of the system C, M consisted of transport cost matrix  $C = [c_{ij}]$  and vector  $M = [a_1, a_2, \dots, a_m; b_1, b_2, \dots, b_n]$  representing receivers' demands and suppliers' supplies (where:  $m$  – number of suppliers,  $n$  – number of receivers). It should be on mind that optimization is possible when C, M system meets the equation:

$$\sum_{i=1}^m a_i = \sum_{j=1}^n b_j, \quad (1)$$

where:  $i = 1, 2, \dots, m$ ;  $j = 1, 2, \dots, n$ .

#### Calculation methodology

- 1) Firstly, the Vogel's number should be calculated for particular rows and columns within transport cost matrix. For rows, the number holds value equal to the difference between two the lowest (representing the lowest costs) elements present in a given row. In the case of columns, the situation is analogous – Vogel's number is a difference between two the lowest values in a given column.
- 2) In subsequent step aiming at assigning the transport size to particular routes, four actions should be performed:
  - selection of a row or a column, for which calculated Vogel's number holds maximum value. Various cases can arise at that step, which may affect further procedure; (i) it may be a situation when the highest Vogel's number is achieved both for a row and a column, and matrix element present at the intersection represents the lowest costs; (ii) another situation consists in that the element present at the intersection of the row and the column does not represent the lowest costs; (iii) the case if the highest Vogel's number is achieved for several rows or columns at the same time; (iv) another situation differing from the previous one in that the element present at the intersection of the row and the column does not represent the lowest costs; such case is met when the highest Vogel's number is achieved for several rows and columns at the same time.



- selection of the element that contains the lowest costs and belongs to a row or a column selected in previous step. Existence of any of above described case, requires special procedure: (i) common assignment both for a row and a column should be introduced in place where element representing the lowest costs is present; (ii) there is a discretion in introducing the assignment to the row or the column where element representing the lowest costs is present; (iii) the case allows for introducing the assignment to any of matrix element, regardless of where the element representing the lowest costs is present;
  - assignment of the highest possible number of transport quantity to the transport costs matrix element selected in previous action;
  - cancelling the column (columns) or row (rows), for which the assignment made the receiver's (receivers') demands or supplier's (suppliers') supplies are met.
- 3) Calculating the Vogel's number for particular rows and columns (without cancelled ones).
  - 4) Repeating second and third steps until all assignments are made, i.e. achieving preliminary flow matrix  $X = [x_{ij}]$ .
  - 5) Calculating value of  $Z_x$  function [Bocchino 1975, Krawczyk 2001, Shenoy 1998, Khanna 2009, Bandopadhyaya 2007]:

$$Z_x = \sum_{i=1}^m \sum_{j=1}^n c_{ij} x_{ij}. \quad (2)$$

### GRAPH-MATRIX METHOD

The Graph-Matrix Method is one of the second-phase method during the optimization procedure.

Verifying if preliminary flow matrix achieved in previous actions has been properly created should be carried out prior to this method applying. The verification can be performed applying following criteria:

$$\sum_{j=1}^n x_{ij} = a_i, \quad (3)$$

$$\sum_{i=1}^m x_{ij} = b_j, \quad (4)$$

where:  $i = 1, 2, \dots, m$ ;  $j = 1, 2, \dots, n$ .

#### Calculation methodology

- 1) Creating the matrix graph by means of connecting all nodes; nodes can be connected only in vertical or horizontal directions.
- 2) Evaluating the type of basis solution represented by preliminary flow matrix achieved in the first step. It is extremely important, because the necessary and sufficient condition for the method to be applied states that any preliminary solution has to be the basic of the first or the second type. In order to set the type of the basic solution, it should be checked whether: (i) number of nodes of the graph constructed using the flow matrix equals to  $m + n - 1$ ; (ii) graph is consistent; (iii) graph does not contain any cycle; (iv) graph's nodes

correspond to positive node elements of the flow matrix; (v) all –no-node elements of the matrix are null. If all above conditions are met, the flow matrix  $X$  is a basic solution of the first type; otherwise, the matrix is no basic solution. Then, it is necessary to make transformation aiming at achieving the basic solution of the second type, which consists in distinguishing the null elements of discussed matrix as node elements to get their  $m + n - 1$  number. The distinguishing should be made in such a way to make graph stretched on those nodes consistent and not containing any cycle.

- 3) Making some actions aiming at verifying the optimization criterion for a given flow matrix; the process consists of the following steps:
  - creating the equivalent null matrix of costs  $C^1$  by means of finding some constants  $u_i$  and  $v_j$ , which added to particular rows ( $u_i$ ) and columns ( $v_j$ ) would bring all node elements of the matrix to zero. In order to make procedure easier, action should be begun from the separate node element in a given row or a column. If the node element is separate in a column, number equal to that element should be subtracted from the row, which results in finding the first  $u_i$ . If the node element is separate in a row, number equal to that element should be subtracted from the column, which results in finding the first  $v_j$ .
  - creating the equivalent null matrix  $C^1$  by means of adding previously found values  $u_i$  and  $v_j$  to particular rows and columns of the cost matrix  $C$ .
  - verifying the optimization criterion for the flow matrix  $X$ . According to a theorem, the flow matrix  $X$  is optimum for transportation problem, if positive values of its elements correspond to elements from equivalent null matrix  $C^1$ , value of which is zero, while other elements are not negative.
- 4) If a given matrix appears not to be optimum flow matrix for transportation problem, it is necessary to execute step 4 consisting in making some corrections in flow matrix aiming at reducing the value of  $Z_x$  function. First, the lowest element among all negative ones in equivalent null matrix of costs  $C^1$ , should be selected. If there are several such elements, any of them can be selected. Then, a node with corresponding selected element, should be incorporated into the graph, which results in creating the graph spanned on  $m + n$  nodes and containing a simple cycle. Next, a cycle should be found and a set of nodes that belongs to it should be divided into two subsets  $A_1(+)$  and  $A_2(-)$ : node that was incorporated to the previous action has to be assigned to subset  $A_1(+)$ , while every two adjacent nodes are assigned to other subsets. Then, iteration should be performed, which is based on making some changes in transport size values. These changes consist in subtracting the assignment corresponding to the lowest of elements  $x_{ij}$  at nodes of subset  $A_2(-)$  and assigning to nodes of subset  $A_1(+)$ , which in consequence cancels the cycle.
- 5) Calculating the value of  $Z_x$  function using the same formula that was applied in Vogel's Approximation Method.
- 6) Repeating the actions of steps 3 to 5 for newly created flow matrices ( $X_1, X_2, \dots, X_k$ ) until the optimum matrix is achieved [Całczyński 1992, Natarajan, Balasubramani, Tamilarasi 2005].

## RESULTS

Execution of optimization methods is going to be presented in practice using the example of goods distribution between warehouses "H" (localized in: Lublin, Chełm, Ostrów Lubelski, and Ryki) and supplied shops "S" (situated in: Łęczna, Fajslawice, Łuków, Bychawa, and Kazimierz

Dolny). The transportation costs on particular routes have been set as the product of the transport fee rate (3.80 PLZ/km) and doubled distance between given enterprises (km). Levels of receivers' demand ( $a_i$ ) and suppliers' supplies ( $b_j$ ) have been randomly selected.

When Vogel's Approximation Method was applied, the calculation procedure is following:

Table 1. The C, M system (highlighted fragment is matrix of costs C)

	$S_1$	$S_2$	$S_3$	$S_4$	$S_5$	$a_i$
$H_1$	190	273,6	722	243,2	433,2	200
$H_2$	425,6	311,6	1238,8	570	942,4	90
$H_3$	190	418	547,2	585,2	638,4	30
$H_4$	668,8	752,4	615,6	722	334,4	90
$b_j$	100	50	80	60	120	410

Table 2. The C, M system improved with calculated values of Vogel's numbers (first step of the procedure)

		0	38	68,4	326,8	98,8	
		$S_1$	$S_2$	$S_3$	$S_4$	$S_5$	$a_i$
53,2	$H_1$	190	273,6	722	243,2	433,2	200
114	$H_2$	425,6	311,6	1238,8	570	942,4	90
228	$H_3$	190	418	547,2	585,2	638,4	30
281,2	$H_4$	668,8	752,4	615,6	722	334,4	90
	$b_j$	100	50	80	60	120	410

Table 3 presents bold characters representing the route, where transport is going to be realized; number in the superscript stands for the transport size through a given route.

Table 3. The C, M system after the second-step procedure

		0	38	68,4	326,8	98,8	
		$S_1$	$S_2$	$S_3$	$S_4$	$S_5$	$a_i$
53,2	$H_1$	190	273,6	722	<b>243,2<sup>60</sup></b>	433,2	200
114	$H_2$	425,6	311,6	1238,8	570	942,4	90
228	$H_3$	190	418	547,2	585,2	638,4	30
281,2	$H_4$	668,8	752,4	615,6	722	334,4	90
	$b_j$	100	50	80	60	120	410

Due to a fact that further procedure aiming at making the assignment, proceeds the same way, it was omitted.

Table 4. Preliminary flow matrix X (achieved by making all assignments)

	S <sub>1</sub>	S <sub>2</sub>	S <sub>3</sub>	S <sub>4</sub>	S <sub>5</sub>	a <sub>i</sub>
H <sub>1</sub>	190 <sup>30</sup>	273,6	722 <sup>80</sup>	243,2 <sup>60</sup>	433,2 <sup>30</sup>	200
H <sub>2</sub>	425,6 <sup>40</sup>	311,6 <sup>50</sup>	1238,8	570	942,4	90
H <sub>3</sub>	190 <sup>30</sup>	418	547,2	585,2	638,4	30
H <sub>4</sub>	668,8	752,4	615,6	722	334,4 <sup>90</sup>	90
b <sub>j</sub>	100	50	80	60	120	410

Values of Z<sub>i</sub> functions according to dependence (2) amounted to 159 448 PLZ.

Applying the Graph-Matrix Method, calculations start from creating the preliminary flow matrix.

Table 5. Preliminary flow matrix X with spanned matrix graph

	S <sub>1</sub>	S <sub>2</sub>	S <sub>3</sub>	S <sub>4</sub>	S <sub>5</sub>
H <sub>1</sub>	190 <sup>30</sup>	273,6	722 <sup>80</sup>	243,2 <sup>60</sup>	433,2 <sup>30</sup>
H <sub>2</sub>	425,6 <sup>40</sup>	311,6 <sup>50</sup>	1238,8	570	942,4
H <sub>3</sub>	190 <sup>30</sup>	418	547,2	585,2	638,4
H <sub>4</sub>	668,8	752,4	615,6	722	334,4 <sup>90</sup>

Matrix C<sup>1</sup> included in Table 6 contains negative elements, hence the preliminary flow matrix is not the optimum.

Table 6. The C<sup>1</sup>, X system

	S <sub>1</sub>	S <sub>2</sub>	S <sub>3</sub>	S <sub>4</sub>	S <sub>5</sub>
H <sub>1</sub>	0 <sup>30</sup>	197,6	0 <sup>80</sup>	0 <sup>60</sup>	0 <sup>30</sup>
H <sub>2</sub>	0 <sup>40</sup>	0 <sup>50</sup>	281,2	91,2	273,6
H <sub>3</sub>	0 <sup>30</sup>	342	-174,8	342	205,2
H <sub>4</sub>	577,6	775,2	-7,6	577,6	0 <sup>90</sup>

Table 7. The  $C^1, X$  system with highlighted the lowest negative element

	$S_1$	$S_2$	$S_3$	$S_4$	$S_5$
$H_1$	$0^{30}$	197,6	$0^{80}$	$0^{60}$	$0^{30}$
$H_2$	$0^{40}$	$0^{50}$	281,2	91,2	273,6
$H_3$	$0^{30}$	342	<b><math>-174,8^0</math></b>	342	205,2
$H_4$	577,6	775,2	-7,6	577,6	$0^{90}$

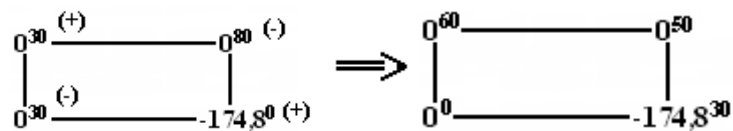


Fig. 1. Changes during iterations

Table 8. The  $C^1, X$  system after iterations

	$S_1$	$S_2$	$S_3$	$S_4$	$S_5$
$H_1$	$0^{60}$	197,6	$0^{50}$	$0^{60}$	$0^{30}$
$H_2$	$0^{40}$	$0^{50}$	281,2	91,2	273,6
$H_3$	0	342	<b><math>-174,8^{30}</math></b>	342	205,2
$H_4$	577,6	775,2	-7,6	577,6	$0^{90}$

Like for Vogel's Approximation Method, the procedure has been shortened by repeating actions.

Table 9. Final version of the  $C^1, X$  system

	$S_1$	$S_2$	$S_3$	$S_4$	$S_5$
$H_1$	$0^{60}$	197,6	7,6	$0^{60}$	$0^{80}$
$H_2$	$0^{40}$	$0^{50}$	288,8	91,2	273,6
$H_3$	167,2	509,2	$0^{30}$	509,2	372,4
$H_4$	577,6	775,2	$0^{50}$	577,6	$0^{40}$

Table 10. Final flow matrix X

	$S_1$	$S_2$	$S_3$	$S_4$	$S_5$	$a_i$
$H_1$	190 <sup>60</sup>	273,6	722	243,2 <sup>60</sup>	433,2 <sup>80</sup>	200
$H_2$	425,6 <sup>40</sup>	311,6 <sup>50</sup>	1238,8	570	942,4	90
$H_3$	190	418	547,2 <sup>30</sup>	585,2	638,4	30
$H_4$	668,8	752,4	615,6 <sup>50</sup>	722	334,4 <sup>40</sup>	90
$b_j$	100	50	80	60	120	410

Value of  $Z_x$  function for calculations made by means of Graph-Matrix Method was 153 824 PLZ.

## CONCLUSIONS

The two-step procedure possible to be used at optimization of a transport realized between the demand and supply points, has been presented. In the first step, the preliminary flow matrix X has been achieved, for which value of  $Z_x$  function amounted to 159 448 PLZ. Two iterations has been performed in the second step. The first one consisted in incorporation of  $C^1$  matrix element of 174.8 value (the lowest negative element of the matrix) into the graph and making some shifts in the transport quantities of the graph elements included in a cycle. That operation has resulted in assigning the value 30 to previously incorporated  $C^1$  matrix element and non-profitable route with the same transport size assigned has been canceled. The second iteration was identical; however it referred to the lowest negative matrix  $C^1$  element that remained after zeroing previous the lowest negative element of that matrix (according to procedure leading to verification of the optimization criterion). Like for previous iteration, the transport size of 50 value has been assigned to incorporated element and non-profitable route has been eliminated. These changes have led to achieving the final matrix (optimum), for which  $Z_x$  function held value of 153 824 PLZ. It means that changes can allow for achieving the savings during the transportation tasks at the level of 5 624 PLZ.

Above method appeared to be efficient for solving the transportation tasks, the example of which was presented in the paper.

## REFERENCES

1. Bandopadhyaya L. 2007.: Topics in Linear Programming and Games Theory. Northern Book Centre. New Delhi.
2. Basiewicz T., Gołaszewski A., Rudziński L. 2007.: Oficyna Wydawnicza Politechniki Warszawskiej. Warszawa.
3. Bernard T. W. 1999.: Introduction to Management Science. Prentice Hall.
4. Bocchino W. A. 1975.: Systemy informacyjne zarządzania. Narzędzia i metody. Wyd. Naukowo – Techniczne, Warszawa.

5. Burski Z., Mijalska-Szewczak I. 2008.: Evaluation of energy-consumption in the vehicles of EU international communication infrastructure. TEKA KMiER. PAN o/Lublin.
6. Całczyński A. 1992.: Metody optymalizacyjne w obsłudze transportowej rynku. Państwowe Wydawnictwo Ekonomiczne. Warszawa.
7. Jacyna M. 2009.: Modelowanie i ocena systemów transportowych. Oficyna Wydawnicza Politechniki Warszawskiej. Warszawa.
8. Jain T. R., Aggarwal S. C. 2009.: Business Mathematics and Statistics. V. K. (India) Enterprises. New Delhi.
9. Kasana H. S., Kumar K. D. 2004.: Introductory operations research: theory and applications. Springer. Berlin.
10. Khanna R.B. 2009.: Quantitative Techniques for Managerial Decisions. PHI Learning. New Delhi.
11. Krawczyk S. 2001.: Metody ilościowe w logistyce przedsiębiorstwa. Tom II. Wyd. C.H. Beck. Warszawa.
12. Marczuk A. 2009.: A computer system for optimisation of soft fruit transportation in diffused purchasing networks. Eksploatacja i Niezawodność – Maintenance and Reliability. Warszawa.
13. Natarajan A. M., Balasubramani P., Tamilarasi A. 2005.: Operations Research. Pearson Education. Singapore.
14. Pang P.N.T. 2004.: Essentials of manufacturing engineering management. iUniverse. Lincoln.
15. Sen R. P. 2010.: Operations Research: Algorithms And Applications. PHI Learning. New Delhi.
16. Shenoy G. V. 1998.: Linear programming: methods and applications. Second editions. New Age Interantional. New Delhi.
17. Srinivasan G. 2007.: Operations research: Principles and applications. PHI Learning. New Delhi.
18. Tiwari N. K., Shandilya S. K. 2006.: Operations Research. Prentice-Hall of India. New Delhi.
19. Towpik K., Gołaszewski A., Kukulski J. 2006.: Infrastruktura transportu samochodowego. Oficyna Wydawnicza Politechniki Warszawskiej. Warszawa.
20. Zielińska E., Lejda K. 2010.: Ecological problems of transport vehicles. TEKA KMiER. PAN o/Lublin.

#### OPTIMALIZACJA TRANSPORTU PRZY WYKORZYSTANIU METODY GRAFÓW MACIERZOWYCH

**Streszczenie.** Celem pracy było przedstawienie postępowania właściwego dla rozwiązywania zadania transportowego. Działania optymalizacyjne przeprowadzono w dwóch etapach. W pierwszym z nich uzyskano wstępną macierz przepływów, na podstawie informacji o wielkości popytów odbiorców i podaży dostawców oraz wartości kosztów przewozów. W drugim etapie dokonano przesunięć we wstępnej macierzy przepływów, uzyskanej w etapie pierwszym. Zmiany te doprowadziły do uzyskania macierzy optymalnej, dla której funkcja  $Z_x$  przyjęła najniższą wartość. Przedstawiona metoda okazała się być skuteczna przy rozwiązywaniu zadań transportowych określonego typu.

**Słowa kluczowe:** transport, optymalizacja, metoda aproksymacyjna Vogela, metoda grafów macierzowych.

## CHANGES OF SPECIFIC MECHANICAL ENERGY DURING EXTRUSION-COOKING OF POTATO STARCH

Marcin Mitrus, Tomasz Oniszczyk, Leszek Mościcki

Department of Food Process Engineering, Faculty of Production Engineering,  
University of Life Sciences, Doświadczalna 44, 20-280 Lublin, Poland,  
marcin.mitrus@up.lublin.pl

**Summary.** The simplest method of physical modification of starch is extrusion-cooking. Changes of the extruder efficiency and specific mechanical energy (SME) during extrusion-cooking of potato starch are presented in the paper. Extrusion-cooking process was characterised by good efficiency. The output depended mainly on the extruder screw speed and starch moisture content, less on process temperature. It ranged between the 11.3 kgh<sup>-1</sup> and 28 kgh<sup>-1</sup> depending on process parameters. SME measurements showed that extrusion-cooking of potato starch is related with rather low energy input ranged from 0.083 to 0.275 kWhkg<sup>-1</sup>. Significant impact on the values of the SME had a screw speed, very little impact had a moisture content of the raw material.

**Key words:** potato starch, extrusion-cooking, efficiency, specific mechanical energy.

### INTRODUCTION

Extrusion-cooking technique is widely used in food processing for production of various types of food such as snacks, meat analogs, pet food and aquafeed. In general terms, extrusion-cooking of the raw material of plant origin is the extrusion of bulk material under high pressure and high temperature. This causes the significant changes in physical and chemical quality of the processed material. During baro-thermal treatment, material is mixed, compacted, compressed, liquefied and plasticity in the end zone of the extruder. Extrusion pressure can reach up to 20 MPa and temperature of the slurry to 200 °C. The scope of physical and chemical changes in processed raw materials depends mainly on the assumed parameters of the extrusion-cooking process and the construction of the extruder [4, 9, 14, 15].

Native starch is used in different industrial sectors, however, due to some disadvantages (eg. insolubility in cold water), its use is severely limited. Disadvantages of native starch can be reduced or even eliminated, through its modification by various methods [5, 11, 20]. The simplest method of physical modification of starch is thermal or baro-thermal treatment. As a result of heating the grain structure is destroyed and there is a partial starch gelatinization. During this process hydrogen bonds, that stabilize the tertiary and quaternary conformational structure of macromolecules, are disrupted [17]. Various forms of drying, extrusion or high pressure treatment are used for this purpose [1, 8, 11, 20].



Due to environmental considerations native and modified starches are now attracting increased attention as raw materials in the production of biodegradable plastics. Extrusion-cooking technique can be successfully applied for this purpose [6, 16].

## MATERIALS AND METHODS

The basic material for investigations was potato starch Superior type produced by the Food Industry Plant "PEPEES" S.A. in Lomza (Poland). Its moisture content was 17%. During our investigations the 4 levels of moisture content of raw material (17, 20, 25 and 30%) were used. In order to obtain expected moisture content, starch was mixed with sufficient amount of water. The obtained samples were stored for 24h in air tight polyethylene bags at room temperature to make whole sample material homogeneous.

Extrusion-cooking of potato starch was carried out using a modified single screw extrusion-cooker TS-45 (Polish design) with  $L / D = 16$ . The die with one opening of 3 mm diameter was used. Extrusion-cooking was carried at different temperature (100, 120 and 140 °C), using a variable speed of the screw (60, 80, 100, 120 rpm) [13].

The extruder output was measured as a mass of the extrudate produced during 10 minutes; measurements were performed in 6 replications.

Power consumption measurement was performed with a standard method using wattmeter connected to the extruder electric panel [7, 10, 12, 18, 19]. The obtained results were converted to an index of specific mechanical energy consumption (SME) after the following formula:

$$\text{SME} = \frac{n \cdot P \cdot O}{n_m \cdot Q} [\text{kWhkg}^{-1}], \quad (1)$$

where:  $n$  - screw rotations [ $\text{min}^{-1}$ ],  
 $n_m$  - maximal screw rotations [ $\text{min}^{-1}$ ],  
 $P$  - power [kW],  
 $O$  - engine loading [%],  
 $Q$  - extruder output [ $\text{kg h}^{-1}$ ].

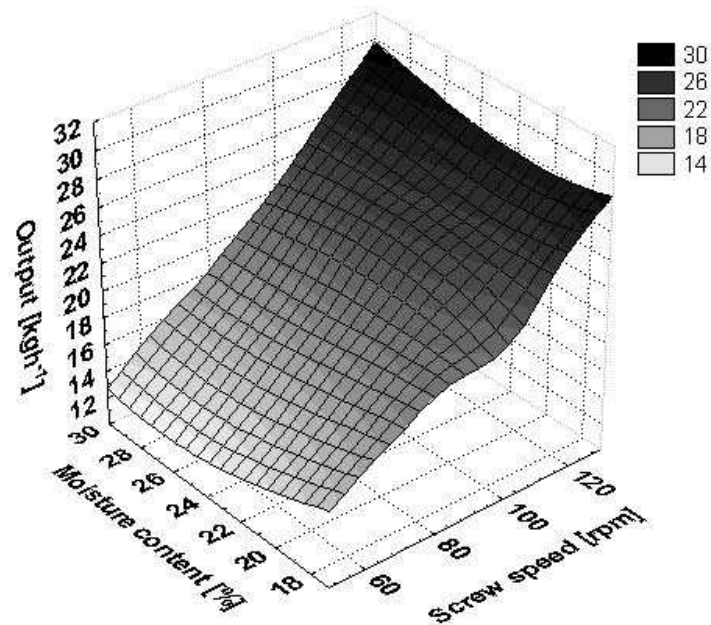


Fig. 1. Changes of the process output during potato starch extrusion-cooking at 100 °C

## RESULTS

Extrusion-cooking of the potato starch was characterised by good efficiency, ranged between 11.3 kg h<sup>-1</sup> and 28 kg h<sup>-1</sup> dependently of process parameters used. Changes in extruder output depended mainly on the extruder screw speed and starch moisture content, less on process temperature.

During processing potato starch with moisture content ranged from 20% to 30% the higher process temperature caused a decrease of the extrusion-cooking efficiency. Generally we can say that the highest output was recorded at 100 °C with one exception the case when the starch of 17% moisture content was processed. The highest output of 28 kg h<sup>-1</sup> was observed during extrusion-cooking at 140 °C.

Measurements have shown that the increase of the extruder screw speed increased the efficiency of the extrusion-cooking (fig. 1 and 2). This effect was observed in the whole range of applied temperature.

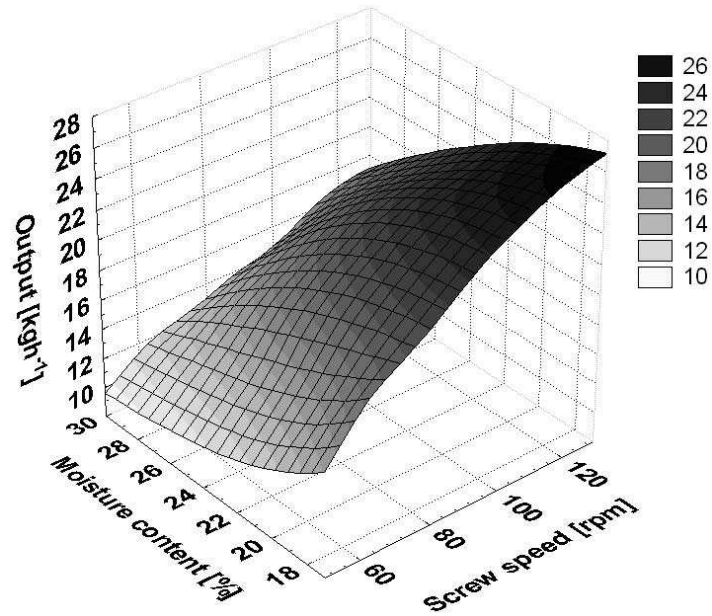


Fig. 2. Changes of the process output during potato starch extrusion-cooking at 120 °C

During processing at 100 °C, an initial decrease and then increase of the process efficiency with increase of starch moisture content was observed. In the course of processing at temperatures: 120 and 140 °C it was found that water addition decreased the extruder capacity (fig. 2).

Application of extrusion cooking technique for plant starch processing needs a very significant factor - determination of specific mechanical energy (SME) necessary to obtain product mass unit. Della Valle et al. [2, 3] processing the potato starch on twin screw extrusion-cooker indicated that SME changed within the interval 0.1 to 0.32 kWhkg<sup>-1</sup>.

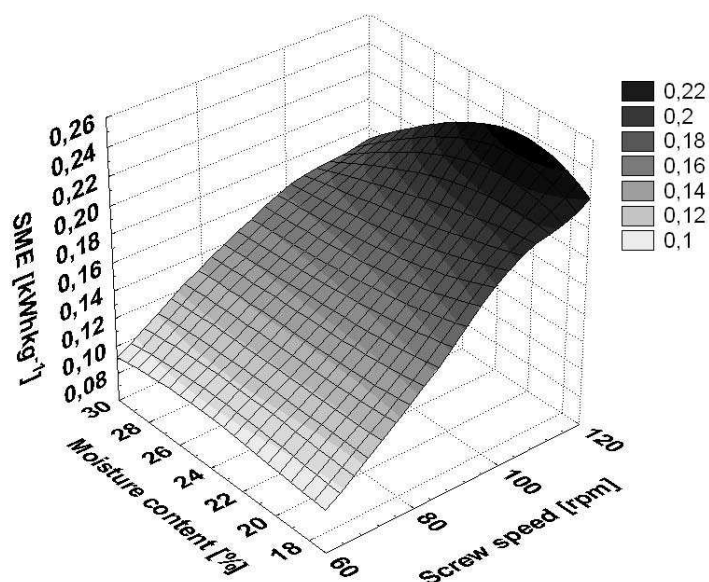


Fig. 3. SME changes during potato starch extrusion-cooking at 100 °C

The present authors' studies showed that the moisture content of the raw material and extruder screw rotation speed exerted a substantial impact on SME during extrusion-cooking of potato starch. The research revealed that the values of SME were within a range 298.8-990 kJkg<sup>-1</sup> (0.083-0.275 kWhkg<sup>-1</sup>). The lowest energy consumption was observed during the extrusion-cooking of potato starch at 140 °C. The highest SME was recorded during the extrusion-cooking at a temperature of 100 °C (at moisture content of 17 and 20%) and at 120 °C (moisture content 25 and 30%). Screw rotational speed increase caused rise in mechanical energy consumption, independently of the process temperature (fig. 3).

Effect of moisture content on the SME was inconclusive. When carrying out the process at 100 °C with lower screw speed (60-80 rpm) minimal changes in mechanical energy consumption was observed with increase in starch moisture content. Higher moisture content of the starch caused SME decrease when higher screw speed (100-120 rpm) was used. When processed at higher temperature an increase of moisture content of starch increased the rate of the SME (fig. 4). It was most likely caused by increasing of the viscosity of processed slurry. Due to the presence of water the starch melts and underwent liquefaction, resulting in lower glass transition temperature.

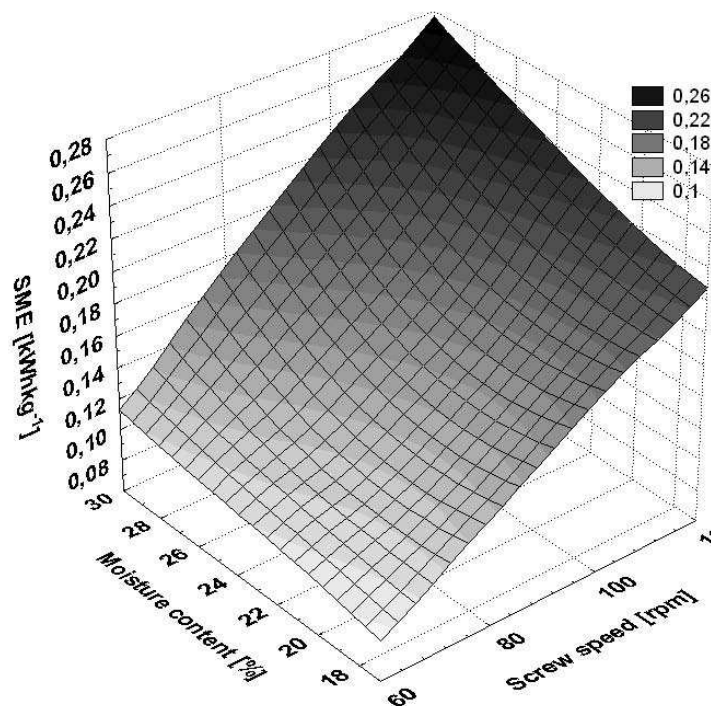


Fig. 4. SME changes during potato starch extrusion-cooking at 120 °C

## CONCLUSIONS

Extrusion-cooking process of the potato starch was characterised by good efficiency. It ranged between 11.3 kgh<sup>-1</sup> and 28 kgh<sup>-1</sup> dependently of the process parameters.

Changes in the extruder output depended mainly on the extruder screw speed and starch moisture content, less on process temperature.

Modification of starch by extrusion-cooking technique is characterized by relatively low specific mechanical energy consumption a range from 298.8 to 990 kJkg<sup>-1</sup> (0.083-0.275 kWhkg<sup>-1</sup>). Significant impact on the values of the SME had a screw speed, very little a moisture content of the raw material.

## Acknowledgments

This scientific work was supported by Polish Ministry of Science and Higher Education funds on science in the years 2009-2011 as a research project NN 313065936.

## REFERENCES

1. Błaszczak W., Valverde S., Fornal J., 2005.: Effect of high pressure on the structure of potato starch, *Carbohydrate Polymers*, 59, 377-383.
2. Della Valle G., Boche Y., Colonna P., Vergnes B., 1995.: The extrusion behaviour of potato starch, *Carbohydrate Polymers*, 28, 255-264.
3. Della Valle G., Vergnes B., Colonna P., Patria A., 1997.: Relations between rheological properties of molten starches and their expansion behaviour in extrusion, *Journal of Food Engineering*, 31, 277-296.
4. Harper J. M., 1981.: *Extrusion of Foods*, Boca Raton: CRC Press.
5. Igura N., Katoh T., Hayakawa I., Furio Y., 2001.: Degradation profile of potato starch melts through a capillary tube viscometer, *Starch*, 53, 623-628.
6. Janssen L.P.B.M., Moscicki L., 2009.: *Thermoplastic Starch. A Green Material for Various Industries*, Weinheim, Wiley-VCH.
7. Janssen L.P.B.M., Moscicki L., Mitrus M., 2002.: Energy aspects in food extrusion-cooking, *International Agrophysics*, 16, 191-195.
8. Kawai K., Fukami K., Yamamoto K., 2007.: Effects of treatment pressure, holding time, and starch content on gelatinization and retrogradation properties of potato starch-water mixtures treated with high hydrostatic pressure, *Carbohydrate Polymers*, 69, 590-596.
9. Mercier C., Linko P., Harper J.M., 1998.: *Extrusion cooking*, St. Paul, American Association of Cereal Chemists, Inc.
10. Mitrus M., 2005.: Changes of specific mechanical energy during extrusion cooking of thermoplastic starch. TEKA Commission of Motorization and Power Industry in Agriculture, 5, 152-157.
11. Mitrus M., 2010.: Modyfikacja skrobi pszennej metodą ekstruzji, In Witrowa-Rejher D., Lenart A., Rybczyński R. (Eds.), *Wpływ procesów technologicznych na właściwości materiałów i surowców roślinnych*, Lublin, Wydawnictwo Naukowe FRNA, 107-112.
12. Mitrus M., Moscicki L., 2009.: Extrusion-Cooking of TPS. In Janssen L.P.B.M., Moscicki L. (Eds.), *Thermoplastic Starch. A Green Material for Various Industries*, Weinheim, Wiley-VCH, 149-157.
13. Mitrus M., Wójtowicz A., Mościcki L., 2010.: Modyfikacja skrobi ziemniaczanej metodą ekstruzji, *Acta Agrophysica*, 16(1), 101-109.
14. Mościcki L., Mitrus M., Wójtowicz A., 2007.: *Technika ekstruzji w przemyśle rolno-spożywczym*, Warszawa, PWRiL.
15. Singh S., Gamlath S., Wakeling L., 2007.: Nutritional aspects of food extrusion: a review, *International Journal of Food Science & Technology*, 42, 916-929.
16. Souza R.C.R., Andrade C.T., 2002.: Investigation of the gelatinization and extrusion processes of corn starch, *Advances in Polymer Technology*, 21, 17-24.
17. Van den Einde R., Bolsius A., Van Soest J., Janssen L.P.B.M., Van der Goot A., Boom R., 2003.: The effect of thermomechanical treatment on starch breakdown and the consequences for the process design, *Carbohydrate Polymers*, 55, 57-63.
18. Wolf B., 2010.: Polysaccharide functionality through extrusion processing, *Current Opinion in Colloid & Interface Science*, 15, 50-54.
19. Wójtowicz A., Mitrus M., 2010.: Effect of whole wheat flour moistening and extrusion-cooking screw speed on the SME process and expansion ratio of precooked pasta products, *TEKA Commission of Motorization and Power Industry in Agriculture*, 10, 517-526.
20. Yan H., Zhengbiao G.U., 2010.: Morphology of modified starches prepared by different methods, *Food Research International*, 43, 767-772.

### ZMIANY ENERGOCHŁONNOŚCI PODCZAS EKSTRUZJI SKROBI ZIEMNIACZANEJ

**Streszczenie.** Najprostszą metodą fizycznej modyfikacji skrobi jest ekstruzja. W pracy przedstawiono wyniki pomiarów wydajności i energochłonności procesu ekstruzji skrobi ziemniaczanej. Proces ekstruzji skrobi ziemniaczanej charakteryzował się wysoką wydajnością. Zmiany wydajności ekstrudera zależały głównie od zmian prędkości obrotowej ślimaka ekstrudera i wilgotności skrobi, w mniejszym stopniu od temperatury procesu. Wydajność zmieniała się w granicach 11.3-28 kg h<sup>-1</sup> w zależności od zastosowanych parametrów procesu. Wyniki badań wskazują, że procesu ekstruzji skrobi ziemniaczanej związany jest z relatywnie niską energochłonnością (0.083-0.275 kWh kg<sup>-1</sup>). Znaczący wpływ na zmiany SME miała prędkość ślimaka ekstrudera, niewielki wpływ miała wilgotność przetwarzanej skrobi.

**Słowa kluczowe:** skrobia ziemniaczana, ekstruzja, wydajność, energochłonność.

## EXTRUSION-COOKING OF WHEAT STARCH

Marcin Mitrus, Agnieszka Wójtowicz

Department of Food Process Engineering, Faculty of Production Engineering,  
University of Life Sciences, Doświadczalna 44, 20-280 Lublin, Poland,  
marcin.mitrus@up.lublin.pl

**Summary.** During the study the impact of extrusion-cooking process parameters on the wheat starch physical properties changes was investigated. The process was characterized by small energy consumption within a range 270-1069 kJkg<sup>-1</sup>. Extrusion-cooking technique allows creating the degree of gelatinization of processed starch. It is possible to achieve low or high level of gelatinization depending on the process parameters. Expansion index of the extrudates decreased with increase of wheat starch moisture content. It was found that the use of the extrusion process resulted in increase of water absorption and cold water solubility of starch. The highest value of WAI was 690% and WSI was 19%.

**Key words:** wheat starch, extrusion cooking, specific mechanical energy, gelatinization, solubility, water absorption.

### INTRODUCTION

Starch plays an important role in many industries, especially in food and feed sector. In practice, native starches are not simply suitable for any specific application. Therefore, various starch modification techniques have been developed for food and non-food applications. The most popular methods of starch modification are chemical methods.

In recent years, it was found that in many cases, especially in the food industry, chemically modified starch can be replaced by extrusion-cooked starch. Food extrusion has been practiced for more than 50 years with early developments in the preparation of ready-to-eat cereals [8]. During the extrusion, physicochemical transformation of starch take place without any additional chemicals. Baro-thermal treatment causes gelatinisation of starch. This process is accompanied by rupture of intermolecular bonds, resulting in rupture of starch grains and significantly increase of water absorption [4, 9, 11, 12, 13, 14].

The degree of changes in starch depends on properly selected process parameters and the residence time of raw material in the extruder. This allows to affect on the properties of the obtained modified starches, including degree of gelatinization and viscosity of the gels [2, 18].



## MATERIALS AND METHODS

Wheat starch Meritena 200 type was produced by SYRAL BELGIUM N.V. (Belgium). Its moisture content was 11,8 %. During the extrusion-cooking process the 4 levels of moisture content of raw material (17, 20, 25 and 30%) were used. In order to obtain expected moisture content, starch was mixed with sufficient amount of water and stored for 24h in air tight polyethylene bags at room temperature to make whole sample material homogeneous.

Extrusion-cooking of potato starch was carried out using a modified single screw extrusion-cooker TS-45 (Polish design) with L/D = 16. The die with one opening with a diameter of 3 mm was used. During the study three temperature of extrusion process (100, 120 and 140 °C) and a variable speed screw (60, 80, 100, 120 rpm) were used.

During the extrusion-cooking process energy consumption was measured with a wattmeter connected to the extruder and the specific mechanical energy (SME) input was calculated [7, 10, 20].

$$SME = \frac{n \cdot P \cdot O}{n_m \cdot Q} [\text{kWhkg}^{-1}], \quad (1)$$

where: n - screw rotations [ $\text{min}^{-1}$ ],  
 $n_m$  - maximal screw rotations [ $\text{min}^{-1}$ ],  
 P - power [kW],  
 O - engine loading [%],  
 Q - extruder output [ $\text{kg h}^{-1}$ ].

Degree of starch gelatinization was measured by enzymatic method with diastase in accordance with Polish standard PN-A-79011-11:1998 [15].

Cross-sectional expansion index was determined as the diameter of extrudates divided by the diameter of the matrix opening [11]. Measurements were done in 10 repetitions.

Water absorption index was determined according to the method of Anderson et al. [1] with own modification. The extrudates were crushed using a laboratory mill to particles with a diameter less than 0.3 mm. A 0.7 g ground sample was suspended in 7 ml of distilled water at 20°C in a tared centrifuge tube, stirred intermittently over a 10 min period. The resulting suspension was centrifuged at rotational speeds 250  $\text{s}^{-1}$  for 10 minutes in T24D type centrifuge. The supernatant liquid was poured into a tared evaporating dish. The remaining gel was weighted and the WAI was calculated as:

$$WAI = \frac{m_g}{m_s} \cdot 100[\%], \quad (2)$$

where:  $w_g$  - weight of gel [g],  
 $w_s$  - weight of dry sample [g].

Measurements were performed in 3 replications.

Water solubility index was determined from the amount of dried solids recovered during evaporation of supernatant obtained from the WAI analysis according to the method of Harper [5]. Results were calculated from formula:

$$WSI = \frac{w_{ds}}{w_s} \cdot 100[\%], \quad (3)$$

where:  $w_{ds}$  - weight of dry solids in supernatant [g],  
 $w_s$  - weight of dry sample [g].

Measurements were performed in 3 replications.

## RESULTS

Application of extrusion cooking technique for plant starch needs a determination of specific mechanical energy (SME) necessary to obtain product mass unit. As Bindzus et al. [3] hold when wheat, maize and rice starch was processed at twin screw extruder the SME values changed in the range 0,081–0,365 kWhkg<sup>-1</sup>. Wiedmann and Strobel [19] in their investigations on the extrusion of wheat TPS recorded the SME ranging from 0,1 to 0,55 kWhkg<sup>-1</sup> depending on material moisture.

The use of extrusion-cooker TS-45 equipped with additional cooling system allowed to keep a stable conditions during wheat starch modification. Extrusion-cooking of the wheat starch was characterised by low mechanical energy consumption (SME) within a range 270-1069.2 kJkg<sup>-1</sup> (0.075-0.297 kWhkg<sup>-1</sup>). Changes in SME depended mainly on the extruder screw speed and starch moisture content, less on process temperature (fig. 1).

Screw rotational speed increase caused rise in mechanical energy consumption, independently of the process temperature. Effect of moisture content on the SME was inconclusive. When carrying out the process at 100 °C and 120 °C the higher moisture content of the starch caused SME increase. During wheat starch extrusion-cooking at 140 °C the higher moisture content of the starch caused SME decrease.

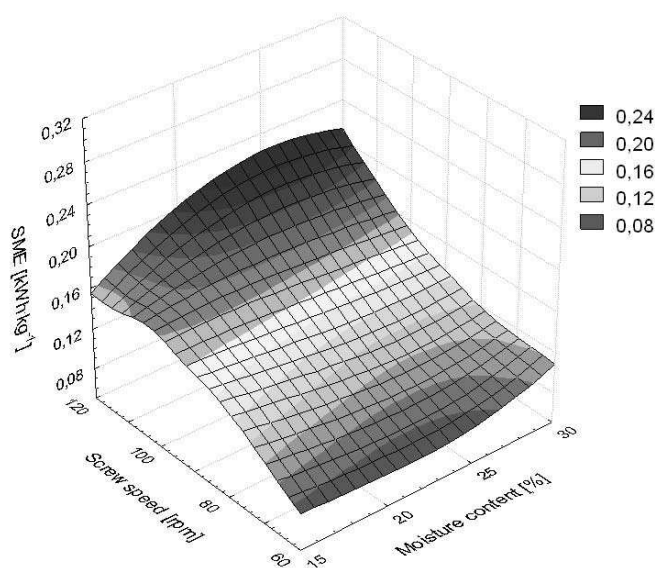


Fig. 1. SME changes during wheat starch extrusion-cooking at 100 °C

The highest degree of gelatinization (100%) was recorded for starch extruded at 100 °C at the moisture content 17%. The lowest degree of gelatinization (69.8%) was recorded for starch extruded at 120 °C at the moisture content 30%. During the studies, independent of the extrusion process parameters, decrease of the degree of starch gelatinization with starch moisture content increase was observed. The research revealed that the degree of starch gelatinization increased with increase extruder screw speed for wheat starch processed at temperature 100 and 140 °C. When carrying out the process at 120 °C the higher extruder screw speed caused decrease in degree of gelatinisation (fig. 2).

Measurements of the expansion index of extruded wheat starch showed that its value decreases with moisture content increase (fig. 3). Extruder screw speed increase caused increase of expansion index. This is a common phenomenon for the most of the extrudates. Extrudates were characterized by a typical structure, resembling a honeycomb structure. Values of the expansion index ranged between 2.7 and 6.2.

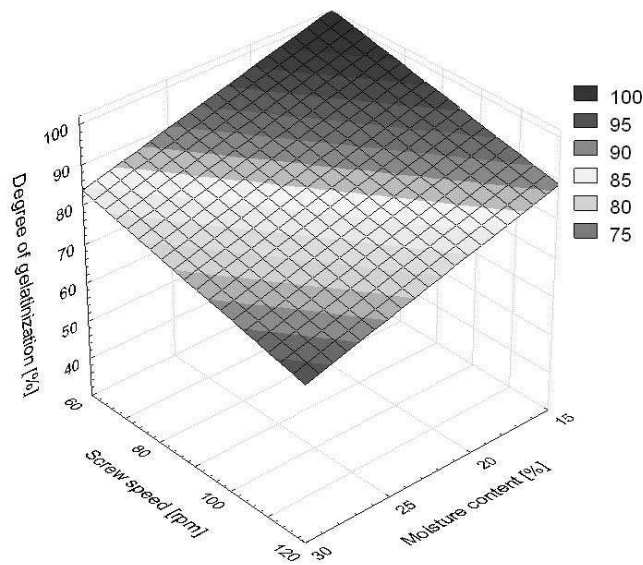


Fig. 2. Degree of gelatinisation changes for wheat starch extrusion-cooked at 120 °C

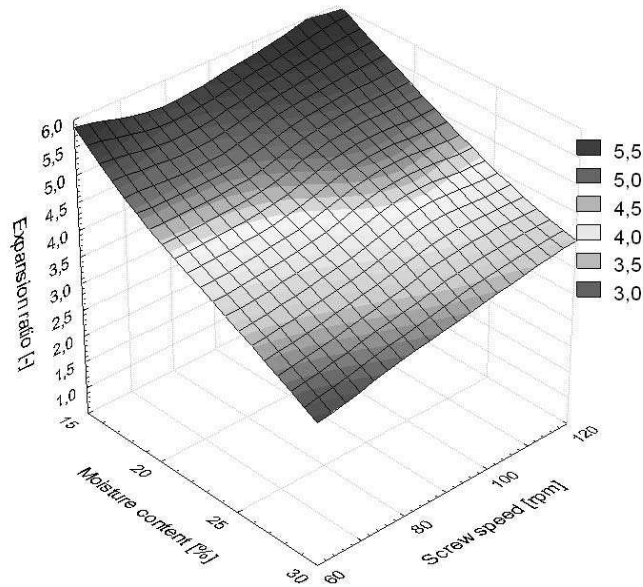


Fig. 3. Expansion index changes during wheat starch extrusion-cooking at 120 °C

According to Ryu and Ng [17] the moisture content in the feed material influences the rheological properties of the melt and builds up the vapor pressure. This causes extensive flash-off of internal moisture when the melt exits the die. However, the viscosity of the melt affects bubble growth as well as shrinkage of generated bubbles. The viscosity of the melt at higher moisture content is lower, thus bubble shrinkage and collapse are increased when steam is flashing at the exit. The viscosity of the melt and the glass transition temperature during the setting of air bubble inside extrudates influenced bubble collapse. Bubble collapse during bubble setting was increased with higher moisture of melt, since melt with higher moisture or lower viscosity had a lower glass transition temperature. Thus, the expansion was decreased in a melt with higher moisture content.

Native wheat starch has WAI approximately 184% and WSI approximately 0.24%. The study showed that the baro-thermal modification of starch significantly effects on its water absorption and solubility in cold water.

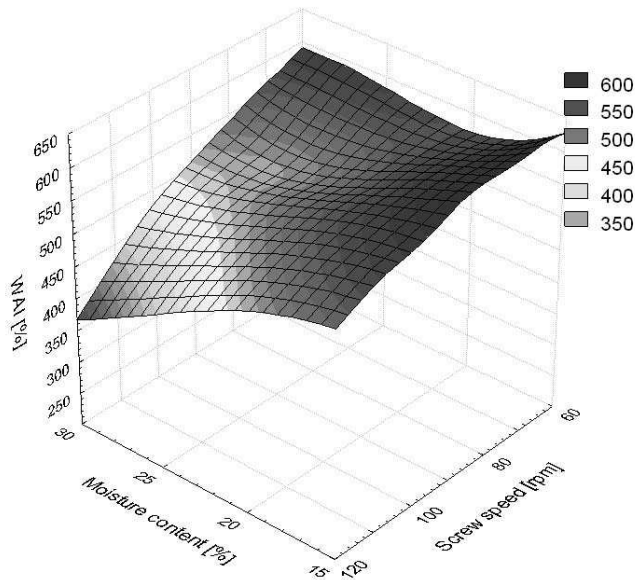


Fig. 4. Wheat starch WAI changes during extrusion-cooking at 100 °C

With the increase in moisture content of processed wheat starch the decrease of water absorption was observed (fig. 4). During extrusion-cooking at 100 and 120 °C the higher extruder screw speed caused WAI decrease. The researches carried out at temperature 140 °C revealed that extruder screw speed increase caused an initial increase (60-80 rpm) and then decrease (100-120 rpm) in modified starch water absorption. WAI values of the extruded wheat starch ranged from 369 to 690% and generally did not deviate from the values obtained for a typical starch extrudates [8].

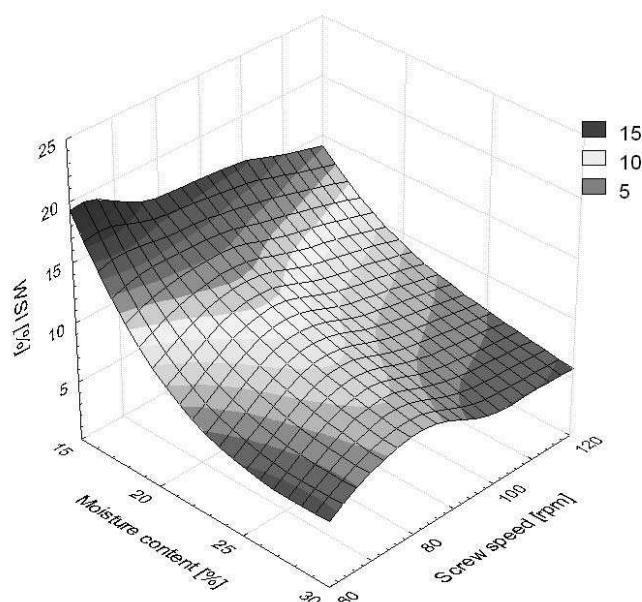


Fig. 5. Wheat starch WSI changes during extrusion-cooking at 140 °C

The research showed that the starch moisture content increase caused reduction of extruded starch WSI (fig. 5). Similar effects of decreasing moisture on WSI have been reported earlier for starch, maize grits and wheat flour [16]. During the studies initial increase (60-80 rpm) and then decrease (100-120 rpm) in modified starch solubility with extruder screw speed increase was observed. WSI values of the extruded wheat starch ranged from 3.8 to 19%. The changes of the solubility of starch were related with changes in the process of gelatinization and starch degradation due to starch moisture content increase. At low to intermediate moisture content and high temperature, the water contained in starch might behave like a lubricant [6]. Degradation of starch progressed by increasing extruder screw speed at low moisture content because less lubricant (water) was available.

## CONCLUSIONS

In the light of obtained results following conclusions can be overtaking:

1. Modification of wheat starch by extrusion-cooking technique is characterized by relatively low specific mechanical energy consumption, ranged from 270 to 1069.2 kJkg<sup>-1</sup> (0.075-0.297 kWhkg<sup>-1</sup>). Significant impact on the values of the SME had a screw speed and a moisture content of the raw material.
2. Extrusion-cooking technique allows creating the degree of gelatinization of processed starch. It was possible to achieve low or high level of gelatinization depending on the process parameters. This is especially important for food and feed applications.
3. Expansion index of wheat starch largely depended on the parameters of the extrusion process. Its value decreased with moisture content increase while increased with screw speed increase.

4. The extrusion process of starch increased the water absorption and cold water solubility. WAI values of the extruded wheat starch ranged from 369 to 690% while WSI ranged from 3.8 to 19%. These changes were closely related to the course of the process of starch gelatinization and degradation and their extent depends on the extrusion parameters used.

### Acknowledgments

This scientific work was supported by Polish Ministry of Science and Higher Education funds on science in the years 2009-2011 as a research project NN 313065936.

### REFERENCES

1. Anderson, R.A., Conway, H.F., Peplinski A.K., 1970.: Gelatinization of corn grits by roll cooking, extrusion cooking and steaming, *Starch*, 22, 130-134.
2. Andersson Y, Hedlund B., 1991.: Extruded wheat flour: correlation between processing and product quality parameters, *Food Quality And Preference*, 2, 201-216.
3. Bindzus W., Livings S.J., Gloria – Hernandez H., Fayard G., van Lengerich B., Meuser F., 2002.: Glass transition of extruded wheat, corn and rice starch, *Starch*, 54, 393-400.
4. Hagenimana A., Ding X., Fang T., 2006.: Evaluation of rice flour modified by extrusion cooking, *Journal of Cereal Science*, 43, 1, 38-46.
5. Harper J. M., 1981.: *Extrusion of Foods*, Boca Raton: CRC Press.
6. Igura N., Katoh T., Hayakawa I., Furio Y., 2001.: Degradation profile of potato starch melts through a capillary tube viscometer, *Starch*, 53, 623-628.
7. Janssen L.P.B.M., Moscicki L., Mitrus M., 2002.: Energy aspects in food extrusion-cooking, *International Agrophysics*, 16, 191-195.
8. Mercier C., Linko P., Harper J.M., 1998.: *Extrusion cooking*, St. Paul, American Association of Cereal Chemists, Inc.
9. Miladinov, V.D.; Hanna, M.A., 2001.: Temperatures and ethanol effects on the properties of extruded modified starch, *Industrial Crops and Products*, 13, 1, 21-28.
10. Mitrus M., 2005.: Changes of specific mechanical energy during extrusion cooking of thermoplastic starch. TEKA Commission of Motorization and Power Industry in Agriculture, 5, 152-157.
11. Mościcki L., Mitrus M., Wójtowicz A., 2007.: *Technika ekstruzji w przemyśle rolnospożywczym*, Warszawa, PWRiL.
12. Moscicki L., 2011.: *Extrusion-cooking technique: Applications, theory and sustainability*, Weinheim, Wiley-VCH.
13. Nabeshima M., Grossmann M., 2001.: Functional properties of pregelatinized and cross-linked cassava starch obtained by extrusion with sodium trimetaphosphate, *Carbohydrate Polymers*, 45, 347-353.
14. Quing B., Ainworth P., Tucker G., Marson H., 2005.: The effect of extrusion conditions on the physiochemical properties and sensory characteristics of rice-based expanded snacks, *Journal of Food Engineering*, 66, 283-289.
15. PN-A-79011-11:1998, *Food concentrates – Test methods – Determination of degree of starch gelatinization (in Polish)*.
16. Singh N., Smith A.C., 1997.: A comparison of wheat starch, whole wheat meal and oat flour in the extrusion cooking process, *Journal of Food Engineering*, 34, 15-32.

17. Ryu G.H., Ng P.K.W., 2001.: Effects of selected process parameters on expansion and mechanical properties of wheat flour and whole cornmeal extrudates, *Starch*, 53, 147-154.
18. Van den Einde R., Bolsius A., Van Soest J., Janssen L.P.B.M., Van der Goot A., Boom R., 2003.: The effect of thermomechanical treatment on starch breakdown and the consequences for the process design, *Carbohydrate Polymers*, 55, 57-63.
19. Wiedmann W., Strobel E., 1991.: Compounding of thermoplastic starch with twin-screw extruders, *Starch*, 43, 138-145.
20. Wolf B., 2010.: Polysaccharide functionality through extrusion processing, *Current Opinion in Colloid & Interface Science*, 15, 50-54.

### EKSTRUZJA SKROBI PSZENNEJ

**Streszczenie.** W trakcie badań określano wpływ parametrów procesu ekstruzji na zmiany fizycznych właściwości skrobi pszennej. Proces ten charakteryzuje się niską energochłonnością w zakresie 270-1069 kJkg<sup>-1</sup>. Technika ekstruzji umożliwia kreowanie stopnia skleikowania przetwarzanej skrobi. Możliwe jest uzyskanie niskiego lub wysokiego stopnia skleikowania skrobi w zależności od zastosowanych parametrów procesu. Stopień ekspandowania ekstrudatów malał wraz ze wzrostem wilgotności skrobi pszennej. Stwierdzono, że zastosowanie procesu ekstruzji powoduje wzrost absorpcji wody i rozpuszczalności skrobi w zimnej wodzie. Najwyższa wartość WAI wynosiła 690% a WSI 19%.

**Słowa kluczowe:** skrobia pszenna, ekstruzja, energochłonność, kleikowanie, rozpuszczalność, absorpcja wody.

## POSSIBILITIES OF APPLICATION OF MODERN SI ENGINES IN AGRICULTURE

Janusz Mysłowski\*

\*West –Pomeranian Technological University

**Summary.** In the article the development of modern engines with spark ignition has been presented based on their operational parameters. Comparison with the parameters of modern engines used in agriculture has been conducted and based on the usefulness of evaluated engines has been determined.

**Key words:** engine, operation parameters.

### INTRODUCTION

Flexibility of combustion engine says about its ability to adapt to variable loading and rotational speed. For traction engines it is very important rating in regard to their operational possibilities. Great intensity of road traffic forces the use of engines intended for automotive vehicles with large mass, which can influence on reduction of movement's smoothness as a result of slight elasticity of the engine. Numerical term for engine elasticity coefficient. It can be determined based on the external characteristic of engine [1,2], in the way presented below :

$$E = e_M e_n = \frac{M_{o\max}}{M_N} \frac{n_N}{n_{Mo\max}}, \quad (1)$$

gdzie:  $e_M$  – elasticity of rotational moment,  
 $e_n$  - extension of rotational speed,  
 $M_{o\max}$  - maximal rotational moment engine,  
 $M_N$  - rotational moment suitable for nominal power,  
 $n_{Mo\max}$  - rotational speed of the Maximal rotational power,  
 $n_N$  - nominal rotational speed.

The first module of the product presents the elasticity of the rotational moment and it depends on the course of the engine's rotation moment. The course depends on such factors as : characteristic parameters of approaching arrangement, characteristic of camshaft, characteristic of power supply arrangement. Through the change of above mentioned parameters we can influence the course of the rotational moment's curves in the direction desired by the user, in order to make the engine well



adapted to carry out its tasks. Particular in concerns the engines in agricultural applications. The way of improvement's realization of the elasticity of the rotational moment depends on executive possibilities and analysis of probability of a given solution in case of specific engine.

The possibilities of changing the second module of the product are closely related to the changes of the first module and it depends on dislocation of position of the maximum of the rotational moment curve. From the position of that maximum depends the extension of rotational speed and influencing it we can control the engine's elasticity effectively. Taking under consideration obtained values of elasticity by the cars' engines of the newest generation it can be said that considerable more profitably were presented engines with self - ignition and direct injection for which the average value of the total elasticity came to  $E = 2,905$  ( $e_M = 1,449$  and  $e_n = 2,005$ ), while for engines with the spark ignition it came to  $E = 1,647$  ( $e_M = 1,136$  and  $e_n = 1,450$ ) [2,3]. The Mitsubishi Company was the first company which used the engines with spark ignition and with direct injection in model Carisima 1.8 GDI and the economical advantages of the engine work expressed by low fuel consumption as for the engines with spark ignition had decided about it. The profile of the time density of the fuel consumption is presented in Fig.1.

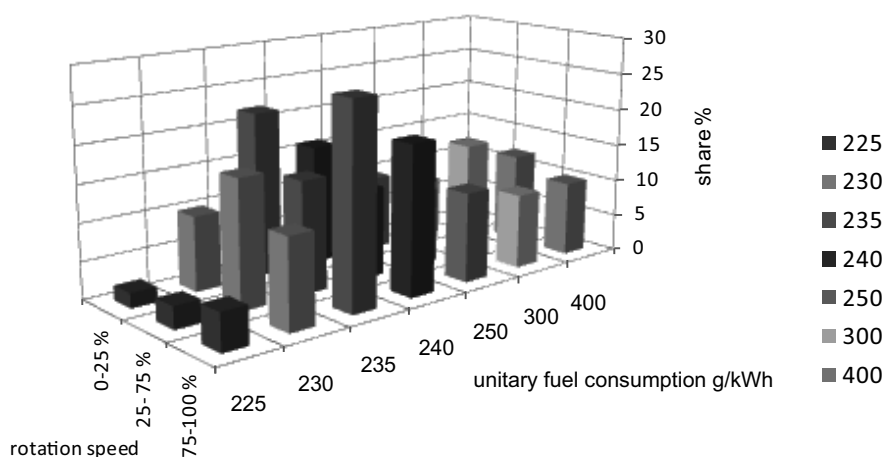


Fig. 1. The profile of the time density of fuel consumption of the Mitsubishi 1.8 GDI [4] engine

In that figure it is clearly seen, that the values of the unitary fuel consumption of described engine are very near the values obtained by the compression-ignition engines which are powering cars. The biggest percentage share of fuel consumption is located in the range from 230 to 240 g/kWh and is low as for the petrol engines. However, the total elasticity of that was low and it came to just  $E = 1,582$ . Further searches of improvements of the engines' operating parameters with the spark ignition were directed to the area where their economicalness and elasticity would be improved with the use of turbo supercharger. Previously, that supercharge encountered some obstacles in the form of too high exhaust gases temperatures which were influencing the vitality of turbocompressors as well their low follow up with changes the engine loading.

## NEW PETROL ENGINES

Operation of the Volkswagen Concern which aim is to bring to general use of the petrol engines with direct injection has brought positive results, and the series of superturbocharged engines designet TFSI ( old sign) engines the pulsating drive of turbo-compressor has been used , dividing the outlet collector into two parallel parts.

The rotors of turbo-compressor having diameters equal to 37 or 41 mm, gives very low inertiion, ans at the same time short response time for the exhaust gases impulses. It allows to reach the rotational speed up to 220 000 1/min, what it is not possible to achieve in turbo – compressor of truck engine.

Table 1.Parameters of petrol engine' work with the direct injection of Volkswagen Concern

1.	Model	1,4 FSI AUX	1,4TFSI CAXC	1,4 TSI BLG	2,0 TFSI AXX	3,0 V6 TFSI
1.	Type	In - line	In – line	In – line	In - line	V - type
2.	Number of cylinder	4	4	4	4	6
3.	D	76,5 mm	76,5 mm	76,5 mm	82,5 mm	84,5 mm
4.	Number of valves	16	16	16	16	24
5.	$V_{ss}$	1390 cm <sup>3</sup>	1390 cm <sup>3</sup>	1390 cm <sup>3</sup>	1984 cm <sup>3</sup>	2995 cm <sup>3</sup>
6.	$\epsilon$	12	10	10	10,5	10,5
7.	$N_e/n$	63 kW 5000 1/min	92 kW 5000 1/min	125 kW 6000 1/min	147 kW 5700 1/min	213 kW 5000 1/min
8.	$M_o/n$	130 Nm 3500 1/min	200 Nm 1500 1/min	240 Nm 1750 1/min	280 Nm 1800 1/min	420 Nm 2500 1/min
9.	Supercharging	–	Turbo	Turbo + mech Eaton	Turbo	Turbo + Mech Roots
10.	Dim.L.O.	95/98	95/98	98	95/98	95/98

Permanent progress in constructional solutions of turbocharged petrol engines of VW/Audi Concern can be traced based on corporation of unit power ( its increase ) of that engines, what is presented in Fig.2, and the elasticity of the engines describet in Table 1,has been presented in Table 2.

Table 2.Flexibility of the Volkswagen Group petrol engines

1.	Model	1,4 FSI AUX	1,4TFSI CAXC	1,4 TSI BLG	2,0 TFSI AXX	3,0 V6 TFSI
1.	$e_M$	1,079	1,137	1,205	1,136	1,031
2.	$e_n$	1,428	3,333	3,428	3,333	2,000
3.	E	1,542	3,789	4,130	3,786	2,063

The values of the unitary fuel consumption of the discussed group of petrol engines within the form of the time-density profile, presented on figures 3 and 4, what allowed for further consid-

eration over comparison of their working parameters with the parameters of compression – ignition engines used in agriculture.

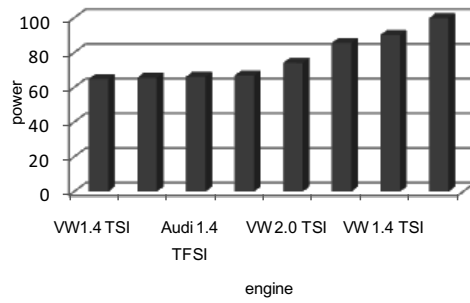


Fig. 2. Unitary powers petrol engines VW/Audi kW/dm³

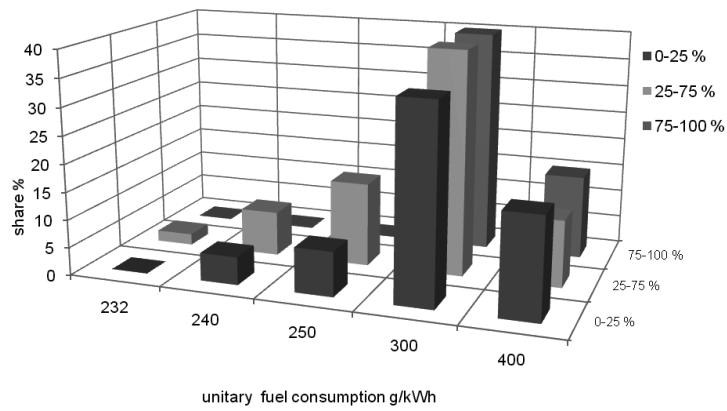


Fig. 3. The time-density profile of the Opel 1.6 16V engine in the form of bar set-up

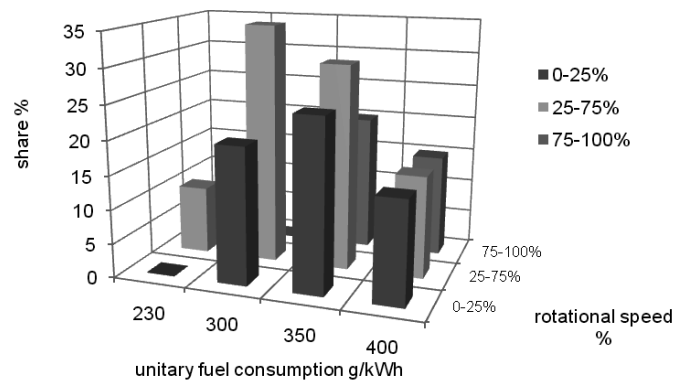


Fig. 4. Time-density characteristic of VW 1.0 engine In the form of bar set-up

### WORKING PARAMETERS OF AGRICULTURAL ENGINES

As the evaluation criterion assumed the engines' elasticity, while for older models its values were given in table 3. Based on the data given in Table 3, we can say that the average elasticity of the agricultural engines of modern petrol engines which is equal to 3,062. In regard to the elasticity of rotational moment that comparison looks much better, because it was better for older agricultural engines (1,195) in comparison with the elasticity of the rotational moment of petrol engines equal to 1,118, and that parameter is very crucial during the operation of the agricultural engines.

Table 3. The elasticity of the agricultural engines [5]

Engine	Average value of $e_M$	Average value of $e_n$	E
Ursus S-312C	1,146	1,223	1,401
Ursus S-4002	1,054	1,334	1,406
Ursus AD3.152	1,162	1,615	1,876
Ursus AD3.152 UR	1,168	1,607	1,877
Ursus A4.236	1,098	1,538	1,689
Ursus A4.248	1,160	1,428	1,656
New Holland 1.85	1,330	1,769	2,352
Renault Ceres 95	1,239	1,437	1,780
Same Silver 90	1,286	1,786	2,296
Steyr 9086	1,291	1,534	1,980
Valmet 865	1,092	1,448	1,581
Zetor 8540	1,313	1,571	2,062
<b>Average</b>	<b>1,195</b>	<b>1,524</b>	<b>1,830</b>

For better picture of evaluated situation, the working parameters of tractors manufactured by wide – world known company John Deere have been presented. It's the company which produces tractors engines with power level ranging from 59 kW to 254 kW. These are not very strained engines in comparison to the engines with spark ignition enclosed in figure 2, because the volumetric power indicator for them ranges from 20,29 to 35,84 kW/dm<sup>3</sup>, but the politics of the company is directed for large durability of these engines but not their straining.

Table 4. Elasticity of John Deere agricultural engines [6]

Engine	$e_M$	$e_n$	E
John Deere 6620SE	1,693	1,533	2,595
John Deere 6330	1,366	1,277	1,745
John Deere 6320	1,336	1,533	2,048
John Deere 66920SE	1,513	1,437	2,174
<b>Average</b>	<b>1,484</b>	<b>1,445</b>	<b>2,140</b>

Comparing modern compression – ignition engines used in agriculture, it can be noticed significant increase of elasticity of the rotational moment for up to 24 %, upon insignificant decrease of elasticity of the rotational speed, it gives the rise of total elasticity for about 17 %. As an example, the characteristic of one of the engines described in Table 4 has been presented below. The improvement of the elasticity of tractors engines is clear, there is no doubt about it, however still the evaluation of their work economicalness must be made, which is lower than the compression – ignition engines of road vehicles, but for petrol engines very modern ones, as it was shown before, still is pretty far way to catch up with the tractors engines. That difference is estimated on the level between 15 and 25 %. The attention is paid to fact of constant unitary consumption  $g_c$  (Fig.5) on the external characteristic on the considerable useful space of rotational speed, what is much more essential indicator in relation to the tractor engines, for sure more important than their elasticity.

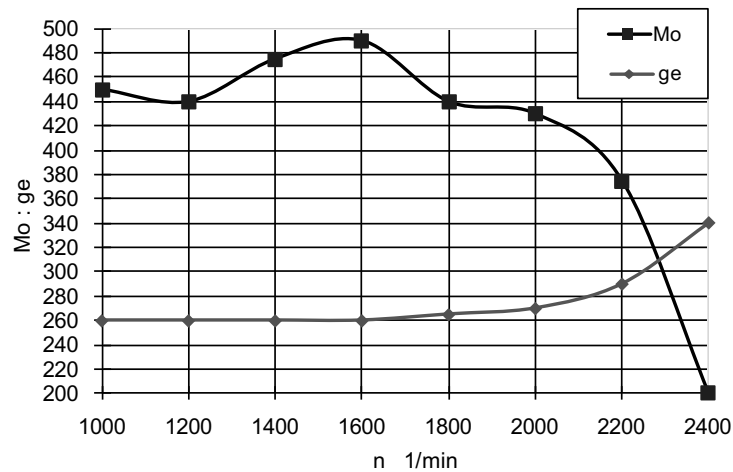


Fig. 5. The external characteristic of John Deere 66 920 SE engine

## CONCLUSIONS

Presented review of operating parameters of supercharged petrol engines with the spark ignition, despite huge construction progress, impinging on the exploational indicators does not induce to propaganda their use as a drive of agricultural vehicles. Different operational conditions do not

require a large elasticity of engines which is required because of traffic on public roads. In agricultural vehicles, greater pressure is put on the ability of implementing work (rotational moment and eventually increase of the coefficient of its elasticity) as well as work economicalness expressed by low fuel consumption. Because of that, those two parameters were taken under consideration while conducting this analysis.

#### REFERENCES

1. Dębicki M.: Teoria samochodu. Teoria napędu. WNT Warszawa 1969.
2. Mysłowski J., Kołtun J.: Elastyczność tłokowych silników spalinowych. WNT Warszawa 2000.
3. Mysłowski J.: comparative analysis of operation flexibility of direct injection diesel engines and spark-ignition engines. TEKA MOTORYZACJI I ENERGETYKI ROLNICTWA, POLSKA AKADEMIA NAUK Oddział w Lublinie, Volume II, Lublin 2002.
4. Mysłowski J.: Pojazdy samochodowe. Doładowanie silników. WKiŁ Warszawa 2011.
5. Mysłowski J., Mysłowski J.: Ocena właściwości eksploatacyjnych doładowanych silników rolniczych. MOTROL, Motoryzacja i Energetyka Rolnictwa. PAN Oddział w Lublinie. Tom 10/2008.
6. Instrukcja obsługi silnika John Deere 6620SE.

#### MOŻLIWOŚCI ZASTOSOWANIA NOWOCZESNYCH SILNIKÓW ZI W ROLNICTWIE

**Streszczenie.** W artykule przedstawiono rozwój nowoczesnych silników o zapłonie iskrowym w oparciu o ich parametry operacyjne. Przeprowadzono porównanie z parametrami współczesnych silników stosowanych w rolnictwie i na tej podstawie określono przydatność ocenianych silników.

**Słowa kluczowe:** silnik, parametry operacyjne.

## NEGATIVE IMPACT OF MOTORIZATION ON THE NATURAL ENVIRONMENT

Jaromir Mysłowski

Department of Mechanical Engineering and Mechatronics at the West Pomeranian  
University of Technology, Al.Piastów 19, 70-310 Szczecin, Poland.

**Summary.** The paper presents a growing threat to the natural environment caused by the avalanche growth in the number of trucks and cars within the urban areas and beyond their borders. Based on the example of the Szczecin agglomeration - located at the crossroads of the east-west and north-south transit routes - selected harmful components associated with the use of trucks and their negative impact on the human lives and functioning of the ecosystem in Poland have been discussed.

**Key words:** engine, exhaust gas smokiness.

### INTRODUCTION

The dynamic increase in the number of cars within urban agglomerations and beyond them and trucks in the domestic and international traffic have caused increasing threat to the environment. The situation has forced to adapt the existing motor transport infrastructure and the transport means themselves to the new needs and possibilities. New engine designs that meet the most stringent European standards and regulations are produced. Companies develop the existing designs and invent entirely new ones - different from the existing solutions.

These attempts are focused on meeting the three basic assumptions:

- low fuel consumption,
- low toxicity of exhaust gases,
- good dynamic properties (engine response),

The strong emphasis on the environmental protection, international arrangements and unusual weather phenomena and anomalies occurring in different parts of the world have indicated that this is the right way[1]. We cannot avoid the increased traffic of vehicles with conventional drive, and a gradual reduction of green areas determining the air quality and maintaining a balance in the ecosystem. Therefore, the research has been continued on improving the operational parameters, the quality of exhaust gases and increasing the pro-ecological awareness in the society [2,4].

## 1. SZCZECIN – URBAN AGGLOMERATION THREATENED BY MOTORIZATION

An efficient response to the growing environmental pollution as the result of impact of the transport means requires the necessary knowledge and reliable research. For this purpose, data about their harmfulness, expressed in measurable units, have been sought as well as the trends governing such interaction. On the basis of the example of a measurement system operating in Szczecin one can trace how such measurements of the area pollution and actions to minimise its effects are organised. The selection of measuring points is related to the intensity of traffic and the main transport routes passing through the urban agglomeration, which is a quite typical area as far as the organisation of transport designed to meet the needs of the population is concerned. Based on the previous experience with the operational testing carried out at the Faculty of Automotive Vehicles Operation of the Technical University of Szczecin, and now the West Pomeranian University of Technology, it has been found that apart from the traffic accident such impact is the most visible and felt in relation to trucks in the form of dust and exhaust gases production [4,10].

The selection of Szczecin is not accidental - its geographical location at the crossing of transit routes from the north to the south and from the west to the east already in the ancient times contributed to its dynamic development and great importance. Also at the present times, the existing and the planned routes passing nearby have provided opportunities for the development of the transport infrastructure, but at the same time the threats for the people and the environment have increased.

The phenomena occurring in Szczecin can be applied to other agglomerations, through which the transit transport goes, and that do not have ring roads to channel that traffic and divert it to the outskirts. That is why the experimental studies have been carried out on the express road S-3 (E 65) (Gorzow Wielkopolski - Szczecin in the direction of the port of Swinoujscie). The results of the operational studies, supported by the engine testing on test stands can be used in developing the future-oriented concept for the land connection of the Scandinavia with the Balkans, e.g. with the Swinoujscie - Jakuszyce motorway as the shortest connection from the Baltic to the Balkans.

A major reconstruction of the transport infrastructure of the city undertaken recently is precisely aimed at clearing the arteries, introduction of modern solutions and widely understood protection of the environment and the health and life of the residents.

## 2. MEASUREMENTS OF AIR POLLUTION IN SZCZECIN

In order to properly protect the environment, decisions have been taken as to constant measurements to monitor the pollution levels. For this purpose, automatic measurement stations have been installed in selected places. The place of measurement in Szczecin has been located in the immediate vicinity of the road with the traffic intensity of about 50 000 vehicles per day. The station measures the momentary concentration of nitrogen oxides, carbon monoxide and sulphur dioxide. An additional factor determining the location is the highest value of noise level at this point ( $L_{eq} = 81 \dots 85$  dB) on the road map of acoustic noise for the city of Szczecin [8,10]. The diagram of the measuring station operation is shown in Fig.1.



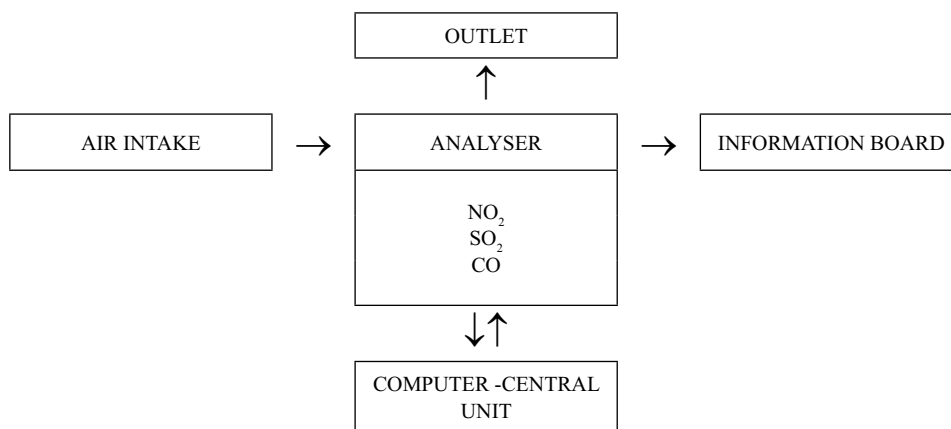


Fig. 1. Diagram of measuring station operation [8]

### 3. POLLUTION MEASUREMENT RESULTS

In 2005, three new automatic air-pollution monitoring stations were opened in Szczecin. The first station in the Andrzejewski Street, Fig.2.2, is designed to measure the urban background, where the representativeness of the measurement station is:

- SO<sub>2</sub> - several kilometres,
- NO, NO<sub>2</sub>, NO<sub>x</sub> - a few hundred metres,
- PM<sub>10</sub> - a few hundred metres,
- O<sub>3</sub> - several kilometres.

Another station at the Rodła Square is the station for the traffic air pollution measurements, where the representativeness of the measurement station is:

- SO<sub>2</sub> - a few kilometres,
- NO, NO<sub>2</sub>, NO<sub>x</sub> - a few hundred metres,
- PM<sub>10</sub> - a few hundred metres,
- C<sub>6</sub>H<sub>6</sub>, C<sub>7</sub>H<sub>8</sub>, C<sub>8</sub>H<sub>10</sub> - a few hundred metres,
- CO - a few hundred metres.

The last of them is in the northern part of the city, in the Łączna Street (impact of Z.Ch. "Police" Chemical Plant)

The representativeness of the measuring station in the Łączna Street is as follows:

- SO<sub>2</sub> - several km,
- NO, NO<sub>2</sub>, NO<sub>x</sub> - several kilometres,
- PM<sub>10</sub> - several kilometres,
- CO - several kilometres.

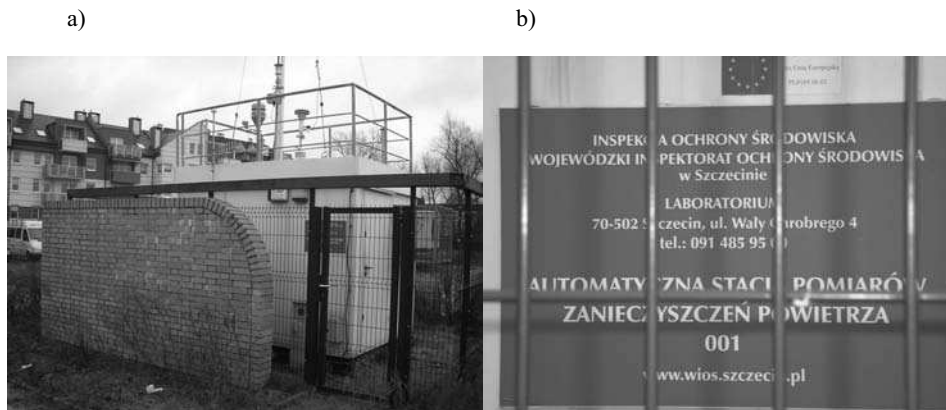


Fig. 2. a, b Measuring station in the Andrzejewski Street in Szczecin [9]

The presented results of the studies concerning the measurements of air pollution caused by the traffic of motor vehicles in Szczecin can be generalised by changing from the time density characteristics to the linear characteristics through calculation of the arithmetic mean value of the sum of the weighted average (Fig.3). This will allow to track the trends accompanying the composition of particular pollutants in the air over the recent years and to predict their possible contents.

Based on the previous studies, the characteristics has been carried out of the annual average air pollution in the agglomeration of Szczecin, which is shown in Fig.3.

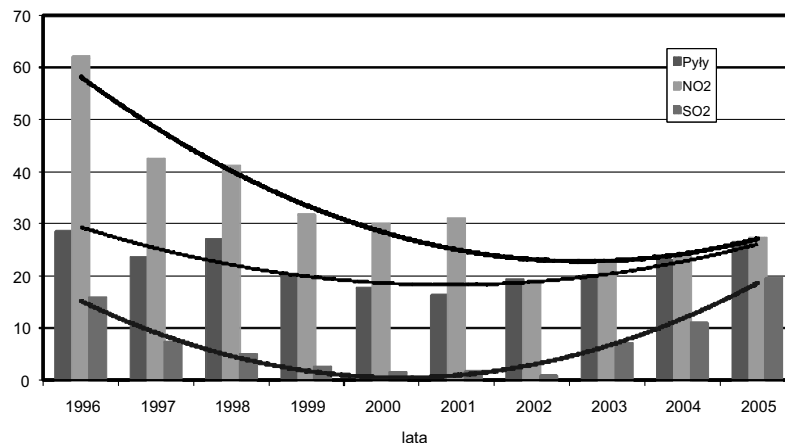


Fig. 3. Curve of annual air pollution in the urban agglomeration of Szczecin in  $\mu\text{g}/\text{m}^3$  [5]

**Legend:** Pyły: dust Lata: years

All the curves representing the basic components of the air pollution show the decreasing trend and then the increasing one. With regards to the suspended particulates, their content in the air decreases till 2001, when it reaches the minimum and then increases, although it has not yet reached the permissible value. This situation has been caused by a growing number of trucks transiting through Szczecin and the lack of a ring road that would relieve the city centre areas.

#### 4. OPERATIONAL PARAMETERS OF TESTED ENGINES

Operational fuel consumption is determined on the basis of road tests that are carried out in certain traffic conditions, with constant or variable speed. This value is dependant on the parameters of the vehicle and the engine as well as many operational factors, such as:

- technical condition of the engine, components and mechanisms of the vehicle,
- weight and distribution of carried passengers, luggage and cargo,
- properties of the road, its shape and type, the quality and condition of pavement,
- traffic conditions,
- atmospheric conditions.

The most general rate of the economic efficiency of the engine operation (economy of a vehicle) is the fuel consumption measured in  $\text{dm}^3/100 \text{ km}$ . However, this is an indicative rate and not very precise one, which does not take into account the operating conditions such as speed, duration of driving, load, road condition and operation time. With regards to the engines, there is a more accurate rate - specific fuel consumption - which sometimes is also given in technical descriptions, especially of heavy-duty trucks [3,6,7].

The specific fuel consumption expressed in  $\text{g/kWh}$  ( $\text{g/HP}$ ) indicates what fuel weight (and the chemical energy contained in it) is to be converted into mechanical work to produce one kilowatt-hour by the engine. This rate is advantageous as it is not dependant on the engine capacity (its size) and the type of used fuel, and thanks to that it is possible to compare different engines designed for different purposes, powered by both petrol and diesel fuel, or fuels of plant origin.

Dependencies between selected parameters determining the engines and pollution generated by them have been presented below [5].

Table 1. Dependence between the response of engines and content of particulates in the air

No.	Engine	Average response	Content of PM 10 $\mu\text{g}/\text{m}^3$	Correlation coefficient
1.	DAF	1.947	18	0.981446
2.	Volvo	1.982	17	
3.	Scania	2.021	19	
4.	Renault	2.053	20	
5.	Mercedes-Benz	2.212	23	
6.	IVECO	2.406	26	

The dependencies between the response of engines and content of particulates in the air are very strong and demonstrate strong relationship between the assessed parameters.

Table 2. Dependence between specific fuel consumption and SO<sub>2</sub> content in the air

No.	Engine	Average g <sub>s</sub> g/(kWh)	SO <sub>2</sub> content μg/m <sup>3</sup>	Correlation coefficient
1.	Renault	191.0	2.0	0.929226
2.	Mercedes	191.4	2.1	
3.	Scania	191.7	1.0	
4.	IVECO	191.9	7.0	
5.	Volvo	192.0	11.0	
6.	DAF	193.6	19.5	

The obtained correlation coefficient is as high as for the dependence g<sub>s</sub> – PM10.

In turn, the dependence between the specific fuel consumption and the content of nitrogen oxides in the atmospheric air has been shown in Table 3

Table 3. Dependence between specific fuel consumption and NO<sub>2</sub> content in the air

No.	Engine	Average g <sub>s</sub> g/(kWh)	NO <sub>2</sub> content μg/m <sup>3</sup>	Correlation coefficient
1	Renault	191.0	30	-0.13388
2.	Mercedes	191.4	31	
3.	Scania	191.7	18	
4.	IVECO	191.9	23	
5.	Volvo	192.0	24	
6.	DAF	193.6	27	

The absolute value of the correlation coefficient indicates a very weak dependence between the assessed parameters, and the negative value indicates that along with the increase in the specific fuel consumption, the content of nitrogen dioxide in the air decreases as a result of combustion processes in automotive engines.

## CONCLUSIONS

Increased truck traffic in urban agglomerations is characterised by high intensity of emission of harmful substances. There are many methods of protecting the natural environment - one of the most important ways is to reduce the traffic congestion by diverting trucks to ring roads, which prevents them from entering the city centres and residential districts. Combined with the proper organisation of the flow streams of vehicles as well as application of the “green wave” and acoustic screens it provides the expected results - maintained smoothness of traffic flow, stabilised speed of the stream of vehicles, reduction of fuel consumption and decrease in the number of accidents.

Based on the analysis of pollutants and operating parameters of the tested engines it can be stated that diverting the truck traffic to the outside of the urban centres is an effective and proven

method of protecting the environment. The increase in the number of utility vehicles causes that this development trend is currently being implemented, but it requires expenditures for the development and reconstruction of the existing infrastructure of the road transport.

The example of other European countries has shown that the expenditures spent for the environmental protection will bring the expected benefits in terms of improving the functioning of the ecosystem and in solving problems of the road transport. The intended and achievable long-term effect is to protect the human health and environment in the region.

#### REFERENCES

1. Chłopek Z.: Ecological aspects of Rousing bio-ethanol fuel to Power combustion engines. *Eksploatacja i Niezawodność* Nr 3 (35) 2007.
2. Chłopek Z.: The estimation of from internal combustion engines fuelled by bio-ethanol. *COMBUSTION ENGINES* 1/2008.
3. Koniuszy A.: The use of luster analysis method foe the development of static load cycles of diesel engines in non road vehicles. *COMBUSTION ENGINES* 4/2008.
4. Merkisz J.: Impact of motorisation on environmental pollution. Technical University of Poznań Publishing House, Poznań, 1995.
5. Mysłowski J: Impact of motorisation air pollution on human health. Scientific Issue of BAME Kaliningrad. Kaliningrad 2009.
6. Mysłowski J: Influence of dynamic powered diesel engines for fumigation of exhaust gasses. Scientific Issue of KGTU Kaliningrad. Kaliningrad 2008.
7. Mysłowski J: Alternative fuels for combustion engines, search for new ways of powered. Scientific Issue of KGTU Kaliningrad. Kaliningrad 2008.
8. Rewaj R.: The annual report on the atmospheric air pollution by traffic in Szczecin – the Harbour Gate area. State Inspection of Environmental Protection - Provincial Inspectorate for Environmental Protection in Szczecin, Library of Environmental Monitoring, Szczecin 1996.
9. Rewaj. R.: Measurements of the traffic pollution of the environment. Provincial Inspectorate for Environmental Protection. Szczecin, 2006.
10. The Ordinance of the Minister of Environment of 26<sup>th</sup> of November 2002 on the scope of the procedure for submission of information relating to the air pollution (*Journal of Laws* No. 204, item 1727).

#### NEGATYWNY WPŁYW MOTORYZACJI NA ŚRODOWISKO NATURALNE

**Streszczenie.** W artykule przedstawiono narastające zagrożenia dla środowiska naturalnego spowodowane lawinowym wzrostem ilości samochodów ciężarowych i osobowych w obrębie aglomeracji miejskich i poza ich granicami. Na przykładzie aglomeracji Szczecina- położonego na skrzyżowaniu dróg tranzytowych wschód –zachód i północ -południe omówiono poszczególne szkodliwe składniki związane z eksploatacją pojazdów ciężarowych oraz ich negatywny wpływ na życie ludzi i funkcjonowanie ekosystemu w Polsce.

**Słowa kluczowe:** silnik, gazy wylotowe.

## ANALYSIS OF THE CONTINUITY OF ELECTRIC ENERGY SUPPLY IN POLAND

Krzysztof Nęcka

Department of Power Engineering and Agricultural Processes Automation,  
Agricultural University of Cracow  
Balicka Str. 116B, 30-149 Kraków, Poland  
e-mail: krzysztof.necka@ur.krakow.pl

**Summary.** The continuity of electricity supply to consumers located within the territory of individual Distribution System Operators in Poland was analysed. A concentration analysis was also performed, which allowed for the separation of Distribution System Operators who are similar in terms of the indices related to electricity supply interruptions recorded in 2010. These were divided into four groups.

**Key words:** concentration analysis, power supply continuity, electric energy, Distribution System Operator.

### INTRODUCTION

Introduction of Directive 2003/54/EC of the European Parliament and of the Council, concerning common rules for the internal market in electricity and Regulation 1228/2003 on conditions for access to the network for cross-border exchanges in electricity has led to separation of the commercial and distribution activities of Power Distribution Companies. The Energy Law of July 1, 2007, however, allows free choice of electricity suppliers to all consumers of electricity in Poland. The result of deregulating the power sector is that electric energy is now considered as a product which, as any other goods on the market, is dependent on technical and economic criteria [Hanzelka, Kowalski 1999; Hanzelka, Wasiak, Pawełek 1998].

Unless the parties of a supply contract agree upon the individual quality parameters of electric energy, standards shall apply as laid down in the *Regulation of December 20, 2004* [Dz. U. z 2004 nr 2, poz. 5 i 6] and the *PN-EN50160* standard, which contains some more indices. The continuity of electric energy supply can be evaluated, among others, based on: the mean time of long interruption, average number of long and short term interruptions [Trojanowska 2007, 2008; Trojanowska, Nęcka 2010]. A full list of indices applied in practice and their determination methods are described in the subject literature [Paska 2004].

Under the normal operating conditions of a distribution network, the number of energy supply interruptions may be from several tens to several hundreds a year [Strzałka 2003]. The lack of continual supply of power causes a loss for the industry and discomfort to individual users. According to the information published by EPRI (Electrical Power Research Institute), the annual loss in

the US industrial sector, due to poor quality of electric energy and supply disruptions, is ca. USD 16 bln [Janiczek, Wasiluk-Hassa, Samotyj 1999]. In Poland, no such comprehensive studies have been made, yet due to the poor condition of the power distribution infrastructure, it can be assumed that the loss is also very high [Niewiedział, Niewiedział]. Power supply continuity is, therefore, a crucial factor for the choice of products and services in a competitive market for electric energy.

The aim of the present paper was to analyse the continuity of electricity supply to consumers located within the territory of individual Distribution System Operators (DSO) in Poland.

### MATERIAL AND METHODS

SAIDI, SAIFI, MAIFI indices were applied to analyse the continuity of electric power supply based on supply interruptions in 2010 which, according to the Regulation of the Minister of Economy of May 4, 2007, as amendment, has been published by individual distribution system operators on their websites. The territorial diversity of power supply reliability was evaluated based on concentration analyses using the agglomeration method, which belongs to the group of hierarchical methods, as well as the k-average method, one of the most important non-hierarchical methods.

### RESULTS

In Poland, eight Distribution System Operators are currently established supplying electrical energy to almost 16.5 million consumers. Figure 1 shows their respective service territories. The only exception to this is the DSO PKP Energetyka, which covers almost the entire country.



Fig. 1. Service territory of individual Distribution System Operators

Źródło: <http://centrum-energetyczne.pl/o-nas/obszar-dzialania>

Based on the Regulation of the Minister of Economy of May 4, 2007, as amended, a distribution system operator, by March 31 of each year, must publish the following energy supply interruption indices established for the previous calendar year:

1. **SAIDI** (the system average interruption duration index for long and very long term interruptions) – expressed in minutes per subscriber per annum, being a sum of the products of duration and the number of subscribers affected by the consequences of such interruptions during a year, divided by the total number of subscribers serviced,
2. **SAIFI** (the system average interruption frequency index for long and very long term interruptions) – being the number of subscribers affected by the consequences of such interruptions during a year, divided by the total number of subscribers serviced,
3. **MAIFI** (the momentary average interruption frequency index for short term interruptions) – being the number of subscribers affected by the consequences of such interruptions during a year, divided by the total number of subscribers serviced.

Pursuant to the Regulation, the DSO establishes the first two indices separately for planned interruptions, i.e. due to the power distribution systems maintenance schedule, and for any unplanned interruptions (due to distribution system breakdowns). They should also be published with and without the inclusion of catastrophic interruptions, i.e. those lasting longer than 24 hours.

The values of the indices for power supply interruptions to subscribers in Poland in 2010 are given in Table 1.

Table 1. Values of the indices for power supply interruptions in 2010

		Value				
		mini- mum	average	maxi- mum	variability factor [%]	
Indicator	SAIDI [min./ sub./year]	planned	3,91	119,61	212,20	58
		unplanned including catastrophic interruptions	19,67	322,45	644,00	56
		unplanned not including catastrophic interruptions	13,99	276,28	579,87	55
	SAIFI [sub./ sub.]	planned	0,01	0,63	1,15	55
		unplanned including catastrophic interruptions	0,09	3,21	5,03	43
		unplanned not including catastrophic interruptions	0,09	3,19	5,02	43
MAIFI [sub./sub.]		0,03	3,46	8,87	72	

According to the calculations, the average duration of long and very long term interruptions, including the catastrophic interruptions, all over Poland is ca. 422 minutes per annum. This varies in a broad range from 25 minutes for the areas serviced by PKP Energetyka to 812 minutes for the service areas of ENION S.A. The average SAIDI value has, for many years, been at a similar, very high level. In other European countries, its value in the years 2004-2006 varied from 23 min./year in Germany and the Netherlands, 30 min./year in Austria to 267 min./year in Portugal and 300 min./year in Slovakia. Higher values were found in Estonia and Romania, 469 and 1187 min./year, respectively [Attachment 9]. In 2010, higher frequency of very severe short term interruptions, i.e. with the duration from 1 second to 3 minutes, was observed. Each subscriber on average suffered



3.46 short term interruptions and 3.21 long term interruptions. The maximum values, however, were twice as high, 8.87 and 5.03 [sub./sub.], respectively.

Great diversification was also found in the analyzed parameters, depending on the prevalence in a given urban or rural area. The situation can be studied by analysing the information presented separately for DSO PGE Łódź Miasto and PGE Łódź Teren. For rural areas, a 6.7 hour increase in the annual duration of long and very long term interruptions was observed. However, the SAIFI index value for rural area was lower by 1.54 [sub./sub.]. The differences noted can be explained by the different nature of the systems.

A concentration analysis was then performed, aimed at separate Distribution System Operators similar in terms of the indices related to electricity supply interruptions recorded in 2010 and combining them in uniform groups. The concentration analysis was performed with the agglomeration method, which belongs to the group of hierarchical methods. The DSO grouping was performed with the Ward method, which, for separating concentrations, uses the inter-class variance minimisation principle, and between the objects, according to the recommendations of Sagan and Łapczyński [2009], the Euclidean distance was calculated. This method was chosen as it is considered to be the most effective in reproducing the actual data structures [Sokołowski 1992]. The effect of such algorithm in the form of a hierarchical tree is shown in Figure 2.

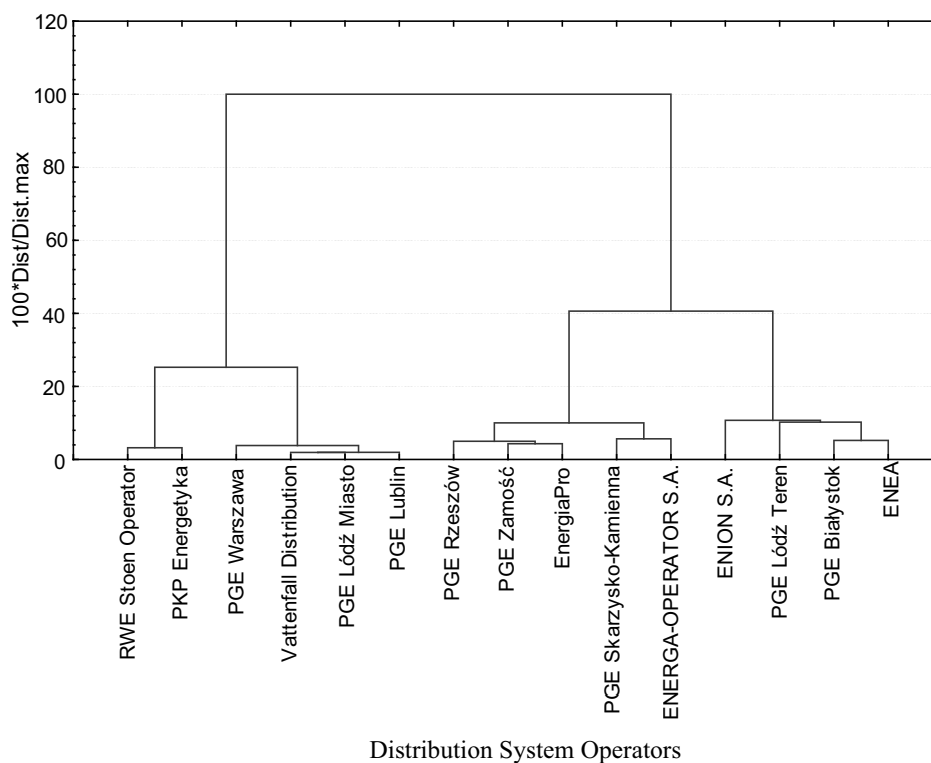


Fig. 2. Similarity agglomeration diagram of individual DSOs for the indices regarding electric energy supply in 2010

An optimum number of concentrations was determined by analysing the agglomeration distance graph (Fig. 3) for the subsequent joining stages at the point of its first noticeable increment, which was observed in the 12<sup>th</sup> step. Calculations performed with the k-average method proved the previous analyses and allowed for the separation of 4 DSO concentrations with the greatest similarity scale. The calculated mean values of individual indices characterising the continuity of power supply in individual groups are listed in Table 2.

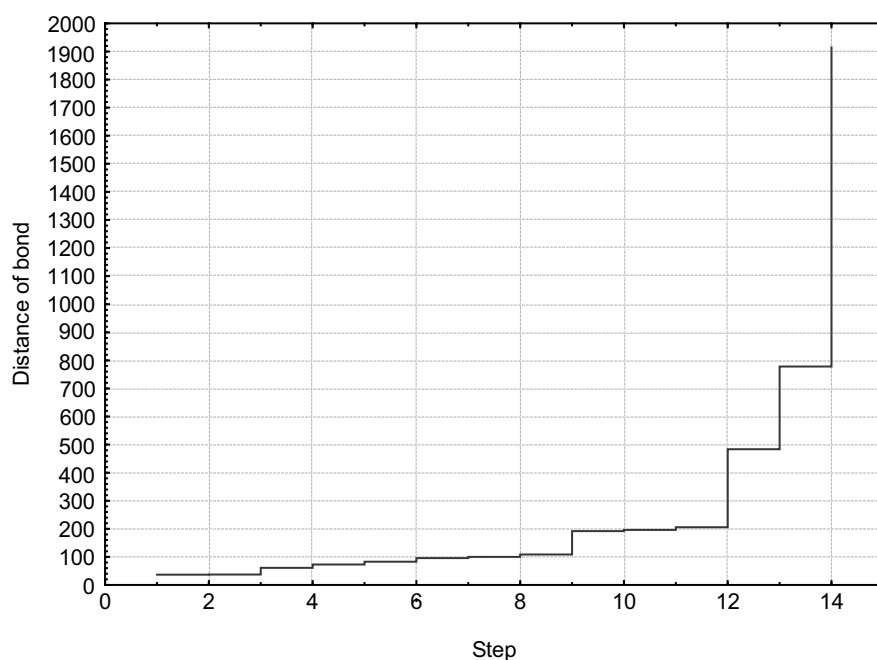


Fig. 3. Course of lining distance during linking stages

Table 2. Mean values of the indices for power supply interruptions in 2010 in individual groups

		Concentration				
		I	II	III	IV	
Indicator	SAIDI [min./sub./year]	planned	4,82	74,26	174,55	153,7
		unplanned including catastrophic interruptions	43,67	181,81	363,64	551,00
		unplanned not including catastrophic interruptions	33,04	179,18	289,96	477,90
	SAIFI [sub./sub.]	planned	0,03	0,52	0,79	0,84
		unplanned including catastrophic interruptions	0,65	3,17	3,76	3,85
		unplanned not including catastrophic interruptions	0,65	3,17	3,72	3,82
	MAIFI [sub./sub.]		0,24	4,13	3,86	3,90

Two power distributors, i.e. RWE Stoen Operator S.A. and PKP Energetyka, were categorised as the first concentration, characterised by the lowest values of indices describing power supply continuity. The mean interruption time in that concentration was 48 min./year. Also, the average frequencies of short and long term interruptions in that concentration were the lowest – 0.24 and 0.68 [sub./sub.], respectively. All the distributors operating in urban areas were categorised under the first and second group, characterised by the lowest indices of long term power supply interruptions. However, in the last group, including DSOs: ENEA, ENION, PGE Białystok and PGE Łódź Teren, operating mainly in rural areas, the highest indices, characterised by long term interruptions were observed. The mean value of the SAIDI index increased to 704.7 [min./sub./year], whereas the SAIFI index reached the value of 4.69 [sub./sub.]. Only the MAIFI parameter value in that group was close to the first concentration and was 3.90 [sub./sub.].

## CONCLUSIONS

According to the performed calculations, an electricity subscriber in Poland may expect at least 5 unplanned power supply interruptions in a year of total duration of up to 10.7 h.

The values of the indices characterising the continuity of power supply in areas serviced by individual Distribution System Operators varied considerably. An average value of the variability factor was almost 55 %, varying from 43 % for the SAIFI index to 72 % for the MAIFI.

Although the power supply reliability indices are published, individual subscribers still have limited access to the information regarding their regions. It appears reasonable to publish these indices with the division into subscribers located in urban and rural areas.

## REFERENCES

1. Dyrektywa 2003/54/WE Parlamentu Europejskiego i Rady dotycząca wspólnych zasad dla wewnętrznego rynku energii elektrycznej i uchylenia dyrektywę 96/92/WE.
2. Hanzelka Z., Kowalski Z. 1999.: Kompatybilność elektromagnetyczna (EMC) i jakość energii elektrycznej w dokumentach normalizacyjnych. JUEE, IV(1).
3. Hanzelka Z., Wasiak I., Pawełek R. 1998.: Normalizacja jakości energii elektrycznej w Polsce. Jakość energii elektrycznej i wyrobów elektrotechnicznych. IV Konferencja Naukowo-Techniczna. Świnoujście.
4. Janiczek R., Wasiluk-Hassa M., Samotyj M. 1999.: How much does power quality cost: views from both sides of the meter; International Conference Electrical Power Quality and Utilisation". September. Cracow. Poland.
5. Niewiedział E., Niewiedział R.: Aktualny stan elektroenergetycznych sieci dystrybucyjnych w Polsce z punktu widzenia bezpieczeństwa zasilania odbiorców. [online]. [dostęp 14-07-2011]. Dostępny w Internecie: <http://24ktp.pl/Dokumenty/Aktualny%20stan%20elektroenergetycznych%20sieci%20dystrybucyjnych.pdf>.
6. Paska J. 2004.: Jakość zasilania. *Elektroenergetyka* 4. s. 1–10.
7. Polska Norma. PN-EN 50160. Parametry napięcia zasilającego w publicznych sieciach rozdzielczych.
8. Rozporządzenie (WE) nr 1228/2003 Parlamentu Europejskiego i Rady z dnia 26 czerwca 2003 r. w sprawie warunków dostępu do sieci w odniesieniu do transgranicznej wymiany energii elektrycznej.

9. Rozporządzenie Ministra Gospodarki z dnia 20 grudnia 2004 r. w sprawie szczegółowych warunków przyłączenia podmiotów do sieci elektroenergetycznych, ruchu sieciowego i eksploatacji sieci oraz standardów jakościowych obsługi odbiorców. Dz.U. z 2004 r. nr 2, poz. 5 i 6.
10. Rozporządzeniem Ministra Gospodarki z dnia 4 maja 2007 r. w sprawie szczegółowych warunków funkcjonowania systemu elektroenergetycznego Dz. U. Nr 93, poz. 623 z dnia 29 maja 2007.
11. Rozporządzeniem z dnia 21 sierpnia 2008 r. zmieniające rozporządzenie w sprawie szczegółowych warunków funkcjonowania systemu elektroenergetycznego Dz. U. Nr. 162, poz. 1005 z dnia 9 września 2008.
12. Sagan A., Łapczyński M. 2009.: Techniki segmentacji w badaniach rynkowych. Materiały szkoleniowe StatSoft Polska.
13. Sokołowski A. 1992.: Empiryczne testy istotności w taksonomii. Akademia Ekonomiczna w Krakowie. Zeszyty Naukowe. Kraków.
14. Trojanowska M. 2007.: Analiza statystyczna ciągłości dostaw energii elektrycznej odbiorcom z terenów wiejskich województwa małopolskiego. Problemy inżynierii rolniczej. Nr 3. S. 43-48.
15. Trojanowska M. 2008.: Analiza stanu technicznego sieci niskiego napięcia na terenach wiejskich podkarpacia. MOTROL 10. s. 131-135.
16. Trojanowska M., Nęcka K. 2010.: Identyfikacja wskaźników opisujących niezawodność zasilania energią elektryczną odbiorców wiejskich. TEKA Komisji Motoryzacji i Energetyki Rolnictwa. Vol X. Lublin. s. 475-483.
17. Ustawa z dnia 10 kwietnia 1997 r. Prawo energetyczne. Dz.U. z 1997 r. nr 54 wraz z późniejszymi zmianami.
18. Załącznik nr 9 – Przerwy w dostawie energii elektrycznej i należne odbiorcom bonifikaty. [online]. [dostęp 14-07-2011]. Dostępny w Internecie: <http://www.szczecin.uw.gov.pl/Aktualnosci/Documents/Za%C5%82%C4%85cznik%20nr%209.pdf>  
<http://centrum-energetyczne.pl/o-nas/obszar-dzialania>.

## ANALIZA CIĄGŁOŚCI DOSTAW ENERGII ELEKTRYCZNEJ NA TERENIE POLSKI

**Streszczenie.** Przeprowadzono analizę ciągłości dostaw energii elektrycznej odbiorcom zlokalizowanym na terenie poszczególnych Operatorów Systemów Dystrybucyjnych w Polsce. Wykonano również analizę skupień, która doprowadziła do wyodrębnienia Operatorów Systemów Dystrybucyjnych podobnych do siebie ze względu na wartości wskaźników dotyczących przerw w dostawie energii elektrycznej zarejestrowanych w roku 2010 i podzielono je na cztery grupy.

**Słowa kluczowe:** analiza skupień, ciągłość zasilania, energia elektryczna, Operator Systemu Dystrybucyjnego.

## USE OF DATA MINING TECHNIQUES FOR PREDICTING ELECTRIC ENERGY DEMAND

Krzysztof Nęcka

Department of Power Engineering and Agricultural Processes Automation,  
Agricultural University of Cracow, Balicka Str. 116B, 30-149 Kraków, Poland  
e-mail: krzysztof.necka@ur.krakow.pl

**Summary.** The project of prediction models was developed in the Data Miner graphic environment, which allows one to determine the hourly electric energy demand for an agricultural and food industry plant. Whilst using data mining techniques, it is not necessary to know apriori the form of the theoretical model of the examined phenomenon; it is also not necessary to meet the assumptions, whilst it is possible to model very complex processes.

**Key words:** data mining, prediction, electric energy, hour request for electric energy.

### INTRODUCTION

The famous astronomer Tycho Brache (1546-1601) and his well-known assistant Johannes Kepler (1571-1630), who was involved both in astronomy and mathematics, are recognized to be forerunners of the data mining technique [Sokołowski 2005]. Brache tried to discover a mathematical formula that would allow prediction of the location of celestial bodies. However, his works were not successful. His student, Kepler, described this in the form of three simple equations, currently known as Kepler's laws.

Among others, Roy [1957] and Tukey [1962] wrote in the 1960s about the necessity of increasing the dynamics of searching for non-parametric methods, for which it would not be necessary to meet burdensome assumptions.

Since that time, very dynamic development of data mining techniques has taken place, as well as many definitions of this issue have been formed and modified over time. Berry, Linoff [1997, 2000] define data mining as a process of examining and analysing large amounts of data in order to discover meaningful patterns and rules. Hand et al [2001], think that data mining is an analysis of usually large, previously collected data sets in order to discover new regularities and describe data in a new way, which is understandable and useful for their owner.

The process of data modelling using data mining proposed in the 1990s by representatives of three companies (production from Germany, statistical from Great Britain and telecommunication from Denmark) was adopted as a standard and covers six phases: a) understanding of the problem, b) recognizing the data, c) preparing the data, d) modelling, e) evaluation of the model, f) implementation of the model.

In this technique, it is not necessary to know a priori the form of the theoretical model of the examined phenomenon. It is also not necessary to meet the assumptions, but this does allow for modelling of very complex processes. The obtained models are usually very complex, and their interpretation is difficult or even impossible for man. They are analysed as black boxes, where input data is introduced and a correct prediction is expected as the output. They also enable one to apply traditional models, though usually issues related to the assumptions are analysed less restrictively. The quality of built models is evaluated mostly by the accuracy of predictions counted in the test set. Because of this, the techniques may be practically used to solve prediction issues [Dęmski 2007; Fijołek i in. 2010; Sokołowski 2007; Sokołowski, Pasztyła 2004; Tadeusiewicz 2006; Trojanowska, Nęcka 2009].

Transformation of the power sector into a market oriented economy in Poland, which took place in 2007 [Dyrektywa 2003/54/WE], caused that electric energy is currently treated as a market product. Due to necessity of balancing demand and supply in real time, this is a very specific product for which the increase of prediction quality is practical both for its suppliers and receivers. Accurate evaluation of electric energy demand within individual hours of the day simply translates into financial results for a company. If the receiver uses any other quantity of energy than planned and ordered within a given hour, the generated difference must be balanced at the balancing market. However, discrepancies between the energy price in a negotiated contract and at the dynamic balancing market may reach even one hundred per cent [Ciepiela 2007].

The goal of the paper was to build the most effective prediction system using the data mining technique that would enable modelling the hourly electric energy demand in agricultural and food industry plants due to the assumed quality measures.

## MATERIAL AND METHODS

The goal of the paper was realized based on the results of own examinations performed using the AS-3 grid parameter analyser within the period from May 2010 to April 2011. This consisted in continuous measurement and recording of average 15-minute loads with active power and parameters characterizing the voltage quality in the transformer station supplying the District Dairy Cooperative. The examined company is located in the southern part of Poland, within the area of electric energy distribution provided by ENION GRUPA TAURON S.A. It is involved in the production of milk for consumption, dairy drinks, butter, cottage cheese and other dairy products, buying, for production purposes, from 15 to 17 million litres of milk every year. It is supplied with electric energy from a transformer and distribution station with 15/0.5kV of rated power 630 kVA, and the total power of installed electric receivers is 330 kW.

By means of transfer of data from the AS-3 grid parameter analyser to the computer, a database was created in a form that allows its reading and further processing in the *Statistica 9.1* program for statistical analysis of data.

## EXAMINATION RESULTS

### **Analysis of load variability.**

Realization of the goal of the paper was preceded by an analysis of load variability in the examined plant. It allowed for the collection of general information on the variability of the examined time series, selection of potential control variables and discovery of the outliers.

At first, an analysis was made of the monthly variability of electric energy demand. The course of changes in energy consumption within individual months is presented in the Fig. 1.

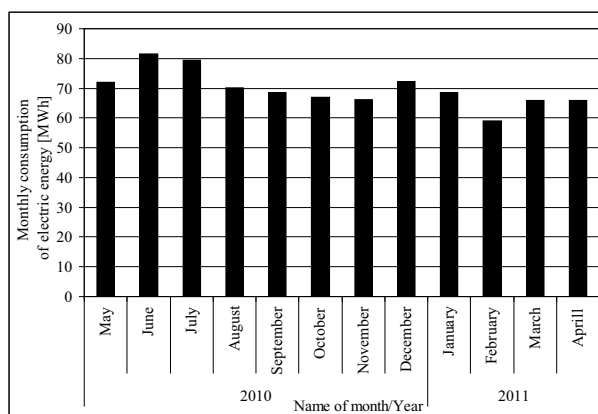


Fig. 1. Monthly consumption of electric energy

From the performed statistical analysis, the results show that monthly consumption of electric energy changes within a range from ca. 60 MWh to 80 MWh. The calculated value of the correlation coefficient has shown the existence of a statistically important dependence between the month and energy consumption. Therefore, the month was accepted as the potential control variable.

The performed analysis of daily energy consumption similarity enabled separation of two characteristic days of the week, i.e. the working day and the non-working day, showing the highest similarity of load form [Nęcka 2011 a]. Therefore, it is advisable to divide the time series into two sets, i.e. working days and non-working days and to create separate prediction models.

Fig. 2 presents the hourly variability of load within a winter and summer month.

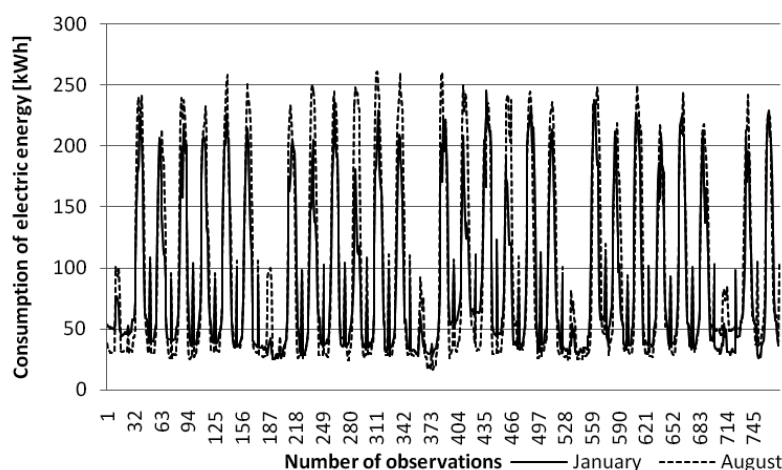


Fig. 2. Course of hourly demand for electric energy during the winter month (January) and the summer month (August)

In Fig. 2 as well as in the entire examined period, no outliers were recorded. However, the seasonality of the electric energy demand is visible. In order to identify the seasonality, an autocorrelation analysis was performed examining the correlation between the values of the time series of data separated from each other by  $k$  points  $ACF(k)=CF(x,x,k)$  (Fig. 3).

Fig. 3a presents the strong dependence between current electric energy consumption and its value one hour earlier. The value of the correlation coefficient for these two measurements is 0.94. Such a strong dependence between the variables enables one to assume that introduction at the input of the model of a variable delayed by one hour results in estimates burdened with minimal error. However, because of the specificity of the Polish energy market, the minimum value of delay that can be used practically is 41 hours [Gładysz 2009].

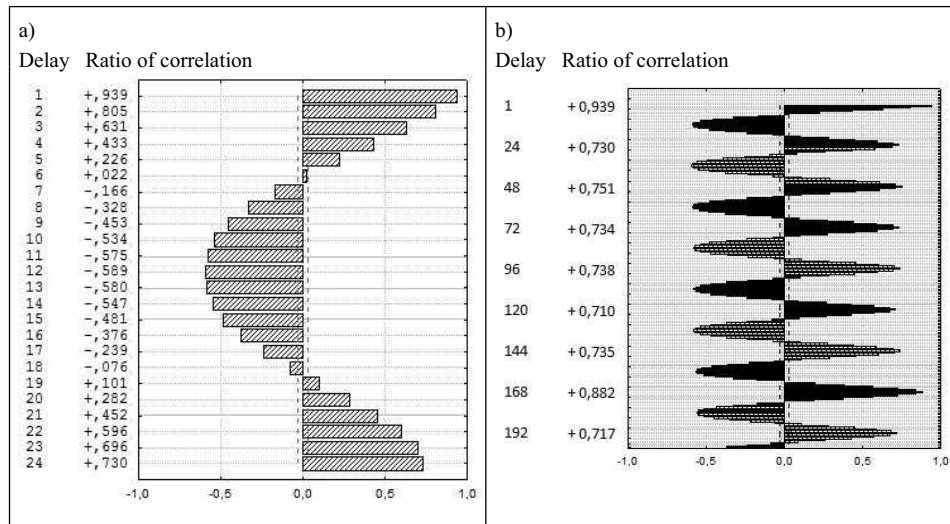


Fig. 3. Autocorrelation graph: (a) for  $k = 24$  (b) for  $k = 200$

Fig. 3b presents the course of the autocorrelation function for delay  $k$  equal to 200 hours. This shows sequences repeated in cycles, in which the amplitude decreases very slowly. The period of the basic cycle is 24 hours. An increase of the correlation coefficient for a delay of 168 hours to the value of 0.88 is clear, which indicates an occurrence not only of daily seasonality, but also weekly. Hence, it is justified to predict the hourly electric energy demand based on previous observations.

Moreover, results of the performed analyses [Nęcka 2011 b] showed that averaged profiles of energy consumption within individual days of the week and parameters characterizing the voltage quality delayed by one or a few seasonal periods are also statistically essential variables influencing electric energy demand.

### Construction of prediction models in the Data Miner operation environment

Before starting the construction of prediction models, the input data was divided to two sets. The first set, being the teaching one, was created based on 18816 observations recorded within the first period of examinations. The second set, the so-called test set, was created based on 2976 observations recorded within the last period of performed examinations. The time horizon for all



predictions developed was 48 hours due to the requirements put on participants of the electric energy market in Poland.

To develop prediction models that allow for the determining of hourly electric energy demand, a project was generated in the *Statistica Data Miner* graphic environment, of which an example for working days is presented in Fig. 4.

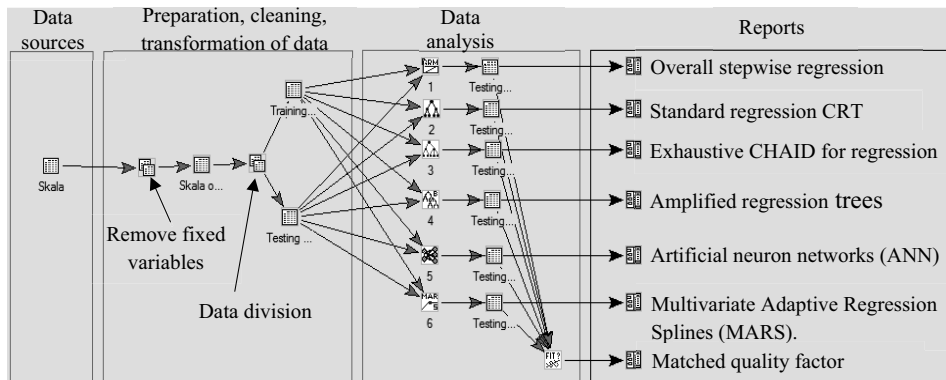


Fig. 4. Project of prediction models generated in the *Statistica 9.1 Data Miner* graphic environment for working days

The workspace in *Statistica 9.1 Data Miner* is divided into four sections that correspond to the four stages of the *Data Mining* project:

- *Data sources*: Specification of location of files that include data to be used during the process of further modelling.
- *Preparation, cleaning, transformation of data*: The node named *Remove fixed variables* allows automatic elimination of input variables that assume one value only. The *Data division* block is responsible for dividing data into a teaching and test set based on the coding variable saved in the prepared input file.
- *Data analysis*: In the generated template of the design enabling prediction of hourly electric energy demand, the following models were used: 1 - overall stepwise regression; 2 - standard regression CRT tree; 3 - exhaustive CHAID for regression; 4 - amplified regression trees; 5 - artificial neuron networks (ANN); 6 - Multivariate Adaptive Regression Splines (MARS). A detailed description of individual models can be found in the literature [Koronacki, Ćwik 2005; Hastie i in. 2001; Kot, Jakubowski, Sokołowski 2011; Tadeusiewicz 1993].

Having started the project based on the selected methods, the program runs a proper number of analyses and generates 5 models that allow for the prediction of hourly electric energy demand. It also creates a new source of data for each model, which includes the results of its application for the test set. Rapid quality evaluation of the generated models and their comparison based, among other things, on the average quarterly error, average absolute error and correlation coefficient is possible thanks to the *Matched quality factor* node.

- *Reports*: After completion of calculations, results summarizing individual analyses in the form of sheets are placed in the workspace of *Data Mining* projects.

### Evaluation of the predicting models

The problem of the quality of the developed prediction is one of the most important issues related to prediction. Absolute average error, absolute average error modulus, absolute average-quarterly error, relative error of prediction, average relating percentage error, standard deviation of error, Janus coefficient, Thiel coefficient are commonly used as measures of errors [Cieślak 1999; Gajda 2001; Trojanowska, Nęcka 2009; Zeliaś i in. 2003].

Within the scope of evaluation of the developed predictions, their accuracy was checked (Tab. 1) by determining the following coefficients counted for the test set:

- *Mean Error – ME:*

$$ME = \frac{1}{n} \cdot \sum_{i=1}^n (E_t - E_t^*) \quad (1)$$

- *Mean Absolute Error – MAE:*

$$MAE = \frac{1}{n} \cdot \sum_{i=1}^n (|E_t - E_t^*|) \quad (2)$$

- *Mean Absolute Percentage Error – MAPE:*

$$MAPE = \frac{1}{n} \cdot \sum_{i=1}^n \frac{|E_t - E_t^*|}{E_t} \cdot 100\% \quad (3)$$

- *Standard Deviation of Errors –SDE:*

$$SDE = \sqrt{\frac{1}{n-1} \cdot \sum_{i=1}^n (E_t - E_t^*)^2} \quad (4)$$

- *Ratio of correlation –  $r_{E_t, E_t^*}$ :*

$$r_{E_t, E_t^*} = \frac{\sum_{i=1}^n (E_t - \overline{E_t}) \cdot (E_t^* - \overline{E_t^*})}{\sqrt{\sum_{i=1}^n (E_t - \overline{E_t})^2} \cdot \sqrt{\sum_{i=1}^n (E_t^* - \overline{E_t^*})^2}} \quad (5)$$

where:

$E_t$  – actual value of electric energy consumption in hour  $t$ ,

$E_t^*$  – predicted value of electric energy consumption in hour  $t$ ,

$\overline{E_t}$  – mean actual value of electric energy consumption in hour  $t$ ,

$\overline{E_t^*}$  – mean predicted value of electric energy consumption in hour  $t$ ,

$n$  – number of the last observation of the predicted variable.

Table 1. Comparison of the quality of predictions generated using the selected methods

Method	Measure of error				
	ME [kWh]	MAE [kWh]	MAPE [%]	SDE [kWh]	$r_{E,E_i}$
Overall stepwise regression	-1,03	10,31	14,40	15,07	0,98
Standard regression CRT	-4,79	15,47	19,47	21,85	0,94
Exhaustive CHAID for regression	-2,33	12,02	16,61	17,13	0,97
Amplified regression trees	-2,74	12,29	16,52	17,41	0,97
Artificial neuron networks (ANN);	-1,39	10,98	15,40	16,77	0,97
Multivariate Adaptive Regression Splines (MARS)	-1,19	10,31	14,23	15,25	0,98
Combined prognosis	-2,24	10,81	13,23	11,34	0,97

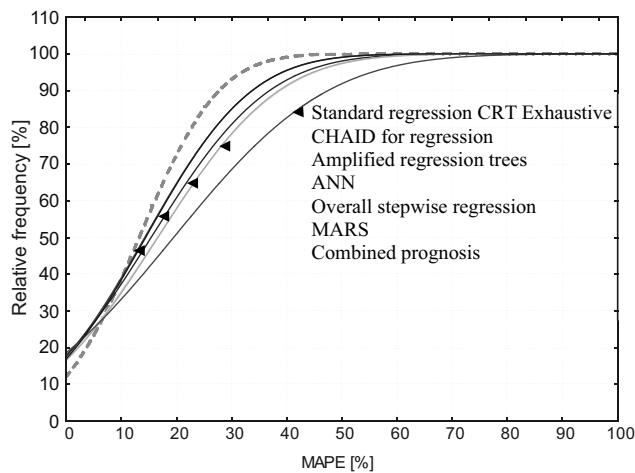


Fig. 4. Cumulative distribution of prediction model errors for the test set

### CONCLUSIONS

The lowest values of coefficients indicating the prediction error for teaching data was obtained in the case of the MARS model; however, the overall stepwise regression made it possible to generate a prediction of comparable quality. In both cases, whilst predicting hourly electric energy demand, we are wrong by ca. 14% on average, and the correlation coefficient value is very high and amounts to 98%.

From the analysis of absolute average error results that all models generated within the examined period of time, overestimated the energy demand by 1 to almost 5 kWh on average. Whilst predicting demand per a given hour of the day, we are mistaken by up to 10 kWh in the case of the stepwise regression and MARS model, and by almost 16 kWh in the case of standard CRT trees.

One percentage reduction of the average relative error of prediction is obtained for the combined prognosis determined as an average value from individual models. A significant reduction of errors with higher values is characteristic for this prediction.

In order to perform the analyses one more time, e.g. after a change of parameters of individual models or after linking new data, it is sufficient to start the previously generated project template, and the entire calculation process shall be completed automatically.

Monthly consumption of electric energy. Name of month/year. Number of observations. Measure of error. Relative frequency.

## REFERENCES

1. Berry M., Linoff G. 1997.: *Data Mining Techniques for Marketing, Sales and Customer Support*, Wiley, Hoboken, NJ.
2. Berry M., Linoff G. 2000.: *Mastering Data Mining*, Wiley, Hoboken, NJ.
3. Ciepela D. 2007.: Koszty bilansowania – zmora klienta. [online]. [dostęp 27-01-2011]. Dostępny w internecie: [http://energetyka.wnp.pl/tpa/poradnik\\_jak\\_zmienic\\_dostawce\\_energii/koszty-bilansowania-zmora-klienta,3359\\_2\\_0\\_1.html](http://energetyka.wnp.pl/tpa/poradnik_jak_zmienic_dostawce_energii/koszty-bilansowania-zmora-klienta,3359_2_0_1.html).
4. Cieślak M. 1999.: *Prognozowanie gospodarcze. Metody i zastosowanie*. Wydawnictwo Naukowe PWN. Warszawa.
5. Demski T. 2007.: Przykład prognozowania z wykorzystaniem metod data mining. [online]. [dostęp 27-01-2011]. Dostępny w internecie: [http://www.statsoft.pl/czytelnia/artykuly/Przyklad\\_prognozowania.pdf](http://www.statsoft.pl/czytelnia/artykuly/Przyklad_prognozowania.pdf).
6. Dyrektywa 2003/54/WE Parlamentu Europejskiego i Rady dotycząca wspólnych zasad dla wewnętrznego rynku energii elektrycznej i uchylenia dyrektywę 96/92/WE oraz rozporządzeni 1228/2003 w sprawie warunków dostępu do sieci w transgranicznej wymianie energii elektrycznej.
7. Fijorek K., Mróz K., Niedziela K., Fijorek D. 2010.: Prognozowanie cen energii elektrycznej na rynku dnia następnego metodami data mining, *Rynek Energii*, nr 12.
8. Hand D., Mannila H., Smyth P. 2001.: *Principles of Data Mining*, MIT Press, Cambridge.
9. Hastie T., Tibshirani R., Friedman J. 2001.: *The Elements of Statistical Learning. Data mining, Inference and Prediction*. Springer Verlag.
10. Gładysz B. 2009.: Metoda określania wielkości kontraktów na energię elektryczną. *Badania operacyjne i decyzje*. Nr 3. Wrocław.
11. Gajda J. B. 2001.: *Prognozowanie i symulacja a decyzje gospodarcze*. Wydawnictwo C.H. BECK. Warszawa.
12. Kot S., Jakubowski J., Sokołowski A. 2011.: *Statystyka*. Wydawnictwo DIFIN. ISBN 978-83-7641-349-5.
13. Nęcka K. 2011a.: Analiza sezonowości obciążeń w zakładzie przemysłu rolno-spożywczego. (Złożona do druku w *Technika Rolnicza Ogrodnicza Leśna*).
14. Nęcka K. 2011b.: Wykorzystanie modeli regresyjnych do prognozowania godzinowego zapotrzebowania na energię elektryczną w zakładzie przemysłu rolno-spożywczego. (Złożona do druku w *Technika Rolnicza Ogrodnicza Leśna*).
15. Roy S. N. 1957.: *Some Aspects of Multivariate Analysis*, Wiley, New York.
16. Sokołowski A. 2007.: Data minind – automat czy metoda naukowa ? [online] [dostęp 24-04-2011] Dostępny w Internecie: [http://www.statsoft.pl/czytelnia/8\\_2007/Sokolowski05.pdf](http://www.statsoft.pl/czytelnia/8_2007/Sokolowski05.pdf).

17. Sokołowski A., Pasztyła A. 2004.: Data mining w prognozowaniu zapotrzebowania na nośniki energii. [online]. [dostęp 27-04-2011]. Dostępny w Internecie: <http://www.statsoft.pl/czytelnia/prognozowanie/04energia.pdf>.
18. Tadeusiewicz R. 2006.: Data mining jako szansa na relatywnie tanie dokonywanie odkryć naukowych poprzez przekopywanie pozornie całkowicie wyeksploatowanych danych empirycznych. [online] [dostęp 24-04-2011] Dostępny w Internecie: [http://www.statsoft.pl/czytelnia/8\\_2007/Tadeusiewicz06.pdf](http://www.statsoft.pl/czytelnia/8_2007/Tadeusiewicz06.pdf).
19. Tadeusiewicz R. 1993.: Sieci neuronowe. Akademicka Oficyna Wydawnicza. Warszawa.
20. Trojanowska M., Nęcka K. 2009.: Wykorzystanie data mining do prognozowania obciążeń szczytowych wiejskich stacji transformatorowych Международная Конференция ЭНЕРГОБЕЗОПЕЧЕНИЕ И БЕЗОПАСНОСТЬ. Wydawnictwo Orłowskiego Państwowego Uniwersytetu Rolniczego ОрелГАУ, s.308-310, Oriel k/Moskwy (Rosja).
21. Trojanowska M., Nęcka K. 2009.: The use of alternative regression models to determine peak loads in rural transformer stations. ТЕКА Komisji Motoryzacji i Energetyki Rolnictwa Vol. IX. Lublin. s. 364-369.
22. Tukey J. 1962.: The Future of Statistics, Annals of Mathematical Statistics, 33, 1-67.
23. Zeliaś A. 1997.: Teoria prognozy. PWN. Warszawa.

#### WYKORZYSTANIE TECHNIK DATA MINING DO PROGNOZOWANIA ZAPOTRZEBOWANIA NA ENERGIĘ ELEKTRYCZNĄ

**Streszczenie.** Opracowano w środowisku graficznym Data Miner projekt modeli predykcyjnych, pozwalających na wyznaczenie godzinowego zapotrzebowania na energię elektryczną dla zakładu przemysłu rolno-spożywczego. Dzięki wykorzystaniu w nim technik data mining nie jest wymagana znajomość apriori postaci modelu teoretycznego analizowanego zjawiska, nie jest również konieczne spełnienie założeń i możliwe jest modelowanie bardzo złożonych procesów.

**Słowa kluczowe:** data mining, prognoza, energia elektryczna, godzinowe zapotrzebowanie na energię.

## APPLICATION OF NICKEL SUPERALLOYS ON CASTINGS FOR CONVENTIONAL ENERGY EQUIPMENT ITEMS

Zenon Pirowski

Foundry Research Institute,  
Poland, 31-418 Krakow, 73 Zakopiańska Street

**Summary.** The actions that can mitigate the adverse effects of various energy crises are continuous improvements in the efficiency of power generation plants. This can be achieved by carrying out the processes at an always higher temperature and pressure, and in a more aggressive environment than the parameters used so far. Such requirements cannot be satisfied any longer by the iron-based alloys, even the best ones. Therefore, multi-component alloys based on nickel and cobalt start to be the materials of choice. On the other hand, new materials of higher performance life are searched for all the time.

Jointly with its American partners, the Foundry Research Institute in Krakow carries out the research works which, among others, aim at the conversion of both material and technology from structures forged and welded in nickel superalloys to cast elements for operation under the most demanding conditions of the power plants of a new generation. A part of the research is done under an “A-USC - NICKEL” American programme, to participation in which the Foundry Research Institute has been invited. Within this programme, the initial studies have already been carried out to master the technique of melting and casting the Inconel 740 alloy and preliminary material testing has been performed on the ready castings. It has been stated, among others, that with the temperature increase, particularly above 700°C, this alloy when used as a cast material is characterised by a definitely less drastic decrease of tensile strength than the same alloy subject to plastic forming.

**Key words:** cast nickel superalloys, manufacturing technology, mechanical properties, microstructure, dispersion hardening.

### INTRODUCTION

Notwithstanding the development of power industry based on different methods of energy generation, the prevailing technique continues to be that which uses coal as a main source of energy. Forecasts in this field predict that this situation will continue in coming decades, as evidenced by the repeated oil and gas crises, not to mention the recent events in Japan.

The actions that can mitigate the adverse effects of such crises are continuous efforts to increase the efficiency of power plants and develop the techniques of coal gasification. By increasing the efficiency of plants from 37% to 46%, and by raising the temperature to 760°C and pressure to 35 MPa, the amount of the emitted CO<sub>2</sub> is reduced by 22% (Figure 1). The amount of other pollut-

ants introduced to the environment decreases as well. The consequence is cost reduction and less of waste disposed to the environment.

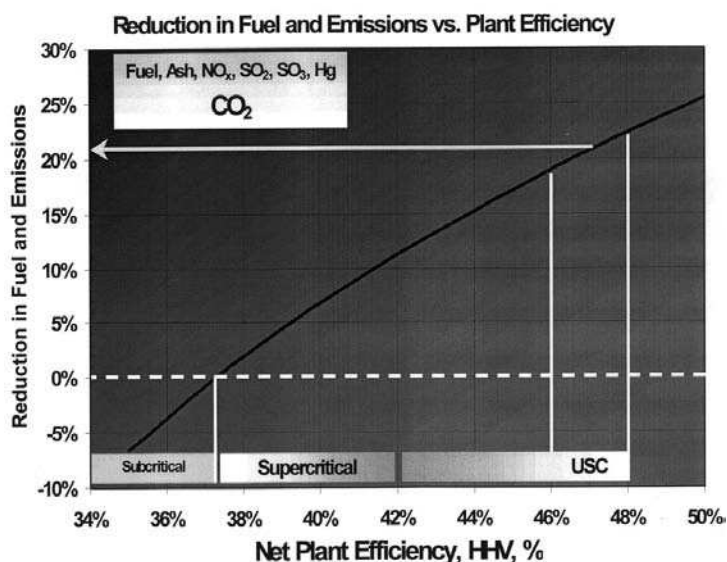


Fig. 1. Effect of operational efficiency of power plants on the emission rate of greenhouse gases (according to data obtained from an American partner – co-executor of the project)

In Poland the share of coal plants in electricity production is over 90%. Therefore, introduction of technological innovations is the action of strategic importance for operation of the national economy and energy security in our country.

Coal processing techniques, both simple consisting in its combustion, as well as complex, such as e.g. gasification, require plants, which include cast parts operating at very high temperatures and in aggressive environments. Increasing the operational efficiency of these devices is a way to reduce the emissions of  $\text{CO}_2$  and other pollutants. This can be obtained by conducting the processes at always higher temperatures and pressures, and in more aggressive media than those used up to now. These requirements cannot be satisfied by the iron-based alloys, even by those of the best quality, and therefore complex superalloys based on nickel and cobalt are applied. They can carry loads at temperatures higher even than 80% of their melting point and in much more aggressive environments. These materials include, among others, nickel superalloys. Within this family of alloys, new materials of improved performance life are developed. The cooperation of materials scientists with designers and process engineers results in the creation of new equipment, more efficient and thus more friendly to the environment.

The Foundry Research Institute in Krakow, jointly with its American partners, has been conducting a research, the main objective of which is to investigate the possibilities of conversion of both material and technology from structures forged and welded in nickel superalloys to cast elements for operation under the most demanding conditions of the power plants of a new generation. A part of the research is done under an “A-USC - NICKEL” American programme, to participation in which the Foundry Research Institute has been invited.

## RESEARCH MATERIAL

After agreements made with the U.S. partners, it has been decided to start the research with the Inconel 740 alloys.

Inconel 740 is a new nickel-chromium-cobalt superalloy. It is solution heat treated and aged, which makes it precipitation hardened with the dispersed inclusions of the second phase. It has been developed for high temperature operation in the automotive and energy industries. Its use increases the service life of boilers, pipes, valves and exhaust systems for diesel engines.

The nickel alloy matrix is solution hardened with an addition of cobalt. During operation at high temperatures, the additions of niobium, aluminium and titanium in the form of precipitates coherent with the matrix of  $\gamma'$  phase dispersion harden the alloy.

Inconel 740 has excellent resistance to high-temperature corrosion. The high content of chromium makes this alloy resistant to oxidation, carburisation and sulphurising, while the high content of nickel and low level of iron make it resistant at high temperatures to the effect of halides (salts of hydrogen halide acids: fluorides, chlorides, bromides and iodides).

In the case of alloys used for coal-fired boilers, a resistance to the corrosive effect of coal dust is also required, and it is Inconel 740 that can satisfy this requirement.

## RESEARCH

Nickel alloys are a group of materials which in the liquid state tend to react strongly with the ceramic material of both crucible and foundry mould.

At the present stage of studies, the work has been started on the selection of optimum ceramic materials which contact the liquid Inconel 740 alloy. The first idea was to use for melting an induction furnace with an inert crucible lining (based on  $Al_2O_3$ ) and as a moulding material – the ceramics with silicate binders. Yet, the obtained test ingots contained some defects, i.e. the discontinuities present in the cast material, mainly in the form of non-metallic inclusions, often forming very large oxide films.

Nickel superalloys, Inconel 740 included, contain a significant amount of the alloying additives of aluminium and titanium (often more than 2%). These elements at high temperatures are highly reactive and “willingly” combine with oxygen. Therefore, a very important metallurgical treatment during melting is reducing to maximum the content of oxygen dissolved in liquid alloy. For this purpose, the methods such as deoxidising with special magnesium-containing deoxidisers and restricted access of air to the melt surface (argon protecting atmosphere) were applied. As charge materials, technically pure metals, ferroalloys and master alloys were used.

The applied metallurgical treatments (deoxidation, pressure reduction, argon protection) reduced the severity of casting defects due to a very high reactivity of molten nickel alloy with the atmosphere of furnace chamber and the ceramic material of crucible and mould. The pouring temperature did not exceed 1600°C. Table 1 shows the chemical composition of the resulting test melt.



Table 1. Chemical compositions of Inconel 740 made by the Foundry Research Institute and according to literature data

Source	Content of elements; wt.%										
	C	Cr	Mo	Co	Al	Ti	Nb	Mn	Si	Fe	Ni
Experiment <sup>1)</sup>	0,10	25,0	0,40	20,0	0,70	1,80	1,60	0,25	0,57	2,50	rest
Commercial <sup>2)</sup>	0,03	25,0	0,50	20,0	0,90	1,80	2,00	0,30	0,50	0,70	rest
Literature <sup>3)</sup>	0,032	23,0	0,40	19,27	0,70	1,69	1,87	0,28	0,47	0,7	rest
	0,074	25,3	0,59	19,91	0,84	2,00	2,05	0,30	0,52	2,1	

<sup>1)</sup> melt made at the Foundry Research Institute,

<sup>2)</sup> leaflet published by Special Metals,

<sup>3)</sup> B. A. Baker, G. D. Smith: Corrosion Resistance of Alloy 740 as Superheater Tubing in Coal-Fired Ultra-Supercritical Boilers, Special Metals Corporation.

After melting, test moulds were poured with the examined alloy and during its solidification the thermal analysis was carried out.

The results of the thermal analysis of the solidifying Inconel 740 alloy are shown in Figure 2. They are helpful in selecting the heat treatment parameters.

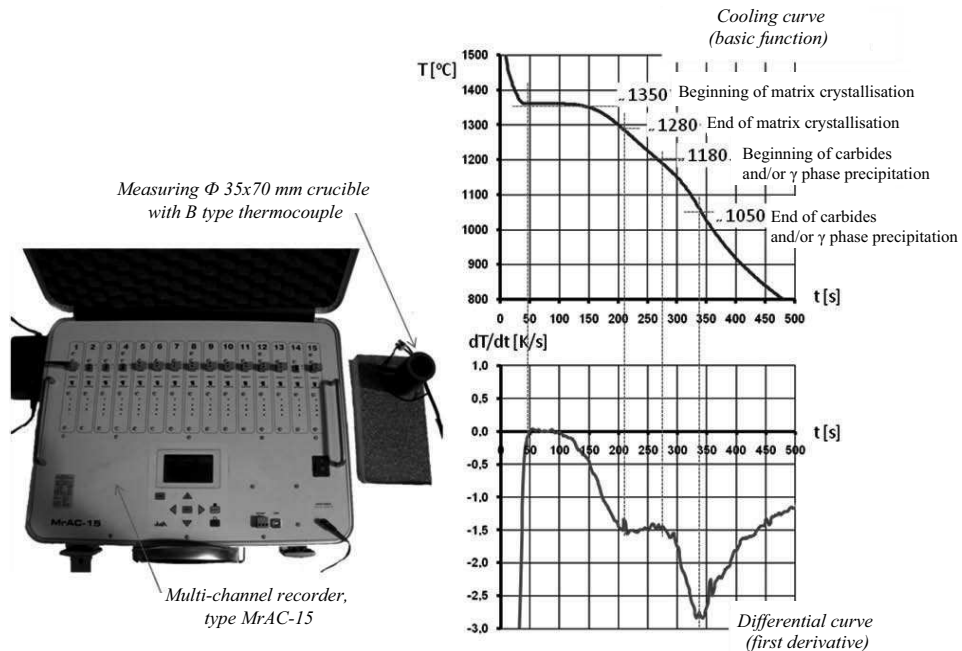


Fig. 2. Thermal analysis of the solidifying Inconel 740 alloy

The cast Inconel 740 alloy has been subjected to materials testing. To perform the tests it was necessary to first select the time and temperature parameters of the heat treatment process.

After the metallographic examinations and hardness and microhardness testing (tests were performed on alloy after different variants of heat treatment), it was decided that the best, in terms of the required properties, heat treatment process would be that depicted in Figure 3. Consequently, before mechanical tests, samples were subjected to this heat treatment.

The applied metallurgical treatments reduced only the severity of internal defects in the cast alloy. To minimise their impact on the results of the tests and examinations, samples were subjected to non-destructive testing, first, and selected for further studies, next. Based on the results of the X-ray examinations, places in the samples with no apparent discontinuities were found. Despite this, in some specimens after rupture, the defects still appeared. Other samples were examined by tomography on CT computers of two types (Figure 4).

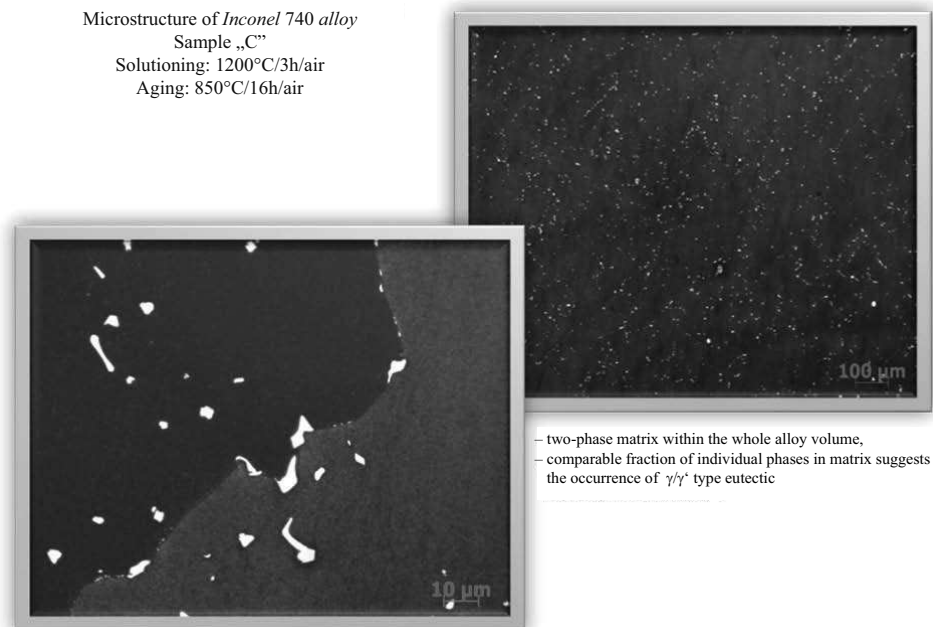


Fig. 3. Microstructure of specimen „C”

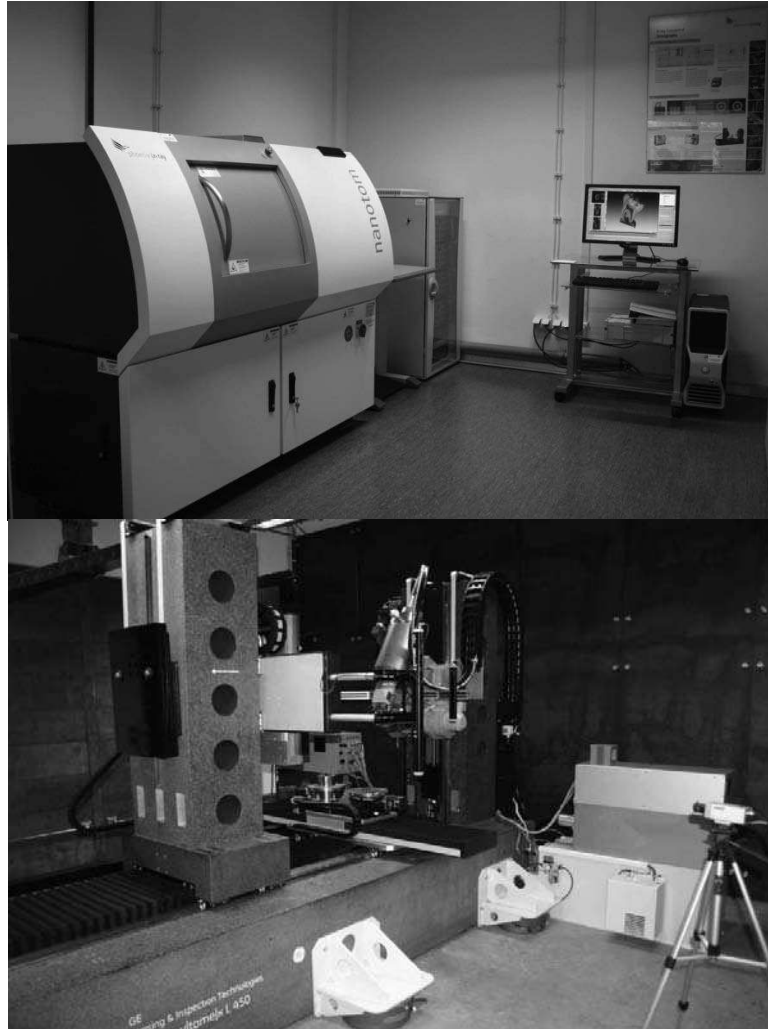


Fig. 4. Nanotom 180 NF (left) and V | Tome | X - L 450 (right)

The tomography done with Nanotom 180 NF (maximum voltage on tube - 180 kV) revealed no internal defects. The reason was that the radiation emitted by the tube was absorbed by the tested material to the extent that made the assessment of internal metal structure impossible. However, the examinations done with tomograph V | Tome | X - L 450 (maximum voltage on tube - 450 kV) revealed the presence of internal discontinuities in the examined sample material. For mechanical testing, samples with the least visible internal defects were selected (Figure 5).

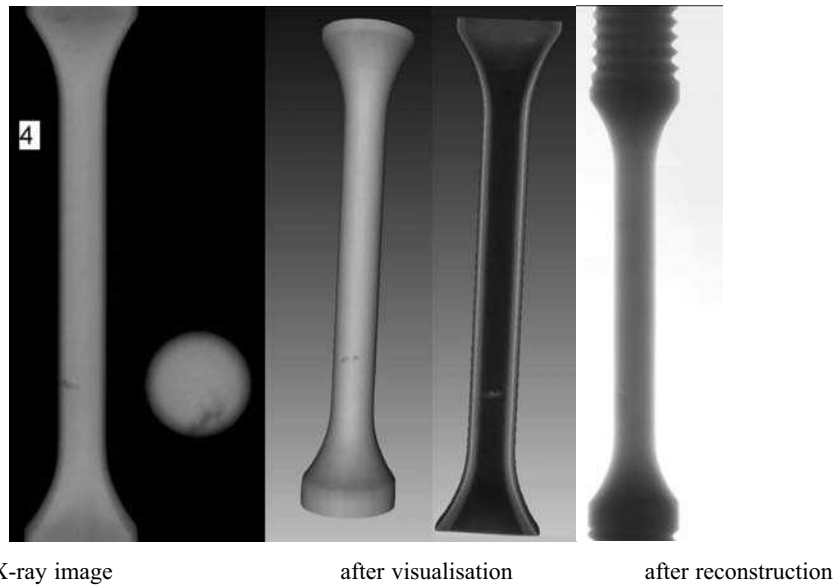


Fig. 5. Examples of the results of non-destructive testing with V | Tome | X - L 450 tomograph (possible occurrence of minor material discontinuities in the lower part of specimen)

The selected samples were subjected to high-temperature mechanical testing. Analysis of the obtained results (Figure 6) shows that, under the conditions of the Foundry Research Institute in Cracow, the production of nickel superalloys characterised by satisfactory high-temperature properties is quite feasible.

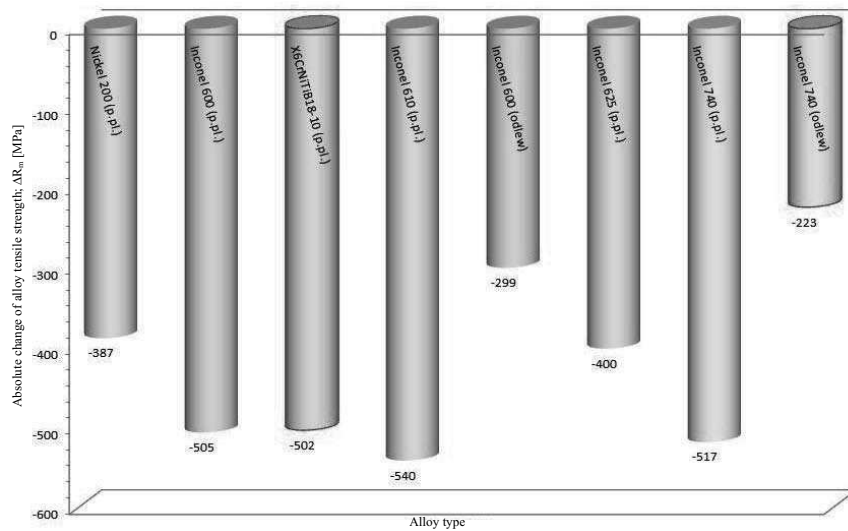


Fig. 6. Changes of tensile strength in selected alloys within the temperature range of 20-800°C  
p.pl. – wrought, odlew - cast

Obtained at different temperatures (20°C, 500°C, 700°C and 800°C) results of the tensile test and their comparison with literature data show that cast Inconel 740 (own research) and Inconel 600 (literature data) have lower tensile strength than their wrought counterparts, but with increased temperature of measurement the drop in the value of this parameter is less drastic in cast alloys. This becomes particularly evident at a temperature above 700°C due to loss of the work hardening effect.

Among the comparable alloys, with temperature increasing in the range of 20-800°C, the least drastic decrease in tensile strength revealed the, cast at the Foundry Research Institute, Inconel 740 alloy ( $\Delta R_m = - 223$  MPa), while for wrought Inconel 740 alloy (literature data), this difference was  $\Delta R_m = - 517$  MPa.

Hence the conclusion follows that by replacing wrought alloys with cast nickel superalloys in structures operating at extra high temperatures, the weight of these elements can be effectively reduced.

## CONCLUSIONS

1. The conducted heat treatment (solutioning and aging) had a significant effect on microstructure of the tested *Inconel 740* alloy and on hardness and microhardness of the austenitic matrix.
2. The highest degree of hardening, and hence the increase in hardness of *Inconel 740* alloy was obtained by solution heat treatment at 1200°C for 3 h, followed by aging at 850°C for 16 h.
3. The results of tensile testing obtained at different temperatures (20°C, 500°C, 700°C and 800°C), when compared with literature data, have proved that cast *Inconel 740* and *Inconel 600* alloys have lower tensile strength than alloys after plastic forming, but with increasing temperature of measurement the drop in the value of this parameter is less drastic in alloys cast. This becomes particularly evident at a temperature above 700 °C.
4. Among the compared alloys, with temperature increasing in a range of 20 - 800°C, the mildest decrease in tensile strength had the, made at the Foundry Research Institute, cast alloy ( $\Delta R_m = - 223$  MPa), whereas for wrought Inconel 740 alloy (literature data) this difference was  $R_m = - 517$  MPa.
5. The use of parts cast from nickel superalloys for extra high temperature performance instead of wrought alloy structures can reduce the weight of the elements and increase their service life.

## REFERENCES

1. Z. Pirowski: Nikiel i jego stopy specjalnego przeznaczenia; monografia; Instytut Odlewnictwa; in print.
2. B. A. Baker, G. D. Smith: Corrsion Resistance of Alloy 740 as Superheater Tubing in Coal-Fired Ultra-Supercritical Boilers, Special Metals Corporation.
3. E. Rusin: Dobór parametrów obróbki cieplnej nadstopu niklu typu Inconel 740 w celu uzyskania odpowiedniej morfologii wydzielań dyspersyjnych; Uniwersytet Pedagogiczny; Kraków 2010; praca magisterska realizowana w Instytucie Odlewnictwa.
4. M. Blicharski: Inżynieria materiałowa – stal; WNT; Warszawa 2004.
5. K. Przybyłowicz: Metaloznawstwo; WNT; Warszawa 2007.

6. Z. Pirowski: Zwiększenie odporności na zużycie erozyjne dwufazowego staliwa Cr-Ni przez dodatek azotu i innych pierwiastków międzywęzłowych; *Archiwum Technologii Maszyn i Automatykacji*. Komisja Budowy Maszyn PAN Oddział w Poznaniu; vol. 26; nr 1; s. 1005-121; Poznań 2008.
7. Z. Stefański, Z. Pirowski i inni: Próby technologiczne wykonywania odlewów ze stopów niklu; *Praca statutowa Instytutu Odlewnictwa*; Zlec. 3671/00; Kraków 1995.
8. J. M. Svoboda: *Nickel and Nickel Alloys*; ASM Handbook - Casting; vol. 15; 10th Edition; ASM Metals Park; Ohio 1993; pp. 815-823.
9. L. L. Faulkner: *Nickel Alloys*; Edited by Ulrich Heubner; Marcel Dekker Inc.; New York – Basel 1998.
10. *Stainless Steel World*. Internet materials: <http://www.stainless-steel-world.net/pdf/11022.pdf>.
11. A. Onoszko, K. Kubiak, J. Sieniawski: Turbine blades of the single crystal nickel based CMSX-6 superalloy; *Journal of Achievements in Materials and Manufacturing Engineering*; vol. 32, 2009; pp. 66-69.
12. L.A. Dobrzański: *Materiały metalowe. Stopy niklu i kobaltu*; IMiB; Gliwice 2007.
13. J. Ericsson i inni: *High – Temperature Materials in Gas Turbines*; Elsevier SC. Public. Comp.; Amsterdam 1974; s. 315-340.
14. L. Swadźba, M. Śnieżek i inni: Żarowytrzymałe stopy, obróbka cieplna oraz powłoki ochronne stosowane na elementy turbin gazowych; SECO/WARWICK; VII Seminarium Szkoleniowe „Nowoczesne trendy w obróbce cieplnej”; Świebodzin 3003.
15. *Advanced Materials and Coatings for Combustion Turbines*; Ed. V. P. Swaminathan and N. S. Cheruvu; Prop. of ASM 1993 Materials Congress, Materials Week'93; Pittsburg 1993.
16. Pirowski Z., Gościański M.: Construction and technology of production of casted shared for rotating and field ploughs; TEKA Commission of Motorization and Power Industry in Agriculture Lublin University of Technology the Volodymir Dahl East-Ukrainian National University of Ługańsk; 2009; v. IX; s. 231-239.
17. Bibus Metals; Oferta handlowa; Internet materials: [http://www.bibusmetals.pl/?k=strony\\_p&m=78&ns=19&pns=19](http://www.bibusmetals.pl/?k=strony_p&m=78&ns=19&pns=19).
18. High-temperature, high-strength. Nickel base alloys; Nickel Development Institute; 1995 Supplement; N° 393; Internet materials: <http://www.stainless-steel-world.net/pdf/393.pdf>.
19. Special Metals Corporation, Huntington, West Virginia, USA; Oferta handlowa; Internet materials: <http://www.specialmetals.com/products/index.php>.
20. CASTI Metals Red Book. Nonferrous Metals; Fourth Edition; CASTI Publishing Inc.; Edmonton 2003.
21. Stainless Foundry & Engineering, Inc.; Oferta handlowa; Internet materials: <http://www.stainlessfoundry.com>.
22. Gina Advanced Materials Co., Ltd; Oferta handlowa; Internet materials: [http://www.gina.com.cn/en/pro/en\\_pro1\\_3.asp](http://www.gina.com.cn/en/pro/en_pro1_3.asp).
23. F. R. N. Nabarro, H. L. de Villiers: *The Physics of creep*; CRC Press; 1995.
24. J. R. Davis: *ASM Specialty Handbook: nickel, cobalt and their alloys*; ASM International 2000.
25. M. J. Luton: *Abstract of Conference High Temperature Alloys for Gas Turbines*; Liege 1986.

The study was done under an international non-cofinanced project No. 721/N-NICKEL/2010/0

## ZASTOSOWANIE NADSTOPÓW NIKLU NA ODLEWY ELEMENTÓW KONWENCJONALNYCH URZĄDZEŃ ENERGETYCZNYCH

**Streszczenie.** Elementem mogącym łagodzić skutki różnych kryzysów energetycznych jest ciągle zwiększanie sprawności urządzeń energetycznych. Można to uzyskać prowadząc procesy technologiczne w coraz wyższej temperaturze, ciśnieniu i agresywniejszym środowisku niż stosowane dotychczas. Takim wymogom nie mogą sprostać już stopy na bazie żelaza, nawet najlepsze z nich pod tym względem. Sięga się tu po wieloskładnikowe stopy na bazie niklu i kobaltu. Powstają wciąż nowe tworzywa o coraz większej trwałości eksploatacyjnej. Instytut Odlewnictwa w Krakowie wspólnie z partnerami amerykańskimi prowadzi prace badawcze, których celem jest między innymi dokonanie konwersji materiałowej i technologicznej konstrukcji kuto-spawanych wykonywanych z nadstopów niklu, na elementy odlwane z przeznaczeniem do pracy w najtrudniejszych warunkach eksploatacyjnych urządzeń energetycznych nowej generacji. Jest ona realizowana między innymi w ramach amerykańskiego programu „A-USC – NICKEL”, do prac, w którym został zaproszony Instytut Odlewnictwa. W ramach tych prac wykonano już wstępne badania polegające na opanowaniu techniki topienia i odlewania stopu Inconel 740 oraz przeprowadzono wstępne badania materiałowe wykonanych odlewów. Stwierdzono między innymi, że ze wzrostem temperatury, zwłaszcza powyżej 700 °C, stop ten, jako stop odlewniczy wykazuje zdecydowanie mniejszy spadek wytrzymałości na rozciąganie niż analogiczny stop przerabiany plastycznie.

**Słowa kluczowe:** odlewnicze nadstopy niklu, technologia wytwarzania, właściwości mechaniczne, mikrostruktura, umocnienie dyspersyjne.

## AN INNOVATIVE AND ENVIRONMENTALLY SAFE METHOD TO MANUFACTURE HIGH-QUALITY IRON CASTINGS FOR POSSIBLE USE AS ELEMENTS OF AGRICULTURAL MACHINES

Andrzej Pytel, Zbigniew Stefański

Foundry Research Institute, Cracow, Poland

**Summary.** The article presents the experience related with the manufacture of utility castings poured in bentonite-bonded sands on a pilot stand. The technological guidelines were presented for the ductile iron castings weighing 40 kg and 10 kg. For individual castings, the mould technology has been developed, cross-sections of the gating and feeding systems were calculated, and pilot pattern equipment was designed. The results of mechanical tests and structure examinations were discussed. The work will continue within the framework of the project No. POIG.01.03.01-12-061/08-00. The technology currently developed relates to high-quality cast iron with spheroidal and vermicular graphite without and with the addition of alloying elements, including also the grade resistant to thermal fatigue. The idea is to simplify the methods used so far for the manufacture of cast iron subjected to spheroidisation or vermicularisation in a ladle and replace them with an in-mould treatment. These steps are expected to improve the ecological conditions, reduce the fume and glare effects related with magnesium treatment, and improve the process economics. The innovative method, discussed in this work and developed further under the above mentioned project, can be successfully used for casting various elements of the agricultural machinery, resulting in increased mechanical properties of the cast elements, longer life on performance and improved magnesium recovery.

**Keywords:** ductile iron, vermicular graphite cast iron, foundry mould, filters, spheroidisers, inoculants, castings for agriculture.

### INTRODUCTION

Various issues related with casting of parts for machinery and equipment as a result of the operations of inoculation, spheroidisation, vermicularisation and filtration in foundry mould are the subject of research carried out by the Foundry Research Institute in Cracow. The basic assumption in the research is that the processes of spheroidisation, vermicularisation and inoculation, also with the use of ceramic filters, are carried out in a foundry mould [1, 2, 3]. The problems of in-mould inoculation and filtration are described in the reference literature [4, 5, 6]. The, introduced in this article, method of cast iron spheroidisation combined with in-mould inoculation and filtration is an original solution among the existing similar technologies as it allows for the simultaneously conducted spheroidisation (vermicularisation), inoculation and filtration of metal, and is substantially different from the methods of cast iron spheroidisation [7] and vermicularisation [8] carried out in a ladle.



## PURPOSE AND SCOPE OF RESEARCH

The aim of the studies was to examine the feasibility of making pilot castings with spheroidisation treatment, inoculation and filtration carried out simultaneously in a foundry mould [9-12], to review the ecological aspects of the process, and to examine the chemical composition, the degree of magnesium recovery, the mechanical properties and structure of thus obtained cast iron [13,14].

In the previously conducted studies, an attempt was made to check the feasibility of spheroidisation, inoculation and filtration of molten cast iron in a foundry mould to pour 6 kg weighing test ingots [15-21]. Here, the main problem was to develop and improve further this technique of spheroidisation and inoculation. The research carried out focussed on the following issues:

- materials were selected to make the spheroidising-filtrating and inoculating-filtrating sets,
- gating systems with reaction chambers for the casting treatment were designed,
- moulds adjusted to the designed sets and to the specific castings were prepared,
- test melts were carried out, followed by spheroidising treatment and inoculation, both conducted in a foundry mould,
- the feasibility of making safely large castings according to the newly developed method was checked,
- the fume and glare effect during spheroidisation was eliminated, and process ecology as well as health and safety conditions were considerably improved,
- the process performance when making utility castings was checked in terms of the metal properties, structure, magnesium recovery in casting, etc.

## MAKING PILOT CASTINGS

Base iron was melted in a RADYNE medium frequency induction furnace in a crucible of 80 kg capacity (basic lining). As mentioned previously, the screen frame weighing 40 kg net and rams weighing 10 kg each were cast. The chemical composition of the base iron and of the cast iron after in-mould spheroidisation is compared in Table 1.

Table 1. Chemical composition of base cast iron and of cast iron after in-mould spheroidisation and inoculation

Melt and sample designation	Cast iron chemical composition, %					
	C	Si	Mn	P	S	Mg
1(w)/R/O	3,40	1,75	0,42	0,035	0,010	-
R/O	3,15	2,50	0,42	0,035	0,010	0,055
2(w)/2s	3,60	1,75	0,48	0,040	0,020	-
2/s	3,50	2,25	0,46	0,045	0,025	0,070
3w/1v	3,60	1,75	0,48	0,040	0,020	-
1v	3,25	2,35	0,46	0,040	0,020	0,060

Note: Symbol (w) denotes base cast iron

A pattern of the screen frame with fragment of the gating system ready for moulding is shown in Figure 1.

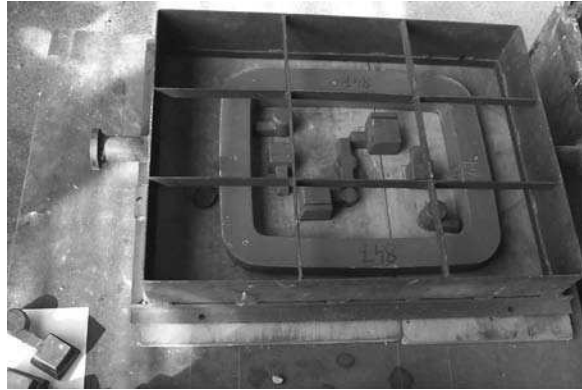


Fig. 1. Pattern of screen frame casting ready for moulding

The ready moulds were poured with molten metal at a temperature of 1440°C. The time of pouring was 23 sec. for the cast frame and 15 sec. for the cast ram. Pouring proceeded calmly and during tests no fume and glare effects related with the spheroidisation process were observed. After cooling, castings were knocked out from the mould and subjected to visual inspection. Figures 2 and 3 show a casting of the frame with gating system and reaction chambers and castings of the rams with cast-on technological samples for testing of the metal properties.



Fig. 2. View of the lower part of casting with a set of chambers for spheroidisation and inoculation



Fig. 3. Castings of rams with gating systems and reaction chambers

Figure 4 shows castings of rams after de-gating.



Fig. 4. Photographs of rams after de-gating

#### TYPES OF TESTS PERFORMED AND QUALITY OF METAL OBTAINED

Tests performed on the cast material used for the screen frame and rams included:

- analysis of chemical composition,
- observations under the microscope (graphite precipitates, structure of metal matrix),

- mechanical properties ( $R_m$ ,  $A_5$ , HB),
- visual inspection of the cut pieces of castings.

## RESULTS

The results of this study are provided in Tables 1 – 3.

Table 1 compares the initial chemical composition of the base iron with the chemical composition of the same cast iron after spheroidisation in a foundry mould using spheroidising-filtrating and inoculating-filtrating sets (castings of the frame and ram). Table 2 compares the results of mechanical tests carried out on sample castings.

Table 2. Mechanical properties of the examined cast iron

Sample designation	Basic mechanical properties of the examined cast iron		
	$R_m$ , MPa	$A_5$ , %	HB/5/750
R/0/A	552	12,8	145
R/0/B	555	12,0	149
2A	526	16,3	163
2B	559	14,4	153
2/O/A	572	12,3	167
2/O/B	575	11,7	166
1/A	513	15,7	150
1/B	458	6,4	136

Note: symbol O denotes samples turned out from castings

Table 3. The results of microstructural examinations of cast iron

No.	Sample designation	Graphite microstructure	Matrix microstructure
1.	R/O	VA5	Pf1, P6
2.	2	VA6	Pf1, P6
3.	1	VA6	P0

Table 3 contains the results of examinations of the structure of graphite and metal matrix in iron castings. A photograph of the cast iron structure obtained during the conducted tests is given as an example in Figure 5 (precipitates of graphite and metal matrix).

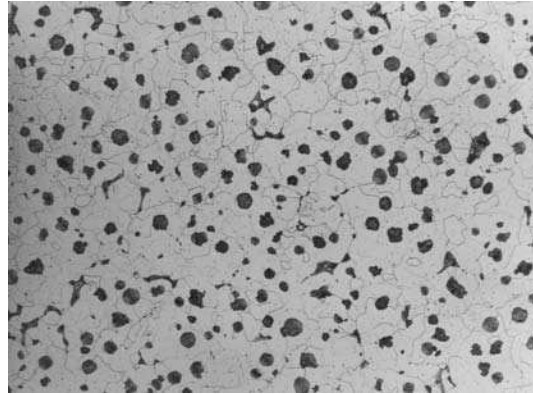


Fig. 5. Microstructure of sample 1; etched section, 100x

All tests and examinations were carried out in accordance with standards valid in this respect:

- determination of cast iron microstructure: PN-75/H-04661,
- characteristics of the graphite precipitates in cast iron: PN-EN ISO 945,
- tensile test for metals: PN-EN ISO 6892-1,
- Brinell hardness measurement: PN-EN ISO 6506-1.

## CONCLUSIONS

1. In cast iron obtained as a result of the conducted studies, the magnesium content was from 0.055% to 0.070%. Compared to ladle spheroidisation, the method presented here enabled reducing the quantity of the added master alloy by about 40%.
2. Graphite microstructure of the type VA5 and VA6 was obtained. In microstructure of the metal matrix, the content of pearlite was up to P6. No cementite was detected.
3. A very good tensile strength of 458–575 MPa, combined with high elongation  $A_5$  (from 6.4 to 16.6%) and a hardness of 136–167 units HB was obtained in the samples.
4. No adverse effects, like violent reaction and metal ejection from mould were observed during the process of in-mould spheroidisation. The spheroidisation carried out in a foundry mould proceeded without any visible fume and glare effects. Changes introduced to the design of the gating system and reaction chambers, as well as the application of reducing atmosphere contributed to the good results of the tests.
5. Casting quality was very good; no internal and surface defects were observed.
6. The obtained test results have proved that it is possible to successfully make iron castings as a result of the spheroidisation treatment and inoculation carried out in foundry mould using spheroidising-filtrating and inoculating-filtrating sets.
7. The course of the tests performed and the results obtained have been positive; it seems that the developed technology is very promising and as such should be developed in future.
8. The presented method can serve in the manufacture of cast iron components or spare parts for agricultural machinery, replacing less durable castings of EN-GJL-200, 250 grades with EN-GJS-400 (600) grades.

## REFERENCES

1. Pytel A., Stefański Z.: Opracowanie i wypróbowanie zestawów do nowej metody wermikularyzacji, sferoidyzacji i modyfikacji żeliwa. Etap I. Opracowanie i wypróbowanie zestawów sferoidyzująco-filtrujących i modyfikująco-filtrujących oraz przeprowadzenie prób. Praca statutowa IOd, zlec. 2014/00, Kraków 2003.
2. Pytel A., Z. Stefański.: Żeliwo z grafitem wermikularnym otrzymane w formie odlewniczej. Wybrane badania. *Odlewnictwo-Nauka i Praktyka. Zeszyt Specjalny 2004, Nr 2*, s.45-50.
3. Pytel A., Stefański Z.: Wybrane aspekty zabiegu wermikularyzowania żeliwa w formie odlewniczej. *Archiwum odlewnictwa PAN, Rok 2006, Rocznik 6, Nr 18 (1/2), Katowice 2006.*
4. Lerner Y.S., Aubrey L.S., Craig D., Margaria T.: In-mould treatment processes in iron foundry practice. Part 1. *Foundry Trade Journal. December 2002*, s. 24-27.
5. Lerner Y.S., Aubrey L.S., Craig D., Margaria T.: In-mould treatment processes in iron foundry practice. Part 2. *Foundry Trade Journal. January 2003*, s. 28-31.
6. Konieczny A.: Modyfikowanie żeliwa w formie odlewniczej z zastosowaniem systemu modyfikująco-filtrującego INFER. *Przegląd Odlewnictwa 2002*, nr 7-8, s. 265-269.
7. Pirowski Z., Gościański M.: Konstrukcja i technologia wytwarzania odlewanych lemieszów do pługów obracalnych i zagonowych; MOTROL – Motoryzacja i Energetyka Rolnictwa; Lublin 2009; t. 11, s. 159-167.
8. Pytel A., Sękowski K.: Struktura i własności wytrzymałościowe niskostopowego żeliwa wermikularnego. 7th International Scientific Conference. Achievements in mechanical and materials engineering. Gliwice-Zakopane, 1998
9. Fraś E., Kusztal J., Podrzucki C.: Zagadnienia modyfikacji żeliwa w formie odlewniczej. *Zeszyty naukowe AGH 1974*, nr 60, s. 9.
10. Piaskowski J.: Żeliwo sferoidalne perlityczne uzyskane bez dodatków stopowych i obróbki cieplnej. *Przegląd Odlewnictwa 1992*, nr 1, s. 27.
11. Olszowska Sobieraj B., Sobieński K.: Wpływ niektórych parametrów mikrostruktury na właściwości żeliwa sferoidalnego. *Zeszyty naukowe AGH nr438, Metalurgia i Odlewnictwo, 1974*, z. 59, s.41.
12. Yuovo A., Alhainen J., Eklund P.: Formuły matematyczne dla określenia struktury i właściwości mechanicznych żeliwa sferoidalnego. *Przegląd Odlewnictwa 1992*, nr 1, s. 22.
13. Możdżeń M., Olszowska-Sobieraj B.: Możliwość sterowania parametrami mikrostruktury żeliwa sferoidalnego w odlewach cienkościennych za pomocą modyfikacji w formie. *Przegląd Odlewnictwa 1999*, nr2, s.55-59.
14. Cizek L., Grant W., Vondrak V.: Optymalizacja właściwości mechanicznych żeliwa sferoidalnego. *Przegląd Odlewnictwa 1997*, nr 5, s.137.
15. Piech K.: Ceramiczne filtry piankowe, charakterystyka i zastosowanie. *Przegląd Odlewnictwa 1995*, nr 1, s. 32-35.
16. Bachny L., Sladek A., Hofman H.: Przyczynek do zagadnienia filtrowania żeliwa sferoidalnego. *Przegląd Odlewnictwa 1999*, nr 3, s. 94-98.
17. Klekowicki K.: Piankowe filtry ceramiczne w formach na linii DISAMATIC. *Przegląd Odlewnictwa 1999*, nr 6, s. 226-229.
18. Aślanowicz M., Ościłowski A., Stachańczyk J., Filtracja ciekłych metali z użyciem filtrów produkcji FERRO-TERM, *Przegląd Odlewnictwa 2002*, nr 9-10, s. 324-327.
19. Aślanowicz M., Ościłowski A., Stachańczyk J.; Polskie doświadczenia w procesie filtracji ciekłych tworzyw metalowych. *Przegląd Odlewnictwa 2002*, nr9.

20. Stachańczyk J., Aslanowicz M.: „Zestaw INFERR - ocena prób przemysłowych”, Acta Metallurgica Slovaca 2002.
21. Jonuleit M., Weiser E.: Zdefiniowane własności. Modyfikacja w formie żeliwa sferoidalnego (GJL) i żeliwa szarego z grafitem płatkowym (GJL); Giesserei- Erfahrungsust 2007 nr 12, s. 46-52.

**This work was supported by Structural Funds under the Operational Programme Innovative Economy for the years 2007 – 2013, Measure 1.3.**

#### INNOWACYJNA I EKOLOGICZNA METODA WYKONYWANIA ODLEWÓW Z ŻELIWA WYSOKOJAKOŚCIOWEGO Z MOŻLIWOŚCIĄ WYKORZYSTANIA W ELEMENTACH MASZYN ROLNICZYCH

**Streszczenie.** W artykule przedstawiono doświadczenia wykonania odlewów użytkowych w formach w masach bentonitowych na stanowisku doświadczalnym. Zaprezentowano założenia technologiczne dla odlewów z żeliwa sferoidalnego o masie 40 kg i 10 kg. Dla poszczególnych odlewów opracowano technologię formy, obliczono przekroje układu wlewowego i zasilającego wykonano omodelowanie próbne. Omówiono rezultaty przeprowadzonych prób, wytrzymałości materiału odlewów i jego struktury. Prace są w dalszym ciągu kontynuowane w ramach prowadzonego projektu: POIG.01.03.01-12-061/08-00. Rozwijana obecnie technologia dotyczy żeliwa wysokojakościowego sferoidalnego i wermikularnego bez dodatków pierwiastków stopowych, jak również z dodatkiem pierwiastków stopowych, także odpornego na zmęczenie cieplne. Ideą zagadnienia jest uproszczenie dotychczasowych metod wytwarzania odlewów z żeliwa poddawanego procesowi sferoidyzacji lub wermikularyzacji w kadzi i zastąpienie procesem sferoidyzacji w formie odlewniczej. Dzięki temu poprawiają się warunki ekologiczne, ograniczone są efekty zadymienia i efekty pirotechniczne związane z reakcją magnezu a także ekonomią procesu. Omówiona w pracy i rozwijana innowacyjna metoda również w projekcie może być z powodzeniem wykorzystana do odlewania różnych elementów maszyn rolniczych powodując zwiększenie właściwości wytrzymałościowych odlewnych elementów, trwałości a także zwiększenia uzysku magnezu w prowadzonym procesie.

**Słowa kluczowe:** żeliwo sferoidalne, żeliwo z grafitem wermikularnym, forma odlewnicza, filtry, sferoidyzatory, modyfikatory, odlewy dla rolnictwa.

## SELECTED MECHANICAL PROPERTIES OF TPS FILMS STORED IN THE SOIL ENVIRONMENT.

Andrzej Rejak, Leszek Mościcki

Department of Food Process Engineering, Lublin University of Life Sciences

**Summary.** The results of measurements of susceptibility to biodegradation and the effect of storage in soil on the mechanical properties of thermoplastic starch films obtained from blends of starch, glycerol and emulsifiers. Studies have shown a varied influence of the blend compositions, extrusion conditions and storage on the scope and efficiency of biodegradation of the products.

**Key words:** biodegradation, mechanical properties, blends, storage.

### INTRODUCTION

Biodegradable plastics, which are a mixture of natural polymers, mainly starch (so-called thermoplastic starch - TPS) and cellulose are produced so far on a small scale. Nowadays products present on the market are *de facto quasi*-biodegradable, is still underway to obtain material fully biodegradable in the environment, which may be used in the manufacture of disposable utensils, gardening and packaging film and/or for the manufacture of garbage bags. The use of biodegradable plastics packaging industry is limited mainly because of financial reasons, due to higher production cost compared to traditional materials and because of the still numerous technical imperfections [4, 5, 6, 7, 8].

### MATERIALS AND METHODS

Research on the process of TPS film extrusion with the addition of emulsifiers with an assessment of basic physical properties of the products obtained was carried out in laboratories of the Department of Food Process Engineering (KIP) of the Lublin University of Life Sciences in 2009-2010.

The film was extruded from TPS pellets on a specially designed laboratory line using blowing technique. That line was performed by SAVO Ltd. Co. from Warsaw (Fig. 1).

TPS pellets were made by extrusion-cooking (baro-thermal treatment commonly used in food sector) in a modified single screw extrusion-cooker TS-45 (ZMCh Metalchem Gliwice, PL). Compound consisted of potato starch (ZPZ Łomża), glycerol (Odczynniki Chemiczne Lublin) and polymers: I - Octene-1 Plastomer EXACT TM 8201, and II - EVA Copolymer (Exxonmobil Chemical LTD, UK) having excellent strength parameters and water resistance (Tab. 1).



The extrusion-cooking process was conducted in the temperature range 90-130oC, with a screw rotation from 60 to 120 rpm.

Strength and mechanical properties tests were conducted in accordance with the current methodology of research [2].



Fig. 1. TPS film blowing in KIP laboratory [8]

Table 1. Composition of compound

Pellets/specification	Composition [%]
Probe SP	Potato starch - 77
	Emulsifier I - 1
	Glycerol - 22
Probe 2SP	Potato starch - 68
	Emulsifier I. - 12
	Glycerol - 20
Probe 3SP	Potato starch - 72
	Emulsifier II. - 8
	Glycerol - 20
Probe 4SP	Potato starch Skrobia - 68
	Emulsifier II.- 12
	Glycerol - 20

During film extrusion the film tubes with a diameter of 150 to 700 mm and thickness from 0.15 to 0.6 mm were obtained, depending on the composition of the pellets. Film extrusion process parameters are given in Table 2.

Table 2. Terms of TPS film extrusion

Probe	Screw rpm	Motor load [A]	Temperature in an extruder's zones [°C]						
			Barrel				Die		
			I	2	3	4	I	II	III
SP	70	8	110	84	130	122	130	140	120
2SP	70	12	117	88	135	122	130	149	125
3SP	70	11,8	116	89	138	124	134	145	121
4SP	70	6,6	114	91	177	130	139	142	122

The resultant film samples were evaluated for biodegradability in soil by using a simplified methodology based on our experiences and described in many works. Film samples before storage as well as during it were periodically tested for mechanical properties in universal testing machine Zwick BDO-FB 0.5TH ; the moisture content of films was also determined in individual stages during storage.

## RESULTS

One of the main factor of the biodegradation of film is its susceptibility to moisture absorption during storage in the soil at the landfill or in natural conditions and loss of strength characteristics . Table 3 presents the results of measurements of moisture content changes during the film stored in the soil; the measurement results of basic mechanical characteristics are presented in graphic form (Figure 1-8).

Table 3. Humidity films in various stages of storage

Moisture content [%] /probe	SP	2SP	3SP	4SP
Moisture after extrusion	9,5	6,5	6,31	6,87
Moisture priori storage	10,6	8,7	8,9	9,8
Moisture after 20 days	60,3	52,5	54,1	56,3
Moisture after 40 days	64,4	52,9	61,1	59,8
Moisture after 60 days	spread	65,8	64,8	69,6

The resistance to puncture foil was carried out in four stages. In the first stage, measurements were made immediately after manufacture, the second stage, after 20 days at the film in the ground, the third after 40 days at the film in the land, while in the fourth stage after 60 days of burying the

film. Examination of these samples allowed us to determine the force required to rupture, maximum stress and elongation at the puncture from the destruction of the sample as well as the degree of biodegradability.

Based on the results of research can be said that, the film received from SP, 2SP, 3SP, 4SP pellets, despite the tensile strength is relatively resistant to puncture. Maximum puncture force ranged from 7.73 N to 16.82 N, whereas the elongation at destruction ranged from 4.51% to 4.71%.

After 20 days of stay in the ground, the film moisture content ranged from 54.1% to 60.3% was the most durable 2SP film, where the maximum puncture force was 2.59 N and 5.93% elongation, and proved to be the weakest SP film, where the maximum penetration force was 0.94 N and 4.53% elongation. It was found that humidity had a decisive influence on films (Table 3).

After 40 days of storage, the maximum force of penetration ranged from 0.79N to 0,49 N, while the elongation at destruction ranged from 6.66% to 7.04%.

2 months storage resulted in total destruction of the sample films of SP and 4SP, they were not suitable for testing (see Fig. 9 and 11). Samples of 2SP (Fig. 10) and 3SP films showed maximum force of penetration: respectively 0.33 N and 0.23 N and extending from the destruction amounted to 6.68% and 6.6%.

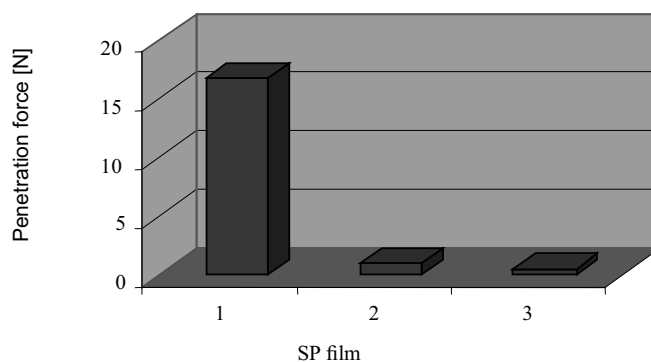


Fig. 1. Comparison of penetration forces of SP film. 1 - test results after production, 2 - after 20 days, 3 - after 40 days of storage

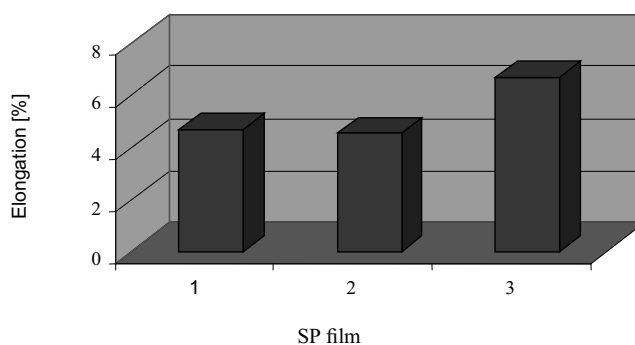


Fig. 2. Comparison of susceptibility for elongation of SP film. 1 - test results after production, 2 - after 20 days, 3 - after 40 days of storage

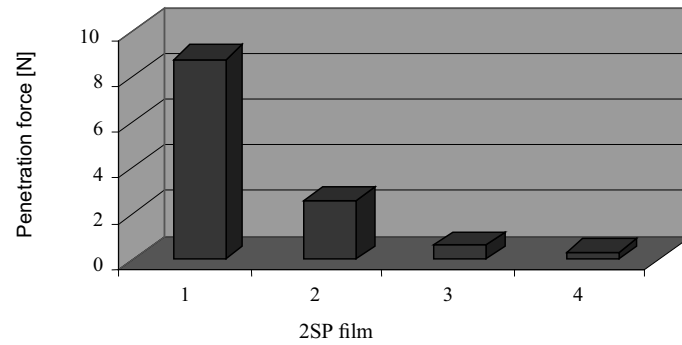


Fig. 3. Comparison of penetration forces of 2SP film. 1 - test results after production, 2 - after 20 days, 3 - after 40 days, 4 - after 60 days of storage

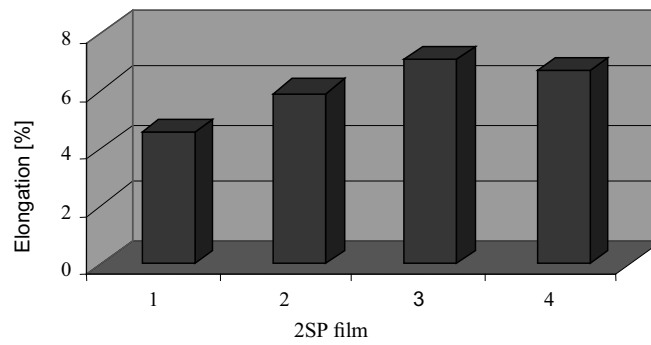


Fig. 4. Comparison of susceptibility for elongation of 2SP film. 1 - test results after production, 2 - after 20 days, 3 - after 40 days, 4 - after 60 days of storage

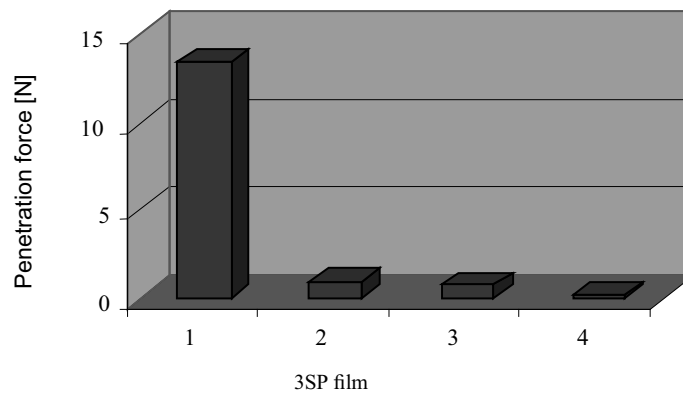


Fig. 5. Comparison of penetration forces of 3SP film. 1 - test results after production, 2 - after 20 days, 3 - after 40 days, 4 - after 60 days of storage

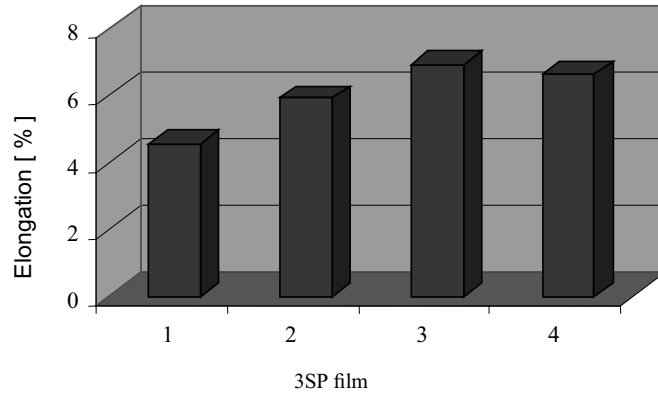


Fig. 6. Comparison of susceptibility for elongation of 3SP film. 1 - test results after production, 2 - after 20 days, 3 - after 40 days, 4 - after 60 days of storage

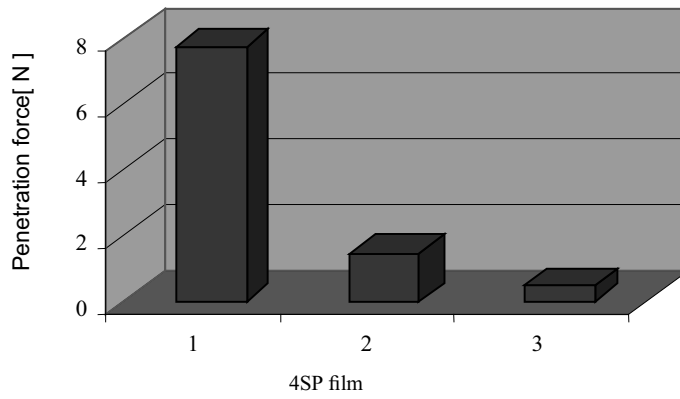


Fig. 7. Comparison of penetration forces of 4SP film. 1 - test results after production, 2 - after 20 days, 3 - after 40 days of storage

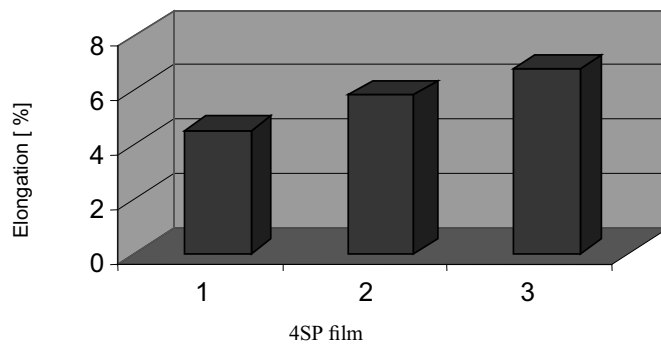


Fig. 8. Comparison of susceptibility for elongation of 4SP film. 1 - test results after production, 2 - after 20 days, 3 - after 40 days of storage

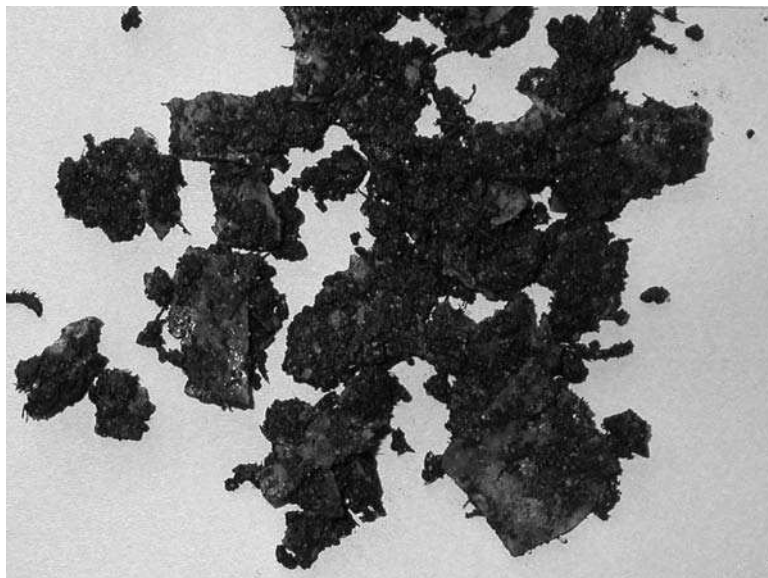


Fig. 9. Film SP after 60 days of storage [8]

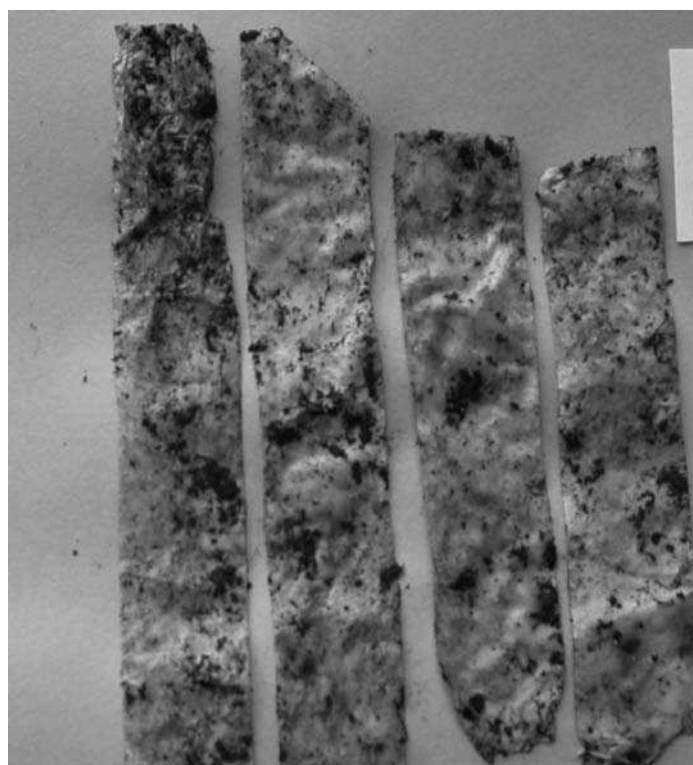


Fig. 10. Film 2SP after 60 days of storage [8]



Fig. 11. Film 4SP after 60 days of storage[8]

## CONCLUSIONS

The analysis of the obtained results of mechanical properties of extruded TPS films stored in the soil showed that:

- Susceptibility of film on the biodegradation depended on the composition of raw mixes (including the participation of emulsifier) and extrusion conditions.
- In addition to the storage time was also important the moisture content of soil where samples were stored.
- The best characteristics in terms of mechanical properties had film samples obtained from a mixture of 2SP containing 20% glycerol and 12% emulsifier.
- The most biodegradable were films produced from a mixture of SP - emulsifier free and 4SP processed at the highest baro-thermal conditions. In both cases, the decisive factor was the nature of changes occurring in starch during the manufacturing process and storage time.

## REFERENCES

1. Błędzki A.K., Fabrycy E.: Polimery biodegralne. Tom 37, nr 8, 1992.s. 343-350.
2. Broniewski T. i inni.: Metody badań i ocena właściwości tworzyw sztucznych. WNT, Warszawa, 2000.
3. Janssen L., Mościcki L. (eds): Thermoplastic Starch, Wiley-VCH, 2009
4. Leszczyński W.: Materiały opakowaniowe z polimerów biodegradowalnych, Przemysł Spożywczy, 8, 2001.
5. Mościcki L., Wojtowicz A.: Kierunki rozwoju opakowań ekologicznych, Zeszyty Naukowe Politechniki Opolskiej, Nr kol.254/2000, s.177-184.

6. Rejak.A., Mościcki L.: Biodegradable foil extruded from thermoplastic starch, Teka Komisji Motoryzacji i Energetyki Rolnictwa, 6/2006, s.123-130.
7. Rejak A.: Badania właściwości fizycznych skrobiowych folii biodegradowalnych. Acta Agrophysica, 9(3), 2007. S. 747-754.
8. Rejak A.: Archiwum prywatne.
9. Rupiński S.: Polimery biodegradowalne. „Plastics Review”, 5/2004.
10. Sikora R.: Przetwórstwo tworzyw wielkocząsteczkowych. WNT, Warszawa, 1993.
11. Trznadel M.: Biorozkładalne materiały polimerowe, Polimery, nr 9/1995, s.485-492.
12. Żakowska H.: Recykling opakowań poużytkowych z tworzyw sztucznych w Polsce. Opakowania. 46(6), s.44-47.
13. Żakowska H.: Biodegradowalne materiały opakowaniowe przydatne do utylizacji przez kompostowanie, Przemysł Spożywczy, nr 8, 2000.
14. PN-81/C-89032.
15. PN-72/C-89096.
16. PN-81/C-89096.
17. PN-81/P-50129.

#### WYBRANE WŁAŚCIWOŚCI MECHANICZNE FOLII SKROBIOWYCH SKŁADOWANYCH W GLEBIE

**Streszczenie.** W pracy przedstawiono wyniki pomiarów podatności na biodegradowalność oraz wpływu przechowywania w glebie na wybrane właściwości mechaniczne folii otrzymanej z mieszanek skrobi termoplastycznej z udziałem gliceryny i emulgatorów. Badania wykazały zróżnicowany wpływ kompozycji mieszanek, warunków wytłaczania oraz przechowywania na zakres i efektywność biodegradacji badanych produktów.

**Słowa kluczowe:** biodegradowalność, właściwości mechaniczne, mieszanki, przechowywanie.



## THE ANALYSIS OF POSSIBILITY OF ENERGY RECOVERY DURING CONVECTIVE DRYING OF PAPRIKA

Stanisław Rudy, Andrzej Krzykowski, Dariusz Dziki,  
Paweł Kozak, Zbigniew Serwatka

Department of Thermal Technology, University of Life Sciences in Lublin,  
Doświadczalna 44, 20-280 Lublin, Poland

**Summary.** In this paper, the enthalpy and the possible amount of energy recovery during paprika (cv. Kier) convective drying were determined. The drying was made for two velocities of the drying factor ( $0.3$  and  $0.5 \text{ m s}^{-1}$ ) and for four temperature levels ( $50$ ,  $55$ ,  $60$ , and  $65^\circ\text{C}$ ). The results showed that for all the independent variables the enthalpy of air leaving the dryer decreased during the drying time. At the respective air flow velocities, the air at the temperature of  $65^\circ\text{C}$  had the highest enthalpy and the air at the temperature of  $50^\circ\text{C}$  the lowest one. An increase of air flow velocity caused an increase in enthalpy, especially at the beginning of the process. The highest amount of energy ( $2,1 \text{ kJ}\cdot\text{s}^{-1}$ ), can be recovered during the drying of paprika at the temperature of  $50^\circ\text{C}$ , and at the air flow velocity of  $0.5 \text{ m}\cdot\text{s}^{-1}$ .

**Key words:** convective drying, heat flux, enthalpy, paprika.

### Nomenclature:

$\varphi$ - relative air humidity,  
 $\rho_{1+x}$  - air density after leaving the dryer [ $\text{m}^3/\text{kg}$ ],  
 $c_{pg}$  - specific heat of dry air [ $\text{kJ}/(\text{kg}\cdot\text{K})$ ],  
 $c_{pw}$  - specific isobaric heat of water vapour [ $\text{kJ}/(\text{kg}\cdot\text{K})$ ],  
 $i_{1+x}$  - enthalpy of one kilogram of dry air and enclosed steam [ $\text{kJ}/\text{kg}$ ],  
 $p_0$  - ambient pressure [ $\text{Pa}$ ],  
 $p_w$  - saturation pressure of air [ $\text{Pa}$ ],  
 $Q$ - heat flux [ $\text{kJ}/\text{s}$ ],  
 $r_0$ - heat vaporization of water at the triple point temperature [ $\text{kJ}/\text{kg}$ ],  
 $R_w, R_g$  - individual gas constant of steam and dry air, respectively [ $\text{J}/\text{kgK}$ ],  
 $t$ - temperature [ $^\circ\text{C}$ ],  
 $T$ - temperature [ $\text{K}$ ],  
 $V$ - volumetric flow rate of medium [ $\text{m}^3/\text{s}$ ],  
 $x$ - absolute humidity [ $\text{kg H}_2\text{O}/\text{kg}$  of dry air].

## INTRODUCTION

The highest amount of energy needed for the support of the drying process is consumed for heating of drying air and for water evaporation from material [Mujumdar 2007, Ivanova et al. 2001, Benali et al. 2006, Rudy 2009]. At the constant air flow velocity the intensity of water evaporation is the highest at the beginning of the process and decreases with the drying time [Flink 1977, Pabis 2007, Ratti 2001, Koyuncu et al. 2004, 2007].

The energy recovery from hot air during the convective drying can be made in a few ways. The simplest method is the recirculation of part of drying air leaving the drier. This method is used when at the beginning of the process the higher relative humidity of the air is required [Sokhansanj, Wood 1991, Savoie 2006, Didukh, Kirchuk 2007, Jech et al. 2006].

The air removed from the system can be used for pre-heating and preliminary drying the raw material before the process. Another method of heat recovery in the drying industry is the use of different kinds of diaphragm heat exchangers or air-air heat pumps. The process of heat recovery by using heat exchangers is more difficult to realize, however, it makes possible the recovery of low relative air humidity [Prvulovic et al. 2001, Atkins et al. 2010, Budin et al. 1996, Conde 1997, Ho et al. 2001, Tippayawong et al. 2009, Soylemez 2006].

## MATERIALS AND METHODS

The aim of this study was to evaluate the influence of temperature and flow velocity of the drying air on the possible amount of thermal energy recovery from moist air after leaving the convective dryer.

The investigations of the convective drying process of sweet paprika (cv. Kier) were performed for two drying flow velocities, namely 0.3 and 0.5 ms<sup>-1</sup>, at the temperature of 50, 55, 60, and 65°C. The velocity and temperature of drying air were measured behind the drying material.

Before being dried, the material was cut into 0.5 mm thick cubes. Paprika was dried up to the 12% (w.b.) moisture level. The convection dryer's load was 25 kg/m<sup>2</sup>. The enthalpy of moist air after leaving the dryer was calculated as follows:

$$i_{1+x} = c_{pg} \cdot t + x \cdot (c_{pw} \cdot t + r_0). \quad (1)$$

The absolute humidity of air was calculated according to the equation:

$$x = 0,622 \cdot \frac{\varphi \cdot p_w''}{p - \varphi \cdot p_w''}. \quad (2)$$

The constant value of absolute humidity of air (0.4) was assumed in the calculations. The absolute humidity of air after leaving the convective dryer was determined, taking into consideration the amount of evaporated water per unit of drying time.

With regard to the fact, that measurements of mass loss of the dried material were carried out at 20 min time intervals, it was assumed, that constant water content evaporated between the measurements. The amount of heat possible to recover from the drying air was calculated as follows:

$$\dot{Q} = \dot{V} \cdot \rho_{1+x} \cdot (i_{1(1+x)} - i_{2(1+x)}), \quad (3)$$

where:

$$\rho_{1+x} = \frac{1}{T} \cdot \left( \frac{\phi \cdot P_w''}{R_w} + \frac{P_0 - \phi \cdot P_w''}{R_g} \right) \quad (4)$$

The volumetric flow rate of drying air was calculated as product of air flow velocity and surface drying screen area. The air enthalpy after passing through heat exchanger was determined for constant value of air temperature equal to 20°C.

The convection drying was conducted using a vertical air-flow dryer. The heating assembly of the dryer consisted of three heating elements and, more specifically, of heaters in chamotte casings, with the total strength of 6.9 kW. The heating element of this dryer consists of three heaters in chamotte casings. One of these heaters is connected to the circulation system of the temperature regulator. The axial ventilator, powered by an electric engine with a multi-stage regulation of rotation, ensured the air flow. The convective dryer diagram was shown in Fig. 1.

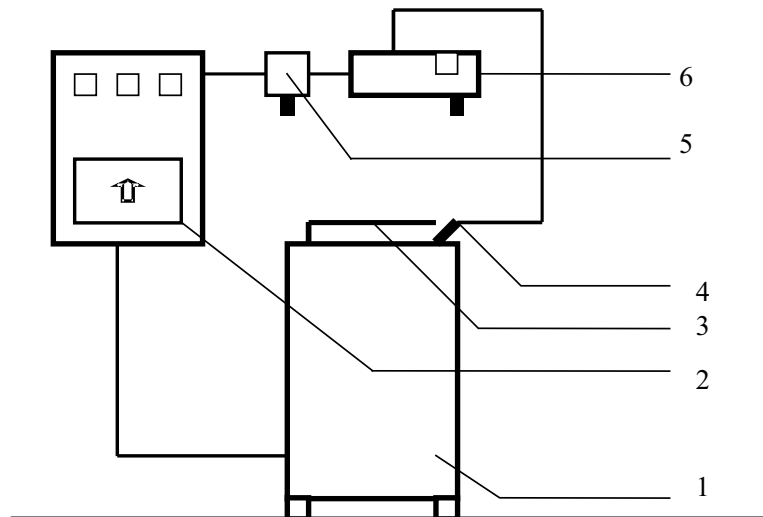


Fig. 1. The scheme of measuring stand for convective drying: 1 – dryer, 2 – switchboard, 3 – screen, 4 – contact thermometer, 5 – contactor, 6 – stabilizer

## RESULTS AND DISCUSSION

The drying curves of paprika, obtained on the basis of experimental data in different drying conditions were shown in Figures 2 and 3. The regression equations described the changes in weight of the material during drying were presented in Tables 1 and 2.

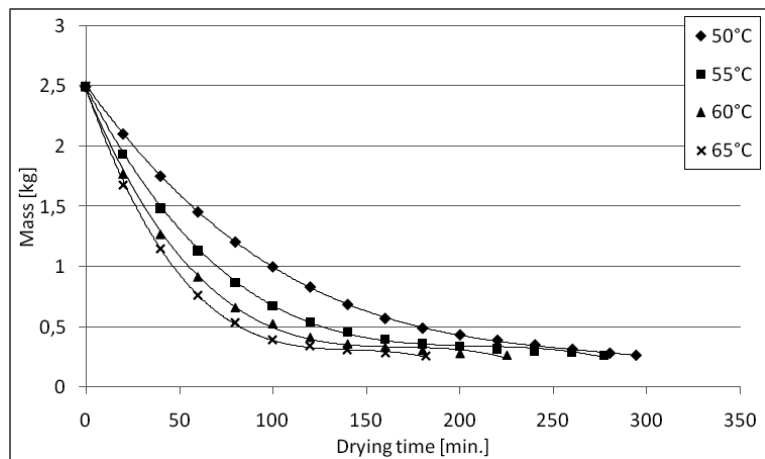


Fig. 2. Convective drying curves of paprika (air flow velocity 0,3 m/s)

Table 1. Regression equations described the relations between the changes in weight of the material and convective drying time (air flow velocity 0,3 m/s)

t [°C]	The regression equation	R <sup>2</sup>
50	$m = -9 \times 10^{-8} \times x^3 + 7 \times 10^{-5} \times x^2 - 0,0216 \times x + 2,5045$	1
55	$m = -2 \times 10^{-7} \times x^3 + 0,0001 \times x^2 - 0,03 \times x + 2,4871$	0,997
60	$m = -4 \times 10^{-7} \times x^3 + 0,0002 \times x^2 - 0,0374 \times x + 2,4681$	0,998
65	$m = -7 \times 10^{-7} \times x^3 + 0,0003 \times x^2 - 0,0445 \times x + 2,4839$	0,999

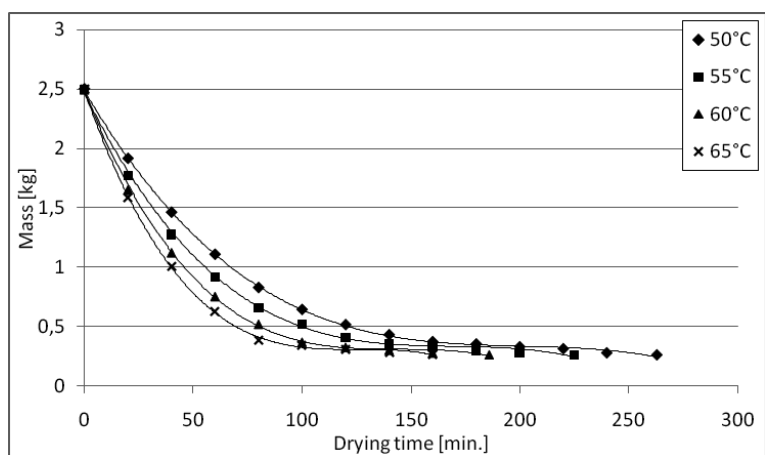


Fig. 3. Convective drying curves of paprika (air flow velocity 0,5 m/s)

Table 2. Regression equations described the relations between the changes in weight of the material and convective drying time (air flow velocity 0,5 m/s)

t [°C]	The regression equation	R <sup>2</sup>
50	$m = -3 \times 10^{-7} \times x^3 + 0,0002 \times x^2 - 0,0312 \times x + 2,4889$	0,999
55	$m = -4 \times 10^{-7} \times x^3 + 0,0002 \times x^2 - 0,0373 \times x + 2,4697$	0,999
60	$m = -7 \times 10^{-7} \times x^3 + 0,0003 \times x^2 - 0,0449 \times x + 2,476$	0,998
65	$m = -10^{-6} \times x^3 + 0,0004 \times x^2 - 0,0523 \times x + 2,4927$	0,999

The highest weight losses were obtained at the beginning of the drying process. This tendency was found for two air flow velocities (at each temperature level). The amount of water evaporated from paprika suddenly decreased after exceeding half of drying time. At each air flow velocity the intensity of water removal increased with the air temperature.

An increase of air flow velocity from 0,3 m×s<sup>-1</sup> to 0,5 m×s<sup>-1</sup> caused intensification of the drying process.

The changes of enthalpy of moist air (determined on the basis of equation 1) after leaving the convective dryer in relation to the drying time were presented in Figures 4 and 5. The regression equations describing these changes during the drying process were presented in Tables 3 and 4.

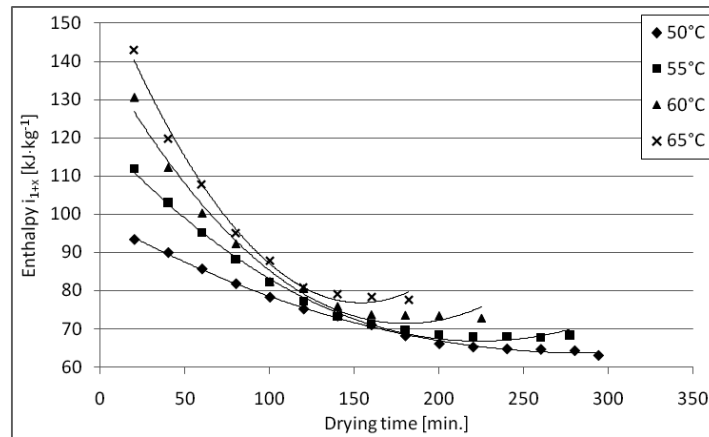


Fig. 4. Enthalpy of moist air in relation to drying time (air flow velocity 0,3 m/s)

Table 3. Regression equations describing the relations between the enthalpy of moist air and drying time (air flow velocity 0,3 m/s)

t [°C]	The regression equation	R <sup>2</sup>
50	$i_{1+x} = 0,0004 \times x^2 - 0,2433 \times x + 98,578$	0,997
55	$i_{1+x} = 0,0011 \times x^2 - 0,4781 \times x + 120,2$	0,996
60	$i_{1+x} = 0,0022 \times x^2 - 0,7808 \times x + 141,69$	0,986
65	$i_{1+x} = 0,0036 \times x^2 - 1,0934 \times x + 160,86$	0,993

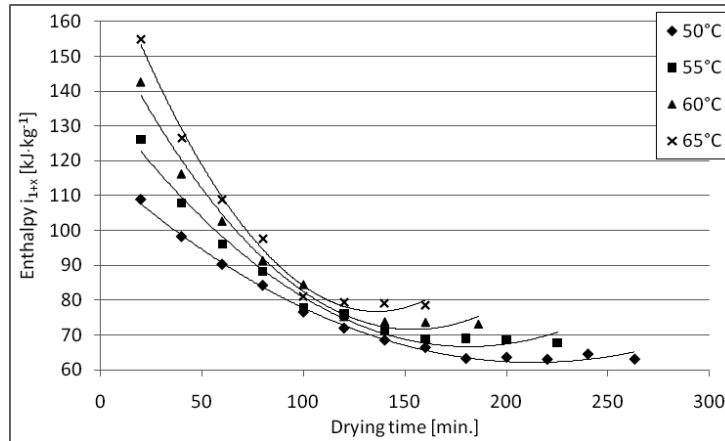


Fig. 5. Enthalpy of moist air in relation to drying time (air flow velocity 0,5 m/s)

Table 4. Regression equations describing the relations between the enthalpy of moist air and drying time (air flow velocity 0,5 m/s<sup>1</sup>)

t [°C]	The regression equation	R <sup>2</sup>
50	$i_{1+x} = 0,0012 \times x^2 - 0,5184 \times x + 117,46$	0,995
55	$i_{1+x} = 0,0022 \times x^2 - 0,7805 \times x + 137,37$	0,996
60	$i_{1+x} = 0,0037 \times x^2 - 1,1516 \times x + 160,28$	0,989
65	$i_{1+x} = 0,0057 \times x^2 - 1,5467 \times x + 181,91$	0,993

For all the considered independent variables the enthalpy of air decreased with the function of convective drying time. Such character of drying curves is conditioned by intensity of water evaporation from drying material.

The highest enthalpy was obtained for drying air removed from the dryer at the highest temperature from the measurement range (65°C). This tendency was found for two air flow velocities. The lowest enthalpy was observed for air obtained after drying at 50°C. An increase of air flow velocity caused an increase of air enthalpy at the beginning of the drying process. However, at the end of the drying the flow velocity had no influence on the enthalpy.

The changes of heat flux (determined on the basis of equation 3), possible to recover from moist air after leaving the convective dryer, in relation to the drying time were presented in Figures 6 and 7. The regression equations describing these changes during the drying process were presented in Tables 5 and 6.

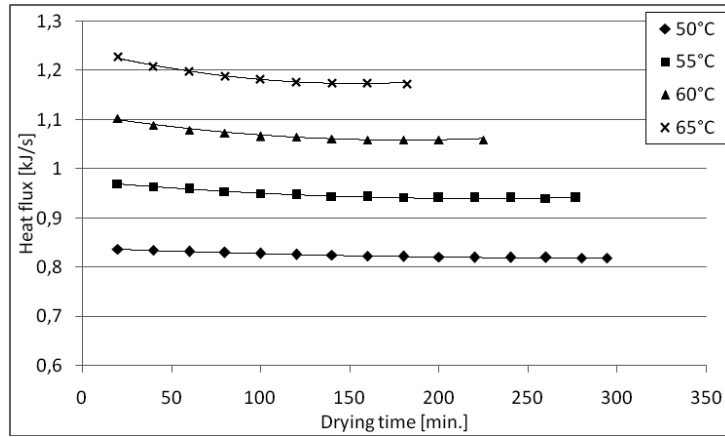


Fig. 6. Heat flux possible to recover for moist air in relation to drying (air flow velocity 0,3 m/s)

Table 5. Regression equations describing the relations between the heat flux and drying time (air flow velocity 0,3 m/s)

t [°C]	The regression equation	R <sup>2</sup>
50	$Q = 2 \times 10^{-7} \times x^2 - 0,0001 \times x + 0,8395$	0,997
55	$Q = 7 \times 10^{-7} \times x^2 - 0,0003 \times x + 0,9754$	0,996
60	$Q = 2 \times 10^{-6} \times x^2 - 0,0006 \times x + 1,1101$	0,986
65	$Q = 3 \times 10^{-6} \times x^2 - 0,0009 \times x + 1,2418$	0,994

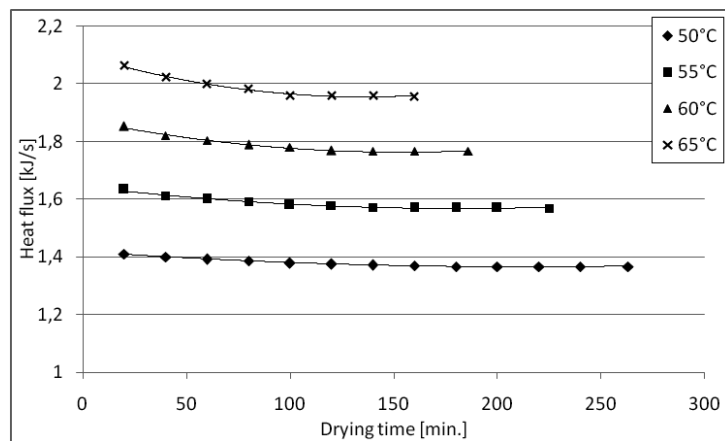


Fig. 7. Heat flux possible to recover for moist air in relation to drying (air flow velocity 0,3 m/s)

Table 6. Regression equations describing the relations between the heat flux and drying time (air flow velocity 0,3 m/s)

t [°C]	The regression equation	R <sup>2</sup>
50	$Q = 10^{-6} \times x^2 - 0,0005 \times x + 1,4185$	0,995
55	$Q = 2 \times 10^{-6} \times x^2 - 0,0009 \times x + 1,646$	0,986
60	$Q = 5 \times 10^{-6} \times x^2 - 0,0014 \times x + 1,8748$	0,989
65	$Q = 8 \times 10^{-6} \times x^2 - 0,0021 \times x + 2,1003$	0,993

The highest amount of energy in the unit of time, at about  $2,06 \text{ kJ} \times \text{s}^{-1}$ , can be recovered from the drying air after leaving the convective dryer at the beginning of the process, at the air flow velocity of  $0,5 \text{ m} \times \text{s}^{-1}$ , and at the highest used temperature.

For all the considered independent variables the heat flux possible to recover from the drying air decreased during the drying process

The increase of air flow velocity caused a significant increase of heat flux of moist air. At the temperature of  $65^\circ\text{C}$  and at the beginning of the process, the value of heat flux is higher by about  $0,8 \text{ kJ} \times \text{s}^{-1}$ . For both the air flow velocities, the highest heat flux possible to recover from the drying air is obtained for the highest temperature used, and the lowest for the lowest value of the drying air temperature.

Figure 8 presents the total quantity of heat possible to recover during the drying process (from the air leaving the convective dryer) in relation to temperature and air flow velocity.

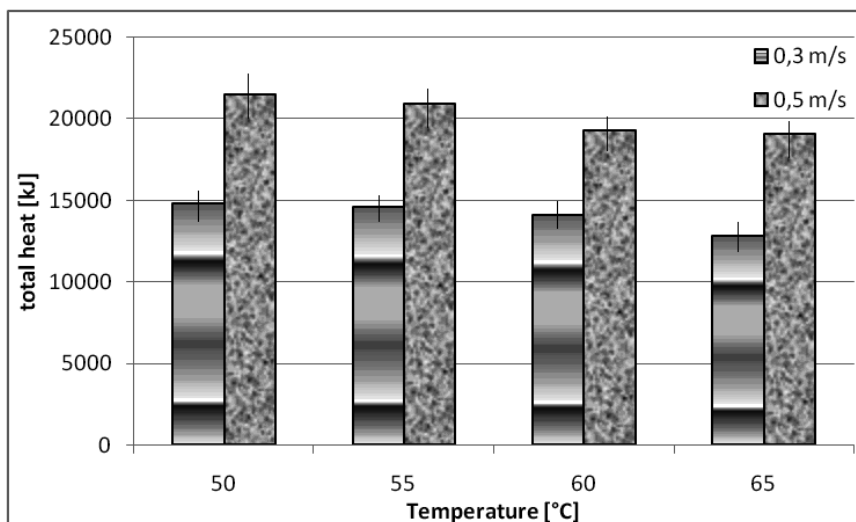


Fig. 8. The total quantity of heat which can be recovered during the convective drying process in relation to temperature and air flow velocity

For each temperature level, the higher amount of total heat can be recovered from the drying air for the higher flow velocity. It is caused by a higher amount of air passing through the dryer in



the unit of time. At the respective air flow velocities, the possible amount of heat recovery decreased with the increase of drying temperature. It was caused by the shortening of the drying time with the increase of drying air temperature. The highest amount of heat can be recovered from the air at the temperature of 50°C and at the air flow velocity of 0.5 m×s<sup>-1</sup>.

## CONCLUSIONS

On the basis of the carried out analysis concerning the possibility of heat recovery during the convective drying process of paprika, the following conclusions can be formulated:

1. For all the considered independent variables, the enthalpy of air leaving the dryer decreased during the drying time. At the respective air flow velocities, the highest enthalpy occurred at the air temperature of 65°C, and the lowest one at the air temperature of 50°C. The increase of air flow velocity caused the increase in enthalpy, especially at the beginning of the process.
2. The heat flux possible to recover from the drying air decreased as the drying time increased. The increase of air flow velocity caused the increase of heat flux in all the measured range. The increase of temperature caused the increase of the amount of heat carried off in the unit of time.
3. The total possible amount of heat energy recovery from the drying air is higher for the higher air flow velocity (at the respective temperature) and decreases with the increase of drying temperature (at the respective air flow velocity).
4. The highest amount of energy, reaching about 2,06 kJ×s<sup>-1</sup>, can be recovered during the drying of paprika at the temperature of 50°C, and at the air flow velocity of 0.5 m×s<sup>-1</sup>.

## REFERENCES

1. Atkins, M., Walmsley, M.R. and Neale, J.R., 2010.: Integration potential of milk powder plants using conventional heat recovery options, *Chem. Eng. Trans.*, 21, s. 997-1002.
2. Benali M., Amazouz M.: "Drying of vegetable starch solutions on inert particles: Quality and energy aspects", *Journal of Food Engineering*, Volume 74, 2006, pp. 484-489.
3. Budin B., Mihelic-Bogdanic A., Filipan V.: Energy conservation using a recuperative drying process. *Energy Convers. Mgmt Vol 37*, No 9, 1996, pp. 1393-1399.
4. Conde M. R.: Energy conservation with tumbler drying in laundries. *Applied Thermal Engineering Vol 17*, No 12, 1997, pp. 1163- 1172.
5. Didukh V., Kirchuk R.: Optimization of immovable material layer at drying. *TEKA Kom. Mot. Energ. Roln. - OL PAN 7 2007*, pp. 81-85.
6. Flink J.: Energy analysis in dehydration processes. *Food Technology*, Volume 31, 1977, pp. 77-84.
7. Ho J.C., Chou S. K., Mujundar A.S., Hawlader M.N.A., Chua K.J.: An optimization framework for drying of heat- sensitive products. *Applied Thermal Engineering Vol 21*, 2001, pp. 1779- 1798.
8. Ivanova, D.; Andonov, K.: "Analytical and experimental study of combined fruit and vegetable dryer". *Energy Conversion and Management*, Volume: 42, Issue: 8, May, 2001, pp. 975-983

9. Jech J., Angelovič M., Poničan J., Židek B., Žitňák M.: Evaluation of drying-plant schief cbs 16-4 power parameters at drying maize. TEKA Kom. Mot. Energ. Roln. - OL PAN 6A 2006, pp. 92–100.
10. Koyuncu, T.; Pinar, Y.; Lule, F.: “Convective drying characteristics of azarole red (*Crataegus monogyna* Jacq.) and yellow (*Crataegus aronia* Bosc.) fruits”, *Journal of Food Engineering*, Volume: 78, Issue: 4, February, 2007, pp. 1471-1475.
11. Koyuncu, T.; Serdar, U.; Tosun, I.: “Drying characteristics and energy requirement for dehydration of chestnuts (*Castanea sativa* Mill.)”, *Journal of Food Engineering*, Volume: 62, Issue: 2, April, 2004, pp. 165-168.
12. Mujumdar, A. S.: “An overview of innovation in industrial drying: current status and R&D needs”, *Transport in Porous Media* Volume, 66, Issue: 1-2, January 2007, pp. 3 – 18.
13. Pabis S.: Theoretical models of vegetable drying by convection, *Transp Porous Med* (2007) 66: s. 77-87.
14. Prvulovic, S., Tolmac, D. and Lambic, M.: Determination of energetic characteristics of convection drying place on pneumatic transportation material, *Journal of Process Technique*, Vol. 1. 70-74, 2001.
15. Ratti C.: “Hot air and freeze-drying of high value foods: a review”, *Journal of Food Engineering*, Volume 49, 2001, pp. 311-319.
16. Rudy S.: Energy consumption in the freeze - and convection-drying of garlic. TEKA Kom. Mot. Energ. Roln. - OL PAN 9 2009, pp. 259–266.
17. Savoie P., Joannis H.: Bidirectional drying of baled hay with air recirculation and cooling. *Canadian Biosystems Engineering* 48 2006: 3.53-3.59.
18. Sokhansanj, S. Wood H.: Simulation of thermal and disinfestation characteristics of a forage dryer. *Drying Technology* 9 1991: 643-656.
19. Soylemez M.S.: Optimum heat pump in drying systems with waste heat recovery. *Journal of Food Engineering* 74 (2006) 292–298.
20. Tippayawong N., Tantakitti C., Thavornun S., Peerawanitkul V.: Energy conservation in drying of peeled longan by forced convection and hot air recirculation. *Biosystems Engineering* 104 (2009), pp. 199-204.

## ANALIZA MOŻLIWOŚCI ODZYSKIWANIA ENERGII W PROCESIE KONWEKCYJNEGO SUSZENIA PAPRYKI

**Streszczenie.** W pracy określono entalpię oraz ilość energii cieplnej możliwej do odzyskania w procesie konwekcyjnego suszenia papryki. Suszenie konwekcyjne zostało przeprowadzone przy dwóch prędkościach przepływu czynnika suszącego oraz na czterech poziomach temperatury. Na podstawie przeprowadzonych badań można stwierdzić, że dla wszystkich zmiennych niezależnych entalpia powietrza opuszczającego suszarkę maleje w czasie trwania suszenia. Przy danej prędkości przepływu największą entalpię posiada powietrze o temperaturze 65°C, natomiast najniższą o temperaturze 50°C. Wzrost prędkości przepływu powietrza powoduje wzrost jego entalpii, zwłaszcza na początku trwania procesu. Największą ilość ciepła, wynoszącą około 21,5 MJ, można odzyskać prowadząc proces suszenia w temperaturze 50°C przy prędkości przepływu 0,5 m×s-1.

**Słowa kluczowe:** Suszenie konwekcyjne, strumień ciepła, entalpia, papryka.

## EFFECT OF DIFFERENT VARIANTS OF PRETREATMENT OF WHEAT GRAIN ON THE PARTICLE SIZE DISTRIBUTION OF FLOUR AND BRAN

Leszek Rydzak, Dariusz Andrejko

University of Life Sciences in Lublin, Poland

**Summary.** The paper presents the results of a study on the particle size distribution of flour and bran obtained as a result of milling of wheat grain with the application of vacuum impregnation and IR heating as the preliminary treatments. The grain was prepared for the milling through the combined application of vacuum impregnation at 5 and 100 kPa and of IR treatment at temperatures of 150 and 180°C during 90 and 150 s in different variants. It was found that the manner of grain preparation for milling had an effect on the particle size distribution of the products of the milling process. The consecutive application of the processes of vacuum impregnation and IR heating caused a significant increase in the level of bran fraction with larger particle sizes, which may indicate effectiveness of the proposed preliminary treatment of wheat grain prior to milling.

**Key words:** vacuum impregnation, infrared radiation treatment, milling, wheat, particle size distribution.

### INTRODUCTION

In cereal processing grain moisture is one of the fundamental criteria of estimation of its status and technological value. That parameter is of particular importance in the production of flour. Hence the production processes of various products of that industry frequently involve moistening operations. The moistening is conducted at various stages of the technological sequence: immediately after the cleaning of granular materials (prior to milling), or after milling and before various processes, mainly thermal [Jankowski 1988].

The moistening of grain causes a number of various changes. The inner structure of kernels changes. The forces binding proteins and starch are reduced, and the kernel structure gets damaged through the appearance of strains caused by the various levels of swelling of the particular components [Obuchowski et al. 1981, Skonecki i et al. 2010].

Grain moistening is one of the most important pretreatments before the proper technological processes. Contact with water is the starting point for a number of physical and chemical transformations [Maskan 2001].

Among other things, grain moistening is conducted prior to the milling of wheat and rye in order to plasticise the seed coat and to separate it from the parenchyma. Well moistened kernels are such whose whole external surface (seed coat) is uniformly moistened, irrespective of the amount

by which the grain moisture has been increased [Kowalewski 1992, Dziki et al. 2004, Opielak et al. 2004, Dziki et al. 2005, Grochowicz et al. 2006].

Jurga [1997] reports that grain to be subjected to milling or husking should be characterised by moisture difference between the parenchyma and the seed coat. That difference should about 2%. Too great a difference in moisture between the seed coat and the parenchyma has an unfavourable effect on the milling properties of grain, as it causes an increase in grain elasticity and plasticity, which leads to an increase in the unit energy requirements in the course of milling.

Within the scope of this study, the grain material was moistened with the technique of vacuum impregnation which permits notable intensification of the process of mass exchange in the solid-liquid system, the consequence of which is uniform moistening of the grain in the external layers of the kernels, without wetting the parenchyma [del Valle et al. 1998, Betoret et al. 2003, Chiralt et al. 2001, Guamis et al. 1997, Gonzalez et al. 1999, Chafer et al. 2003, Fito et al. 1996, Fito et al. 2001]. However, grain subjected to vacuum impregnation is characterised by too high moisture levels, in some cases even exceeding 20%, to be directly subjected to milling. Hence the proposal to apply the technique of infrared radiation treatment (micronisation) that guarantees the possibility of obtainment of virtually any desired grain moisture level prior to the milling and ensures favourable changes in the structure of the kernels. Another advantage of the process is the fact that the times of grain exposure to infrared radiation are very short (up to 3 min), which minimises the energy consumption.

The objective of the study was to determine the effect of vacuum impregnation and IR radiation treatment on the particle size distribution of flour and bran which is one of the fundamental criteria in the evaluation of the process of milling.

## PURPOSE AND METHODS

The experimental material was wheat grain cv. Koksa and Torca. The grain was moistened to several levels of initial moisture content. The milling of the grain was performed on a laboratory mill Quadrumat Junior. It is a four-roller laboratory mill with an aspiration system and a drum sifter. The milling of a grain sample using this mill corresponds to the milling parameters obtained in industrial mills. Determinations of grain material moisture prior to and after the moistening, and of the flour and bran obtained as a result of the milling, were made with the over-dry method in accordance with the standard PN-86/A-74011. Grain moistening was conducted in sealed containers. A laboratory balance with an accuracy of  $10^{-2}$ g was used to weigh portions of 500 g of each kind of grain, the portions were placed in the containers, and then water was added in such amounts as to obtain the required levels of grain moisture. Then the containers with the grain material were sealed, shaken and placed in a refrigerator for a period of 72 hours.

### **Impregnation of wheat grain**

The process of grain impregnation was conducted in a chamber with a volume of ca.  $2 \text{ dm}^3$ , coupled to a vacuum pump permitting the regulation of pressure within the chamber within the range of 5-100 kPa. The chamber was immersed in the water bath of an ultra-thermostat which permitted the process to be conducted under various temperature conditions. To ensure complete immersion of all kernels, they were placed in a container made of wire mesh. The level of pressure in the chamber was recorded by means of a vacuum gauge. The cover of the chamber was additionally equipped with a system of valves connecting the chamber with the vacuum pump and a water reservoir. The tight sealing at the interface between the chamber and the cover was achieved by means of a gasket greased with vaseline.

After placing the vacuum chamber in the ultra-thermostat, the temperature of the process of grain moistening was set. The temperature of 15°C was applied. The water wetting the grain was at a temperature similar to that of the temperature in the chamber. The differences between those temperatures were within  $\pm 2^\circ\text{C}$ . After the temperature in the chamber stabilised, a container with a weighed portion of grain material, with a weight of ca. 40 grams, was placed in it.

Next, when the hydraulic hoses were filled with water, the chamber was closed and, after opening the valve connecting with the vacuum pump, the pressure in the chamber was set. The pressure levels applied in the study were 5 kPa and 100 kPa – atmospheric pressure (control treatment). When the pressure stabilised, the valve connecting with the water reservoir was closed. Each time the grain sample was flooded with a portion of water with volume of ca. 0.2 dm<sup>3</sup>. In the course of flooding the grain sample with water, a slight increase of the pressure in the chamber was observed as the chamber filled with the water. The control sample was moistened following a similar procedure, but under the conditions of atmospheric pressure.

When the grain sample was fully flooded, the pressure was rapidly brought up to the atmospheric pressure. Grain samples were taken immediately after the impregnation (after about 30 seconds of contact with water).

The measurement system is presented in Fig. 1.

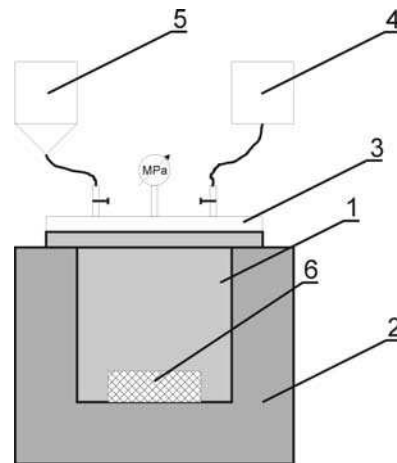


Fig. 1. Schematic of the measurement system for the study of the process of vacuum impregnation of grain: 1 – vacuum chamber, 2 – ultra-thermostat, 3 – cover, 4 – vacuum pump, 5 – water reservoir, 6 – container with grain material

### Grain heating with IR radiation

The process of grain heating with IR radiation was conducted with the help of a device designed and constructed by Andrejko [2004]. The main elements of the system (Fig. 2) are frame 1, belt conveyor and a heating system with stepless temperature adjustment. The grain material is pursued into chute 3, equipped with a shutter, and then it is fed onto the belt of the conveyor (single layer). The material on the conveyor belt is moved to the heating zone 8, where it is subjected to treatment with infrared radiation. The conveyor is powered by a DC electric motor with a voltage regulator permitting smooth adjustment of the belt speed within the range from  $5 \times 10^{-3} \text{ m} \times \text{s}^{-1}$  to

$7 \times 10^{-2} \text{ m} \times \text{s}^{-1}$  (the material remains in the heating zone for 15 to 200 s, respectively). The conveyor belt material is characterised by considerable resistance to high temperatures (up to  $250^\circ\text{C}$ ) and low IR transmittance (ca. 10%). The device is equipped with two heating heads 2 (each with 4 IR radiators); the upper head, positioned above the belt, and the lower head, located beneath the belt.

For heat treatment of small grains it is sufficient to use only the upper head. When heating large seeds, e.g. those of white lupine, it is recommended that the lower head is also switched on. In such a case the belt of the conveyor should be replaced with a belt of  $\phi = 0.1 \text{ mm}$  copper wire, with square mesh of 1 mm side. Such a wire mesh has IR transmittance of over 90%.

IR radiation is emitted by 8 individually supplied radiators (4 in each section). Those are temperature radiators, built of ceramic material, supplied with mains power (230V), and their power rating is 400W. In their spectrum the share of visible radiation is at a level of a fraction of one percent (dark emitters). Due to their design (flat panel emitters) they provide uniform heating at all points of the surface of the conveyor belt within the heating zone. Mean temperature of the emitter surface is ca.  $500^\circ\text{C}$ , and the emitted wavelength is  $\lambda = 2.5\text{-}3.0 \text{ }\mu\text{m}$ .

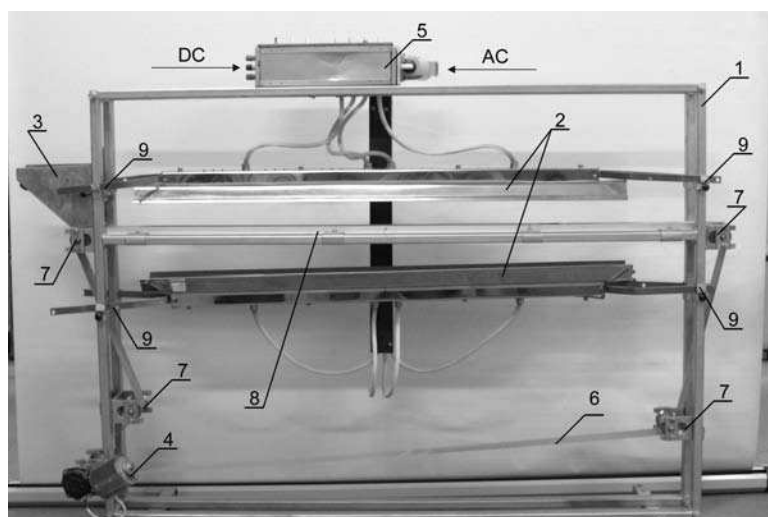


Fig. 2 Laboratory device for IR treatment of granular plant materials; 1 – frame, 2 – heating head with 4 IR radiators with individual power supply, 3 – filling chute, 4 – DC motor, 5 – control module, 6 – conveyor belt, 7 – rollers, 8 – heating zone, 9 – adjustment of heating head position

### Particle size distribution determination

Flour and bran screening was performed using the Retsch vibratory sieve shaker AS 200. It is equipped with an electromagnetic drive system producing 3D throwing motions, which causes uniform distribution of the material screened over the whole sieve area. Very simple operation and short screening times with very high separation efficiency are the advantages of the sieve shaker.

The screening was conducted at vibration amplitude of 2.20 mm and measurement time of 2 minutes. The adopted parameters of sifting result from earlier studies on the effect of the parameters of the sieve shaker operation on the separation efficiency of granular mixtures. The sieves applied were Vogel sieves with elongated apertures with dimensions of 1.60x25, 1.70x25, 2.20x25, 2.50x25

and 2.80x25 mm. The weight of a screened sample was 300 g. The measurements were performed in five replications.

Moreover, sieve analysis was performed for flour and bran acquired through milling. The sifting was made using sieves with square mesh, suitable for flour and bran.

## RESULTS AND DISCUSSION

The results of the analyses performed within the scope of the study are presented graphically in Figures 3-4.

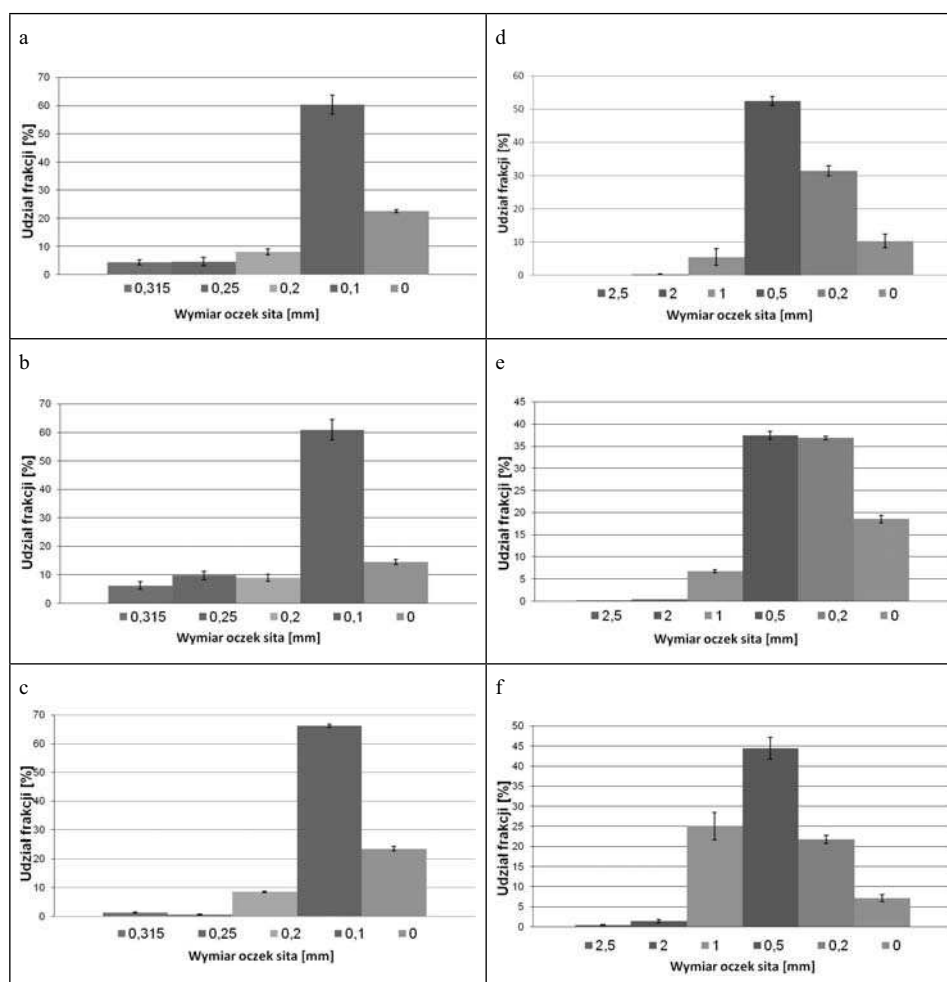


Fig. 3. Results of sieve analysis of flour and bran obtained through milling of wheat grain cv.

Torka, a, b, c – flour, d, e, f – bran,

a, d – flour and bran from zero sample (control) b, e – flour and bran from grain after micronisation at 150 °C for 90 s. c, f – flour and bran from grain after impregnation at 5 kPa and micronisation at 150 °C for 150 s

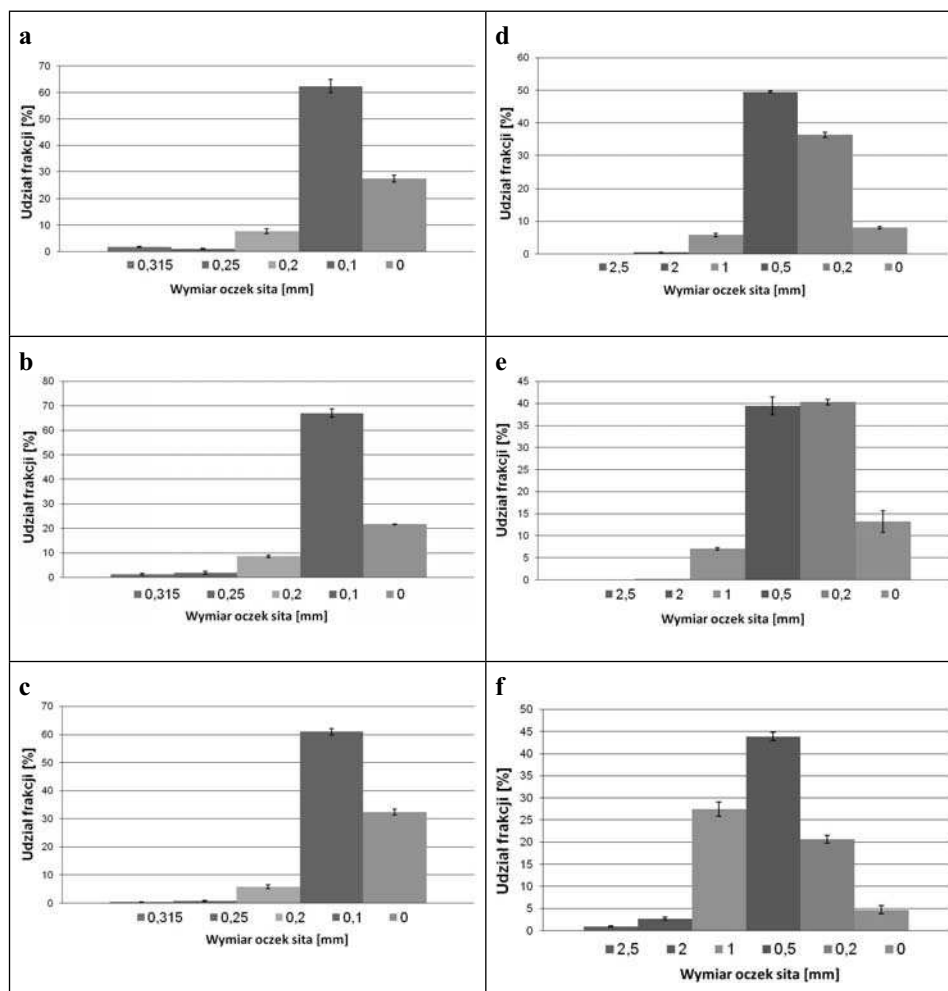


Fig. 4. Results of sieve analysis of flour and bran obtained through milling of wheat grain cv. Koksa, a, b, c – flour, d, e, f – bran, a, d – flour and bran from zero sample (control) b, e – flour and bran from grain after micronisation at 150 °C for 90 s, c, f – flour and bran from grain after impregnation at 5 kPa and micronisation at 150 °C for 150 s

After analysing the results obtained one can note that in all cases studied the size of the bran particles produced was affected by the process of impregnation preceding the milling, causing an increase in their size. The fraction obtained on the sieve with mesh size of 1 mm was several times greater after grain impregnation at 5 kPa than in the other cases. Analysis of the particle size distribution of flour revealed that, irrespective of the preliminary treatments applied, its changes were not as pronounced as was the case with bran.



## CONCLUSIONS

The study and the analysis of the results permitted the formulation of the following conclusions:

- Preliminary treatment of wheat grain consisting in the application of micronisation or impregnation and micronisation affects the particle size distribution of both the flour and the bran.
- Greater changes were observed in the case of bran. The moistening of grain, followed by short-time drying (micronisation) causes the seed cover to become elastic and not to crumble. Hence, after the application of both pretreatment processes, the mean size of bran particles increases significantly.

## REFERENCES

1. Andrejko D. 2004.: Zmiany właściwości fizycznych nasion soi pod wpływem promienionowania podczerwonego. Rozprawy Naukowe. AR w Lublinie. Zeszyt 288.
2. Betoret N., Puente L., Diaz M.J., Pagan M.J., Garcia M.J., Gras M.L., Martinez-Monzo J., Fito P. 2003.: Development of probiotic-enriched dried fruits by vacuum impregnation. *Journal of Food Engineering*. 56. s. 273-277.
3. Chafer M., Gonzales-Martinez C., Ortola M.D., Chiralt A., Fito P. 2001.: Orange peel products obtained by osmotic dehydration. *Osmotic dehydration and Vacuum Impregnation. Application in Food Industries*. Lancaster Technomic Publishing Co. s. 93-106.
4. Chiralt A., Fito P., Barat J.M., Andres A., Gonzalez-Martinez C., Esriche I., Camacho M.M. 2001.: Use of vacuum impregnation in food salting process. *Journal of Food Engineering*. 49. s. 141-151.
5. Dziki D., Laskowski J. 2004.: The energy-consuming indexes of wheat kernel grinding process. *TEKA Komisji Motoryzacji I Energetyki Rolnictwa*. IV.
6. Dziki D., Laskowski J. 2005.: Influence of selected factors on wheat grinding energy requirements. *TEKA Komisji Motoryzacji I Energetyki Rolnictwa*. V.
7. Fito P., Andres A., Chiralt A., Pardo O. 1996.: Coupling of hydrodynamic mechanism and deformation relaxation phenomena during vacuum treatments in solid porous-liquid systems. *Journal of Food Engineering*. 27. s. 229-240.
8. Fito P., Chiralt A., Barat J.M., Andres A., Martinez-Monzo J., Martinez-Navarrete. 2001.: Vacuum impregnation for development of new dehydrated products. *Journal of Food Engineering*. 49. s. 297-302.
9. Gonzales Ch., Martinez-Navarrete N. Chiralt A., Fito P. 1999.: Drying behaviour of Manchego type cheese throughout ripening. *Drying '98*. s. 1251-1258.
10. Grochowicz J., Andrejko D. 2006.: Effect of the moisture content on energy consumption at grinding of lupine seeds. *TEKA Komisji Motoryzacji I Energetyki Rolnictwa*. VI.
11. Guamis B., Trujillo A.J., Ferragut V., Chiralt A., Andres A., Fito P. 1997.: Ripening Control of Marchengo Type Cheese Salted by Brine Vacuum Impregnation. *Int. Dairy Journ.* 7:185-192.
12. Jankowski S., Surowce mączne i kaszowe, Wydawnictwo Naukowo-Techniczne, Warszawa, 1988.
13. Jurga R. 1997.: *Przetwórstwo zbóż cz.I*. WSiP. Warszawa.
14. Kowalewski W. 1992.: Przydatność krajowych nawilżaczy intensywnych. Ocena na podstawie badań CLTPIPZ. *Przegl Zboż. Młyn.* 7:2-3.

15. Maskan M. 2001.: Effect of maturation and processing on water uptake characteristics of wheat. *Journ. of Food Eng.* 47:51-57.
16. Obuchowski W., Gąsiorowski H., Kołodziejczyk P. 1981.: Twardość ziarna pszenicy jako kryterium jego jakości. *Post. Nauk Roln.* 5:97-108.
17. Opielak M., Andrejko D., Komsta H. 2004.: The influence of thermal processing with infrared rays on the elementary energy consumption in grinding wheat grains. *TEKA Komisji Motoryzacji I Energetyki Rolnictwa*. IV.
18. Skonecki S., Laskowski J. 2010.: Effect of particle size fragmented wheat on energy requirements in the process of extrusion. *TEKA Komisji Motoryzacji I Energetyki Rolnictwa* X.
19. Valle del J.M., Aranguiz V., Diaz L. 1998.: Volumetric Procedure to Assess Infiltration Kinetics and Porosity of Fruits by Applying a Vacuum Pulse. *Journ. of Food Eng.* 38:207-221.

#### WPLYW RÓŻNYCH WARIANTÓW PRZYGOTOWANIA ZIARNA PSZENICY NA SKŁAD GRANULOMETRYCZNY MĄKI I OTRĄB

**Streszczenie.** W pracy zaprezentowano wyniki badań składu granulometrycznego mąki i otrąb otrzymanych w wyniku przemiału ziarna pszenicy z zastosowaniem impregnacji próżniowej i ogrzewania promieniowaniem podczerwonym jako obróbki wstępnej. Ziarno przygotowano do przemiału przez zastosowanie połączonych zabiegów impregnacji próżniowej w ciśnieniu 5 i 100 kPa oraz obróbki promieniowaniem podczerwonym w temperaturze 150 i 180 °C i czasie 90 i 150 s w różnych wariantach. Stwierdzono, że sposób przygotowania ziarna do przemiału ma wpływ na skład granulometryczny produktów przemiału. Zastosowanie kolejno po sobie następujących procesów impregnacji i ogrzewania promieniowaniem podczerwonym powodowało znaczny wzrost ilości frakcji otrąb o większych wymiarach cząstek, co może świadczyć o skuteczności proponowanej obróbki ziarna przed przemiałem.

**Słowa kluczowe:** impregnacja próżniowa, obróbka promieniowaniem podczerwonym, przemiał, pszenica, skład granulometryczny.

## EFFECT OF VACUUM IMPREGNATION AND INFRARED RADIATION TREATMENT ON ENERGY REQUIREMENTS IN WHEAT GRAIN MILLING

Leszek Rydzak, Dariusz Andrejko

University of Life Sciences in Lublin, Poland

**Summary.** The paper presents the results of a study on the energy requirements of the process of wheat grain milling. The grain was prepared for the milling through the application of combined treatments of vacuum impregnation at pressures of 5 and 100 kPa and IR treatment at temperatures of 150 and 180°C during 90 and 150 s in various variants. It was found that the method of grain preparation for milling affected the energy consumption. The consecutive application of the processes of impregnation and micronisation caused an increase in the energy requirements of the grain milling process. That energy requirement was higher in the case of grain impregnation at 5 kPa.

**Key words:** energy consumption, vacuum impregnation, infrared radiation treatment, milling, wheat.

### INTRODUCTION

In cereal processing grain is frequently subjected to various processes related with a change in its moisture content. Grain moistening causes a number of various changes. The inner structure of kernels changes. The forces binding proteins and starch are reduced, and the kernel structure gets damaged through the appearance of strains caused by the various levels of swelling of the particular components [Obuchowski et al. 1981].

Increase in the moisture of maize grains by as little as 1.5% already causes the appearance of internal damage. The extent of the damage increases with increasing moisture and attains its maximum after 8 hours of grain contact with water [Wu et al. 1988]. The cause of the damage to grain structure is excessively fast imbibition of water due to the low initial moisture level [Sivritepe et al. 1995].

In the course of soaking of wheat grain there takes place intensive lateral cracking of the parenchyma. The appearance of such cracks leads, in consequence, to a reduction in the kernel hardness index [Grundas et al. 1998]. Among other strength properties of grain that are affected by the process of moistening we should also mention the decrease, by half, of the value of the modulus of elasticity [Singh et al. 2001].

Moistening reduces the mechanical strength of cereal grain. That decrease is observed at moisture levels above 11% [Obuchowski et al. 1985]. Whereas, there takes place an increase in the energy requirements for grain fragmentation. In the case of wheat kernels, that parameter doubles in value within the moisture range of 10 – 18% for soft wheat cultivars, and for durum wheat cultivars – increases 1.5-fold [Jurga 1997, Dziki et al. 2004, Opielak et al. 2004, Dziki et al. 2005, Grochowicz et al. 2006].

In the cereal industry a variety of equipment is used for the realisation of the process of grain moistening. Their operation consists in sprinkling a grain deposit with a specific amount of water which is then distributed on the surface of the kernels by means of various methods (e.g. the Bühler or the Vibronet systems). In such an approach to the process the uniformity of grain moistening is far from perfect. However, the approach is highly convenient from the technological point of view, as it permits relatively easy determination of the final moisture level at the end of the process. It does, however, present a number of difficulties, which is evident in the fact that at large processing plants the technological process provides even for triple moistening of the same grain material prior to the milling. Such a philosophy of realisation of the process of grain moistening enforces, moreover, long periods of grain tempering. In the case of durum wheat the duration of grain tempering may be even 36 hours.

In the study presented here the grain material was moistened using the vacuum impregnation technique, one of the new techniques in food processing, permitting notable intensification of the process of mass exchange in the solid-liquid system, which causes uniform moistening of kernels in their outer layers, without wetting the parenchyma [del Valle et al. 1998, Betoret et al. 2003, Chiralt et al. 2001, Guamis et al. 1997, Gonzalez et al. 1999, Chafer et al. 2003, Fito et al. 1996, Fito et al. 2001]. However, grain subjected to vacuum impregnation is characterised by too high moisture levels, in some cases even exceeding 20%, to be directly subjected to milling. Hence the proposal to apply the technique of infrared radiation treatment (micronisation) that guarantees the possibility of obtaining of virtually any desired grain moisture level prior to the milling and ensures favourable changes in the structure of the kernels. Another advantage of the process is the fact that the times of grain exposure to infrared radiation are very short (up to 3 min), which minimises the energy consumption.

The objective of the study was to determine the effect of vacuum impregnation and IR radiation treatment on the energy consumption in the process of milling.

## PURPOSE AND METHODS

The experimental material was wheat grain cv. Koksa and Sukces. The grain was moistened to several levels of initial moisture content. The milling of the grain was performed on a laboratory mill Quadrumat Junior presented in Fig. 1.



Fig. 1. Laboratory mill Quadrumat Junior

It is a four-roller laboratory mill with an aspiration system and a drum sifter. The milling of a grain sample using this mill corresponds to the milling parameters obtained in industrial mills. Determinations of grain material moisture prior to and after the moistening, and of the flour and bran obtained as a result of the milling, were made with the over-dry method in accordance with the standard PN-86/A-74011. Grain moistening was conducted in sealed containers. A laboratory balance with an accuracy of  $10^{-2}$ g was used to weigh portions of 500 g of each kind of grain, the portions were placed in the containers, and then water was added in such amounts as to obtain the required levels of grain moisture. Then the containers with the grain material were sealed, shaken and placed in a refrigerator for a period of 72 hours.

During the milling, the energy consumption of the process of fragmentation of wheat grain in the laboratory mill Quadrumat Junior was measured with the help of a Lumel PP83 transducer.

### Impregnation of wheat grain

The process of grain impregnation was conducted in a chamber with a volume of ca.  $2 \text{ dm}^3$ , coupled to a vacuum pump permitting the regulation of pressure in the chamber within the range of 5-100 kPa. The chamber was immersed in the water bath of an ultra-thermostat which permitted the process to be conducted under various temperature conditions. To ensure complete immersion of all kernels, they were placed in a container made of wire mesh. The level of pressure in the chamber was recorded by means of a vacuum gauge. The cover of the chamber was additionally equipped with a system of valves connecting the chamber with the vacuum pump and a water reservoir. The tight sealing at the interface between the chamber and the cover was achieved by means of a gasket greased with vaseline.

After placing the vacuum chamber in the ultra-thermostat, the temperature of the process of grain moistening was set. The temperature of  $15^\circ\text{C}$  was applied. The water wetting the grain was at a temperature similar to that of the temperature in the chamber. The differences between those temperatures were within  $\pm 2^\circ\text{C}$ . After the temperature in the chamber stabilised, a container with a weighed portion of grain material, with a weight of ca. 40 grams, was placed in it.

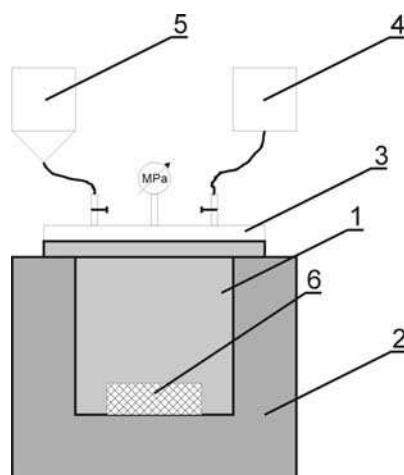


Fig. 2. Schematic of the measurement system for the study of the process of vacuum impregnation of grain: 1 – vacuum chamber, 2 – ultra-thermostat, 3 – cover, 4 – vacuum pump, 5 – water reservoir, 6 – container with grain material

Next, when the hydraulic hoses were filled with water, the chamber was closed and, after opening the valve connecting with the vacuum pump, the pressure in the chamber was set. The pressure levels applied in the study were 5 kPa and 100 kPa – atmospheric pressure (control treatment). When the pressure stabilised, the valve connecting with the water reservoir was closed. Each time the grain sample was flooded with a portion of water with volume of ca. 0.2 dm<sup>3</sup>. In the course of flooding the grain sample with water, a slight increase of the pressure in the chamber was observed as the chamber filled with the water. The control sample was moistened following a similar procedure, but under the conditions of atmospheric pressure.

When the grain sample was fully flooded, the pressure was rapidly brought up to the atmospheric pressure. Grain samples were taken immediately after the impregnation (after about 30 seconds of contact with water).

The measurement system is presented in Fig. 2.

### Grain heating with IR radiation

The process of grain heating with IR radiation was conducted with the help of a device designed and constructed by Andrejko [2004]. The main elements of the system (Fig. 3) are frame 1, belt conveyor and a heating system with stepless temperature adjustment. The grain material is pursued into chute 3, equipped with a shutter, and then it is fed onto the belt of the conveyor (single layer). The material on the conveyor belt is moved to the heating zone 8, where it is subjected to treatment with infrared radiation. The conveyor is powered by a DC electric motor with a voltage regulator permitting smooth adjustment of the belt speed within the range from  $5 \times 10^{-3} \text{ m} \times \text{s}^{-1}$  to  $7 \times 10^{-2} \text{ m} \times \text{s}^{-1}$  (the material remains in the heating zone for 15 to 200 s, respectively). The conveyor belt material is characterised by considerable resistance to high temperatures (up to 250°C) and low IR transmittance (ca. 10%). The device is equipped with two heating heads 2 (each with 4 IR radiators); the upper head, positioned above the belt, and the lower head, located beneath the belt.

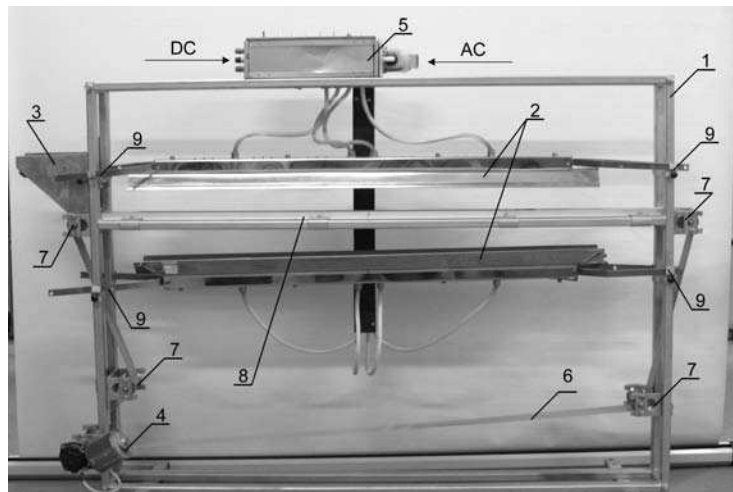
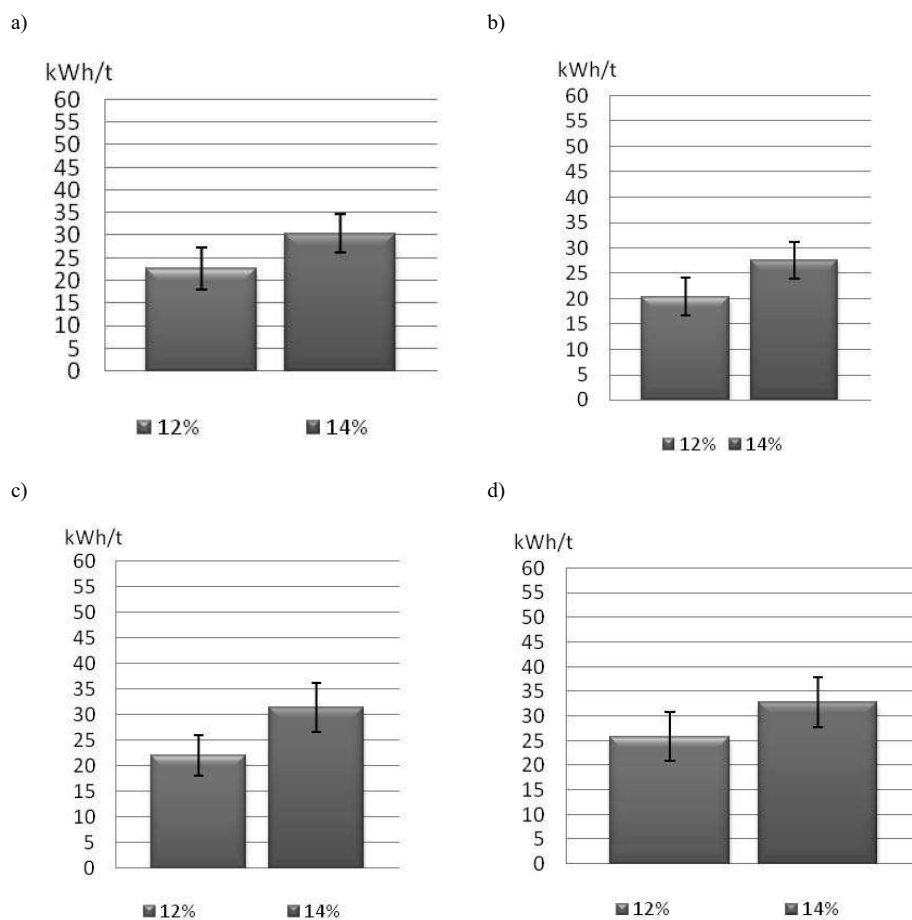


Fig. 3. Laboratory device for IR treatment of granular plant materials; 1 – frame, 2 – heating head with 4 IR radiators with individual power supply, 3 – filling chute, 4 – DC motor, 5 – control module, 6 – conveyor belt, 7 – rollers, 8 – heating zone, 9 – adjustment of heating head position

For heat treatment of small grains it is sufficient to use only the upper head. When heating large seeds, e.g. those of white lupine, it is recommended that the lower head is also switched on. In such a case the belt of the conveyor should be replaced with a belt of  $\varphi = 0.1$  mm copper wire, with square mesh of 1 mm side. Such a wire mesh has IR transmittance of over 90%.

IR radiation is emitted by 8 individually supplied radiators (4 in each section). Those are temperature radiators, built of ceramic material, supplied with mains power (230V), and their power rating is 400W. In their spectrum the share of visible radiation is at a level of a fraction of one percent (dark emitters). Due to their design (flat panel emitters) they provide uniform heating at all points of the surface of the conveyor belt within the heating zone. Mean temperature of the emitter surface is ca. 500°C, and the emitted wavelength is  $\lambda = 2.5\text{-}3.0$   $\mu\text{m}$ .

## RESULTS AND DISCUSSION



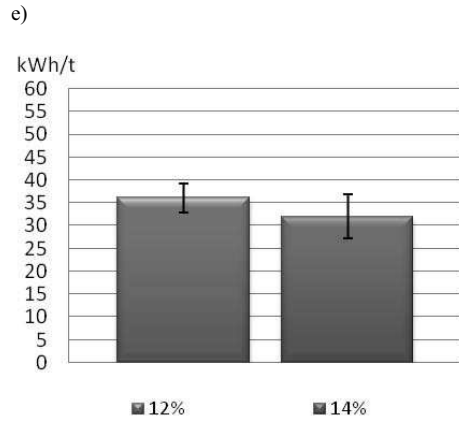
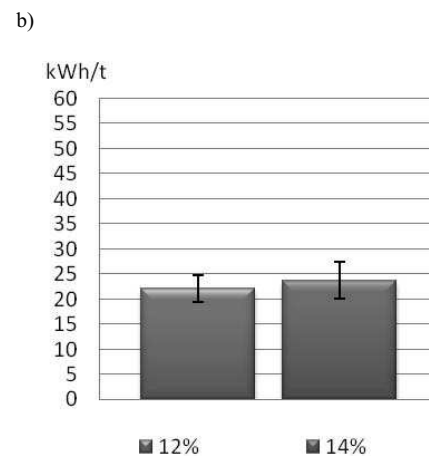
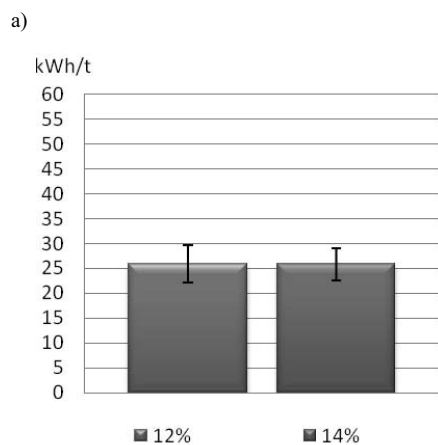


Fig. 4. Effect of consecutive processes of impregnation and micronisation on energy requirements of the process of milling of wheat grain cv. Kokska. Initial moisture of the grain samples - 12%,14%:

- Zero sample, grain not subjected to any treatment,
- Impregnation of grain at atmospheric pressure, micronisation for 90 s,
- Impregnation of grain at atmospheric pressure, micronisation for 150 s,
- Vacuum impregnation of grain at 5 kPa, micronisation for 90 s,
- Vacuum impregnation of grain at 5 kPa, micronisation for 150 s.

Figure 4 presents the effect of the consecutive processes of impregnation and micronisation on the energy requirements for the milling of wheat grain cv. Kokska, with initial moisture content of 12% and 14%. Grain subjected to impregnation and micronisation showed a slight increase in energy requirements, only the sample with initial moisture of 12%, subjected to impregnation at 5 kPa and micronised for 150 seconds displayed a significant increase in milling energy requirements. Measurement for grain with initial moisture of 16% was impossible due to the high plasticity of the material, which precluded the operation of the laboratory mill.





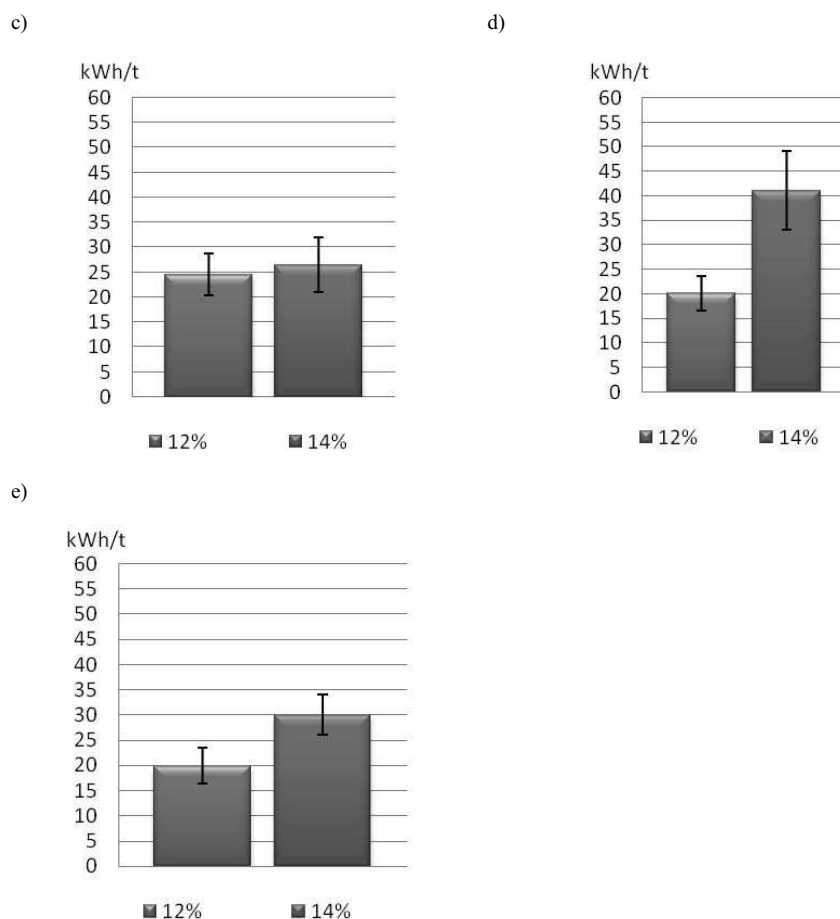


Fig. 5. Effect of the process of micronisation and of the consecutive processes of impregnation and micronisation on energy requirements of the process of milling of wheat grain cv. Sukces. Initial moisture of the grain samples - 12%,14%:

- Zero sample, grain not subjected to any treatment,
- Impregnation of grain at atmospheric pressure, micronisation for 90 s,
- Impregnation of grain at atmospheric pressure, micronisation for 150 s,
- Vacuum impregnation of grain at 5 kPa, micronisation for 90 s,
- Vacuum impregnation of grain at 5 kPa, micronisation for 150 s.

Figure 5 presents the results of measurements of energy requirements of the process of milling of samples of wheat grain cv. Sukces. Grain samples with initial moisture content of 12% and 14% could be tested, while the experiment with grain sample with initial moisture of 16% was impossible due to the high plasticity of the material, which caused the laboratory mill to block. In all the cases an increase was observed in the energy requirements for the milling process, the highest after the application of vacuum impregnation at 5 kPa.

## CONCLUSIONS

The results obtained permitted the formulation of the following conclusions:

1. Preliminary treatment of wheat and rye grain consisting in micronisation at 150°C for 90 and 150 s caused a slight increase in the amount of energy required for the milling of 1 ton of the material.
2. Consecutive application of the processes of impregnation and micronisation caused an increase in the energy requirements for the process of milling. That requirement was greater in the case of the application of vacuum impregnation.
3. Impregnation of grain with initial moisture content of 16% resulted in an excessive level of moisture of the material, with resultant increase in its plasticity, which made it impossible to conduct the milling of the grain.

## REFERENCES

1. Andrejko D. 2004.: Zmiany właściwości fizycznych nasion soi pod wpływem promienionowania podczerwonego. *Rozprawy Naukowe. AR w Lublinie. Zeszyt 288.*
2. Betoret N., Puente L., Diaz M.J., Pagan M.J., Garcia M.J., Gras M.L., Martinez-Monzo J., Fito P. 2003.: Development of probiotic-enriched dried fruits by vacuum impregnation. *Journal of Food Engineering.* 56. s. 273-277.
3. Chafer M., Gonzales-Martinez C., Ortolá M.D., Chiralt A., Fito P. 2001.: Orange peel products obtained by osmotic dehydration. *Osmotic dehydration and Vacuum Impregnation. Application in Food Industries.* Lancaster Technomic Publishing Co. s. 93-106.
4. Chiralt A., Fito P., Barat J.M., Andres A., Gonzalez-Martinez C., Esriche I., Camacho M.M. 2001.: Use of vacuum impregnation in food salting process. *Journal of Food Engineering.* 49. s. 141-151.
5. Dżiki D., Laskowski J. 2004.: The energy-consuming indexes of wheat kernel grinding process. *TEKA Komisji Motoryzacji i Energetyki Rolnictwa.* IV.
6. Dżiki D., Laskowski J. 2005.: Influence of selected factors on wheat grinding energy requirements. *TEKA Komisji Motoryzacji i Energetyki Rolnictwa.* V.
7. Fito P., Andres A., Chiralt A., Pardo O. 1996.: Coupling of hydrodynamic mechanism and deformation relaxation phenomena during vacuum treatments in solid porous-liquid systems. *Journal of Food Engineering.* 27. s. 229-240.
8. Fito P., Chiralt A., Barat J.M., Andres A., Martinez-Monzo J., Martinez-Navarrete. 2001.: Vacuum impregnation for development of new dehydrated products. *Journal of Food Engineering.* 49. s. 297-302.
9. Gonzales Ch., Martinez-Navarrete N. Chiralt A., Fito P. 1999.: Drying behaviour of Manchego type cheese throughout ripening. *Drying '98.* s. 1251-1258.
10. Grochowicz J., Andrejko D. 2006.: Effect of the moisture content on energy consumption at grinding of lupine seeds. *TEKA Komisji Motoryzacji i Energetyki Rolnictwa.* VI.
11. Grundas S., Godecki M., Miś A., Borkowska H., Styk B. 1998.: Charakterystyka cech technologicznych ziarna uszkodzonego mechanicznie w wyniku nawilżania. *Biul. Inst. Agrofiz. PAN.* 1:23-26.
12. Guamis B., Trujillo A.J., Ferragut V., Chiralt A., Andres A., Fito P. 1997.: Ripening Control of Marchengo Type Cheese Salted by Brine Vacuum Impregnation. *Int. Dairy Journ.* 7:185-192.
13. Jurga R. 1997.: *Przetwórstwo zbóż cz.I. WSiP. Warszawa.*

14. Obuchowski W., Gąsiorowski H., Kołodziejczyk P. 1981.: Twardość ziarna pszenicy jako kryterium jego jakości. *Post. Nauk Roln.* 5:97-108.
15. Obuchowski W. 1985.: Twardość ziarna pszenicy: znaczenie technologiczne i czynniki oddziaływujące na tę właściwość. *Rocz. AR Poznań.* 152:9-53.
16. Opielak M., Andrejko D., Komsta H. 2004.: The influence of thermal processing with infrared rays on the elementary energy consumption in grinding wheat grains. *TEKA Komisji Motoryzacji I Energetyki Rolnictwa.* IV.
17. Singh H., Singh N., Kaur L., Saxena S.K. 2001.: Effect of sprouting conditions on functional and dynamic rheological properties of wheat. *Journ. of Food Eng.* 47:23-29.
18. Sivritepe H.O., Dourado A.M. 1995.: The effect of seed moisture content and variability on the susceptibility of pea seeds to soaking injury. *Sci. Hort.* 61:185-191.
19. Valle del J.M., Aranguiz V., Diaz L. 1998.: Volumetric Procedure to Assess Infiltration Kinetics and Porosity of Fruits by Applying a Vacuum Pulse. *Journ. of Food Eng.* 38:207-221.
20. Wu P.C., Eckhoff S.R., Chung D.S., Converse H.H. 1988.: Breakage Susceptibility of Rewetted and Blended Corn Samples. *Trans of the ASAE.* 31(5):1581-1584.

#### WPLYW IMPREGNACJI PRÓŻNIOWEJ I OBRÓBKII PROMIENIOWANIEM PODCZERWONYM NA ENERGOCHŁONNOŚĆ PRZEMIAŁU ZIARNA PSZENICY

**Streszczenie.** W pracy zaprezentowano wyniki badań energochłonności procesu przemiału ziarna pszenicy. Ziaro przygotowano do przemiału przez zastosowanie połączonych zabiegów impregnacji próżniowej w ciśnieniu 5 i 100 kPa oraz obróbki promieniowaniem podczerwonym w temperaturze 150 i 180 °C i czasie 90 i 150 s w różnych wariantach. Stwierdzono, że sposób przygotowania ziarna do przemiału ma wpływ na energochłonność. Zastosowanie kolejno po sobie następujących procesów impregnacji i mikronizacji powodowało wzrost zapotrzebowania energii na proces przemiału. Zapotrzebowanie to było większe w przypadku zastosowania impregnacji w ciśnieniu 5 kPa.

**Słowa kluczowe:** energochłonność, impregnacja próżniowa, obróbka promieniowaniem podczerwonym, przemiał, pszenica.

## COMPUTATIONAL DOMAIN DISCRETIZATION AND ITS IMPACT ON FLOW FIELD AROUND THE SPARK PLUG IN SI ENGINE

Marcin Sosnowski

Institute of Technical Education, Faculty of Mathematics and Natural Sciences  
Jan Długość University in Czestochowa, Aleja Armii Krajowej 13/15, 42-218 Czestochowa  
m.sosnowski@ajd.czyst.pl

**Summary.** The discretization of computational domain is a crucial factor influencing the conformity of numerical and experimental research results. The paper presents the comparison of results obtained for the same numerical setup but with different mesh types: hexahedral, tetrahedral and polyhedral mesh. The computational domain was the sector of constant volume combustion chamber with a spark plug. The results presented in the form of velocity and  $Y^+$  contour plots prove that the applied mesh type significantly influences the results and therefore the conformity of numerical and experimental research results.

**Key words:** spark ignition engine, numerical modelling, mesh type, computational domain discretization, computational fluid dynamics.

### INTRODUCTION

The flow field around spark plug impacts the spark discharge in spark ignited (SI) engines [1]. Ignition resulting from spark discharge between spark plug electrodes is a crucial factor which strongly influences the combustion process [2, 3]. As a consequence the flow field around the spark plug significantly affects engine work repeatability and toxic components concentration in exhaust gases [4, 9]. That is why proper modelling of flow field in the vicinity of spark plug is extremely important because it significantly influences results of SI engine work cycle numerical modelling and conformity of numerical and experimental research results [5, 6, 7].

Very often the numerical solution is mesh-dependent, which allows to claim that the discretization of computational domain seems to be one of the key factor, which affects the simulation results. Three mesh types were used to prove the above mentioned thesis. These types are (Fig. 1):

- hexahedral mesh,
- tetrahedral mesh,
- polyhedral mesh.

The hexahedral (HEX) mesh is considered as the most reliable one because its numerical diffusivity is the lowest of all the mesh types describes in the paper. The disadvantage of HEX mesh

is the fact, that it is difficult to generate such mesh in case of complicated geometry. On the other hand, tetrahedral (TET) mesh is the most diffusive one but it is relatively easy to generate it even in case of complicated geometry. The polyhedral (POLY) mesh seem to combine the advantages of both HEX and TET mesh as its numerical diffusivity is comparable to HEX mesh and it is as easy to be generated as the TET mesh.

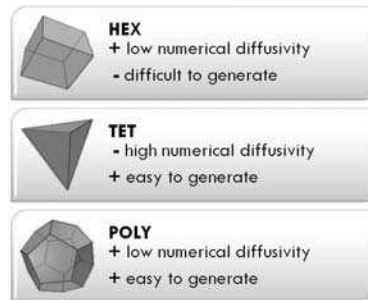


Fig. 1. Mesh types and its basic characteristics

## THE COMPUTATIONAL DOMAIN AND BOUNDARY CONDITIONS

The computational domain is a sector of constant volume combustion chamber with a spark plug depicted in Fig. 2. HEX (Fig. 3) and TET (Fig. 4) meshes were generated for the same geometry and the seed setting were identical in each case. The POLY (Fig. 5) mesh was generated automatically on the basis of TET mesh using FLUENT software.

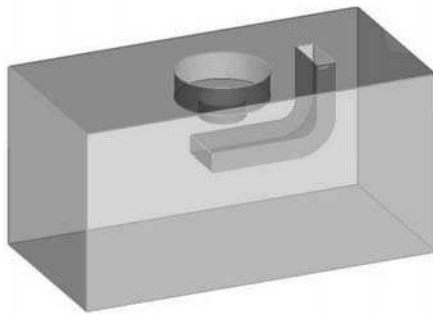


Fig. 2. The computational domain: constant volume combustion chamber with spark plug

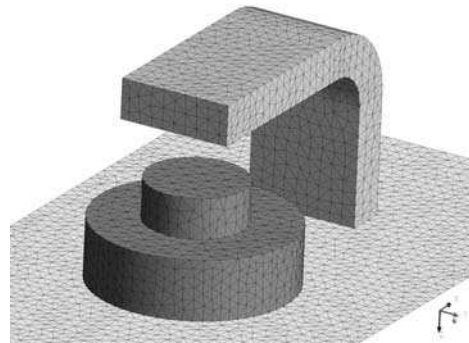


Fig. 3. The computational domain discretization with the use of HEX mesh

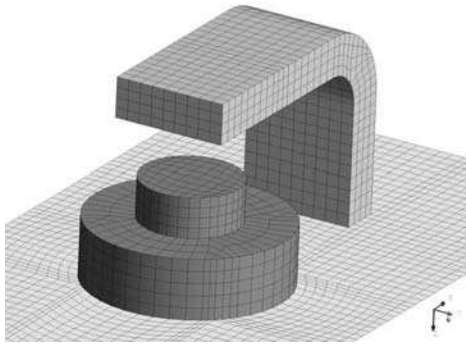


Fig. 4. The computational domain discretization with the use of TET mesh

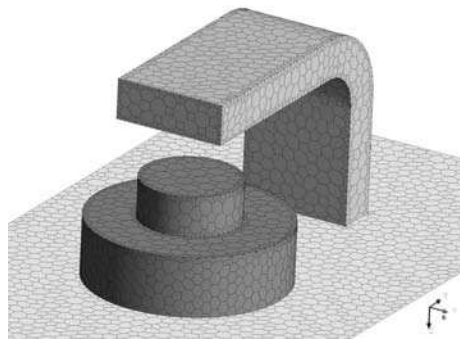


Fig. 5. The computational domain discretization with the use of POLY mesh

The number of elements in case of each mesh type is shown in Fig. 6. Number of HEX elements was almost 11 times lower comparing to TET mesh regardless the fact that the seed settings were the same for each mesh type. Converting TET mesh to POLY reduced the number of elements almost 6 times.

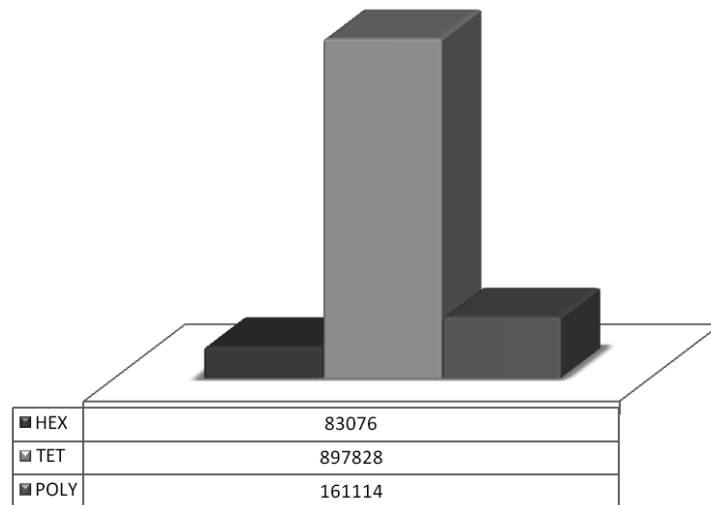


Fig. 6. The number of elements in case of each mesh type

The value of resultant air-fuel mixture flow velocity measured with the use of anemometer located in place of spark plug in S320 engine at the piston position corresponding to ignition moment measured in [8] was determined to be at the level of 8 m/s. Therefore constant and uniform flow field of above mentioned velocity value and direction parallel with the X axis was declared as boundary condition at the borders of computational domain coplanar to YZ plane (Fig. 7).

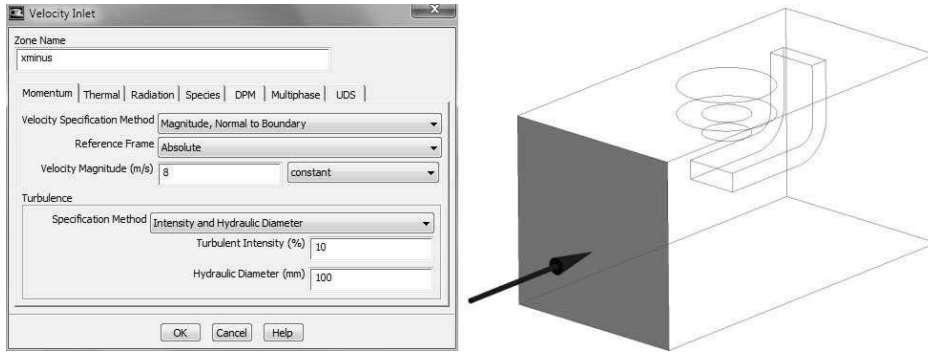


Fig. 7. Boundary condition setup

MODELLING RESULTS

The numerical modelling results are presented as velocity contour plots in the XZ plane (Fig. 8) and  $Y^+$  on the surfaces representing the engine head and the spark plug (Fig. 9) obtained for all three mesh types analyzed in the paper.

The  $Y^+$  is a non-dimensional wall distance from the wall to the first mesh point and can be defined as follows:

$$Y^+ = \frac{U_* Y}{\nu}$$

where:

- $U_*$  - friction velocity at the nearest wall,
- $Y$  - distance to the nearest wall,
- $\nu$  - local kinematic viscosity of the fluid.

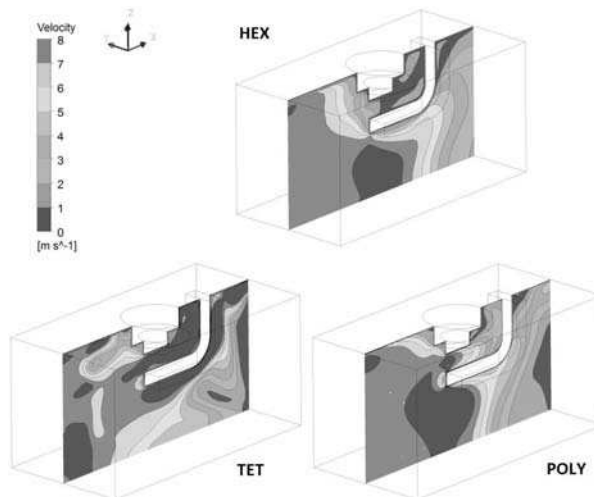


Fig. 8. Velocity contour plots in XZ plane for each of the analyzed mesh types

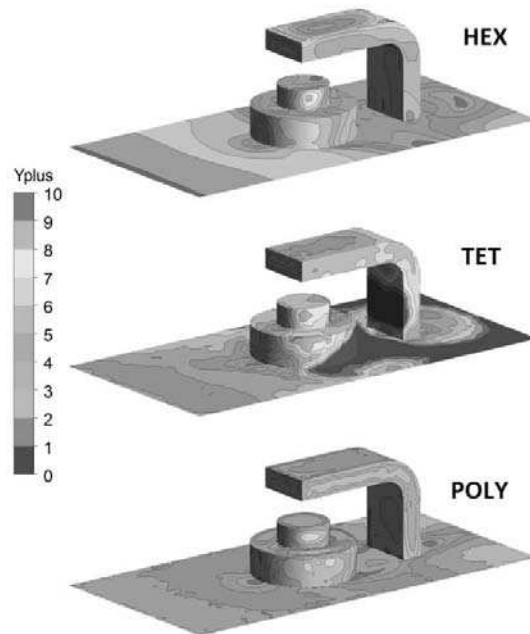


Fig. 9.  $Y^+$  contour plots for each of the analyzed mesh types

## CONCLUSIONS

The numerical modelling results presented as velocity contour plots for each of the analyzed mesh types reveal that the velocity distribution in the XZ plane obtained with the use of POLY mesh is more consistent with the HEX mesh than the results obtained for the TET mesh. However differences in the volume between spark plug electrodes are significant even for HEX and POLY mesh.

In case of  $Y^+$  (similarly as for the velocity), acquired results reveal that the distribution obtained with the use of POLY mesh is more consistent with the HEX mesh than the results obtained for the TET mesh. The differences are caused by the local velocity values and the height of the first mesh layer from the wall, which are used to calculate the  $Y^+$ .

The results prove that the computational domain discretization significantly influence the numerical modelling results. That is why the mesh type should be wisely chosen for the specific cases and the proper seed size must be declared.

Another issue, which has to be further examined, is the boundary layer. The proper values of  $Y^+$  depend on the kind of solver settings (wall-function or wall-integration) as well as the seed size near the wall. Therefore, the seed size should be chosen separately for each of the analyzed mesh types in order to obtain mesh-independent solution and then the solutions for HEX, TET and POLY mesh should be compared.

## REFERENCES

1. Franke A.: Diagnostics of electrical phenomena in gases for the monitoring of spark-ignited combustion, Lund Institute of Technology, Lund University, 2000.



2. Herweg R., Maly R.R.: A fundamental model for flame kernel formation in SI engines, SAE Paper 922243, 1992.
3. Jamrozik Arkadiusz, Kociszewski Arkadiusz, Sosnowski Marcin, Tutak Wojciech; Simulation of combustion in SI engine with prechamber; XIV UKRAINIAN POLISH CONFERENCE "CAD in Machinery Design Implementation and Educational Problems"; Polyana; 2006.
4. Kociszewski Arkadiusz, Jamrozik Arkadiusz, Sosnowski Marcin, Tutak Wojciech: Computational analysis and experimental research into lean mixtures combustion in multi-spark plug SI engine; EUROPEAN KONES 2006, 32nd International Scientific Congress on Powertrain and Transport Means; Warsaw, Lublin, Naleczow; 2006.
5. Sosnowski Marcin: Ignition model and its impact on flame kernel formation in SI engine; Edukacja Techniczna i Informatyczna, 2009.
6. Sosnowski Marcin: Modelowanie i analiza przebiegu wyładowania iskrowego w silniku z zapłonem wymuszonym; Prace Instytutu Lotnictwa, Warszawa, 2009.
7. Sosnowski Marcin: Rejestracja optyczna wyładowania iskrowego przy różnych parametrach przepływowych medium gazowego pomiędzy elektrodami świecy zapłonowej; Edukacja Techniczna i Informatyczna, 2009.
8. Tutak W.: Modelowanie zawirowania świeżego ładunku w komorze spalania tłokowego silnika spalinowego, Praca doktorska, 2002.
9. Tutak Wojciech, Jamrozik Arkadiusz, Kociszewski Arkadiusz, Sosnowski Marcin: The experimental research of the three-dimensional turbulence field in combustion chamber of internal combustion engine; EUROPEAN KONES 2006, 32nd International Scientific Congress on Powertrain and Transport Means; Warsaw, Lublin, Naleczow; 2006.

#### DYSKRETYZACJA DOMENY OBLICZENIOWEJ I JEJ WPŁYW NA POLE PRZE- PŁYWU WOKÓŁ ŚWIECY ZAPŁONOWEJ W SILNIKU NISKOPRĘŻNYM

**Streszczenie.** Dyskretyzacja domeny obliczeniowej jest kluczowym czynnikiem wpływającym na zgodność wyników badań numerycznych i eksperymentalnych. W pracy przedstawiono porównanie wyników uzyskanych dla tych samych ustawień numerycznych, ale dla różnych rodzajów siatki: siatka sześciokątna, czworosienna i wielosienna. Obliczeniowa domena obejmowała sektor stałej objętości komory spalania ze świecą zapłonową. Wyniki przedstawione w postaci prędkości i obrysów  $Y^+$  dowodzą, że zastosowany typ siatki znacząco wpływa na wyniki, a zatem również na zgodność wyników badań numerycznych i eksperymentalnych.

**Słowa kluczowe:** silnik niskoprężny, modelowanie numeryczne, typ siatki, dyskretyzacja domeny obliczeniowej, obliczeniowa dynamika płynów.

## DYNAMIC POTENTIAL OF PASSABLENESS OF THE AGRICULTURAL TRACTION-TRANSPORT TECHNOLOGICAL MACHINE WITH A HYDRODRIVE OF WHEELS

Georgij Tajanowskij\*, Wojciech Tanas\*\*

\* The Belarussian National Technical University,

\*\* University of Life Sciences in Lublin, Poland

**Summary.** In article the technique and results of research of traction-dynamic characteristics of a harvester with a hydrodrive of wheels is stated. In the papers the methodology of study the agriculture machine with hydrostatical wheel as well as the estimation of its drawing properties. The stress distribution of drive wheels, wheel slip and changes of machine weight was presented. The computing project of agriculture machine was realized which contain: working pressure in driving set, wheel slip, drawing force, velocity and power of engine.

**Key words:** agriculture machine, hydrostatical drive, stress distribution, drawing and dynamical characteristics.

### INTRODUCTION

Creation of any agricultural harvester is interfaced to the rational coordination of work of all internal subsystems taking into account real interaction of the machine with an environment. In this connection it is necessary to consider in a complex working process of a harvester, considering influence of loadings of its technological modules on indicators of operational properties.

Technological forward semihinged modules of harvesters include undermining passive or active working bodies, bodies scraps, crushing, rejection, removal of a tops of vegetable and others, in case of machines for cleaning of root crops: a potato, carrots, onions, a beet, or - harvesters at grain-harvesting machines and machines for cutting and crushing of the plants, separating and transporting mechanisms [1, 2, 3, 5, 6, 8, 10]. Power resistance from the working bodies co-operating with soil and plants [3, 4, 7, 9, 11], makes essential impact on traction dynamics of all machine. Besides, in the course of work the machine changes the weight, at bunker filling, that also influences properties of the machine.

Wide penetration a hydrovolume drive on modern agricultural harvesters is caused by its essential advantages, in comparison with machines with step mechanical transmissions. However traction-dynamic properties of such machines differ from machines with step mechanical transmissions and are less studied [12, 13, 14, 15].

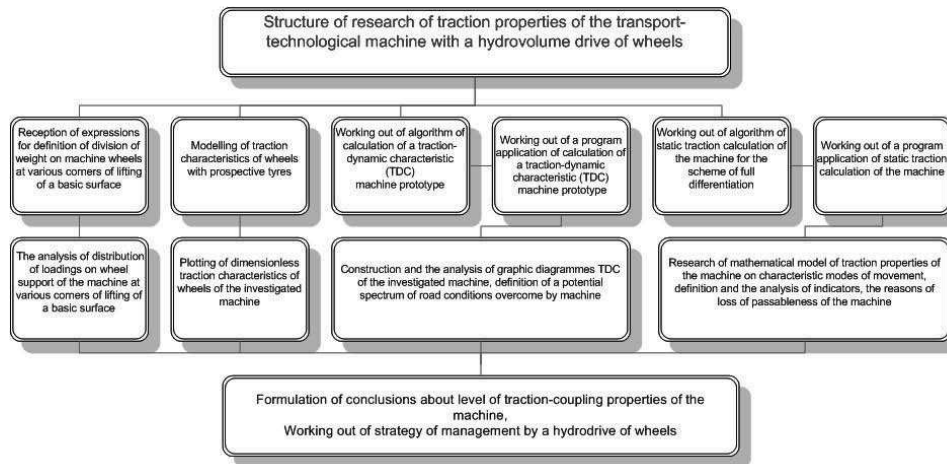


Fig. 1. Algorithm of research of traction-dynamic potential of the machine

In connection with considerable change of normal loadings on wheels of the harvester having the memory bunker, in the course of cleaning, moving across the field and on distant transport represents scientific and practical interest research of traction characteristics of a harvester with a hydrovolume drive of wheels. On the basic operating modes of such machines the drive of wheels from one pump under the scheme 4K4 with full differentiation is used.

The purpose of given article consists in definition of traction-dynamic characteristics of a harvester taking into account specificity of distribution of normal loadings on wheels of leading bridges and their valid slipping, as makes difference of this work from the known.

The block diagramme of algorithm of research of traction-dynamic properties of a harvester with a hydrovolume drive of wheels according to an object in view is resulted in figure 1.

## DISTRIBUTION OF NORMAL LOADINGS TO MACHINE WHEELS

Tjagovo-coupling properties of a harvester are in many respects defined by normal loadings to a basic surface on wheels. Distribution of these loadings depends on a number of factors: the design-layout scheme of running system; masso-geometrical parametres: positions of the centre of weights, the moments of inertia concerning axes of cross-section and longitudinal-angular fluctuations; characteristics of rigidity and geometrical parametres of tyres; deformation characteristics and characteristics of microprofiles of a basic surface on trajectories of movement of wheels of different boards and harvester bridges; a mode of movement of the machine; influences of the technological module aggregated with machine at working and transport positions [7, 11, 13].

More often the harvester has statically definable running system with a shaking beam of the bridge of operated wheels. Expressions of reactions in support of wheels of the machine which settlement scheme is shown in figure 2 are for such a case received.

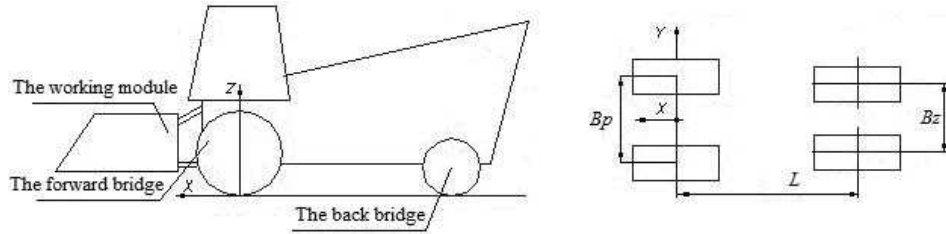


Fig. 2. The scheme of a transport technological harvester

The example of a copy of the screen of the monitor with calculation listing in a program application of symbolical mathematics with initial data of one of possible variants of a harvester and settlement expressions depending on a corner of lifting of basic surface  $\alpha$  is resulted in figure 3.

By results of calculation schedules of dependences of distribution of normal loadings on wheels of a harvester for various conditions of the memory bunker and position of the technological module (figures 4-6) are constructed.

In figures 4-6 among schedules the curve only for one of wheels of the back bridge of operated wheels, as normal loadings on a wheel of other board same is shown.

$g := 9.81$ $\alpha := \begin{pmatrix} 0 \\ 2 \\ 4 \\ 6 \\ 8 \end{pmatrix} \cdot \text{deg}$		<b>Weight parameters of the machine, [ N ]</b> $B_p := 2.720$ : Track of the forward bridge, M $L := 5.250$ : Interaxial base, M $M_{kom0} := 25340$ : Weights with the empty bunker, kg		$X_c := 2.265$ $Y_c := -0.0483$ $Z_c := 1.672$ Co-ordinates of the centre of weights with the empty bunker and the lifted working module	
$\alpha = \begin{pmatrix} 0 \\ 0.03 \\ 0.07 \\ 0.1 \\ 0.14 \end{pmatrix}$		$R_{1lev} := 0.5 \cdot g \cdot M_{kom0} \cdot \left[ \cos(\alpha) \cdot \left( 1 - \frac{X_c}{L} + 2 \cdot \frac{Y_c}{B_p} \right) - \frac{Z_c}{L} \cdot \sin(\alpha) \right]$ $R_{1prav} := 0.5 \cdot g \cdot M_{kom0} \cdot \left[ \cos(\alpha) \cdot \left( 1 - \frac{X_c}{L} - 2 \cdot \frac{Y_c}{B_p} \right) - \frac{Z_c}{L} \cdot \sin(\alpha) \right]$		$R_{1lev} = \begin{pmatrix} 66255.06 \\ 64833.23 \\ 63332.41 \\ 61754.42 \\ 60101.2 \end{pmatrix}$ <b>Normal loading of a forward left wheel, N</b> $R_{1prav} = \begin{pmatrix} 75083.5 \\ 73656.29 \\ 72139.34 \\ 70534.5 \\ 68843.72 \end{pmatrix}$	
$R_{1most} := R_{1lev} + R_{1prav}$ $R_{1most} = \begin{pmatrix} 141338.56 \\ 138489.51 \\ 135471.74 \\ 132288.92 \\ 128944.93 \end{pmatrix}$		$R_{2most} := (X_c \cdot \cos(\alpha) + Z_c \cdot \sin(\alpha)) \cdot g \cdot \frac{M_{kom0}}{L}$		$R_{2most} = \begin{pmatrix} 107246.84 \\ 109944.45 \\ 112508.11 \\ 114934.7 \\ 117221.26 \end{pmatrix}$	
$R_{2lev} := 0.5 \cdot R_{2most}$ $R_{2prav} := 0.5 \cdot R_{2most}$		$R_{2lev} = \begin{pmatrix} 53623.42 \\ 54972.23 \\ 56254.06 \\ 57467.35 \\ 58610.63 \end{pmatrix}$ $R_{2prav} = \begin{pmatrix} 53623.42 \\ 54972.23 \\ 56254.06 \\ 57467.35 \\ 58610.63 \end{pmatrix}$			

Fig. 3. Listing of calculation of normal loadings on harvester wheels

Apparently from figures 4-6, wheels of running system are exposed at work to considerable change of loadings, that essentially affects traction efforts developed by them and traction properties of the machine as a whole.

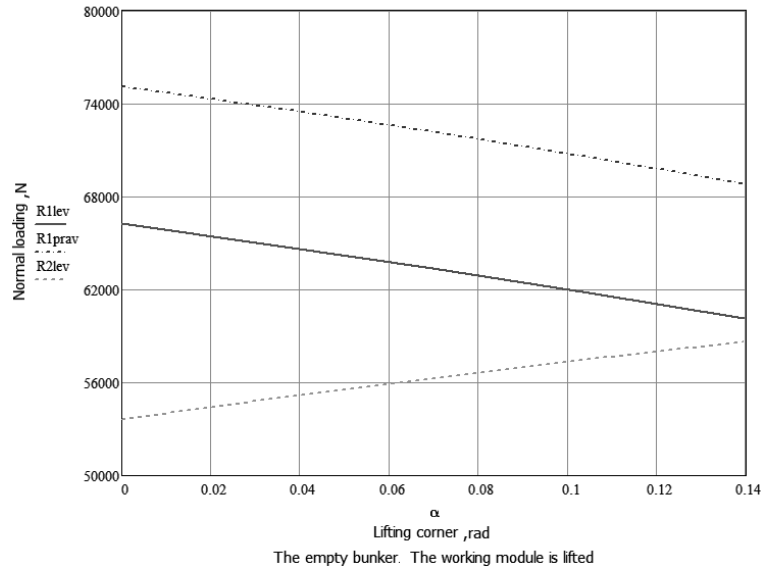


Fig. 4. Normal loadings on harvester wheels at the empty bunker and the lifted forward working module

As follows from figures 4-6, with growth of a corner of lifting of a surface of movement of a wheel of the back bridge of operated wheels are loaded in addition also their normal loading approaches with similar loadings of forward wheels, both at the empty bunker, and at full, but in case of the lifted forward technological module.

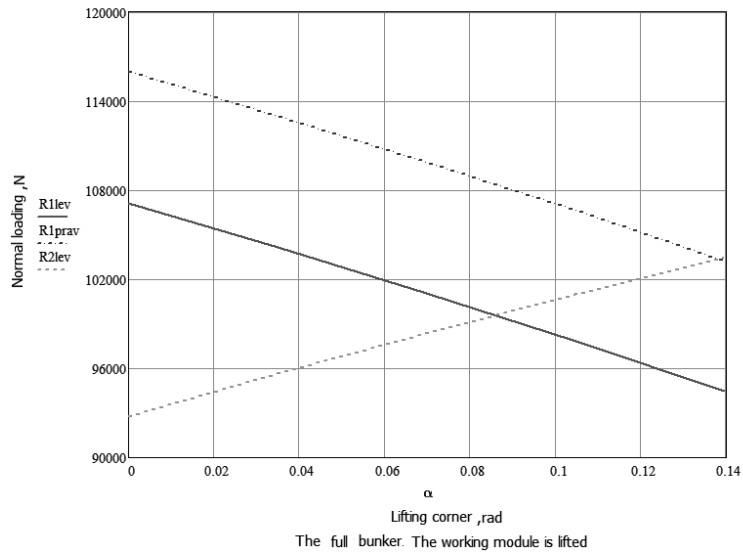


Fig. 5. Normal loadings on harvester wheels at the full bunker and the lifted forward module

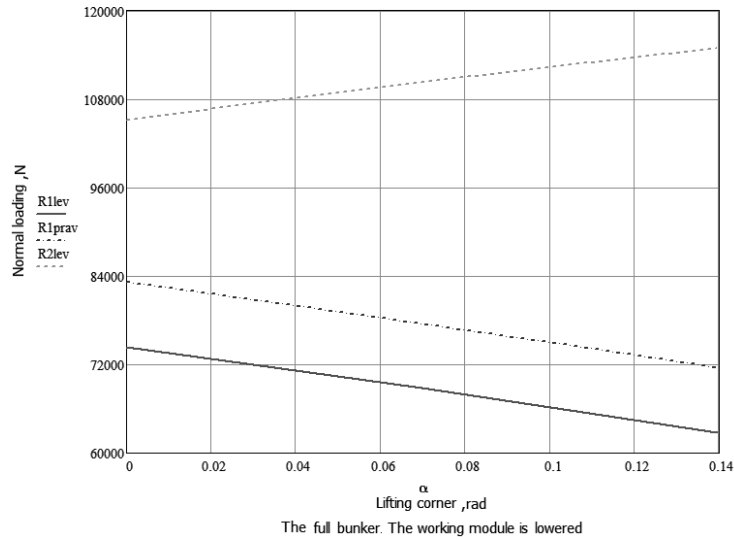


Fig. 6. Normal loadings on harvester wheels at the full bunker and the lowered forward module

At lowering of the forward module and its interaction with soil loading essentially increases by back wheels. With growth of a corner of lifting of a surface weeding this redistribution of loadings it is aggravated. Various loadings on wheels of the left and right board are caused by discrepancy of the centre of weights of the machine with its longitudinal a vertical plane of symmetry of running system of the machine that is connected with feature of placing of the process equipment on a considered variant of a harvester.

#### TRACTION-DYNAMIC POTENTIAL OF THE HARVESTER

Passableness of the harvest wheel machine is a difficult technical quality which is shown in its work to destination in interaction with environment through properties of passableness which characterise the ability of the machine caused by set of systems of its design and their interrelations, to carry out reliable safe overcoming of the set limited working space of the movement which are in a certain condition of structure (figure 7). In this figure the most widespread measuring instruments of properties of passableness are resulted.

PROPERTIES OF PASSABLENESS

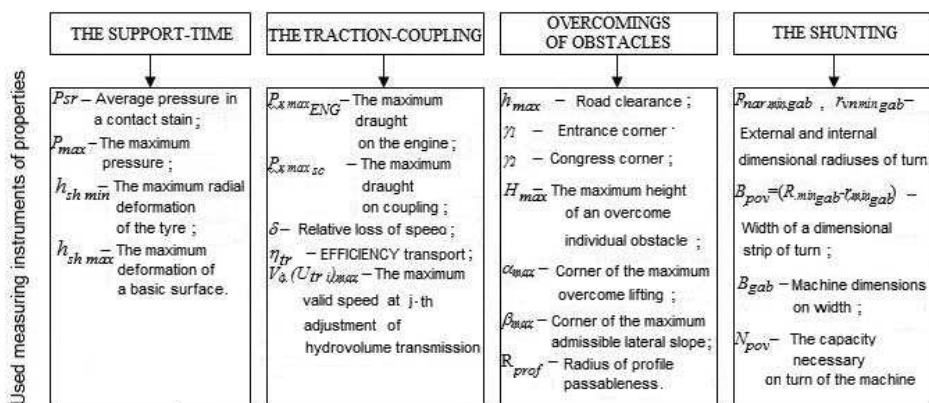


Fig. 7. Structure and most often used measuring instruments of properties of passableness

At the lifted forward working module of the machine its settlement scheme is resulted in figure 8.

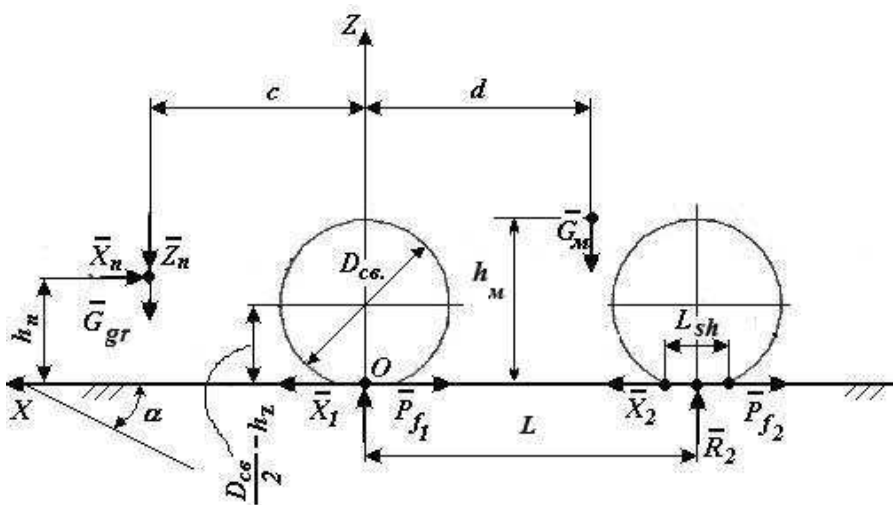


Fig. 8. the Settlement scheme of a harvester in transport position for a complex estimation of passableness

$G_{gr}$  - weight lifted in transport position the forward technological module;

$G_M$  - harvester weight;

$L_{sh}$  - length of a stain-contact of a wheel with a ground

The equations of static balance of a harvester at the established speed of movement look like:

$$\left. \begin{aligned} \sum X = 0: -X_n + X_1 - R_1 \cdot f_1 + X_2 - R_2 \cdot f_2 &= 0, \\ \sum Z = 0: -Z_n + G_{gr} + R_1 - G_M + R_2 &= 0, \\ \sum M_O = 0: (Z_n + G_{gr}) \cdot C - X_n \cdot h_{II=n} - G_M \cdot d + R_2(a+b) &= 0. \end{aligned} \right\} \quad (1)$$

At the lifted forward technological module and maintenance of absence of a kinematic mismatch of district speeds of wheels of leading bridges we can write down:

$\varphi_1 = \varphi_2 = \varphi$  - operating ratio of chain weight of leading bridges of the machine;  
 $\delta_1 = \delta_2 = \delta$  - slipping of driving wheels of the machine;

$$\left. \begin{aligned} X_1 = R_1 \cdot \phi; X_2 = R_2 \cdot \phi; X_n = 0; Z_n = 0, \text{ then } P_{f_1} = R_1 \cdot f_1; P_{f_2} = R_2 \cdot f_2, \\ \phi = \frac{R_1 \cdot f_1 + R_2 \cdot f_2}{R_1 + R_2}; R_2 = \frac{G_M \cdot d - G_{gr} \cdot C}{L}, \\ R_1 = G_M + G_{gr} - R_2; \varphi = \varphi_{\max} (1 - e^{-\kappa_{sh} \cdot \delta}), \end{aligned} \right\} \quad (2)$$

whence

$$\delta = -\frac{1}{\kappa_{sh}} \cdot \ln(\varphi_{\max} - \varphi). \quad (3)$$

The indicator of potential of passableness looks like [4]:

$$P = \sqrt[3]{P_{sc} \cdot P_{op} \cdot P_N},$$

where:  $P_{sc}$  - a passableness indicator on coupling,

$P_{op}$  - an indicator of basic passableness,

$P_N$  - A passableness indicator on the engine capacity  $N_n$ ,

$$P_{sc} = 1 - \frac{P_{\kappa}}{P_{\kappa \max}}; P_{op} = 1 - \frac{P_{sr}}{[P_{sr}]_{dop}}; P_N = 1 - \frac{N}{N_n}. P_{op} = 1 - \frac{P_{sr}}{[P_{sr}]_{dop}}; P_N = 1 - \frac{N}{N_n}. \quad (4)$$

$$\left. \begin{aligned} P_{\kappa} = (R_1 + R_2) \cdot \phi; P_{\kappa \max} = (R_1 + R_2) \cdot \varphi_{sc}; P_{sc} = 1 - \frac{\varphi}{\varphi_{sc}}, \\ h_{z_i} = \frac{R_i}{2} \cdot \frac{1}{\pi \cdot p_{w_i} \cdot \sqrt{B_{sh_i} \cdot D_{ch_i}}}; L_{sh_i} = \sqrt{\frac{D_{ch}^2}{4} - h_{z_i}^2}, \\ S_{k_i} = B_{sh_i} \cdot L_{sh_i}; P_{st_i} = \frac{R_i}{2 - S_{k_i}}; P_{op} = 1 - \frac{P_{sr \max}}{[P_{sr}]_{dop}}. \end{aligned} \right\} \quad (5)$$

Taking into account the accepted designations capacity  $N$  spent for movement, is equal:

$$N = (X_n + R_1 \cdot f_1 \cdot \cos \alpha + R_2 \cdot f_2 \cdot \cos \alpha + G_M \cdot \sin \alpha) \cdot V, \quad (6)$$

where:  $V = \frac{\pi \cdot n_d}{30 \cdot U_{TR_i}} \cdot r_{ri}^o$ ,



$$\delta = 1 - \frac{V_d}{V}; \quad V = \frac{V_d}{1 - \delta}; \quad V_d = V \cdot (1 - \delta). \quad (7)$$

The capacity lost on slipping of wheels, is equal:  $N_d = N \cdot \delta$ ,

$$\left. \begin{aligned} N_n &= \frac{\pi \cdot n_{d_{nom}}}{30} \cdot M_{d_{nom}}, \\ \text{At } X_n &= 0; \quad N = N_f + N_\alpha + N_\delta, \\ (N_f + N_\alpha) &= N \cdot (1 - \delta); \quad P_N = 1 - \frac{N}{N_n}, \end{aligned} \right\} \quad (8)$$

$$\text{Transport EFFICIENCY of the machine: } \eta_{trm} = \frac{N_{f_{gr}}}{N}. \quad (9)$$

where capacity on overcoming of resistance to movement:

$$N_f = G_{gr} (f \cdot \cos \alpha + \sin \alpha) \cdot V_{dp} \quad (10)$$

As a result of calculation of all intermediate sizes value  $P$  pays off.

For an estimation of traction-dynamic potential of the wheel machine widely use as a measuring instrument dynamic factor  $D$  [1]:

$$D = \frac{P_k - P_w}{G}, \quad (11)$$

where:  $P_k$  - a total tangent force of wheels of running system;  $P_w$  - force of resistance of air;  $G$  - machine weight.

Thanks to high general EFFICIENCY modern aksial-piston hydromachines even more often find application in hydrovolume drives of wheel running systems of technological multipurpose machines. For a design stage carrying out of research of traction-coupling properties of such machines is necessary, for the purpose of a choice of rational parametres of a drive of wheels, algorithms of management by hydromachines in characteristic working conditions of running system.

In case of work of hydromotors of a drive of wheels from one pump under the scheme of full differentiation the total traction effort of driving wheels of the machine essentially depends on coupling conditions of separate wheels and resistance to their movement. And this effort is limited by a wheel which is in the most adverse conditions: with the least vertical loading, coupling and the greatest resistance to movement. Such conditions lead to sharp growth of its slipping, decrease in total draught of all wheels and, frequently, to loss of passableness of the machine.

For maintenance of demanded draught the control system of a hydrodrive realises various algorithms. Necessity of check of their efficiency at a design stage demands working out of adequate mathematical model of working process of a hydrovolume drive. Thus it is necessary to consider real traction characteristics of the wheels equipped with pneumatic tyres then the mentioned model will allow to trace continuously true values of pressure and expenses of a working liquid in system, slippings of each of the wheels, the valid speed of the machine, all components of expenses of capacity on movement of the machine and other target sizes depending on parametres of the machine, conditions of movement, position of controls by hydromachines of a hydrovolume drive and the machine engine (figure 1).

By a known technique traction-dynamic characteristics in the beginning have been calculated on the computer (TDC) a harvester with a hydrovolume drive [1] at work with the wheel formula 4K2 and 4K4. Results of calculations are resulted in figures 9,10.

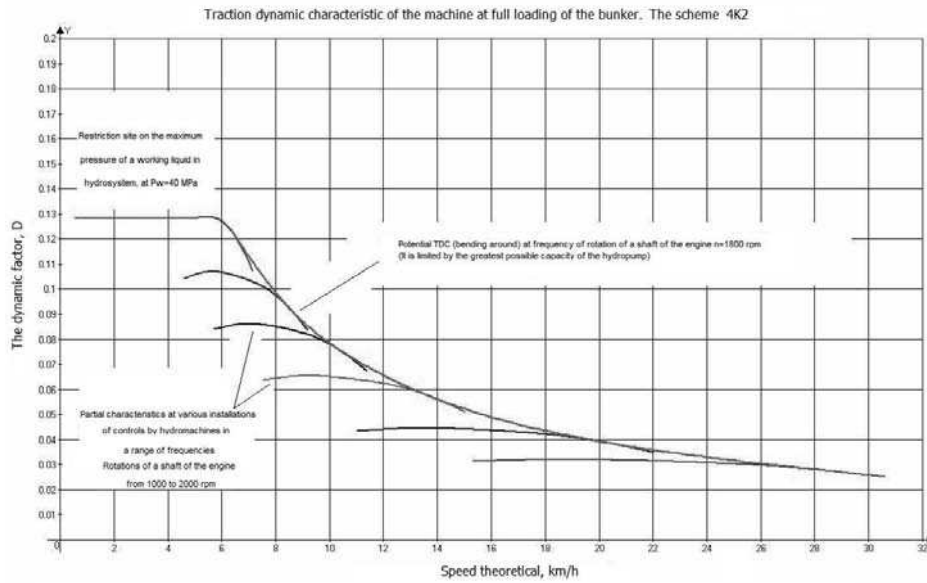


Fig. 9. TDC a harvester at work under the scheme 4K2

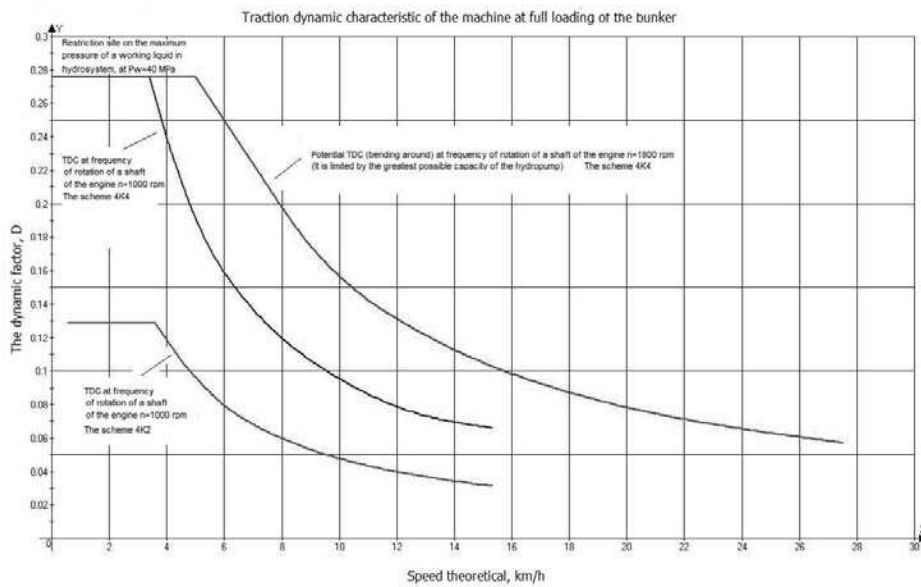


Fig. 10. TDC a harvester at work under the scheme 4K4

As follows from the characteristic, the dynamic factor for the scheme 4K2 at full loading of the bunker does not exceed value 0,13, and at work under the scheme 4K4 - 0,28 and is limited by

admissible pressure of a working liquid in pressure head highways of a hydrodrive of hydromotors of a drive of wheels.

On TDC have defined the maximum corners of overcome lifting  $\alpha_{ij}$ , being set by factor of resistance to movement of the machine and solving the trigonometrical equation. For concrete j-th point TDC:

$$D_{j \max} = f_i \cdot \cos \alpha_{ij} + \sin \alpha_{ij}, \tag{12}$$

where:  $f_i$  - factor of resistance to machine movement on the given site of a surface of movement which is equal to the sum of factor of resistance movement machines and specific, on a unit of weight of the machine, technological resistance  $P_{\text{tech}}$ . The forward module:

$$f_i = f_{ki} + P_{\text{tech}}/G_k \Sigma. \tag{13}$$

Unknown values of corners  $\alpha_{ij}$  at set  $D_{j \max}$  and  $f_i$  can be defined a numerical method, for example in a program application of symbolical mathematics, or to calculate under the formula:

$$\alpha_{ij} = \arcsin (D_{j \max} \cdot \cos (\arctg f_i)) - \arctg f_i. \tag{14}$$

In figures 11 and 12 schedules of dependences of the maximum corners of lifting of a surface of movement overcome by a harvester are resulted, at work under the scheme 4K4 with the hung out forward module.

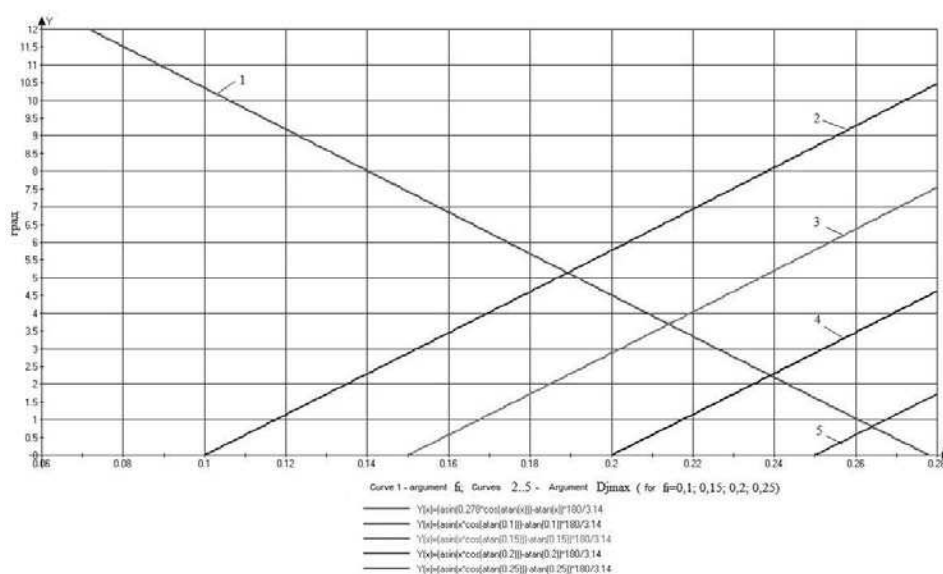


Fig. 11. The diagram for definition of corners of overcome liftings

And the curve 1 reflects dependence  $\alpha_{ij}(f)$  at the maximum value of the dynamic factor for the specified condition of the machine in a spectrum of road conditions, resistance to movement of

wheels of the machine on which is not exceeded by values 0,28 that corresponds really meeting. In heavy road conditions the machine is capable to overcome lifting no more than 3,2 degrees. Curves  $2.5 - \alpha_{ij}(D)$  - in figure 11 are received for surfaces of movement with values  $f_p$ , accordingly the equal: 0,1; 0,15; 0,2; 0,25, depending on the dynamic factor which the harvester can have, that is to the maximum value - 0,278.

TDC a harvester allows to define values of theoretical speeds of movement, traction efforts so and spent capacity, pressure in pressure head highways of motors, the spectrum on weight of overcome road conditions, and represents result of traction-dynamic calculation. The loading traction characteristic at a small range of resistance of giving of the technological module is not informative.

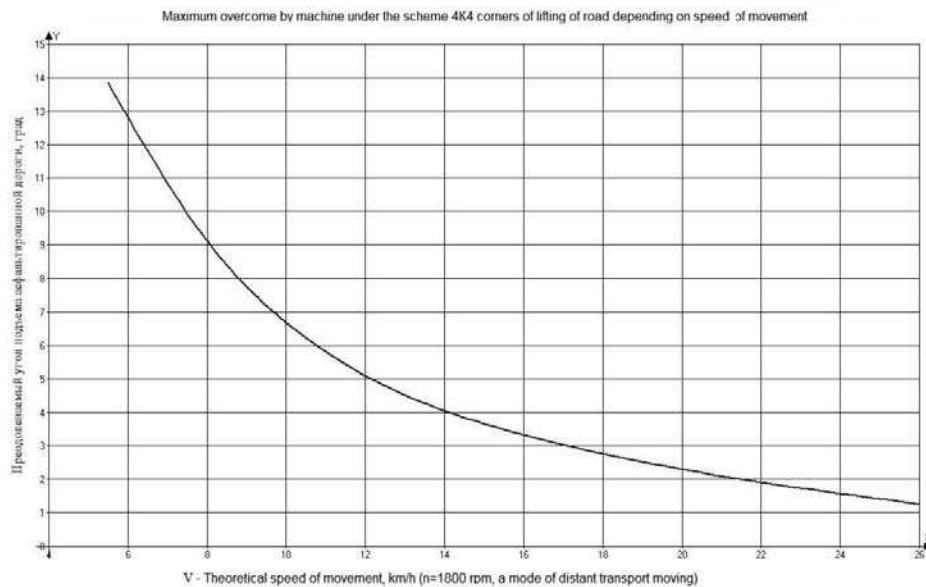


Fig. 12. Influence of theoretical speed on corners of overcome liftings

### STATIC TRACTION CALCULATION OF A HARVESTER WITH A HYDROVOLUME DRIVE OF WHEELS

Research of distribution of traction forces on wheels, slippings of wheels and high-speed losses of capacity of the machine for the scheme of full differential communication of pumps with motors and distributions of vertical loadings on wheels on various surfaces of movement makes a subject of static traction calculation of the machine, which has been executed on algorithm specially developed by authors to consider true values of pressure in hydrosystem of a drive and slipping of each of driving wheels.

Taking into account calculated earlier for a studied variant of division of weight of a harvester on wheels and accepted maximum resolved on a drive of wheels of capacity of the engine in 340 kw it is executed on the resulted algorithm (figure 1) the analysis of traction indicators of a harvester. Calculations in the developed program application in a package of symbolical mathematics were spent depending on a corner of lifting of a surface of movement for following five basic regular modes of movement across the field, and also on the asphalted road on distant transport.

Parametres of modes the following: 1st technological mode - a field,  $n=1400$  rpm, the empty bunker, 4K4, the full differentiation, the lowered forward module, volume of hydropumps - maximum, volume of hydromotors - maximum; 2nd technological mode - the same, but with the full bunker; 3rd mode - short technological transport moving across the field,  $n=1400$  rpm, the empty bunker, 4K4, the full differentiation, the lifted forward module, volume of hydropumps - maximum, volume of hydromotors - maximum; 4th mode - the same, as in previous, but with the full bunker; 5th mode - asphalt,  $n=1800$  rpm, the empty bunker, 4K4, the full differentiation, the lifted forward module, distant transport moving, volume of hydropumps - maximum, volume of hydromotors - minimum.

In connection with absence of results of traction tests of tyres of wheels of the machine their traction characteristics have been constructed by calculation by the developed technique for two surfaces of movement: a field and the asphalted road.

Results of static traction calculation of the machine are presented in table 1. As follows from table 1, on coupling of one of driving wheels with a ground the machine reaches restrictions only on the first mode at coal of lifting of a surface of the field, exceeding 6 degrees. On modes 2, 4 and 5 restrictions come at various corners of lifting of a surface of movement or on pressure in a pressure head highway of a hydrodrive, or because of the big machine of the capacity exceeding capacity of the established engine demanded for movement.

At machine work under the scheme of full differentiation each wheel has the values of slipping, angular and theoretical speed. In this connection restriction of the maximum corner of overcome lifting on coupling owing to insufficiency of total draught wheels in each concrete case will be defined by one of wheels system which the first will reach absolute value of slipping, as it is visible from table 1.

Table 1. Results of traction calculation of a harvester

Lif-ting corner, degr.	Pressure in hydro-system of a drive of wheels, kPa	Relative loss of speed of a wheel the forward left wheel	Relative loss of speed of a wheel the forward right wheel	Relative loss of speed of a wheel, back left/rights wheels	Total draught of wheels, kN	Speed reality, km/h	Power engine on a drive of wheels, kW
1 mode							
0	17999,224	0,262	0,21	0,186	53,36	5,387	158,228
2	20332,403	0,319	0,24	0,198	60,277	5,19	178,633
4	22644,750	0,407	0,28	0,21	67,132	4,898	197,929
6	24933,449	0,598	0,33	0,223	73,917	4,222	207,732
8	27195,712	1,0	0,41	0,237	80,624	0	231,436
2 mode							
0	29399,051	0,197	0,182	0,188	87,156	5,532	250,186
2	33533,686	0,228	0,206	0,201	99,413	5,398	285,372
4	37631,406	0,267	0,235	0,214	111,561	5,238	320,244

6	41687,219	0,321	0,273	0,227	123,585	5,034	354,759
8	45696,184	0,405	0,325	0,241	135,470	4,737	388,875
3 mode							
0	17689,627	0,153	0,144	0,209	52,442	5,579	150,539
2	20485,029	0,169	0,157	0,229	60,729	5,461	174,328
4	23255,472	0,187	0,171	0,249	68,943	5,335	197,904
6	25997,583	0,207	0,187	0,27	77,072	5,198	221,24
8	28708,019	0,232	0,206	0,292	85,107	5,047	244,306
4 mode							
0	29082,473	0,154	0,148	0,202	86,217	5,598	247,492
2	33678,228	0,171	0,163	0,219	99,842	5,485	286,602
4	38232,951	0,191	0,18	0,236	113,345	5,365	325,363
6	42741,093	0,214	0,199	0,254	126,709	5,233	363,727
8	47197,162	0,242	0,223	0,272	139,920	5,087	401,649
5 mode							
0	17319,848	0,047	0,046	0,066	19,070	22,831	189,504
2	24864,972	0,053	0,05	0,075	27,377	22,667	272,059
4	32379,802	0,059	0,056	0,083	35,652	22,496	354,282
6	39855,182	0,065	0,061	0,092	43,882	22,315	436,074
8	47282,005	0,073	0,067	0,100	52,060	22,123	517,334

## CONCLUSIONS

Developed and realised as information technology the technique of a design estimation of t<sub>g</sub> dynamic potential of a harvester with a hydrovolume drive of wheels allows to accept correctly its rational parametres and to investigate traction properties of a wide class of similar machines taking into account the valid slipping of driving wheels on a movement surface.

## REFERENCES

1. Butenin N.V., Lunts Ya.L, Merkin D.R.: Course of Theoretical Mechanics, Vol.2 Dynamics, Nauka Moscow, 1985.
2. Dreszer K.A. and others: Napedy hydrostatyczne w maszynach rolniczych. PIMR Poznan, 2005.
3. Guskov V.V., N.N. Velev, J. E.: Atamanov and other. Tractors: theory/ - M.: Engineering, 1988. – 376 p.

4. Krasowski E. (red.), 2005.: Kinematyka i dynamika agregatów maszynowych. Działy wybrane. Ropczyce Wyższa Szkoła Inżynieryjno-Ekonomiczna w Ropczycach.
5. Kuzmitski A.V., Tanas W.: Ground stress modeling. TEKA Komisji Motoryzacji i Energetyki Rolnictwo PAN, Lublin 2008/ T. VIII, p. 135-140.
6. Mielnikow S.W.: Experiment planning in research on process in agriculture (in Russian). Leningrad, Kolos, 1980.
7. Osiecki A.: Hydrostatyczny napęd maszyn. WNT, Warszawa, 2004.
8. Petrov V.A. Hydrovolume transmissions of self-propelled machines. - M: Mechanical engineering, 1988. - 248 p.
9. Pietrow G.D.: Potatoes harvester, Mashinostrojenije, Moskwa 1984.
10. Stryczek S.: Napęd hydrostatyczny, t. I Elementy. Wyd. IV. WNT, Warszawa, 1997.
11. Sukach M., Lisak S., Sosnowski S.: Kinematic analysis of the working process of trencher. TEKA Komisji Motoryzacji i Energetyki Rolnictwo PAN, Lublin 2010/ T. X, p. 425-431.
12. Szydelski Z.: Napęd i sterowanie hydrauliczne w pojazdach i samojezdnych maszynach roboczych. WNT, Warszawa, 1993.
13. Tajanowskiy Georgij, Tanas Wojciech.: Distribution of loadings in transmission traction power means with all driving wheels and with system of pumping of trunks at work with hinged instruments // Teka komisji of motorization and power industry in agriculture./ Polish Academy of sciences branch in Lublin/ Volume VII, Lublin, 2007, page 217-224.
14. Tajanowskiy Georgij, Tanas Wojciech.: The analysis of regular wheel loadings distribution at a statically unstable running system if an agricultural machine on a rough surface. TEKA Komisji Motoryzacji i Energetyki Rolnictwo PAN, Lublin 2010/ T. X, p. 464-474.
15. Under the editorship of Guskov V.V., 1987.: Hydro-pneumo automatic device and a hydro-drive of mobile cars. Minsk.: Higher School. – 310 page.

#### METODYKA OCENY WŁAŚCIWOŚCI UCIAĞOWYCH MASZYNY ROLNICZEJ Z HYDROSTATYCZNYM NAPĘDEM KÓŁ JEZDNYCH

**Streszczenie.** W publikacji przedstawiono metodykę badań i oceny właściwości uciągowych oraz uciągowo-dynamicznych charakterystyk maszyny rolniczej z hydrostatycznym napędem kół jezdnych. Przy opracowaniu metodyki uwzględniono specyfikę rozkładu normalnych obciążeń na koła mostów napędowych, ich rzeczywistego poślizgu i możliwości weryfikacji algorytmów sterowania napędem kół przy zmiennej masie maszyny. Przedstawiono projekt obliczeniowy maszyny rolniczej obejmujący: ciśnienie robocze w hydrostatycznym układzie napędowym, indywidualny poślizg kół napędowych, siłę uciągu, prędkość roboczą i moc silnika przeznaczoną na napęd kół.

**Słowa kluczowe:** maszyna rolnicza, napęd hydrostatyczny, obciążenia normalne, charakterystyki uciągowo-dynamiczne.

## ENERGY CONSUMPTION IN THE MOTION OF THE VEHICLE WITH ELECTRIC PROPULSION

Piotr Tarkowski, Ewa Siemionek

Lublin University of Technology, Faculty of Mechanical Engineering  
20-618 Lublin, Nadbystrzycka 36 Str.  
e-mail: p.tarkowski@pollub.pl, e.siemionek@pollub.pl

**Summary.** In the article, energy balance of the wheeled vehicle is discussed. Also, detailed analysis of factors determining energy consumption of the motion is provided. It comprises basic phases of the motion, as well as different cases when the vehicle realizes a complex speed profile. The conception of carrying out energy balance of the vehicle with electric propulsion was used for a car model with the electric motor of direct current and for a two-wheeled vehicle with the triphase asynchronous motor placed in the front wheel.

**Key words:** energy consumption, electric vehicle, energy balance, electric propulsion.

### INTRODUCTION

The subject of energy analysis of the wheeled vehicle motion are factors determining the total expense of energy, as well as the demand for electric energy drawn from the battery. The starting point of the analysis is energy balance of the vehicle moving according to the determined speed profile. The main element of the balance is energy consumption of the motion which reflects the demand for energy on propelled wheels necessary for the realization of the assumed speed profile – it is the basic quantity determining the uptake of electric energy from the battery.

If the motion of the vehicle with electric propulsion is analysed as the result of particular energy transformations, one should take into consideration the way of delivering energy necessary for its realization, which can consist in:

- delivering energy from the engine through the power transmission system to the propelled wheels,
- using disposable kinetic energy (obtained earlier in the phase of acceleration) for overcoming resistance in retarded motion,
- using potential energy of the vehicle for overcoming resistance to motion while driving down the slope.

The following cases of the motion can be distinguished depending on the way it is forced by particular longitudinal forces:

- motion forced exclusively by the action of driving force; it includes acceleration and driving at constant speed,



- motion on the sloping road forced by the component of gravity force ( $G \cdot \sin \alpha$ ),
- retarded motion caused by the shortage of driving force, i.e. when  $F_N < F_{OP}$  coasting ( $F_N = 0$ ),
- braking with the use of brakes causing the dissipation of kinetic energy [Silka 1995,1997,2002].

### ENERGY BALANCE OF THE CAR

In energy balance of the electric wheeled vehicle (covering a particular road section), the total energy delivered to the motor in the form of electric energy taken from  $E_{el}$  battery is the sum of: energy on propelled wheels (i.e. energy consumption of the motion) balancing resistance to motion, energy losses in the motor and in the system of propulsion transmission, and also energy consumed by the engine while idling, e.g. during braking or at stops. Thus:

$$E_{EL} = E + \Delta E_s + \Delta E_{pc} + \Delta E_j, \quad (1)$$

where:  $E$  - energy consumption of the motion,  $\Delta E_s$  - losses which occurred during the processing of energy in the motor,  $\Delta E_{pc}$  - losses which occurred during the transmission of energy from the motor to the propelled wheels,  $\Delta E_j$  - energy delivered to the motor while idling, i.e. without the transmission of propulsion to the wheels .

Energy consumption of the motion is the amount of propelling energy delivered to the wheels exclusively in the phases of propulsion; because while driving with the disconnected wheel propulsion, resistance to motion is overcome at the expense of kinetic energy acquired during acceleration. It follows that the drive forced by torque transmitted from the motor to the wheels is considered the basic condition of the wheeled vehicle motion; therefore energy consumption of the motion is an important energy parameter.

Energy consumption of the motion is the amount of energy used to overcome: rolling resistance  $E_t$ , air resistance  $E_p$ , grade resistance  $E_w$ , and also energy used to increase kinetic energy of the vehicle  $E_K$ :

$$E = E_t + E_p + E_w + E_K. \quad (2)$$

Contrary to rolling resistance and air resistance, which are always present, grade resistance appears periodically. Energy used to overcome this resistance is equal to the gain in potential energy of the vehicle and may be partially recovered while descending the slope; at the same time the battery is recharged.

While covering a longer section of the road with variable speed, when the speed profile consists of a series of modules (including acceleration, fixed motion and braking), energy consumption of the motion is determined by the sum:

$$E = \sum \int_0^{L_N} (F_{OP})_N ds + \sum E_K. \quad (3)$$

Kinetic energy and potential energy of the vehicle are acquired exclusively at the expense of energy delivered from the electric motor to the wheels, during acceleration and overcoming the slope, respectively. In retarded motion, depending on the type of forcing, resistance is overcome partly or wholly at the expense of kinetic energy. In the case of commonly used friction brakes, the process of braking consists in the dissipation of considerable amount of kinetic energy, which as

a result of friction changes into heat discharged into the environment. At the same time, the remaining part of this energy is used to overcome resistance to motion on the braking path. Substituting equation (2) to energy balance equation (1) leads to:

$$E_{EL} = E_t + E_p + E_w + E_K + \Delta E_s + \Delta E_{pc} + \Delta E_j. \quad (4)$$

Energy consumption of the motion, according to equation 2, is the sum of energy expenditure for overcoming resistance to motion and also for overcoming inertial force during acceleration. After the equivalence of work and energy has been taken into consideration, either component of energy consumption of the motion can be expressed as the product of force and distance:

$$E_t = mg \int_0^{L_N} f_t ds = \bar{F}_t L_N, \quad (5)$$

$$E_p = K \int_0^{L_N} v^2 ds = \bar{F}_p L_N, \quad (6)$$

$$E_w = mg \int_0^{L_{NW}} \sin \alpha ds = \bar{F}_w L_{NW}, \quad (7)$$

$$E_K = m\delta \int_0^{L_A} a ds = \bar{F}_b L_A, \quad (8)$$

where:  $a$  - acceleration,  $ds$  - path differential,  $f_t$  - rolling resistance coefficient,  $E_t$ ,  $E_p$ ,  $E_w$  - energy used to overcome resistance to the motion of rolling, air and grade, respectively,  $E_K$  - kinetic energy, - rolling, air and grade resistance, respectively, - force of inertia,  $K=c_x A \rho$  - air resistance coefficient,  $L_A$  - length of path in the acceleration phase,  $L_N$  - total length of path in the propelling phase,  $L_{NW}$  - length of path covered in overcoming the slope,  $m$  - vehicle mass,  $v$  - vehicle speed,  $\alpha$  - angle of longitudinal path inclination,  $\delta$  - coefficient of rotating masses.

In the most general case, the driving cycle consists of several modules with the speed profile as shown in Figure 1. Points u and p denote the beginning of the deceleration phase and braking phase, respectively (with the engine disconnected from the propulsion system); point k denotes the end of a given module and the beginning of the next.

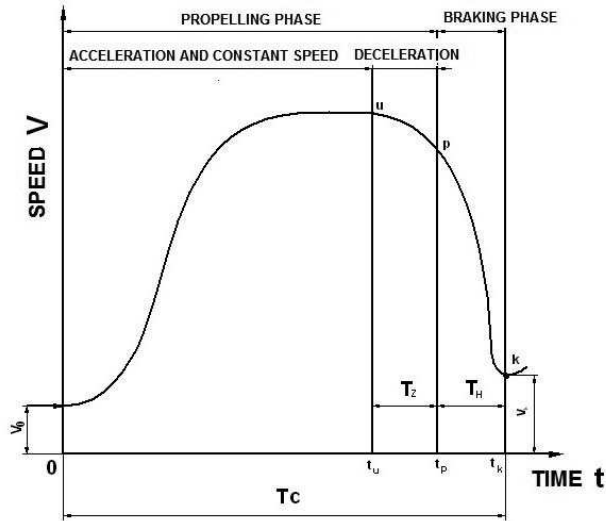


Fig. 1. Speed profile of a single module [Siłka 1998]

Where:

$0 \div t_u$  - acceleration phase + phase of driving at constant speed, subscript N,

$t_u \div t_p$  - deceleration phase, subscript Z,

$t_p \div t_k$  - braking phase, subscript H (where  $t_k = T_c$ ).

If these denotations are used, energy consumption in the motion of a single module equals:

$$E_i = mgf_i(L_N + L_z) + K(\vartheta_N L_N + \vartheta_z L_z) + m/2(v_p^2 - v_0^2), \quad (9)$$

where:  $f_i$  - rolling resistance coefficient,  $K$  - air resistance coefficient,  $L_z$  - path of deceleration phase,  $m$  - vehicle mass,  $\vartheta_N$  - mean square value of speed in the propelling phase,  $\vartheta_z$  - mean square value of speed in the deceleration phase.

The speed profile of a wheeled vehicle covering an adequately long section of the path consists of a bigger or smaller number of modules, depending on external factors, including features of the path and conditions of the motion. In such a case, energy consumption of the motion is the sum of energy consumptions of particular modules [Madej 2004, Prochowski 2005, Siłka 1998].

## EXPERIMENTAL STUDIES

In order to verify experimentally relationships between the parameters of speed profile and energy consumption per unit, road tests of the electric car model and the two-wheeled vehicle with electric propulsion were conducted in the Department of Motor Vehicles at the Technical University of Lublin. The tests comprised multiple drives of vehicles in real traffic conditions, according to various complex speed profiles, with a simultaneous registration of kinematic parameters of the motion and measurements of energy consumed by batteries.

During acceleration, due to the action of the forcing signal  $U$  on the electric vehicle, the flow of electric current with intensity  $I$  was initiated. The intensity of this process and the obtained final value of angular velocity  $\omega$  of the engine shaft (Fig. 2) depended on the value of applied voltage  $U$ , as well as on external and internal resistance to motion  $M_m$ . In the course of the experiment, the following values were recorded: voltage on battery terminals, angular velocity  $\omega$  of the engine shaft and the intensity of current  $I$  flowing in the electric circuit. The second controlling value, which is torque  $M_m$ , was not measured directly during the tests. It was determined from dependences (10) and (11).

$$M_m = F_t r + M_{STR}, \quad (10)$$

$$F_t = mgf_r, \quad (11)$$

where:  $F_t$ -rolling resistance,  $r$  - radius of the circle,  $M_{STR}$  - moment of internal losses in the power transmission system,  $m$  - total mass of the vehicle,  $g$ -gravitational acceleration,  $f_r$  - rolling resistance coefficient [Grzeżożek 2003, Merkisz 2007, Orzełowski 1995, Śmieszek 2000].

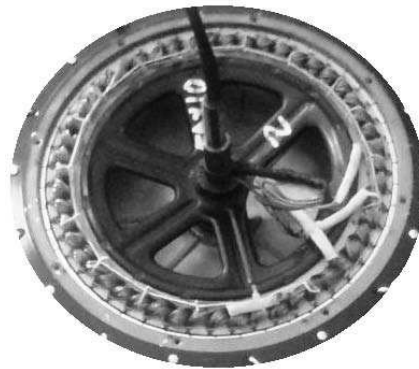


Fig. 2. View of the electric engine of the two-wheeled vehicle

In the course of conducted tests, besides direct measurements of voltage  $U$ , current intensity  $I$  and angular velocity  $\omega$  of the engine shaft, a number of additional steps were carried out. These steps were necessary to determine chosen structural parameters of the tested object, to verify proper operation of the measuring system, as well as to enable carrying out the process of estimation of some values occurring in dependences (10) and (11). Therefore, the studies which were carried out were divided into the following stages:

1. Preliminary studies. Within the range of these studies there were: the measurement of vehicle mass, determining parameters characterizing batteries used in tests, determining design parameters of vehicles, such as gears and rolling radius of wheels, and checking proper functioning of the measuring system.
2. The study of acceleration process and steady motion. These studies were carried out for different supply voltages and for different total masses of vehicles.
3. The coasting test. These tests consisted in accelerating vehicles with different total masses, and then determining motion retardation occurring during their free coasting.

For the purpose of registering data derived from measurements, a set consisting of the portable Notebook computer and the USB Basic data acquisition card ( 8ch, 14-Bit) from National

Instruments were used. The system was connected to the tested vehicle by means of electric wires. The view of the tested two-wheeled vehicle is shown in Figure 3.

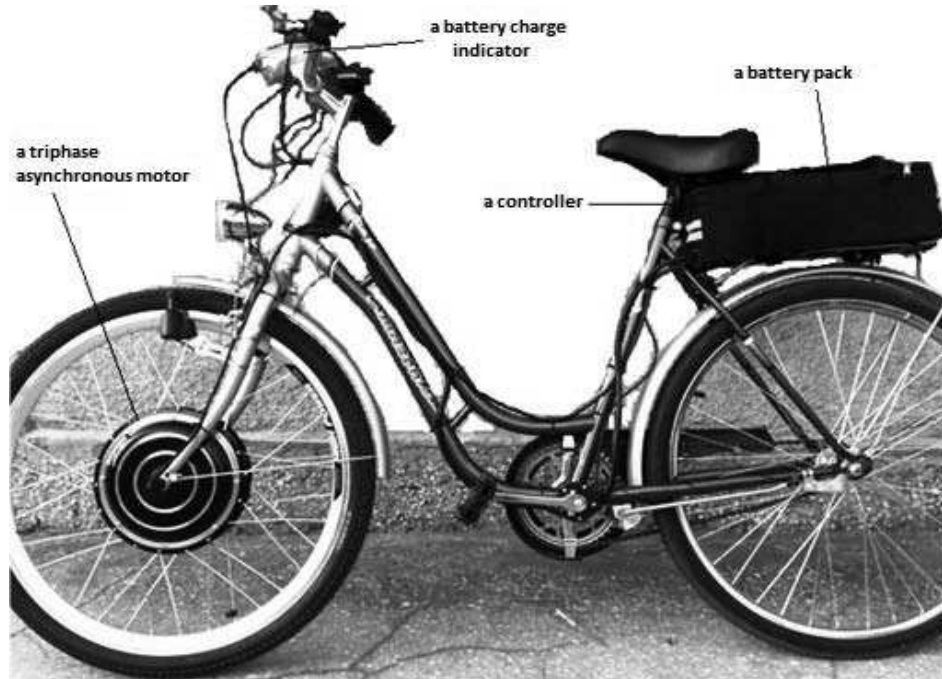


Fig. 3. View of the two-wheeled vehicle with electric power transmission system

## CONCLUSIONS

In conclusion, it can be stated that the studies which were carried out make it possible to determine energy consumption associated with the motion of the electric vehicle.

On the basis of carried out registration of supply voltage and current consumed by the motor and the control system, it is possible to determine the power drawn from the fully charged battery and the maximum range of the drive. In further research, procedures enabling the full use of properties of electric motors and electrochemical batteries in the realization of the motion with a complex speed profile will be worked out .

## REFERENCES

1. Grzeżożek W., Adamić-Wójcik I., Wojciech S.: Komputerowe modelowanie dynamiki pojazdów samochodowych, Wydawnictwo Politechniki Krakowskiej, Kraków 2003.
2. Madej J.: Teoria ruchu pojazdów szynowych, Oficyna Wydawnicza Politechniki Warszawskiej, Warszawa 2004.
3. Mamela J., Bról S., Jantos J.: Estymacja charakterystyk układu napędowego na podstawie pomiaru przyspieszenia samochodu, Wydawnictwo Politechniki Opolskiej, Opole 2008.

4. Merkisz J., Mazurek S., Pielecha J.: Pokładowe urządzenia rejestrujące w samochodach, Wydawnictwo Politechniki Poznańskiej, Poznań 2007.
5. Orzełowski S.: Eksperymentalne badania samochodów i ich zespołów, WNT, Warszawa 1995
6. Prochowski L.: Mechanika ruchu, WKŁ, Warszawa 2005.
7. Siłka W.: Analiza wpływu parametrów cyklu jezdnyego na energochłonność ruchu samochodu, PAN, Teka Komisji Naukowo-Problemovej Motoryzacji 1642-1639 z14, Kraków 1998.
8. Siłka W.: Analiza energochłonności ruchu samochodu ze zmienną prędkością, Wydawnictwo WSInż., Opole 1995.
9. Siłka W.: Energochłonność ruchu samochodu, WNT, Warszawa 1997.
10. Siłka W.: Teoria ruchu samochodu, WNT, Warszawa 2002.
11. Śmieszek M.: Ruch i zapotrzebowanie na energię automatycznie kierowanego pojazdu transportowego – kołowego robota mobilnego, Oficyna Wydawnicza Politechniki Rzeszowskiej, Rzeszów 2000.

#### ENERGOCHŁONNOŚĆ RUCHU POJAZDU Z NAPĘDEM ELEKTRYCZNYM

**Streszczenie.** W artykule rozważono bilans energetyczny pojazdu kołowego oraz podano szczegółową analizę czynników decydujących o energochłonności ruchu, obejmującą podstawowe fazy ruchu oraz różne przypadki realizacji przez pojazd złożonego profilu prędkości. Koncepcję przeprowadzenia bilansu energetycznego pojazdu z napędem elektrycznym przeprowadzono dla modelu samochodu z silnikiem elektrycznym prądu stałego oraz pojazdu jednośladowego z trójfazowym silnikiem asynchronicznym umieszczonym w przednim kole.

**Słowa kluczowe:** energochłonność, pojazd elektryczny, bilans energetyczny, napęd elektryczny.

## FORECAST MODELS OF ELECTRIC ENERGY CONSUMPTION BY VILLAGE RECIPIENTS OVER A LONG-TERM HORIZON BASED ON FUZZY LOGIC

Małgorzata Trojanowska<sup>\*)</sup>, Jerzy Małopolski<sup>\*\*)</sup>

Agricultural University of Cracow, Balicka Str. 116B, 30-149 Kraków, Poland

<sup>\*)</sup>Department of Power Engineering and Agricultural Processes Automation

<sup>\*\*)</sup>Department of Agricultural Engineering and Informatics,

e-mail: malgorzata.trojanowska@ur.krakow.pl; jerzy.malopolski@ur.krakow.pl

**Summary.** In this work, four fuzzy models of yearly electric energy consumption were constructed and differed from one another in the method of inference and/or the shape of the fuzzy set membership function. The suitability of models for forecasting was evaluated on the basis of analysis of acceptability and accuracy of forecasts determined based on the constructed models. The most accurate predictions were those determined on the basis of Mamdani model.

**Key words:** electric energy, long-term forecasting, fuzzy models.

### INTRODUCTION

Long-term forecasts of annual electric energy consumption by village recipients are of practical significance in technical as well as economic terms. They are the initial stage for planning strategic development of electric energy infrastructure in a given area. Changes in agricultural production and the living standards of villages require modernization and development of electric energy devices in villages. These alterations are becoming harder to predict under the conditions of the market economy, which often decreases the capability of executing a forecast of good quality for demand of electric energy over a long-term horizon.

A significant problem is also the acquisition and simulation of a sufficient amount of data. This problem arises when forecasts are carried out based on end-use or econometric models. This is why models based only on analysis of time series are used more often, but with the utilization of new tools and methods, such as the artificial intelligence method. Models built based on the artificial intelligence method can be very useful in cases where the principle describing cause and effect relationships in a given system is not known. Methods based on fuzzy logic belong to the group of artificial intelligence methods.

The aim of this work was to elaborate on fuzzy models of annual consumption of electric energy by village recipients and to evaluate the suitability of these models for long-term forecasting.

## MATERIAL AND METHODS

The realization of the aim of the work was carried out based on the statistics of electric energy sales by a selected distribution company from southeastern Poland.

The following fuzzy models of systems with one input and one output were considered in this work [Mamdani 1974, 1977; Małopolski, Trojanowska 2009a, 2009b; Mielczarski i in. 1998; Pedrycz 1984, 1993; Piegat 1999; Takagi, Sugeno 1985; Trojanowska, Małopolski 2004, 2007, 2009]: Mamdani models (M models) with Gaussian membership functions in the input space of the model, Takagi-Sugeno models (TSg models) with Gaussian membership functions in the input space of the model, Takagi-Sugeno models (TSt models) with trapezoidal membership functions in the input space of the model, relational models (Rel models) with trapezoidal and triangular membership functions in the input space of the model.

In these models, selection of the fuzzy set membership function as well as the methods of defuzzification was carried out, using the method discussed in the works of Trojanowska and Małopolski [2004, 2007, 2009a, 2009b].

## RESULTS

The experiments carried out so far of long-term forecasting have indicated that the set of input data from the history of the forecasted process should include at least 15 years [Dobrzańska 1998, 2002]. Shorter periods of observation do not make it possible to bring out the developmental dynamics of the process.

Figure 1 shows the course of yearly electric energy consumption by recipients from the rural regions of southeastern Poland over the next 26 years. During this period of time, the consumption of electric energy was initially characterized by a significant rising trend, as a result of which the demand for energy increased nearly two-fold over 6 years. After that period, the consumption of electric energy began to decrease. The increasing trend soon recurred, but it was so slight that only now have sales of electric energy to village recipients by the studied distribution company reached the level from over twenty years before.

In the work, among 26 sets of data regarding yearly consumption of electric energy, 22 were used for construction of forecasting models and verifications of acceptability of forecasts calculated on the basis of these models. The last four sets of data served to evaluate the accuracy of forecasts.

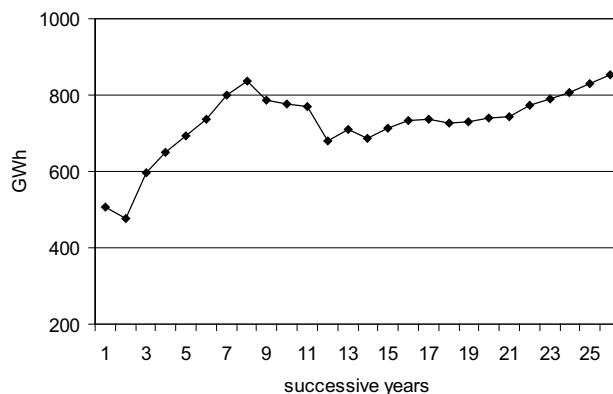


Fig. 1. The course of annual consumption of electric energy by village recipients in southeastern Poland



Due to the nonstationary course of yearly consumption of electric energy, fuzzy models describing the functional dependency  $y = f(x)$  were determined, where  $y$  is the increment of electric energy consumption during a given year, and  $x$  is the increment of consumption of electric energy in the previous year. The method of coupled gradients was used for the optimization of the fixed structure model [Osowski 1996], and the constructive principle was used for the selection of the best model [Piegat 1999].

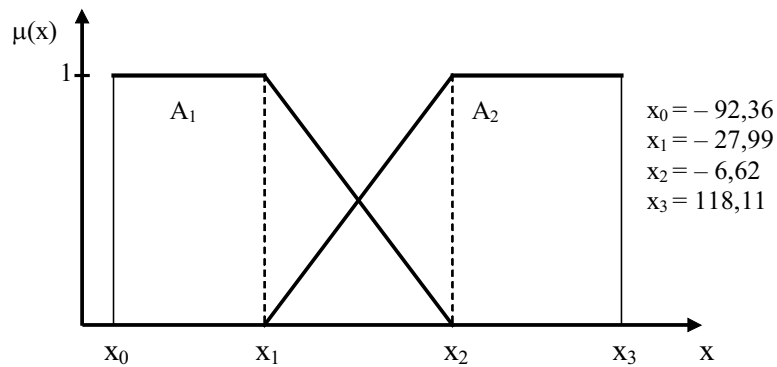
The rule bases in the open form of the Mamdani model are as follows:

$$\begin{aligned} \text{R1: IF } (x \text{ near } -38,31) \text{ THEN } (y \text{ near } 25,55), & \quad (1) \\ \text{R2: IF } (x \text{ near } -4,74) \text{ THEN } (y \text{ near } -92,36), & \\ \text{R3: IF } (x \text{ near } -1,37) \text{ THEN } (y \text{ near } -92,36), & \\ \text{R4: IF } (x \text{ near } 38,60) \text{ THEN } (y \text{ near } -45,31), & \\ \text{R5: IF } (x \text{ near } 42,48) \text{ THEN } (y \text{ near } 54,76), & \end{aligned}$$

and for the Takagi-Sugeno model with Gaussian membership functions in the input space of the model:

$$\begin{aligned} \text{R1: IF } (x \text{ near } -14,09) \text{ THEN } (y = 39,68 + 0,12x), & \quad (2) \\ \text{R2: IF } (x \text{ near } -2,61) \text{ THEN } (y = -154,73 + 1,35x), & \\ \text{R3: IF } (x \text{ near } 4,86) \text{ THEN } (y = 24,13 - 1,49x). & \end{aligned}$$

The courses of membership functions and rule bases of the TSt type Takagi-Sugeno model are shown in Figure 2, and those of the relational model in Figure 3.



$$\begin{aligned} \text{R1: IF } (x \text{ is } A_1) \text{ THEN } (y = 91,17 + 0,85x) & \quad (3) \\ \text{R2: IF } (x \text{ is } A_2) \text{ THEN } (y = -15,89 + 0,75x) & \end{aligned}$$

Fig. 2. Courses of membership functions and rule base for the Takagi-Sugeno model (TSt)

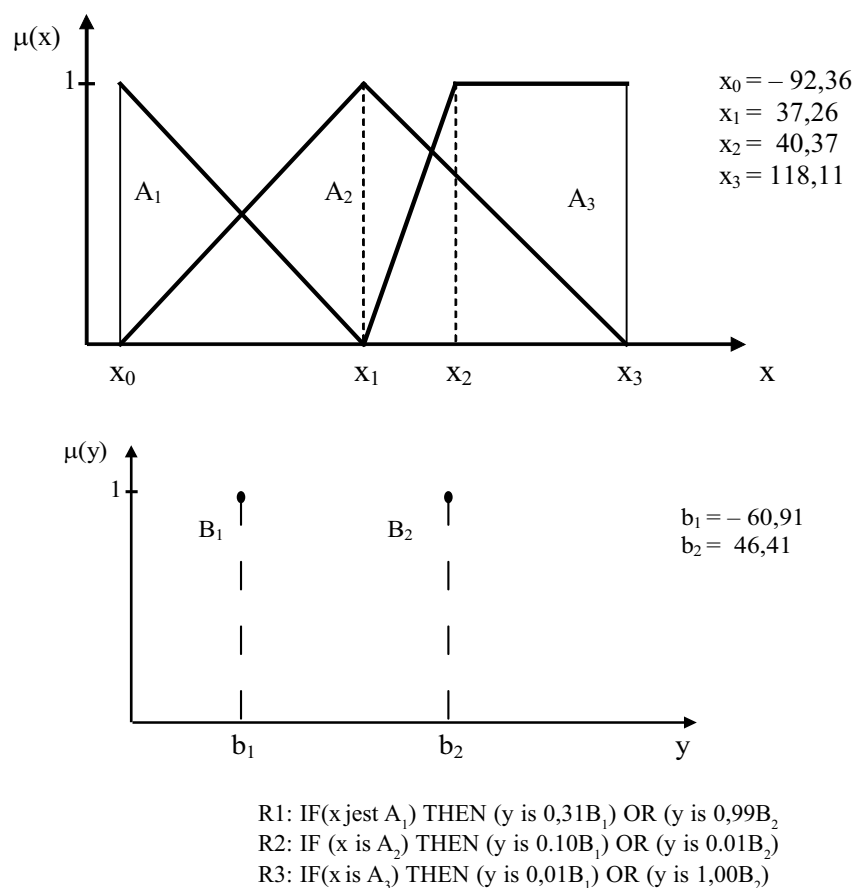


Fig. 3. Courses of membership functions and rule base for the relational model

### MODELING CONSUMPTION OF ELECTRIC ENERGY EVALUATION OF FORECAST QUALITY

#### Forecast acceptability

Within the scope of evaluation of acceptability of forecasts of electric energy consumption, the results of the executed forecasting procedures were compared with real process executions. Specifically, time courses of the determined real consumption of electric energy and expired forecasts of this consumption based on the constructed models were observed through analysis of their matching (Fig. 4), and the mean absolute percentage error (MAPE) values were determined as the most often used measurement of acceptability of electric energy demand forecasts.

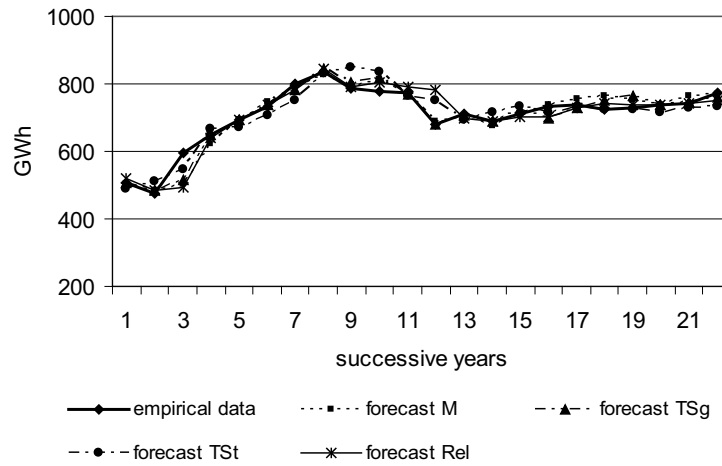


Fig. 4. Expired forecasts of annual electric energy consumption

Errors were determined from the dependency [Dittman 2002]:

$$MAPE = \frac{1}{n} \sum_{t=1}^n \frac{|y_t - \hat{y}_t|}{y_t} \cdot 100 \quad (5)$$

where:  $y_t$  - real electric energy consumption during year  $t$ ,  
 $\hat{y}_t$  - electric energy consumption forecast for the year  $t$ ,  
 $n$  - number of observations used for elaboration of the model ( $n=22$  years).

The values of these errors are listed in Table 1. The errors of all forecasts are slight, which confirms the satisfactory matching of all the models to the real sales of electric energy, allowing for the acknowledgement of all the elaborated forecasts as being acceptable.

Table 1. Comparison of the acceptability of forecasts of yearly consumption of electric energy

Model	M	TSg	TSt	Rel
MAPE [%]	2,23	2,10	3,87	2,86

### Forecast accuracy

The accuracy of forecasts is determined after the expiration of the period for which the forecast was determined, and the degree of forecast accuracy is measured using ex post errors [Cieślak 1999].

In the work, the Theil coefficient ( $I^2$ ) and the Janus coefficient ( $J^2$ ) were used for evaluation of forecast accuracy along with the MAPE error, which was determined for the empirical range of forecast verification.

The Theil coefficient was calculated from the dependency [Zeliaś i in. 2004]:

$$I^2 = \frac{\sum_{t=n+1}^T (y_t - y_t^*)^2}{\sum_{t=n+1}^T y_t^2}, \quad (6)$$

where:  $y_t^*$  - forecast of electric energy consumption for the period  $t > 22$  years,  $T=26$  years.

$\sqrt{I^2}$  provides information of what the total relative prediction error is during the period of empirical forecast verification, without regard as to what caused this error.

In turn, the Janus coefficient serves to test the validity of the model and is described by the formula [Zeliaś i in. 2004]:

$$J^2 = \frac{\frac{1}{T-n} \sum_{t=n+1}^T (y_t - y_t^*)^2}{\frac{1}{n} \sum_{t=1}^n (y_t - \hat{y}_t)^2}. \quad (7)$$

A comparison of forecast accuracy is included in Table 2.

Table 2. Comparison of the accuracy of forecasts of yearly consumption of electric energy

Year	Real value	Model M	Model TSg	Model TSt	Model Rel
23	791,321 GWh	797,422 GWh	754,211 GWh	777,025 GWh	756,588 GWh
24	807,689 GWh	816,872 GWh	786,432 GWh	790,042 GWh	788,261 GWh
25	831,212 GWh	833,24 GWh	807,398 GWh	804,094 GWh	807,474 GWh
26	853,328 GWh	856,763 GWh	820,247 GWh	832,993 GWh	823,349 GWh
MAPE	-	0,64 %	3,52 %	2,41 %	3,29 %
I	-	0,71 %	3,60 %	2,48 %	3,36 %
J <sup>2</sup>	-	0,01	0,25	0,12	0,22

The executed calculations showed that all the estimated models are still valid ( $J \leq 1$ ) and in each case, the main reason for the occurrence of forecast errors was prediction load (at 78 to 96 percent).

Analysis of prediction accuracy was decidedly the most advantageous for forecasts determined based on the Mamdani model. In this case, 78% of the slight ex post total forecast error was caused by prediction load, approx. 9% by insufficient forecasting elasticity, and 13% by insufficient prediction of turning points.

Despite the small forecasting ex post error determined based on the Mamdani model, it can be considered as what should be done for forecasts made using this method to be even more accurate, all the more that full correctness was observed. It was proven that all four forecasts were overestimated (Fig. 5). Forecasts can then be simply corrected, e.g. through decreasing each forecast by the mean value of the observed prediction load, that is by about 5.2 GWh.

Correction of the forecast (Fig. 3) caused a decrease of all standards of forecast quality (MAPE=0.30%, I=0.33%,  $J^2=0.002$ ).

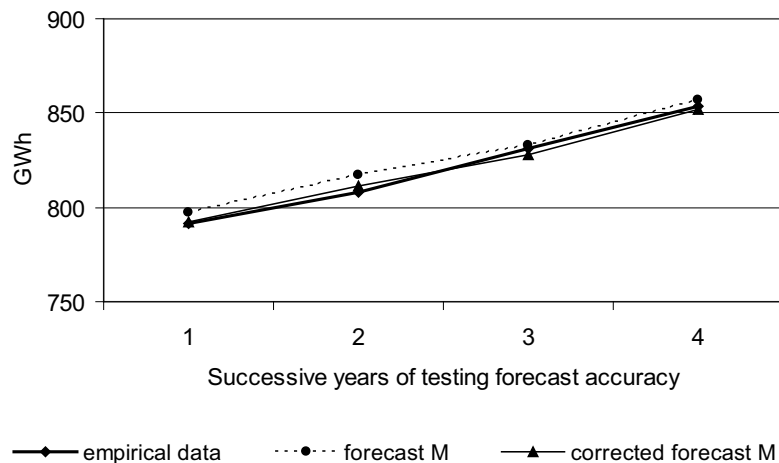


Fig. 5. Courses of yearly real electric energy consumption and forecasts before and after correction during the period of empirical forecast verification

## CONCLUSIONS

The obtained test results confirmed the suitability of the fuzzy forecast models with Mamdani, Takagi-Sugeno and relational inference types presented in the work for prediction of annual demand for electric energy of village recipients. All the determined forecasts based on the elaborated models can be acknowledged as good due to the fact that ex post forecasting errors did not exceed 5%. The overwhelming majority of these errors were caused by prediction load, which can easily be overcome.

Out of all the forecasts, the ones that were decidedly the most accurate were proven to be those determined based on Mamdani models.

## REFERENCES

1. Cieślak M. (red.). 1999.: Prognozowanie gospodarcze. Metody i zastosowania. WN PWN Warszawa.
2. Dittman P. 2003.: Prognozowanie w przedsiębiorstwie. Oficyna Ekonomiczna, Kraków.
3. Dobrzańska I. 1998.: Prognozowanie elektroenergetyczne w świetle wymagań kodeksu planowania rozwoju systemu przesyłowego. Materiały V Konferencji Naukowo-Technicznej: Rynek energii elektrycznej REE'98. Nałęczów, 323 – 326.
4. Dobrzańska I. (red.). 2002.: Prognozowanie w elektroenergetyce. Zagadnienia wybrane. Wyd. Pol. Częstochowskiej, Częstochowa.
5. Małopolski J., Trojanowska M. 2009a.: Modele rozmyte zapotrzebowania na moc dla potrzeb krótkoterminowego prognozowania zużycia energii elektrycznej na wsi. Część I. Algorytmy wyznaczania modeli rozmytych. Inżynieria Rolnicza 5 (114), 185-191.
6. Małopolski J., Trojanowska M. 2009b.: Modele rozmyte zapotrzebowania na moc dla potrzeb krótkoterminowego prognozowania zużycia energii elektrycznej na wsi. Część II. Opracowanie predykcyjnych modeli relacyjnych. Inżynieria Rolnicza 5 (114), 185-191.

7. Mamdani E. H. 1974.: Applications of fuzzy algorithms for control of simple dynamic plant. Proceedings IEEE , No. 121(12). s. 1585–1588.
8. Mamdani E. H. 1977.: Applications of fuzzy algorithms to approximate reasoning using linguistic synthesis. IEEE Transactions on Computers 1977, vol. C–26, No.12. s. 1181–1182.
9. Mielczarski W., Michalik G., Khan M.E. 1998.: Fuzzy modeling of load demand in the residential systems. Heidelberg, New York.
10. Piegat A. 1999.: Modelowanie i sterowanie rozmyte. AOW EXIT. Warszawa.
11. Osowski S. 1996.: Sieci neuronowe w ujęciu algorytmicznym. WNT. Warszawa.
12. Pedrycz W. 1984.: An identification algorithm in fuzzy relational systems. Fuzzy Sets and Systems, No. 13, 153–167.
13. Pedrycz W. 1993.: Fuzzy control and fuzzy systems. New York: John Wiley and Sons.
14. Takagi T. Sugeno M. 1985.: Fuzzy identification of systems and its applications to modeling and control. IEEE Transactions on Systems, Man, and Cybernetics, vol. 15, No. 1, pp. 116-132.
15. Trojanowska M., Małopolski J. 2004.: Zastosowanie teorii zbiorów rozmytych w prognozowaniu zapotrzebowania na energię elektryczną na terenach wiejskich. Inżynieria Rolnicza nr 4 (59), 263-267.
16. Trojanowska M., Małopolski J. 2007.: Krótkoterminowe prognozowanie zapotrzebowania na energię elektryczną odbiorców wiejskich przy wykorzystaniu modeli Mamdaniego. Problemy Inżynierii Rolniczej nr 3, 35-42.
17. Trojanowska M., Małopolski J. 2009.: Wykorzystanie modeli Takagi-Sugeno do krótkoterminowego prognozowania zapotrzebowania na energię elektryczną odbiorców wiejskich. Inżynieria Rolnicza nr 1 (110), s. 325-330.
18. Zeliaś A., Pawełek B., Wanat S. 2004.: Prognozowanie ekonomiczne. WN PWN Warszawa.

#### MODELE PROGNOSTYCZNE ZUŻYCIA ENERGII ELEKTRYCZNEJ PRZEZ ODBIORCÓW WIEJSKICH W DŁUGIM HORYZONCIE CZASOWYM OPARTE NA LOGICE ROZMYTEJ

**Streszczenie.** W pracy zbudowano cztery modele rozmyte rocznego zużycia energii elektrycznej różniące się między sobą typem wnioskowania lub/i kształtem funkcji przynależności zbiorów rozmytych. Przydatność modeli do predykcji oceniono na podstawie analizy dopuszczalności i trafności prognoz wyznaczonych w oparciu o zbudowane modele.

Najbardziej trafne okazały się prognozy wyznaczone w oparciu o modele Mamdaniego.

**Słowa kluczowe:** energia elektryczna, prognozowanie długoterminowe, modele rozmyte.

## THE ANALYSIS OF MIXING DEGREE OF GRANULAR PRODUCTS WITH THE USE OF MICROTRACERS

Kazimierz Zawiaślak, Józef Grochowicz\*, Paweł Sobczak

Department of Food Engineering and Machines, University of Life Sciences in Lublin, Poland  
Doświadczalna 44, 20-236 Lublin, e-mail: kazimierz.zawislak@up.lublin.pl

\*University of Hotel Catering and Tourism Management, Warsaw, Poland

**Summary.** Paper presents the results of investigations on the mixing process of six mineral blends of similar physical properties. Mixing process was realized in the mixers of various construction and capacity. Different mixing duration and filling degree of the mixers were used. The uniformity of mixtures was determined indirectly, by means of microtracers introduced into mixture: the uniformity of their distribution in mixed material was determined after each mixing cycle.

**Keywords:** mixing, homogeneity, microtracers.

### INTRODUCTION

Mixing of loose, granular materials is a very complex process, where the mixed compounds are distributed by random, chaotic motion of the particles. Mixing process is realized in various mixers, different in the type, shape of agitator, technological parameters etc. [Boss 1987, Dreszer et al. 2007].

Mixing process is strongly affected by the physical properties (such as the density, moisture content, average particle size, the angle of repose, slip angle and shape of the particles) of the components. Moreover, the kinetics of mixing process depends on its realization conditions as well as on the construction of mixing assembly [Rachowiecki A. 1991, Grochowicz, Walczyński 2004, Kulig, Laskowski 2008, Dżiki, Laskowski 2006].

The objective of mixing process consists in achieving such a state of mixture where its particles are situated in random positions. After achieving the maximum mixing degree, obtained system often stratifies tending to stable equilibrium state, where the particles of the same physical properties take up a definite location in the bed. Such a phenomenon is defined as segregation [Williams 1976]. Basic parameter to evaluating the quality of this process is the mixing degree that may be described [Rose 1959], by the relationship:

$$M = 1 - \frac{s}{\sigma_0}, \quad (1)$$

where:

M – mixing degree,  
 s – standard deviation after mixing,  
 $\sigma_0$  – standard deviation in state of primary segregation.

The numerical value of mixing degree ranges within the interval from 0 to 1, where value 0 denotes the mixture non-mixed, while value 1 – the system perfectly mixed. Adequate definition of the quality scale may be expressed by evaluation of the mixing state [Boss 1987].

The kinetic model of mixing process for heterogenous grainy materials was also proposed [Rose 1959]:

$$\frac{dM}{dt} = A(1 - M) - B\phi, \quad (2)$$

where:

M – mixing degree,  
 A i B – constants depended on the mixed compounds,  
 $\Phi$  – potential of segregation.

According to Rose, the potential of segregation may range within  $-1$  and  $+1$ ; depending on the initial compound distribution in the mixer and its relation with mixing degree, the M may be expressed as follows:

$$M = 1 - \Phi^2. \quad (3)$$

In investigations on evaluating the mixing degree, the proper material sampling and sample analysis are an important factor. Sampling should be representative, what is attainable only at an assumption that the samples were taken from measuring points uniformly distributed in whole volume of the mixture. The problems of sampling and sample analysis were considered by a number of scientists [Ciftici et al. 2002, Eisenberg et al. 1992, Heidenreich et al. 2000, Laurent et al. 2002, Lindley 1991].

The accuracy of mixing process analysis depends also on the size of tested sample. In feed processing industry the size of material sample is specified by adequate standard regulations [Kwiatk et al. 2004, Matuszek, Tukiendorf 2008]. Boss determined the condition of minimum sample dimension i.e. it must contain at least as many particles that, in case of ideal mixing, the component occurring in lowest concentration is represented in the sample by at least one particle. Therefore, the small samples provide a strong dispersion, whereas too much ones may suggest better homogenization of the mixture than it really is [Boss 1987, Williams 1976, Putier 2001].

Usually the mixtures used in feed processing industry are multicomponent, where each component represents different physical properties; thus, achieving their satisfactory blend may be often very difficult. Determination of basic mixing parameters, such as mixing duration for given type of the mixer, is an important element deciding on the quality of final product [Fan 1970, Rollins et al. 1995, Królczyk, Tukiendorf 2008].

## OBJECTIVE OF RESEARCH

The studies aimed at checking the possibilities of evaluating feed mixture homogeneity with the use of Mocrotracer<sup>TM</sup> F – Blue.










MATERIALS AND METHODS

Investigations were carried out in four horizontal band mixers and one vertical conical of planetary type. According to technical specification mixing effectiveness of the machines was 1:10000.

Tests were conducted in accordance with the ASAE Standard (No.S303) describing the testing procedures of mixing effects. According to this procedure from each batch of mixed material 10 samples of 80 g weight were taken.

The Microtracer™ F-Blue at a rate of 50g per 1 ton of mixture was used for tracing. 1 g of microtracer contains 25000 particles. At such a number of particles and 100% mixture homogeneity, a 80g mixture sample should contain 100 microtracer particles. Specific characteristics are showed in the table 1.

Table 1. Amount and mass of microtracers

Kind of microtracer	Mass of 100 units [g]	The biggest size [mm]	Photo	
Blue	0,0029 0,0029 0,0029 0,0031	505,30		
		288,22		
		416,16		
		246,09		
		543,25		
		259,67		
		288,02		
239,13				
Average	<b>0,00295</b>	<b>348,23</b>		
Standard deviation	0,0000086	114,4132		
Red	0,0034 0,0032 0,0034 0,0029	296,35		
		301,61		
		281,02		
		264,00		
		343,02		
		182,04		
		156,74		
Average	<b>0,003225</b>	<b>260,6829</b>		
Standard deviation	0,000204634	62,26671		

The microtracer, after initial mixing with soyabean meal was supplied directly to the mixer just after its filling. Samples of 80g weight taken for determination of the mixing degree were sepa-

rated in the Rotary Detector (model BL-89, series XO-7) for snatching the microtracers. The tracer test involves pouring a feed sample through a "Rotary Detector" laboratory magnetic separator isolating the tracer on a small filter paper. For a quantitative estimate of the tracer and by inference the medication, one demagnetizes the magnetic material and sprinkles it onto a larger filter paper wetted with the appropriate developer (50% ethanol) to yield a paper with countable spots.

Material for tests included the mixtures marked by letters: A, B, F.

Scope of the tests:

- mineral mixtures A and B, mixing duration – 3, 5 and 7 minutes, mixer capacity 400 liters, horizontal mixer, filling 100%,
- mineral mixture F, mixing duration 5, 6, 7, 8, 10 min., mixer capacity 1500 liters, horizontal mixture, filling 100%.

Following physical parameters were determined for all the mixtures: angle of repose, slip angle, bulk density, shaken density, moisture content, mean geometric size of the particle.

Obtained measurement results were statistically analyzed and variation coefficient was determined as a criterial value evaluating the quality of mixing process.

Time of emptying was checked for all the mixers, next the frequency of sampling was assigned.

Exceptionally, the samples for determination of the mixing degree from mixture marked by letter A were received at constant capacity. It allows to determine the whole received sample.

## RESULTS AND DISCUSSION

Selected physical parameters of the mixtures tested, significant for the process of mixing are presented in table 2. The test were carried out in accordance with obligatory standards.

Table 2. Physical characteristics of investigated mixtures

Mixture	Angle of repose [°]	Slip angle [°]	Bulk density [kg·m <sup>-3</sup> ]	Shaken density [kg·m <sup>-3</sup> ]	Moisture content [%]	Mean geometric size of particle d <sub>g</sub> [mm]
A	38	24,50	1448	1468	2,10	0,42
B	37	23,75	1235	1270	1,95	0,47
F	30	33	1188	1237	2,3	0,49

Mean geometric size of the particle tested mixtures ranged from 0,42 to 0,49 mm, whereas the bulk density was within the range of 1188 – 1448 kg·m<sup>-3</sup>. Above results enabled to count the tested mixtures among powdery products.

**Measuring results of mixing efficiency – mixture A** Table 3 presents the investigation results concerning the occurrence of microtracer particles in the samples and calculated on this basis variation coefficients for the tested mixture.

Obtained results showed that the optimum mixing duration enabling to get homogenous product for the mixture of given raw material composition, amounts to 5 min. Either, the shortening of mixing time or its elongation cause a disadvantageous changes in mixture homogeneity.

Table 3. Number of microtracer particles in particular samples – the mixture A

Sample	Number of microtracer particles in the sample		
	4min.	5min.	7min.
1	153	157	153
2	156	140	152
3	165	134	157
4	157	158	175
5	137	152	137
6	129	134	142
7	157	130	161
8	168	159	138
9	177	139	134
10	130	147	146
Mean	152,9	145	149,5
SD	16,148	11,005	12,713
CV	<b>10,561</b>	<b>7,5897</b>	<b>8,5034</b>

#### Test results for the mixture B

The results of testing the homogeneity of mixture B are given in tables 4 and 5.

Table 4. Number of microtracer particles in particular samples after mixing over 4 min – the mixture B

Sample	Number of microtracer particles in the sample		
	4 min.	5 min.	7 min.
1	103	108	117
2	123	110	105
3	93	121	100

4	121	125	108
5	91	123	99
6	92	91	115
7	79	100	106
8	114	110	123
9	132	117	125
10	114	107	125
Mean	<i>106,2</i>	<i>111,2</i>	<i>112,3</i>
SD	17,145	10,665	10,034
CV	<b>16,144</b>	<b>9,5905</b>	<b>8,9348</b>

#### Testing results for mixture F

Investigations included several mixing durations, i.e. 5, 6, 7, 8, 10 min. in order to assign the time necessary to getting the homogeneity consistent with the standard requirements for premixes. The results are presented in table 5.

Table 5. Values of CV coefficient for particular mixing duration of the mixture F

Sample/mixing duration	5	6	7	8	10
	Number of microtracer particles				
1	73	101	86	126	86
2	85	81	92	112	107
3	85	103	129	113	89
4	93	108	97	115	99
5	128	106	92	98	83
6	94	106	99	107	101
7	133	112	91	106	118
8	109	89	91	99	101
9	105	85	87	96	77
10	81	90	78	105	103
Mean	<i>98,6</i>	<i>98,1</i>	<i>94,2</i>	<i>107,7</i>	<i>96,4</i>
SD	19,957	10,857	13,555	9,1415	12,429
CV	<b>20,24</b>	<b>11,067</b>	<b>14,389</b>	<b>8,4879</b>	<b>12,894</b>

The test results showed that the adequate homogeneity characterized by CV below 10% was achieved after 8 min. mixing duration (table 5). Thus, it is suggested – at production of premixes in tested mixer type – to employ the mixing duration of 8 min.

## CONCLUSIONS

The investigations concerning determination of homogeneity for 6 mixtures from mixtures from various mixers by means of the microtracers showed that this method is useful to analysis of mixing process in production plants. The method enables fast reaction during technological process running, thus it eliminates the risk of producing mixtures of non-standard parameters.

## REFERENCES

1. Boss J. 1987.: Mixing of grainy material. PWN. Warsaw, Poland.
2. Ciftici I., Ercan A. 2002.: Effect of diets with different mixing homogeneity on performance and carcass traits of broilers. Department of Animal Science, Ankara University, Turkey, 1-14.
3. Dreszer K., Pawłowski T., Zagajski P. 2007.: The process of grain relocation with screw conveyors. TEKA Kom. Mot. Energ. Roln., 7, 86-96.
4. Dżiki D., Laskowski J. 2006.: Influence of wheat grain mechanical properties on grinding energy requirements. TEKA Kom. Mot. Energ. Roln., 6A, 45-52.
5. Eisenberg S. and Eisenberg D., 1992.: Closer to perfection. Feed Management, 11, 8-20.
6. Fan L.T., Chen S.J., Watson C.A. 1970.: Solid mixing. Ind. Eng. Chem, 62, 7, 53-69.
7. Grochowicz J., Walczyński S. 2004.: The effect of some technological factors on the consumption of energy at mixing granular materials. TEKA Kom. Mot. Energ. Roln., 4, 71-76.
8. Heidenreich E., Strauch W. 2000.: Decisive factors for solids mixing process in compound feed production. Part 2. Feed Magazine, 7-8, 286-292.
9. Królczyk J., Tukiendorf M. 2008.: Research on the impact of mass fractions of multi-element granular structure on the mixing process. Int. Agrophysics, 22, 45-52.
10. Kulig R., Laskowski J. 2008.: Energy requirements for pelleting of chosen feed materials with relation to the material coarseness. TEKA Kom. Mot. Energ. Roln., 8, 115-120.
11. Kwiatek K. and Korol W. 2004.: Base of sample receiving for animal feeding In laboratory scale. Feed Industry, 9, 9-14.
12. Laurent B.F.C., Bridgwater J., Parker D.J. 2002.: Convection and segregation in a horizontal mixer. Powder Technology, 123, 9-18.
13. Lindley J.A. 1991. Mixing processes for agricultural and food materials: 1 Fundamentals of mixing. J. Agric. Eng. Res., 48, 153-170.
14. Matuszek D., Tukiendorf M. 2008.: Application of roof shaped and double cone inserts in mixing of granular elements in the flow process. Int. Agrophysics, 22, 147-150.
15. Putier F. 2001.: Assessment of homogeneity of compound feed. Feed Magazine, 3, 98-108.
16. Rachowiecki A. 1991.: Stochastic model of grainy mixers segregation. Scientific Books of Polytechnic in Szczecin, 30, 83-89.
17. Rollins D.K., Faust D.L., Jabas D. 1995.: A superior approach to indices in determining mixture segregation. Powder Technology, 84, 277-282.
18. Rose H.E. 1959.: A suggested equation relating to the mixing of powders and its application to the study of the performance of certain types of machine. Trans. Inst. Chem. Eng, 37, 47-64.
19. Standard ASAE no S303.

20. Williams J.C. 1976.: The segregation of the particle materials. A Review, Powder Technology, 15, 245-251.

#### ANALIZA STOPNIA WYMIESZANIA PRODUKTÓW SYPKICH Z ZASTOSOWANIEM MIKROSKAŹNIKÓW

**Streszczenie.** W pracy przedstawiono wyniki badań procesu mieszania sześciu mieszanek mineralnych o zbliżonych właściwościach fizycznych. Proces mieszania prowadzono w mieszarkach o różnej pojemności i konstrukcji. Stosowano różne czasy mieszania i stopnie wypełnienia mieszarki. Jednorodność mieszanek określano pośrednio przez wprowadzenie do mieszanki mikroskaźników (microtracers) i oznaczenie równomierności ich rozmieszczenia po cyklu zmieszania.

**Słowa kluczowe:** mieszanie, homogenność, mikroskaźniki.

## OIL PRESSURE DISTRIBUTION IN VARIABLE HEIGHT GAPS

Tadeusz Złoto, Konrad Kowalski

Institute of Machine Technology and Production Automation  
Czestochowa University of Technology

**Summary.** The paper deals with problems connected with oil flow in variable height gaps in hydraulic machines. On the basis of the Navier-Stokes equations and the continuity equation, equations describing pressure in the gap were determined. The results of calculating pressure distribution in variable height gaps (both confuser and diffuser types) are presented, depending on oil viscosity and relative motion of one of the gap walls.

**Key words:** variable-height gap, hydraulic oil, pressure distribution.

### INTRODUCTION

In pumps and engines within hydraulic systems pairs of surfaces can be found separated by gaps filled with oil [Ivantysyn and Ivantysynova 2001, Stryczek 1984]. Phenomena occurring in the gaps affect the operation of hydraulic systems, for instance energy loss affects the overall efficiency. Thus, taking such factors into consideration is essential in designing hydraulic machines [Lasaar 2000, Osiecki 2004, Podolski 1981, Szydelski and Olechowicz 1986].

A gap in hydraulic machines is an oil-filled space between the two surfaces of neighbouring parts. The distance between the surfaces, referred to as height, is typically of a few micrometers size and of various shapes [Baszta 1966, 1971].

The liquid flow in the gap is a leakage, which can occur in the following cases:

- when there is a pressure difference between the two ends of the gap, in which case it is a pressure flow;
- when one of the surfaces moves with respect to the other, in which case it is a friction flow;
- when pressure difference and surface motion co-occur, in which case it is a pressure-friction flow [Nikitin 1982].

Fig. 1 presents a division of flat gaps. A parallel positioning of the surfaces is an ideal case, but in practice, due to manufacturing imprecision or load asymmetry, variable-height gaps are much more frequent. Among the variable-height gaps, confuser gaps can be distinguished, in which the height decreases with the flow direction, and diffuser gaps, in which the height increases with the flow direction [Trifonow 1974].

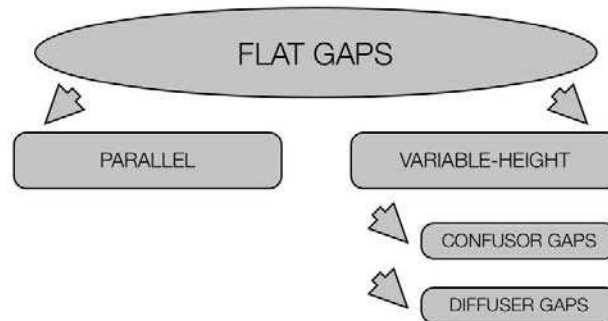


Fig. 1. Division of flat gaps

#### APPLYING THE NAVIER-STOKES EQUATIONS FOR DETERMINING OIL PRESSURE DISTRIBUTION IN A GAP

Fluid motion is described by means of the Navier-Stokes equations, also known as the motion equations, or the momentum equations. Usually, the flow continuity equation is also applied. For an oil-filled flat gap, it is most convenient to represent those equations in the Cartesian coordinate system  $x, y, z$  as [ Kondakow 1975, Osipow 1966]:

$$\frac{\partial v_x}{\partial t} + v_x \frac{\partial v_x}{\partial x} + v_y \frac{\partial v_x}{\partial y} + v_z \frac{\partial v_x}{\partial z} = \nu \left( \frac{\partial^2 v_x}{\partial x^2} + \frac{\partial^2 v_x}{\partial y^2} + \frac{\partial^2 v_x}{\partial z^2} \right) - \frac{1}{\rho} \frac{\partial p}{\partial x}, \quad (1)$$

$$\frac{\partial v_y}{\partial t} + v_x \frac{\partial v_y}{\partial x} + v_y \frac{\partial v_y}{\partial y} + v_z \frac{\partial v_y}{\partial z} = \nu \left( \frac{\partial^2 v_y}{\partial x^2} + \frac{\partial^2 v_y}{\partial y^2} + \frac{\partial^2 v_y}{\partial z^2} \right) - \frac{1}{\rho} \frac{\partial p}{\partial y}, \quad (2)$$

$$\frac{\partial v_z}{\partial t} + v_x \frac{\partial v_z}{\partial x} + v_y \frac{\partial v_z}{\partial y} + v_z \frac{\partial v_z}{\partial z} = \nu \left( \frac{\partial^2 v_z}{\partial x^2} + \frac{\partial^2 v_z}{\partial y^2} + \frac{\partial^2 v_z}{\partial z^2} \right) - \frac{1}{\rho} \frac{\partial p}{\partial z}. \quad (3)$$

The left-hand sides of equations (1 ÷ 3) represent the inertia forces of the operating agent whereas the right-hand sides represent viscosity forces and pressure of oil [Bukowski 1975, Walczak 2006].

The continuity equation is:

$$\frac{\partial v_x}{\partial x} + \frac{\partial v_y}{\partial y} + \frac{\partial v_z}{\partial z} = 0. \quad (4)$$

On the basis of Fig. 2 the current height  $h$  of the gap was determined at the distance  $x$  from the beginning of the coordinate system:

$$h = (h_2 - h_1) \frac{x}{l} + h_1. \quad (5)$$



Assuming that the oil flows in the direction of the  $x$  axis, the gap type depends on the heights  $h_1$  and  $h_2$ . If  $h_1 > h_2$ , it is a confusor gap, if  $h_1 < h_2$ , it is a diffuser gap. If  $h_1$  and  $h_2$  are equal, it is a parallel gap.

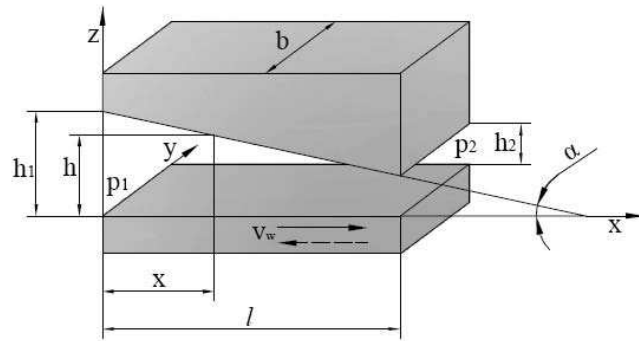


Fig. 2. Diagram of a flat confusor gap

It is assumed that oil, whose viscosity is determined by the dynamic viscosity coefficient  $\mu$  being under the constant pressure gradient, flows through a flat cline gap confined by impenetrable, perfectly smooth and inelastic walls. The upper wall is stationary and the lower wall, being subject to external forces, counteracts resistance due to oil viscosity, and moves with constant horizontal velocity  $v_w$  with respect to the stationary wall. The motion of the particles of incompressible oil with the turn of the  $x$  axis is steady, constant and rectilinear. After adopting the assumptions:  $v_x = v_x(x,z)$ ,  $v_y = 0$  and  $v_z = 0$ , equations (1 ÷ 4) become simplified:

$$v_x \frac{\partial v_x}{\partial x} = \nu \left( \frac{\partial^2 v_x}{\partial x^2} + \frac{\partial^2 v_x}{\partial z^2} \right) - \frac{1}{\rho} \frac{\partial p}{\partial x}. \quad (6)$$

$$0 = \frac{\partial p}{\partial y}, \quad (7)$$

$$0 = \frac{\partial p}{\partial z}, \quad (8)$$

$$\frac{\partial v_x}{\partial x} = 0. \quad (9)$$

It follows from (6 ÷ 9) that  $v_x = v_x(z)$  and  $p = p(x)$ .

Thus, the motion of oil in the gap is represented by the following differential equation:

$$0 = \nu \frac{\partial^2 v_x}{\partial z^2} - \frac{1}{\rho} \frac{\partial p}{\partial x}. \quad (10)$$

With the dynamic viscosity coefficient  $\mu$ :

$$\mu = \nu \rho. \quad (11)$$

Equation (10) becomes:

$$\frac{\partial^2 v_x}{\partial z^2} = \frac{1}{\mu} \frac{\partial p}{\partial x}. \quad (12)$$

And after integrating equation (12) twice:

$$v_x = \frac{1}{\mu} \frac{\partial p}{\partial x} \frac{z^2}{2} + C_1 z + C_2. \quad (13)$$

The integration constants  $C_1$  and  $C_2$  were determined on the basis of the following boundary conditions:

$$v_x = v_w \text{ for } z = 0, \text{ and } v_x = 0 \text{ for } z = h.$$

Ultimately, the formula for flow velocity in the gap is:

$$v_x = \frac{1}{2\mu} \frac{\partial p}{\partial x} (z^2 - hz) - \frac{v_w}{h} z + v_w. \quad (14)$$

The oil flow intensity occurring in a gap of the height  $b$  can be represented as:

$$Q = b \int_0^h v_x dz. \quad (15)$$

Then, substituting (14) into (15):

$$Q = -\frac{1}{12\mu} \frac{\partial p}{\partial x} b h^3 + v_w \frac{h}{2} b. \quad (16)$$

The pressure distribution  $p(x)$  of oil in a gap can be found from the following equation [Ivantysynova 2009]:

$$p(x) = \int \frac{\partial p}{\partial x} dx. \quad (17)$$

The differential  $\partial p/\partial x$  was obtained from (16):

$$\frac{\partial p}{\partial x} = \frac{6\mu v_w}{h^2} - \frac{12\mu Q}{bh^3}. \quad (18)$$

Substituting (18) into equation (17):

$$p(x) = \int \left( \frac{6\mu v_w}{h^2} - \frac{12\mu Q}{bh^3} \right) dx. \quad (19)$$

When equation (5) is taken into account, equation (19) becomes:

$$p(x) = \int \left[ \frac{6\mu v_w}{\left( (h_2 - h_1) \frac{x}{l} + h_1 \right)^2} - \frac{12\mu Q}{b \left( (h_2 - h_1) \frac{x}{l} + h_1 \right)^3} \right] dx. \quad (20)$$

Then, after integrating equation (20):

$$p(x) = \frac{6\mu v_w}{(h_2 - h_1)l} \cdot \frac{1}{(-1)} \cdot \frac{(h_2 - h_1)}{l} \cdot \frac{1}{x + h_1} - \frac{12\mu Q}{b \cdot (h_2 - h_1)l} \cdot \frac{1}{(-2)} \cdot \frac{1}{\left[\frac{(h_2 - h_1)}{l}x + h_1\right]^2} + C. \quad (21)$$

The integration constant  $C$  was obtained on the assumption that pressure at the entrance to the gap is  $p_1$  (when  $x = 0$   $p = p_1$ ). Thus, the integration constant  $C$  is:

$$C = p_1 + \frac{6\mu v_w l}{(h_2 - h_1)h_1} - \frac{6\mu Q l}{b(h_2 - h_1)h_1^2}, \quad (22)$$

and the pressure distribution  $p(x)$  of oil in the gap is:

$$p(x) = \frac{6\mu l}{h_2 - h_1} \left( -\frac{v_w}{h} + \frac{Q}{bh^2} + \frac{v_w}{h_1} - \frac{Q}{bh_1^2} \right) + p_1. \quad (23)$$

The difference  $h_2 - h_1$  can be obtained by transforming equation (5):

$$h_2 - h_1 = (h - h_1) \frac{l}{x}. \quad (24)$$

Then, substituting (24) into equation (23):

$$p(x) = \frac{6\mu x}{h - h_1} \cdot \left( v_w \frac{h - h_1}{h_1 h} + \frac{Q}{b} \cdot \frac{h_1^2 - h^2}{h_1^2 h^2} \right) + p_1. \quad (25)$$

After transformations, formula (25) becomes:

$$p(x) = \frac{6\mu x}{h_1 h} \cdot \left( v_w - \frac{Q}{b} \frac{h + h_1}{hh_1} \right) + p_1. \quad (26)$$

After substituting the boundary conditions  $x = l$ ,  $p = p_2$  and  $h = h_2$  into equation (26) a formula for the oil flow intensity in the gap was obtained:

$$Q = \frac{(p_1 - p_2) \cdot b \cdot (h_1 \cdot h_2)^2}{6\mu l \cdot (h_1 + h_2)} + \frac{v_w \cdot b \cdot h_1 \cdot h_2}{h_1 + h_2}. \quad (27)$$

When equations (27) and (26) are taken into consideration, the equation of oil pressure distribution in a variable-height gap finally becomes:

$$p(x) = \frac{6\mu x}{h_1 h} \cdot \left[ v_w - \left( \frac{(p_1 - p_2)(h_1 \cdot h_2)^2}{6\mu l \cdot (h_1 + h_2)} + v_w \frac{h_1 \cdot h_2}{h_1 + h_2} \right) \frac{h + h_1}{h \cdot h_1} \right] + p_1. \quad (28)$$

### RESULTS OF SIMULATION EXPERIMENTS ON OIL PRESSURE DISTRIBUTION IN A VARIABLE-HEIGHT GAP

The simulation experiments on oil pressure distribution in a variable-height gap were conducted by means of the available computer programs.

The following input data were assumed in the computations:

- pressure at the gap entrance  $p_1 = 16$  [MPa],
- pressure at the gap exit  $p_2 = 0$  [MPa],
- gap length  $l = 0,030$  [m],
- gap height  $b = 0,015$  [m],
- dynamic viscosity coefficient within the range of 0,0122 to 0,0616 [Pas],
- relative velocity of one of the walls – 5 to 5 [m/s].

The entrance and exit heights for the confusor gap are  $h_1 = 36$  [ $\mu\text{m}$ ] and  $h_2 = 12$  [ $\mu\text{m}$ ], respectively, and for the diffuser gap  $h_1 = 12$  [ $\mu\text{m}$ ] and  $h_2 = 36$  [ $\mu\text{m}$ ].

Fig. 3 presents oil pressure distributions for flow in a confusor gap (the convex curve), a parallel gap (the linear pressure) and a diffuser gap (the concave curve).

Fig. 4 presents oil pressure distributions for friction flows caused by a relative motion of one of the walls in a confusor and diffuser gaps, depending on the velocity.

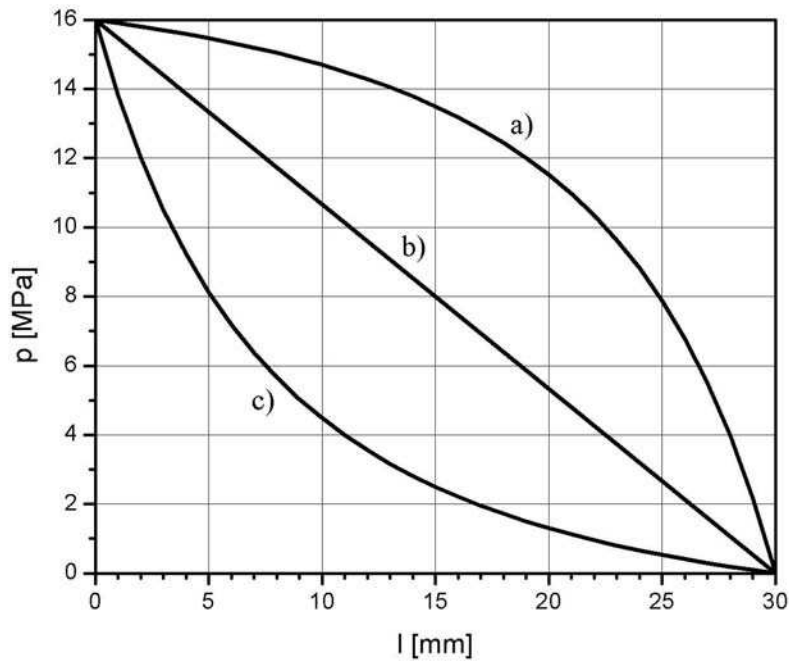


Fig. 3. Oil pressure distributions for pressure flows in a flat gap  
a) confusor gap, b) parallel gap, c) diffuser gap

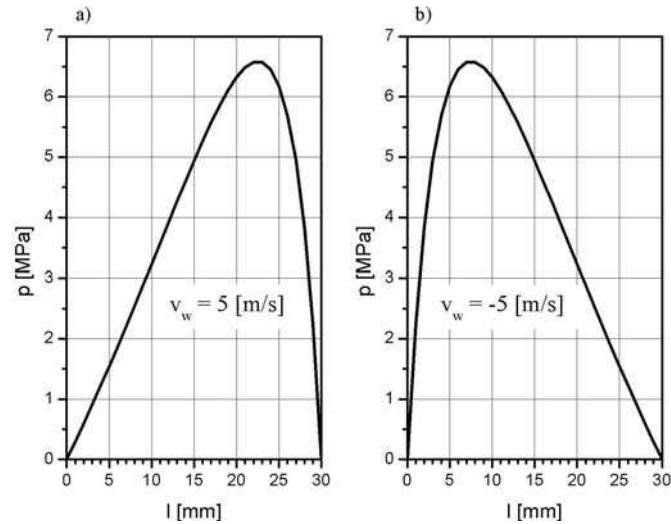


Fig. 4. Oil pressure distributions in a variable-height gap for friction flows depending on the velocity of the lower wall for a) confusor gap, b) diffuser gap

An interesting case of flow in a variable-height gap is the pressure-friction flow caused both by the pressure difference and the relative motion of one of the walls.

Fig. 5 presents oil pressure distributions in a gap depending on the dynamic viscosity coefficient, with relative motion of one of the walls in the direction of the flow, for confusor and diffuser gaps.

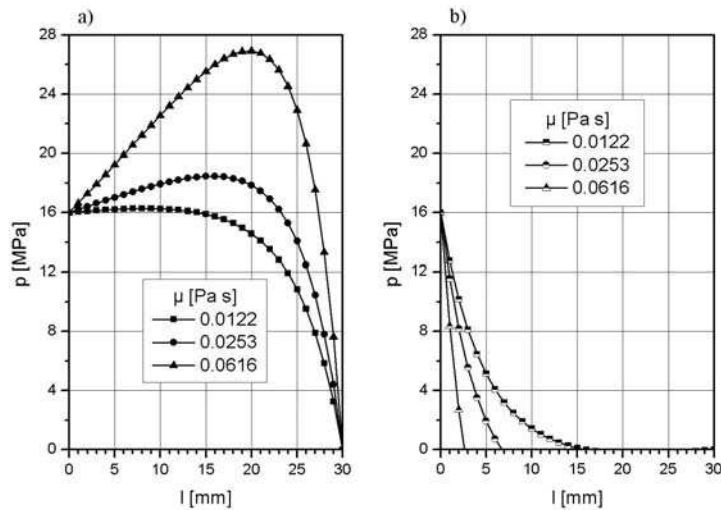


Fig. 5. Oil pressure distributions in the gap depending on the dynamic viscosity coefficient with the relative motion of the lower wall in the direction of the flow ( $p_1 = 16$  MPa,  $p_2 = 0$  MPa,  $v_w = 5$  m/s) for a) confusor gap, b) diffuser gap

Fig. 6 shows oil pressure distributions in a gap with relative motion of one of the walls in the opposite direction to the flow, depending on the dynamic viscosity coefficient for confusor and diffuser gaps.

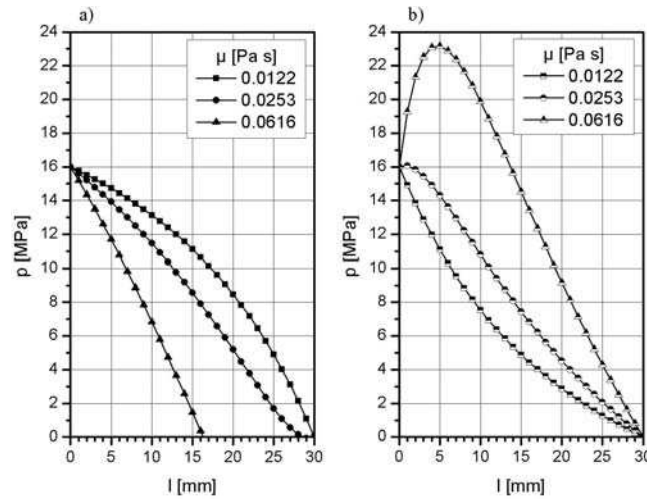


Fig. 6. Oil pressure distributions in a gap depending on the dynamic viscosity coefficient with the lower wall moving in the direction opposite to the flow ( $p_1 = 16$  MPa,  $p_2 = 0$  MPa,  $v_w = -5$  m/s) for a) confusor gap, b) diffuser gap

Figs. 7 and 8 present oil pressure distributions in gaps depending on the relative velocity of one of the walls for confusor and diffuser gaps, respectively.

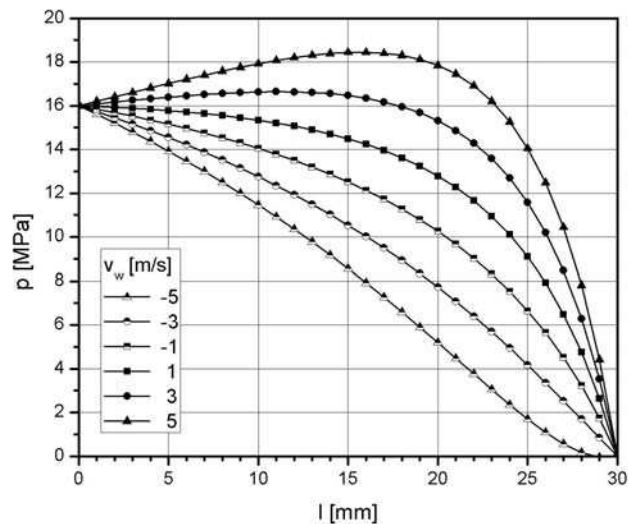


Fig. 7. Oil pressure distributions in a confusor gap depending on the relative velocity  $v_w$  of the lower wall ( $p_1 = 16$  MPa,  $p_2 = 0$  MPa)

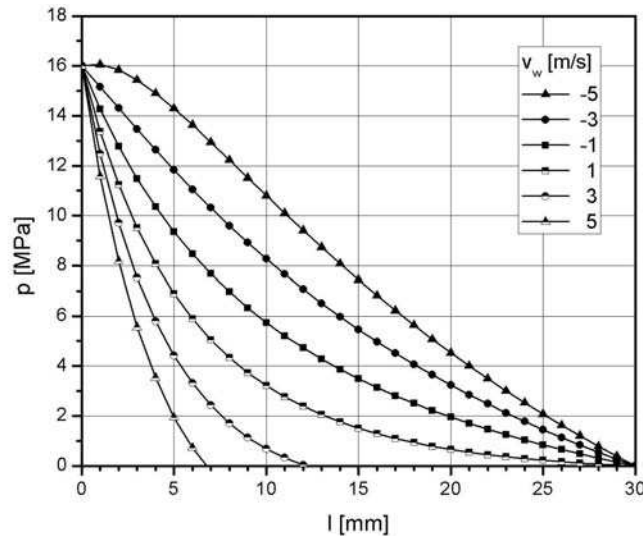


Fig. 8. Pressure distributions in a diffuser gap depending on the relative velocity  $v_w$  of the lower wall ( $p_1 = 16$  MPa,  $p_2 = 0$  MPa)

The analysis of oil pressure distributions in variable-height gaps demonstrates that in confusor type gaps the pressure increases along the gap, whereas in diffuser type gaps the pressure drops, compared to the pressure in a parallel gap.

## CONCLUSIONS

The conducted analyses lead to the following conclusions:

1. The computation model assumed in the study makes it possible to find pressure distributions in flat variable-height gaps.
2. The pressure distribution depends by and large on the dynamic viscosity of oil and relative motion of one of the walls.
3. As compared to a parallel gap, confusor type gaps show increase in oil pressure, whereas diffuser type gaps show decrease in oil pressure.
4. Oil flow in variable-height gaps will be subject to further investigation.

## REFERENCES

1. Baszta T.M., 1966.: *Hydraulika w budowie maszyn*. Poradnik. WNT, Warszawa.
2. Baszta T.M., 1971.: *Maszynostroitel'naja gidraulika*. Maszynostrojenie, Moskwa.
3. Bukowski J., 1975.: *Mechanika płynów*. PWN, Warszawa.
4. Ivantysyn J., Ivantysynova M., 2001: *Hydrostatic Pumps and Motors*. Academia Books International. New Delhi.
5. Ivantysynova M., 2009.: *Design and Modeling of Fluid Power Systems*. Purdue University.
6. Kondakow L. A., 1975.: *Uszczelnienia układów hydraulicznych*. WNT, Warszawa.

7. Lasaar R., 2000.: The Influence of the Microscopic and Macroscopic Gap Geometry on the Energy Dissipation in the Lubricating Gaps of Displacement Machines. Proc. of 1-st FPNI-PhD Symposium. Hamburg.
8. Nikitin G.A., 1982.: Szczielewyje i labirintnyje upłotnienia gidroagregatow. Maszynostrojenie, Moskwa.
9. Osiecki A., 2004.: Hydrostatyczny napęd maszyn. WNT, Warszawa.
10. Osipow A.F., 1966.: Objemnyje gidrowliczeskie maszyny. Maszynostrojenie, Moskwa.
11. Podolski M.E., 1981.: Upornyje podszipniki skolżenia. Leningrad.
12. Stryczek S., 1984: Napęd hydrostatyczny. Elementy i układy. WNT, Warszawa.
13. Szydelski Z.: Olechowicz J., 1986.: Elementy napędu i sterowania hydraulicznego i pneumatycznego. PWN, Warszawa.
14. Trifonow O.N., 1974.: Gidrawliczeskie systemy mietałorieżuszczych stankow. MSI, Moskwa.
15. Walczak J., 2006.: Inżynierska mechanika płynów. Wyd. Politechniki Poznańskiej, Poznań.

#### ROZKŁADY CIŚNIENIA OLEJU W SZCZELINACH PŁASKICH O ZMIENNEJ WYSOKOŚCI

**Streszczenie.** W opracowaniu przedstawiono problematykę związaną z przepływami oleju przez szczeliny płaskie o zmiennej wysokości występujące w różnego rodzaju maszynach hydraulicznych. Na podstawie równań Naviera-Stokesa i równania ciągłości wyznaczono zależności określające ciśnienie panujące wzdłuż szczeliny. Przedstawiono rezultaty obliczeń rozkładów ciśnienia w szczelinach o zmiennej wysokości konfuzorowych i dyfuzorowych w zależności od lepkości oleju i ruchu względnego jednej ze ścianki tworzącej szczelinę.

**Słowa kluczowe:** szczelina zmiennej wysokości, olej hydrauliczny, rozkłady ciśnienia.



## OIL LEAKAGE IN A VARIABLE-HEIGHT GAP BETWEEN THE CYLINDER BLOCK AND THE VALVE PLATE IN A PISTON PUMP

Tadeusz Zloto, Damian Sochacki

Institute of Machine Technology and Production Automation  
Czestochowa University of Technology

**Summary.** The paper analyses the flow intensity of oil leakages in a variable-height gap between the cylinder block and the valve plate in an axial piston pump. The analysis is carried out for various zones of the valve plate depending on the inclination angle of the cylinder block and the dynamic viscosity coefficient of oil.

**Key words:** oil leakage, variable-height gap, piston pump.

### INTRODUCTION

Due to their capability of operating at high pressures and powers, piston pumps are characterized by high values of energy efficiency coefficients, computed as the ratio of power to mass or volume [Osiecki 2004, Stryczek 1984]. Because of that they have found numerous applications in various branches of industry, especially in machines with complex functions, high efficiency and yield requirements. This, in turn, creates a demand for continuous development towards improving exploitation parameters of those machines by modernizing their construction.

In a pump operating in real conditions, due to variable moments resulting from hydrostatic load and relief forces, the cylinder block takes a non-parallel position with respect to the valve plate and the gap between them is of variable height [Ivantysyn and Ivantysynova 2001, Jang 1997, Kaczmarek and Rutanski 1982, Pasyнков 1976 ], as shown in Fig. 1.

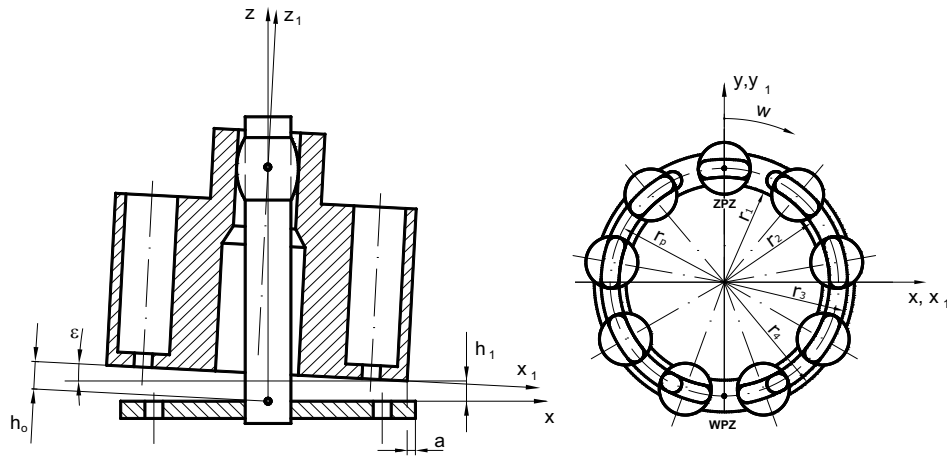


Fig. 1. Variable-height gap with a non-parallel cylinder block

During the pump's operation oil leaks outside and inside the valve plate, which affects, among other things, the volumetric efficiency of the pump [Jerszow and Kariew 1979, Zloto 2007].

In the present paper numerical methods are employed for determining the flow intensity of oil leaks in various zones of the valve plate in an axial piston pump.

#### COMPUTATION MODEL OF FLOW INTENSITY OF OIL LEAKS IN A VARIABLE-HEIGHT GAP

It was assumed that the gap between the rotating cylinder block and the valve plate is of variable height. Assumptions concerning the oil flow in the gap are as follows [Nikitin 1982, Osipow 1966]:

- the flow is laminar,
- the surfaces are rigid and do not undergo deformation,
- the gap's height is small and completely filled with oil,
- the tangent stress is Newtonian,
- the liquid is noncompressible,
- the liquid inertia forces are negligible.

A model of gap flows between the cylinder block and the valve plate is shown in Fig. 2.

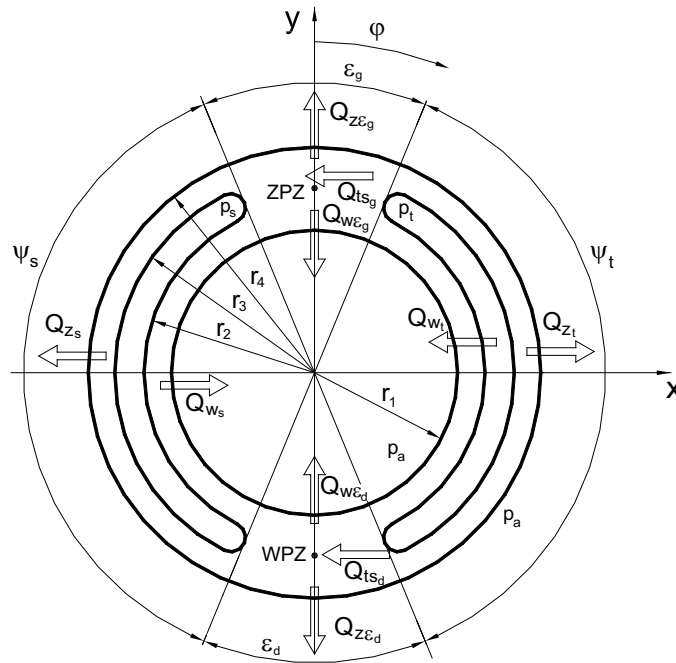


Fig. 2. Model of gap flows

In the pressure zone  $\psi_t$  and the suction zone  $\psi_s$ , the liquid flows outside the valve plate  $Q_{z_t}$  and  $Q_{z_s}$ , and into the valve plate  $Q_{w_t}$  and  $Q_{w_s}$ . In the upper and lower transition zones there are also centrifugal flows  $Q_{z\varepsilon_g}$  and  $Q_{z\varepsilon_d}$ , as well as centripetal flows  $Q_{w\varepsilon_g}$  and  $Q_{w\varepsilon_d}$ . Between the pressure and suction zones there are peripheral flows  $Q_{ts_g}$  and  $Q_{ts_d}$ .

In each of the zones the flow intensity of oil leaks was computed as the elementary product of the gap cross-section area and the mean flow velocity in accordance with:

$$Q = P \frac{1}{n} \sum_{i=0}^n (v_r)_{sr_i}, \quad (1)$$

where:

$P$  – the total area of the gap cross-section,

$n$  – the number of interpolation intervals,

$(v_r)_{sr_i}$  – the mean flow velocity.

The cross-section area was obtained on the basis of the numerical method of squaring interpolated trapeziums [Majchrzak and Mochnacki 1994] according to:

$$P = l_n \left[ \frac{h(r, \varphi_0) + h(r, \varphi_n)}{2} + \sum_{i=1}^{n-1} h(r, \varphi_i) \right], \quad (2)$$

where:

$h(r, \varphi)$  – the gap height at a given radius and angle,

$\varphi_0$  – the angle at the beginning of a given zone,

$\varphi_n$  – the angle at the end of a given zone,

$n$  – the number of intervals in the method of squaring interpolated trapeziums,  
 $l_n$  – the length of an interval in the numerical method.  
 The gap height for a given cross-section was obtained from:

$$h = -r \sin \varphi \cdot \cos \delta \cdot \operatorname{tg} \varepsilon - r \cos \varphi \cdot \sin \delta \cdot \operatorname{tg} \varepsilon + R \operatorname{tg} \varepsilon + h_1, \quad (3)$$

where:

$r$  – the current radius of a given cross-section,

$\varphi$  – the angle of a given flow cross-section,

$\varepsilon$  – the inclination angle of the cylinder block,

$\delta$  – the angle between the axis  $x$  and the smallest height  $h_1$  of the gap,

$R$  – the radius of the cylinder block.

The accuracy of results obtained in the computation model depends on the number  $n$  of intervals in the numerical method of squaring interpolated trapeziums [Zloto and Nagorka 2009]. Fig. 3 presents the accuracy of results depending on the assumed number of intervals: the more intervals, the more accurate the results.

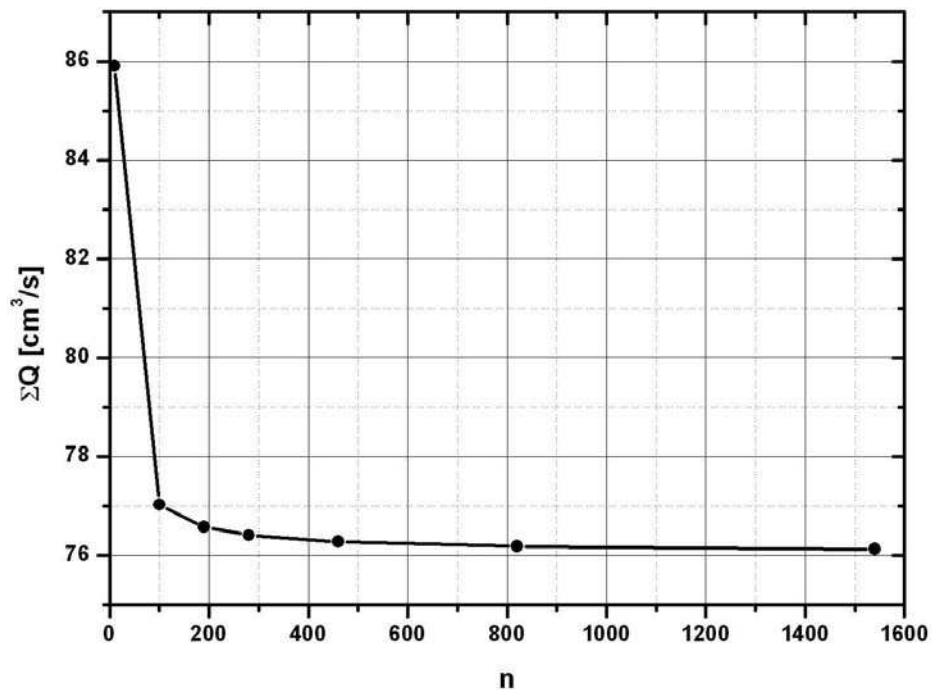


Fig. 3. Values of the flow intensity depending on the number of intervals assumed in the numerical method

The total flow intensity of oil leaks in a variable-height gap was computed according to the algorithm presented in Fig. 4.

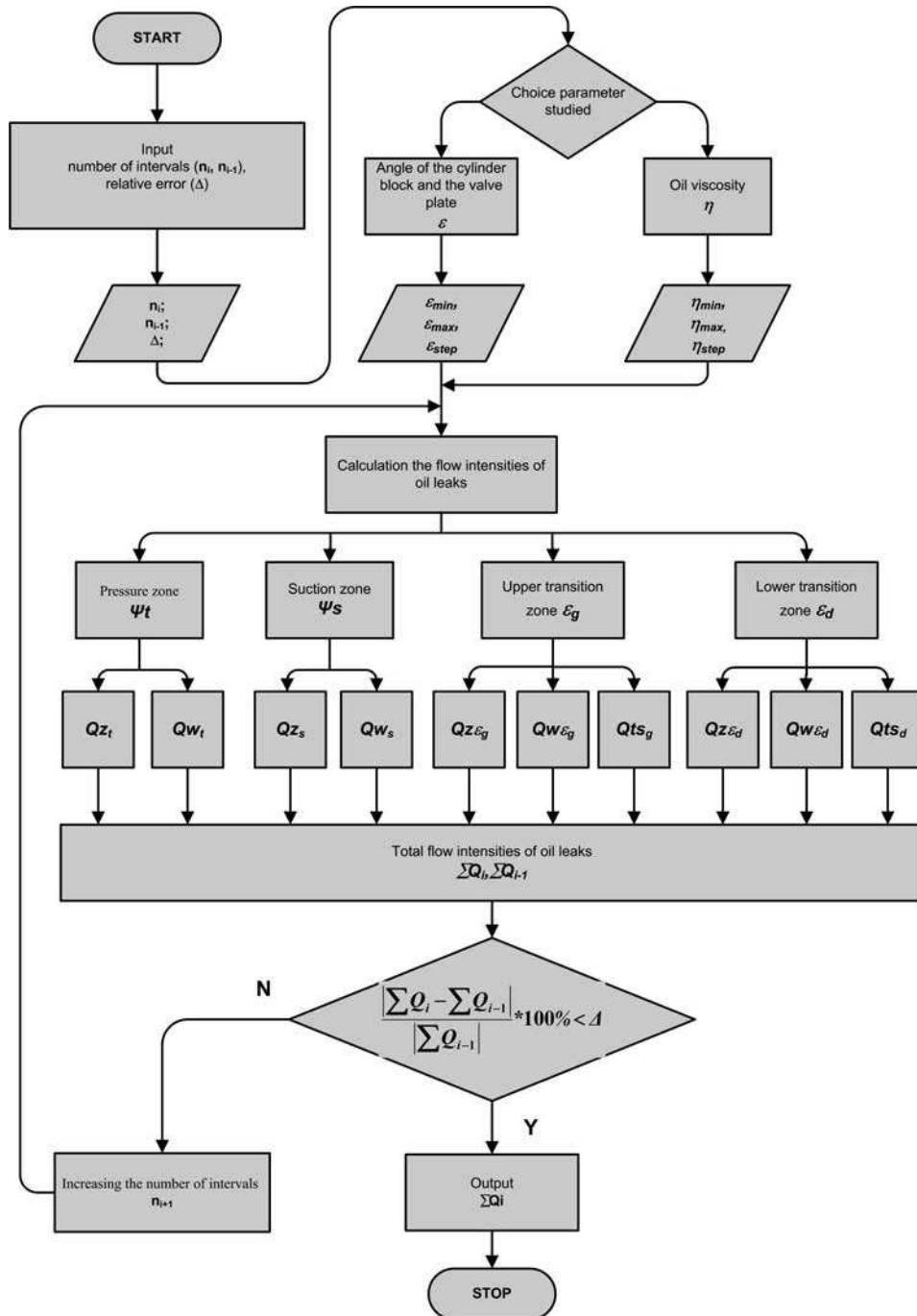


Fig. 4. Algorithm for numerical computation of the leak flow intensity

## RESULTS OF COMPUTATIONS CARRIED OUT IN THE STUDY

The above-described computation model was utilized for the analysis of the total leak flow intensity depending on the angle  $\varepsilon$  of the cylinder block inclination and the dynamic viscosity coefficient  $\eta$  of oil.

The following data was assumed in the model:

- the pressure in the pressure zone  $p_i = 32$  MPa,
- the pressure in the suction zone  $p_s = 0.1$  MPa,
- the pressure outside and inside the valve plate  $p_o = 0$  MPa,
- the angular velocity of the cylinder block  $\omega = 157$  rad/s,
- the angle  $\delta = 0,785$  rad with respect to the axis  $x$  of the smallest gap height  $h_1$ ,
- the angle of the cylinder block inclination with respect to the valve plate  $\varepsilon = 0,000523$  rad,
- the minimal gap height  $h_1 = 2 \times 10^{-6}$  m,
- the characteristic radii of the valve plate of a pump are  $r_1 = 0,0284$  m,  $r_2 = 0,0304$  m,  $r_3 = 0,0356$  m i  $r_4 = 0,0376$  m.

Fig. 5 presents the percentage shares of oil leak intensity in the particular zones of the valve plate. As can be seen, the greatest leaks are in the upper transition zone of the valve plate, and the smallest at the suction zone.

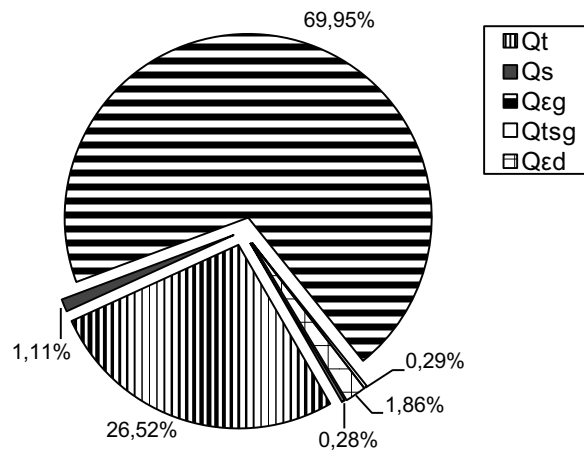


Fig. 5. Percentage shares of oil flow intensities at the particular zones of the valve plate

Figs. 6 and 7 show total values of oil leak flow intensity depending on the inclination angle of the cylinder block and on the dynamic viscosity coefficient of oil, respectively.

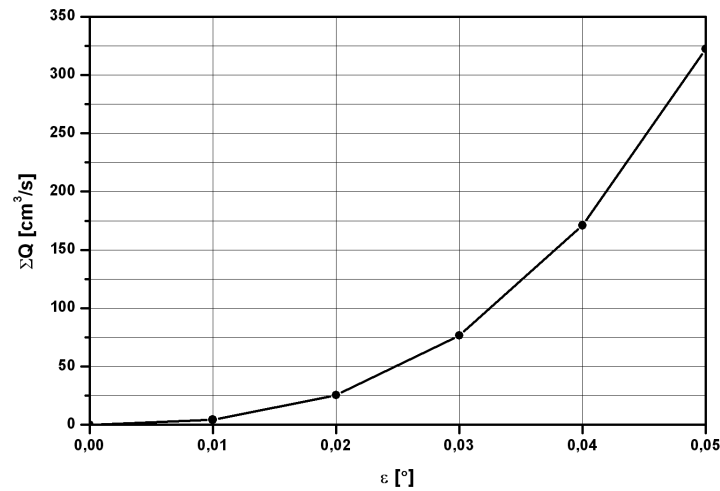


Fig. 6. Values of total flow intensities of oil leaks depending on the inclination angle of the cylinder block

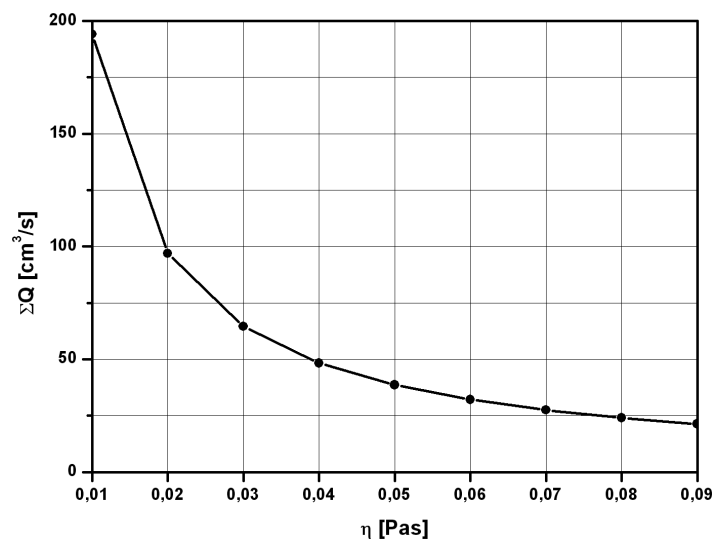


Fig. 7. Values of total flow intensities of oil leaks depending on the dynamic viscosity coefficient of oil

Figs. 6 and 7 depict the significant influence of the inclination angle of the cylinder block and of the dynamic viscosity coefficient of oil on the total values of oil leaks.

## CONCLUSIONS

On the basis of the carried out study, the following conclusions can be formulated.

1. The developed computation model is suitable for the analysis of the flow intensity of oil leaks in the particular zones of the valve plate.

2. The highest percentage of the leak flow intensity occurs in the upper transition zone.
3. The impact of the cylinder block inclination angle and of the dynamic viscosity coefficient on the total values of leak flow intensity is significant.

#### REFERENCES

1. Ivantysyn J., Ivantysynova M., 2001.: Hydrostatic Pumps and Motors. Academia Books International. New Delhi.
2. Jang D.S., 1997.: Verlustanalyse an Axialkolbenheiten. Dissertation. RWTH, Aachen.
3. Jerszow B.I., Kariew G.P., 1979.: Razpredelitel aksialnykh gidromaszin s rawienstwom utieczek w naprawleniach wnutriennowo i narużnowo pojaskow. Wiestnik Maszynostrojania nr 10.
4. Kaczmarek R., Rutański J., 1982.: Pompy wielotłoczkowe osiowe. Pomiar grubości szczeliny w rozdzielaczu z wykorzystaniem indukcyjnych czujników pomiarowych. Przegląd Mechaniczny nr 23 – 24.
5. Majchrzak E., Mochnacki B., 1994.: Metody numeryczne. Podstawy teoretyczne, aspekty praktyczne i algorytmy. Wydawnictwo Politechniki Śląskiej, Gliwice.
6. Nikitin G.A., 1982.: Szczielewyje i labirintnyje upłotnienia gidroagregatow. Maszynostrojanie, Moskwa.
7. Osiecki A., 2004.: Hydrostatyczny napęd maszyn, WNT, Warszawa.
8. Osipow A.F., 1966.: Objemnyje gidrowliczieskie maszyny. Maszynostrojanie, Moskwa.
9. Pasynkow R. M., 1976.: Wlijanie pieriekosa cylindrowo bloka na rabotu torcowowo raspriedielitiela aksialno-porszniewoj gidromasziny. Wiestnik Maszynostrojania nr 10.
10. Stryczek S., 1984.: Napęd hydrostatyczny. Elementy i układy., WNT, Warszawa.
11. Złoto T, Nagorka A., 2009.: An efficient FEM for pressure analysis of oil film in a piston pump. Applied Mathematics and Mechanics, Springer Vol. 30, No.1.
12. Złoto T., 2007.: Przecieki oleju w rozrządzie tarczowym pompy wielotłoczkowej osiowej. Hydraulika i Pneumatyka nr 6.

#### PRZECIEKI OLEJU W SZCZELINIE O ZMIENNEJ WYSOKOŚCI POMIĘDZY BLOKIEM CYLINDROWYM I TARCZĄ ROZDZIELACZA POMPY TŁOKOWEJ

**Streszczenie.** W pracy przedstawiono analizę natężenia przepływu przecieków oleju w szczelinie o zmiennej wysokości pomiędzy blokiem cylindrowym i tarczą rozdzielacza pompy wielotłoczkowej osiowej. Analizę przeprowadzono dla różnych stref tarczy rozdzielacza w zależności od kąta pochylenia bloku cylindrowego i współczynnika lepkości dynamicznej oleju.

**Słowa kluczowe:** przecieki oleju, szczelina o zmiennej wysokości, pompa tłokowa.



## OPERATIONAL RELIABILITY MODEL OF THE PRODUCTION LINE

Grzegorz Bartnik, Andrzej W. Marciniak

Department of Technology Fundamentals, University of Life Sciences in Lublin, Poland  
grzegorz.bartnik@up.lublin.pl; Andrzej.marciniak@up.lublin.pl

**Summary.** The proposed model has been created for the purpose of risk analysis in the production of a medical device. The requirement for risk management and risk analysis is articulated both in ISO 13485 and MDD Directive 93/42. The presented method of risk modeling is exemplified by risk analysis in the production of a medical device, namely a dental composite.

**Key words:** probabilistic networks, knowledge engineering, reliability.

### INTRODUCTION

The concept of operational reliability model is related to the treatment of computer models as a way of knowledge representation. In this approach a model is treated as an engineering product, whose basic form of application is to build it in the information infrastructure of production processes management system. Such a reliability model requires certain functional properties and operational scenarios.

To meet these requirements it needs to broaden the conceptual system of classical reliability engineering with conceptual models used in knowledge engineering and artificial intelligence. In the context of the reliability concept, we refer not only to the machinery and equipment but the entire production process (process reliability), and reliability is treated as an aspect of predictability and repeatability of processes.

Application of knowledge engineering to reliability modeling has the effect that the model is created on the way through the transition from the representation of knowledge expressed in natural language to the form expressed in a formal and executable language. In this process of knowledge translation, machine learning algorithms based on previously gathered empirical facts play an important role. The model functions as a knowledge base (or part thereof) answering the questions asked by the user or another system. It is important that these responses are generated through automated inference mechanisms and not just a simple search. Achieving this functionality requires the use of special knowledge representation languages.

In the case of reliability models functioning as knowledge representation system their ability is required of conceptual integration with classical reliability theory. This requirement is fulfilled

to a large extent by the language of Bayesian networks. Hence their use in the reliability modeling of a production line.

### OBJECT AND METHOD OF RELIABILITY MODELING

Application of Bayesian networks to reliability modeling is shown on the example of a medical device production line. Products in that category are subject to special requirements arising inter alia from the European Directive MDD93/42 and the ISO 13485 standard. In the process of medical devices manufacturing must be consciously and rationally justified by the methods used for risk management. Reliability model of the production process is treated as one of the main elements of risk management system.

The production process in this case is cyclical and the production cycle is a sequence of specific actions (operations) leading to the final product that meets the relevant standards and requirements of the user. The structure of that process is shown in Figure 1.

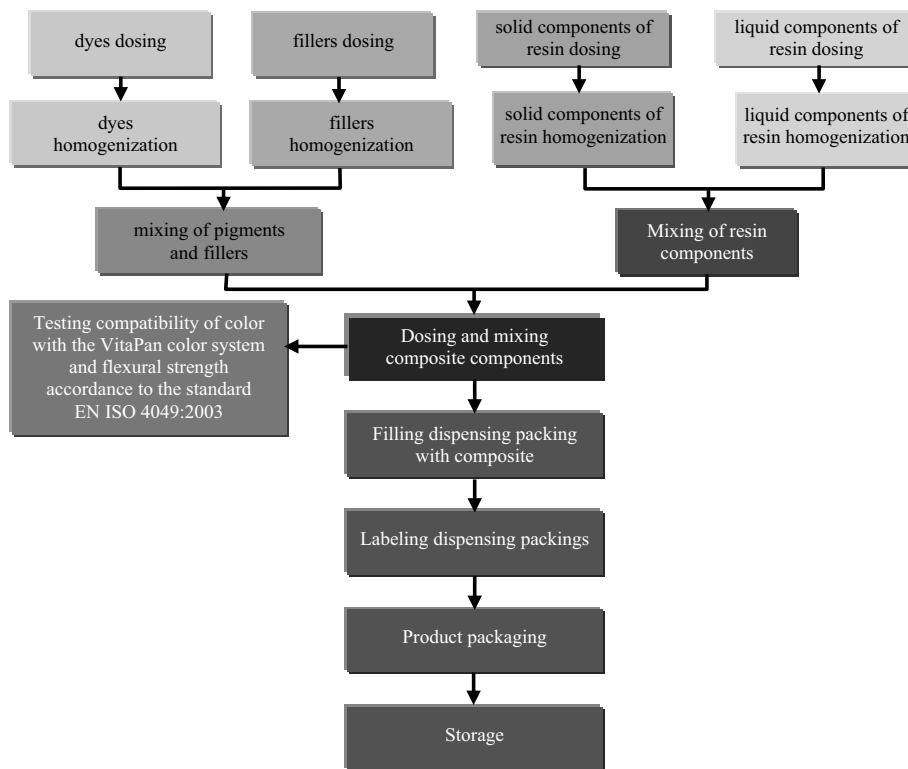


Fig. 1. Structure of dental composite manufacturing process

The conceptualization of reliability process in this case consists of product requirements specification of each operation by projecting back the final product requirements and then identification of the events conditioning the fulfillment of requirements specific for each operation.

In the classical reliability engineering, reliability model of the considered process would most likely be created in the technique of event trees or fault trees. An example of such a model is shown in Figure 2. Each operation involves nodes representing the occurrence of adverse events or non-occurrence required events and deterministic fusion node representing the cumulative effect of these events (Fig. 3).

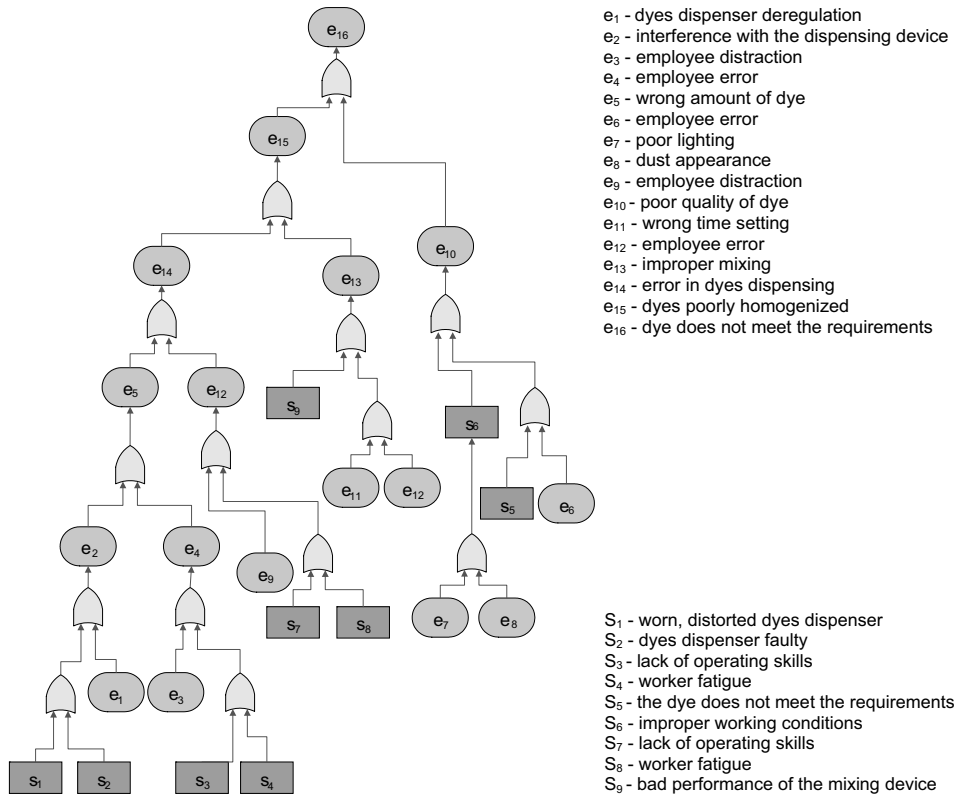


Fig. 2. Elementary Bayesian network

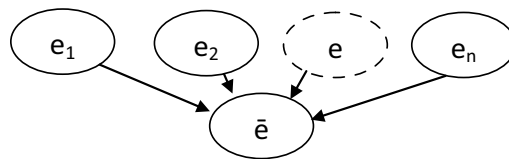


Fig. 3. Elementary Bayesian network

If any of the events alone is sufficient for the failure of the operation, then the resulting node “ $e$ ” can be modeled as an operation “Noisy-Or”, being a probabilistic counterpart of the logical “OR”. The additional expressiveness can be achieved by applying the operations “Noisy-Or” of “leakage” (leakage), which is interpreted as the probability that the result of the technological operations will be negative, although not all the required events which occurred were negative. In



successful completion of each operation, and the likelihood of successful completion of the process by obtaining a final product complying with the requirements.

## CONCLUSIONS

The paper presents the problem of process reliability modeling using Bayesian networks technology. Models made in this technology meet the requirements of being a knowledge representation system, that is, have the characteristic of adaptability, i.e. automatic tuning the model to the specific environment of its use by machine learning on empirical examples. Such models can be used to asking questions concerned with risk management in production processes and getting answers by inference mechanisms prediction and explanation.

## REFERENCES

1. Bartnik G. Marciniak A.: Modelowanie ryzyka identyfikacji krytycznych punktów kontroli w łańcuchach żywności. Zarys inżynierii systemów bioagrotechnicznych, część 3b pod redakcją Leszka Powierzy, P.P.-H „DRUKARNIA” Sp.z.o.o. Sierpc, s.401-420, Płock 2007.
2. Bartnik G., Kusz A., Marciniak A.: Dynamiczne sieci bayesowskie w modelowaniu procesu eksploatacji obiektów technicznych. Inżynieria Wiedzy i Systemy Ekspertowe, t. II, str. 201-208, Oficyna Wydawnicza Politechniki Wrocławskiej, Wrocław 2006.
3. Jansen F. V.: An introduction to Bayesian Networks. Taylor&Francis, London 1996.
4. Marciniak A., Maksym P.: Model wspomaganie działań interwencyjnych w sytuacji zagrożenia uprawy pszenicy ozimej. Inżynieria Wiedzy i Systemy Ekspertowe, t. II, str. 353-361, Oficyna Wydawnicza Politechniki Wrocławskiej, Wrocław 2006.
5. Marciniak A.: Projektowanie systemu reprezentacji wiedzy o rolniczym procesie produkcyjnym. Rozprawy naukowe Akademii Rolniczej w Lublinie, Wydział Inżynierii Produkcji, zeszyt 298, WAR 2005.
6. Murphy K. P.: Dynamic Bayesian Networks. 2002. <http://www.ai.mit.edu/~murphyk>.
7. Pearl J.: Probabilistic reasoning in intelligent systems: networks of plausible reasoning. Morgan-Kaufman Publ. Inc. 1988.

## MODEL OPERACYJNO-NIEZAWODNOŚCIOWY LINII PRODUKCYJNEJ

**Streszczenie.** Zaproponowany model utworzony został dla potrzeb analizy ryzyka przy produkcji wyrobu medycznego. Wymóg zarządzania ryzykiem i przeprowadzania analizy ryzyka występuje zarówno w normie ISO 13485 jak i dyrektywie MDD 93/42. Przedstawiona została metoda modelowania ryzyka dla potrzeb przeprowadzania analizy ryzyka przy produkcji wyrobu medycznego, jakim jest kompozyt stomatologiczny.

**Słowa kluczowe:** sieci probabilistyczne, inżynieria wiedzy, niezawodność.

## APPLICATION OF THE OPERATIONAL RELIABILITY MODEL TO THE RISK ANALYSIS IN MEDICAL DEVICE PRODUCTION

Grzegorz Bartnik<sup>1</sup>, Grzegorz Kalbarczyk<sup>2</sup>, Andrzej W. Marciniak<sup>1</sup>

<sup>1</sup>Department of Technology Basics, Faculty of Production Engineering,  
University of Life Sciences in Lublin

grzegorz.bartnik@up.lublin.pl; andrzej.marciniak@up.lublin.pl

<sup>2</sup>Laboratory of Dental Pharmacology ARKONA, info@arkonadent.com

**Summary.** We present an application of the Bayesian network model to the risk analysis of the operational reliability of the dental composite material production line. The model is a computational tool meeting the risk management requirements formulated in the directive MDD 93/42 and the standard ISO 13485 concerning medical devices.

**Keywords:** probability networks, risk analysis, reliability

### INTRODUCTION

This paper is devoted to the application of mathematical approach of Bayesian networks to model process reliability of production lines. The starting point of this work is the computational model, which we have recently developed [Bartnik, Marciniak 2011]. The model has the properties of the adaptive data base using the algorithms of machine learning applied to the sets of systematically stored empirical data to calibrate model parameters. This approach allows for addressing specific questions using automatic inference mechanisms. The operational reliability (process reliability) is defined as the probability that the product obtained in the production satisfies appropriate standards, customer and legislative demands. Fulfilling all these demands depends on many random factors, which may significantly influence the quality of the final product.

### MODEL AND METHODS

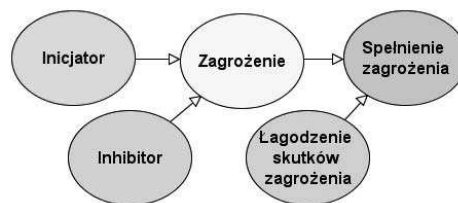
The object of our study is a technological line for production of dental composite materials.

Production process is referred to as a sequence of the operations leading to the final product. During each operation there are external factors, related to the operator or machines used, which may endanger the results by causing the so called hazard initiating event. However, an occurrence of

the initiating event does not necessarily lead to the production of an invalid final product, especially if hazard inhibiting events are possible (hazard inhibitors).

Hazard situations may lead to the danger scenario with a given probability. The results of the hazard depend on the possibility of the events mitigating the negative effects. One established method to model such systems is to use Bayesian networks. The model we apply is based on 5 nodes connected by the cause-effect relations (for details see Fig. 1).

For each operation of the technological process after the identification of a hazard, one or several such diagrams can be created, depending on the number of different types of hazard specific for the given operation. Information fusion concerning a single operation can be done using the “noisy or” gate.



Legend: Inicjator-Initiator; Zagrozenie-Risk; Spełnienie zagrożenia- Risk occurrence; Inhibitor- Inhibitor; Łagodzenie skutków zagrożenia- Mitigating the effects of hazard

Fig. 1. A basic model of risk

In agreement with the European directives and related standards, the system of the risk analysis and management should enable the answering of the questions of two categories:

- risk prediction for each type of hazard.
- prediction of the most probable causes and identification of the hazard sources for each specified defect of the final product.

These questions belong to the category of the risk prediction and shall explain the reasons of the hazard. Risk management is based on the decision making in dependence on the response to the questions formulated above.

## RESULTS

In this paper we apply the computer model of the process reliability of the production line to the case of dental composite materials production. In the remainder of this section we show how the model may be applied to answer specific questions on the quality of the final product.

In Fig. 2 we present a part of the Bayesian network demonstrating a predictive reasoning leading to answering the question concerning a possibility of receiving by a customer of a product that does not meet the requirements, given the probabilities of the causes of such event.

We consider the following example for the production line under consideration: Let the prior probability of using wrong pigments be equal to 2,023%, the prior probability of a dosage error be equal to 0,759%, and the prior probability of an improper mixing equals 0,670%. If the result of the strength test is positive with the probability 1,143% and the color test is negative with the probability 96,125% (the result that does not eliminate the product during the test phase), then the probability that the customer receives a defective product is equal to 10,504%.

Fig. 3 is devoted to the response of our model for a given probability that the customer receives a product not meeting the requirements, defined at an acceptable level of 0,118%. In other words, the aim of the model is to establish the maximal level of the risk of the events "wrong pigments", "dosage error", and "improper mixing" taking place with the probabilities 0,083%, 0,009% and 0,008%, respectively, which result in the event "wrong color" with the probability 0,049%.

In Fig. 5 we present a typical scheme of the model realization allowing for an investigation of the observed effects using the specification of the most probable causes. Assuming that the event "the customer receives a product which does not meet the requirements" is taking place for sure (with the probability 100%), and it is due to the occurrence of the event "wrong color" with the probability 100%, we specify the probability distributions of the network nodes preceding the node "wrong color":

- The wrong pigments with the probability 59,043%
- The dosage error with the probability 22,137%
- The improper mixing with the probability 19,815%.

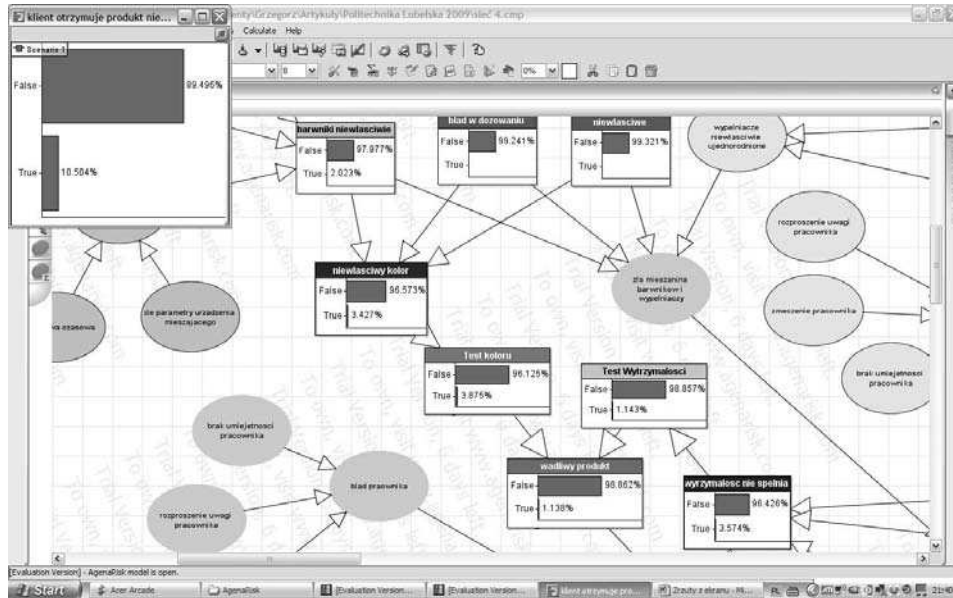


Fig. 2. Response of the network to the question about the probability of the event "the customer receives the product which does not meet the requirements" given the probabilities of the possible causes.





## CONCLUSIONS

The operational reliability model given in the form of the Bayesian network can be used to analyze the risk of obtaining of a final product that does not meet the requirements. Mechanisms of predictive and diagnostic reasoning typical for the Bayesian networks allow for the answering of specific questions posed in the risk analysis. In this paper we presented an example of this approach applied to the technological line of the dental composite material.

## REFERENCES

1. Bartnik G., Marciniak A.: operational reliability model of the production line, Teka Komisji Motoryzacji i Energetyki Rolnictwa Polskiej Akademii Nauk Oddział w Lublinie (przyjęty do druku lipiec 2011).
2. Bartnik G., Kusz A., Marciniak A.: Dynamiczne sieci bayesowskie w modelowaniu procesu eksploatacji obiektów technicznych. Inżynieria Wiedzy i Systemy Ekspertowe, t. II, str. 201-208, Oficyna Wydawnicza Politechniki Wrocławskiej, Wrocław 2006.
3. Jansen F. V.: An introduction to Bayesian Networks. Taylor & Francis, London 1996.
4. Marciniak A., Maksym P.: Model wspomaganie działań interwencyjnych w sytuacji zagrożeń uprawy pszenicy ozimej. Inżynieria Wiedzy i Systemy Ekspertowe, t. II, str. 353-361, Oficyna Wydawnicza Politechniki Wrocławskiej, Wrocław 2006.
5. Marciniak A.: Projektowanie systemu reprezentacji wiedzy o rolniczym procesie produkcyjnym. Rozprawy naukowe Akademii Rolniczej w Lublinie, Wydział Inżynierii Produkcji, zeszyt 298, WAR 2005.
6. Murphy K. P.: Dynamic Bayesian Networks. 2002. <http://www.ai.mit.edu/~murphyk>.
7. Pearl J.: Probabilistic reasoning in intelligent systems: networks of plausible reasoning. Morgan-Kaufman Publ. Inc. 1988.
8. Bartnik G. Marciniak A.: Modelowanie ryzyka identyfikacji krytycznych punktów kontroli w łańcuchach żywności. Zarys inżynierii systemów bioagrotechnicznych, część 3b pod redakcją Leszka Powierzy, P.P.-H „DRUKARNIA” Sp.z.o.o. Sierpc, s.401-420, Płock 2007

## ZASTOSOWANIE MODELU OPERACYJNO-NIEZAWODNOŚCIOWEGO W ANALIZIE RYZYKA W PROCESIE PRODUKCJI WYROBU MEDYCZNEGO

**Streszczenie.** Przedstawiono zastosowanie modelu stworzonego dla potrzeb analizy ryzyka przy produkcji kompozytu stomatologicznego w odpowiedzi na wymagania zarządzania ryzykiem i przeprowadzania analizy ryzyka występujące w normie ISO 13485 oraz dyrektywie MDD 93/42 dotyczących wyrobów medycznych.

**Słowa kluczowe:** sieci bayesowskie, analiza ryzyka, niezawodność

## TABLE OF CONTENTS

<b>Anatoliy Boyko, Kostyantyn Dumenko</b> RESEARCH ON RELIABILITY OF SUBSYSTEMS OF GRAIN HARVESTING COMBINE.....	5
<b>Norbert Chamier-Gliszczyński</b> MODELLING OF TRAFFIC FLOW IN AN URBAN TRANSPORTATION SYSTEM.....	12
<b>Norbert Chamier-Gliszczyński</b> SELECTED ASPECTS OF MODELLING OF SUSTAINABLE URBAN TRANSPORTATION SYSTEM .....	19
<b>Adam Drosio, Marek Klimkiewicz, Remigiusz Mruk</b> ENERGETIC AND TECHNOLOGICAL ANALYSIS OF THE PROCESS OF OIL PRESSING FROM WINTER RAPE .....	25
<b>Mieczysław Dziubiński, Jacek Czarnigowski</b> MODELLING AND VERIFICATION FAILURES OF A COMBUSTION ENGINE INJECTION SYSTEM .....	38
<b>Andrzej Gil, Piotr Kowalski, Krzysztof Wańczyk</b> REDUCING ENERGY CONSUMPTION DURING MANUFACTURE OF SEMI-FINISHED COMPONENTS OF THE PLANETARY GEAR THROUGH THE USE OF CASTINGS MADE BY RAPID PROTOTYPING .....	53
<b>Bożena Gładyszewska, Anna Ciupak</b> A STORAGE TIME INFLUENCE ON MECHANICAL PARAMETERS OF TOMATO FRUIT SKIN.....	64
<b>Krzysztof Gołacki, Paweł Kołodziej</b> IMPACT TESTING OF BIOLOGICAL MATERIAL ON THE EXAMPLE OF APPLE TISSUE.....	74
<b>Wawrzyniec Gołębiowski, Tomasz Stoeck</b> TRACTION QUALITIES OF A MOTOR CAR FIAT PANDA EQUIPPED WITH A 1.3 16 V MULTIJET ENGINE .....	83
<b>Aleksander Karwiński, Zdzisław Żółkiewicz</b> APPLICATION OF MODERN ECOLOGICAL TECHNOLOGY LOST FOAM FOR THE IMPLEMENTATION OF MACHINERY.....	91

<b>Jarosław Knaga, Tomasz Szul</b>	
ANALYSIS OF WATER-WATER TYPE HEAT PUMP OPERATION IN A BUILDING OBJECT .....	100
<b>Arkadiusz Kociszewski</b>	
MODELLING OF THE THERMAL CYCLE OF SI ENGINE FUELLED BY LIQUID AND GASEOUS FUEL .....	109
<b>Anna Kowalska</b>	
RECRUITING AND USING AGRICULTURAL BIOGAS .....	118
<b>Milosław Kozak</b>	
AN APPLICATION OF BUTANOL AS A DIESEL FUEL COMPONENT AND ITS INFLUENCE ON EXHAUST EMISSIONS .....	126
<b>Paweł Kozak, Dariusz Dziki, Andrzej Krzykowski, Stanisław Rudy</b>	
OPTIMIZATION OF ENERGY CONSUMPTION IN THE FREEZE DRYING PROCESS OF CHAMPIGNON ( <i>AGARICUS BISPORUS L</i> ) .....	134
<b>Andrzej Krzykowski, Stanisław Rudy, Paweł Kozak, Dariusz Dziki, Zbigniew Serwatka</b>	
INFLUENCE OF BLANCHING AND CONVECTIVE DRYING CONDITIONS OF PARSLEY ON PROCESS ENERGY CONSUMPTION .....	142
<b>Izabela Kuna-Broniowska, Bożena Gładyszewska, Anna Ciupak</b>	
A COMPARISON OF MECHANICAL PARAMETERS OF TOMATO'S SKIN OF GREENHOUSE AND SOIL-GROWN VARIETIES .....	151
<b>Elżbieta Kusińska, Agnieszka Starek</b>	
MECHANICAL PROPERTIES OF TEXTURE OF MIXED FLOUR BREAD WITH AN ADMIXTURE OF RYE GRAIN .....	162
<b>Andrzej Kusz, Piotr Maksym, Andrzej W. Marciniak</b>	
BAYESIAN NETWORKS AS KNOWLEDGE REPRESENTATION SYSTEM IN DOMAIN OF RELIABILITY ENGINEERING .....	173
<b>Urszula Malaga-Toboła</b>	
OPERATING COSTS OF FARM BUILDINGS IN SELECTED ECOLOGICAL HOLDINGS .....	181
<b>Andrzej Marczuk, Wojciech Misztal</b>	
OPTIMIZATION OF A TRANSPORT APPLYING GRAPH-MATRIX METHOD .....	191
<b>Marcin Mitrus, Tomasz Oniszczuk, Leszek Mościcki</b>	
CHANGES OF SPECIFIC MECHANICAL ENERGY DURING EXTRUSION-COOKING OF POTATO STARCH .....	200

---

<b>Marcin Mitrus, Agnieszka Wójtowicz</b>	
EXTRUSION-COOKING OF WHEAT STARCH .....	208
<b>Janusz Mysłowski</b>	
POSSIBILITIES OF APPLICATION OF MODERN SI ENGINES IN AGRICULTURE.....	216
<b>Jaromir Mysłowski</b>	
NEGATIVE IMPACT OF MOTORIZATION ON THE NATURAL ENVIRONMENT.....	223
<b>Krzysztof Nęcka</b>	
ANALYSIS OF THE CONTINUITY OF ELECTRIC ENERGY SUPPLY IN POLAND .....	230
<b>Krzysztof Nęcka</b>	
USE OF DATA MINING TECHNIQUES FOR PREDICTING ELECTRIC ENERGY DEMAND.....	237
<b>Zenon Pirowski</b>	
APPLCATION OF NICKEL SUPERALLOYS ON CASTINGS FOR CONVENTIONAL ENERGY EQUIPMENT ITEMS.....	246
<b>Andrzej Pytel, Zbigniew Stefański</b>	
AN INNOVATIVE AND ENVIRONMENTALLY SAFE METHOD TO MANUFACTURE HIGH-QUALITY IRON CASTINGS FOR POSSIBLE USE AS ELEMENTS OF AGRICULTURAL MACHINES .....	256
<b>Andrzej Rejak, Leszek Mościcki</b>	
SELECTED MECHANICAL PROPERTIES OF TPS FILMS STORED IN THE SOIL ENVIRONMENT. ....	264
<b>Stanisław Rudy, Andrzej Krzykowski, Dariusz Dziki, Paweł Kozak, Zbigniew Serwatka</b>	
THE ANALYSIS OF POSSIBILITY OF ENERGY RECOVERY DURING CONVECTIVE DRYING OF PAPRIKA .....	273
<b>Leszek Rydzak, Dariusz Andrejko</b>	
EFFECT OF DIFFERENT VARIANTS OF PRETREATMENT OF WHEAT GRAIN ON THE PARTICLE SIZE DISTRIBUTION OF FLOUR AND BRAN .....	283
<b>Leszek Rydzak, Dariusz Andrejko</b>	
EFFECT OF VACUUM IMPREGNATION AND INFRARED RADIATION TREATMENT ON ENERGY REQUIREMENTS IN WHEAT GRAIN MILLING .....	291

<b>Marcin Sosnowski</b>	
COMPUTATIONAL DOMAIN DISCRETIZATION AND ITS IMPACT ON FLOW FIELD AROUND THE SPARK PLUG IN SI ENGINE .....	300
<b>Georgij Tajanowskij, Wojciech Tanas</b>	
DYNAMIC POTENTIAL OF PASSABLENESS OF THE AGRICULTURAL TRACTION-TRANSPORT TECHNOLOGICAL MACHINE WITH A HYDRODRIVE OF WHEELS .....	306
<b>Piotr Tarkowski, Ewa Siemionek</b>	
ENERGY CONSUMPTION IN THE MOTION OF THE VEHICLE WITH ELECTRIC PROPULSION.....	320
<b>Małgorzata Trojanowska, Jerzy Małopolski</b>	
FORECAST MODELS OF ELECTRIC ENERGY CONSUMPTION BY VILLAGE RECIPIENTS OVER A LONG-TERM HORIZON BASED ON FUZZY LOGIC .....	327
<b>Kazimierz Zawiślak, Józef Grochowicz, Paweł Sobczak</b>	
THE ANALYSIS OF MIXING DEGREE OF GRANULAR PRODUCTS WITH THE USE OF MICROTRACERS .....	335
<b>Tadeusz Złoto, Konrad Kowalski</b>	
OIL PRESSURE DISTRIBUTION IN VARIABLE HEIGHT GAPS .....	343
<b>Tadeusz Złoto, Damian Sochacki</b>	
OIL LEAKAGE IN A VARIABLE-HEIGHT GAP BETWEEN THE CYLINDER BLOCK AND THE VALVE PLATE IN A PISTON PUMP .....	353
<b>Grzegorz Bartnik, Andrzej W. Marciniak</b>	
OPERATIONAL RELIABILITY MODEL OF THE PRODUCTION LINE.....	361
<b>Grzegorz Bartnik, Grzegorz Kalbarczyk, Andrzej W. Marciniak</b>	
APPLICATION OF THE OPERATIONAL RELIABILITY MODEL TO THE RISK ANALYSIS IN MEDICAL DEVICE PRODUCTION.....	366